Energy Storage and its Strategic Impacts on the Power Network

A Thesis

SUBMITTED IN FULFILMENT OF THE REQUIREMENTS FOR THE DEGREE OF

DOCTOR OF PHILOSOPHY

By

MOHAMMAD TAUFIQUL ARIF

To

School of Engineering and Technology
Higher Education Division

Central Queensland University

Australia

March 2013

To the environment friendly future power network

Abstract

Modern power systems are moving towards accommodating more and more renewable energy (RE) into the grid to minimize greenhouse gas (GHG) emission from energy sector. Large scale adoption of solar photovoltaic (PV) and wind turbine creates instability in the power system network due to the intermittent nature of these sources. Major problem associated with these sources are fluctuation in energy level or even unavailability of useful energy, minimum or no supply of energy during peak demand, moreover integration of these sources in different phases can cause phase unbalance and power quality (PQ) issues in the network. Energy Storage (ES) is considered to be the solution to overcome these PQ problems by buffering a sizeable portion of energy generated by different intermittent RE sources during low demand time and export it back into the network as required.

Recent developments and advances in ES and power electronics technologies are making storage technologies viable for modern power applications. It can play a major role in supplementing peaking power generation to meet short period peak load demand. However the integration of ES is not straight forward and also depends on the network capacity and capability. Moreover lack of standard regulations also increases the risk of ES integration into the power network. Large scale integration of ES could increase the risk of additional harmonics in the network, change in voltage regulation, change in distribution transformer loading condition, could develop islanding situation and eventually change the PQ condition of the network.

The research presented in this thesis investigated the impacts of the integration of large scale ES with the low voltage (LV) distribution netowrk (DN). Various standards and regulations practiced by the utility operators were investigated. Experiment was conducted and impatcs on the network was indentified with increased solar PV. Experiments were conducted at the CSIRO's renewable energy integration facility in Newcastle. Experimental result was analysed and similar model was developed to compare the results. In order to investigate the impacts of the large scale ES integration with the grid, a large section of Ergon Energy distribution network was accurately designed and developed using PSS SINCAL with the real network data. Network under eight zone substations were individually analysed and further investigation was carried out for the overall large network with various network configuration.

The investigation results showed that ES supported load demand when RE was not available, also stored excess energy when load demand was low. It was noted that ES supported load when energy generation from RE sources fluctuated and also improved phase unbalance condition. Furthermore, ES improved network voltage level and eventually helps in voltage regulations. By integrating ES, the load on network element such as distribution transformer (DT) and cable or conductor reduced, which eventually increased network capacity. However, ES works as a current source and connected to the network through inverter that injects harmonic current into the network. Harmonic current introduces harmonic voltage in the network. ES supports load demand therefore with the reduced flow of load current causes increase in total harmonic distortion (THD) in the network. It was also observed that this increase in THD was highest at the LV side of the DN, however the effects passed through the high voltage (HV) side of DN to the HV sub-transmission and transmission network as well.

This research also estimated the required ES for a typical residential load considering solar and wind resource data of Rockhampton, Australia. Furthermore economical and environmental significance of ES was investigated. Therefore, this research provides the knowledge of ES impacts on power network of various sizes and capacities. Moreover, this research opens the scope for further research to minimize the harmonic impacts of ES.

Energy Storage and its Strategic Impacts on the Power Network

Table of Contents

LIST OF FIGURES

LIST OF TABLES

LIST OF ABBREVIATIONS

AC	:	Alternating Current
Ah	:	Ampere-hour
AMI	:	Advanced Metering Infrastructure
AMR	:	Automated Meter Reading
ANSI	:	American National Standard Institute
AS	:	Australian Standard
BER	:	Berserker
BESS	:	Battery Energy Storage Systems
BOM	:	Bureau of Meteorology
BSS	:	Bulk Supply Substations
BUS		Power network bus
CAES	:	Compressed Air Energy Storage
CHP	:	Combined Heat and Power
COE	:	Cost of Energy
CRF	:	Capital Recovery Factor
CS	:	Central Store
CSIRO	:	Commonwealth Scientific and Industrial Research Organisation
CSP	:	Concentrated Solar Power
CST	:	Canning Street
DAQ-DB	:	Data Acquisition from Distribution board
DAQ-PV	:	Data Acquisition from PV
DC	:	Direct Current
DER	:	Distributed Energy Resources
DFD	:	Distribution Feeder Database
DFT	:	Discrete Fourier Transform
DG	:	Distributed Generation/ Generators
DINIS	:	Distribution Network Information System
DL	:	Distribution Line
DN	:	Distribution Network
DNSP	:	Distribution Network Service Providers
DoD	:	Depth-of-Discharge
DoE	:	Department of Energy
DR	:	Distributed Resources
DS	:	Distribution Substations
DT	:	Distribution Transformer
DVR	:	Dynamic Voltage Restorer
EDLCs	:	Electrochemical Double-Layer Capacitors
EIA	:	Energy Information Administration, USA.
EMI	:	Electromagnetic Interference
EPRI	:	Electrical Power Research Institute
EPS	:	Electrical Power System
ES	:	Energy Storage

ESS	:	Energy Storage System
FACTS	:	Flexible AC Transmission Systems
FBs	:	Flow-Battery
FC	:	Fuel Cell
FES	:	Flywheel Energy Storage
FFT	:	Fast Fourier Transform
FRN	:	Frenchville
GHG	:	Green House Gas
GIS	:	Geographic Information System
GW	:	Giga Watt
GWh	:	Giga Watt-hour
HES	:	Hydrogen Energy Storage
HOMER	:	Hybrid Optimisation Model for Electric Renewable
HPT	:	High-Pressure Turbine
HV	:	High Voltage
HVDC	:	High Voltage Direct Current
Hz	:	Hertz
IEA	:	International Energy Agency
IEC	:	International Electro technical Commission
IEEE	:	Institute of Electrical and Electronics Engineers
kg	:	Kilogram
km	:	Kilometre
kV	:	Kilo Volt
KVA	:	Kilo Volt Ampere
KVAR	:	Kilo Volt Ampere Reactive
kW	:	Kilo Watt
kWh	:	Kilo Watt-hour
LC	:	Load Curve
LCR	:	Lakes Creek
LF	:	Load Flow
Li-ion	:	Lithium-ion
LPT	:	Low-pressure Turbine
ltr	:	Litre
LV	:	Low Voltage
m	:	meter
m^2	:	Square meter
m^3	:	Cubic Meter
MDOD	:	Maximum Depth of Discharge
MEMS	:	Micro-Electro Mechanical System
MV	:	Medium Voltage
MVA	:	Mega Volt Ampere
MW	:	Mega Watt
MWh	:	MegaWatt-hour
NaS	:	Sodium-sulphur
NASA	:	National Aeronautics and Space Administration

NiCd	:	Nickel-Cadmium
Ni-MH	:	Nickel-Metal Hydride
NPC	:	Net Present Cost
NREL	:	National Renewable Energy Laboratory
NSW	:	New South Wales
NZS	:	New Zealand Standard
^{o}C	:	Degree Celsius
O&M	:	Operation and Maintenance
PAN	:	Pandoin
PCC	:	Point of Common Coupling
PERG	:	Power Engineering Research Group
PF	:	Power Factor
PHS	:	Pumped Hydro/Hydroelectric Storage
PHK	:	Parkhurst
POC	:	Point of Connection
POE	:	Point of Evaluation
PQ	:	Power Quality
PSB	:	Polysulphide Bromide battery
PSS/SINCAL	:	Power System Simulator/Siemens Network Calculation
PTS	:	Power Transformation System
PV	:	Photovoltaic
p.u.	:	per unit
RE	:	Renewable Energy
REIF	:	Renewable Energy Integration Facility
RES	:	Renewable Energy Sources
RF	:	Renewable Fraction
RGL	:	Rockhampton Glenmore
RMS	:	Root Mean Square
RSH	:	Rockhampton South
SCES	:	Super Capacitors Energy Storage
sec	:	Second
SLG	:	Single Line to Ground
SMES	:	Superconducting Magnetic Energy Storage
SOC	:	State Of Charge
SWER	:	Single Wire Earth Return
TAC	:	Total Annualized Cost
TES	:	Thermal Energy Storage
THD	:	Total Harmonic Distortion
THDi	:	Total Harmonic Current Distortion
THDv	:	Total Harmonic Voltage Distortion
ToU	:	Time of Use
TWh	:	Tera Watt-hour
U_{hi}	:	Harmonic Emission Vector
US	:	United States
U.S.	:	United States

U.S.A	:	United States of America
V	:	Volt
V_{FL}	:	Voltage at full load
V_n	:	Rated Voltage
V_{NL}	:	Voltage at no load
VPS	:	Virtual Power Station
VR	:	Voltage Regulation
VRB	:	Vanadium Redox Battery
W	:	Watts
Wh	:	Watt-hour
WT	:	Wind Turbine
yr	:	Year
ZnBr	:	Zinc Bromide Battery
ZS	:	Zone Substations
$	:	Dollar

Acknowledgements

I am delighted to acknowledge those who have encouraged me and contributed in many ways during my progress and towards the completion of this research.

Firstly, I would like to express my sincere gratitude to my Principal Supervisor Dr Amanullah M Than Oo for his continuous guidance, assistance and encouragements during this research. I deeply appreciate his effort in providing me the opportunity of teaching and learning experience. I would also like to show my generous appreciation to my Associate Supervisor Dr A B M Shawkat Ali for his valuable suggestions and guidance throughout this research.

I am thankful to CQUniversity, Rockhampton, Australia for the award of research scholarship to pursue this study. I want to express my special thanks to the Power Engineering Research Group (PERG) and Office of Research at CQUniversity for their support in various ways.

I would like to express my special thanks to David Cornforth, Project Leader, Energy Technology, CSIRO and Tim Moore, Project Engineer at CSIRO Energy Centre to provide scope to use CSIRO Renewable Energy Integration Facility and to guide conducting the experiments. I would also like to thank Ergon Energy (Rockhampton Branch) for providing support in various ways in developing the power network model of Rockhampton. I want to express my special thanks to Anthony Cran, Senior Engineer, Distribution and Planning at Ergon Energy for his help during the development of Rockhampton Power network model and providing access to the DINIS model and Google Earth model of Ergon Energy for Rockhampton city.

I am indebted to Ulrike Sachs of Siemens AG, Infrastructure & Cities Sector, Smart Grid Division and Michael Göttlinger of SimTec Softwareentwicklung GmbH and also to Geordie Mitchell of Hill Michael to learn PSS SINCAL. I am also grateful to Gilbert Jin of SMA Technology for providing various inverter data. I would also like to acknowledge the support of GM Shafiullah in various ways during my time in CQUniversity.

Above all, I would like to express my special thanks and appreciation to my wife Shamima Moazzem, my son Aayan Tausiq Arif, my parents and parents-in-law for their patience, understanding, scarifies and encouragements during this research.

Declaration of Originality

I, Mohammad Taufiqul Arif, declare that the PhD thesis entitled —"Energy Storage and its Strategic Impacts on the Power Network" has not been previously submitted either in whole or in part for a degree at CQUniversity or any other tertiary institution. To the best of my knowledge and belief, the material presented in this thesis is original except where due reference is made in text. The length of this thesis is no more than 100,000 words, exclusive of tables, figures, appendices and references.

Redacted

Mohammad Taufiqul Arif

March 28, 2013

Copyright Statement

Redacted

(Mohammad Taufiqul Arif)
28 March 2013

List of Publications

Book Chapters

1. **Mohammad Taufiqul Arif**, Amanullah M. T. Oo, A B M Shawkat Ali, "Estimation of Energy Storage and its Feasibility Analysis", Energy Storage - Technologies and Applications, Dr. Ahmed Zobaa (Ed.), DOI: 10.5772/52218, InTech, 2013
2. **Mohammad Taufiqul Arif**, Amanullah M. T. Oo, A B M Shawkat Ali, "Energy Storage - Applications and Advantages" accepted for the Book Titled "Smart Grid: Opportunities, Developments and Trends", Springer London, 2013.
3. GM Shafiullah, Amanullah M. T. Oo, A B M Shawkat Ali, Peter Wolfs, **Mohammad Taufiqul Arif**, "Renewable Energy Integration - Opportunities and Challenges" accepted for the Book Titled "Smart Grid: Opportunities, Developments and Trends", Springer London, 2013.

Journals

4. **Mohammad Taufiqul Arif**, Amanullah M. T. Oo, A B M Shawkat Ali, "Integration of Renewable Energy Resources into the Distribution Network - A Review on Power Quality Requirement", International Journal on Energy and Power (IJEP), Science and Engineering Publishing Company, 1(2), P. 37-48, 2012, (ISSN online: 2169-4931)
5. **Mohammad Taufiqul Arif**, Amanullah M. T. Oo, A B M Shawkat Ali, GM Shafiullah, "Significance of Storage on Solar Photovoltaic System - a Residential Load Case Study in Australia", accepted in the International Journal of Smart Grid and Renewable Energy (SGRE), Scientific Research. Vol.4 No. 2, May 2013.
6. **Mohammad Taufiqul Arif**, Amanullah M. T. Oo, A B M Shawkat Ali, "Role of Energy Storage on Distribution Transformer loading in Low Voltage Distribution Network", accepted in the International Journal of Smart Grid and Renewable Energy (SGRE), Scientific Research. Vol.4 No. 2, May 2013.
7. **Mohammad Taufiqul Arif**, Amanullah M. T. Oo, A B M Shawkat Ali, "Investigation of Energy Storage Systems, it's Advantage and Requirement in Various Locations in Australia", accepted in the International Journal of Renewable Energy (JRE), Hindawi Publishing Corporation, 2013.

8. **Mohammad Taufiqul Arif**, Amanullah M. T. Oo, A B M Shawkat Ali, “Impacts of Storage and Renewable Energy Integration into the Low Voltage Distribution Network”, submitted to the IEEE Transactions on Smart Grid, 2013.
9. **Mohammad Taufiqul Arif**, Amanullah M. T. Oo, A B M Shawkat Ali, “Renewable Energy and Energy Storage Impacts on Power Network - Experimental and Simulation Investigation”, submitted to the IEEE Transactions on Smart Grid, 2013.
10. **Mohammad Taufiqul Arif**, Amanullah M. T. Oo, A B M Shawkat Ali, “Energy Storage Impacts on Distribution Network”, submitted to the international Journal of Renewable Energy, Elsevier, 2013.

Conference Papers

11. **Mohammad Taufiqul Arif**, Amanullah M. T. Oo, A B M Shawkat Ali, GM Shafiullah, “Impacts of storage and solar photovoltaic on the distribution network”, Australasian Universities Power Engineering Conference (AUPEC2012) in Denpasar-Bali, Indonesia 26-29th September, 2012
12. GM Shafiullah, **Mohammad Taufiqul Arif**, Amanullah M. T. Oo, ABM Shawkat Ali "Meeting Energy Demand and Global Warming by Integrating Renewable Energy into the Grid," Australasian Universities Power Engineering Conference (AUPEC 2012), Bali, Indonesia, 26-29 September 2012.
13. GM Shafiullah, **Mohammad Taufiqul Arif**, Amanullah M. T. Oo, ABM Shawkat Ali, Salahuddin Azad, and Tim Moore, "Experimental Analysis of Harmonics on Utility Grid with PV Penetration," In the proceedings of the International Conference on Electrical and Computer Systems, Ontario, Canada, 24-26 August, 2012
14. Luke Teather , **Mohammad Taufiqul Arif**, GM Shafiullah, Amanullah M. T. Oo, “A Study of the Impacts of Electric Vehicles on Rockhampton's Distribution Network”, In the proceedings of the International Conference on Electrical and Computer Systems, will be held in Ottawa, Ontario, Canada, 26-24 August, 2012
15. **Mohammad Taufiqul Arif**, Amanullah M. T. Oo, A B M Shawkat Ali, Md. Fakhrul Islam, “Significance of Storage and feasibility analysis of Renewable energy with storage system”, in the proceedings of the IASTED International Conference on Power and Energy Systems (Asia PES 2010), Page 90-95, Nov 24-26, 2010, in Phuket, Thailand

Chapter 1

Thesis Overview

1.0 Introduction

Renewable energy (RE) generation continues to grow worldwide [1] [2] to reduce energy related CO_2 emission and to support the additional electricity demand. Like many countries around the world, Australia has set up its renewable energy target to receive 20% of energy from RE sources by 2020 [3, 4]. However, there are numerous challenges in fully capturing renewable energy and integrating it with the grid. The daily energy profile, fluctuating characteristics of solar and wind energy limits its capability to support a timely load demand. A clear solution is the adoption and integration of an Energy Storage System (ESS) with these intermittent RE. ESS can store the unused energy and support the load demand. For increased penetration of solar and wind energy, a large-scale ESS is required. Traditionally, the transmission and distribution network was designed for one-way power flow; however, integration of large-scale storage with large-scale RE introduces bidirectional dynamic power flow in the network, which causes changes in distribution transformer (DT) loading and fluctuation in the network. Inverter integrated storage and RE causes harmonic emission into the network. Voltage regulation and harmonics are the two vital power quality elements for a distribution network (DN), especially for a weak network like the Rockhampton DN in Queensland, Australia. Therefore, this thesis investigates the impacts of storage compared to the standard allowable limit for DN. The economical and environmental benefits of ESS are also explained.

Section 1.1 illustrates the background and importance of this research. Section 1.2 identifies the problems of the present system. Justification of this research is therefore illustrated in section 1.3. The aims and objective of this thesis are described in section 1.4.

The contribution of this thesis is outlined in section 1.5, and its scope and limitations are presented in section 1.6. Finally, concluding remarks are presented in section 1.7.

1.1 Background and Significance

Electricity demand is increasing globally with infrastructural development and improved lifestyles. According to the International Energy Agency's prediction in 2010, world primary energy demand will increase 40% by 2030 [5]. The Energy Information Administration (EIA) [6] anticipated that the world net electricity generation would increase by 87%, i.e. from 18.9 trillion kWh in 2007 to 35.2 trillion kWh in 2035. In Australia, Queensland's electricity demand will continue to grow more than 3.5% per year [7]. Energy related carbon dioxide emissions in the world will increase 43%, i.e. from 29.7 billion metric tons in 2007 to 42.4 billion metric tons in 2035 [6]. In Australia, the energy sector is a major contributor of greenhouse gas (GHG) emission [8]. Therefore, to meet the increased electricity demand and to lower the GHG emission, RE generation is increasing globally. Solar photovoltaics (PV) and wind turbine are the fastest growing power-generation technologies in the world. Figure 1.1 and 1.2 show the growth of solar PV and wind energy in the world.

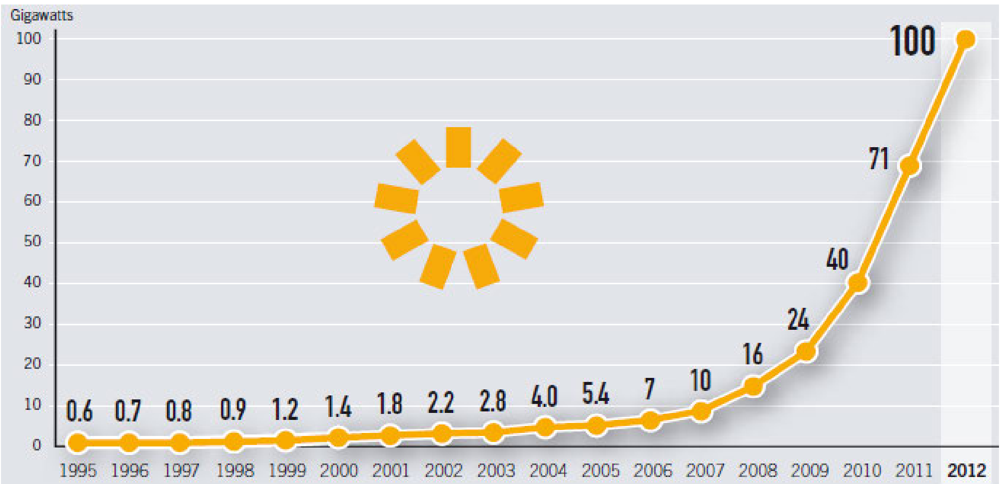

Figure 1:1 Global Solar PV capacity (1995-2012) [2]

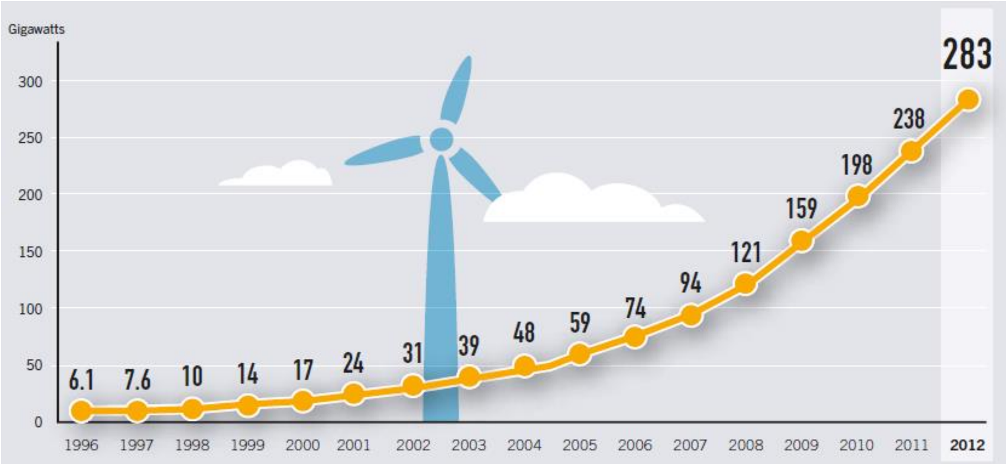

Figure 1:2 Global Wind Power capacity (1996-2012) [2]

Increasing electricity generation from PV and wind is a concern to distribution utilities in the areas in terms of over-voltage/under-voltage on low-voltage (LV) distribution networks, back-feeding to the distribution transformer or even the distribution regulator due to dynamic power flow [9], and contribution to harmonic interference within the network [10]. However, the generation profiles of solar and wind are limited for part of the daily load profile [11] which could create a potential imbalance in load demand and energy supply. Moreover, intermittency and fluctuations are natural phenomena of these sources [12]. Utility operators in Europe expressed concern of harmonics emission, effects on voltage regulation, and islanding due to high penetration of PV into weak grid [13]. Wind turbine integration into the grid can introduce voltage fluctuation, flicker, harmonics and voltage unbalance [14, 15].

Several studies indicated that storage could overcome problems associated with solar and wind energy. Technological development increases demand of energy storage to use with intermittent RE. Large-scale storage allows RE producers to store surplus energy, to supply to the grid when load demand increases, and also to balance supply and demand. In Australia, approximately 10% of Queensland's electricity network has been built to support only the extreme peak loads [7] and maintains costly short-term generators to support peak demand. By integrating proper sized ES with RE, this peak load demand can be minimized and can reduce the cost of energy. The distribution network in Queensland, Australia covers a large geographical area. Some distant areas are connected via single wire earth return (SWER) network, and loads are not uniformly distributed according to the line length. Moreover, due to seasonal variation, load demand also goes very high during peak demand time. This uneven load distribution and load demand makes Queensland's distribution network very vulnerable.

Several studies have been conducted with regard to integrating large-scale PV or wind energy into the grid [13, 16], and there are some examples in large-scale storage installation for specific application [17]. Most of these studies were simulation-based with preset network architecture, and only a few used a small-scale practical network. There is little or no research literature available for a unique distribution network like the Queensland distribution network. The installation of various sizes of PV and wind energy into the network along with various sizes of storage to support various capacity loads in the grid could complicate charging and discharging of different sizes of storage. Small-scale storage in the network could be exhausted quickly, which may force continuous dynamic power flow in the network. This could keep the distribution transformer busier, and fluctuation can lead to the higher network level which in turn leads to voltage regulation problems. Intermittent fluctuating energy from solar PV and wind energy and inverters with power electronics all introduce harmonics into the network. It is expected that inverter-integrated storage with continuous charging and discharging is likely to introduce more harmonics into the network.

Therefore, this research concentrates on investigating the voltage regulation and harmonics issues in the network by integrating large-scale storage into the network. This study is conducted exclusively for Ergon Energy distribution network based in Rockhampton. It is a city of more than 100,000 population. The DN in Rockhampton supports an approximate load of 193 MVA[18] and divided into 11 zone substations. This study also analyses the economic and environmental implications of storage in supporting solar PV and wind energy. It is likely that the distribution network in Rockhampton will have to accept large-scale RE and storage to support future load demand; therefore, this study is very significant for future network stability.

The findings of this research will help utilities to take necessary measures before large-scale integration of storage and RE into the network. This will eventually help in building an environment-friendly, sustainable power system for the future.

1.2 Problem Definition

In Queensland, Australia, peak electricity demand generally occurs between 4:00PM and 8:00PM, when most householders return home and turn on energy intensive appliances [7]. However, during peak demand time, RE such as solar and wind is unable to generate energy. Therefore, in heavily penetrated PV & wind energy systems in the network, storage is the key enabler to support future load demand especially in peak demand period and to extend the use of RE.

The daily profile of solar and wind energy requires to have storage to support the load demand. It is more critical when the fluctuation level ramps the energy output such that load cannot consume, or there is not enough output to support the load. Therefore, storage plays a key role in buffering excess energy and supply in quick time. Based on the data [11, 19], Figure 1.3 shows the conditions where storage can play the key role in supporting the load during morning and evening. Neither solar or wind energy profile matched with either residential or commercial load in Rockhampton.

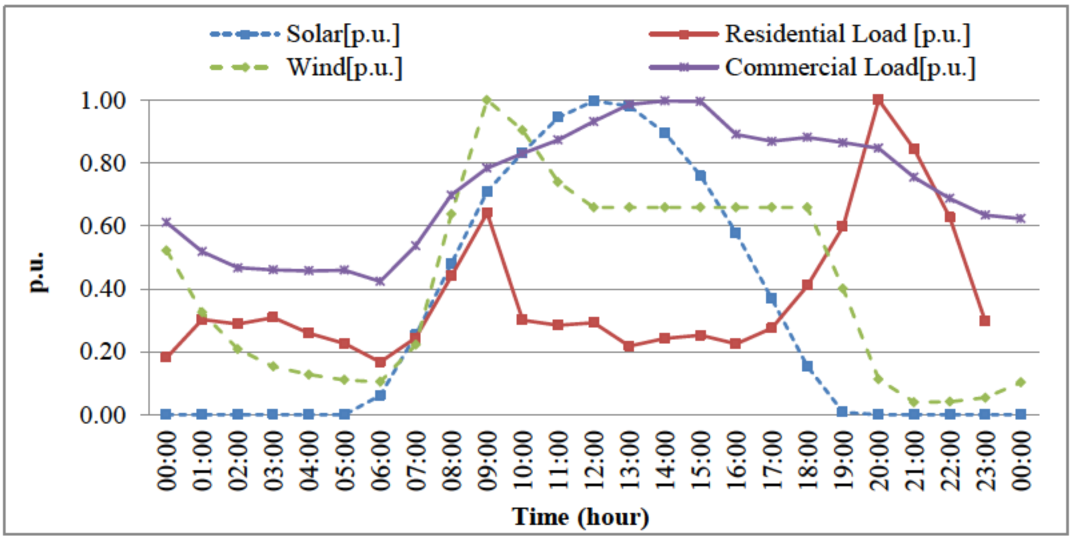

Figure 1:3 Daily Solar & Wind energy, residential load and commercial load in per unit in Rockhampton

But the operation of large storage is not straightforward in the network when solar and wind energy penetration increases. Integration of energy storage depends on the load size, RE generation, distance from load, size of storage and how storage is connected to the network. Load demand and RE generation are variable, which in turn varies the charging and discharging conditions of energy storage. In addition, connection orientation of RE and storage can unbalance the voltage or power at a certain node and its associated load elements. Moreover, inverter and power electronics add harmonics to the network; therefore, storage connected to the network through inverters also may cause additional harmonics to the network. However, various capacity storage systems in various node points in the large network will influence one another in voltage deviation, loading on feeder transformers or distribution transformers, phase unbalance condition and in harmonics emission in the network. The distribution network in Queensland, Australia is distributed in vast geographical areas and combines three phase networks with a single phase SWER network. Therefore, the large-scale integration of storage, solar PV and wind in this network can have impacts at an intensified level.

1.3 Justification of the Study

The generation of electricity from solar PV and wind turbine is increasing for various reasons and several positive attributes accelerate its development. Several utility operators in various developed countries included a range of energy from solar and wind into their power network and expressed various concerns like voltage regulation, harmonics, islanding and reactive power problem [13]. These installations are limited in size and storage was not included; therefore, peak demand and fluctuation demands are met by conventional sources, which include additional generation from conventional sources and cause a significant release of GHG into the atmosphere. There are few large-scale storage installations in different utility networks in various countries for load shifting purpose only [17]; therefore, the uncertainty and energy fluctuations were not experienced by these configurations. The Australian power network has little to no experience either with large-scale integration of solar or wind energy or with large energy storage systems. However in Australia, generation from solar PV and wind is increasing. Therefore, it is imminent that large-scale storage will be required for better utilization of solar and wind output. Investigation is urgently required to identify the impacts of such systems that are already addressed by other countries, and also to make necessary rectifications before large-scale storage and RE can fully be integrated with the grid.

1.4 Aim and Objectives of the Thesis

Energy storage system (ESS) can act as a load or source of energy. It connects with a power supply from conventional sources and renewable sources into the grid at the point of common coupling (PCC). The grid then receives a supply from all these sources simultaneously or from different sources at different times. Abrupt changes in weather conditions bring fluctuations in solar and wind energy output, which in turn introduces fluctuation in the network. Storage responds to minimize the fluctuation, which requires multiple charge-discharge sequences; as a consequence, loading on DT also changes. Moreover, inverter and power electronics adds harmonics to the network. As discussed earlier, a weak network is prone to various power quality problems and dynamic power flow accelerates these problems.

The purpose of this study is to identify the impact of large-scale storage on the power network. As the power network in Queensland is weak compared to others, and the location of solar PV and wind energy generation will be distributed over different points in the DN, small scale storage as well as large-scale storage will be integrated in the near future. However, the load flow of the total network is based on the load demand, and RE generation and storage condition can influence the desired performance of the network. Therefore, this thesis investigates the two power quality indices (Voltage regulation and harmonics) after integrating storage to support solar PV and wind energy. Moreover, it explains the estimation of required storage for a particular load profile along with economical and environmental benefits due to storage. The major objectives are:

- To estimate the ES for a typical load to integrate with PV or wind energy in Aaustralia
- To investigate economical and environmental significance of ES
- To develop a large power network model for detailed analysis
- To conduct experimental investigation and extend range of investigation in network model
- To identify the impacts of ES in terms of voltage regulation and harmonic distortion in various network configurations

1.5 Methodology and Contribution of the Thesis

After assessing a range of literature, technical reports, experimental results and the experiences of other utilities regarding RE, its potential, the importance of energy storage and its advantages, this study presents the potential of ESS and limitations of large-scale integration of renewable energy. In order to accomplish the objective, the Rockhampton distribution network was selected, and solar and wind data was collected from Bureau of Meteorology (BoM) [11]. In order to understand the impacts on network, an experiment was conducted using the Renewable Energy Integration Facility (REIF) at CSIRO in Newcastle, Australia. Load data of the Rockhampton distribution network was collected from Ergon Energy, the utility operator in Rockhampton. Ergon Energy has an extensive model of the network built in DINIS (Distribution Network Information System) software package. However, DINIS is unable to model PV, wind and storage systems. LV network for an unbalanced system was also not possible in DINIS for harmonic distortion calculation. Therefore, an accurate distribution network was developed using PSS SINCAL which allows the integration of RE and ESS.

Figure 1.4 shows the Rockhampton distribution network in DINIS and Figure 1.5 shows the same in GoogleEarth. The GIS model built in GoogleEarth contains end load information, line parameters and the detailed location of each network element.

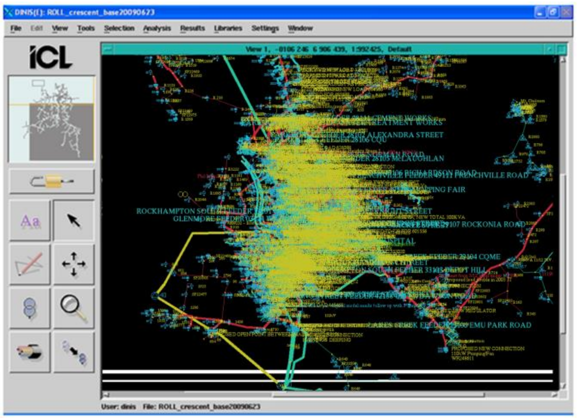

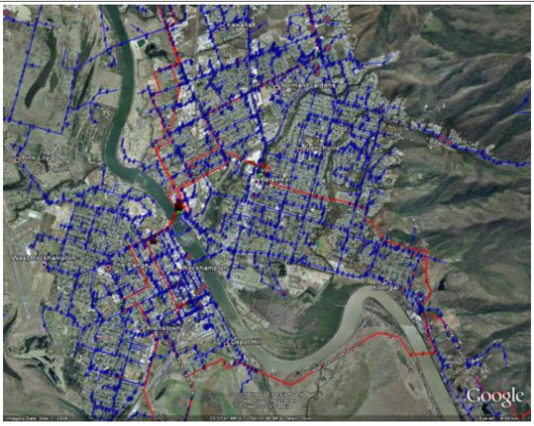

Figure 1:4 Rockhampton DN in DINIS **Figure 1:5 Rockhampton DN in Google Earth**

The research was initiated by estimating the required storage with solar and wind energy application for a particular load in Rockhampton, Australia. However the detailed methodology is classified in the following three areas:

1.5.1 Estimation and Significance of Energy Storage

To meet load demand, proper-sized generation is required. Electrical energy generated from solar and wind is sometimes unable to meet the load demand and sometimes exceeds the load demand. Excess electricity neither can be used by load nor it can be stored in storage if solar/wind generator and storage size is not properly estimated. This event occurs when the ES such as; Battery State of Charge (SOC) exceeds its maximum allowable value and the solar/wind output power exceeds load demand. The amount of wasted/lost energy can be avoided or reduced by proper choice of battery and PV/Wind generation sizes. PV panel size and the battery size have different impacts on the indices of performance, and proper balance between the two is necessary [20]. By comparing load and energy generated from solar and wind energy in Rockhampton, required storage is estimated. Furthermore significance of ESS is also illustrated.

1.5.2 Development of the Network Model

In order to identify the impacts of large-scale storage on DN, an accurate network model was developed using PSS SINCAL for Rockhampton DN. The initially existing network in DINIS was converted to SINCAL and was verified with the existing GIS model in Google

Earth. By comparing the SINCAL model with DINIS and the GoogleEarth GIS model, the errors generated during conversion were rectified and the SINCAL database was populated with correct information of the present distribution network of Rockhampton. SINCAL offers a full range of analysis methods from standard load flow to enhanced dynamic simulation for balanced and unbalanced network. It also deals with voltage level from high voltage (HV) to low voltage (LV). PSS SINCAL offers a full range of network modelling, including unbalanced network structures and new smart grid elements such as wind turbine, Solar PV, Battery (storage) etc. for network analysis.

Figure 1.6 shows the Rockhampton distribution network developed in PSS SINCAL, which includes all parameter values and geographical locations. The development of the network model initiated from the experimental configuration and finally building the complete power network of Rockhampton.

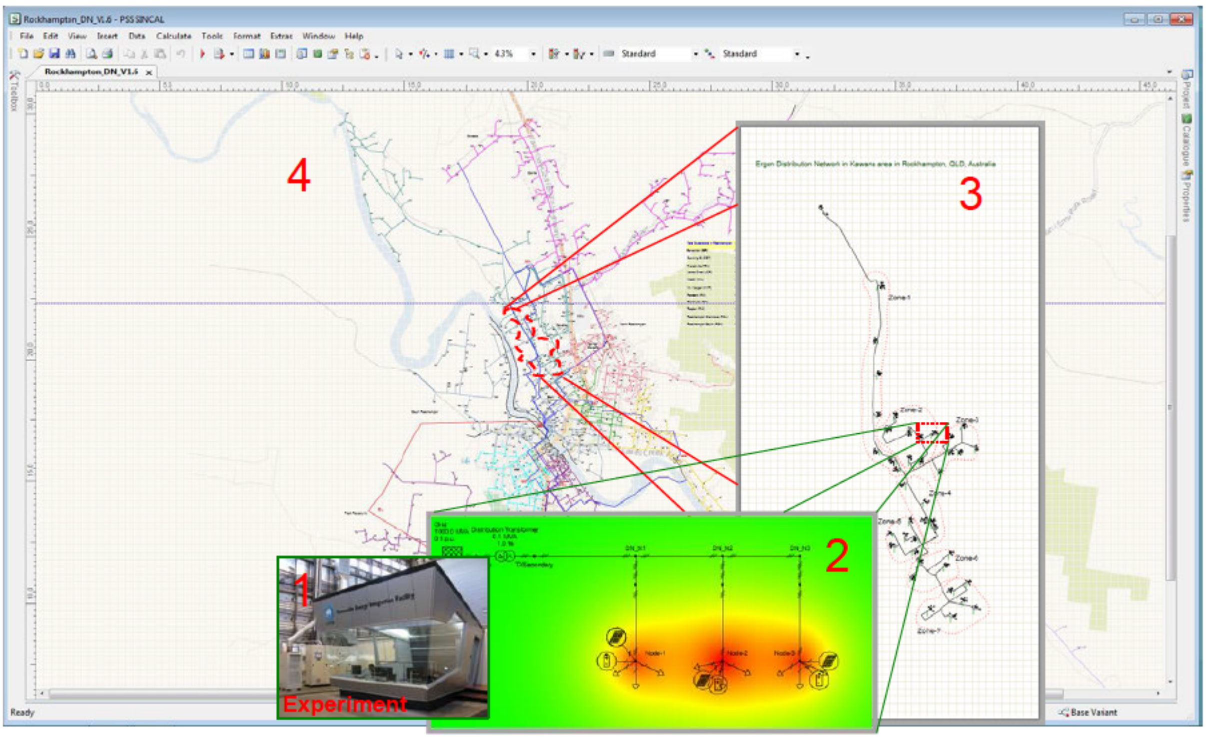

Figure 1:6 Development of Rockhampton distribution network model in SINCAL

1.5.3 Identification of Impacts

Traditionally, network planning was based on load flow simulation. However, due to the element of smart grids or renewable generation, it is no longer reasonable to study one particular load flow for a network. Instead, the time-varying load profile for a day (if not a month or year) needs to be evaluated. The load profile shows the load of every interval desired for the total duration.

After validation of the network model of Rockhampton, load flow simulation was done in an unbalanced system to investigate the voltage deviation at different nodes due to the integration of energy storage after solar PV, wind energy into the LV network. The investigation result was compared with the standard limit set by AS-4777 [21] and local utility limit [22, 23]. Load profile (load curve) simulation was conducted to investigate the storage response to voltage fluctuation due to the fluctuation of energy from solar PV or wind turbine.

Harmonic distortion in voltage or current waveform is caused by the impact of nonlinear load or generating sources connected by inverters. Harmonics due to single-phase distorting loads spread across the three phases and excessive level of harmonics due to single-phase load/source can overload the neutral line, which causes overheating of the neutral conductor [24]. High levels of total harmonic distortion (THD) can cause thermal effects and overload the neutral conductor, as well as disturbance to the electronic equipment. High penetration of RE in LV-DN can cause single-phase loading, which introduces harmonics [12]. Moreover, inverters and their switching are a possible source of harmonics. DC elements and switching devices (inverters with storage and solar PV/wind and switching controller) add harmonics in addition to various load harmonics. Therefore harmonic impacts on the network due to storage and RE were investigated and compared with the limit set by AS-4777 [21] and Energex and Ergon standard [22].

The impact on network is different in small-scale and large-scale integration. Therefore, investigation was done from single distribution transformer loading to a medium network (Kawana suburb) and finally a complete power network of Rockhampton; as shown in Appendix A-2.

1.6 Scope and Limitation of the Study

There is no large scale storage system integrated with RE in the Australian power network; therefore, there was no measured data to compare. However, the findings of this study are very significant and can be used as a reference for future study.

1.7 Outline of the Thesis

The thesis is organized in the following seven chapters:

Chapter 1 describes general background and motivation of this study. Key technology, research objective, methodologies and contribution of this study are discussed.

Chapter 2 provides detailed background of this research, values of storage and importance with RE applications. Various energy storage systems (ESS), standards and integration into the grid are explained briefly. Various studies of the current time and experience of several utility operators are also explained and identified the research scope.

Chapter 3 outlines the estimation of required storage for a particular load in Australia. This chapter also identifies the significance of storage in terms of environment and economics for the same load profile.

Chapter 4 explains the details of network model development in PSS SINCAL. Storage, load, PV and wind turbine allocation in various network points are described. Residential and commercial load profiles in per unit (p.u.) were developed. Solar PV and wind turbine output was converted to per unit for the location of Rockhampton. Various modelling scenarios and strategies are explained considering small, medium and large networks.

Chapter 5 illustrates detailed technical analysis of voltage deviation due to storage integration into the grid. Storage was integrated into the network after introducing solar PV or wind turbine in the low voltage distribution network. First, voltage deviation was analysed from the experimental results after adding solar PV into the micro-grid at the integration facility in CSIRO. Simulation was done in three different conditions in small, medium and large-scale network environment.

Chapter 6 explains the detailed technical analysis of harmonic emission into the grid. Initially, experimental results were analysed for harmonics due to solar PV integration into the micro-grid at CSIRO. Simulation was carried out in different network sizes and harmonic distortion due to energy storage was identified.

Chapter 7 summarizes the outcome of this research and illustrates the significance of the contribution. Future scope for this research is also discussed in this chapter.

Chapter 2

Literature Review

2.0 Introduction

This chapter presents the background of this research and outlines its context relative to the energy challenges particularly in Australia. The challenges include: structure of the present transmission and distribution network; extensive use of fossil fuel, which emits pollutant gas into the air; lack of standard guidelines to integrate renewable energy into the grid; and widely distributed load. On the other hand, the availability of vast open land and geographical location shows the potential of solar and wind energy in Australia. There is little research done in large-scale integration of intermittent RE in Australia, which demands the large-scale integration of energy storage for a reliable and stable power supply. This chapter explains the structure of the distribution network in section 2.1, and various energy sources in section 2.2. Distributed energy generation is described in section 2.3. Various storage technologies are explained in section 2.4. Regulatory standards to integrate RE and integration of storage with the grid are explained in section 2.5. Various research and development in integrating RE and storage into the grid was investigated, and the scope of this research is defined in section 2.6. Concluding remarks are made in section 2.7.

2.1 Distribution Network

The present electricity network is a complicated integration of multiple stages, from generation to transmission, transmission to distribution, and finally to the consumers. The high voltage (HV) transmission network transfers the bulk of electricity at voltages above 110kV to the bulk supply substations (BSS). In Queensland, Australia, BSS supply power to the zone substations (ZS) and large customers via 33 kV, 66 kV, 110 kV and 132 kV networks operate as radial, parallel radial or meshed network [25, 26] as shown in Figure 2.1.

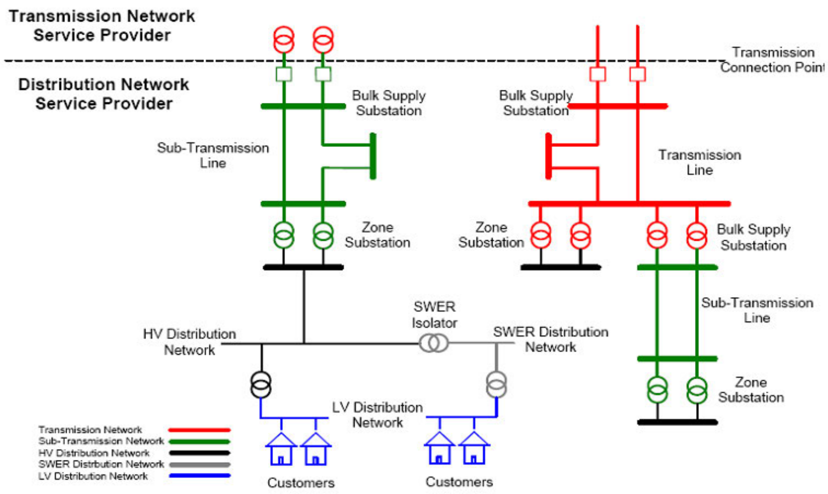

Figure 2:1 Power Distribution Network [25]

ZS supplies to the distribution network (DN) by stepping down the voltage to 11 kV, 22 kV or 33 kV. ZS provides protection and control to the local DN. In Australia, DN is a combination of, HV, SWER (Single Wire Earth Return) and LV networks. The distribution network service providers (DNSP) have to meet certain regulated voltages that are supplied to the customer via distribution transformer (DT). The standard voltages associated with DN are:

- HV DN: 11 kV, 22 kV and sometimes 33 kV
- LV DN: 415 V (Line-Line)/240 V (Line-Ground)
- SWER: 11 kV, 12.7 kV and 19.1 kV

Power network or grids are designed to transmit electricity generated by large conventional power plants. Electricity generated from various renewable sources use synchronous or asynchronous generators except for solar PV. PV uses an inverted rectifier to connect the power flow to the grid. Various capacity transformers interconnect distribution to transmission network, loads to the distribution network. In a DN, the voltage falls in the direction of current flow due to resistance and inductance of the cable as shown in Figure 2.2 [27].

Energy generation from renewable sources requires an installation of the plant in locations where enough supply is available—for example, better wind speed and solar radiation for wind turbine and PV plants respectively. Therefore, installations of RE applications are expected to connect at various local points of the distribution network. In contrast to large power plants, renewable plants have less capacity and are integrated into the low-voltage side of the DN. When such decentralized RE integration increases into the LV side of the DN, power flows to the HV side of DN and introduces bidirectional power flow in the network. As a consequence, the voltage level rises at the point of RE connection. Voltage rise aggravates when more and more such distributed generators integrate, especially into the weak grid.

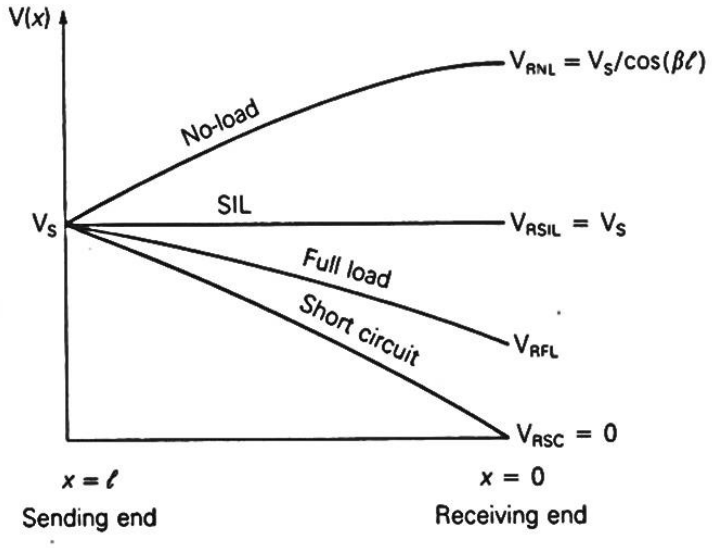

Figure 2:2 Voltage profile from source to end load [27]

The trend of energy supply from renewable sources in the medium- or low-voltage network is highly visible. The popular rooftop solar PV is mostly installed to meet residential customer needs and connected at the LV DN. Although the size of this single customer is very small, the combined total demand is significant. Similarly, the combined total solar PVs installed in these houses have great influence on the total network performance. Distributed wind turbines are also connected to the LV DN. The combined maximum capacity of all RE installations connected without a dedicated transformer must remain <30% of the rated capacity of the DT [28]. Akatsuka Motoki et al. [29] mentioned that fluctuation in the output of a megawatt class PV system may disturb stable operation of the power system. The integration of many decentralized RE generators can be concentrated to form a virtual plant to increase efficiency by actively storing excess energy and help in grid management. The structure of DN in Australia, especially DN in Queensland is greatly distributed over large geographical areas which make the grid weak compared to the large urban grids in developed countries. Moreover, energy source plays a critical role in the development of future power networks.

2.2 Energy Sources

Energy that has been used from ancient times is known as conventional or traditional energy. Primary sources include coal, natural gas and oil. These carbon-based energy sources are non-renewable, meaning they will run out at some point. These energy sources burn and convert into heat energy that is used to run the generator to produce electricity. This process emits GHG as a by-product. Electricity demand increases with time and development. Around 242 TWh of electricity (including off-grid) was generated in Australia in 2009-10 where, renewable contribution was only 19.7 TWh, or almost 8.15% [30] as shown in Table 2.1 and Figure 2.3.

Table 2:1 Australian Electricity generation by fuel, in 2009-10

Name (Fuels used)		Generation (TWh)	% Used
Black coal	:	124.5	51.53%
Brown coal	:	56.0	23.17%
Natural gas	:	36.2	14.98%
Petroleum Oil	:	2.7	1.11%
Other	:	2.5	1.03%
Hydro	:	12.5	5.17%
Wind	:	4.8	1.98%
Solar	:	0.3	0.12%
Biomass		1.2	0.49%
Biogas		0.9	0.37%
Total	:	241.6	100%

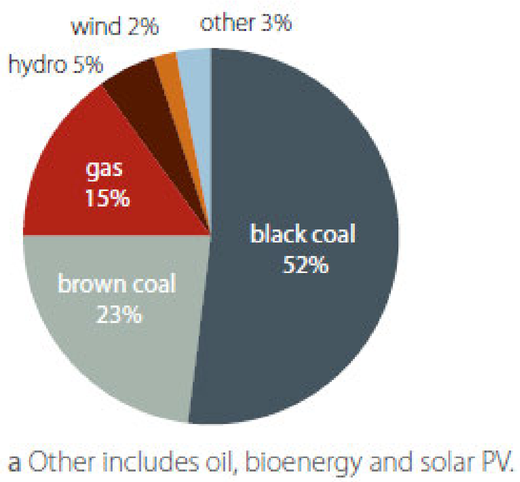

Figure 2:3 Australia's Electricity generation by Fuels in 2009-10 [30]

The dependency on coal makes Australia one of the largest GHG-emitting countries. According to the National Greenhouse Gas Inventory (Kyoto protocol accounting framework), it is found that the energy sector is the major contributor to GHG emission in Australia [31].The energy sector alone contributed 73.93% of GHG emission in overall

Australia and 62.71% in Queensland. Table 2.2 illustrates the carbon-dioxide equivalent emission in 2009 in Australia and in Queensland. In 2009, GHG inventory total in Australia increased by 13.79% compared to 2000. Global energy-related CO_2 emission will rise 43%, from 29.9 billion metric tons in 2007 to 42.4 billion metric tons in 2035 as predicted by EIA [6]. To reduce GHG emission and the environmental threat due to global warming, Kyoto protocol was adopted by most nations. They agreed to reduce GHG emission by at least 5% below the 1990 level by 2008 to 2012[32]

Table 2:2 National GHG Inventory Total, Carbon dioxide equivalent emission 2009 [31]

	Category	CO_2-e emission Giga-gram (1,000 Tonnes)	
		Australia	Queensland
1	National GHG Inventory total	564,542.63	155,129.42
2	**Energy**	**417,354.98**	**97,283.18**
3	Industrial Processes	29,617.03	5,722.59
4	Agriculture	84,745.63	26,935,81
5	Waste	14,075.39	3,179.01
6	Land use, Land-use change and Forestry KP	18,749.60	22,008.82

Therefore, there is an urgent need especially for Australia to search for alternative energy sources that are free from GHG emission. RE offers alternative sources of energy that are generally pollution-free, climate-friendly, unlimited, naturally replenished, technologically effective and environmentally sustainable.

2.2.1 Limitation of Present Network

The network structure in Queensland supports single-phase load, 3 phase load, and large critical load, although Ergon Energy, a local operator, also manages a few off-grid networks. Queensland also faces unique challenges as a result of its vast geographic area and highly decentralized population, particularly in regard to ensuring a cost-effective and reliable supply of electricity to remote and sparsely populated regions through its SWER network.

Most of the present transmission and distribution networks are not able to provide intelligent data essential for a modern grid operation. Moreover, the present power system mostly depends on the fossil fuels—especially coal—which contributes to GHG emission and eventually has a detrimental impact on the environment. While RE integrates into the network, supply and demand must be balanced for proper operation of power systems. Supply can come directly from generation or energy storage. The present power system's limitations can be summarized as:

- Electricity generation greatly depends on conventional sources like coal, gas or oil;
- Produces enough GHG which emits to the nature and increases the threat of global warming;
- Large generation systems are very difficult to change the production level quickly;
- Widely distributed, small-size loads make the network weak, which has high line loss;
- As a storage system is not available in the present system, the generation system always runs on higher than demand to meet the requirement. In the process, a large amount of extra fossil fuel burns which adds additional GHG emission;
- Integration of multiple generation systems are strictly demand based and costly;
- Present network is generally a one-way power flow only.

2.2.2 Renewable Energy

As illustrated earlier, the energy sector is a major contributor of GHG emission, especially in Australia. Moreover, the price of conventional energy sources is increasing gradually. To reduce GHG emission and cost of energy by ensuring the everlasting free source of energy, large-scale RE integration into the grid is the global demand for future electric energy. Most developed countries have set the goal to integrate electricity from RE sources; likewise Australia, has set its vision, by 2020 to integrate 20% electricity from RE sector, i.e. 45,000GWh of electricity from RE sector by 2020[1, 3, 4, 33]. Australia also committed to reaching a national GHG emission target of 60% below 2000 levels by 2050 [34].

Renewable sources include solar, wind, hydro, tides, geothermal and biomass. Burning biomass also emits GHG [35] as well as geothermal energy, although this emission is less significant compared to the burning of fossil fuels[36]. Among all these RE sources, hydroelectricity is the most matured one and around 15% of electricity was generated from this source globally in 2008[1]. Tidal power stations are very limited and development specifically depends on suitable locations. Hydropower and geothermal energy are also site-specific and comparatively expensive to build. Compared to all other types of RE sources, solar and wind are available at any location in any part of the world. However, one of the main concerns of these sources is the intermittency, which is very critical for the reliability and stability of power system operations.

2.2.2.1 Renewable Energy Potential of Australia

Compared to most other countries, Australia's solar resource is equal to the world's best. The annual average solar exposure is greater than 6kWh/m^2/day (2,200kWh/m^2/year), as shown in Figure 2.4 [37]. Yearly average sunshine hours vary from 5 to 10 hours and maximum area is over 8 hours [38]. Due to various natural factors like day/night cycle, location, cloud movement, temperature, air pressure and sun/moon effects on earth, the energy intensity from solar radiation fluctuates. Figure 2.5 shows the solar radiation fluctuation level for the year 2009 in Rockhampton, Australia [11].

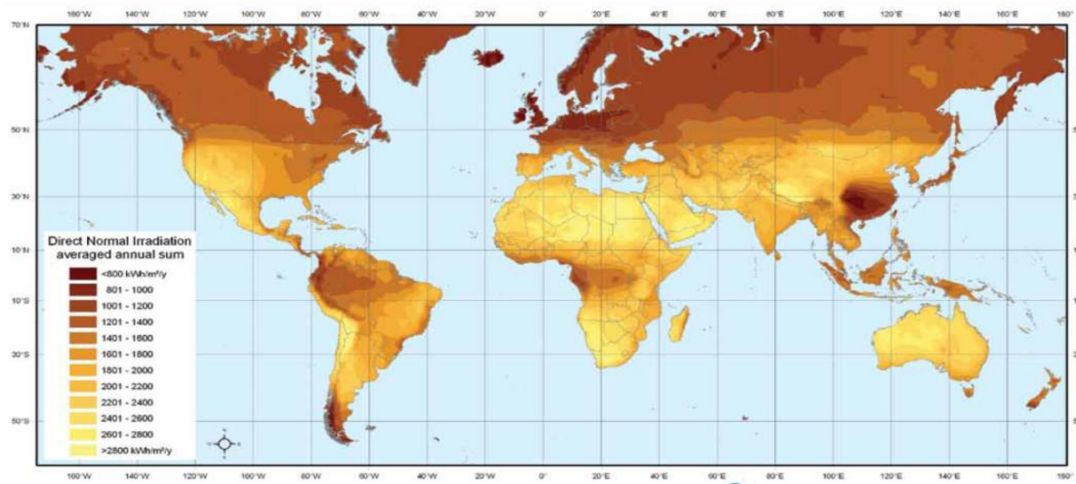

Figure 2:4 Solar Power Potential[39]

Having the advantage of vast open land and large coastal areas, Australia has one of the highest commercially exploitable wind resources per capita in the world, as shown in Figure 2.6 [37, 40, 41]. Like solar radiation, wind speed also fluctuates due to several natural factors. The data collected in 2011 from Bureau of Meteorology [11], as depicted in Figure 2.7, shows the fluctuation of wind speed in Rockhampton.

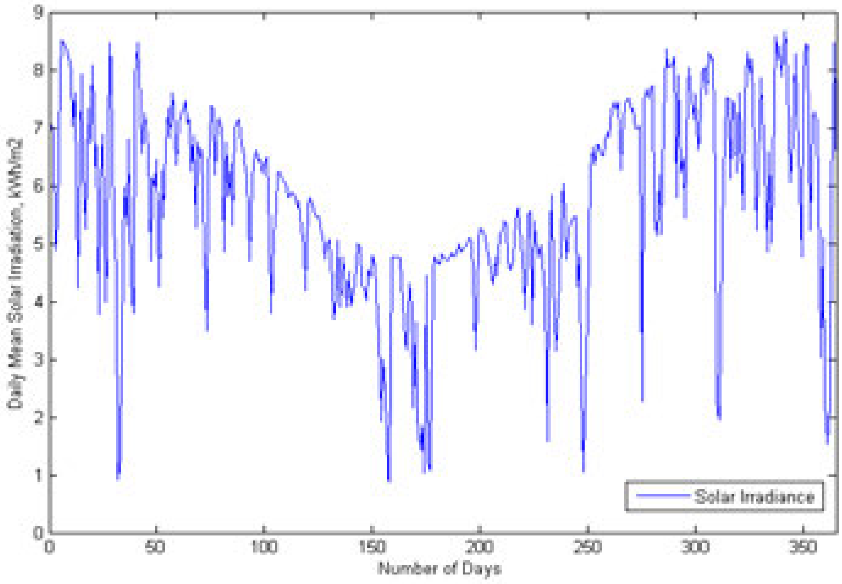

Figure 2:5 Daily solar radiation of Rockhampton, Australia

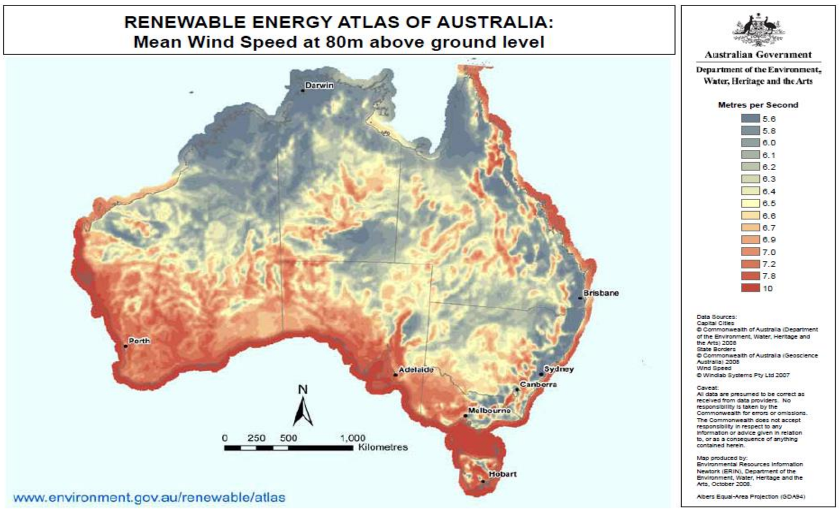

Figure 2:6 Wind speed map of Australia [35, 38]

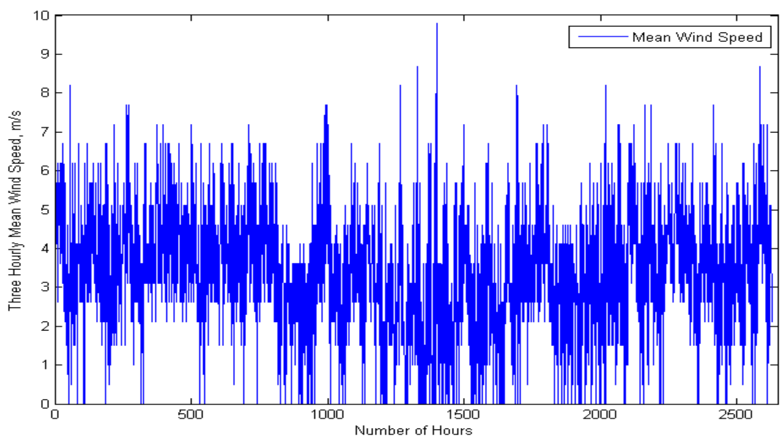

Figure 2:7 Three hourly wind speed of Rockhampton area, Australia

The potential locations of solar and wind energy are distributed in various parts of Australia, and the intermittent nature of fluctuation exists everywhere. Installation of solar and wind energy systems at distributed locations is known as distributed energy generation.

2.3 Distributed Energy Generation

Distributed generation describes electric power generation that is geographically distributed and is located closer to the load—or in some cases, at the customer's premises. The generation capacity of distributed generation is much smaller compared to the conventional power plant. Renewable energy, co-generation plants, and standby generators are considered as distributed generators (DG) [42]. Traditionally in a radial network, power flows only in one direction. Network operators are now facing difficulties while integrating DGs within the existing power network. The standard and tolerance of the existing grid does not cater for bi-directional power flow and affects voltage regulation, stability and harmonics. Figure 2.8 illustrates the concept of active power flow from DGs into the network that causes in reserve of the conventional power flow from source to load.

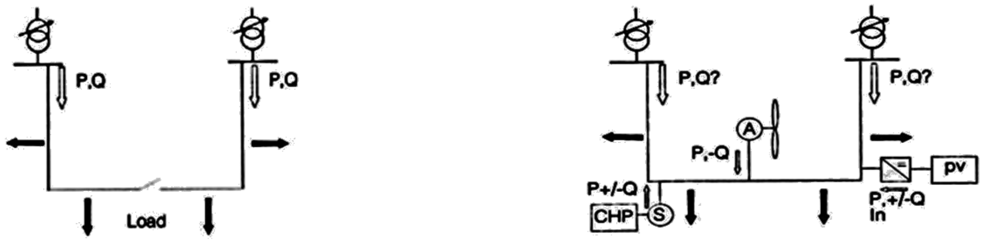

a. Power flow- conventional b. Power flow - after integrating DG

Figure 2:8 Power flow in distribution network without and with DGs [9]

2.3.1 Benefits of Distributed Energy Generation

Some positive attributes that make DGs a definite choice for power networks is:

- Can be used on location without an intrinsic cost penalty, compared to the cost of bulk power of traditional generation (if demand is matched with generation);
- Can offer voltage or power (active/reactive) support;
- Reduces capacity demand of transmission and distribution network, which reduces load on transformer and conductor;
- Improves cost penalty due to grid failure.

Two primary RE technologies integrated into the distribution level are rooftop solar PV and wind turbines. However, managing generated electricity from these sources requires a place to store electricity when excess energy is generated, and also to hold as a supply for a later time. Therefore storage is also considered as a distributed generator. For typical load, a storage-integrated grid connected to PV and wind systems presents a sustainable and economically viable solution [43-45]. Large-scale energy storage or grid energy storage lets energy producers store surplus electricity to a temporary electricity storage site, which becomes an energy producer when electricity demand becomes greater. Grid energy storage is especially important for matching supply and meeting energy demand from RE over a 24-hour period.

2.3.2 Importance of Energy Storage in Power Network

The supply of energy from solar and wind are not continuous and may change energy intensity at any time due to natural factors like day/night cycle, location, cloud, temperature, air pressure, sun and moon effects on earth etc. Due to these factors, it is not possible to achieve continuous supply from solar and wind and also, the level of energy is subject to fluctuate. Thus, a storage-integrated PV or wind system is the solution to overcome the major challenges introduced by the intermittent nature of RE.

Figure 2.9 shows the measured fluctuation extremes from solar PV, which indicates how fast these changes can occur [46].

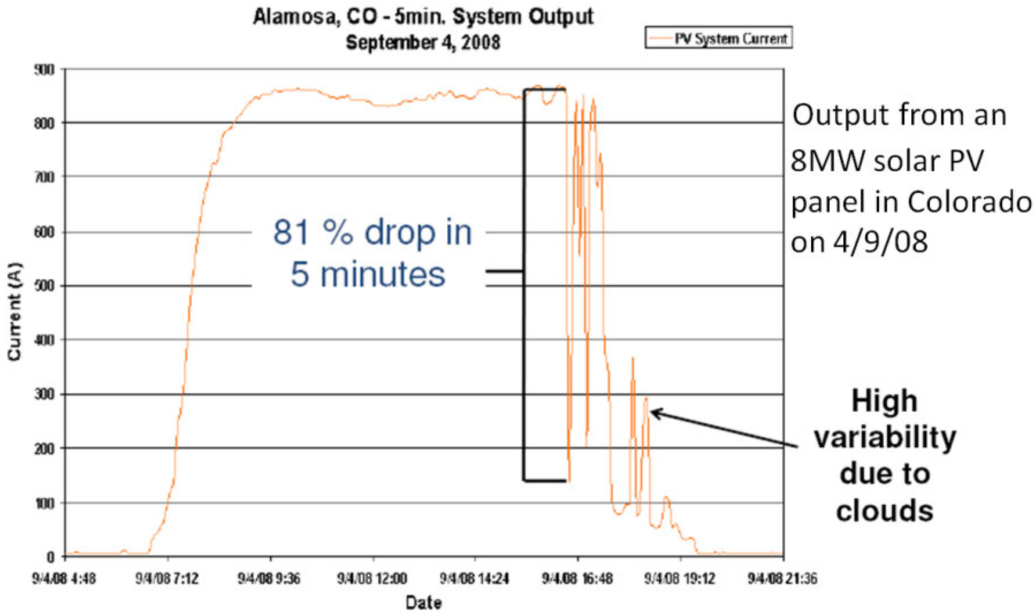

Figure 2:9: Variability nature of solar energy

Similarly, wind power turbulence refers to fluctuation in wind speed on a relatively fast time-scale, typically approximately less than 10 minutes. Turbulence intensity depends on roughness of ground surface, height, topographical features and thermal behaviour of the atmosphere. The maximum wind speed of 141 km/hr was measured at Bellambi Point (near Wollongong), NSW in Australia at 5:30PM as shown in Figure 2.10 [47].

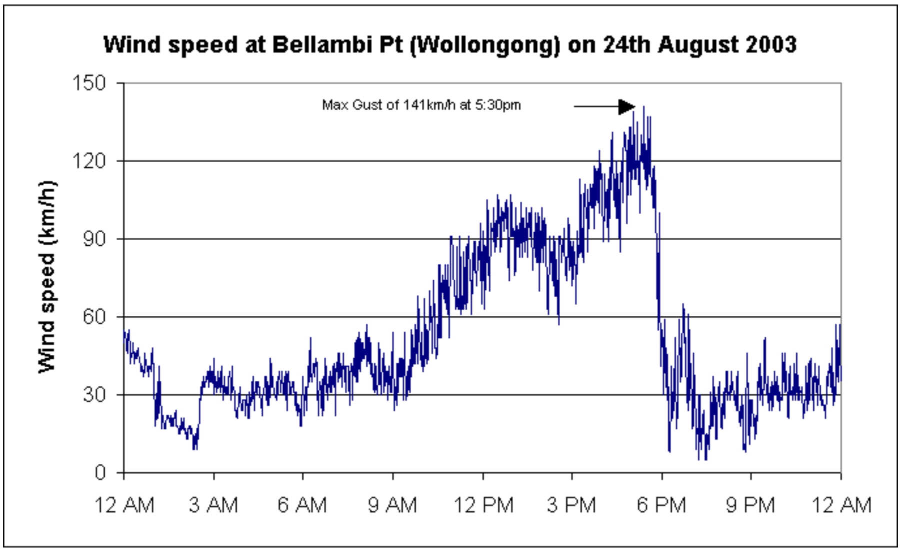

Figure 2:10 Wind speed variation at Bellambi Point near Wollongong, NSW[47]

Wind turbine output varies with wind speed; even at the best wind speed sites, power output varies dramatically from hour to hour and minute to minute. However, the grid must respond to load demand. According to Eon Netz, one of the grid managers in Germany, the amount of back-up power required was 80% [48], which was the maximum output observed from all of their wind power facilities together. Therefore, to support the load demand from PV and wind during fluctuations, storage is required to balance the load demand. There are different storage technologies suitable for different applications.

2.4 Energy Storage Technologies

Different ES technologies coexist and different characteristics make them suitable for different applications. ES is now seen more as a tool to improve power quality in power systems, assist in power transfer and to enhance system stability. Recent developments and advances in ES and power electronics technology make ES applications a feasible solution for modern power applications. In an AC (alternating current) system, electrical energy cannot be stored electrically. However, energy can be stored by converting and storing it electrochemically, electromagnetically, kinetically or as potential energy. Each ES technology contains a power conversion unit. Two factors characterize the application of ES technology. One is the amount of energy that can be stored, and the other is the rate of energy transferred to/from the storage device.

ES technologies can be classified according to energy and power density, response time, cost, lifetime, efficiency and operating constraints. Different forms of ES systems that include pumped hydro storage (PHS), compressed air energy storage (CAES), thermal energy storage (TES), and flywheel, hydrogen, different type of batteries, capacitors, and superconducting magnetic energy storage (SMES) are suitable for different types of applications. Different ES systems are explained below:

i. Battery Energy Storage Systems (BESS)

The battery is one of the most cost-effective ES technologies available today for storing energy electrochemically. BESS is a modular technology and one of the more promising storage technologies for power applications such as regulations, protection, spinning reserve and power factor correction [49]. Battery storage requires DC (Direct Current) electricity; therefore, a converter is required to interface with the AC system.

There are a number of battery technologies under consideration for large-scale application. Lead-acid batteries are an established and mature technology that can be designed for bulk ES or for rapid charge or discharge application. Other battery technologies are nickel-metal hydride (Ni-MH), nickel-cadmium (Ni-Cd), lithium-ion (Li-ion), sodium-sulphur (NaS) and flow-battery (FBs). There are three types of FBs: Vanadium Redox battery (VRB), Polysulphide Bromide battery (PSB) and Zinc Bromide battery (ZnBr).

However, there are limitations to BESS. For instance, lead-acid batteries are sensitive to operating temperatures and the best operating temperature is about 27ºC, which has a depth-of-discharge (DoD) limit and charge/discharge cycle limit. NaS batteries need to be kept at temperatures above 270 ^{o} C. VRBs have a lower power density.

Lead-acid Lithium-ion Vanadium-Redox

Figure 2:11: Different battery technologies

The largest lead-acid battery installed in California has a capacity of 10MW/40MWh [50]. Nonetheless, no detailed report is available on how this storage system provides support for the overall operation of the power system. The largest NaS battery has a rating of 9.6MW/64MWh, whereas the largest VRB has a rating of 1.5MW/1.5MWh [50]. Few battery technologies are shown in Figure 2.11.

ii. Superconducting Magnetic Energy Storage (SMES)

SMES is a device that stores energy in a magnetic field generated by the DC current flowing through a superconducting coil. The inductively stored energy (E in joules) and the rated power (P in watts) are the common specifications of SMES, and can be expressed by Equation 2.1 [51]:

$$E = \frac{1}{2} L I^2 \qquad P = \frac{dE}{dt} = LI\frac{dI}{dt} = VI \tag{2.1}$$

where L is the inductance of the coil, I is the DC current flowing through the coil and V is the voltage across the coil. Energy can be drawn from SMES almost as an instantaneous response and can be stored or delivered over periods ranging from a fraction of a second to several hours.

SMES has a fast response and high efficiency (charge-discharge efficiency over 95%). Possible applications of SMES includes load levelling, voltage stability, dynamic stability, transient stability, frequency regulation, transmission capacity enhancement and power quality improvement [51]. However, the SMES system is still costly compared to other ES technologies. It is sensitive to temperature and can become unstable in temperature changes.

iii. Super Capacitors Energy Storage (SCES)

Capacitors store accumulated positive or negative electric charges on parallel plates separated by dielectric materials. Capacitance (C) is represented by the relationship between stored charge (q) and voltage between plates (V). Capacitance depends on the area of the plates (A), distance between plates (d) and permittivity of the dielectric (ε) as shown in Equation 2.2 [51].

$$q = CV \quad C = \frac{\varepsilon A}{d} \quad E = \frac{1}{2}CV^2 \tag{2.2}$$

The amount of energy can be increased by increasing capacitance or voltage between the plates. However, voltage depends on the withstand strength of the dielectric, which is also impacted by the distance between plates. The total voltage change when charging or discharging capacitors can be shown by Equation 2.3[51]. C_{tot} and R_{tot} are the total capacitance and resistance respectively, from a combined series/parallel configuration of capacitor cells to increase total capacitance and total voltage level.

$$dV = i \times \frac{dt}{C_{tot}} + i \times R_{tot} \tag{2.3}$$

Capacitors are used in many AC or DC applications. Capacitors are often used as very short-term storage with power converters. DC capacitors are used as large-scale energy storage on distribution dynamic voltage restorer (DVR) that compensates for temporary voltage sags on the power distribution systems [52]. The disadvantage of capacitor is its low energy density.

Ceramic hyper-capacitors have both fairly high voltage withstand capacity (about 1kV) and high dielectric strength. Ultra-capacitors are double-layer capacitors that have increased storage capacity and are suitable for high peak-power, low-energy applications. Electrochemical double-layer capacitors (EDLCs) work similarly as conventional capacitors but have very high capacitance ratings, long life cycle and better efficiency.

iv. Flywheel Energy Storage (FES)

FES stores energy in a rotatory mass. Flywheel can be used to store energy for power systems when coupled to an electric machine such as a synchronous generator. Stored energy (*E*) depends on the moment of inertia (*J*) of the rotor and the square of the rotational velocity (ω) of the flywheel. The moment of inertia depends on the radius (*r*), mass (*m*) and length/height (*h*) of the rotor, as shown in Equations 2.4 [51].

$$E = \frac{1}{2} J\omega^2 \qquad J = \frac{r^2 mh}{2} \tag{2.4}$$

FES systems are able to provide very high peak power, high power and energy density and have a virtually infinite number of charge-discharge cycles [53]. Flywheel has been considered for numerous power system applications, including power quality, peak shaving and stability enhancement applications and also for transportation applications. However, it requires cooling and there is power loss during ideal time. Figure 2.12 shows a FES application scheme.

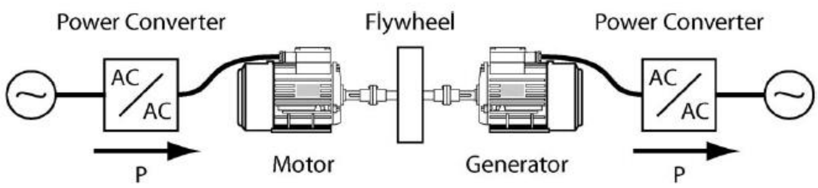

Figure 2:12 General scheme of Flywheel with two machines[53]

v. Thermal Energy Storage (TES)

TES involves storing energy in a thermal reservoir to use at a later time. TES system is suitable for solar thermal power plants, and consists of either synthetic oil or molten salt as heat energy storage collected from a concentrated solar power plant (CSP), as shown in Figure 2.13. CSP with TES can store thermal energy for period up to 15 hours, thus improving flexibility of the grid and facilitating greater penetration of solar energy into the grid. TES can be used to increase the reliability of intermittent RE sources.

Figure 2:13 Concentrated solar power with molten salt as heat storage [54]

vi. Pumped Hydroelectric Storage (PHS)

PHS is a large-scale ESS that uses the potential energy of water developed by the gravitational force. This gravitational force is generated by pumping water from a lower reservoir to an upper reservoir during low demand time, as shown in Figure 2.14. During high demand time, water is released back into the lower reservoir through turbine to produce electricity. The low energy density of PHS requires either a large water body or greater height variation. Even so, PHS provides critical backup during peak demand on the national grid.

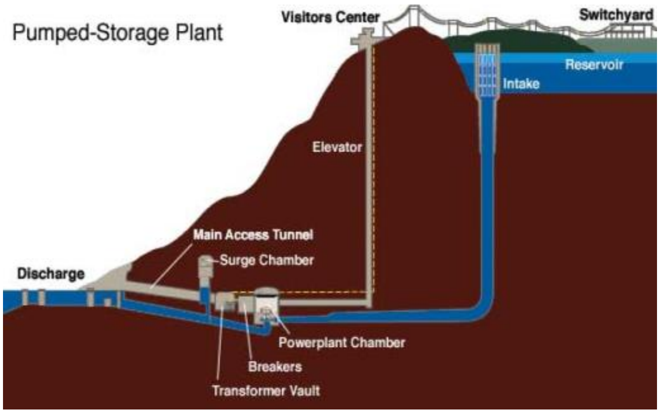

pumped hydroelectric energy storage layout

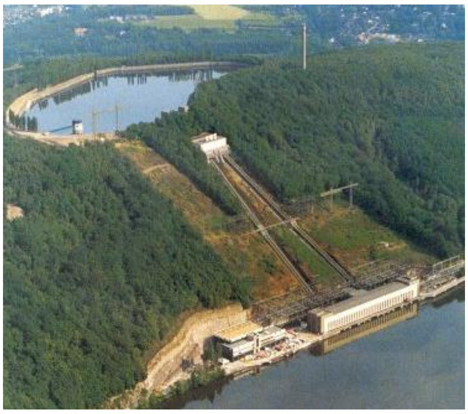
PHS facility at Alaska [55]

Figure 2:14 Pumped hydroelectric storage layout and example

The power capacity (*W*) of PHS is a function of the water flow rate and the hydraulic head, whilst the energy stored (*Wh*) is a function of the reservoir volume and hydraulic head. The power output of a PHS facility can be calculated by Equation 2.5 [56] and the storage capacity of PHS can be calculated by Equation 2.6 [57]:

$$P_c = \rho g Q H \eta \tag{2.5}$$

$$S_c = \frac{\rho g H V \eta}{3.6x10^9} \tag{2.6}$$

P_c is the power capacity in Watts (*W*), ρ is the mass density of water (kg/m^3), g is the gravitational constant (m/s^2), Q is the discharge through the turbines (m^3/s), H is the effective head height (m) and η is the generating efficiency, S_c is the storage capacity in megawatt-hour (MWh), and V is the volume of water that is drained and filled each day (m^3).

PHS is a cost-effective large storage system currently available, although installation requires a specific geographic site. An example of PHS is operated by First Hydro Company in the UK [58] is the Dinorwig Power Station, that is capable of moving from 0 to 1,320MW power injection in 12 seconds. This station can inject 1728 MW for 5 hours [59]. PHS has a comparatively longer lifespan and can respond quickly to support demand. It is ideal for load-levelling applications. It is also suitable for peak load support and frequency regulation.

vii. Compressed Air Energy Storage (CAES)

CAES stores energy as compressed air for later use. It consists of a power train motor that drives the compressor, a high-pressure turbine (HPT), a low-pressure turbine (LPT) and a generator as shown in Figure 2.15. Most commercially implemented CAES systems use an adiabatic storage system to manage heat exchange. CAES use off-peak electricity to compress air; conversely, stored and compressed air is released to operate gas turbine. Gas turbines use compressed air and natural gas; therefore, CAES makes gas turbine more efficient than the conventional gas turbine system. Commercial systems use natural caverns as air reservoirs and installed commercial system capacity ranges from 35 to 300MW.

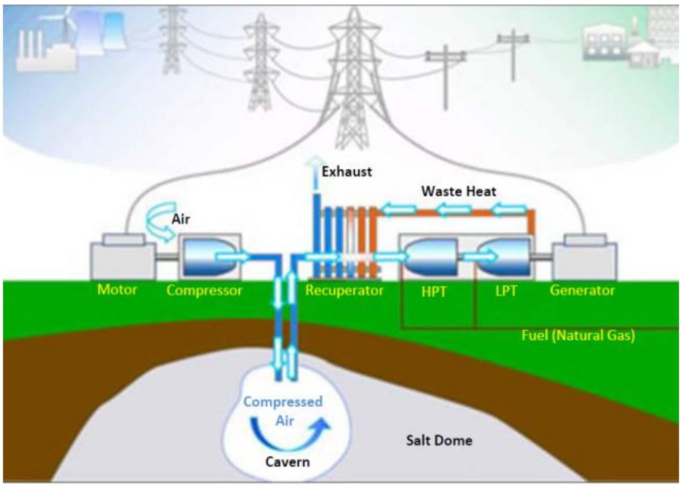

Figure 2:15 Compressed air energy storage

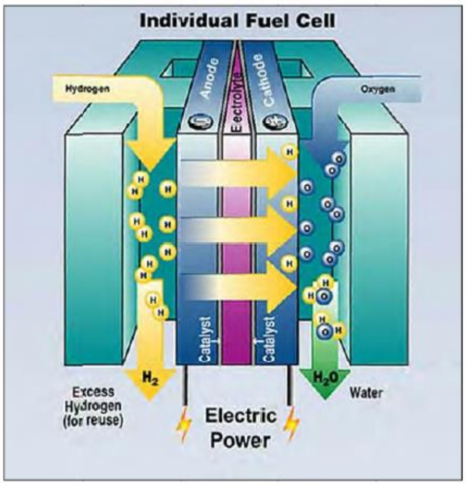

Figure 2:16 Structure of Fuel cell

CAES are considered for applications such as electric grid support for load levelling [53], frequency regulation, load following and voltage control. It is dependent on the specific geographical location for underground reservoir; therefore, installation cost can be high.

viii. Hydrogen Energy Storage (HES)

HES differs from conventional idea of energy storage because it uses separate processes for hydrogen production, storage and use. An electrolyzer produces hydrogen and oxygen from water. A hydrogen fuel cell converts hydrogen and oxygen back into water, releasing energy. The main drawback of HES is that hydrogen is extremely flammable and difficult to store as a pressurized gas. Different strategies of integrating HES with wind and solar energy were proposed in [60].

Fuel Cell (FC): Fuel cell uses stored hydrogen and passes it over the anode (negative) and oxygen over the cathode (positive), causing ions and electrons to form at the anode. The electrons flow through an external circuit that produce electricity while the hydrogen ion passes from the anode to cathode, combining with oxygen to produce water. Figure 2.16 shows the structure of a hydrogen fuel cell.

The characteristics of different ESS described above are summarized below in Table 2.3.

Table 2:3 Energy Storage Systems [53, 59, 61-64]

Type	**Energy efficiency (%)**	**Energy density (Wh/kg)**	**Power density (W/kg)**	**Life (cycles or years)**	**Discharge at rated capacity (hours)**	**Response time (s)**	**Self discharge**
Pumped hydro	70 - 80	0.3	-	20-60 years	1-24+	10	Negligible
CAES	40-50	10-30	-	20-40 years	1-24+	360	low
TES	75	-	-	30 years	-	>10s of minutes	-
SMES	90	10-75	-	>100,000	$2.7X10^{-7}$-0.0022	0.01	10-15%
Flywheel (steel)	85-95	5-30	1000	>20000	$2.7X10^{-7}$-0.25	0.1	Very high
Super Capacitor	80-95	2-5	800-2000	10 years	$2.7X10^{-7}$-1	0.01	5-20%
Lead-acid	65-80	20-35	25	200-2000	0.0027-2+	<1/4 cycle	low
Ni-Cd	60-90	40-60	140-180	500-2500	0.0027-2+	<1/4 cycle	0.2-0.3%
Li-MH	50-80	60-80	220	<3000			high
Li-ion	70-85	100-200	360	500-10000	0.017-2+	<1/4 cycle	1-5%
Li-polymer	70	200	250-1000	>1200			medium
NaS	70-89	120	120	2000-3000	0.0027-2+	<1/4 cycle	-
VRB	80-85	25	80-150	>16000	0.0027-10	<1/4 cycle	negligible
EDLC	95	<50	4000	>50000			Very high
Hydrogen	50	100-150	-	-	-	360	low
Fuel cell	-	-	-	>1000	0.0027-24+	<1/4 cycle	-

In order to support applications that require a combination of high power (for devices with quick response) and high energy (for devices with slow response), a hybrid ESS was proposed in different studies [53]. The following section illustrates the storage category, its applications and advantages.

2.4.1 Classification of Energy Storage Systems

Energy storage will play unique and critical role in the future smart grid development by combining different RE sources capability into the grid. Storage can buffer the power spikes and dips and fluctuations [65]. Highest valued applications of storage identified by EPRI [66] are to maintain commercial and industrial power quality and reliability, to enable stationary and transportable system for grid support. In large-scale application, electrical ES can be divided into three main functional categories such as:

- **Power Quality:** Stored energy applied only for seconds or less to ensure continuity of power quality.
- **Bridging power:** Stored energy applied for seconds to minutes to assure continuity of service when switching from one source of energy to another.
- **Energy Management:** Stored energy used to decouple the timing of energy generation and consumption especially in the application of load levelling. Load levelling involves charging of storage in low demand time and use in peak time, which enables consumers to minimize the total energy cost.

ESS has a number of applications in electrical power systems, especially integrating intermittent RE into the grid. ESS can be classified according to capacity, discharge time, efficiency and capital cost as shown in Figure 2.17 to 2.20 [67]. The cost of storage technologies is changing as they mature. Figure 2.20 shows the cost and energy density of various ESS based on 2002 value.

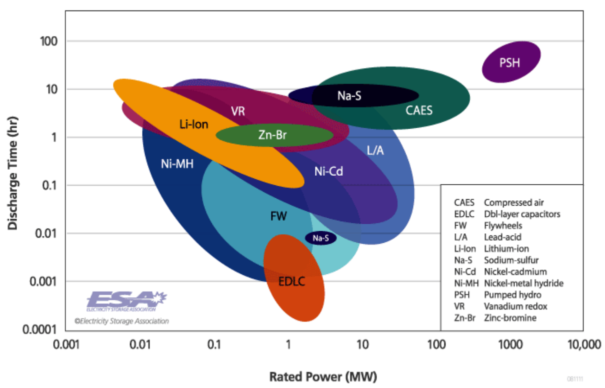

Figure 2:17 Power rating of different storage systems

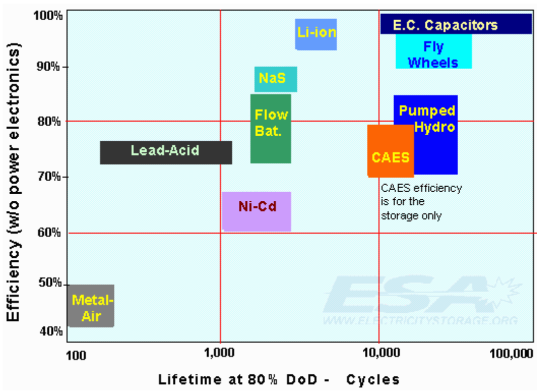

Figure 2:18 Efficiency & life of different ESS

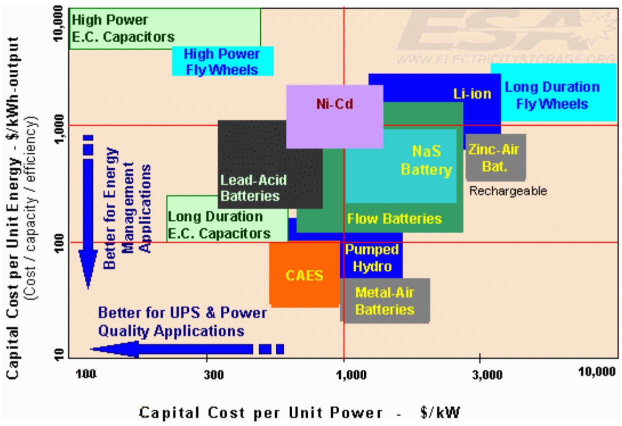

Figure 2:19 Capital cost of different ESS

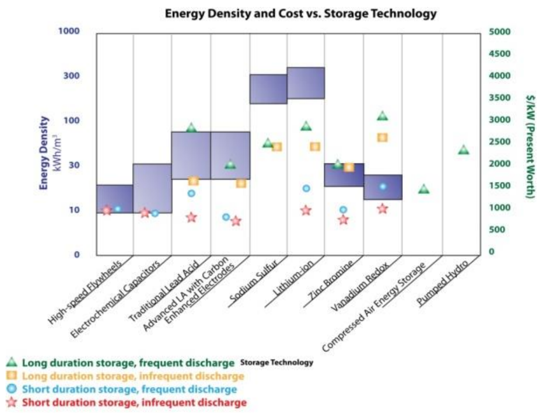

Figure 2:20 Storage technology and cost

2.4.2 Advantages of Energy Storage Systems

Energy storage can revolutionize electric power systems using RE by supporting peak load problem, improving stability and power quality. Storage can be applied with the generation, transmission and in various point of the distribution system, at the customer site or with any particular appliances. ESS, in combination with advanced power electronics applied to intermittent RE sources, provides technical, financial and environmental benefits, which are explained below:

i. Technical benefit of ESS:

ESS can improve performance of the application suitable for eclectic utility and transport system. The main advantage of the ESS is to maintain the grid power at a constant level [68] by contributing in the following ways.

- **Grid voltage support:**

  ESS can provide power to the grid to maintain grid voltage within an acceptable range, especially when RE is integrated.

- **Grid frequency support:**

  Real power provided by the ESS to the grid reduces any sudden large generation imbalance by RE and keeps the grid frequency within allowable limits. Storage plays a significant role in minimizing high frequency power fluctuations [65].

- **Transient stability:**

  ESS reduces power oscillation by injecting or absorbing real power.

- **Load levelling or peak shaving:**

Storing electricity during low demand time and supplying it during peak demand time is known as load levelling, as shown in Figure 2.21. ESS provides freedom in load levelling and peak shaving by moving peak demand into the off-peak period.

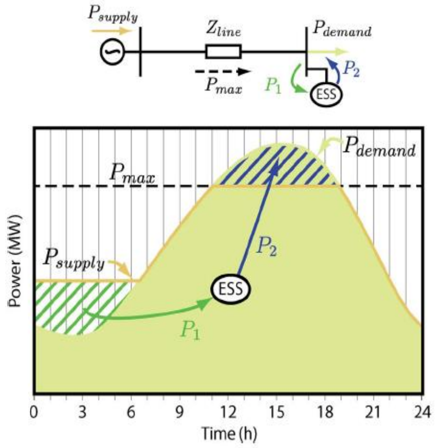

Figure 2:21 Basic concept of load levelling using ESS[53]

- **Spinning reserve:**

ESS can support the generator by providing active power over a given period of time to keep the desired generation capacity.

- **Power quality improvement:**

ESS can mitigate power quality problems such as changes in the magnitude or shape of the voltage or current waveform (including harmonics, power factor, transients, flicker, sag, swell etc).

- **Reliability:**

ESS can reduce the interruption in electric power delivery and improve reliability.

- **Ride through support:**

ESS provides support to the load during system disturbances, such as voltage sag or momentary blackout.

- **Unbalanced load compensation:**

ESS can inject or absorb power to/from individual single-phase unbalanced loads. ESS needs to be connected with a four-wire inverter to support in this situation.

- **Increasing penetration of RE sources:**

The intermittent characteristics of solar and wind energy cause fluctuations in voltage and frequency, which poses a great barrier in large-scale integration of these fast-growing RE sources. Moreover, unbalance in demand and supply becomes eminent due to the nature of solar and wind energy generation. Investigation showed that for every 10% of wind energy penetration into the grid, a 2% - 4% of installed wind capacity of balancing power is required from other sources for stable operation [53], this is also critical for large-scale solar PV integration. ES acts as a buffer that insulates the grid against the frequent and rapid power fluctuations from high penetration of renewable resources [69]. Storage improves the grid penetration of PV energy [70]. A large ESS allows high penetration of wind and solar PV into the grid [59, 71-74].

ii. Financial benefit of ESS:

Although integration of ESS incurs additional cost, however there are various financial benefits, which are explained below:

- **Cost reduction:**

Electricity can be purchased during low demand periods to store and use during high demand periods, so the overall total consumption cost is reduced. Moreover, stored electricity can be sold during high demand. Electricity from RE can be used in a similar fashion to reduce total consumed energy cost.

- **Avoiding additional cost in generation:**

ESS can help in avoiding installation or renting cost of additional generation to support peak load demand.

- **Avoiding additional cost in transmission/distribution:**

ESS can improve the transmission and distribution performance by operating utilities with its capacity, thus avoiding the additional cost of installation to support peak load. Moreover, transmission access/congestion costs can be avoided by the use of ESS.

- **Reduce reliability and power quality related financial loss:**

ESS helps to improve power quality by supporting loads during outage, sag, or flickering. This in turn improves reliability and reduces the penalty cost of the utility operators.

- **Increases revenue from RE generation:**

ESS helps in time-shift in load demand by storing electricity from RE generators and supplying it when needed. This ensures maximum utilization of RE.

iii. Environmental benefit of ESS:

ESS ensures the best utilization of RE, which also reduces the use of conventional energy sources, and consequently reduces GHG emission [74].

Therefore, energy storage technology can play a significant role in maintaining power quality and system reliability [51]. The principle application of ESS is to respond to sudden changes in load; support load during transmission or distribution interruptions; and correct load voltage profiles with rapid reactive power control, which allow generators to operate in balance with the system load at their normal speed [51]. The technical advantages of different ESS are summarized in Table 2.4.

Table 2:4 Applications of different Energy Storage Technologies [68, 75]

Energy storage applications	Pumped hydro	CAES	SMES	Lead-acid	Flow batteries	Flywheels	Super	Hydrogen/ Fuel cell	TES
Load levelling	√	√		√	√			√	√
Load following	√	√		√	√			√	√
Peak generation	√	√		√	√	√		√	√
Fast response spinning reserve	√	√		√	√	√	√	√	
Conventional spinning reserve	√	√		√	√	√		√	
Emergency back-up	√	√		√	√			√	√
Uninterruptible power supply				√	√	√		√	
Transient and end use ride through			√	√	√	√	√	√	√
Transmission & Distribution stabilisation	√	√	√	√	√			√	
RE integration	√	√		√	√	√		√	√
RE back-up	√	√		√	√				√

Proper utilization of ESS depends on various cost involvements with different applications. Cost is one of the key indices in the proper choice of ESS.

2.4.3 Cost of Energy Storage Systems

Selection of suitable ESSs are determined by any or all of the following criteria: lifetime, life cycle, power and energy, self-discharge rate, environmental impact, efficiency, capital cost, storage duration and technical maturity of the storage system. The present cost of storage is considered one of the major barriers to large-scale utilization. The operational cost (maintenance, loss during operation and ageing) and capital investment cost are the most important factors to select a suitable ESS. Efficiency and lifetime also affect the overall cost of the ESS. Table 2.5 summarizes the power or energy related cost of various ESS.

Table 2:5 Cost of various ESSs

Storage technology	Power related cost ($/kW)[75]	Energy related cost ($/kWh)[75]	Power Capacity cost ($/kW)[63]	Storage cost rank
Pumped hydro	600 - 2000	0 - 20	5 - 100	Low [62, 64]
CAES	425 - 480	3 - 10	2 - 50	Low [62]
Lead-acid Battery	200 - 580	175 - 250	50 - 400	Low [62, 64]
Ni-Cd Battery	600 - 1500	500 - 1500	400 - 2400	High [62, 64]
NaS Battery	259 - 810	245	300 - 500	Medium
Li-ion Battery	-	900 - 1300[64]	600 - 2500	High [62]
Vanadium Redox	1250 - 1800	175 - 1000	150 - 1000	Medium
ZnBr	640 - 1500	200 - 400	150 - 1000	Medium
High speed Flywheel	350	500 - 25000	300 - 25,000	High [64]
Super Capacitors	300	20,000 - 82,000	300 - 2000	High [64, 73]
Fuel cell (Hydrogen)	1100 - 2600	2 - 15	425 - 725	Low
SMES	300	2000	1000 - 10,000	High [59, 62]

Per-cycle cost of ESS are 5-80 c/kWh for VRB, 8-20 c/kWh for NaS, 20-100c/kWh for NiCd and 20-100c/kWh for Lead-acid battery [62].

2.4.4 Integration of Energy Storage into the Grid

For off-grid applications, storage has to fulfil the following requirements: (i) the discharge rate has to be larger than or equal to the peak load capacity; (ii) the storage capacity has to be large enough to supply energy for a long time (e.g. night time) and to operate during its autonomy period. IEEE 1013[76] provides recommendations for sizing lead-acid batteries for stand-alone PV systems. If storage is required for a grid connected RE system, autonomy becomes a secondary issue.

The main objectives of introducing ESS to the power utility are to improve system load factor, peak shaving, to provide system reserve, achieve reliability and effectively minimize production cost. Some ESS like battery energy storage systems (BESS), electrochemical double-layer capacitors (EDLC), superconducting magnetic energy storage (SMES), flywheel energy storage (FES) and fuel cell (FC) requires power converter to connect between two different DC voltage level buses, a DC voltage bus and an AC voltage bus or even connect a current source to a voltage bus [53]. To manage the energy flow in bidirectional way and controlling the charging and discharging process of ESS, Power converter with ESS should have the following features:

- High efficiency
- Fast response (frequency regulation applications)
- Stand with high peak power (peak shaving application)
- Manage high rated power (load levelling application)

Integration of RE into the grid can be done at different points of the LV network and through a step-up transformer to the HV network. Based on the load demand near RE generation, storage can be added to the network near the load centre to improve various uncertainties developed by solar and wind energy. For large-scale solar and wind power plants, large-scale storage can be integrated into the network through inverter and transformer. However, for charging and discharging, two-way AC/DC converters are required.

Wind power plants transmit output power to the grid through AC or DC line after stepping up the voltage, as shown in Figure 2.22. A present commercial wind turbine generator has the capacity of 1.5 MW to 3 MW with a rotor diameter of up to 126 m. Such a turbine can produce power at wind speeds of about 3 m/s and a maximum power at around 10 m/s to 13 m/s [16]. Some wind power plants have a capacity comparable to that of a conventional power generator.

A solar PV cell directly converts solar energy into DC electricity. PV modules have a typical capacity of 50 W to 200 W. PV systems is highly modular and capacity ranging from few Watts to tens of megawatts. DC output from PV systems converted to AC by inverter to integrate into the grid. Large-scale PV systems are called PV power stations as shown in Figure 2.23.

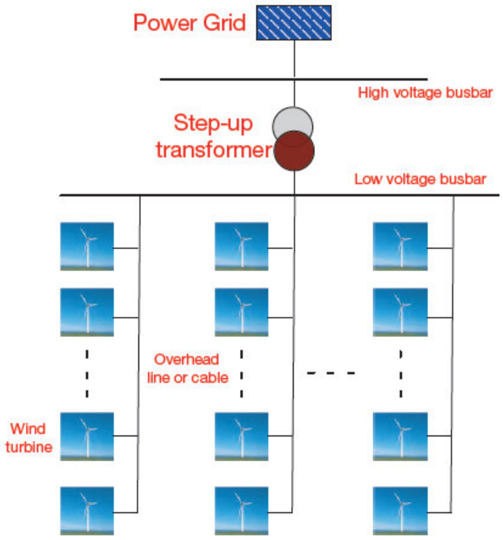

Figure 2:22 Structure diagram of a wind farm [16]

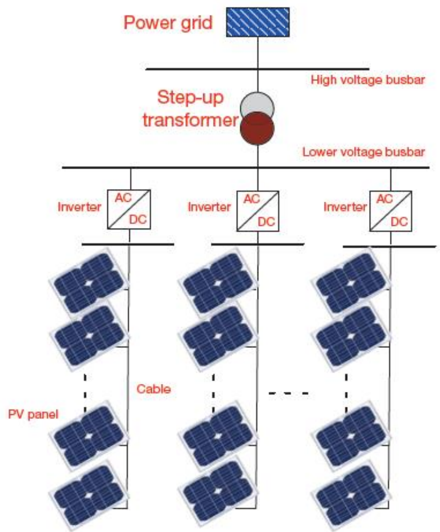

Figure 2:23 Structure of PV power station [16]

As discussed earlier, the integration of DGs at the DN can introduce reverse power flow and can interfere with voltage regulation. Generally, a voltage regulator (a transformer located at the beginning of the feeder) maintains a higher voltage at the beginning of the feeder to ensure adequate voltage at the end of the feeder. By introducing significant power from PV just after the voltage regulator or beginning of the feeder, the end load of the feeder will experience low voltage. If significant power from PV is injected at the end of the feeder, high voltage may occur at the end of the feeder or at the connection point. Figures 2.24 and 2.25 show these scenarios [77].

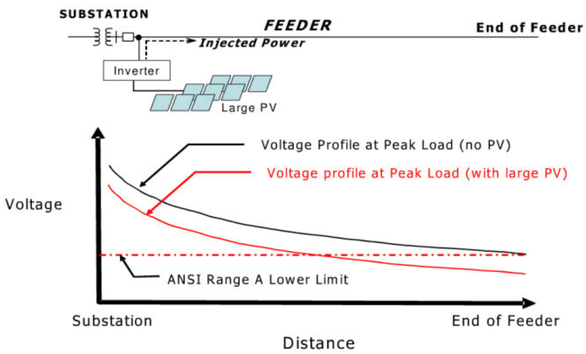

Figure 2:24 Line drop compensation confused by PV generation near the front of regulator

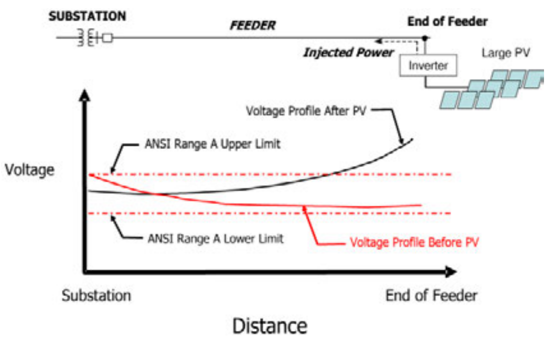

Figure 2:25 High voltage due to large integration of PV near the end of the Feeder

Integrating large-scale RE into the grid brings variability and uncertainty. Constantly balancing the generation and load can improve the flexibility of the power system, which in turn makes the power system reliable and efficient. Flexibility can also be achieved from the load side through demand response. ESS can also improve flexibility by acting as a load or generator [16].

The widest range of uses for large-scale ESS lies in service to the grid operator in order to provide generation flexibility. The best use of storage is as a tool to mitigate variability and uncertainty for the entire grid, rather than for specific load or generation. A project completed in 2011 that consists of 100 MW wind power, 40 MW PV power and 20 MW energy storage as shown in Figure 2.26 [16]. Storage contributed to smoothing output, schedule following, load following and frequency regulation. It also made the wind and PV stations more grid-friendly [16].

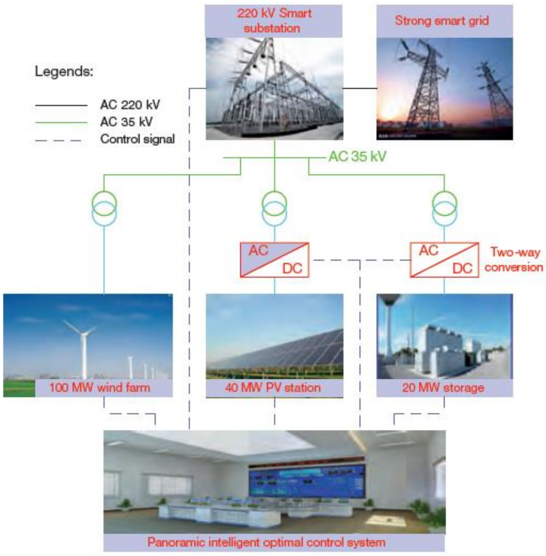

Figure 2:26 Architecture of wind power, solar power, energy storage in a transmission demonstration project

An ESS with Flexible AC Transmission Systems (FACTS) devices adds flexibility to achieve improved transmission system by improving system reliability, dynamic stability, power quality, transmission capacity, and by supporting active and reactive power[51, 78].

There is not yet a concrete standard for integrating bulk and large storage into the grid. However IEEE 1547-2003 [79] provides guidelines to connect distributed resources (DR) such as solar PV, wind and energy storage to the power grid at the distribution level. The importance of ES has been evaluated by forming working groups to develop standard IEEE

P2030.2 for the interoperability of ESS integration with the electric power infrastructure [80]. In Australia AS 4777 [81] provides guidelines to connect DGs to the DN via inverters up to 10kVA for single-phase and 30kVA for three-phase units.

2.5 Investigation of Standards in Integrating Energy Storage into the Grid

The characteristics of RE sources influence the output electricity which is quite variable with time and different than the grid power characteristics, moreover RE sources does not guarantee load and demand management. Therefore, there are a number of power quality (PQ) issues that must be addressed before integrating DG into the power network and regulatory standards play an important role to ensure power qualities. Current practice by local DNSP in ensuring PQ at customer end is somewhat different than various standard guidelines [12]. Comparing AS-4777 with relevant standards and practices and planning by local utility operator to integrate RE in Queensland, Australia the inconsistent PQ indexes are summarized below:

- **Voltage regulation:** AS-4777 [21] indicates single-phase rated voltage as 230 V, ranging from 200 V minimum to 270 V maximum. Three-phase rated voltage is 400 V, with a range minimum of 350 V to a maximum of 470 V. AS-610038 [82] indicates single-phase and three-phase supply voltage as 230 V and 400 V, respectively, with a tolerance between +10% and -6% and a utilization range of +10% and -11%. AS/NZS-61000.3.3 [83] indicated that the system voltage range is 220 V to 250 V. AS-61000.3.100 [84] indicated the single-phase voltage limit as 216 V to 253 V, and three-phase limit as 376 V to 440 V. Ergon Energy currently uses 240 V as its single-phase base voltage. Ergon-Energex have a combined standard [22] stated voltage range as 240 V ± 6% and 415 V ± 6% for single-phase and three-phase respectively.

- **Frequency:** AS-4777 indicates that a 50 Hz system power frequency should not exceed limits ranging from 45 Hz to 55 Hz. Ergon-Energex’s combined standard indicated this range from 49.85 Hz to 50.15 Hz.

- **Harmonics emission:** AS-4777 indicates that harmonic current limits and total current harmonic distortion (THD) up to the 50th harmonic should be less than 5%. IEEE-1547 [79] indicated the same, but for even harmonics of h>16, the limit is different. IEEE-1159 [85] indicated a harmonic voltage limit of 0~20%. The Ergon-Energex combined standard sets its total voltage harmonic limit (THD) to 8%.

- **Power factor:** AS-4777 indicates that the power factor of the inverter shall be in the range from 0.8 leading to 0.95 lagging. However Ergon-Energex combined standard states that the LV system power factor should be greater than 0.8, but not leading.
- **DC offset:** AS-4777 indicates that the DC output current of the inverter shall not exceed 0.5% of rated output current or 5 mA whichever is greater. IEEE-1547 indicates that DGs shall not inject DC current greater than 0.5% of rated output current. IEEE-1159 indicates that DC offset voltage should be in the range of 0 ~ 0.1% of rated voltage.

Photovoltaic planning criteria [23] by Ergon Energy indicated a required PV panel efficiency of 95% and inverter efficiency of 98%. Alteration in DT tapping is not allowed in increased voltage by PV. Allowed voltage rise due to PV at PCC is 1% of the base voltage. Each installation of PV capacity is restricted to 1.3 kW in rural areas for DT up to 50 kVA. In urban areas, the restriction is 4 kW for DT up to 100 kVA.

The findings summarized above clearly indicate that there are gaps in different PQ parameter limits or ranges among different standards and guidelines. This can limit integrating a large number of distributed energy resources (DER) and storage into the DN. Therefore, this research considered AS-4777 as the primary guideline along with Ergon Energy’s parameter limits.

2.6 Investigation of Various Research Works

Storage application falls into two categories: energy application and power application. Long discharge and charge cycles are involved in energy applications such as peak shaving and load levelling. Short period discharge and charge with many cycles are involved in power applications such as: frequency and voltage regulation, power quality, smoothing of renewable energy generation and ramp rate control [17]. For grid stabilization or grid support application, the standard technology of energy storage systems currently consists of large installations of lead-acid batteries. The primary function of grid support is to provide a spinning reserve in the event of power plant or transmission line equipment failure. Current implementation can provide a few minutes of energy; however, overall grid management (including shifting peak load and supporting renewable energy) will require longer duration of storage that can handle greater energy/power ratios [17]. There are few examples of large-scale battery systems in various applications as explained in [17].

As elaborated earlier, utilities face several challenges in integrating solar and wind into the grid and expressed concerns on various PQ issues. Austria, France, Germany, Spain, Netherlands and the United Kingdom are the six countries that represent 98% of installed PV power in the European Union. Technical assessments expressed the following concerns after PV-DG integration into the grid in these countries [13]:

- Harmonic emission by inverters was considered a current and future concern at high penetration of PV.
- Voltage regulation was a big concern for weak grids with high PV penetration, but not for strong urban networks. Different regulations allowed over voltage limits of 5% to 6% by PV plants.
- Network protection was a big concern, as there is lack of direct control on DGs by the DNSP.
- Unintentional islanding due to high penetration of PV-DG was considered a matter of concern.
- In Austria, Spain and the Netherlands, PV-DG penetration limits for LV networks varied between 33% and 75% whereas for medium voltage (MV) networks it was 50%.
- Current standards for PV-DG had improved for harmonic emission, islanding, flickering, penetration limits, interaction of multiple inverters, voltage imbalances, inverter capacitance and coordination of standard safety in LV DN.

The properties of wind turbine generators may increase the PQ related problems [14] and introduce PQ disturbances into the network such as:

- In fixed speed wind turbines, tower effect can introduce flicker [15].
- Induction generators connected directly to the grid may cause heavy transients in

weak distribution grids [15] and wind generators connected through electronic interface may introduce transients during switching.

- Strong wind gusts may cause simultaneous power output fluctuations by a series of wind turbines concentrated in a small area [15], and can cause frequency disturbances.
- Single-phase wind generators are expected to cause voltage unbalance to some extent.
- Reactive power shortages may occur at the wind power plant, which can cause voltage instability [86].
- Wind power may affect the power flow direction in the network & can cause transmission capacity problem [86].

Several studies indicated that storage can overcome problems associated with solar and wind energy. Storage battery size for grid connected PV system was determined by considering the lower and upper bounds of the storage [87]. An investigation showed that battery energy storage could mitigate over voltage and overload problem by voltage regulation and peak shaving. Therefore, it would allow more PVs to integrate without upgrading grid capacity [88].

An investigation on a SWER network in a rural area showed that battery storage boosted the network voltage while voltage fluctuated due to fluctuating PV generation [89]. This investigation was limited only to a single-phase line, and results may not be similar in a three-phase network. The authors [89] suggested the following while considering storage in transmission and distribution applications:

- Energy storage capacity available to the network will determine control of storage unit.
- Feeder R/X ratio determines the reactive power improvement by four-quadrant inverters.
- Storage integrated with PV reduces loading on the network.
- Positioning of storage should be in close proximity to load centre in order to reduce voltage drop in the feeder.

An investigation was done by integrating a high penetration of solar PV and wind energy in an isolated grid in Texas, USA. Results indicated that energy storage can provide a critical role in solar PV and wind energy integration, particularly at penetrations beyond 50% of load demand and when storage increases RE penetration [90]. This study suggested further investigation to understand the grid-level changes by integrating the grid with transmission networks containing existing non-renewable sources.

However, all the literature findings only suggest that storage would be a solution to overcome various issues. Little or no actual research was carried out to further investigate how storage in a real-life scenario can support grid stability and reliability. Furthermore, the risk of integrating large storage into the network was not investigated in a real-life scenario.

2.7 Conclusions

Power systems are the key to any development work. However, the stationary energy sector is the major contributor of GHG emission in Australia. RE is considered to be a major source of future energy. Solar PV and wind are the two most promising sources of RE; however; characteristics of these sources produce energy fluctuation, uncertainty in timely generation and lack of availability for 24 hours a day. Grid integration of PV and wind turbine introduces uncertainty and fluctuations into the power network; therefore, quick-response energy storage must be considered for the stability of the power network. Among various storage systems, quick response battery is suitable to operate with solar and wind energy. There are only a few large storage systems installed to operate solely for load shifting. Only a few storage systems are integrated with intermittent solar and wind energy, and few thermal storage systems are working with concentrated solar power.

There is lack of standard for integrating large-scale RE and storage into the grid. However, the AS-4777 standard describes the necessary parameter limits in integrating DG into the Australian power grid. Moreover, DNSP in Queensland has specific PQ parameters. Various study and utility experiences indicated that solar and wind sources can create problems like voltage regulations, harmonics, islanding, and lowering the power factor in the network. Advantages and applications of storage indicated that storage could overcome various PQ problems. However, there is little research investigating the impacts of storage in a real network. Only a few studies investigated storage with PV or wind energy, but these were limited, with small capacity and small network size. More specific research and experimental investigation is required considering a practical network scenario. Therefore, this thesis will investigate storage response in voltage regulations and harmonics distortion after integrating storage with solar PV and wind energy in a large power network in Rockhampton.

In order to conduct the investigation, initially the estimation of required storage was done using Rockhampton solar and wind data and described in chapter 3.

Chapter 3

Estimation and Significance of Storage

3.0 Introduction

Storage plays a significant role in balancing the intermittent nature of RE. It also allows unused RE to be captured and used when it is needed. Solar and wind are the two most fostered sources of RE. However, due to natural factors, these sources cannot provide steady energy for the whole day and introduce potential unbalance in energy generation and demand. Moreover, PV and wind are not able to meet the full load demand when the RE generators are about to start generating energy. Similarly, the load demand may fall to the lowest level when RE is in the highest mode of the generating stage, which exhibits loss of energy. Therefore, it can be said that RE is unable to generate energy by following the load demand, which is a major limitation in energy management. Storage can assume this critical role for proper energy management. Moreover, storage helps in reducing the intermittent fluctuating nature of RE and improves the PQ. As mentioned in chapter 2, the conventional energy sector is a major contributor of GHG emission. Storage helps in reducing the overall GHG emission by improving RE participation to support load demand. In order to support a substantial amount of timely load demand, RE applications should be designed accordingly.

Residential load, solar radiation and wind speed data of regional Australia were considered for the estimation of required storage [91, 92]. The load demand of the residential load in the Capricornia region of Rockhampton depends on the residents' work time pattern. Overall electricity demand is very high in the evening [7] and also in the morning for the residential load. However, PV cannot generate electricity during the morning or evening. Residents need to purchase costly electricity during peak demand in the evening. Similarly, wind energy is also unable to follow the residential load profile. Therefore, properly estimated storage needs to be integrated to overcome this situation.

Electricity generation varies with the fluctuations of solar radiation, wind speed and available duration of these sources. The load profile and the electricity generation profile do not synchronize most of the time, which keeps the dependency on conventional grid power for major load demand. In order to maximize the use of RE, properly sized storage needs to be integrated for a suitable system. There are several standards available that describe sizing and storage requirements for stand-alone systems. Few other standards considered solar PV, wind turbine, storage as distributed resources (DR) and provide guidelines to connect DR to the grid. Considering guidelines and limitations in various standards, this chapter followed the sizing guidelines for stand-alone systems to estimate the required storage for the grid-connected RE applications.

Therefore, the need for storage systems was explored in order to maximize the use of RE, and estimates the storage capacity required to meet the daily need that will gradually eliminate the dependency on conventional energy sources. The estimation steps presented here to design RE applications, considered daily residential load profile. For the estimation of required size of storage, solar PV and wind turbine were considered as RE resources. Properly sized RE resources combined with properly sized storage are essential for the best utilization of RE in a cost-effective way. This chapter also presents the economical and environmental benefits of storage.

Motivation to estimate required storage is discussed in section 3.1. Section 3.2 discusses estimation steps for required storage. Also explained in this section are the estimation of daily residential load and energy generated in Rockhampton from solar and wind. The significance of storage is explained in section 3.3, and concluding remarks are made in section 3.4.

3.1 Background

Australia is one of the best places for solar and wind energy. Figure 3.1 shows the solar radiation and wind speed of Rockhampton for the year 2009 [11], which is suitable to convert into useful energy. Solar PV and wind turbine are the most popular methods to convert energy from these sources.

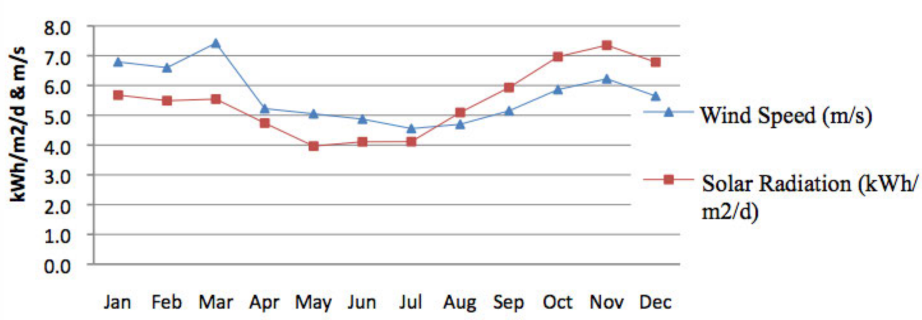

Figure 3:1 Solar radiation and wind speed of Rockhampton for 2009

Solar Power:

A solar PV array is modelled as a device that produces DC electricity in direct proportion to the global solar radiation. The power output from the PV array can be calculated by Equation 3.1[93, 94].

$$P_{PV} = Y_{PV} f_{PV} \left(\frac{\bar{G}_T}{\bar{G}_{T,STC}}\right)\left[1 + \alpha_P\left(T_C - T_{C,STC}\right)\right] \tag{3.1}$$

If there is no effect of temperature on the PV array, the temperature coefficient of the power is zero, thus the above equation can be simplified as Equation 3.2 [93, 94].

$$P_{PV} = Y_{PV} f_{PV} \left(\frac{\bar{G}_T}{\bar{G}_{T,STC}}\right) \tag{3.2}$$

where Y_{PV} - rated capacity of PV array, meaning power output under standard test conditions [kW]; f_{PV} - PV de-rating factor [%]; G_T - solar radiation incident on PV array in current time step [kW/m^2]; $G_{T,STC}$ - incident radiation under standard test conditions [1 kW/m^2]; α_P - temperature coefficient of power [%/^{o}C]; T_C - PV cell temperature in current time step [^{o}C]; $T_{C,STC}$ -PV cell temperature under standard test conditions [25^{o}C]. Performance of PV array depends on derating factors like temperature, dirt and mismatched modules.

Wind Power:

Kinetic energy of wind can be converted into electrical energy by using wind turbine, rotor, gear box and generator. The available power of wind is the flux of kinetic energy, which the air is interacting with rotor per unit time at a cross sectional area of the rotor and that can be expressed [95] as per Equation 3.3:

$$P = \frac{1}{2}\rho A V^3 \tag{3.3}$$

where, *P* is Power output from wind turbine in Watts, ρ is the air density (1.225kg/m^3 at 15^{o}C and 1-atmosphere or in sea level), *A* is rotor swept area in m^2 and *V* is the wind speed in m/s.

The swept area of a horizontal axis wind turbine of rotor diameter (D) in meter (or blade length = D/2) can be calculated by Equation 3.4.

$$A = \pi(\frac{D}{2})^2 \text{ sq.m} \tag{3.4}$$

As power in the wind is proportional to the cube of the wind speed, therefore increase in wind speed is very significant. One way to get more power is by increasing the tower height. Hourly wind speed at different height above ground level can be calculated by the vertical wind profile Equation 3.5 [96, 97]:

$$V_2 = V_1(\frac{H_2}{H_1})^{\propto} \tag{3.5}$$

where v_1 and v_2 are the wind speeds at heights H_1 and H_2 and α is the wind shear component or power law exponent or friction coefficient. A typical value of α is 0.14 for countryside or flat plane area. Equation 3.5 commonly used in United States and the same is expressed in Europe by Equation 3.6 [97]:

$$V_2 = V_1(\frac{\ln(H_2/z)}{\ln(H_1/z)}) \tag{3.6}$$

where, *z* is the roughness length in meters. A typical value of *z* for open area with a few windbreaks is 0.03m.

Temperature has effect on air density which changes the output of wind turbine. Average wind speed globally at 80m height is higher during day time than night time [41].

However, German physicist Albert Betz concluded in 1919 that no wind turbine could convert more than 16/27 or 59.3% of the kinetic energy of the wind into mechanical energy by turning a rotor. This is the maximum theoretical efficiency of rotor, and this is known as the Betz Limit or Betz's Law. This is also called the “power coefficient” and the maximum value is: C_P= 0.59. Therefore, Equation 3.3 can be written as Equation 3.7:

$$P = \frac{1}{2}C_p\rho AV^3 \tag{3.7}$$

Based on the above relation of energy conversion from solar radiation and wind speed, solar PV and wind turbine can be considered from small scale remote systems to large scale grid-connected applications. Grid connected PV or wind turbine with battery as storage can provide future-proof energy autonomy. A recent study on high penetration of PV on present grid, mentioned that energy storage is the ultimate solution for allowing intermittent sources to address utility base load needs [98].

In regional areas of Australia, roof top Solar PV is installed in many residential houses either in off-grid or grid connected configurations and most residential wind turbine are for specific applications in off-grid configuration. In grid connected solar PV systems where storage is not integrated, the energy output from this system does not satisfy to the desired level. Currently installed most of the residential PV systems are designed in such way that even with battery integrated system is not able to support the load in reliable way. Therefore size of storage needs to be properly estimated to support load demand.

The adoption of storage certainly incurs additional cost to the system but the benefits of adding storage has not been clearly assessed. Therefore this chapter aims to achieve two objectives. One is to estimate the required storage for the grid connected PV system, grid connected wind turbine system or combination of grid connected PV and wind turbine system to achieve the maximum daily use of RE. Second objective is to identify the significance of storage on the designed system in terms of environment and economic by comparing the same system with and without storage. The feasibility of the designed system is expressed as, if the Cost of Energy (COE) and Net Present Cost (NPC) are closer to the present system while providing environmental benefits by reducing GHG emission and improving the Renewable Fraction (RF) or improving RE participation.

The following sections estimates required storage for residential load in Rockhampton and also describe the significance of storage.

3.2 Estimation of Required Storage

Improper sized PV/Wind system is unable to meet the load requirements, sometimes electrical energy from RE wasted which neither can be used by the load nor can be stored in battery. The amount of wasted/lost energy can be avoided or reduced by proper choice of battery and PV/Wind generatior sizes. G.B. Shrestha et al. in [20] mentioned that PV panel size and the battery size have different impacts on the indices of performance and proper balance between the two is necessary. A proper match between the installed capacities with the load demand is essential to optimize such installation.

Brahmi Nabiha et al. in [99] presents sizing of mini autonomous hybrid grid, including PV, wind, generator and battery. The performance of any battery, expressed essentially by the voltage, load capacity and SOC or the Depth of Discharge (DOD). The usable energy in a battery can be expressed by Equation 3.8, where *C* is battery capacity and V_{bat} is the battery cell voltage.

$$\mathrm{E_{usable}} = \mathrm{C\ x\ V_{bat}\ x\ DOD_{max}} \tag{3.8}$$

IEEE Std-1013-2007 [76] provides the recommendations for sizing of lead-acid batteries for stand-alone PV systems. This recommended practice provides a systematic approach for determining the appropriate energy capacity of a lead-acid battery to satisfy the energy requirements of the load for residential, commercial and industrial stand-alone PV systems. IEEE Std-1561-2007 [100] provides guideline for optimising the performance and life of Lead-Acid batteries in remote hybrid power systems; which includes PV, wind, and batteries. It also explains the battery sizing considerations for the application. IEEE Std 1547-2003 [101] provides a guideline to connect Distributed Resources (DR), such as PV, wind and storage to the power grid at the distribution level. Grid-connected system sizing for storage-integrated PV system is also explained in [97].

Considering the above standards, sizing practices and guidelines, Figure 3.2 shows the steps for estimation of required storage for steady state residential load [91]. For the ease of this analysis, both PV and Wind turbine are considered to produce DC power. The DC power is converted to AC by an inverter, and the battery is considered as a storage device.

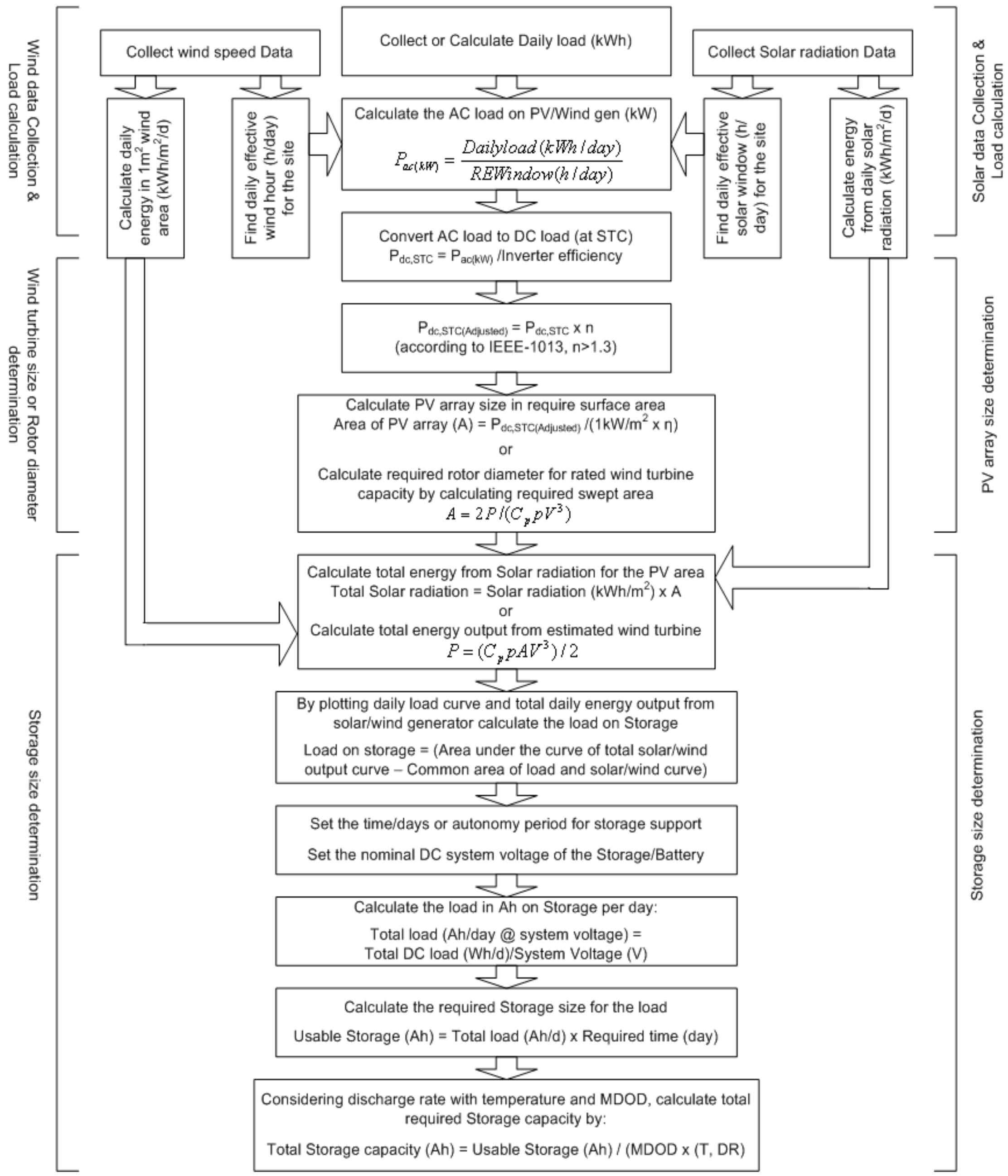

Figure 3:2 Storage size estimation steps [91]

The following steps are summarized for estimation and details are shown in Figure 3.2.

- Step 1: Determine the daily load (ex: a residential house).
- Step 2: Determine the required PV or wind turbine rating for the load.
- Step 3: Determine the daily energy output from the PV array or wind turbine.
- Step 4: Estimate PV array size or wind turbine rotor diameter.

- Step 5: Identify the daily load on storage by comparing the daily energy output from RE (PV or wind turbine) with the daily load.
- Step 6: Estimate the required battery/storage size in Ah for the load on storage.

The following sub-sections describe the estimation of required storage for grid connected PV, wind and hybrid systems considering the residential load of Rockhampton. Daily total load, daily energy output from solar PV and wind turbine were approximated in order to estimate the required storage.

3.2.1 Estimation of Daily Residential Load

The preferred method of determining load is a bottom-up approach in which daily load is anticipated and summed to yield an average daily load. This can be done by multiplying the power rating of all the appliances by the number of hours they are expected to operate during an average day to obtain Watt-hour (Wh) value as shown in Table 3.1. The load data collected from a three-bedroom house in Kawana, Rockhampton in Australia and total land area of the house is 700m^2 where 210m^2 is the building area with available roof space and suitable open space in front. For grid-connected household appliances, the daily average load can also be obtained from monthly utility bills.

Table 3:1 Daily load consumption of a house

Appliances	Rating	Daily time of use	Qty	Daily use (Wh/day)
Refrigerator	602kWh/year (300W)	Whole day	1	1650
Freezer	88W	Whole day	1	880
Electrical Stove	2100W	Morning & Evening (1-2hrs)	1	2100
Microwave Oven	1000W	Morning & Evening (30 min to 1 hr)	1	500
Rice cooker	400W	Evening (30 minutes)	1	200
Toaster	800W	Morning (10 - 30 minutes)	1	80
Ceiling Fan	65W	Summer night (4 -5 hrs) & Holidays	5	1300
Fluorescent light	16W	Night (6 - 8 hours)	20	320
Washing machine (vertical axis)	500W	Weekends (1hr/week)	1	71
Vacuum Cleaner	1400W	Weekends (1hr/week)	1	200
Air conditioner (Window)	1200W	Summer night & Holidays (1hr)	3	1200

TV 32" LCD (Active/Standby)	150/3.5W	Morning & night (4 hrs)	1	670
DVD player (Active/Standby)	17/5.9W	Night (2 hrs)	1	50
Cordless phone	4W	Whole day	1	96
Computer (Laptop)	20W	Night (4 - 5hrs)	1	80
Clothe iron	1400W	Night & Holidays (15 - 30 minutes)	1	350
Heater (Portable)	1200W	Winter night & Holidays (30 minutes)	1	600
Hot Water System	1800W	Whole day(3- 4 hrs)	1	5400
Total:				15,747

Data source: Product catalogue and [97]

The load profile of a residential house varies according to the residents work time pattern. The working nature of the residents of Kawana suburb is such that most of the residents start for work between 7:00AM and 8:00AM and return home between 5:00PM and 6:00PM from Monday to Friday. A 24-hour load profile of a particular day as shown in Figure 3.3. It was found that maximum load demand was in the evening from 6:00PM to 10:00PM and in the morning 8:00AM to 9:00AM.

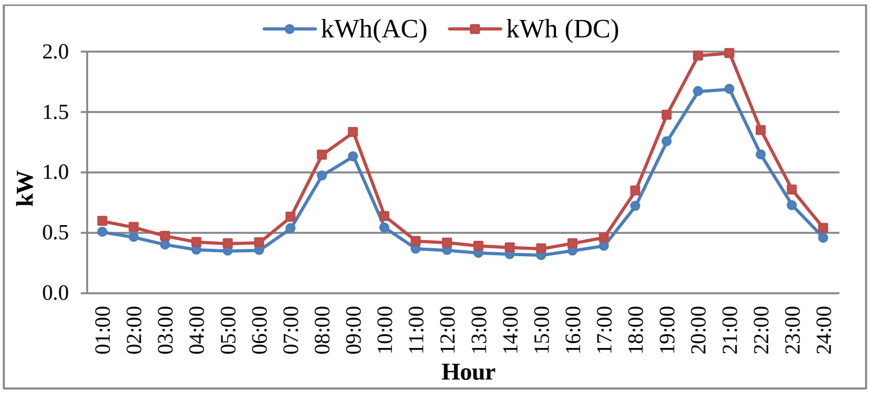

Figure 3:3 Daily Load profile of a Residential house

Hourly load is a time series data set, and the area under the curve is calculated using the trapezoidal method. Therefore, total daily load can be estimated by calculating the area under the load profile curve by trapezoidal method using Equation 3.9.

$$\text{Daily Load} = P_{Load} = \int_{t_1}^{t_{24}} \frac{1}{2}(p_{t_1} + p_{t_2})T_{12}dt \tag{3.9}$$

Where p_{t1} = Load (in kW) at time t =1, p_{t2} = Load (in kW) at time t = 2, T_{12} = time difference between t_1 and t_2 in hour.

Following Equation 3.9, total daily load is the area under the load curve shown in Figure 3.3, which is 15.7 kWh. The equivalent DC load is shown (considering the efficiency of the converter at 85%), which is 18.47 kWh. The average Australian household electricity use is about 16 kWh/day [102].

3.2.2 Estimation of Daily Available Solar Energy

Solar radiation varies with time and season. To estimate available useful solar energy, the worst month solar radiation was used to ensure that the designed system could operate year-round. In Australia, the yearly average sunlight hours vary from 5 to 10 hours/day, and the maximum area is over 8 hours/day [38]. From the collected data, it was found that in Rockhampton, solar radiation over 5.0kWh/m^2/d varies from 08:00AM to 16:00PM; i.e. the sun hour/solar window is 8 hrs/day.

The daily average solar radiation of Kawana suburb in the Capricornia region of Rockhampton city is shown in Figure 3.4. It was found that annual average solar radiation was 5.48 kWh/m^2/day. The lowest monthly average solar radiation was 4.0 kWh/m^2/day in May, and the highest solar radiation was from October to December in 2009. The PV system was designed to supply the entire load considering the worst month solar radiation, which will deliver sufficient energy during the rest of the year.

Figure 3.4 shows the hourly solar radiation of May 07, 2009. Daily total solar energy was estimated by calculating the area under the solar radiation curve using Equation 3.9. Therefore, total solar radiation in May 07, 2009 was 1.582975 kWh/m^2/d. This energy was generated by a PV area of 1m^2. Total solar radiation will increase with the increased surface area of the PV array.

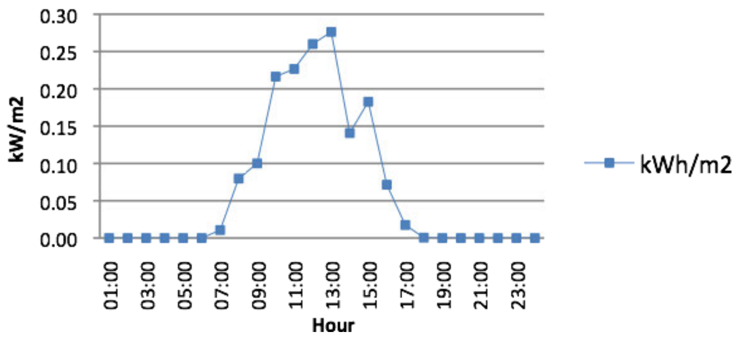

Figure 3:4 Daily Solar radiations on May 07, 2009 in Rockhampton

3.2.3 Estimation of Daily Available Wind Energy

Wind speed varies with different natural factors, time and season. To estimate the available useful wind energy, the worst month wind speed was considered to ensure that the designed system could operate year-round. From the collected data of Rockhampton, it was found that July had the worst wind speed as shown in Figure 3.1. It was found that in 2009, the wind speed of Rockhampton was 6m/s or more for a daily average duration of 10 hours. However, for the month of July and August it was only 5 hours as shown in Table 3.2. Therefore, wind speed data of July was considered for the estimation of daily energy output.

Table 3:2 Wind speed period or window (6m/s or more)

Month	Daily Time period	Time window (hrs)
Jan	06:00 - 20:00	14
Feb	03:00 - 17:00	14
Mar	00:00 - 15:00, 22:00 - 24:00	17
Apr	00:00 - 04:00, 20:00 - 24:00	8
May	16:00 - 24:00	8
Jun	12:00 - 19:00	7
Jul	10:00 - 15:00	5
Aug	07:00 - 12:00	5
Sep	01:00 - 10:00	9
Oct	00:00 - 06:00, 19:00 - 24:00	11
Nov	00:00 - 03:00, 15:00 - 24:00	12
Dec	13:00 - 24:00	11

Three hourly wind speed data, points at 10.4m above sea level were collected [38] for the year 2009, which were then interpolated to get hourly data. At turbine heights of 10m, 40m and 80m, the corresponding wind speeds were shown in Figure 3.5. For energy estimation during July 03, 2009, wind speed data was considered. Corresponding energy was calculated for $1m^2$ of rotor wind area at a rotor height of 40m using Equation 3.7 as shown in Figure 3.6. Total energy output via wind turbine on July 03, 2009 is the area under the curve of Figure 3.6 (11:00AM to 09:00PM) which is 0.232785kWh/m^2/d. Betz limit, gearbox, bearing and generator efficiency were considered and overall efficiency of the wind turbine system was taken to be 25%.

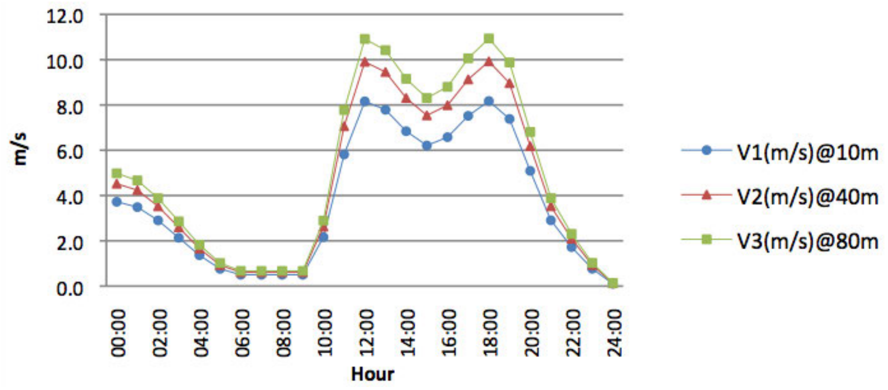

Figure 3:5 Wind speed at 10m, 40m and 80m height at Rockhampton

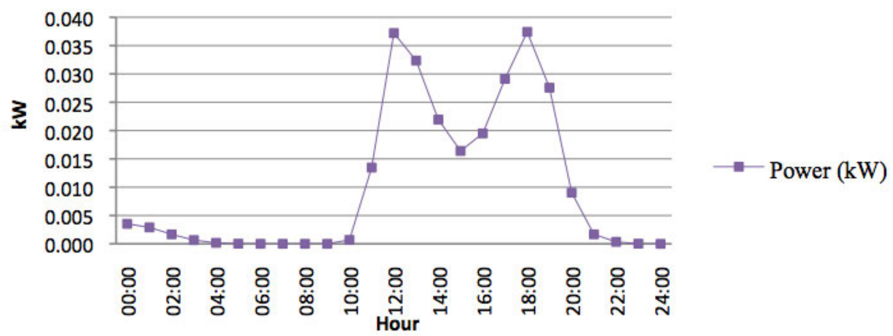

Figure 3:6 Energy converted per m^2 of wind at 40m height wind speed in Rockhampton

3.2.4 Estimation of Storage for Grid-connected Solar PV

The size of the PV array is determined by the daily average load divided by the available solar window, or sun-hours per day. Generally, grid connected PV systems are designed to provide from 10% to 60% of energy needs with the difference being supplied from power utility[103]. However, the PV contribution can be increased to 100% of average regular steady state load. Following the steps presented in Figure 3.2, the estimation starts by calculating required PV size.

Daily load of a three-bedroom house in Rockhampton as calculated in section 3.2.1 is 15.7 kWh/day. Daily extractable solar energy in Rockhampton as calculated in section 3.2.2 as 1.582975 kWh/m^2/day. Therefore, the PV array should support at least 15.7 kWh of load every day at the solar energy rate of 1.582975 kWh/m^2/day. The solar window is 8 hours or more in Rockhampton[38]; therefore, the required PV array rating/capacity for the AC load as:

$$P_{ac}(kW) = \frac{\text{Energy (kWh/day)}}{\text{Solar window (h/day)}} = \frac{15.7}{8} = 1.9625kW$$

The overall efficiency of PV system depends on inverter efficiency (of 95%) [104] and loss due to dirt and mismatch between PV modules. Equivalent DC load can be found by considering the efficiency of the PV system as:

η = inverter efficiency * dirty collector * mismatched modules = 85%

$$P_{dc,STC} = \frac{P_{ac}(kW)}{\eta} = \frac{1.9625}{0.85} = 2.31kW$$

To use battery as storage system, size of the PV array needs to be more than 1.3 times the load [76] in stand-alone configuration. But for the grid connected configuration 1.0 or 1.1 is good enough to avoid over design. For this designed residential load, it was considered 1.1. So the adjusted PV array size for the equivalent DC load becomes:

$$P_{dc,STC(Adjusted)} = 1.1xP_{dc,STC} = 1.1x2.31 = 2.541kW$$

Therefore, for this three bed room house 2.541kW capacity of PV array with proper sized storage required to support its load for 24 hours a day.

For known PV efficiency and for 1kW/m^2 rated PV module, required surface area of the PV array can be calculated. The efficiency of crystal silicon PV module is 12.5% [97], however LG Polycrystalline module efficiency is 13.7% [105], so the surface area becomes:

$$P_{dc,STC} = (1kW/m^2)\text{insolation} * A * \eta$$

$$A = \frac{P_{dc,STC}}{(1kW/m^2)\eta} = \frac{2.541}{1x0.125} = 20.328m^2$$

Therefore 20.328m^2 PV array with efficiency of 12.5% will support the load with sufficient storage size. This PV area is much smaller than the area of the designed house roof area.

The total energy output from 20.328m^2 PV array is used to estimate the required storage for the load. Batteries last longer if they are shallow cycled. The capacity of the battery bank can be calculated by multiplying the daily load on battery by the autonomy day or the number of days it should provide power continuously. The ampere-hour (Ah) rating of the battery bank can be found after dividing the battery bank capacity by the battery bank voltage (ex. 24V or 48V). It is generally not recommended to design for more than 12 days of autonomy for off-grid system and for grid connected system one day autonomy is good.

Total solar energy generated by the 20.328m^2 PV array at the solar radiation rate of Rockhampton is plotted in Figure 3.7 and calculated using Equation 3.9 as 32.17872 kWh which is the area under the PV output curve. Therefore daily PV output is 2.05 times daily total load demand. Now superimpose the DC load curve on the PV output curve to find the load that needs to be supported by the storage as shown in Figure 3.7. The common area under the curve is 6.196kWh which is the area of the load that served by the PV array during day time while charging the batteries as well. The remaining load is (18.47 - 6.196) =12.274kWh/day that needs to be served by the storage. Therefore installed storage with PV should support 0.8 times the daily load demand. This is the daily minimum load on storage. However the design was based on to support total load, therefore the remaining energy from the PV array should be managed by the storage system which is (32.17872 - 6.196) =

25.98272kWh/day. This is the maximum load on storage, if total energy generated by PV array needs to be managed by the storage.

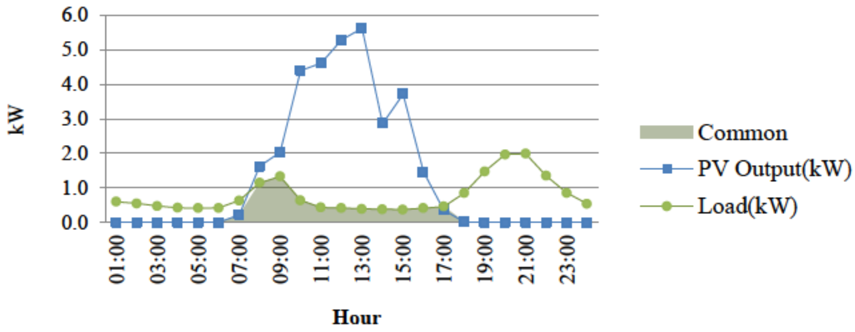

Figure 3:7 Total PV output, total load shows the load on storage

Inverters are specified by their DC input voltage as well as by their AC output voltage, continuous power handling capability and the amount of surge power they can supply for brief periods of time. Inverter's DC input voltage which is the same as the voltage of the Battery bank and the PV array is called the system voltage. The system voltage usually considered as 12V, 24V or 48V. The system voltage for this designed DC system was considered 24V and this system was designed for one day. Therefore, the required battery capacity can be calculated.

$$\text{Daily minimum load on storage in Ah @ system voltage} = \frac{\text{Load (Wh/day)}}{\text{System Voltage}} = \frac{12.274\text{x}10^3}{24} = 511.416\text{Ah/d}$$

$$\text{Daily maximum load on storage in Ah @ system voltage} = \frac{\text{Load (Wh/day)}}{\text{System Voltage}} = \frac{25.98272\text{x}10^3}{24} = 1082.613\text{Ah/d}$$

Energy storage in a battery typically expressed by Ah, at system voltage and at some specified discharge rate. Table 3.3 shows characteristics of several types of batteries.

Table 3:3 Comparison of Battery Characteristics[97]

Battery type	MDOD	Energy Density (Wh/kg)	Cycle Life (Cycles)	Calendar Life (Year)	Efficiencies	
					Ah%	Wh%
Lead-acid, SLI	20%	50	500	1-2	90	75
Lead-acid, golf cart	80%	45	1000	3-5	90	75
Lead-acid, deep-cycle	80%	35	2000	7-10	90	75
Nickel-cadmium	100%	20	1000-2000	10-15	70	60
Nickel-metal hydride	100%	50	1000-2000	8-10	70	65

The Ah capacity of a battery is not only rate-dependent but also depends on temperature. The capacity under varying temperature and discharge rates to a reference condition of C/20 battery (i.e. can discharge for 20 hours) at 25^{o}C is explained in [97]. Lead-acid battery capacity decreases dramatically in colder temperature conditions. However heat is also not good for batteries. In Rockhampton average temperature is above 20^{o}C. The maximum depth of discharge (MDOD) for Lead-acid batteries is 80%, therefore for one day discharge the batteries need to store:

$$\text{Battery storage (minimum)} = \frac{\text{Load (Ah/day) x No of days}}{\text{MDOD}} = \frac{511.416\text{x}1}{0.80} = 639.27\text{Ah}$$

$$\text{Battery storage (maximum)} = \frac{\text{Load (Ah/day) x No of days}}{\text{MDOD}} = \frac{1082.613\text{x}1}{0.80} = 1353.26\text{Ah}$$

The rated capacity of battery is specified at standard temperature. At 25^{o}C, the discharge rate of C/20 battery becomes 96% [97], therefore, finally the required battery capacity becomes:

$$\text{Required minimum Battery storage}(25^{\circ}\text{C,20hour-rate}) = \frac{\text{Battery storage}}{\text{Rated capacity}} = \frac{639.27}{0.96} = 665.90Ah$$

$$\text{Required maximum Battery storage}(25^{\circ}\text{C,20hour-rate}) = \frac{\text{Battery storage}}{\text{Rated capacity}} = \frac{1353.26}{0.96} = 1409.64Ah$$

Thus for 15.7 kWh/d load minimum 665.90 Ah to maximum 1409.64 Ah of storage battery required at system voltage 24 V with 2.541 kW solar PV.

3.2.5 Estimation of Storage for Grid-connected Wind Energy

Following the similar steps of section 3.2.4 (detailed as shown in Figure 3.2), required wind turbine capacity was calculated and then required storage was estimated for the same load of 15.7 kWh/day.

Energy generated by wind turbine at 40m height of 1m^2 rotor wind area was calculated in section 3.2.3, which is 0.232785kWh/m^2/d. The output of the wind turbine needs to be improved such that at least 15.7 kWh of load should be supported each day. It was found that in July, wind speed was 6m/s or above only for 5hrs/day at 10m height, however at 40m hub height wind speed was 6m/s or above for 10hrs/day, therefore the hub height was considered 40m. The required wind turbine capacity for the load can be calculated as:

$$P_{ac}(\mathrm{kW}) = \frac{\mathrm{Load\ (kWh/day)}}{\mathrm{Windwindow\ (h/day)}} = \frac{15.7}{10} = 1.57\mathrm{kW}$$

The storage which is a DC component; it requires inverter to support the load. DC capacity of the wind turbine can be calculated considering inverter efficiency of 90%.

$$P_{dc,STC} = \frac{P_{ac}(\mathrm{kW})}{\eta} = \frac{1.57}{0.90} = 1.744\mathrm{kW}$$

Likewise PV assumption, wind turbine capacity is considered 1.1 times the required load in grid connected configuration, to charge batteries while supporting load. So the adjusted wind turbine capacity for the equivalent DC load becomes:

$$P_{dc,STC(Adjusted)} = 1.1\mathrm{x}P_{dc,STC} = 1.1\mathrm{x}1.744 = 1.92\mathrm{kW}$$

Energy generated by wind turbine on July 03, 2009 was 0.232785kWh/m^2/d. To support total load, rotor swept area needs to be adjusted. Equation 3.7 shows that power output is not linear for increase in rotor diameter. It was found that at 40m rotor height, wind speed varied b/w 6.17m/s to 9.92m/s, therefore average wind speed of 8m/s was considered to calculate the rotor diameter for the rated wind turbine capacity of 1.92 kW. The rotor diameter was calculated (using Equation 3.3 and 3.4) as 5.58m and calculated total energy is 26.355 kWh which is the area under the curve (using Equation 3.9) as shown in Figure 3.8 for the same day. Therefore daily wind turbine output is 1.7 times the daily load demand.

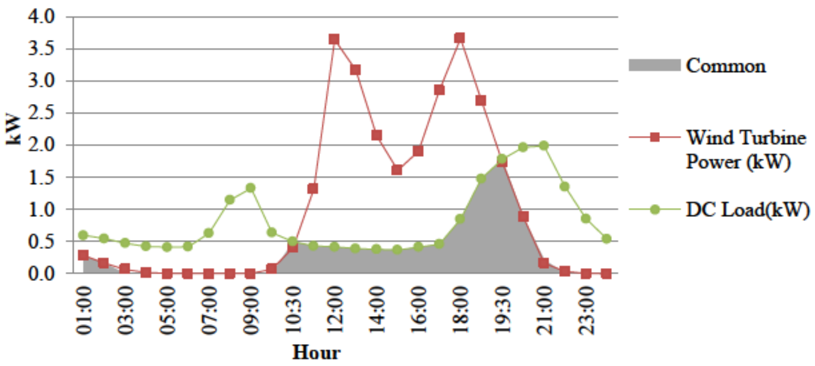

Figure 3:8 Total wind turbine output, total load shows the energy that needs to be stored

Daily load curve was plotted on the daily energy output curve to get the common area or the load that directly supported by the wind turbine which is 7.736 kWh. The remaining (18.47 - 7.736) = 10.734kWh of load needs to be supported by the storage each day. Therefore installed storage with wind turbine should support 0.7 times the the daily load demand. This is the minimum load on storage. However the design was considering to manage 100% load, therefore remaining (26.355 - 7.736) = 18.619kWh of energy must be managed by the storage. This is the maximum load on storage.

Considering the DC system voltage as 24V, load on battery in Ah can be calculated for one day as:

$$\text{Daily minimum load on storage in Ah @ system voltage} = \frac{\text{Load (Wh/day)}}{\text{System Voltage}} = \frac{10.734\text{x}10^3}{24} = 447.25\text{Ah/d}$$

$$\text{Daily maximum load on storage in Ah @ system voltage} = \frac{\text{Load (Wh/day)}}{\text{System Voltage}} = \frac{18.619\text{x}10^3}{24} = 775.79\text{Ah/d}$$

Energy storage in a battery typically represented by Ah, at system voltage and at some specified discharge rate. Considering MDOD for Lead-Acid batteries is 80%, therefore for one day discharge the battery needs to store the energy as:

$$\text{Battery storage (minimum)} = \frac{\text{Load (Ah/day) x No of days}}{\text{MDOD}} = \frac{447.25\text{x}1}{0.80} = 559.0625\text{Ah}$$

$$\text{Battery storage (maximum)} = \frac{\text{Load (Ah/day) x No of days}}{\text{MDOD}} = \frac{775.79\text{x}1}{0.80} = 969.7375\text{Ah}$$

The rated capacity of battery is specified at standard temperature. At 25°C, the discharge rate of C/20 batteries (i.e. discharge for 20 hours), becomes 96% [97], therefore finally required battery capacity becomes:

$$\text{Required minimum Battery storage}(25^{\circ}\text{C},20\text{hour-rate}) = \frac{\text{Battery storage}}{\text{Rated capacity}} = \frac{559.0625}{0.96} = 582.356Ah$$

$$\text{Required maximum Battery storage}(25^{\circ}\text{C},20\text{hour-rate}) = \frac{\text{Battery storage}}{\text{Rated capacity}} = \frac{969.7375}{0.96} = 1010.143Ah$$

Thus for 15.7 kWh/d load minimum 582.356 Ah to maximum 1010.143 Ah of storage battery required at system voltage 24 V with 1.92 kW wind turbine.

3.2.6 Estimation of Storage for Grid-connected Hybrid System

Many studies indicated that hybrid system is always better than any single RE system. However the practical implementation depends on the availability of adequate solar radiation, wind speed and their seasonal variation. Other critical point is adequate space for hybrid system installation and moreover the overall cost of the installation. The study location of this analysis is suitable for both solar and wind energy. It was found that for little variation of wind speed, convertible energy variation is much higher therefore wind energy fluctuation is higher than solar energy. Considering all the scenarios and for the ease of analysis it was considered that 50% of load demand to be supported by solar and 50% by wind energy.

Following the steps in Figure 3.2 and considering the examples shown in sections (3.2.4 and 3.2.5), the required storage is estimated below.

For Solar PV: 50% AC Load is (15.7/2) = 7.85kWh/d

$$P_{ac}(\text{kW}) = \frac{\text{Energy (kWh/day)}}{\text{Solar window (h/day)}} = \frac{7.85}{8} = 0.98125\text{kW}$$

Equivalent DC load can be found by considering the efficiency of the PV inverter as 85%:

$$P_{dc,STC} = \frac{P_{ac}(\text{kW})}{\eta} = \frac{0.98125}{0.85} = 1.1544\text{kW}$$

For this designed residential load, PV capacity considered 1.1 times the load. So the adjusted PV array size for the equivalent DC load becomes:

$$P_{dc,STC(Adjusted)} = 1.1xP_{dc,STC} = 1.1x1.1544 = 1.27kW$$

Therefore it requires 1.27kW capacity of PV array with proper sized storage to support 50% load for 24 hours a day.

Considering the crystal silicon PV module whose efficiency is 12.5% [97], therefore the surface area of PV module becomes:

$$P_{dc,STC} = (1kW/m^2)\text{insolation} * A * \eta$$

$$A = \frac{P_{dc,STC}}{(1kW/m^2)\eta} = \frac{1.27}{1x0.125} = 10.16m^2$$

Therefore $10.16m^2$ of PV area required for this hybrid system. The output energy from this PV module is plotted in Figure 3.9. For the remaining 50% load the required wind turbine is estimated as:

For Wind turbine: 50% AC Load is $(15.7/2) = 7.85$ kWh/d

$$P_{ac}(kW) = \frac{\text{Load (kWh/day)}}{\text{Windwindow (h/day)}} = \frac{7.85}{10} = 0.785 \text{ kW}$$

The inverter considered with this wind turbine of efficiency 90%, therefore the DC capacity becomes:

$$P_{dc,STC} = \frac{P_{ac}(kW)}{\eta} = \frac{0.785}{0.90} = 0.872 \text{ kW}$$

For this designed residential load, wind turbine capacity considered 1.1 times the load. So the adjusted wind turbine size for the equivalent DC load becomes:

$$P_{dc,STC(Adjusted)} = 1.1xP_{dc,STC} = 1.1x0.872 = 0.9592kW$$

Average wind speed of 8m/s was considered to calculate the rotor diameter for the required capacity of wind turbine. For the 0.9592kW capacity wind turbine, the rotor diameter becomes 3.95m and daily energy generated by this wind turbine is plotted in Figure 3.9.

Total energy generated from this hybrid system is 28.12kWh and compared with the DC load it was calculated that the Hybrid system support directly 8.45kWh of load as shown (the common area) in Figure 3.9. Therefore the minimum (18.47 - 8.45) = 10.02kWh of load needs to be supported by the storage system. However the hybrid system was designed to support total load therefore remaining generated energy of (28.12 - 8.45) = 19.67 kWh from hybrid system must be managed by the storage. This is the maximum load on storage.

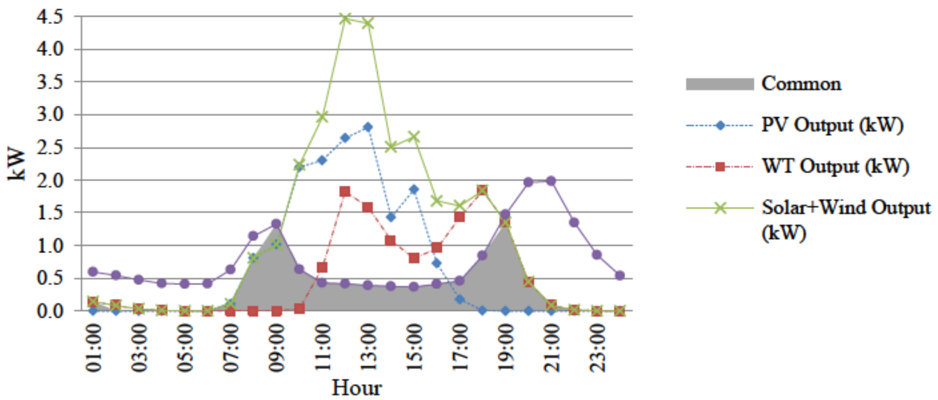

Figure 3:9 Output of hybrid system and total load shows the energy that needs to be stored

Considering the DC system voltage as 24V, load on battery in Ah can be calculated for one day as:

$$\text{Daily minimum load on storage in Ah @ system voltage} = \frac{\text{Load (Wh/day)}}{\text{System Voltage}} = \frac{10.02\text{x}10^3}{24} = 417.50\text{Ah/d}$$

$$\text{Daily maximum load on storage in Ah @ system voltage} = \frac{\text{Load (Wh/day)}}{\text{System Voltage}} = \frac{19.67\text{x}10^3}{24} = 819.58\text{Ah/d}$$

Considered MDOD of Lead-Acid batteries is 80%, therefore for one day discharge the battery needs to store the energy as:

$$\text{Battery storage (minimum)} = \frac{\text{Load (Ah/day) x No of days}}{\text{MDOD}} = \frac{417.50\text{x}1}{0.80} = 521.875\text{Ah}$$

$$\text{Battery storage (maximum)} = \frac{\text{Load (Ah/day) x No of days}}{\text{MDOD}} = \frac{819.875\text{x}1}{0.80} = 1024.843\text{Ah}$$

Temperature effects are considered in the storage requirements for the hybrid systems. At 25^{o}C for C/20 batteries (i.e. 20 hours discharge) the discharge rate is 96%, therefore finally required battery capacity becomes:

$$\text{Required minimum Battery storage}(25^{\circ}\text{C,20hour-rate}) = \frac{\text{Battery storage}}{\text{Rated capacity}} = \frac{521.875}{0.96} = 543.62Ah$$

$$\text{Required maximum Battery storage}(25^{\circ}\text{C,20hour-rate}) = \frac{\text{Battery storage}}{\text{Rated capacity}} = \frac{1024.843}{0.96} = 1067.544Ah$$

Therefore in grid connected configuration to support 15.7 kWh/day load the required minimum and maximum storage with solar PV, Wind turbine and hybrid system are shown in Table 3.4. Minimum storage indicates the required storage that needs to support the daily load. However PV, wind turbine or a hybrid system generates more energy than the daily load requirement. Therefore, maximum storage is required to manage total generated energy either by supporting load or supplying to the grid at a suitable time.

Table 3:4 Required storage in different configurations

Designed system	**Required system capacity**	**Required Storage (at 24V DC system voltage)**	
		Minimum (Ah)	**Maximum (Ah)**
Solar PV system	2.541 kW PV with 20.328m^2 PV array	665.90Ah	1409.64Ah
Wind turbine system	1.92 kW wind turbine with 5.58m rotor diameter	582.356Ah	1010.143Ah
Hybrid system	1.27 kW PV with 10.16m^2 PV array and 0.9592 kW wind turbine with 3.95m rotor diameter	543.62Ah	1067.544Ah

Although the adoption of storage with the RE system adds additional cost to the system, there are some clear benefits of storage that will be explained in the next section.

3.3 Significance of Storage

The advantage of storage is explained below by investigating its influence in environmental and economical contexts in particular RE applications. A computer model was used to identify the significance of storage with solar, wind and hybrid power systems.

3.3.1 Model Development

A model was developed as shown in Figure 3.10. HOMER is the optimisation tool for designing and analysing hybrid power systems and is currently used by users all over the world [106]. Solar PV, wind turbine, storage, inverter, grid and diesel generator were used in different sizes and combinations to determine the optimal configuration to support the load.

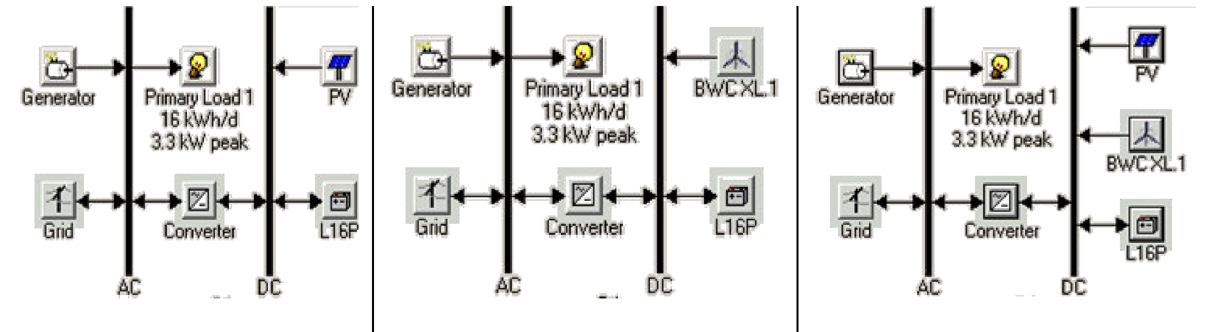

Solar PV configuration	Wind Turbine configuration	Hybrid configuration

Figure 3:10 Simulation model in different configurations

The designed model identified the optimized configuration of storage, PV, wind turbine with a grid or diesel generator for a residential load. It also investigated environmental and economical benefits due to the storage systems. The model was evaluated considering the project lifetime of 25 years. The performance matrices considered are net present cost (NPC) and cost of energy (COE) as economical factors; and renewable fraction (RF) and greenhouse gas (GHG) emission as environmental factors. The model was compared in off-grid and grid connected configurations. The performance matrices are briefly explained below:

Net Present Cost (NPC): The total net present cost of a system is the present value of all the costs that it incurs over its lifetime, minus the present value of all the revenue that it earns over its lifetime. NPC is the main economic output and ranked all optimised systems accordingly. NPC can be represented [106, 107] in Equation 3.10:

$$\mathrm{NPC}(\$) = \frac{\mathrm{TAC}}{\mathrm{CRF}} \tag{3.10}$$

where *TAC* is the total annualized cost (which is the sum of the annualized costs of each system component). The capital recovery factor (*CRF*) is given by Equation 3.11:

$$\mathrm{CRF} = \frac{\mathrm{i}(1+\mathrm{i})^{\mathrm{N}}}{(1+\mathrm{i})^{\mathrm{N}}-1} \tag{3.11}$$

where *N* denotes number of years and *i* means annual real interest rate (%). Model considered annual interest rate rather than the nominal interest rate. The overall annual interest rate considered as 6%.

Cost of Energy (COE): It is the average cost per kWh of useful electrical energy produced by the system. COE can be calculated by dividing the annualized cost of electricity production by the total useful electric energy production and represented [106] in Equation 3.12:

$$\mathrm{COE} = \frac{\mathrm{C_{ann,tot}} - \mathrm{C_{boiler}E_{thermal}}}{\mathrm{E_{prim,AC}} + \mathrm{E_{prim,DC}} + \mathrm{E_{def}} + \mathrm{E_{grid,sales}}} \tag{3.12}$$

where $C_{ann,tot}$ is total annualized cost of the system ($/yr), C_{boiler} is boiler marginal cost ($/kWh), $E_{thermal}$ is total thermal load served (kWh/yr), $E_{prim,AC}$ is AC primary load served (kWh/yr), $E_{prim,DC}$ is DC primary load served (kWh/yr), E_{def} is deferrable load served (kWh/yr) and $E_{grid,sales}$ is total grid sales (kWh/yr).

Emission: Emission is widely accepted and understood environmental index. Greenhouse gases (CO_2, CH_4, N_2O, HFCs, PFCs, SF_6) are the main concern for global warming. In addition SO_2 is another pollutant gas released by coal fired energy system. Emission is measured as yearly emission of the emitted gases in kg/year and emissions per capita in kg/kWh. Model used it as input when calculating the other O&M cost. It was represented in [106] as shown in Equation 3.13:

$$\mathrm{C_{om,other}} = \mathrm{C_{om,fixed}} + \mathrm{C_{cs}} + \mathrm{C_{emission}} \tag{3.13}$$

where $C_{om,fixed}$ is system fixed O&M cost ($/yr), C_{cs} is the penalty for capacity shortage ($/yr) and $C_{emission}$ is the penalty for emission ($/yr).

Renewable Fraction (RF): It is the total annual renewable power production divided by the total energy production. RF can be calculated [108] using Equation 3.14:

$$\mathrm{RF} = \frac{\mathrm{E_{RE}}}{\mathrm{E_{TOT}}} \tag{3.14}$$

where E_{RE} and E_{TOT} are the total energy generated by RE and total energy generated by the system respectively. The overall RF (f_{ren}) can also be expressed[106] by Equation 3.15:

$$\mathrm{f_{ren}} = \frac{\mathrm{E_{ren}+H_{ren}}}{\mathrm{E_{tot}+H_{tot}}} \tag{3.15}$$

where E_{ren} is renewable electric production, H_{ren} is renewable thermal production, E_{tot} is total electrical production and H_{tot} is total thermal production.

3.3.2 Model Data

Load data:

For the simulation of the model, residential load data was considered as explained in section 3.2.1 and the daily average electricity consumption per house is 15.7kWh/day, therefore yearly residential load (AC) becomes 5730kWh/yr. Software model simulates the operation of a system by making energy balance calculation for each of the 8,760 hours of a year. Daily load profile with seasonal variation is shown in Figure 3.11. Daily electricity consumption pattern shows that during morning and evening demand is high.

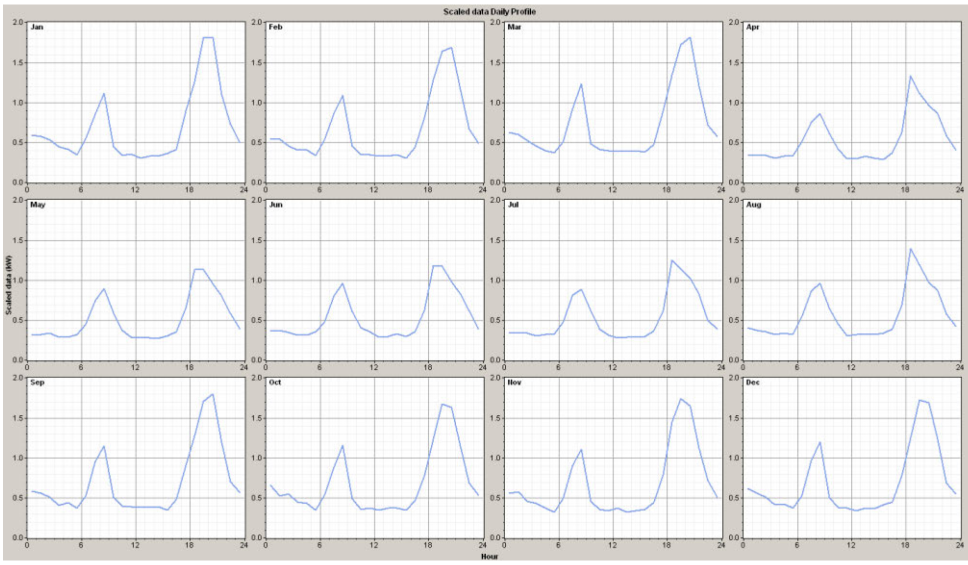

Figure 3:11 Daily Electric load demand in each month

Solar and wind data:

Hourly solar radiation data and three hourly wind speed data was collected from Bureau of Meteorology [38] for the year 2009 and 2010 of station number 039083 for the location of Rockhampton Aero Weather Station (-23.3753^{o}N, 150.4775^{o}E) at 10.4m above the mean sea level. Collected solar radiation data was imported into the model to calculate the daily average value and clearance index. Solar radiation is very high from September to December and clearance index is 0.547 and average daily radiation is 5.467 kWh/m^2/day. May, June and July has the lowest average solar radiation. Moreover collected wind speed data was imported into the model considering weibull factor k= 0.14, auto correlation factor = 0.901, diurnal pattern strength = 0.0271 and hour of peak wind speed = 23. Daily average wind speed is 5.669 m/s. Wind speed was good from October to March and wind speed from June to August is lowest. Daily average solar radiation and wind speed in Capricornia region of Rockhampton city is as shown in Figure 3.12 and 3.13.

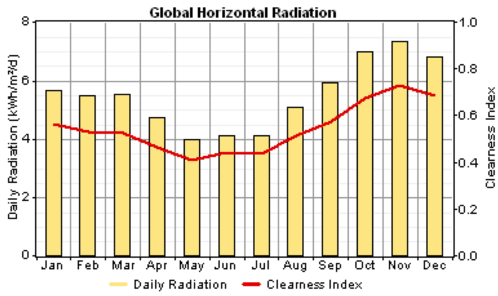

Figure 3:12 Daily average solar radiation

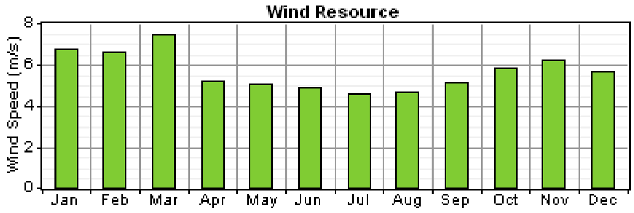

Figure 3:13 Daily average wind speed

Storage:

Battery is one of the fast response storage systems. For this analysis Trojan L16P Battery (6V, 360Ah) at system voltage of 24V DC is used in the model. The efficiency of this battery is 85%, minimum State of Charge (SoC) is 30% [106].

Battery dispatch: Two battery dispatch strategy explained in [109], named ‘load following’ and ‘cycle charging’. In load following strategy, a generator produces only enough power to serve the load, battery charging and supporting deferrable load depends on renewable power sources. In cycle charging strategy, whenever a generator operates it runs at its maximum rated capacity, charging the battery bank with any excess electricity until the battery reaches the specified state of charge. Load following strategy was considered for this analysis for the better utilization of RE.

3.3.3 System Components Cost

Table 3.5 lists the required system components with related costs in Australian currency. PV array, wind turbine, battery charger, inverter, deep cycle battery, diesel generator and grid electricity costs are included for the analysis. PV array including inverter price is available, and found that 1.52kW PV array with inverter costs $3599 [110], also it is found that 1.56kW PV with inverter costs is $4991[111]. However model considered battery charger is included with PV array therefore the PV array cost is listed accordingly in Table 3.5 and inverter costs considered separately.

Table 3:5 Technical Data and Study assumptions

Description	Value/Information
PV array	
Capital cost	$3100.00/kW
Replacement cost	$3000.00/kW
Life Time	25 years
Operation & maintenance cost	$50.00/year
Wind Turbine (BWC XL.1 1 kW DC)	
Capacity	1kW DC
Hub Height	40m
Capital cost	$4000.00
Replacement cost	$3000.00
Life time	25 years
Operation & maintenance cost	$120/yr
Grid electricity	
Electricity price (Off peak time)	$0.30/kWh
Electricity price (Peak time)	$.38/kWh
Electricity price (Super Peak time)	$0.65/kWh
Emission factor	
CO_2	632.0 g/kWh
CO	0.7 g/kWh
Unburned hydrocarbons	0.08 g/kWh
Particulate matter	0.052 g/kWh
SO_2	2.74 g/kWh
NOx	1.34 g/kWh
Inverter	
Capital cost	$400.00/kW
Replacement cost	$325.00/kW
Life time	15 years
Operation & maintenance cost	$25.00/year
Storage (Battery)	
Capital cost	$170.00/6V 360Ah
Replacement cost	$130.00/6V 360Ah
System Voltage	24 volts
Generator	
Capital cost	$2200.00/kW
Replacement cost	$2000.00/kW
Operation & maintenance cost	$0.05/hr
Life time	15000hrs
Fuel cost	$1.53/ltr

SMA Sunny Boy Grid Tie Inverter (7000Watt SB7000US) price is $2823 [112], however Sunny Boy 1700W inverter price is $699 [113]. 1kW BWC XL.1 wind turbine with 24V DC charge controller price is $3560 [114] and 10kW Bergey BWC Excel with battery charging or a grid-tied option the wind turbine cost is $29,250 [115]. Grid electricity cost in Rockhampton was found from the local utility operator's (Ergon Energy) electricity bill [116] and for Tariff-11, it is $0.285/kWh (including GST & service). However carbon tax at the rate of $23/ton of GHG emission increases the electricity bill as well as the cost of conventional energy sources. Thus off-peak electricity cost is considered as $0.30/kWh for this analysis. The price of a Trojan T-105 6V, 225AH (20HR) flooded Lead-Acid battery is $124.79 [117]. The fuel cost for generator is considered at the current price available in Rockhampton, Australia. Table 3.5 shows the unit cost of each component considered in this analysis.

The significance of storage was analysed from the optimised model result to evaluate the environmental and economical advantages of storage in off-grid and grid-connected configurations in fourteen different cases as shown below. All of these cases were analysed using a load of 5730kWh/yr.

Category-1: Off-grid Configuration

Case-1: Diesel Generator only
Case-2: PV with Diesel Generator
Case-3: PV with Storage and Diesel Generator
Case-4: Wind turbine with Diesel Generator
Case-5: Wind turbine with Storage and Diesel Generator
Case-6: Hybrid (PV & Wind turbine) with Diesel Generator
Case-7: Hybrid (PV & Wind turbine) with Storage and Diesel Generator

Category-2: Grid-connected Configuration

Case-1: Grid only
Case-2: PV with Grid and Diesel generator
Case-3: PV with Storage, Grid and Diesel generator
Case-4: Wind turbine with Grid and Diesel generator
Case-5: Wind turbine with Storage, Grid and Diesel generator
Case-6: Hybrid (PV & Wind turbine) with Grid and Diesel generator

Case-7: Hybrid (PV & Wind turbine) with Storage, Grid and Diesel generator

3.3.4 Model Results and Discussion

The optimisation result used various combinations of elements and ranked the optimised model according to NPC. These optimised models support the same load of 5730 kWh/yr and used PV, wind turbine, storage, grid supply, generator at different times in different combinations, which resulted in different levels of emission. In 14 different cases the highest ranked optimised model results are discussed below, and findings are compared for NPC, COE, emission and RF.

3.3.4.1 Category-1: (Off-grid configuration)

Case 1. Diesel generator only:

In this configuration, a 3 kW diesel generator was used to support a total load of 5730kWh/yr, which consumed enough fuel (3535L/yr) to emit a significant amount of GHG and pollutant gases to the air. The generator required frequent maintenance and fuel cost was also high; therefore, NPC was high and COE was $1.857/kWh. This configuration was the costliest and environmentally the most vulnerable.

Case 2. PV with diesel generator configuration:

In this off-grid configuration, the model used 6-kW PV with a 1-kW inverter and a 3-kW diesel generator as required resources. A total of 9,170 kWh/yr of electricity was generated from PV and the diesel generator. PV alone generates 4, 454 kWh/yr, therefore RF became 48.6% but most of the energy from the PV array was wasted. The diesel generator directly supplied 4, 716 kWh/yr to the load, which was 82.30% of load demand. 1014 kWh/yr or 17.69% of load was supported by the PV array through an inverter. Therefore, a significant amount of electricity from the PV array was wasted. Wasted electricity was 3,376 kWh/yr, or 75.79% of total electricity production from PV. To reduce this great amount of loss, this system should have some way to store the energy and subsequently reduce the use of diesel generator.

Case 3. PV with Storage and diesel generator configuration:

In this off-grid configuration model, a 9-kW PV, 24 Trojan L16P batteries (@ 6V, 360Ah) at 24V system voltage with a 2-kW inverter and a 3-kW diesel generator was used. The optimised configuration reduced the use of the diesel generator; 85.58% of the load was supported by PV with storage. Results showed that PV generated more electricity than the load demand, and the batteries stored the excess electricity to maintain the load demand.

The PV generated 6,681 kWh/yr of electricity, of which a good amount of energy was stored in the batteries and used at other times. The total AC load was supported directly by the PV array during the day, and by the batteries during morning and night. The inverter converted 5,217 kWh/yr of DC electricity to AC. The batteries stored 3,367 kWh/yr of energy and supplied 2,886 kWh/yr to support the load. The batteries stored 50.40% of PV-generated energy and supported 50.37% of load, while PV directly supported 35.22% of load. However, 984 kWh/yr of excess energy generated by the PV array (or 14.73%) was wasted which could have been sold to the grid.

Figure 3.14 and 3.15 show the inverter output when the optimised solar PV system supported the load without storage and with storage configuration respectively. It is clear from the figures that storage supports the load when the PV is unable to generate energy.

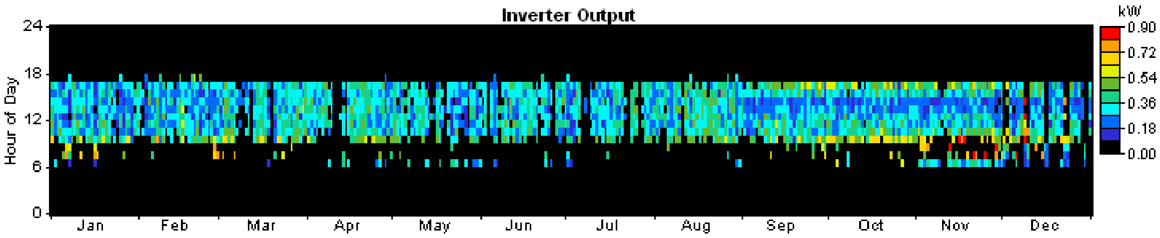

Figure 3:14 Off-grid configuration - Case-2: Inverter output without Storage

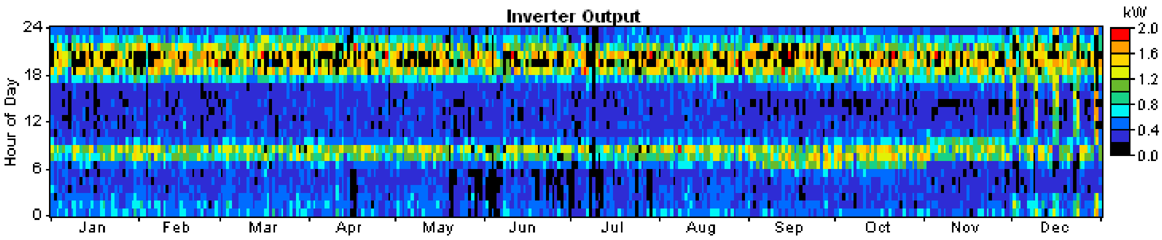

Figure 3:15 Off-grid configuration - Case-3: Inverter output with Storage

Case 4. Wind turbine with diesel generator configuration:

This off-grid configuration used a 6-kW BWC XL.1 wind generator with a 3-kW inverter and a 3-kW diesel generator as required resources to support 5,730 kWh/yr of load. Result showed that, the wind turbine generated much more electricity than the total load demand but could not meet the load demand for a 24-hour period.

A total of 26,137 kWh/yr of electricity was generated from the wind turbine and diesel generator configuration, where 23,268 kWh/yr was generated from the wind turbine (i.e. 89.02% of total production). However, most of it was wasted because the wind turbine supports only 2,861 kWh/yr of load, which is 49.93% of load demand. The diesel generator contributed 2,869 kWh/yr or 50.07% of load demand. However, compared to the total production, the diesel generator‘s contribution was only 10.98%. A total of 20,225 kWh/yr (or 77.38% of total electricity production) was wasted; compared to the total wind turbine output, 86.92% was wasted. By adding storage, this huge loss of energy could be minimized and that could reduce the use of the diesel generator.

Case 5. Wind turbine with storage and diesel generator configuration:

This off-grid configuration model used a 3-kW BWC XL.1 wind generator, 40 Trojan L16P batteries (@ 6V, 360Ah) at 24V system voltage and a 3-kW inverter. This optimised configuration shaded out the diesel generator; 100% of the load was supported by wind turbine and storage. Results showed that the wind turbine generated more electricity than the load demand, and the batteries stored the excess electricity to support load demand at another time.

The wind turbine generated 11,634 kWh/yr of electricity. The inverter converted 6095 kWh/yr of DC electricity to AC. The batteries stored 2,363 kWh/yr of energy and supplied 2,036 kWh/yr to the load. In other words, the batteries stored 20.31% of wind turbine generated energy and supported 35.53% of load. However, 5,212 kWh/yr of excess energy generated by the wind turbine (i.e 44.79% of total generated energy) was wasted that could be sold to the grid.

Figure 3.16 and 3.17 shows the inverter output when the optimised wind system supports the load without storage and with storage configuration respectively. It is clearly shown in the figures that storage supports the load when the wind turbine is unable to generate energy, even though the wind turbine generates more energy than load demand.

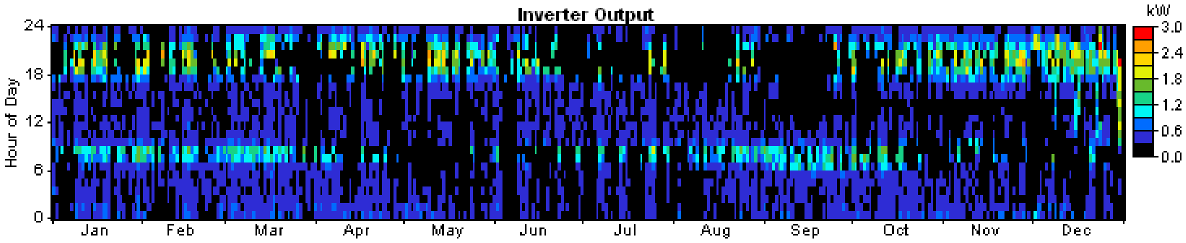

Figure 3:16 Off-grid configuration - Case-4: Inverter output without Storage

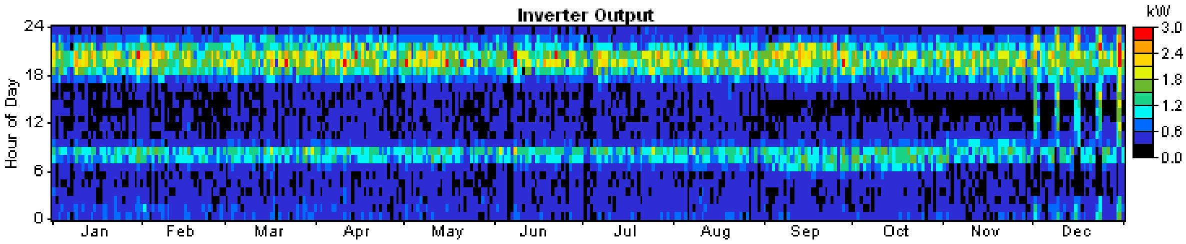

Figure 3:17 Off-grid configuration - Case-5: Inverter output with Storage

Case 6. Hybrid system with diesel generator configuration:

This off-grid hybrid configuration model used a 3-kW PV array, a 5-kW BWC XL.1 wind generator, a 3-kW inverter and a 3-kW diesel generator. Results showed that although PV and wind turbine generated much more electricity than the total load demand, the configuration could not meet the load demand for a 24-hour period.

Total electricity generated from PV, Wind turbine and diesel generator was 24,433 kWh/yr where 2,227 kWh/yr was from PV, 19,390 kWh/yr was from the wind turbine, and 2,816 kWh/yr was from the diesel generator. In terms of percentages, PV contributed 9.1%, the wind turbine contributed 79.35% and the diesel generator contributed 11.53% of total production. In other words, the overall RE contribution was 88.47% of total production. The diesel generator contributed 49.14% of load demand. The inverter converted 3,100 kWh/yr of DC electricity to 2,914 kWh/yr of AC electricity from RE generation, which was 50.85% of load demand. A significant amount of electricity (18,517 kWh/yr) from RE sources was wasted, which was 75.78% of total electricity production and 85.66% compared to the total RE production. Storage could be used to reduce this huge energy loss and to minimize the use of diesel generator.

Case 7. Hybrid system with storage and diesel generator configuration:

This off-grid hybrid configuration model used a 1-kW PV, a 3-kW BWC XL.1 wind generator, a 5-kW inverter and 32 Trojan L16P batteries at 24-V system voltage to support the same load. The hybrid system (PV and wind turbine) output with storage supported 100% load and shaded out the use of the diesel generator. Results showed that storage stored the electricity from the hybrid system and met the load demand 24 hours a day, but a significant amount of energy was wasted that could have been sold to the grid.

A total of 12,376 kWh/yr of electricity was generated from the hybrid system, where 742 kWh/yr (or 6%) was from PV and 11,634 kWh/yr (or 94%) was from the wind turbine. The batteries stored 2,073 kWh/yr and supported 1,788 kWh/yr or 31.20% of load demand. This configuration supplied 100% of the load demand from RE; however, 5,995 kWh/yr or 48.44% of RE-generated electricity was wasted which could have been sold to the grid.

Figures 3.18 and 3.19 show the inverter output in a hybrid RE configuration without and with storage system respectively. It is clear from the figures that even a hybrid system is not able to support load demand completely, while storage supports the load at critical times.

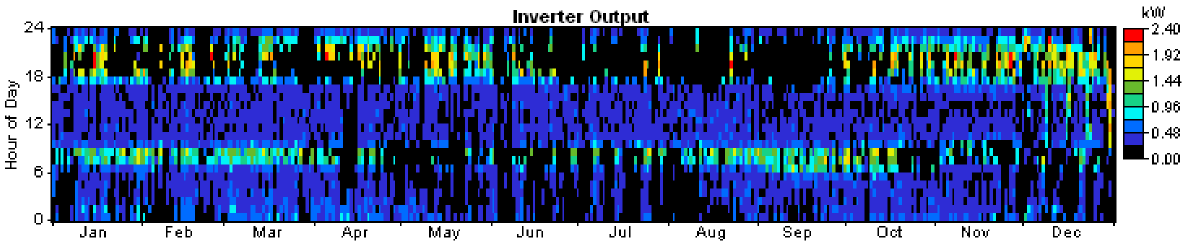

Figure 3:18 Off-grid configuration - Case-6: Inverter output without Storage

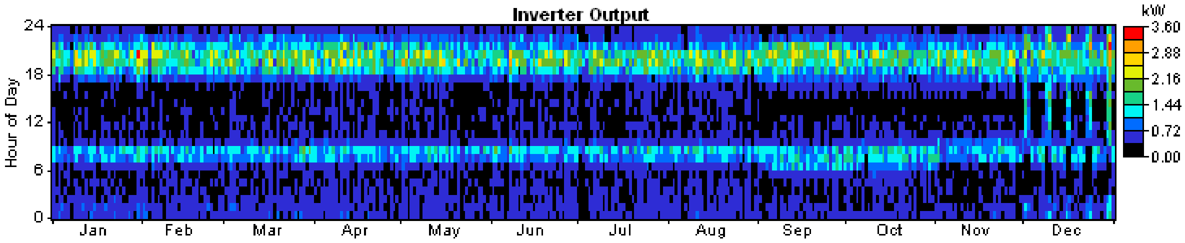

Figure 3:19 Off-grid configuration - Case-7: Inverter output with Storage

Summary of Category-1 or Off-grid configurations:

The results of stand-alone configurations can be summarized that storage improved load support. Storage also reduced GHG emission and the loss of RE-generated electricity, and demonstrated the scope to sell excess energy to the grid. Table 3.6 summarizes these findings from optimised models in different cases. Load support describes the percentage of load supported by RE and storage compared to total load demand. Energy loss describes the percentage of energy loss compared to total RE production.

Table 3:6 Category-1 or off-grid configuration results

	Diesel Generator	**Solar PV**	**Wind turbine**	**Inverter**	**Storage (at 24V DC system voltage)**	**RE use**	
						Load support	**RE energy loss**
Case-2 (PV +Gen)	3kW	6kW	-	1kW	-	17.69%	75.79%
Case-3: (PV+Storage+Gen)	3kW	9kW	-	2kW	24 nos. (2160Ah)	85.58%	14.73%
Case-4 (Wind turbine+Gen)	3kW	-	6kW	3kW	-	49.93%	86.92%
Case-5 (Wind turbine+Storage+Gen)	-	-	3kW	5kW	40 nos. (3600Ah)	100%	44.79%
Case-6 (Hybrid +Gen)	3kW	3kW	5kW	3kW	-	50.85%	85.66%
Case-7 (Hybrid+Storage+Gen)	-	1kW	3kW	5kW	32 nos. (2880Ah)	100%	48.44%

3.3.4.2 Category-2: (Grid-connected configuration)

Case 1. Grid only configuration:

This is the configuration of most residential electricity connections. The grid supplies a total load demand of 5,730 kWh/yr. The grid electricity tariff varies with time, season and application [116, 118]. This configuration model considered 3 different prices of grid electricity, depending on demand time. These are off-peak (0.30$/kWh), peak (0.38$/kWh) and super peak rate (0.65$/kWh). 6:00PM to 7:00PM is considered super peak; 8:00PM to 10:00PM and 8:00AM to 9:00AM are both considered peak times; and the rest are off-peak times. In this case, yearly average COE becomes $0.392/kWh. Because grid electricity comes mainly from conventional sources, a good amount of GHG and pollutant gas emit into the air.

Case 2. PV in a grid-connected configuration:

In this optimised model configuration, the diesel generator was shaded out; however, the PV array still contributed a small portion of load demand. To meet load demand, this model used a 1-kW PV, a 1-kW inverter and a grid supply. A total of 6,429 kWh/yr of electricity was produced, where the grid supplied 5,687 kWh/yr (or 88.46% of total production) and supported 99.25% of the total load demand. The PV array produced 742 kWh/yr (or 11.54% of total production) and supported only 43 kWh/yr, or 0.75% of the load demand. A total of 12 kWh/yr of energy was sold back to the grid. 683 kWh/yr of PV-generated electricity was wasted due to mismatch in timely demand, which could be stored and supplied to the load.

Case 3. PV with storage in a grid-connected configuration:

This configuration of model is very interesting compared to the earlier case; by adding sufficient storage, the system improved the PV contribution for the same load demand. To meet load demand, this model used a 4-kW PV array, 8 Trojan L16P batteries, a 2-kW inverter and a grid supply. A total of 6,107 kWh/yr of electricity was produced, where the grid supplied 3,137 kWh/yr (or 51.36% of total production) and supported 54.75% of the total load demand. The PV array produced 2,969 kWh/yr or 48.62% of total production. Grid sales and loss of energy were insignificant. The batteries stored 1,410 kWh/yr and supplied 1,210 kWh/yr to the load or 21.12% of total load. However the PV array directly supported 1,383 kWh/yr of load, which was 24.14% of total load demand.

Figures 3.20 and 3.21 show the inverter output, with the solar PV in a grid-connected case supported load without and with storage respectively. It is clearly indicated from the figures that storage improves load support by providing load demand during the evening and morning.

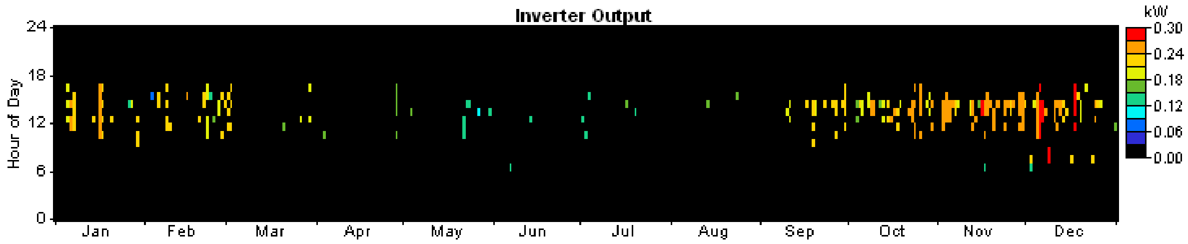

Figure 3:20 Grid-connected configuration - Case-2: Inverter output without Storage

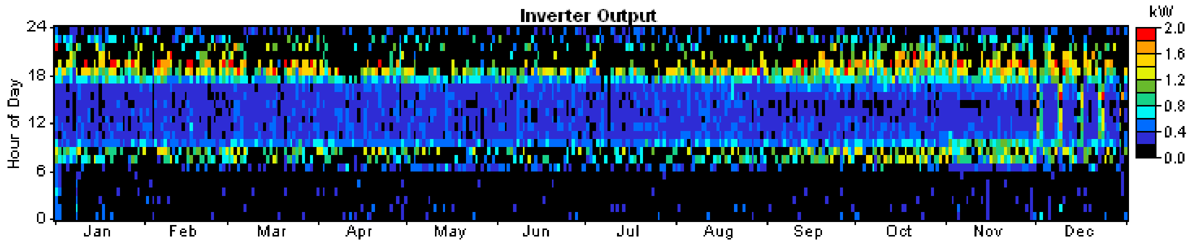

Figure 3:21 Grid-connected configuration - Case-3: Inverter output with Storage

Case 4. Wind turbine in grid-connected configuration:

In this configuration model, the wind turbine generated enough electricity but was unable to meet the timely load demand. Thus, it consumed a significant amount of grid electricity. To meet the load demand, this optimised model used a 2-kW BWC XL.1 wind turbine, a 2-kW inverter and the grid supply. A total of 11,200 kWh/yr of electricity was produced, where the wind generator produced 7,756 kWh/yr or 69.25% of total production. The grid supplied 3,444 kWh/yr (or 30.75% of total production) and 60.1% of load demand. Wind turbine supported 2,286 kWh/yr or 39.89% of load demand. 3,635 kWh/yr or 46.86% of electricity was sold back to the grid. A total of 1,456 kWh/yr (or 18.77% of electricity) was unused.

Case 5. Wind turbine with storage in grid-connected configuration:

This configuration model used a 2-kW BWC XL.1 wind generator, 12 Trojan L16P batteries, a 3-kW inverter and the grid supply. 8,477 kWh/yr of total electricity was produced. The grid supplied only 721 kWh/yr or 8.5% of total production and only 12.58% of total load demand. The wind turbine produced 7,756 kWh/yr which was 91.49% of total production. The batteries stored 2,076 kWh/yr and supplied 1,782 kWh/yr (or 31.1% of total load demand). However, the wind turbine directly supported 3,227 kWh/yr (or 56.32% of total load demand). Total 2,003 kWh/yr or 25.83% of electricity was sold back to the grid and loss of energy was only 0.04%. A significant amount of electricity was consumed from renewable generation, and a good amount of energy was sold back to the grid, reducing overall GHG emission.

Figure 3.22 shows that the wind turbine produced enough electricity and supplied a significant amount of electricity to the grid; however, it was unable to support the full load demand. The inverter converted more electricity from DC to AC when storage supported load demand as shown in Figure 3.23.

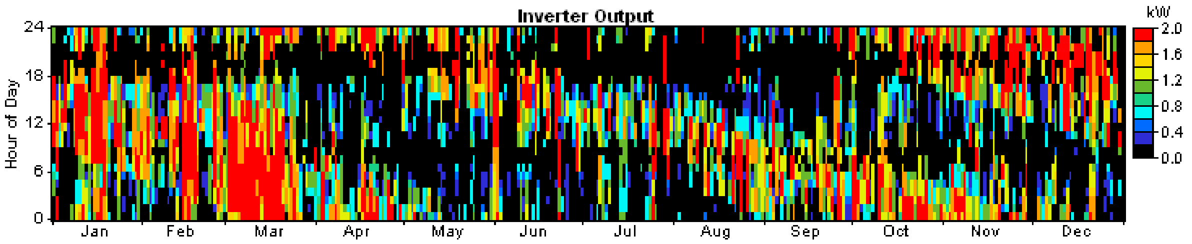

Figure 3:22 Grid-connected configuration - Case-4: Inverter output without Storage

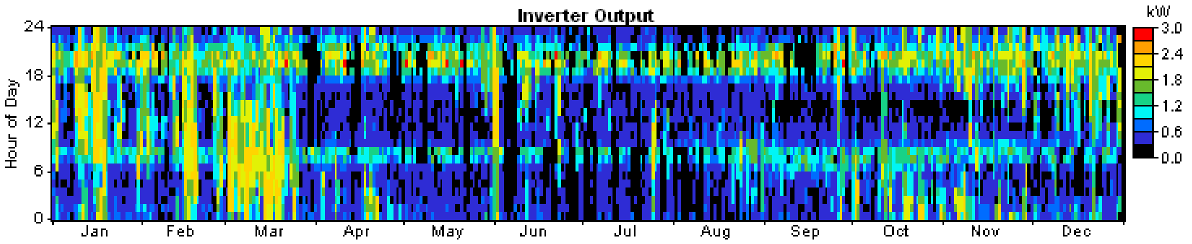

Figure 3:23 Grid-connected configuration - Case-5: Inverter output with Storage

Case 6. Hybrid system without storage in grid-connected configuration:

In this configuration, both the PV and wind turbine were used. This hybrid configuration model used a 1-kW PV, a 2-kW BWC XL.1 wind generator, a 2-kW inverter and a grid supply for the same load of 5730kWh/yr. Results showed that the hybrid system was optimised such that minimum RE components were required but could not meet the load demand for a 24-hour period. A total of 11,765 kWh/yr of electricity was produced, where the grid supplied 3,267 kWh/yr (57.01% of load demand, or 27.76% of total production). The PV and wind hybrid system produced 8,498 kWh/yr, or 72.23% of total production. The hybrid system also supplied 2,463 kWh/yr of electricity, or 42.98% of load demand. However, the hybrid system generated enough electricity and sold 3,966 kWh/yr (or 46.67% of the hybrid-generated electricity) to the grid. Still, 1,658 kWh/yr of electricity was wasted, which was 19.51% of total RE production. This wasted electricity could be utilized and grid use could be minimized by adding storage.

Case 7. Hybrid system with storage in grid-connected configuration:

This hybrid configuration model used a 1-kW PV, a 2-kW BWC XL.1 wind generator, a 3-kW inverter, 12 Trojan L16P batteries and a grid supply. This configuration improved RE contribution to supporting load demand. A total of 8,975 kWh/yr of electricity was produced, where the grid supplied only 477 kWh/yr (5.31% of total production or 8.32% of load demand). The PV generated 742 kWh/yr and the wind turbine generated the most, with 7,756 kWh/yr. That is, RE production was 94.68% of total electricity generation and supported 91.67% of load demand. This hybrid system sold 2,466 kWh/yr (or 29.01% of electricity) back to the grid. Storage helped in improving RE utilization and minimized energy loss. Only 2.84 kWh/yr of electricity was wasted (or 0.03% of hybrid-generated electricity). The batteries stored 2,009 kWh/yr and supported 1,726 kWh/yr of load or 30.12% of load demand.

Figure 3.24 shows the inverter activity in the hybrid system without storage. It is clearly evident that the hybrid system is unable to support load after 18:00PM and in the morning. Storage supports the load during this time as shown in Figure 3.25.

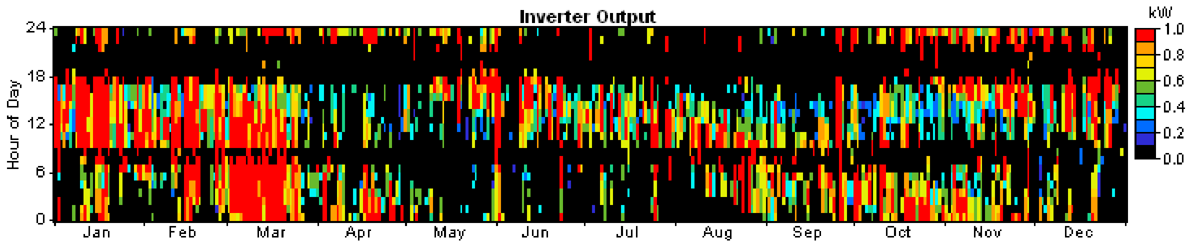

Figure 3:24 Grid-connected configuration - Case-6: Inverter output without Storage

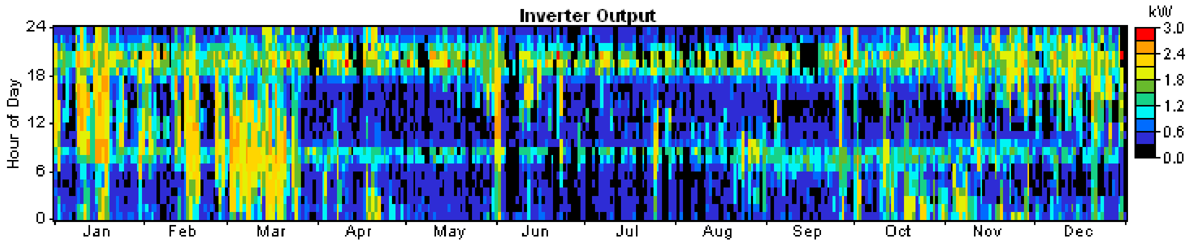

Figure 3:25 Grid-connected configuration - Case-7: Inverter output without Storage

Summary of Category-2 or Grid-connected configurations:

The results of grid-connected configurations can be summarized thusly: storage improved load support. Storage optimised the RE sources by minimizing grid use and loss of energy. Table 3.7 summarizes these findings. Load support is defined as the percentage of load supported by RE and storage compared to total load demand. Energy loss is defined as the percentage of energy loss compared to total RE production. Grid sales are the energy sold to the grid relative to total RE production.

Table 3:7 Category-2 or grid connected configuration results

	PV	**Wind**	**Inverter**	**Storage (at 24V DC system voltage)**	**RE use**		
					Load support	**Grid sales**	**RE energy loss**
Case-2 (PV +Grid)	1kW	-	1kW	-	0.75%	1.62%	92.05%
Case-3 (PV+Storage+Grid)	4kW	-	2kW	8 nos. (720Ah)	24.14%	0.13%	0.22%
Case-4 (Wind turbine+Grid)	-	2kW	2kW	-	39.89%	46.86%	18.77%
Case-5 (Wind turbine +Storage+Grid)	-	2kW	3kW	12 nos. (1080Ah)	87.42%	25.83%	0.04%
Case-6 (Hybrid +Grid)	1kW	2kW	2kW	-	42.98%	46.67%	19.51%
Case-7 (Hybrid+Storage+Grid)	1kW	2kW	3kW	12 nos. (1080Ah)	91.67%	29.01%	0.03%

3.3.4.3 Findings or Results

The optimisation was done in two configuration categories and seven cases in each category. Four different factors were compared in each case. These factors were GHG & pollutant gas emission, RF, COE and NPC. The comparative findings of these factors are explained below.

3.3.4.3.1 GHG and Pollutant gas emission

Figure 3.26 shows GHG and pollutant gas emissions in different case configurations. In the off-grid or stand-alone system, storage eliminated GHG and other pollutant gas emission. In a grid-connected configuration, it was also evident that storage minimized emission by improving RE utilization. By selling excess energy back to the grid, storage further helped in reducing GHG emission from the grid. The reductions are shown as negative values in Figure 3.26.

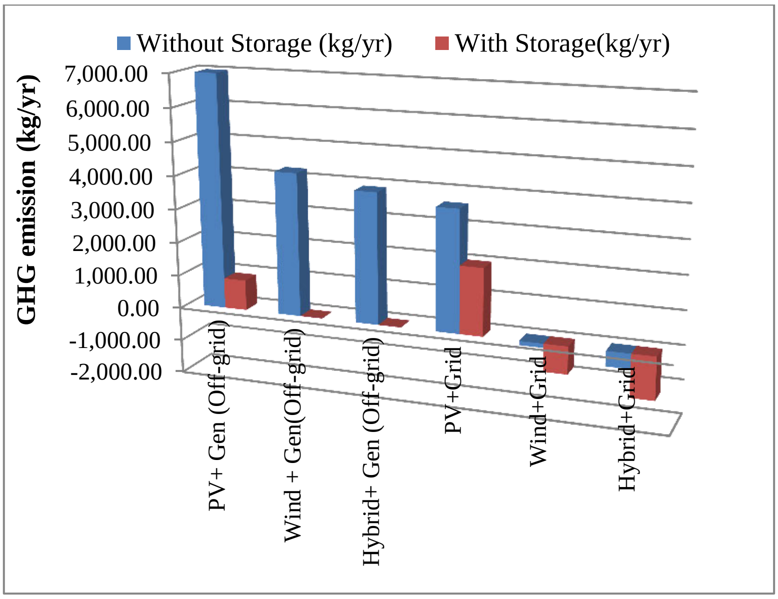

Figure 3:26 GHG and Pollutant gas emission in different cases

3.3.4.3.2 Renewable Fraction (RF)

RF is the measuring index of how much electricity is produced from RE, as a proportion of total production. In a stand-alone system, it was found that storage eliminates the use of diesel generators; thus, RF became 100%. In a grid-connected configuration, storage again improves the RE utilization and RF became as high as 94.7% as shown in Figure 3.27.

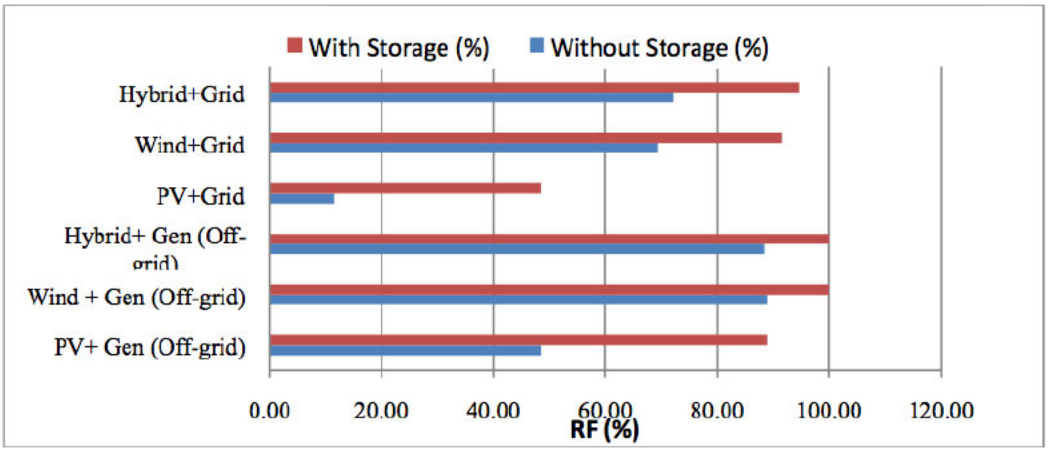

Figure 3:27 RF in different cases

3.3.4.3.3 Cost of Energy (COE)

COE is the cost of per unit energy in $/kWh. The stand-alone configuration involved a costly diesel generator; therefore, the COE was very high. However, adding storage helped to reduce the COE to a reasonable level. In a grid-connected configuration in all combinations of RE sources, storage reduced the COE. In a hybrid system, storage reduced the COE to 0.297$/kWh as shown in Figure 3.28, which was less than the grid only energy cost of 0.392$/kWh.

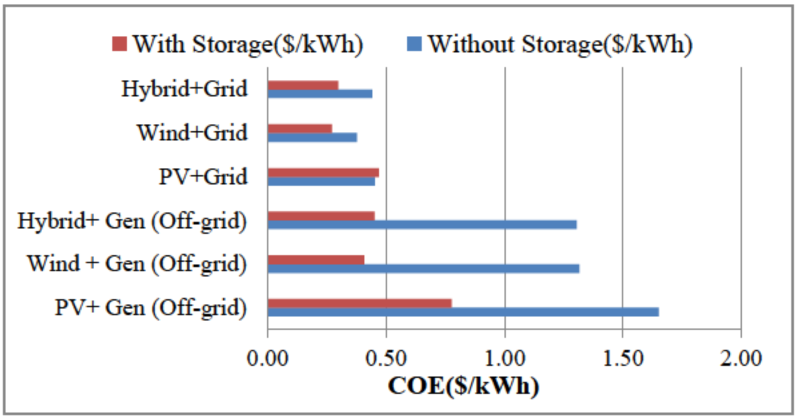

Figure 3:28 COE in different cases

3.3.4.3.4 Net Present Cost (NPC)

NPC represents the present cost of the system. In the stand-alone configuration, NPC was very high. However, storage helped in reducing NPC to an acceptable level by improving the utilization of RE. In a grid-connected configuration, storage helped in reducing NPC, although with PV, the NPC increased marginally as shown in Figure 3.29.

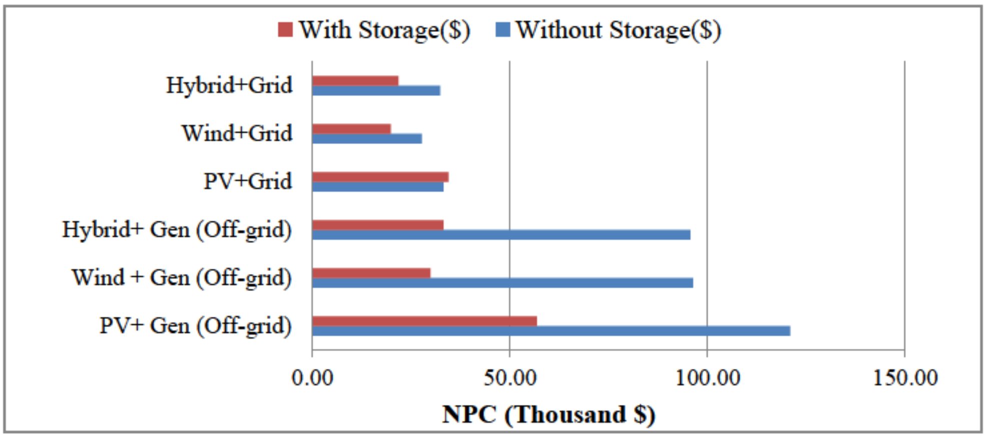

Figure 3:29 NPC in different cases

3.3.4.3.5 Payback Period

Payback was calculated by comparing one system with another. Payback is the number of years in which the cumulative cash flow switches from negative to positive by comparing the storage-integrated model with a non-storage model in a grid-connected configuration. Cash flow in a grid-connected PV with storage system was compared to cash flow in a grid-connected PV base system (without storage). It was found that the payback period is 4.15 years. Similarly, a grid-connected wind generator with storage was compared to a system without storage; the payback period was 2.67 years. In the case of a grid-connected hybrid (PV & wind turbine) system with storage compared to the same without a storage system, it was found that the payback period was 2.05 years. Storage helped in RE utilization by minimizing the use of grid electricity and increasing energy sell-back to the grid. Therefore, it was confirmed that the investment cost of storage integration yields in a very short period of time, as shown in Figure 3.30. In Australia, the solar bonus scheme awarded the price of electricity fed into the grid from RE at a rate of $0.44/kWh [119, 120], which is much higher than the utility rate. This ensures shorter payback period in Australia. Recently, the Australian government introduced a carbon tax that increased the cost of electricity from conventional sources. Storage can help to increase RE utilization and to reduce the overall cost of consumed electricity.

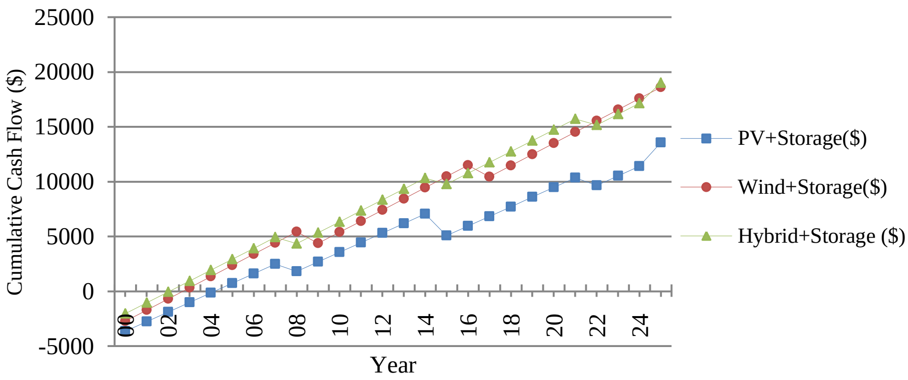

Figure 3:30 Payback period of storage in three cases

3.4 Conclusions

A storage-integrated RE system was analysed for a residential load in Rockhampton, Australia. Estimation of required storage with the RE system for the load was demonstrated. Estimation steps were explained, and the estimation of required storage was done with a grid-connected PV, wind and hybrid systems for a residential load of 15.7kWh/d in Rockhampton. A software model in HOMER was used for the same daily average load of 15.7kWh/d and identified optimised configurations for the required system components. Models were simulated for the required system components for yearly load of 5730kWh/yr, taking into account a 25-year project lifespan and also considering the solar radiation and wind speed data with seasonal variation. The estimation process considered one-day loads and estimated the required system components for the worst month solar radiation and wind speed data. However, the results from both methods were similar, as shown in Table 3.8.

Table 3:8 Required system components in Estimation process and from optimized model

Configuration	Estimation result		Model result	
	PV/Wind	Storage	PV/Wind	Storage
Solar PV system	2.541kW solar PV	(665.90 - 1409.64)Ah	4kW solar PV	720Ah
Wind turbine system	1.92kW wind turbine generator	(582.35 - 1010.14)Ah	2 kW wind turbine generator	1080Ah
PV + Wind Hybrid system	1.27 kW PV + 0.9592kW wind turbine generator	(543.62 - 1067.54)Ah	1 kW PV + 2 kW wind turbine	1080Ah

The significance of storage with RE was analysed by building a model in HOMER. The model was analysed in stand-alone and grid-connected configurations. Analysis was conducted to observe the storage influences over the GHG emission, RF, COE and NPC indexes. It was found by analysing the result from the optimised model that storage has a great influence on improving RE utilisation.

It was evident from the analysis that storage helped significantly in reducing GHG & other pollutant gas emission, reduced COE, improved RF and reduced NPC. Comparing without and with-storage systems models, it was found that in a grid-connected PV system, storage reduced 44.79% of GHG and pollutant gas emission. In grid-connected wind and hybrid systems, storage reduced GHG emission more than 100% by selling extra energy to the grid. A grid-connected configuration storage improved RF; with PV, wind turbine and hybrid systems, the RF was 48.6%, 91.5%, and 94.7%, respectively. Storage reduced COE; in a grid-connected configuration, it was as low as the presently available grid electricity cost. For hybrid and wind systems, the COE was $0.297/kWh and $0.27/kWh respectively. Similarly, storage reduced NPC for PV, wind and hybrid configurations by 3.78%, 28.36%, and 32.69%, respectively. Moreover, the payback time for storage is very short. Thus, a storage- integrated RE system is more feasible for large-scale implementation.

Chapter 4

Network Model Development

4.0 Introduction

Renewable energy generation from solar and wind is largely variable and unable to meet the timely load demand especially the peak demand. The ability to store generated energy from these sources during peak generation periods allow RE generation to be utilised more effectively. Using energy storage, network operators will be able to load shift, peak load support, flatten the fluctuations and improve overall network performance. However, there is little research done on the integration of large scale storage and RE with the power network in Australia.

The power network in Queensland is versatile in many forms. It consists of diverse network configuration to support dispersed load of various capacities. It also has SWER network integrated with the conventional three phase distribution network. Integration of large scale solar, wind energy and storage in this network may cause adverse impact which was not tested before. One of the primary objectives of this thesis is to identify the impacts of the integration of energy storage with the power network.

In order to investigate the impacts on power network, a realistic network model was required to further investigate the impact to the power system network. This model enables to further integrate RE sources and ES into the network. This model provides flexibility to connect these sources and storage in various connection configurations in the power network which is impossible in real life environment. This chapter provides details on the network model which was developed to investigate in details for Rockhampton power network and explained required settings for the model to analyse voltage regulation and harmonics emission. This model can be used for any future analysis by the utility operator in Rockhampton.

Section 4.1 illustrates the power network structure in Queensland, Australia. The network model development processes are explained in section 4.2. Section 4.3 introduces the use of PSS SINCAL to develop a power network model considering various network settings. Four different network setups are described in section 4.4 to identify the impacts of ES on the power network. Final concluding remarks are made in section 4.5.

4.1 Background: Power Network in Queensland

Ergon Energy is the Distribution Network Service Provider (DNSP) in Queensland which was formed by the Queensland Government in 1991 from the then six regional Queensland electricity distributors and subsidiary retailers as shown in Figure 4.1. Figure 4.2 shows the current geographical boundaries of Ergon Energy.

In the early years, electricity was supplied in regional Queensland from local authorities in 6 major areas:

- Far North (Cairns)
- North Queensland (Townsville)
- Mackay Region (Mackay)
- **Capricornia (Rockhampton)**
- Wide Bay (Maryborough)
- South West (Toowoomba)

Coal fired power stations are the main source of electricity in Queensland. Due to the concern of GHG emissions, the government has planned to generate 20% electricity from RE sources, particularly from solar and wind.

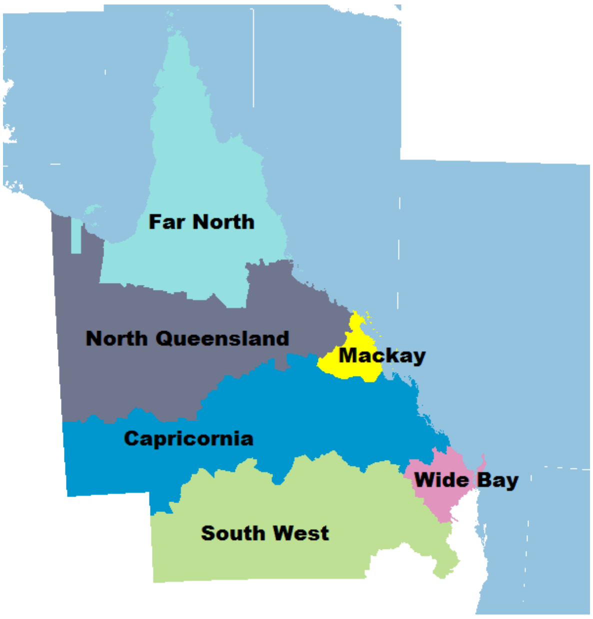

Figure 4:1 Ergon Energy legacy regions

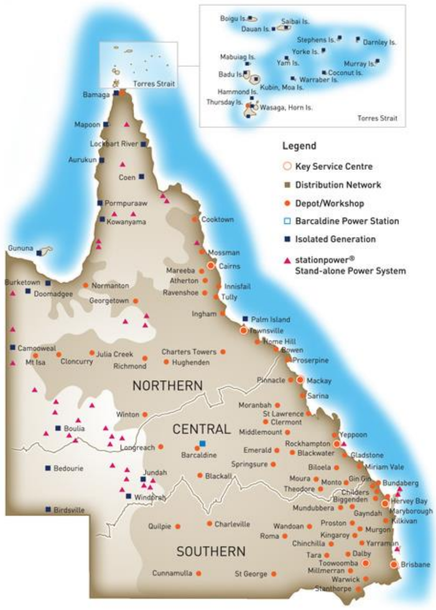

Figure 4:2 Ergon geographical region [1]

The impacts of increased RE utilisation increases the risk of unexpected effects on the utility grid. The associated risk cannot be seen in the present power network as current RE adoption is significantly small and have no significant effect on the DN. Queensland power network is quite different in many forms. Load types are nearly symmetrically distributed in urban areas but industrial heavy loads (few MVA size) are connected along nearby very small loads. Some heavy loads (such as mining site) are distributed in rural areas where loads are not symmetrically distributed thereby power flow in the Queensland network is not uniform. Ergon Energy is the utility operator in most of the areas in Queensland and supplies electricity to around 700,000 customers, operating over an area of 1million square kilometres areas which is around 97% area of Queensland [121]. Ergon Energy's electricity network consists of approximately 150,000 km of power lines and 1 million power poles along with associated infrastructure such as substations and power transformers. Moreover Ergon Energy operates 33 stand-alone power stations that provide electricity to the extremely isolated communities. Ergon Energy was recently involved in electricity generation from renewable energy (RE) sources and is one of Australia's largest purchaser of RE [121]. Figure 4.3 shows the assets of Ergon Energy as of 30 June 2012[122].

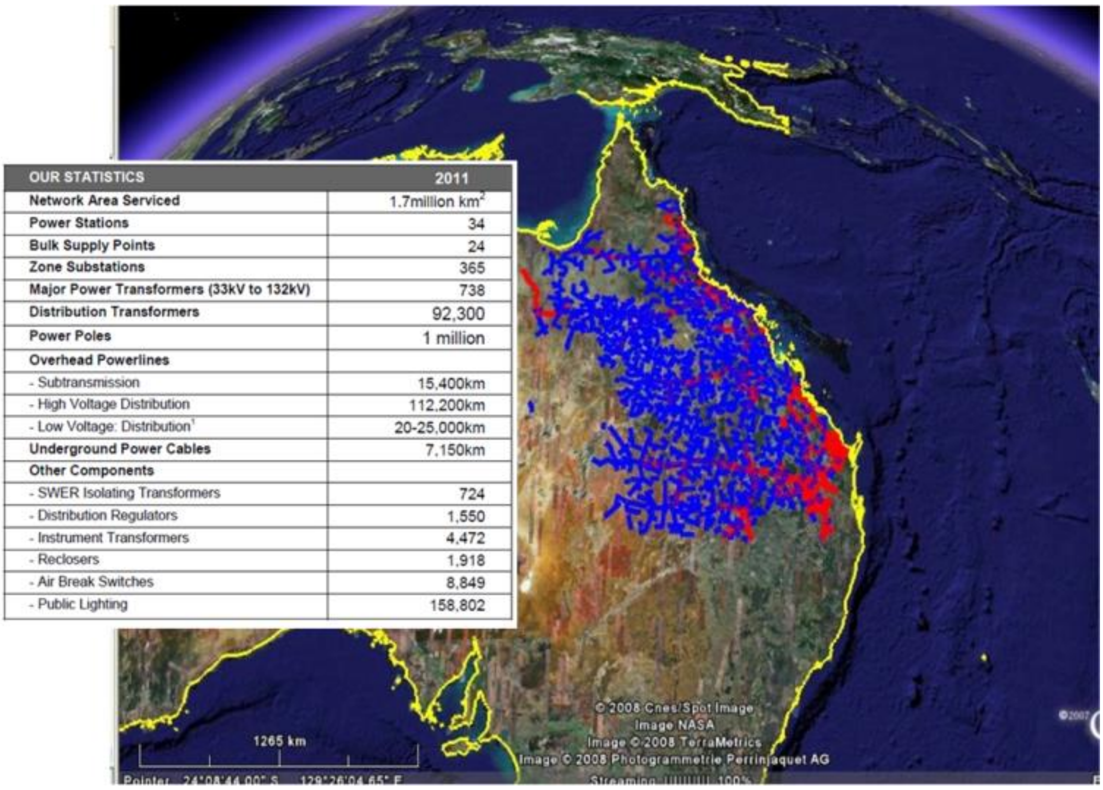

OUR STATISTICS	2011
Network Area Serviced	1.7million km^2
Power Stations	34
Bulk Supply Points	24
Zone Substations	365
Major Power Transformers (33kV to 132kV)	738
Distribution Transformers	92,300
Power Poles	1 million
Overhead Powerlines	
- Subtransmission	15,400km
- High Voltage Distribution	112,200km
- Low Voltage: Distribution[1]	20-25,000km
Underground Power Cables	7,150km
Other Components	
- SWER Isolating Transformers	724
- Distribution Regulators	1,550
- Instrument Transformers	4,472
- Reclosers	1,918
- Air Break Switches	8,849
- Public Lighting	158,802

Figure 4:3 Ergon Energy Power Network and Network Assets [122]

4.1.1 Network Load and Challenges to Electrical Infrastructure

Customer number growth rate in Ergon Energy is an average of 1.7% per year [122] and the peak day load profile of the Ergon Energy network is shown in Figure 4.4. The nature of load demand has impacts on infrastructure utilisation.

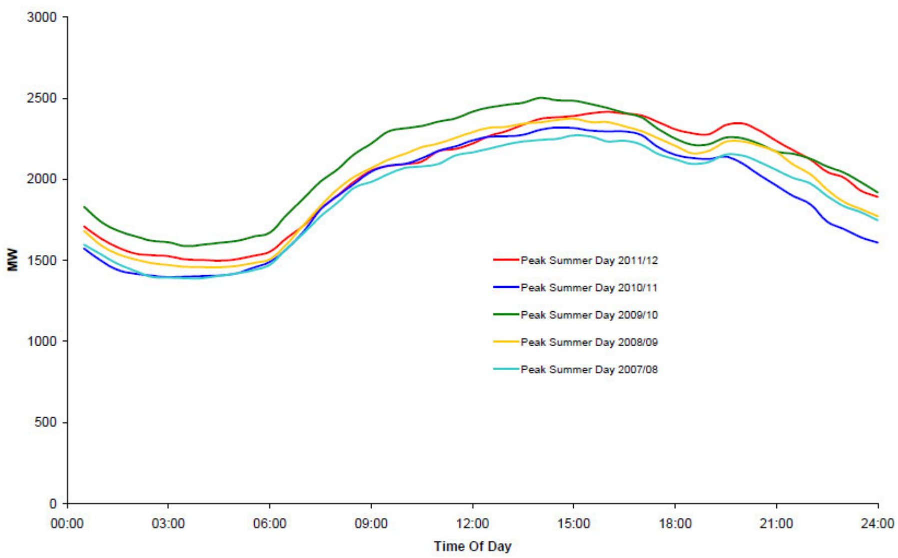

Figure 4:4 Peak day load profile of Ergon Energy network (2007/07 to 2011/12 seasonal year) [122]

The rating of electrical infrastructure is usually dependent on the ambient temperature. Due to the fact that a hot transformer cannot dissipate as much heat on a hot day as it can on a cold day. Equipment that services a peak load is in risk for relatively long periods with high heat therefore cannot service as high a peak load value. Total load profile shown in Figure 4.4 shows the challenges for electrical infrastructures such as [122]:

- Peak loads occur during 12:00PM and 15:00PM i.e. in the hottest part of the day
- Peak loads are not short term and remain high for most of the day and continue up to the evening
- Peak load increases with increase in temperature while the effective rating of the conventional power plant decreases with ambient temperature.

Residential load peak demand occurs in the evening and it is a minimum during the day time, therefore there is considerable discussion about increasing the penetration of household PV generation to reduce the day time peak demand. However, this will not alleviate the evening peak demand without energy storage when residential demand is highest [122] as well as the total load demand is at a peak. At present condition the power network in Queensland faces several PQ related problems.

4.1.1.1 Power Quality Concern

Power flow in Queensland power network is not uniform due to large transmission and distribution line to support distant and remote loads. The network also requires to manage a unique combination of three phase and SWER network. Moreover the recent integration of RE sources of various capacities through distribution network into the power network also considered a prime cause of PQ problem. Ergon Energy has 1,789 Power Quality monitors connected throughout the network which indicated that [122]:

- 27.7% sites recorded over voltage which is outside of regulatory limits.
- 1.8% sites having under voltage that is outside of regulatory limits.
- 1.8% of three phase sites showed unbalanced conditions which is outside the standard.
- Total harmonic distortion (THD) found in several sites was greater than the regulatory limits.

In LV DN continuous work is required to improve voltage unbalance, particularly with rural feeders [122]. Figure 4.5 shows the power quality profile of Ergon Energy from 2006/07 to 2011/12 [122].

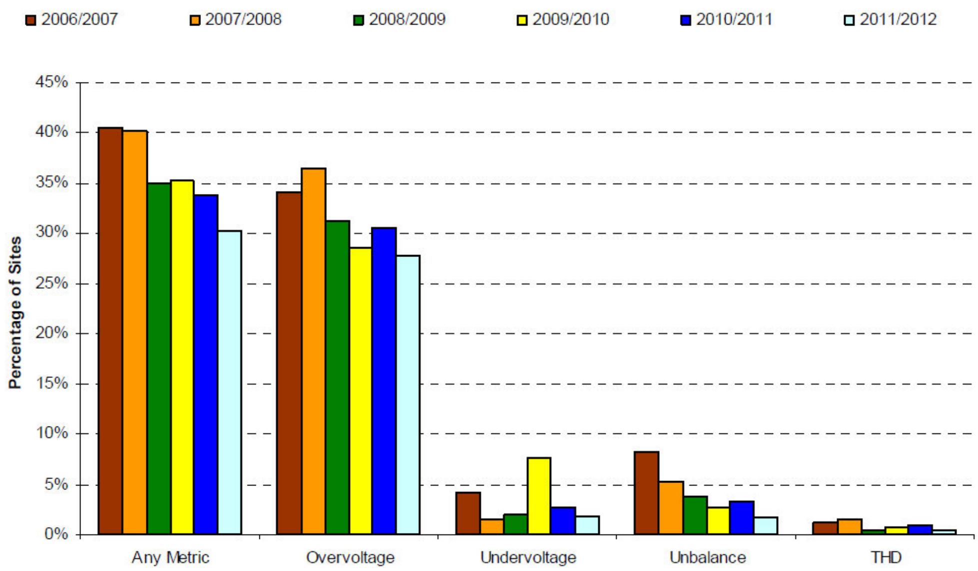

Figure 4:5 Power Quality parameters (Ergon Energy Network) [122]

Therefore it is clear that power network in Queensland is facing two PQ related problems such as; Voltage regulation and Harmonics. By integrating RE and storage, the present level of problems may intensify; therefore it is urgently required to be investigated before large scale integration.

4.1.1.2 RE share of Ergon Energy

As mentioned earlier, GHG emission is a great concern for stationary energy generation. In order to reduce the environmental impact from GHG emissions, Ergon Energy is working with several RE projects in Queensland [121]. At the end of February 2012, the estimated total installed PV capacity in Queensland was 427 MW [123], although it is only a very small part of present load demand.

- Birdsville Geothermal power provides 80kW of electricity to consumers and provides around 30% of the annual electricity needs of Birdsville which is not connected to the national grid.

- Windorah solar farm in Western Queensland has a peak capacity of 130kW, however diesel generators operate to support load during the night and on cloudy days. Small size storage batteries are used for small fluctuations due to brief cloud cover.
- Two wind turbines generate up to 450 kW of electricity which is 5% to 10% of Thursday Island's electricity needs. The tower height is 30m and rotor diameter is 29m.
- Ergon Energy tested a 5kW hydrogen fuel cell in their Cairns workshop. It is intended to support the sparsely populated customers at the end of long rural power lines.

Currently there is no RE projects in Rockhampton although many houses in this area have already installed grid connected roof-top solar PVs and more such installations are expected. This thesis considered Rockhampton as the potential site for investigation.

4.1.2 Site Description

Rockhampton is situated in Central Queensland, on the Tropic of Capricorn [124] and typical temperature range 22°C to 32°C in summer and 9°C to 23°C in winter. This is very sunny area and experiences over 300 days of sunshine each year. Also this city lies within the cyclone risk zone. The present population of Rockhampton is 112,383 and land area is 18,356 km^2 [124]. Figure 4.6 shows the area boundary of Rockhampton region.

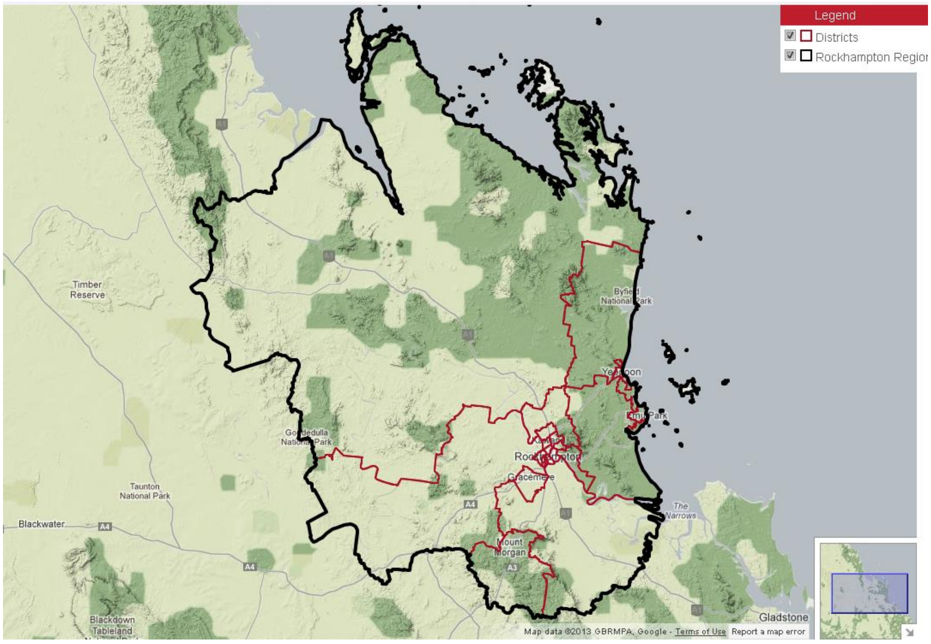

Figure 4:6 Rockhampton Region Map [124]

The coal-fired Stanwell Power Station in Rockhampton has a generation capacity of 1445 MW. In Queensland, Transmission network gets energy supply from various electricity generators through "Power Link" and are connected to the bulk supply substation (BSS). PowerLink is a Government owned corporation that owns, develops, operate and maintains Queensland's high voltage electricity transmission network. The power network in Rockhampton is connected to the transmission network through Rockhampton Glenmore BSS and 11 zone substations (ZS) that distribute electricity to the load through 56 distribution feeders as shown in Table 4.1. ZS supplies 11 kV to Distribution substations (DS) that supplies electricity to end loads through distribution transformer (DT). DT connects the low voltage (LV) loads such as residential or commercial load.

Table 4:1 Zone Substations in Rockhampton power network

Zone Substation	Type	Short name	Capacity	Distribution Feeder
Berserker	ZS	BER	66/11 kV	2
Canning Street	ZS	CST	66/11 kV	5
Frenchville	ZS	FRN	66/11 kV	7
Lakes Creek	ZS	LCR	66/11 kV	6
Malchi	ZS	MAL	66/11 kV	4
Mount Morgan	ZS	MTM	66/11 kV	3
Pandoin	ZS	PAN	66/22 kV/11 kV	4
Parkhurst	ZS	PKH	66/11 kV	7
Raglan	ZS	RAG	66/22 kV	3
Rockhampton Glenmore	BSS, ZS	RGL	132/66/11 kV	8
Rockhampton South	ZS	RSH	66/11 kV	7

Rockhampton distribution network is a major part of the Capricornia region network. From source data of Ergon Energy in 2011 [18], the loading capacity of DT connected from 56 distribution feeders is shown in Figure 4.7 and the maximum utilization of these transformer along feeders are shown in Figure 4.8 and the number of customers in different zone substations are shown in Figure 4.9, where the total number of customer in Rockhampton is 37,941 and total peak load is 194 MVA. There are a total of 1,341 numbers of solar PV installations in Rockhampton and the cumulative PV capacity is shown in Figure 4.10.

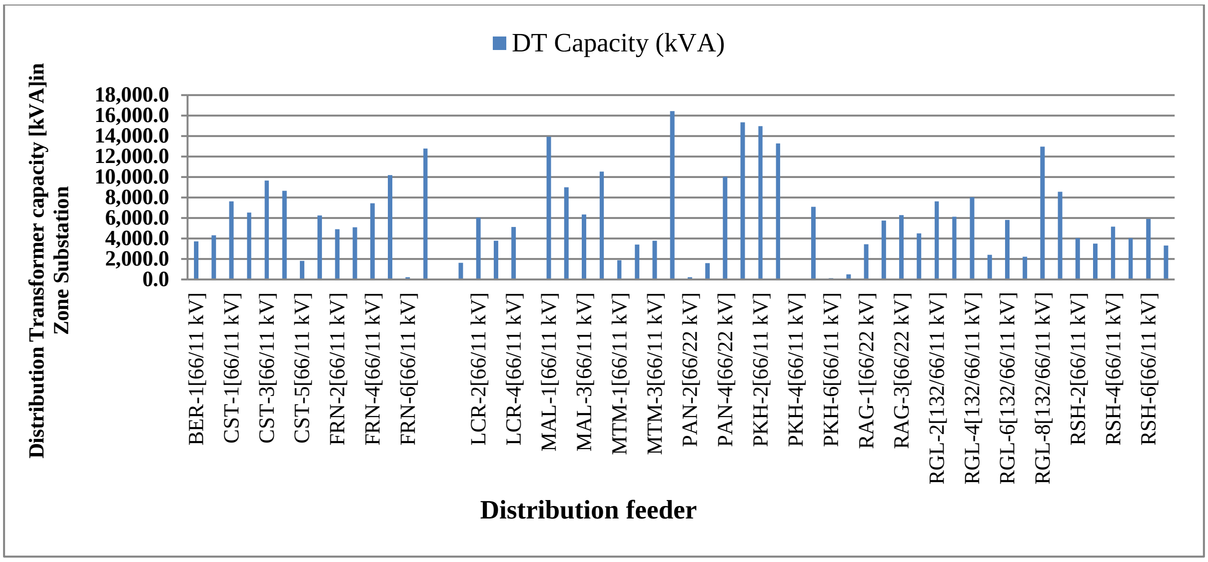

Figure 4:7 Distribution transformer capacities at feeders in zone substations [18]

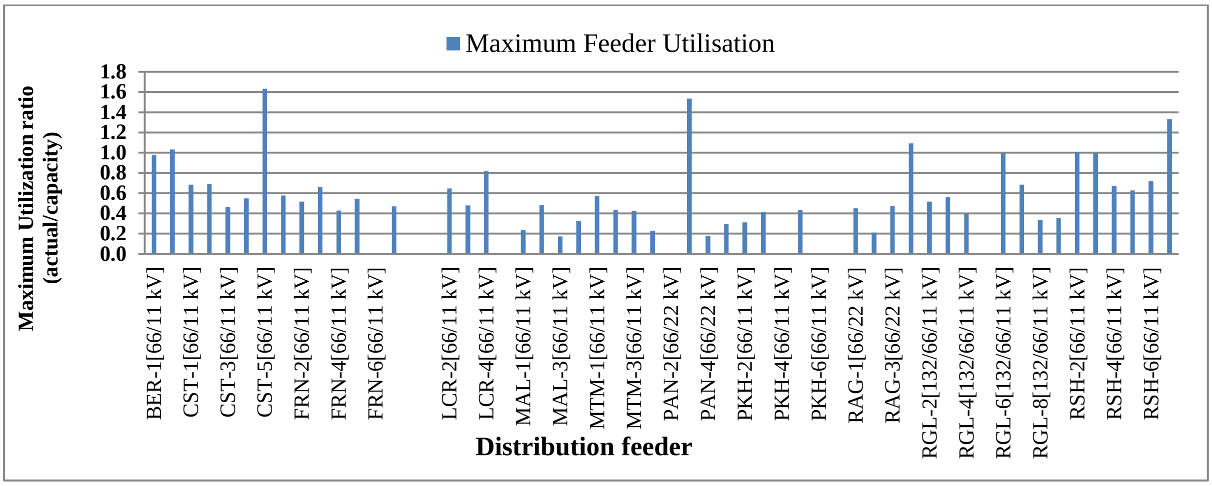

Figure 4:8 Maximum utilization of transformer in Zone substation feeders [18]

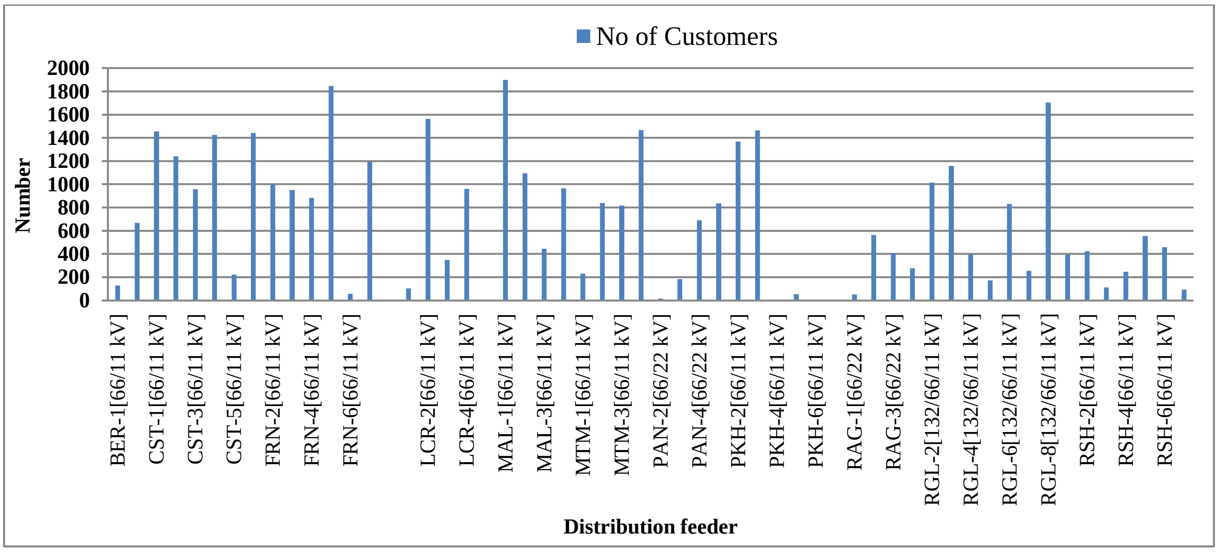

Figure 4:9 Numbers of customers in different zone substations along feeders [18]

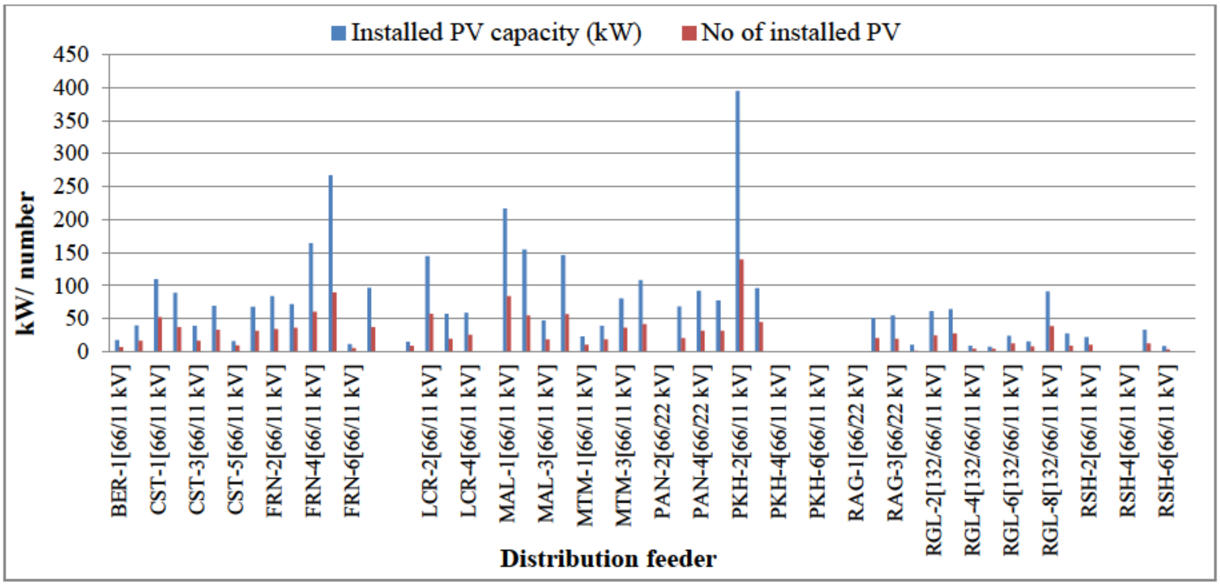

Figure 4:10 Installed Solar PV and numbers of PV customers [18]

Figure 4.11 shows the peak day summer load in Rockhampton [19]. Demand is very high from 08:00AM to 10:00 PM.

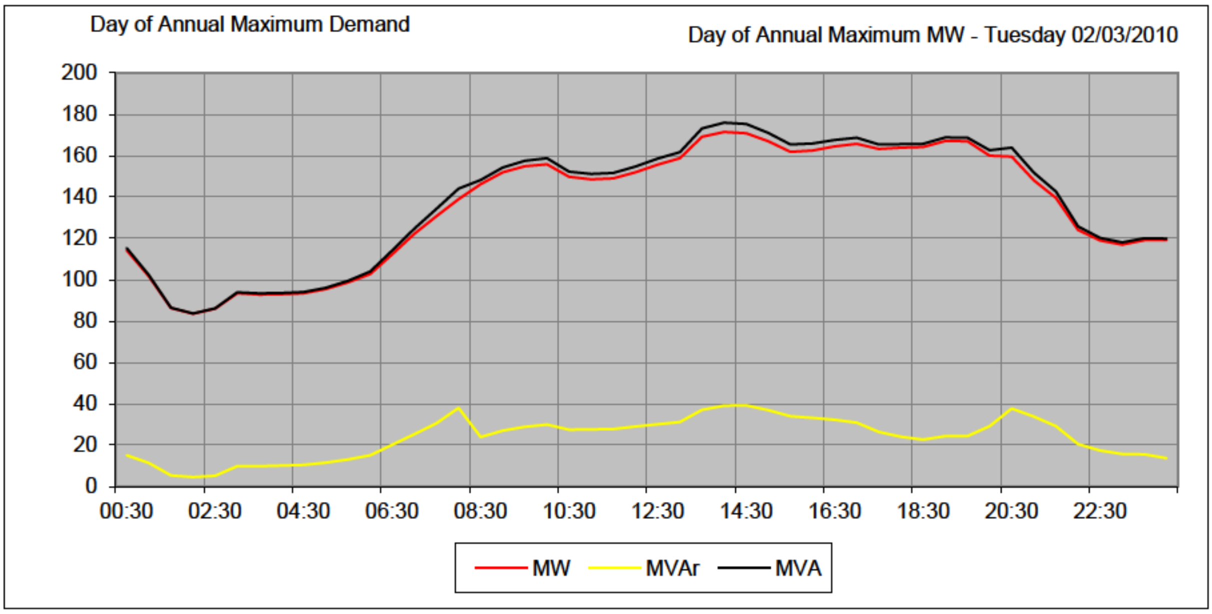

Figure 4:11 Peak day load profile of Rockhampton in 2010 [19]

Present RE installations (Roof-top PV) in Rockhampton are at the LV side and the local operator (Ergon Energy) has no monitoring tool for the LV network. Software tools can provide the scope and capability to investigate any possible effects due to RE integration into the LV network. The accuracy of this investigation depends on the proper network model having suitable control settings. Therefore the development of an accurate power network for

Rockhampton is required so that it can incorporate storage and RE. Also selection of software tools is important that can calculate load flow for fixed loads and time varying dynamic load and also can analyse the harmonic effects.

The next section describes the development of a network model and Rockhampton was chosen as a case study as it has very unique load profile.

4.2 Network Model Development

Power system analysis is essential for generation, load demand management, fault detection and the economic use of power. To make the network reliable and sustainable it becomes necessary to perform load flow analysis. Different iterative methods are commonly used for load flow analysis such as; Newton-Raphson method, Gauss-Seidel method etc. To develop a network model for power network analysis, a suitable software tool is essential. Power flow analysis can be done by various simulation software. For basic power flow analysis MATLAB toolboxes can be used but it has limitations for large power network such as Rockhampton distribution network. Distributed generators such as storage and renewable energy are the new sources (at the distribution network) for power flow analysis, hence identifying a suitable tool was critical to further develop and analyse the network. A number of relevant tools were investigated and identified suitable one as detailed below.

4.2.1 Software Simulation Tool selection

EasyPower is a load flow analysis software that determine active and reactive power, overload and voltage violation problems [125] and optimise system for efficiency. ETAP simulation can be used for prediction, design and the planning of system behavior which includes Arc Flash analysis, short circuit analysis, load flow analysis, motor starting analysis and load analysis [126]. ETAP Renewable Energy Software [127] can design, analyze and operate wind turbine generator, solar PV for grid integration studies. ETAP Smart Grid software allows control, optimize and manage power distribution networks. DINIS (Distribution Network Information System) provides excellent graphical operation and network representation for power analysis. DINIS [128] provides network analysis for 3 phase, 2 phase and single or SWER network however it does not have RE features. PSS SINCAL [129] has the ability to analyze unbalanced systems and harmonic distortion for a modeled system. It also has the capability to represent the network and platform visually. PSS SINCAL has the capability to calculate the following:

- Load flow with the following calculation procedure
  - Admittance matrix
  - Current iteration
  - Newton-Raphson
  - Unbalanced
- Single phase, two phase or three phase short circuit calculation based on VDE/IEC or ANSI or G74
- Unbalanced Load Flow
- Harmonics calculation
- Load Profile or Load curve calculation
- Fault detection

Moreover SINCAL can position the power network in real location in map using latitude and longitude values of nodes to fit the network in Google Earth GIS map which gives better view of the network.

DINIS is used by Ergon Energy to develop the HV distribution network for Rockhampton. There is a conversion tool developed by Hill Michael [130] to transform the DINIS model to the SINCAL model. Conversion is not straight forward as there are various complexities arise due to conversion, which need to be rectified. However conversion provides the similar skeleton of the original model which is very useful for placing the network according to GIS data. Considering the capabilities of SINCAL and the availability of the conversion tool, it helps to select PSS SINCAL as the simulation tool to achieve the objective.

Network development processes are explained below:

4.2.2 Existing Network Model and its Conversion

Ergon Energy is the power utility operator in Queensland, Australia. Ergon energy developed the HV network model using DINIS. The Smallworld and Google Earth model of Ergon Power network were built based on the GIS database and the load information was added in the DINIS model from Distribution Feeder Database (DFD). This existing DINIS model of Rockhampton area was converted to the SINCAL model using Dinis-to-SINCAl converter developed by Hill Michael [130]. Every nodes were checked to ensure the accuracy of the developed and model corrected it as necessary.

Figure 4.12 shows the Rockhampton Distribution Network in DINIS and Figure 4.13 shows the converted model in SINCAL with resized object sizes. All data in SINCAL is saved in table form in Access Database file, therefore changing this value was easily done by the Export/Import facility from the Excel file.

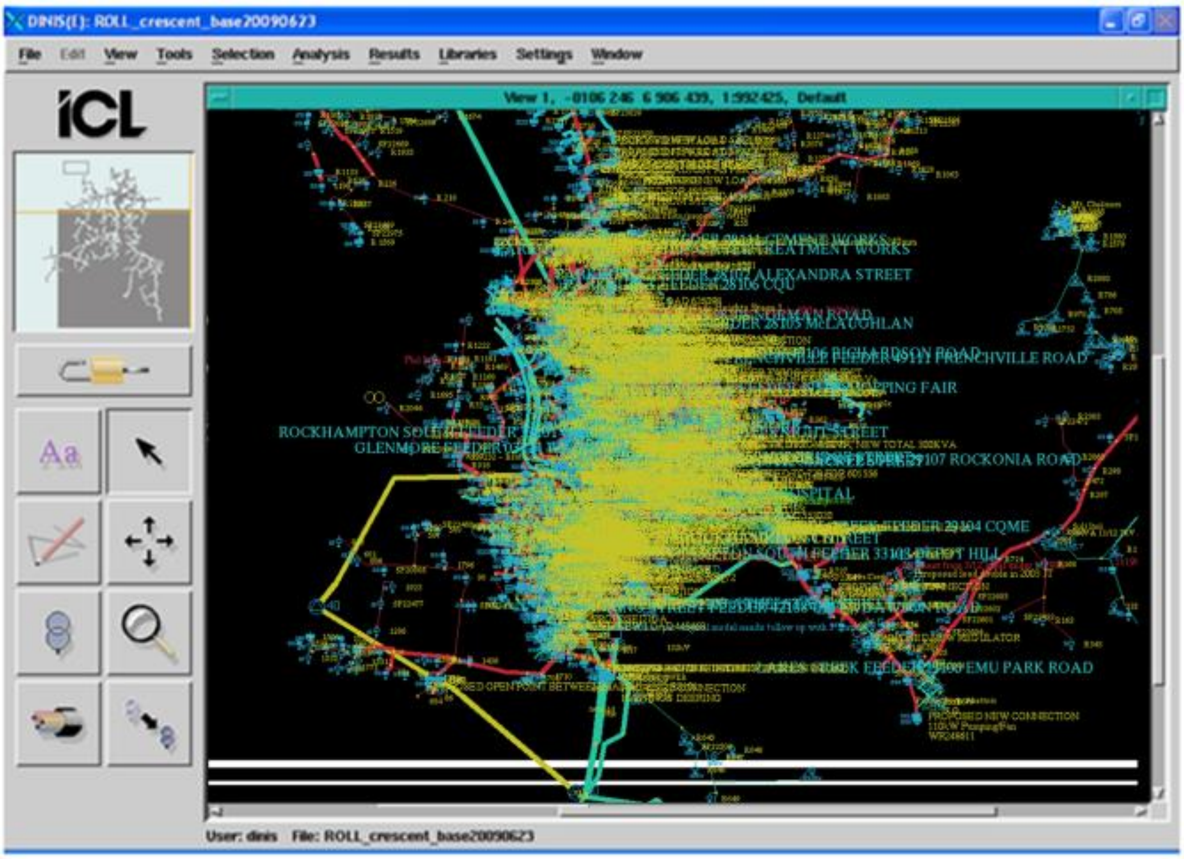

Figure 4:12 Rockhampton Distribution Network in DINIS

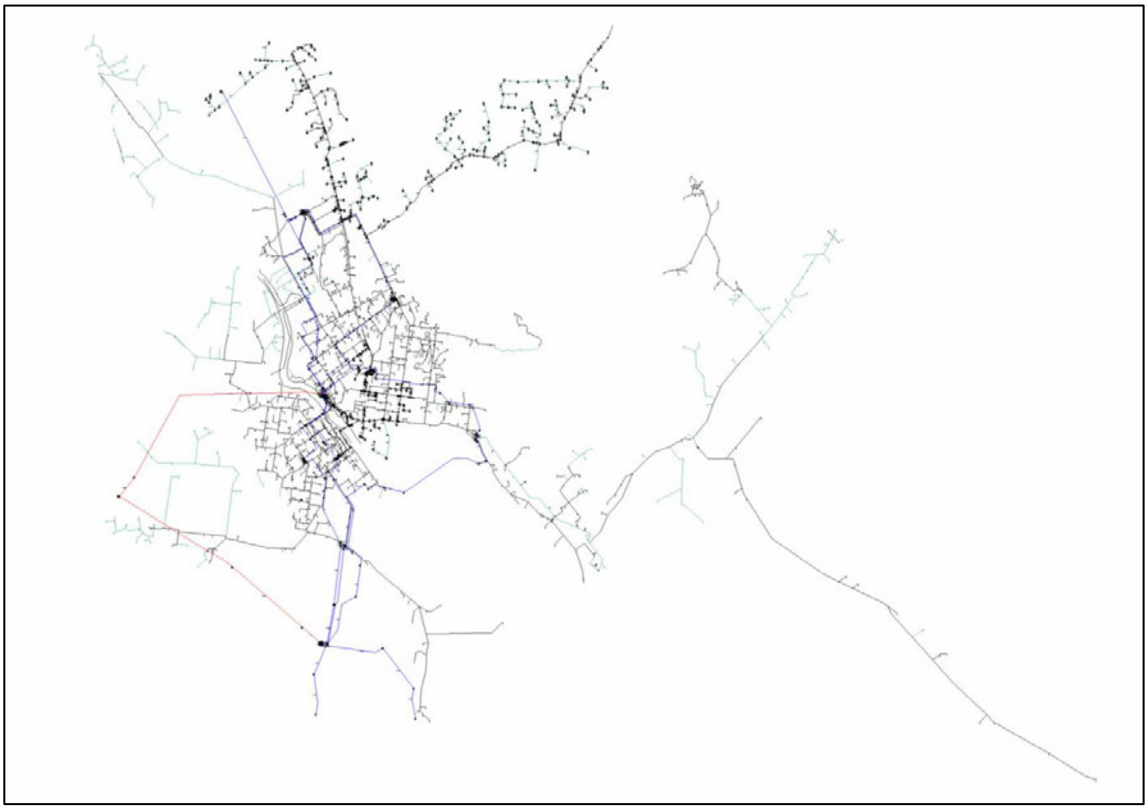

Figure 4:13 Converted Rockhampton Distribution Network in SINCAL

Load, transformer and regulator data was converted, however it was required to convert all line or conductor data from per-unit/km to resistance/km. Transformer winding impedances and zero phase sequence data was completed using the following processes and entered into the SINCAL database. The process of converting line impedance is shown by an example below:

Considering “Moon Conductor 7/4.75 AAC” and the conductor properties in DINIS is as shown in Table 4.2.

Table 4:2 Conductor impedance data in DINIS

Conductor parameter	Value (%/km)
Resistance	23.6
Reactance	29.543
Capacitance Charging	0.000402

Also considering for this example, DINIS uses a base value of 100MVA in the case of 11kV system voltage, therefore impedance is;

$$Z_{base} = \frac{V_{base}{}^{2}}{S_{base}} = \frac{11000^{2}}{100x10^{6}} = 1.21\Omega = 1p.u.$$

As the charging capacitance value is given in %/km and which needs to be converted to nf/km, therefore;

$$z = \frac{1}{2\pi fc}$$

$$C_{base} = \frac{1}{2\pi fZ_{base}} = \frac{1}{2\pi x50x1.21} = 0.00263f$$

Therefore the impedance data in Table 4.2 can be converted as follows and converted values are shown in Table 4.3:

$$\frac{\text{Resistance}}{km} = \frac{R_{pu}}{100}xZ_{base} = \frac{23.6}{100}x1.21 = 0.28556\Omega / km$$

$$\frac{\text{Reactance}}{km} = \frac{X_{pu}}{100}xZ_{base} = \frac{29.542}{100}x1.21 = 0.35747\Omega / km$$

$$\frac{\text{Capacitance}}{km} = \frac{C_{pu}}{100}xC_{base} = \frac{0.000402}{100}x0.00263 = 10.575nf / km$$

Table 4:3 Conductor impedance in SINCAL

Conductor parameter	**Value/km**
Resistance	0.28556 ohm/km
Reactance	0.35747 ohm/km
Capacitance	10.575 nf/km

The converter converts all impedance data and entered into the SINCAL model. Table 4.4 lists some other conductors used in this network and their current ratings and impedance values.

Table 4:4 Different conductor specifications used in the Rockhampton power network

Conductor type	Stranding	Code	Feeder rating (Summer day)	R (ohm/km)	X (ohm/km)	C (nF/km)
AAC	7/4.75	Moon	300A	0.282	0.357	10.575
	7/0.173	Wasp	281A	0.335	0.335	10.412
	7/4.50	Mercury	253A	0.314	0.409	9.133
	19/3.25	Neptune	396A	0.223	0.343	10.845
	19/3.75	Pluto	340A	0.168	0.334	11.156
	19/0.128	Hornet	300A	0.226	0.340	10.838
HDBC	19/2.00	19/2.00	229A	0.367	0.373	9.901
	7/0.104	7/0.104	177A	0.560	0.436	8.397
ACSR GZ	6/1/0.144	Mink	191A	0.484	0.371	10.068
	6/0.186-7/0.062	Dog	230A	0.291	0.404	9.204

The LV network was not available in DINIS, therefore; it was developed using SINCAL for further simulation. Moreover, SWER transformer information such as correct phase value and voltage level was required to input manually. Each and every node was checked for an accurate network model.

4.2.3 Validation of Model Network

The developed network model in PSS SINCAL was verified with the collected data and the existing network model in DINIS along with the existing network information in Google Earth model for Ergon Energy. This verification allowed the model to accurately represent the current power network of the Rockhampton area. Therefore the integration of PV, wind and storage on this network was rightly represented and allowed to identify the possible impacts on the network.

Troubleshooting: During the troubleshooting phase, the network model was verified against all other available information, different settings and parameter limits to ensure that the network is running correctly. This stage eliminated any system irregularities and identified values that are against the expected values to ensure completeness of the network model. Errors were identified and eliminated within varying techniques such as changing system settings and using different parameters. Troubleshooting was essential to complete the network correctly and to accomplish the objectives.

Low Voltage (LV) network: The LV network was not available in the DINIS model of Ergon Energy. LV network information was available in the Google Earth GIS model, which was the total LV load in a node. Due to this limitation the LV network was integrated into the HV network model by using the LV distribution transformer (11kV/415V). The LV load, energy storage and RE were connected on the secondary side (LV side) of the DT.

After fixing all errors during the conversion process and completing simulation settings, latitude and longitude data was added to the Rockhampton Power network so as to position the model in the right geographical location as shown in Figure 4.14. Figure 4.15 shows the Rockhampton city in Google Earth that ensures the developed network is rightly aligned in its geographical position. Figure 4.16 shows the Rockhampton power network in Google Earth.

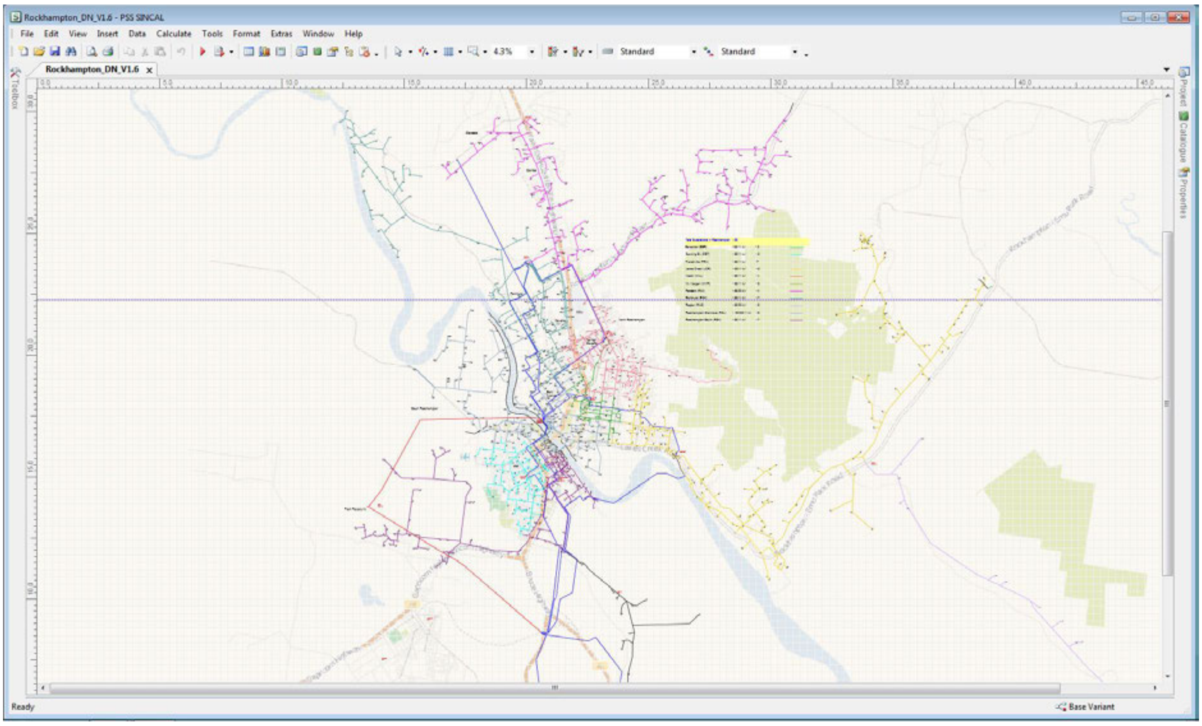

Figure 4:14 Developed Power Network Model of Rockhampton with GIS information

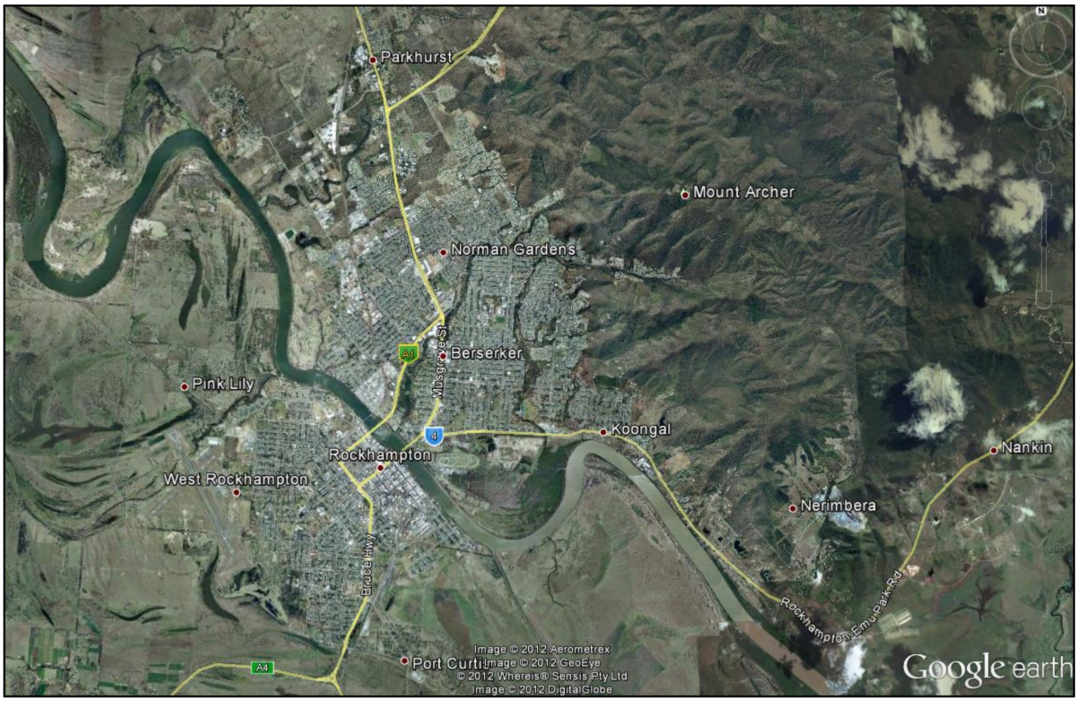

Figure 4:15 Google Earth Map showing Rockhampton City

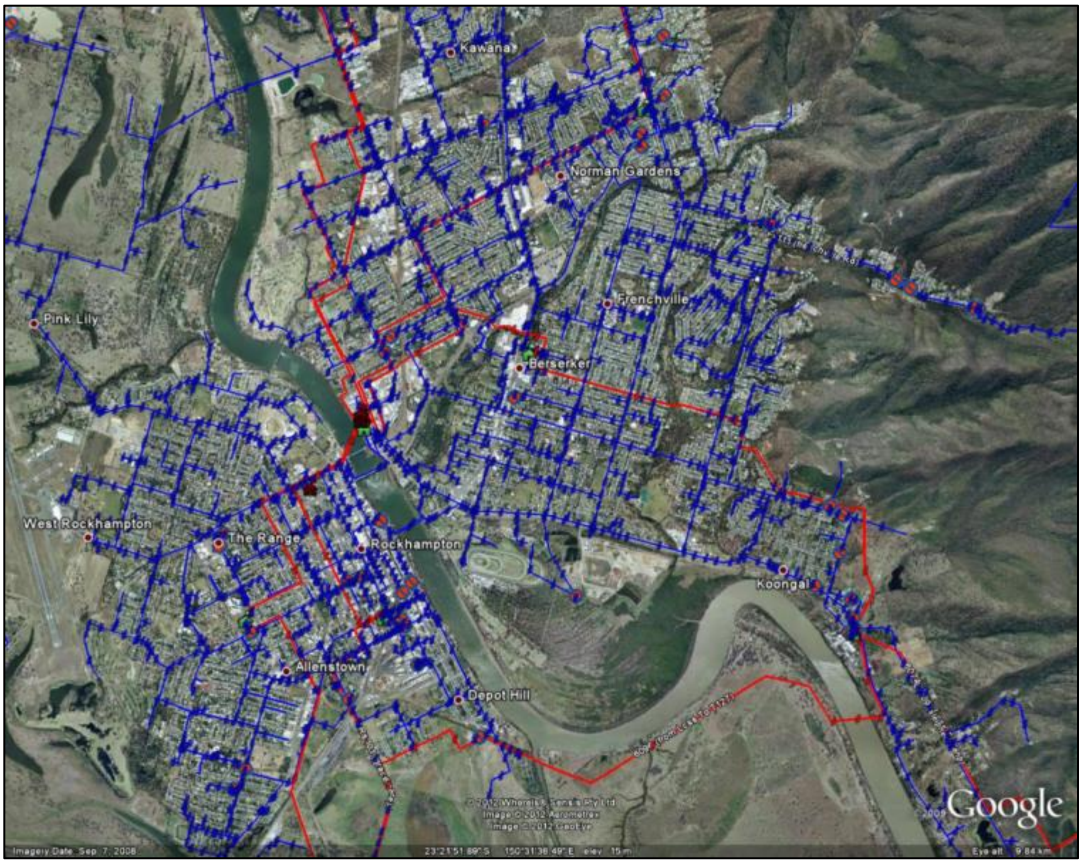

Figure 4:16 Rockhampton Power Network in Google Map

The process of the development of the Rockhampton network model is illustrated in Figure 4.17. It also indicates the stage where impacts can be analysed.

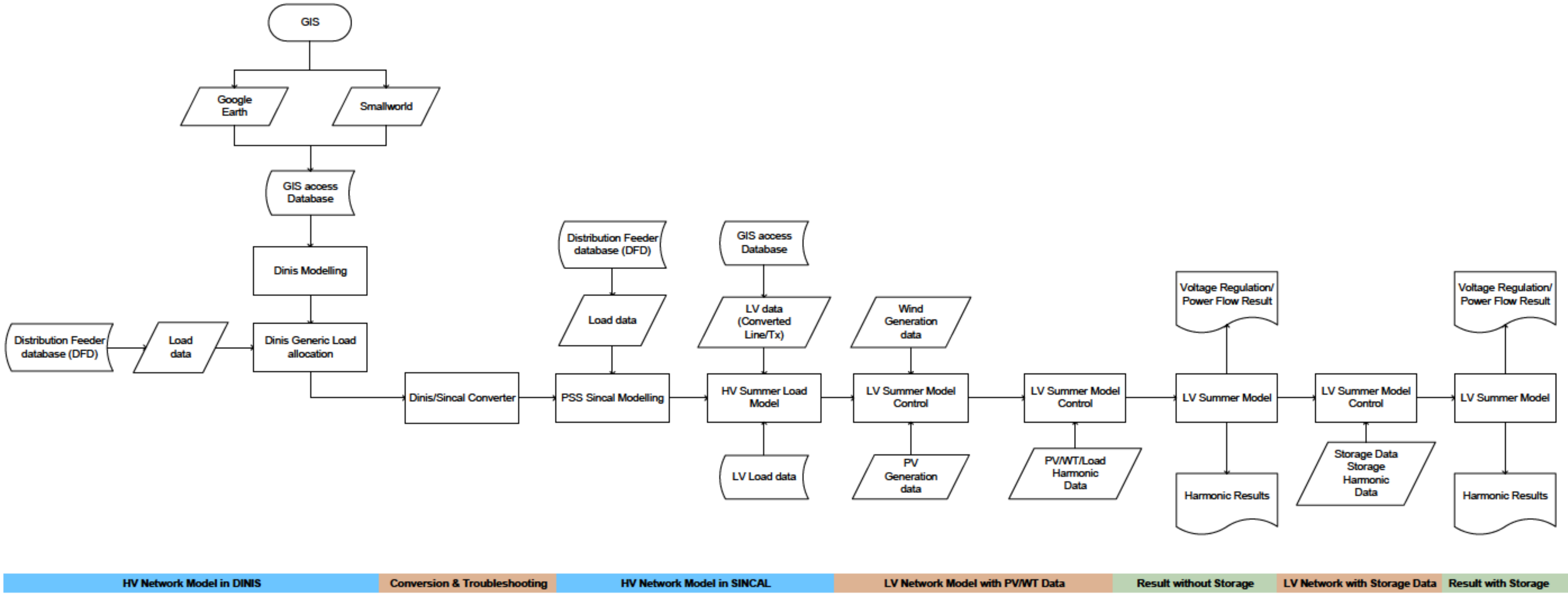

Figure 4:17 Network development process

The following section describes the network building steps, model considerations, controls and input settings which are essential to understand the power network developed in PSS SINCAL.

4.3 Introduction of Network Modeling in PSS SINCAL

This section describes how to develop power networks in the SINCAL environment and Figure 4.18 shows the workspace of this tool. The toolbox, menu bar, working network voltage level, result and view setting, workspace window and message window is shown in Figure 4.18.

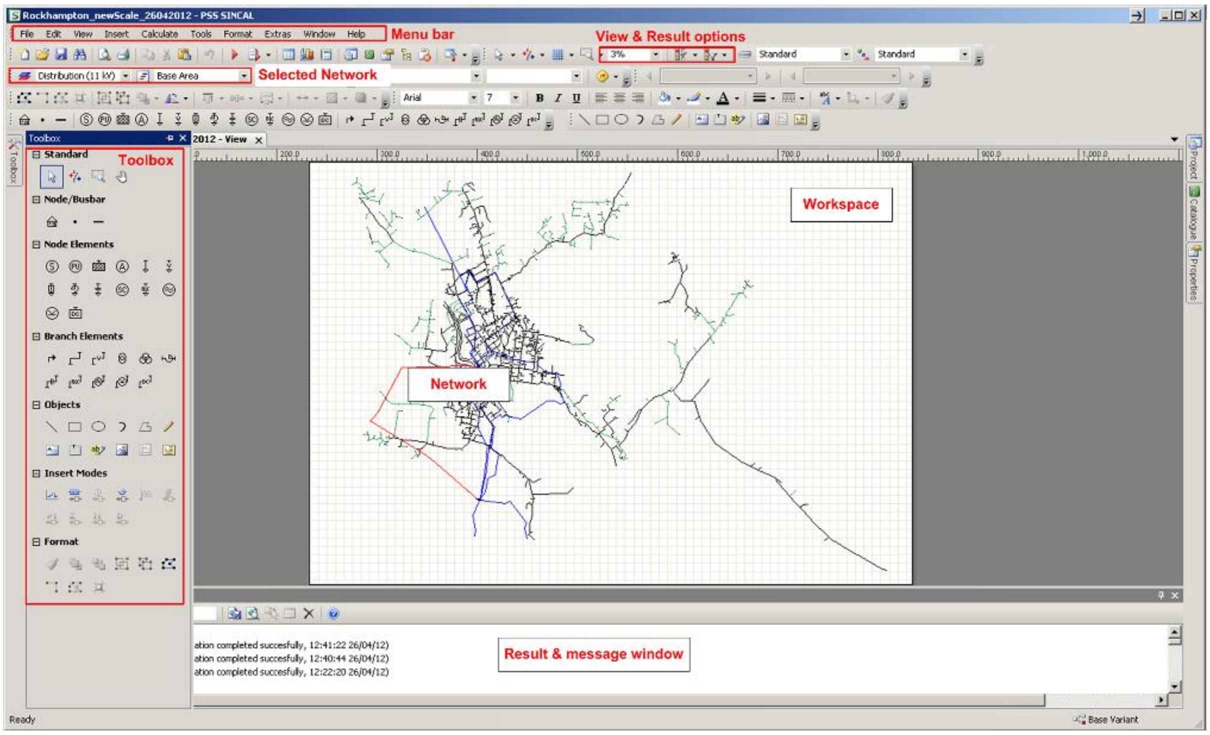

Figure 4:18 Network development space in PSS SINCAL

4.3.1 Elements for Network Development

Building a network starts with setting the network voltage level. Table 4.5 shows the voltage levels used in the Rockhampton power network; however other voltage levels can also be set if required.

Table 4:5 Network Levels

Name	Short Name	Rated Voltage (Vn)
Transmission (132 kV)	132 kV	132.0 kV
Sub-transmission (66 kV)	66 KV	66.0 kV
Distribution (22 kV)	22 kV	22.0 kV
Distribution (11 kV)	11 kV	11.0 kV

SWER (12.7 kV)	12.7 kV	12.7 kV
Low Voltage (415 V)	415 V	415.0 V

After defining the required network level, elements were added in the workspace and connected with the proper conductor or line. Elements in SINCAL are in three groups: Node, Node element and Branch element. Line parameter includes line type, line dimension, length, resistance, reactance, capacitance, rated frequency, rated voltage, thermal current limit, zero-phase sequence data and the phase of the line.

A simple network is shown in Figure 4.19 to describe the required element and control settings. Distribution Transformer (DT) shows two voltage levels in the network. For example, it is considered that the primary side (Tx_Primary) of DT has a 11 kV voltage level and the secondary side (Tx_Secondary) has 415 V, therefore Load is connected to the LV side and the single phase voltage becomes (415/√3) = 240 V. Each of the required elements in the network is described below:

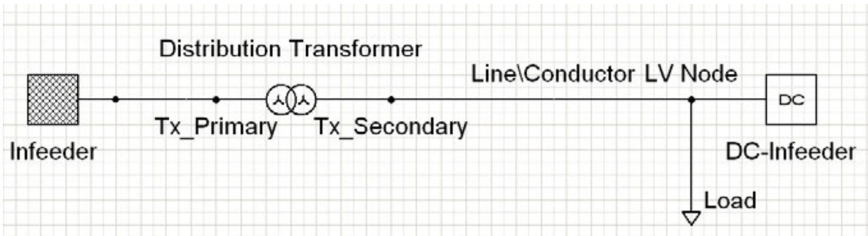

Figure 4:19 A Simple Network

Infeeder:

Infeeder is the element that describes the power input to the network. The required parameters such as minimum and maximum power, resistance and reactance, operating state, power factor and the zero-phase sequence values are required to provide as shown in Figure 4.20.

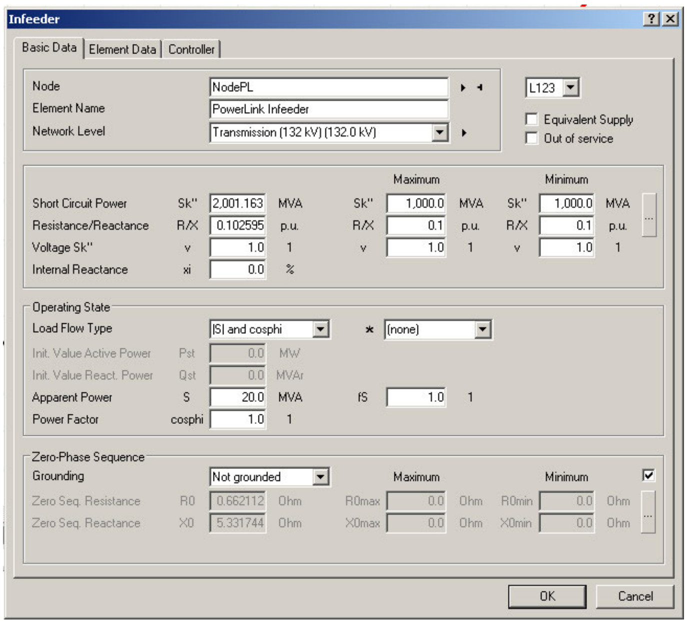

Figure 4:20 Settings for Infeeder

Transformer:

Transformer is one of the basic components in a power network and is connected in various transmission and distribution networks. The parameters that characterise the transformer are those values such as primary/secondary voltage, rated power, short circuit voltage, vector group and the zero-phase sequence value. All the required values and phase data for each transformer are entered into the network as shown in the Figure 4.21. For the analysis of LV DN, the effects on secondary side (LV side) of DT and for HV DN, the effects on primary side of DT needs to be observed.

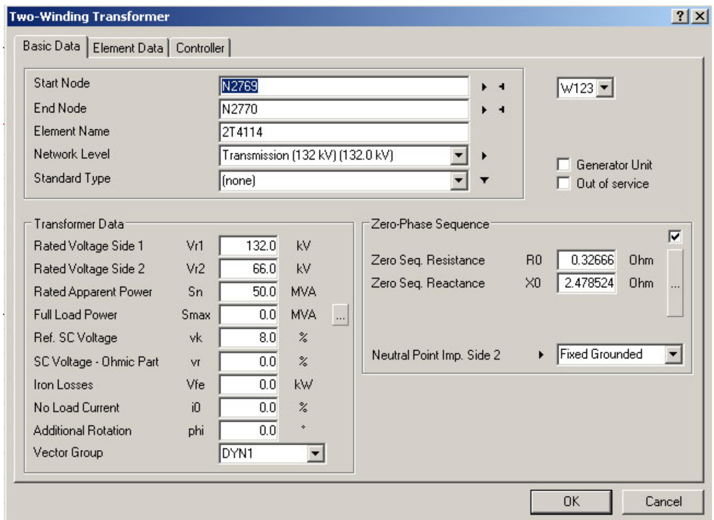

Figure 4:21 Settings for Transformer

Line or Conductor:

Conductor parameters are very important which includes type of conductor, length, impedances, operating voltage, thermal current limit, zero sequence data as shown in Figure 4.22. SINCAL has a conductor database that provides a list of conductor with all required parameters settings, however local settings can be entered. Conductor phases need to be entered according to the connected network settings. A list of conductor parameters is explained in Table 4.4 in section 4.2.2.

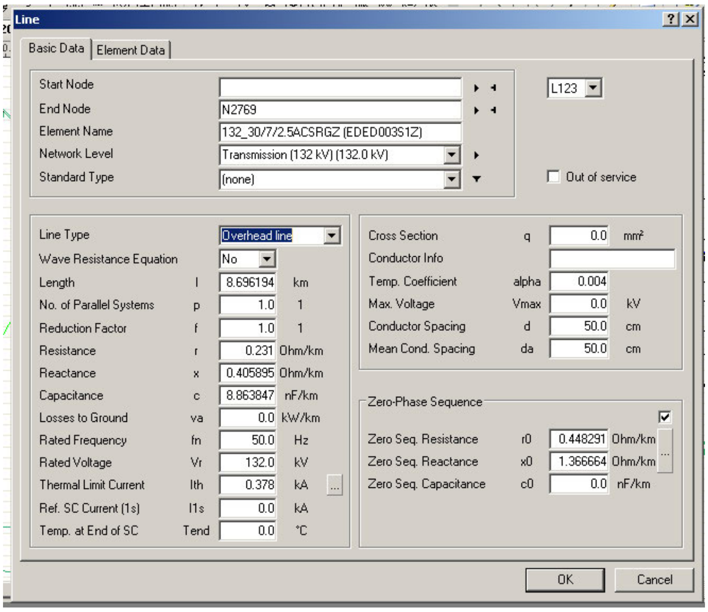

Figure 4:22 Settings for conductors

Load:

The input settings for Load type, Load flow type and Load inputs are required for simulation. Load flow types define behavior of load for load flow (LF) calculations. Load inputs can be in various formats like; (i) active power, reactive power and voltage (ii) apparent power, power factor and voltage (iii) current, power and voltage (iv) active power and current etc. and Factor can be used to multiply the load input values. Asymmetry can be entered by selecting load phase. Load profile provides time varying load data which is required for load curve (LC) calculation. Figure 4.23 shows the input setting of load element.

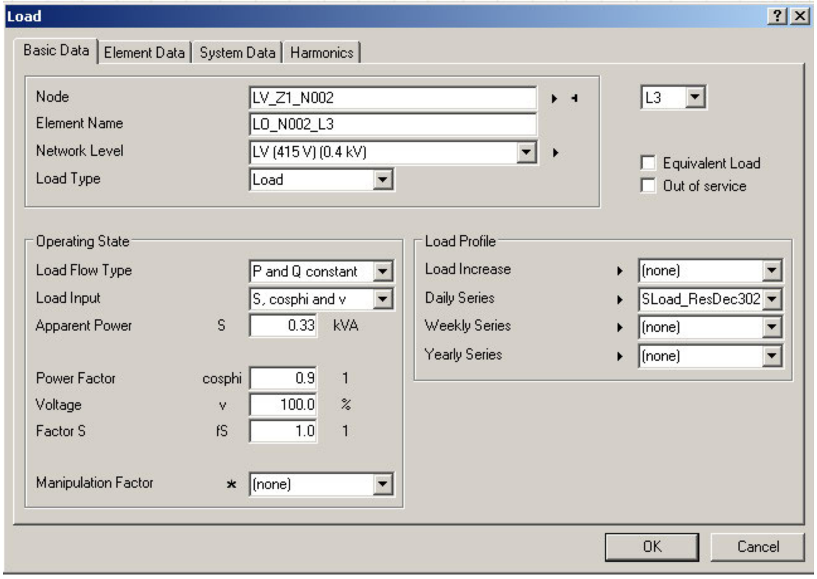

Figure 4:23 Settings for Load

DC-Infeeder:

DC-Infeeder can be a photovoltaic (PV), wind turbine or battery type as shown in Figure 4.24. SINCAL simulates DC-Infeeder as the current source for load flow calculations. As the battery works as storage therefore it can store and supply direct current (DC) during charging and discharging.

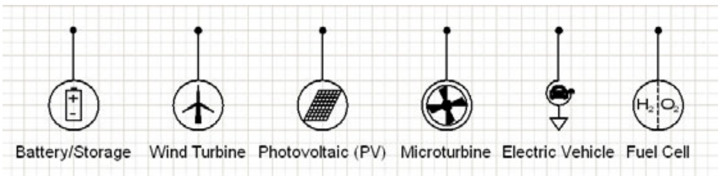

Figure 4:24 Various DC-Infeeders

When DC power is positive, the active power on the alternating current (AC) side is as shown by Equation 4.1 and when DC power is negative, the active power on the AC side is as shown by Equation 4.2 [131].

$$P_{ac} = P_{dc} * fP_{dc} * \left(1 - \frac{P_{ldc}}{100}\right) * \frac{\eta}{100} \tag{4.1}$$

$$P_{ac} = \frac{P_{dc} * fP_{dc}}{\left(1 - \frac{P_{ldc}}{100}\right)} * \frac{100}{\eta} \tag{4.2}$$

Where P_{dc} is the DC power of battery, f_{pdc} is the factor for DC power, P_{ldc} is the loss until inverter and η is the efficiency of the inverter.

The parameters of DC-Infeeder includes DC power, manipulation factor, efficiency of inverter, loss before inverter, reactive power from inverter, rated voltage of inverter, minimum and maximum voltage and connection type. Moreover daily, weekly or yearly load profile can be entered for each of the DC-Infeeder. The settings for DC-Infeeder are shown in Figure 4.25.

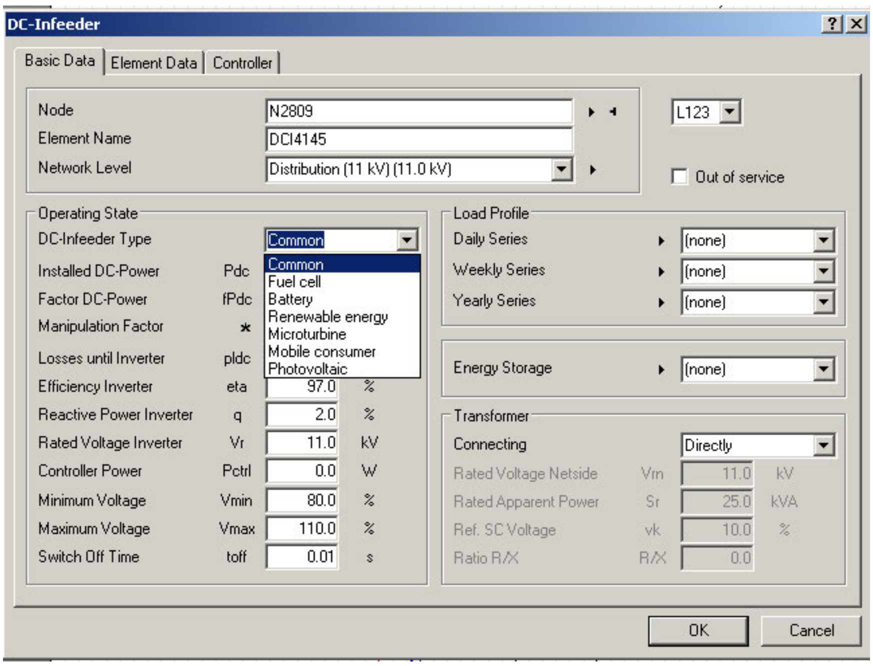

Figure 4:25 Settings for DC-Infeeder

Node/Busbar:

Nodes are the basic elements of a network. The Busbar is a special graphical form of node. All network elements are connected to the node and the branch element connects two or three nodes together.

4.3.2 Calculation Procedures

PSS SINCAL calculates currents in the network from differences in potential of nodes and the impedance between nodes. Load flow calculations calculate current or voltage between nodes. The node point equation creates the following linear Equation 4.3 [131].

$$Y * V = \overline{I} \tag{4.3}$$

where Y is the node-point admittance matrix, V is the vector of node voltages and $\overline{I}$ is the vector of feed currents.

The current vector is filled at the node points where power is added or removed before the equation is solved. SINCAL simulates removal with negative feed current. From each phase voltage, SINCAL calculates the current in the corresponding phase using Ohm's Law. If a phase is not connected, the current is zero. PSS SINCAL converts currents in phases (L1, L2 and L3) to component current using the transformation equation for currents as explained in Equation 4.4 [131].

$$\begin{pmatrix} I_0 \\ I_1 \\ I_2 \end{pmatrix} = \frac{1}{\sqrt{3}} * \begin{pmatrix} 1 & 1 & 1 \\ 1 & a & a^2 \\ 1 & a^2 & a \end{pmatrix} * \begin{pmatrix} I_A \\ I_B \\ I_C \end{pmatrix} \tag{4.4}$$

Where I_0, I_1, I_2 are currents in the positive, negative and zero phase sequence. I_A, I_B and I_C are the phase currents.

PSS SINCAL uses transformation equations for voltages to convert component voltages to the phase voltages as explained in Equation 4.5.

$$\begin{pmatrix} V_0 \\ V_1 \\ V_2 \end{pmatrix} = \frac{1}{\sqrt{3}} * \begin{pmatrix} 1 & 1 & 1 \\ 1 & a & a^2 \\ 1 & a^2 & a \end{pmatrix} * \begin{pmatrix} V_A \\ V_B \\ V_C \end{pmatrix} \tag{4.5}$$

Where V_0, V_1 and V_2 are voltages in positive, negative and zero phase sequences, V_A, V_B and V_C are the phase voltages.

The above calculation of currents and voltages is based on the universal complex transformation matrix as shown below

$$\frac{1}{3} * \begin{pmatrix} 1 & 1 & 1 \\ 1 & a & a^2 \\ 1 & a^2 & a \end{pmatrix} \quad \text{where } a = e^{j\frac{2\pi}{3}}$$

PSS SINCAL uses phase voltages and currents from the final iteration to calculate the power in all phases.

4.3.3 Calculation Method Selection

PSS SINCAL calculation methods provide the option to select desired simulation tool as shown in Figure 4.26. The purpose of this thesis requires the Load Flow (LF), Load Curve (LC) and Harmonic analysis in asymmetrical network configurations.

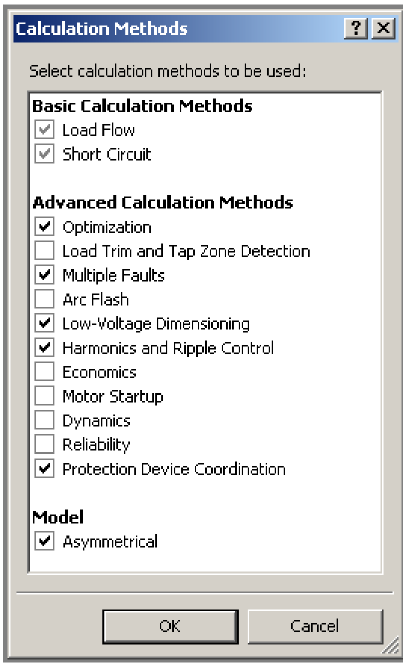

Figure 4:26 Selection of Calculation methods

Calculation settings provide the details for the choice of each of these calculation methods.

4.3.3.1 Settings for LF Calculation

Calculation settings provide the option to select the operating state. “Determine Rating” sets the reference value used to calculate the load. For this simulation “Base Rating” was selected as no additional load values are required. “Asymmetrical” setting was selected to process the asymmetrical network element. "Diagram Creation" setting was set to "Completely" for small network and "Marked" for large networks so as to view the simulation results in diagramatically. "Controller Adjustment" was set "Continuous" for controller positions from integer to any deviating point, to determine the required level easily. For all calculation methods "Zero Sequence Data" is essential and for global setting for this simulation Z_0 was set identical to Z_1 which describes that zero phase sequence data is the same as positive phase sequence data.

Figure 4.27 shows the calculation settings window for Load Flow (LF), Load Curve (LC) and Harmonic/Ripple Control settings.

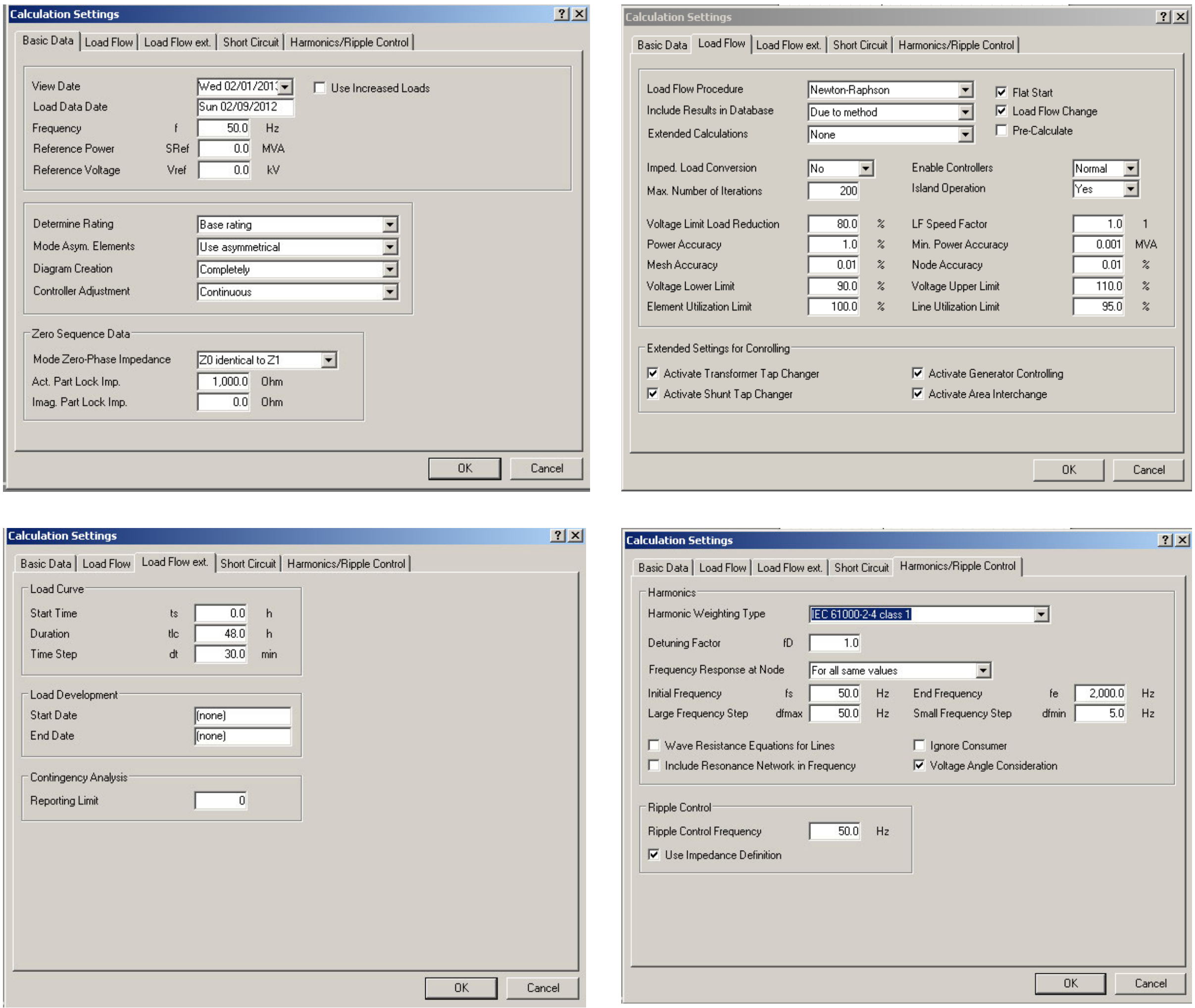

Figure 4:27 Calculation settings window

LF settings specify which simulation procedure is used for calculations. SINCAL provides "Current iteration, Newton-Raphson, Admittance matrix and Unbalanced" procedures for normal LF, biased short circuit, optimal branching, multiple faults, load curve and load development. For this simulation the Newton-Raphson procedure was used. To keep the database size small "Due to method" was selected, that store results according to the simulation method used. In "Extended Calculations" settings, "Load Factor" provides the information about the load limit of the network reached in the range of 0 to 100. "Nodal Transmission Loss Factor" provides the information on how changes in load will affect the total active loss of the network.

Turning on "Load Flow Change" allows calculations to switch between LF procedures appropriate for LF calculation and also to avoid convergence problem. Keeping the impedance load conversion settings to "No" ensures load behavior is fixed as prescribed active and reactive power independent of node voltage. Keeping the impedance load conversion settings to "Normal", converts the load behavior as an ideal impedance load and consumed power changes quadratically with the voltage.

By setting "Enable Controllers" to "No" allows variable network elements only with preset initial values. Setting this to "Normal" enables controller that control network elements within a preset range. Setting this to "Extended" enables addition control function to ensure that power in the network is distributed to all available generators and loads are shaded for overvoltage or under voltage problems.

Maximum number of iteration determines the permissible iteration number to solve the LF problem. "Island Operation" field activates dynamic modeling of generators and Infeeders. This mode requires each connected sub-network should have one slack (generator or infeeder) that assures power balance.

"Voltage limit Load Reduction" field prescribes voltage limit from which load is dynamically reduced with a characteristics curve. This function requires setting the "Extended" option in the "Impedance Load Conversion" field. "LF Speed Factor" controls the convergence speed of the LF procedure and normally the acceleration factor is set to 1.0.

LF result accuracy requires Power accuracy, Min. Power accuracy, Mesh accuracy and Node accuracy field values to be set. If network condition is within the set value, LF results are considered valid. Power accuracy specifies the maximum permissible power fault at the node which was set to 1.0%. Min. power accuracy extends power accuracy fields for nodes with minimal consumption or feed. Mesh accuracy only used with LF calculation for current iteration. Node accuracy sets maximum difference in voltage for nodes between two LF iterations.

Voltage Lower Limit and Voltage Upper Limit specify the permitted voltage range. Element Utilization Limit and Line Utilization Limit control the permitted load limit for the load flow.

"Extended Settings for Controlling" works only if the Enable controller field is not set to "No". Activate Generator controlling enables controlling for synchronous machine and DC-infeeders.

Additional settings for Unbalanced LF Calculation:

This calculation method calculates networks with asymmetrical equipment and asymmetrical transmission elements. Asymmetrical simulation of the network is necessary and requires negative and zero phase sequence data as well as positive phase sequence data. By modifying connection type, individual symmetrical networks become asymmetrical networks.

PSS SINCAL uses symmetrical components to calculate unbalanced load flow. Lines, transformers, coils etc. have series admittance. Consumers, motors, shunt reactors etc. remove current from the network at their nodes. Generators, infeeders etc. feed current into the network at their nodes. If they have constant power SINCAL treat them like consumers.

Asymmetrical load with grounded neutral point or one-phase grounded load only exists in network with four conductors. Zero-phase sequence data are required to enter the fourth conductor. Transformer and generator neutral points close the current through the fourth conductor. Zero-phase sequence data are required for successful asymmetrical load flow calculations.

Network elements can be defined for unbalanced data by assigning the elements connection type. Initially all elements connection type set as symmetrical (all phases) which can be set to asymmetrical by changing connection phasing as shown in Figure 4.28.

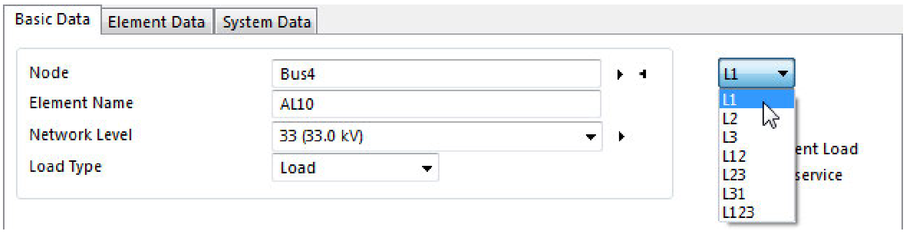

Figure 4:28 Element connection (Phase) settings

4.3.3.2 Settings for LC Calculation

Load curve are load flow calculations with load values that can be modified over time. In addition to their rated values, loads are assigned with load profiles. Load Flow extension tab describes the settings for load curve calculation as shown in Figure 4.27. Start Time and Duration determine the time period for LC calculations. SINCAL performs LF calculations during this period with given Time Step.

LC calculation determines the LF in low voltage distribution network while considering (a) Load profiles, (b) Consumer simultaneity (c) Consumer data for each consumer connection. This assures that load in the network is calculated more exactly and the LC calculation is based on detailed network analysis.

4.3.3.3 Settings for Harmonics Calculation

Harmonic calculation is an effective tool for calculating the following in the electrical transmission and distribution networks:

- Network inlet impedances at any point in a network
- Coupling impedances between any two points in a network
- Harmonic voltage and current distribution

In PSS SINCAL, Harmonics calculates network impedance between a defined starting frequency and an end frequency with frequency step. SINCAL calculates load flow to determine the load current for the harmonic calculations. Supplementary data is required for Harmonics calculations. Voltage source or Current source assigns harmonic voltage and harmonic current at the respective frequency.

4.3.4 Model Simulation and Results

After completing network development and setting all control parameters, the network was run for iterative methods for LF, LC or Harmonics calculations.

Simulation results show the calculation summary in the message window as shown in the Figure 4.29. Warning message indicates about the input data is out of range, which helps to correct the settings of the model. Finally the result can be found in tabular form from database and LC result in graphical form. Harmonic calculation results can be found in tabular form and in graphical form. However tabular form result can be exported for further analysis using other applications

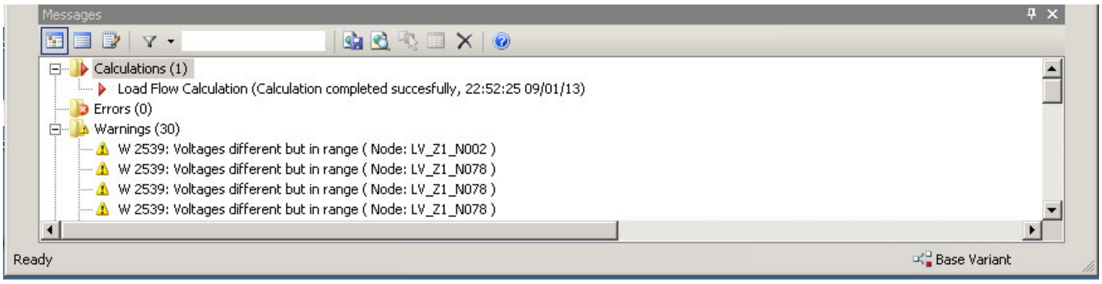

Figure 4:29 Calculation summary window

4.3.5 Standard Limits to Analyse Results

As discussed earlier in chapter 2, there is greater risk in terms of power quality when large scale RE are integrated with the power network, particularly solar and wind energy. Several literatures explained the advantages of energy storage but there is lack of research and demonstration work in integration of large scale storage into the network. The power network of Rockhampton neither experienced large penetration of RE nor large integration of energy storage. However the large integration of distributed generator (DG) is expected in this network to overcome the challenges of GHG emission from conventional energy sources. Therefore this thesis investigated two main power quality indexes (Voltage regulation and harmonics) with large integration of RE with Energy Storage into the power network of Rockhampton.

4.3.5.1 Voltage Regulation

Voltage regulation (VR) is the ability of a system to provide nearly constant voltage level with a wide range of loads. VR can be expressed by Equation 4.6 [132]:

$$VR(\%) = \frac{|V_{NL}| - |V_{FL}|}{|V_{FL}|} x100\% \tag{4.6}$$

Where V_{NL} is the voltage at no load, V_{FL} is voltage at full load. A smaller value of V_R is more beneficial. There are standard limits for V_R to maintain PQ. However there are some difference in voltage variation limits among different standards [12].

AS 60038 Standard [82] describes that, at PCC inverter should supply nominal voltage of 230 V AC for single phase line to neutral and 400 V AC for three phase line to line with a tolerance of +10% and -6% at a frequency of 50Hz. The utilization voltage range is +10%, -11%. However, AS 61000.3.100-2011 [84] provides the limits of steady state supply voltage at the customer connection points for LV (230 V nominal) system as give in Table 4.6.

Table 4:6 LV (230V) Steady state Voltage limits [84]

Steady state voltage measure (10 minutes r m.s)	Voltage limit (P-N)		Voltage limit (P-P)		Single phase 3 wire, centre neutral limit (P-P)	
	Min	***Max***	***Min***	***Max***	***Min***	***Max***
$V_{1\%}$	216V	-	376V	-	432V	-
$V_{99\%}$	-	253V	-	440V	-	506V

AS 4777-2005 standard [21] provides voltage and frequency limits as shown in Table 4.7, for inverter ratings up to 10 kVA for single phase and 30 kVA for three phase DG units to inject electric power to the DN.

Table 4:7 Voltage and frequency limits [21]

Voltage	Voltage limits	
	Single phase	***Three phase***
V_{min}	200 - 230V	350 - 400V
V_{max}	230 - 270V	400 - 470V
Frequency	**Frequency limits**	
f_{min}	45 - 50Hz	
f_{max}	50 - 55Hz	

Energex and Ergon Energy Standard [22], in Queensland, Australia set the nominal voltage and maximum allowable voltage range for voltage regulation as shown in Table 4.8.

Table 4:8 Voltage Ranges and maximum allowable variance [22]

Nominal Voltage	Maximum allowable variance
<1 kV [133] (240V Phase to Neutral 415V Phase to Phase 480V Phase to Phase)	Nominal voltage ± 6%
1 kV - 22kV	Nominal voltage ± 5%
22kV	Nominal voltage ± 10%

Photovoltaic Planning Criteria by Ergon Energy [23] allowed 1% voltage rise at 240V base voltage due to the PV energy system at PCC. Operation of a Wind turbine (WT) may affect the steady-state voltage in the connected network [134]. Operation of solar PV can increase voltage at the connected node during maximum generation time although it depends on the load profile. An installation of multiple WT may be assessed assuming its output power at the PCC [134]. Load flow analysis can assess this effect if WT bring the magnitude of voltage outside the required limit.

Voltage Unbalance:

Voltage unbalance is regarded as a significant PQ problem at the electricity distribution level. In a balanced sinusoidal system, the three phase-to-neutral voltages are equal in magnitude and phase difference from each other is 120 degree. Any difference in that magnitude and/or phase causes system unbalanced. Voltage unbalance is caused by unequal system impedances and unequal distribution of single-phase loads [135]. There are growing concerns, as the increased penetration of single phase DG can overload one phase by unloading other phases which is the common cause of an unbalanced system. Energex and Ergon Energy Standard [22], sets limit for voltage unbalance as shown in Table 4.9.

Table 4:9 Voltage Unbalance [22]

Nominal supply voltage	**Voltage Unbalance**			
	No contingency event	***Credible contingency event***	***General***	***Once per hour***
	30 min average	***30 min average***	***10 min average***	***1 min average***
>100 kV	0.5%	0.7%	1.0%	2.0%
10 kV - 100kV	1.3%	1.3%	2.0%	2.5%
<10kV	2.0%	2.0%	2.5%	3.0%

LF analysis can provide the phase voltage and angle to identify the voltage unbalance condition.

4.3.5.2 Harmonics

Harmonics are the frequencies that are integer multiples of the fundamental frequency. The ratio of the harmonic frequency to the fundamental frequency is the harmonic order. Harmonic distortion in voltage or current waveform differs from that of an ideal sinusoidal waveform and produces waveform distortion. Power system harmonics is receiving a great deal of attention due to the increased portion of non-linear loads or generating sources connected by inverters. Harmonics due to single phase distorting loads spread across the three phases and excessive level of harmonics can overloading and overheating the neutral conductor [24] and also can cause frequency resonance [136]. Harmonic currents injected into the supply system can cause harmonic voltages to rise [137].

A common term that is used in relation to harmonics is total harmonic distortion (THD). The ratio of the r.m.s. value of the sum of all the harmonic components up to a specified order (h) to the r.m.s. value of the fundamental component is termed as total harmonic distortion and expressed by Equation 4.7 [137].

$$THD = \sqrt{\sum_{h=2}^{H}\left(\frac{Q_h}{Q_1}\right)^2} \tag{4.7}$$

where Q represents either current or voltage, Q_1 is the r.m.s. value of fundamental component, h is the harmonic order, Q_h is the r.m.s. value of the harmonic component of order *h* and *H* is the highest order depending on application.

The above equation can be written for current or voltage signal using Equation 4.8 and 4.9[12]

$$THD(i) = \frac{\sqrt{i_2^2 + i_3^2 + i_4^2 + ... + i_{h-1}^2}}{i_1} \tag{4.8}$$

$$THD(v) = \frac{\sqrt{v_2^2 + v_3^2 + v_4^2 + ... + v_{h-1}^2}}{v_1} \tag{4.9}$$

where i_1 and v_1 are the fundamental component of currant and voltage and i_h and v_h are the harmonic components.

High level THD can cause thermal effects on motors, transformers and capacitors causing excessive heating and overloading of the neutral, as well as disturbance of electronic equipments. High penetration of RE in LV-DN can cause single phase loading and leads to the introduction of harmonics. Moreover inverters and its switching are a possible source of harmonics.

Harmonic emission level:

The harmonic emission level into the power system is the magnitude of the harmonic voltage or current vector at each harmonic frequency, which is caused by the considered (RE) installation at the point of evaluation (POE). POE can be the point of connection (POC) or the point of common coupling (PCC) of the installation that introduces harmonics. Harmonic emission vector (U_{hi}) results in increased levels of harmonic distortion on the network ($U_{h(post\text{-}connection)}$) as shown in Figure 4.30. Actual harmonic voltage or current at any point on a system is the result of the vector sum of the individual harmonic components of each source [137].

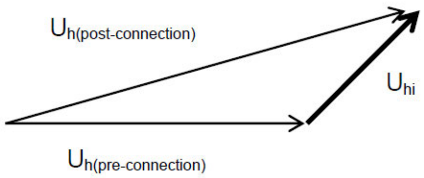

Figure 4:30 Emission vector (U_{hi}) and its contribution to the measured harmonic vector [137]

Harmonic emission should be less than the emission limit set in relevant standard and clauses as discussed below. The significant harmonics (above fundamental) are usually the 3rd, 5th and 7th harmonics [138].

IEEE 1547 [79] describes harmonic current injection at the PCC and shall not exceed the limit given in Table 4.10. Even harmonics are limited to 25% of the odd harmonic limits.

Table 4:10 Maximum harmonic current distortion (%)

Harmonic order (h)	h<11	11≤h<17	17≤h<23	23≤h<35	35≤h	TDD
%	4.0	2.0	1.5	0.6	0.3	5.0

For Grid connected energy systems via inverters, AS 4777-2005 [21] describes harmonic currents of the inverter and shall not exceed the limits shown in Table 4.11 and total harmonic distortion (THD) up to 50th harmonic shall be less than 5%.

Table 4:11 Current harmonic limits (%)

Harmonic order number	Harmonic current Limits (%)
Odd harmonic	
3, 5, 7, and 9	4%
11, 13 and 15	2%
17, 19 and 21	1.5%
23, 25, 27, 29, 31 and 33	0.6%
Even harmonic	
2, 4, 6 and 8	1%
10 - 32	0.5%

Energex and Ergon Energy Standards for network performance[22] in Queensland, Australia describe voltage harmonics for the system voltages up to 35 kV as shown in Table 4.12.

Table 4:12 Harmonic Voltage (in % of nominal voltage)

Odd harmonics				**Even Harmonics**	
Multiple of 3		***Non multiple of 3***			
Order (h)	***% voltage***	***Order (h)***	***% voltage***	***Order (h)***	***% voltage***
3	5.0	5	6.0	2	2
9	1.5	7	5.0	4	1
15	0.3	11	3.5	6	0.5
21	0.2	13	3.0	8	0.5
>21	0.2	17	2.0	10	0.5
		19	1.5	12	0.2
		23	1.5	>12	0.2
		25	1.5		
		>25	0.2+1.3(25/h)		
Total harmonic distortion (THD) = 8%					

The compatibility levels of voltage harmonic are given in [137] and for long term effect THD is 8% and for very short term effect THD is 11%.

4.3.6 Input Data for the Network Model

As explained earlier, for the network model to simulate for LF, LC or Harmonics calculations, load profile for load, energy profile for solar and wind, storage size, DT size and harmonics data for inverters are required.

Load profile data is required to calculate the Load curve simulation or time varying simulation. Summer hourly load data of Rockhampton and hourly energy generated data from PV and wind turbine was used for the daily energy profile. Load profile data was entered in per unit (p.u.) value. Load profile data for load can be entered as load increases, daily series, weekly series or yearly series data.

4.3.6.1 Load Profile for Load Data

Daily load data for residential load type and commercial load type data was considered for the detailed analysis in different cases. Figure 4.31 shows the daily load profile starting from 00:00AM and ends at 23:00AM for residential and commercial load in Rockhampton.

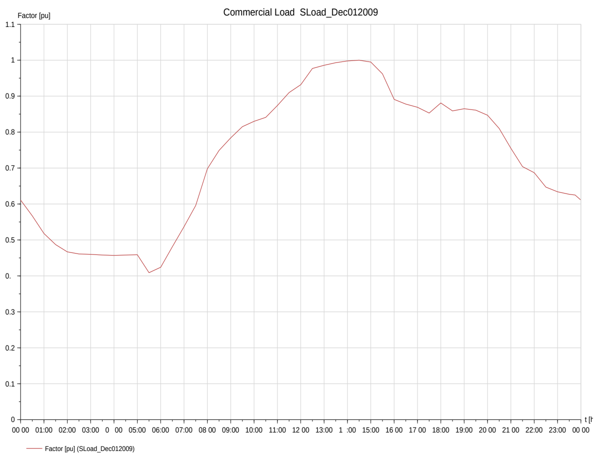

a- Commercial summer load

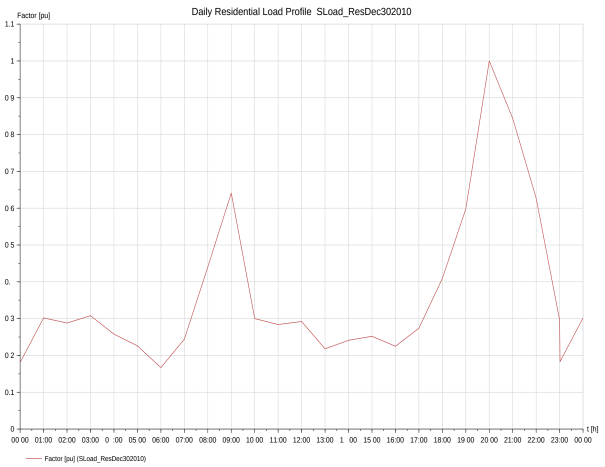

b- Residential summer load

Figure 4:31 Daily Load Profile for various load type in Rockhampton

4.3.6.2 Load Profile for Solar and Wind Energy

Daily solar PV generated energy with hourly data was entered as the energy profile for PV with PV parameter settings. Similarly daily wind turbine generated energy with hourly data was entered with the wind turbine parameter settings. Energy generation from PV and wind turbine was explained in detail inchapter 3 by using Equation 3.1 and 3.3. Various network cases considered in this chapter, solar radiation and wind speed of summer season was considered for greater energy output. Figure 4.32 and 4.33 shows the daily profile of solar and wind energy. Wind turbine rotor diameter was considered 6.2 m and tower height of 20 m and overall output efficiency was considered as 20%. However energy fluctuation was generated considering that there was deep cloud for long time and not enough wind speed for long time and the fluctuated output profile of PV and wind turbine was considered in different case configurations as shown in Figure 4.34 and 4.35.

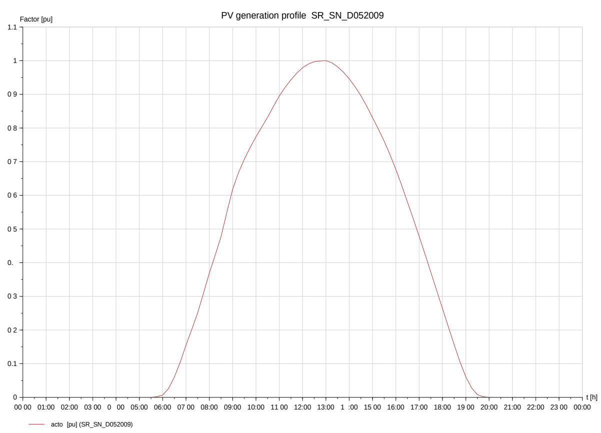

Figure 4:32 Daily PV generation profile in Rockhampton
(11/05/2010 solar radiation Data)

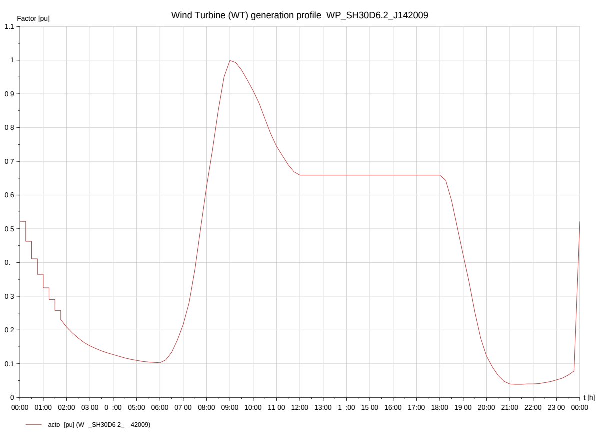

Figure 4:33 Daily Wind generation profile in Rockhampton
(14/01/2010 wind speed data)

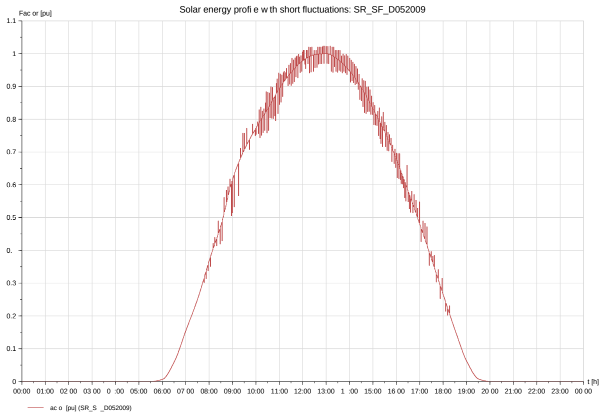

a. Continuous short fluctuation

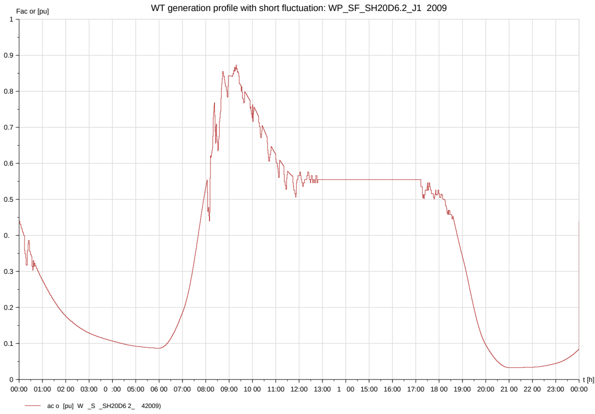

a. Continuous short fluctuation

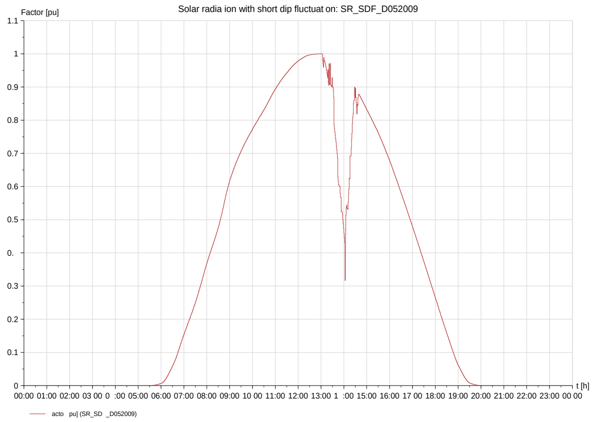

b. Short dip fluctuation

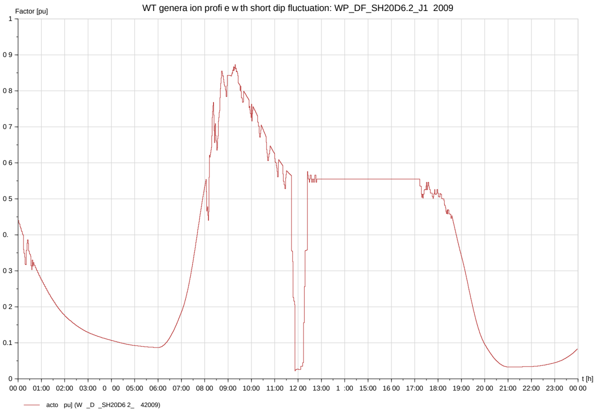

b. Short dip fluctuation

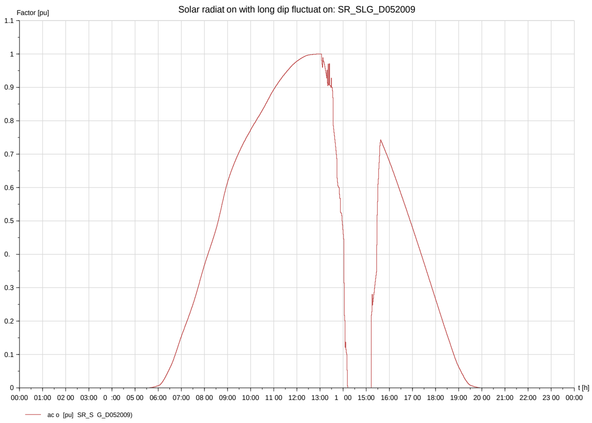

c. Long dip fluctuation

Figure 4:34 Daily PV energy generation profile with Fluctuation

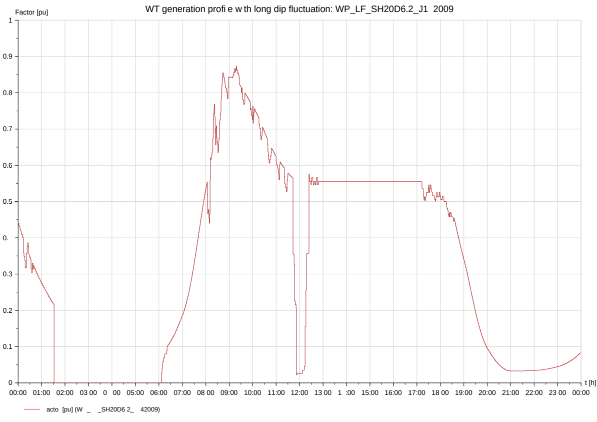

c. Long dip fluctuation

Figure 4:35 Daily Wind energy generation profile with Fluctuation

Figure 4.34 shows the different types of energy fluctuations from Solar PV due to the cloud movement. With varying size and frequency of cloud on the path of solar PV, energy generation fluctuated with continuous short interval as shown in Figure 4.34(a), dip fluctuation for short duration as shown in Figure 4.34(b) and dip fluctuation for longer time as shown in Figure 4.34(c). As the variation in size and frequency of cloud and wind speed is natural phenomena, therefore these profiles in Figure 4.34 and Figure 4.35 were created to observe impact and response of storage in the network.

4.3.6.3 Energy Storage

In SINCAL environment, energy storage is controlled by the power balance at the swing bus. If there is enough power in the network, energy storage stores it and if there is less power in the network, energy storage feeds the stored power into the network. Battery used as energy storage and additional data of storage was entered such as; level of stored energy when storage can start functioning, minimum storage (SOC) and maximum storage capacity however charging and discharging efficiency also entered into the battery/storage parameter as shown in Figure 4.36.

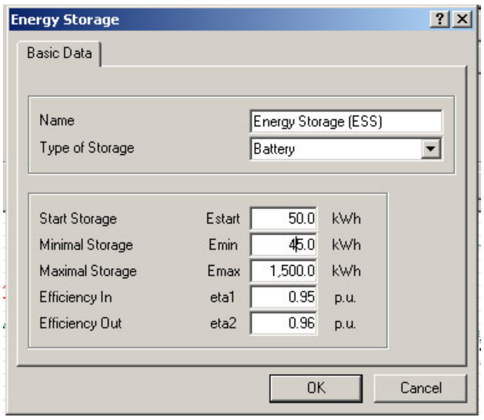

Figure 4:36 Settings for Energy Storage

4.3.6.4 Harmonics Data

To analyse harmonic effect on the network, harmonic emission of load, inverter with PV and Storage and harmonic emission data of converter for wind turbine was entered from available inverter harmonic data and considering maximum standard limits. Figure 4.37 shows the input window of harmonic current data for PV inverter.

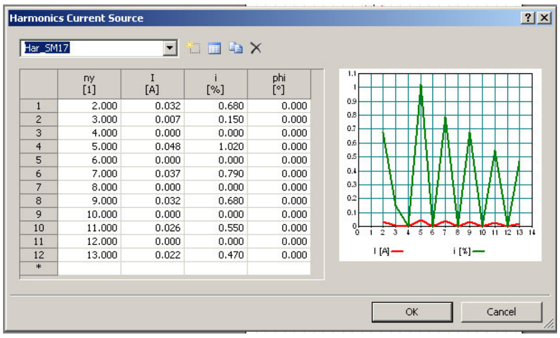

Figure 4:37 Harmonic profile window

Load or equipment is a great source of harmonic current. Equipments are classified in four groups (Class A, B C and D) for the required input current of not more than 16A/phase and their harmonic current limit is mentioned in AS/NZS 61000.3.2 [139]. Single-phase power electronic loads such as desktop computer and home entertainment equipment tend to have high current distortion compared to three-phase power electronic loads [138]. Most of the household equipments are in the class-A type and few are in the class-D type and total harmonic current distortion (THDi) for class-A and class-D equipments up to 25th harmonics is 17.27% and 17.41% respectively [139]. Considering current harmonic limits of class-A equipment, load current harmonics were scaled down to 25% for THDi of 4.30% for the analysis as shown in Table 4.13. SMA Sunny Boy SB5000TL-20 inverter current harmonics limit follows EN 61000-3-12 Class A standard and THDi is 1.08%, moreover SMA Sunny Backup SBU5000 inverter for storage current harmonics is less than 1.8% [140]. AS 61400.21 [134] , EN 50160 [141] and IEC 61000.3.6 [137] mentioned the voltage harmonics limit for LV and medium voltage (MV) network and THD is 8%. Table 4.13 and Table 4.14 shows the harmonic emission data for load, inverter with PV and storage and wind turbine. For large capacity node elements, the harmonic limit was scaled up accordingly based on the data in Table 4.13 and 4.14.

Table 4:13 Harmonic currents of load equipments [33], inverter and harmonic voltage for WT

Harmonic order(n)	**Load (class-A) harmonic current**			**Harmonic current storage inverter**		**Voltage Harmonic for wind turbine**
	Max. [In]	***Considered In[A]***	***In/Il[%]***	***In[A]***	***In/Il[%]***	***Vn/Vl[%]***
2	1.08	0.27	1.6875	0.012942	0.051689	1.2
3	2.3	0.575	3.59375	0228856	0.914052	3.0
4	0.43	0.1075	0.671875	0.005825	0.023265	0.6
5	1.14	0.285	1.78125	0.077436	0.30928	3.6
6	0.3	0.075	0.46875	0.005204	0.020783	0.3
7	0.77	0.1925	1.203125	0.054342	0.217043	3.0
8	0.23	0.0575	0.359375	0.004953	0.019782	0.3
9	0.4	0.1	0.625	0.039527	0.157872	0.9
10	0.184	0.046	0.2875	0.002827	0.011291	0.3
11	0.33	0.0825	0.515625	0.033559	0.134036	2.1
12	0.1533	0.038325	0.23953125	0.002136	0.008533	0.275
13	0.21	0.0525	0.328125	0.027398	0.109427	1.8
14	0.131	0.03275	0.2046875	0.002294	0.009162	0.258
15	0.15	0.0375	0.234375	0.021206	0.084697	0.24

16	0.115	0.02875	0.1796875	0.002799	0.01118	0.246
17	0.132	0.033	0.20625	0.019243	0.076858	1.2
18	0.102	0.0255	0.159375	0.002731	0.010907	0.234
19	0.118	0.0295	0.184375	0.024458	0.097685	1.056
20	0.092	0.023	0.14375	0.002692	0.010752	0.225
21	0.107	0.02675	0.1671875	0.030202	0.120626	0.18
22	0.084	0.021	0.13125	0.002442	0.009752	0.216
23	0.098	0.0245	0.153125	0.033581	0.134122	0.846
24	0.076	0.019	0.11875	0.004731	0.018897	0.2124
25	0.09	0.0225	0.140625	0.031494	0.125787	0.762

Table 4:14 Harmonic current for different PV inverters [140, 142]

Harmonic order(n)	SMA 1.1 KW (THD 3.02%)		SMA 1.7 KW (THD 2.16%)		SMA 5 kW (THD 1.08%)		SMA 10 kW (THD 1.0%)	
	SMA SB1100		*SMA SB1700*		*SMASB5000TL-20*		*SMA SMC10000TL*	
	In[A]	*In/Il[%]*	*In[A]*	*In/Il[%]*	*In[A]*	*In/Il[%]*	*In[A]*	*In/Il[%]*
2	0.01811	0.37	0.0421	0.56	0.0111565	0.05	0.00586581	0.01
3	0.03071	0.63	0.0488	0.65	0.19729	0.91	0.384337	0.90
4	0.01118	0.23	0.0222	0.30	0.00502145	0.02	0.0114444	0.03
5	0.05128	1.06	0.0112	0.15	0.0667554	0.31	0.0512343	0.12
6	0.002751	0.06	0.0102	0.14	0.00448591	0.02	0.00672723	0.02
7	0.05858	1.21	0.017	0.23	0.0468467	0.22	0.0625911	0.15
8	0.005867	0.12	0.0095	0.13	0.00426986	0.02	0.00813819	0.02
9	0.05597	1.15	0.0226	0.30	0.0340753	0.16	0.0666775	0.16
10	0.009943	0.20	0.0238	0.32	0.00243703	0.01	0.00570188	0.01
11	0.04988	1.03	0.0326	0.44	0.0289304	0.13	0.0705687	0.16
12	0.009146	0.19	0.027	0.36	0.00184167	0.01	0.00756474	0.02
13	0.04027	0.83	0.0478	0.64	0.0236188	0.11	0.0593798	0.14
14	0.007046	0.15	0.0252	0.34	0.00197747	0.01	0.00335702	0.01
15	0.03447	0.71	0.0567	0.76	0.018281	0.08	0.0544674	0.13
16	0.004423	0.09	0.0178	0.24	0.00241313	0.01	0.00459997	0.01
17	0.0285	0.59	0.0579	0.78	0.0165892	0.08	0.0395974	0.09
18	0.00258	0.05	0.0085	0.11	0.00235417	0.01	0.0125238	0.03
19	0.02328	0.48	0.0509	0.68	0.0210845	0.1	0.0310429	0.07
20	0.00465	0.10	0.0049	0.07	0.00232081	0.01	0.000246588	0.0
21	0.01913	0.39	0.0385	0.52	0.0260361	0.12	0.0385961	0.09
22	0.004803	0.10	0.0105	0.14	0.00210479	0.01	0.00157224	0.0
23	0.01662	0.34	0.029	0.39	0.0289491	0.13	0.0307978	0.07
24	0.003586	0.07	0.0092	0.12	0.00407872	0.02	0.00835717	0.02
25	0.01558	0.32	0.0219	0.29	0.02715	0.13	0.0350835	0.08

Network development procedure, input parameter and control settings are described in section 4.3 in order to build a power network model. The Rockhampton power network and it’s development in SINCAL is also described. Based on the above description on network development, settings and parameter values for components and input data, four different case scenarios are described below to identify the impacts on the power network.

4.4 Impact Analysis - Experiment and Software Model Investigation

In order to investigate the impacts on large networks, the initial model was developed based on the experimental settings that integrate PV into the network. An extended model was developed considering only a single distribution transformer (DT) load which is a single unit of a large network. Gradually the model was developed based on the real network data of Kawana suburb in Rockhampton. Finally the large Rockhampton power network was considered for analysis which consists of 11 zone substations that supports load through 56 distribution feeders. However, 8 ZS was considered for the model development and simulation as network data for Malchi, Mount Morgan and Raglan ZS power network was not completely available.

Control cases are designed to investigate the voltage regulation (voltage drop or rise) due to PV and wind turbine utilisation and the same with adding energy storage. Harmonic emission due to PV and wind energy utilisation was investigated and the same was investigated after adding storage. Fluctuation of generated energy from PV and wind turbine was integrated and voltage regulation and harmonic emission was investigated with and without energy storage.

The four different network configurations are described below and the modeling results are described in chapter 5 and 6.

4.4.1 Investigation-1: Experiment and Software Model Simulation

Impacts of PV integration on power networks were investigated in an experiment conducted at the Renewable Energy Integration Facility (REIF) of CSIRO in Newcastle, Australia. During the experiment storage were unavailable, therefore a similar setup was developed in PSS SINCAL and later storage was integrated as shown in Figure 4.38 and 4.39 respectively.

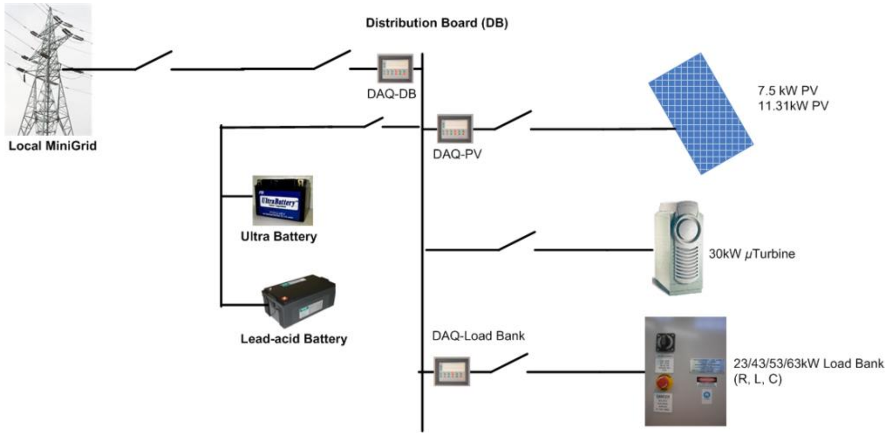

Figure 4:38 Experimental setup at CSIRO

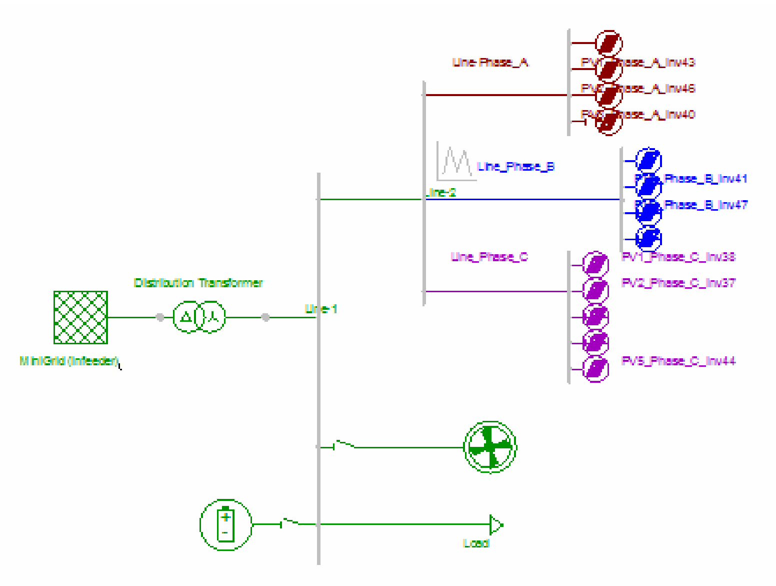

Figure 4:39 Model development mimic of Experiment Setup

4.4.1.1 Experimental Setup

Voltage regulation and harmonic emission on the network has been investigated with varying PV and varying load conditions. The REIF has rapid integration facility that can intelligently detect and solve faults on electricity systems. In its Minigrid facility 1 kW wind turbine, 30 kW gas turbine, 23 kW solar PV, 64 kW load bank and 711 kWh Battery storage (consists of Ultra Battery and Lead-acid battery) was available. For the experiment wind turbine and storage was not available. The typical connection layout is shown in Figure 4.38 considering storage is disconnected. Three distribution boards with three data acquisition systems connect up to 11.31 kW PV, upto 63 kW load and up to 30 kW micro turbine. Two experiments were conducted by integrating 7.5 kW PV and then 11.31 kW PV.

The three-phase voltage at REIF was 430V and phase voltage RMS value is 248V, therefore the voltage waveform peak was at 350V. Switching facility was used in REIF to connect PV, Load, micro turbine and storage to connect or disconnect to the network. Three data acquisition system (DAQ-DB, DAQ-PV, DAQ-Load) collects voltage and current data at 5000 samples per second at the main distribution board, at the node where all PV connected to the network and at the load connected node.

There are 13 single phase inverters (4 in phase A, 4 in phase B and 5 in phase C) of SMA 1100W and SMA 1700W was used to connect up to 11.31 kW PV. SMA is one of the leading type inverter and used with Solar PV at the CSIRO Renewable Energy Integration Facility (REIF). The total installed inverters maximum capacity is 6.2kW, 6.2kW and 6.7kW in phase A, B and C respectively.

4.4.1.2 Model Simulation Network Setup

A software model mimic to the experimental setup was developed and voltage regulation and harmonic emission was analysed. Inverter efficiency was considered to be 91.5% and losses from PV until inverter was considered such that total PV output was 11.31kW and connected with inverter in the following order as shown in Figure 4.40; however total inverter capacity was 19.1kW:

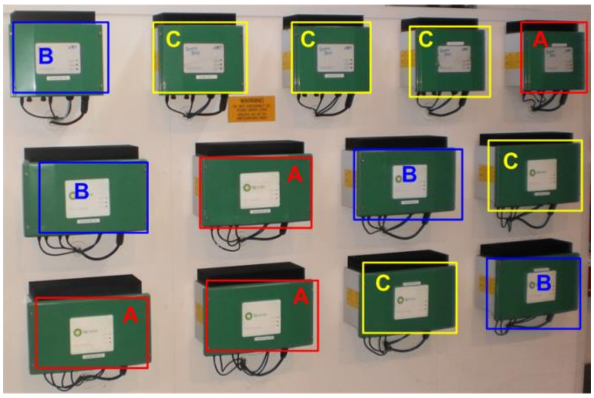

a. Connection layout of 13 inverters with phases at REIF

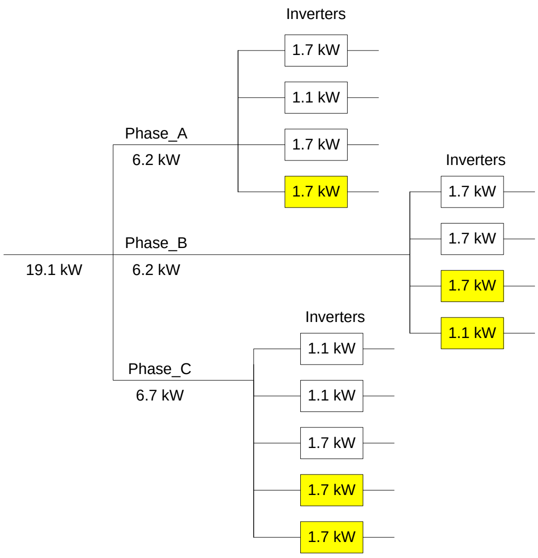

b. Connection of 13 inverter in software model

Figure 4:40 Inverter Connection Layout

PV connected in different phases as inverter in different phases was connected as shown in Figure 4.40. For total PV output of 7.5 kW, in phase-A one 1.7kW inverter, in Phase-B one 1.7kW and one 1.1kW inverter and in Phase-C two 1.7 kW inverter was switched off as shown colored in Figure 4.40 (b). Considering power factor of 0.9 the maximum load becomes (63/0.9) = 70.0 kVA therefore distribution transformer capacity was considered as 100 kVA.

Storage requires enough available power in the network and in the experimental setup PV capacity was much less than the loads demand therefore there was no available power to store. In chapter 3, estimation of required PV and storage size was explained and it was found that to support maximum load demand by PV and storage, PV capacity should be 2.05 times the total daily load demand and storage capacity is 0.8 times the total daily load demand [91]. In order to investigate impacts of storage PV capacity was increased and storage was integrated. Experimental and simulation results on Voltage regulation and harmonic emission is explained in Chapter 5 and 6 respectively.

4.4.2 Investigation-2: Considering a Small Network

Based on the findings of simulation results and experimental results, a small network was developed considering residential loads connected along a service line from a LV DT.

LV distribution network loads are connected along the distribution line and loads at the end of the line receives lower voltage and DT connects all these loads to the HV side of the network. Each DT has a specific loading or utilisation capacity. To ensure quality in power supply up to the end load, DT always operated within their safe operating limit which is set by the distribution network service provider (DNSP). Disturbance in one DT could affect all loads on the distribution line or service line.

Voltage regulation and harmonics emission due to PV, WT and Storage was analysed and a model was developed.

Model setup:

A software model was developed considering that a distribution line from DT was supporting residential load demand of a small area. Residential houses are connected to the single phase line of DN. Figure 4.41 shows road sides view of residential electricity connections from the DN in Rockhampton in Queensland, Australia. As mentioned earlier each residential house peak load demand is 1.72 kW or 1.91 kVA, considering the power factor as cosφ = 0.9. This model considered 5 such houses are connected in each phase in each node and also considered same load for each house. Therefore 15 houses are connected in each node and total of 45 houses are connected in three nodes from the DT with a total load of 85.95 kVA. It was also considered that 5 such houses installed roof top solar PV or WT in each node and connected in Node-1, Node-2 and in Node-3 as shown in Figure 4.42 in distributed connection configuration.

All three nodes are 500m apart from each other. The model was developed in PSS SINCAL indicating RE (initially solar PV and then WT) and storage was connected to the DN through an inverter. It was considered that load was uniformly distributed among three phases in each node before installing RE. Storage was integrated with the RE integrated loads to improve performance and maximise the use of RE. Initially RE (PV or WT), storage was distributed along with load and then centralised integration of RE and storage was applied. Storage is controlled by power balance at the swing bus, if there is too much power in the network, storage will charge and if there is less power available storage will discharge. Other considerations for the model are explained below:

Figure 4:41 Road side view of residential load connected from DT

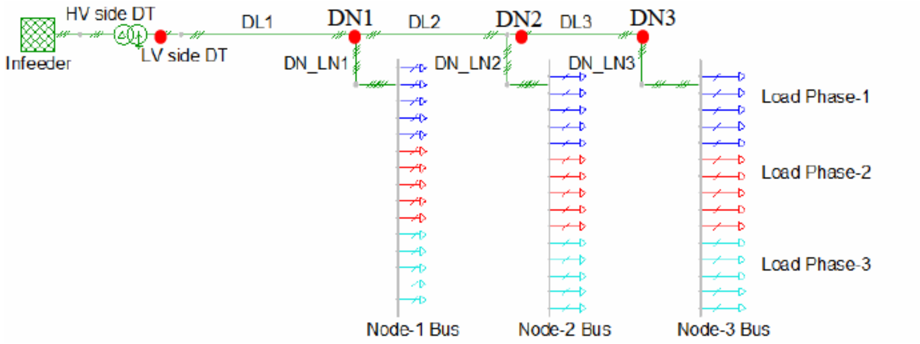

a. Load only connection configuration

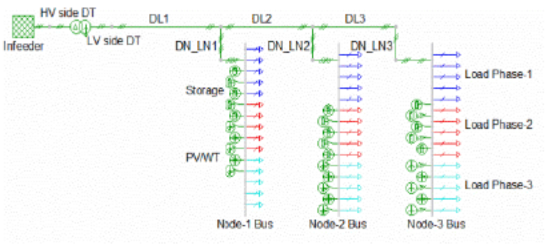

b. PV/WT/Storage - distributed connection

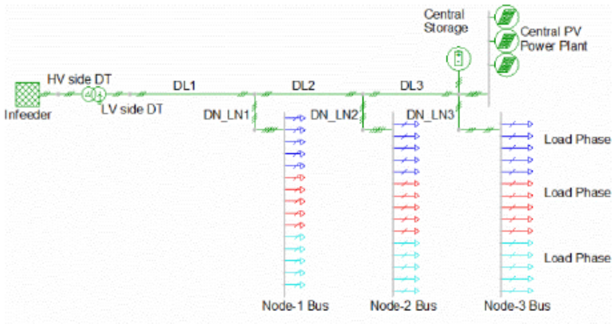

c. PV/WT/Storage - centralized connection

Figure 4:42 A small network model

4.4.2.1 Load Allocation

The average Australian household electricity use is about 16kWh/day [102]. Daily household load profile is based on the working nature of the residents and the average load pattern as shown in Figure 4.31 (b). In Queensland, Australia, peak demand generally occurs between 16:00PM to 20:00PM, when most householders return home and turn on energy intensive appliances [7].

The model considered urban area load with DT (11 kV/415 V) capacity of 100 kVA. LV residential load was considered for unbalanced load flow and time varying load profile for load curve analysis. Load allocation as shown in Table 4.15.

Table 4:15 Load allocation in three nodes

Node	Phase 1		Phase 2		Phase 3	
Node 1,2,3 (DN1, DN2, DN3)	KVA	COSΦ	KVA	COSΦ	KVA	COSΦ
	9.55	0.9	9.55	0.9	9.55	0.9

4.4.2.2 RE and Storage Allocation

Average daily residential load, solar radiation and wind speed in Rockhampton were considered in selecting the required RE capacity. Ergon Energy, the local DNSP in

Rockhampton allows 4 kW capacity of PV for each urban area house. Therefore allowed PV capacity is 210% of the peak load demand of 1.72 kW.

It was found that for the solar radiation, wind speed and residential load in Rockhampton the required daily PV output should be around 2.05 times or for WT around 1.7 times the daily load demand [91] as explained in Chapter 3. In model inverter efficiency was considered as 97% and loss until inverter was considered 5%. For this investigation, it was considered that five houses in node-1 installed 5 kW PV or WT/house, similarly 5 houses in node-2 and 5 houses in node-3. The energy profile for PV and WT is as shown in Figure 4.32 and 4.33. It was considered that storage was installed with the same peak capacity of load, which is 1.72 kW in each house where solar PV or WT was installed. Therefore from a total of 45 houses, 5 houses in each bus connected PV/WT or storage in distributed connected configuration. However in centralised connection configuration 75 kW of PV/WT and 25.8 kW of storage were connected at the end node. Table 16 and 17 shows the installed PV or WT and storage in different nodes.

Table 4:16 Installed solar PV/Wind turbine capacity in different nodes

Node	Phase 1		Phase 2		Phase 3	
	kW	No of house	kW	No of house	kW	No of house
DN1	5	5	-	-	-	-
DN2	-	-	5	5	-	-
DN3	-	-	-	-	5	5

Table 4:17 Installed Storage in different nodes

Node	Phase 1		Phase 2		Phase 3	
	kW	No of house	kW	No of house	kW	No of house
DN1	1.72	5	-	-	-	-
DN2	-	-	1.72	5	-	-
DN3	-	-	-	-	1.72	5

4.4.2.3 Harmonic Data

For harmonic calculations harmonic data of the inverter, WT and load from Table 4.13 and 4.14 were considered.

4.4.2.4 Network Parameter

The single line diagram of the network as shown in Figure 4.42 uses solar PV, wind turbine and storage to support the load demand. The service line in the network connects all the elements and integrates this small network to the large network using DT. The line parameter and DT ratings are shown in Table 4.18.

Table 4:18 Network and line parameters

Operating voltage	**415 V (line- line)/240 V (Line-ground)**
sformer ratingDistribution tran	100kVA, 415 V/11 kV
Number of customer connected	45
Line length from Transformer secondary to end load	1.5 km
Conductor resistance	0.12602 ohm/km
Reactance	0.13486 ohm/km
Zero sequence data	
Resistance	0.57 ohm/km
Reactance	1.5468 ohm/km
Capacitance	4.56 nF/km

Model was simulated in the following configurations and results are explained in chapter 5 and 6.

Case-0: Load only

Case-1: Load with Solar PV

Case-2: Load with PV + Storage

Case-3: Load with Large central PV power plant

Case-4: Load with central PV power plant + Storage

Case-5: Load with Wind turbine (WT)

Case-6: Load with WT + Storage

Case-7: Load with large central WT Power plant

Case-8: Load with central WT Power plant + Storage

4.4.3 Investigation-3: A Small Power Network in Rockhampton

In order to investigate the impacts of storage connected in the LV network, a part of the Rockhampton distribution network was considered which was developed using PSS SINCAL. The power network of Kawana suburb was considered for this analysis. The network is connected through the McLaughlin Street distribution feeder from Parkhurst 66/11kV zone substation with connected distribution transformer capacity is 13,281kVA with 1463 customers connected. Currently DTs are 41% utilised. In this network currently installed PV capacity is 95.8kW where cumulative PV panel output is 86.7kW and maximum installed single PV capacity is 4kW and total 44 customers already installed PV panels.

Model Setup:

This model is a part of the Rockhampton power network and considered only one distribution feeder that is connected from Parkhurst zone substation. Loads along the feeder are shown in Figure 4.43. Load distribution, PV and storage allocation, load profiles and harmonic information are described below.

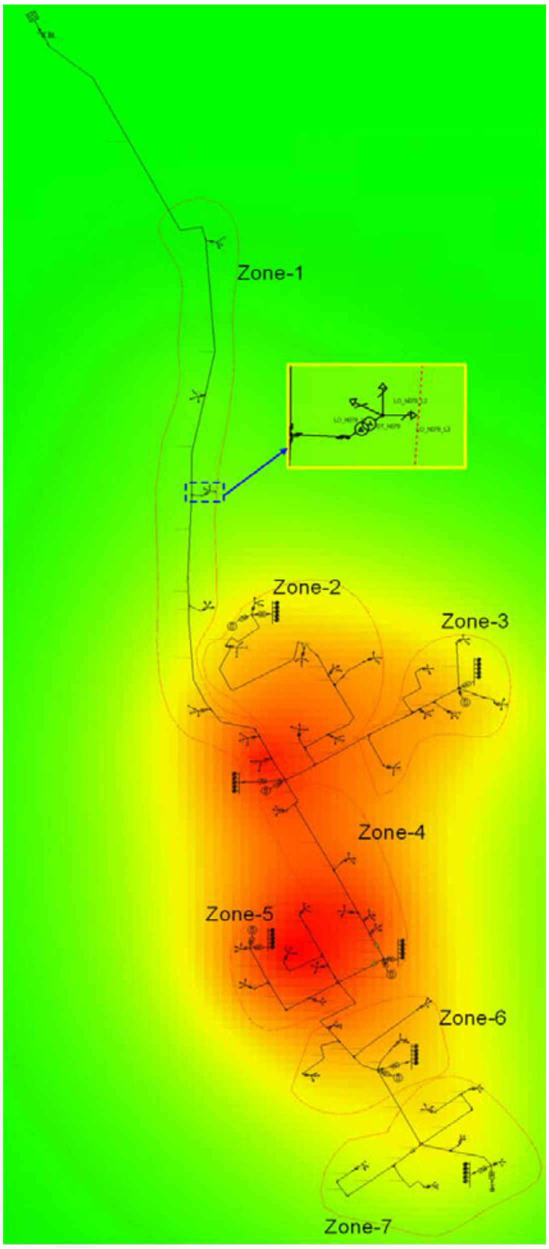

Figure 4:43 Power network of Kawana area

4.4.3.1 Load Allocation

For unbalanced load flow simulation, HV load was transformed to LV load by connecting through a LV DT which was set as 41% loaded. From infeeder to the end load, this network was divided into 7 load zones to observe impacts on different node points of the network. Table 4.19 shows the 3-phase HV side load distribution of the network.

The HV side 3 phase loads were uniformly replaced and distributed by three single phase loads connected through DT (11kV/415V) as shown in Figure 4.43; therefore zone wise load allocation remains same as shown in Table 4.19.

Table 4:19 Load distribution of the network

Zone	Load connected HV side node	Load		Total and % of load
		S[kVA]	Cos(phi)	
Z1	HV_N002	1.0	0.90	1005.722 kVA (18.48%)
	HV_N003	160.388	0.95	
	HV_N007	140	0.90	
	HV_N009	50.917	0.95	
	HV_N010	600.0	0.8	
	HV_N074	2.5	0.90	
	HV_N078	50.917	0.95	
Z2	HV_N014	50.917	0.90	763.755kVA (14.03%)
	HV_N015	50.917	0.95	
	HV_N018	152.751	0.90	
	HV_N019	50.917	0.95	
	HV_N021	152.751	0.90	
	HV_N022	152.751	0.90	
	HV_N023	152.751	0.90	
Z3	HV_N025	127.292	0.95	789.212kVA (14.50%)
	HV_N028	101.834	0.95	
	HV_N029	101.834	0.95	
	HV_N031	152.751	0.95	
	HV_N033	50.917	0.90	
	HV_N036	254.584	0.90	
Z4	HV_N038	152.751	0.80	601.052kVA (11.04%)
	HV_N040	30.55	0.95	
	HV_N041	115.0	0.90	
	HV_N042	150.0	0.90	
	HV_N043	152.751	0.90	
Z5	HV_N047	101.834	0.90	1111.004kVA (20.41%)
	HV_N049	500.0	0.80	
	HV_N051	152.751	0.90	
	HV_N052	101.834	0.90	
	HV_N055	152.751	0.80	
	HV_N056	101.834	0.95	
Z6	HV_N057	101.834	0.95	407.336kVA (07.48%)
	HV_N059	101.834	0.90	
	HV_N061	101.834	0.95	
	HV_N063	101.834	0.95	
Z7	HV_N067	101.834	0.90	763.755kVA (14.03%)
	HV_N068	152.751	0.90	
	HV_N070	152.751	0.90	

	HV_N073	101.834	0.95	
	HV_N076	101.834	0.90	
	HV_N076	101.834	0.90	
	HV_N077	152.751	0.90	

4.4.3.2 Photovoltaic and Storage Allocation

After converting all loads to single phase load, PV capacity was allocated to each node on single phase line with 20%, 50% and 100% of load rating. Similarly, storage was also allocated in 20%, 50% and 100% of load rating. To set the PV and storage capacity, inverter efficiency was also considered.

Load profile:

For load curve analysis load profile of each single phase load, daily average summer solar radiation of Rockhampton and storage capcity were considered. The load considered was the residential load of the typical summer period of Queensland Australia. Load profiles are shown in Figure 4.31 (b) and 4.32 in per unit (p.u.) value.

4.4.3.3 Harmonic Data

All loads and inverters current harmonics data were inserted into the model to calculate the harmonic emission on the DN. Present day inverter efficiency is 93% to 97% [143]. Storage is connected to the grid through an inverter and SMA Sunny-backup SBU5000 inverter THD(i) is <1.8%. Harmonic data is shown in Table 4.13 and 4.14.

Model was simulated in the following configurations and results are explained in chapter 5 and 6.

a. Distributed Integration of RE and ES:

- Load with no PV or storage installed
- Load with PV (20% of load rating)
- Load with PV and storage(20% of load rating)
- Load with PV (50% of load rating)
- Load with PV and storage (50% of load rating)
- Load with PV (100% of load rating)
- Load with installed PV and storage (100% of load rating)

b. Centralised Integration of bulk size RE and ES

4.4.4 Investigation-4: Rockhampton Power Network

Development of the Rockhampton power network was explained in section 4.2 and 4.3. Network building in PSS SINCAL and necessary settings are shown in section 4. The developed Rockhampton power network is divided under 8 zone substations as shown in Figure 4.44.

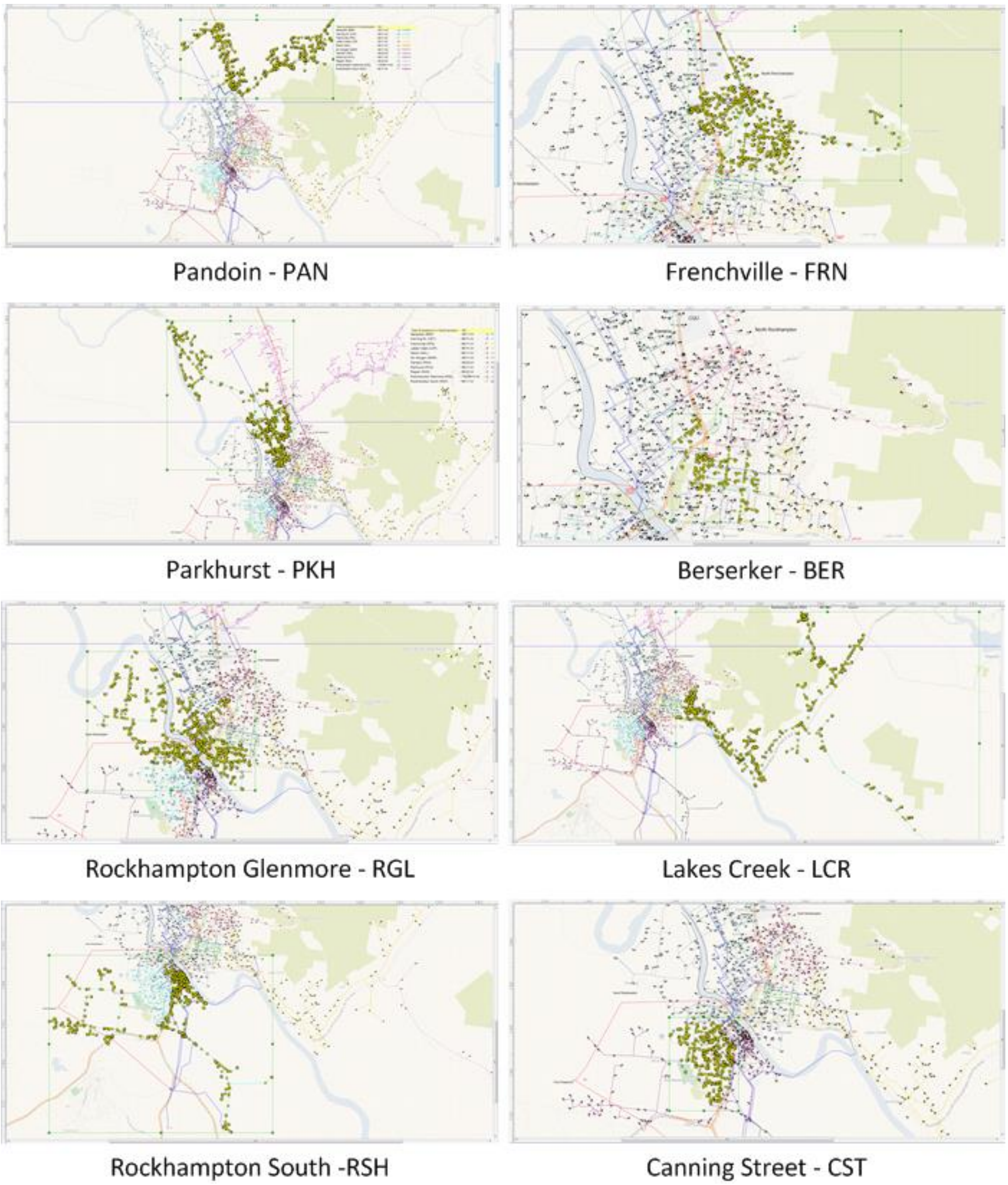

Figure 4:44 Rockhampton Power Network under different Zone substations

Main supply from Power Link connects the Rockhampton Glenmore bulk supply station (BSS) through a 132 kV line and all other zone substations (ZS) linked with BSS through 66/11 kV transformer and connects all feeders under respective ZS. From various points of the feeder, distribution transformer (DT) connect loads with the feeder. For LV loads DT supplies (11 kV/415 V) 415 V line to line or 240 V line to neutral voltage. HV loads are connected to 11 kV line from DT. RE such as solar PV and wind turbine and energy storage such as battery are connected to the LV side of the DT. Figure 4.45 shows the simple connection layout.

The impact analysis model was analysed concentrating on the longest feeder under each ZS. Voltage regulation and Harmonics calculation was done in load only, load with RE and load with RE and storage configurations. As discussed earlier, that storage stores energy only when there is enough power available in the network, therefore this analysis started considering that installed RE (PV or Wind turbine) capacity is same as load, although load profile and RE profile differs. There is total of 1,232 number of HV nodes that connects various capacity loads in the network. Total network load is 168,620 kVA. This load distribution is listed in Appendix-A. DT connecting LV loads are considered 50% loaded or utilised during peak demand.

Harmonic data for load, inverter and storage is already explained and listed in Table 4.13 and 4.14. Conductor parameters are explained in Table 4.4. Load profile for load, solar and wind energy are also explained in sections 4.3.6.1 and 4.3.6.2 as shown in Figure 4.31, 4.32 and 4.33.

The analysis was done starting from end node along the service line towards the ZS under the following configurations:

- Load only (no PV/WT and Storage penetration)
- Load with RE (with PV/WT penetration)
- Load with RE and ES (PV/WT and Storage penetration)

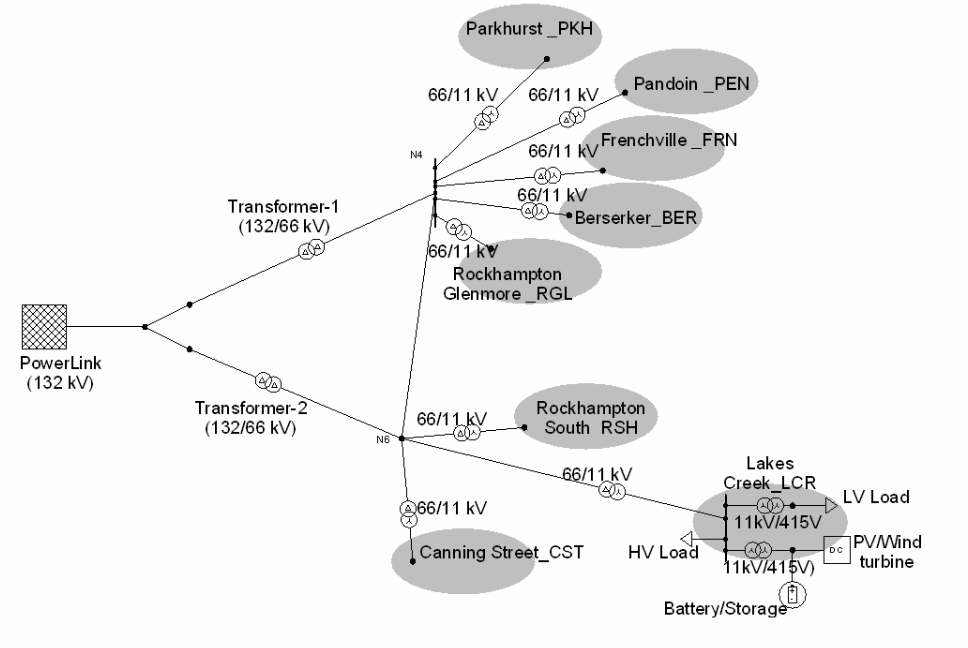

Figure 4:45 Simplistic connection layout from supply to load

The findings are explained in chapters 5 and 6.

4.5 Conclusions

This chapter explained the development of power system network along with its capacity and power quality challenges faced by utility operator Ergon Energy. Voltage regulation and harmonics are the main concerned elements associated with power quality. Thus, this investigation was required to discover the impacts of large scale RE and storage integration into the network. In order to conduct this investigation software simulation was required and the best way to achieve acceptable result is by considering a practical power network with real data. Therefore this chapter describes the development of power network in PSS SINCAL. The network development, required parameter and settings are explained. Moreover, a network model was developed based on the experimental investigation. Four different network models were developed and explain as it analyses voltage regulation and harmonics. The development of this accurate model is the first of its kind which will be very useful for the network engineers to maintain the network more reliably.

Chapter 5

Impacts of Storage on Network Voltage Regulation

5.0 Introduction

A detailed scenario on experimental setup and model setup were described in Chapter 4 considering various network sizes in order to analyse impacts of storage on power network. This chapter discusses the results of experimental and simulation work in terms of voltage regulation (Voltage drop or rise) in the network due to the integration of Energy Storage (ES) with RE into the power network. Four different cases were described in chapter 4 to investigate the impacts of integration of large scale storage and RE sources from small scale to large scale networks. This chapter describes the investigation and results of the following 4 scenarios:

Investigation-1: Voltage variation observation by

A. Experimental Investigation

B. Simulation based on experiment

(i) Without Energy storage

(ii) With Energy storage

Investigation-2: Voltage variation observation in a small distributed load network

Investigation-3: Voltage variation observation in a small Power Network in Rockhampton

Investigation-4: Voltage variation observation in a large Rockhampton Power network

Section 5.1 details the experiment and simulation results. Section 5.2 explains the investigation results of a network segment by integrating RE and storage in distributed and centralised way. Section 5.3 covers a practical network of Kawana in Rockhampton and the results are discussed. Section 5.4 covers the complete power network of Rockhampton. Results are discussed by the separate analysis of 8 Zone Substations (ZS) in Rockhampton and finally the results for the complete power network of Rockhampton are given. Conclusions are made in section 5.5.

5.1 Results and Discussion of Investigation-1

This section covers two parts; (i) results of the experimental investigation and (ii) simulation results without storage and with storage integrated configuration.

5.1.1 Result and discussion - Experimental Investigation

The experimental setup was explained in Chapter 4, as shown in Figure 5.1 (which was shown in Figure 4.38 in Chapter 4).

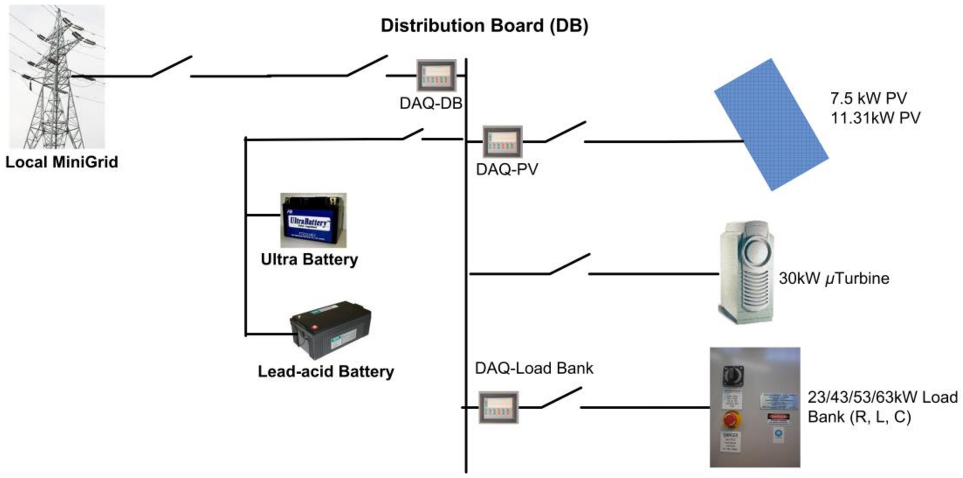

Figure 5:1 Experimental setup at CSIRO

Two experiments were conducted to observe the impacts of increased PV penetration. Phase voltage data was collected at the data acquisition systems in DAQ-DB at 5000 sample/sec for the following two experiments. PV was connected into the network in different sizes in different phases as showed in the inverter connection layout in Figure 4.40 in Chapter 4, but load was connected as 3-phase.

Experiment-1: 7.5 kW PV integration with varying load (23/43/53/63 KW)

Experiment-2: 11.31 kW PV integration with varying load (23/43/53/63 kW)

Voltage data collected from DAQ_DB for both experiments was compared with the expected voltage waveform peak value of 350V. In 3-phase line phase-to-phase voltage at REIF was 430V.

By analysing the experimental results it was found that significant voltage fluctuation occurred into the network, as well the power factor was reduced with the increase of PV penetration. In the experimental network, a maximum of 11.31 kW PV was integrated through inverter which added active power into the network. This has increased active power and reduced the share of reactive power in the network which caused to reduce the power factor. It was also observed that voltage waveform was a bit out of phase as shown in Figure 5.2 and 5.3. Voltage waveform was also not purely sine wave, as the peak has flat head which can cause harmonics into the network.

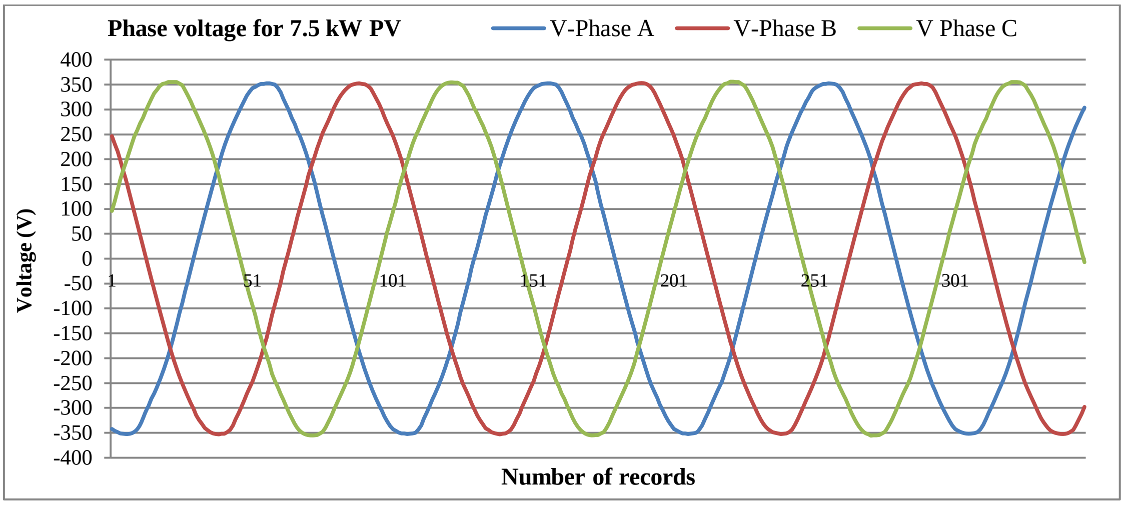

Figure 5:2 Phase voltage after integrating 7.5 kW PV with 63 kW Load in Experiment-1

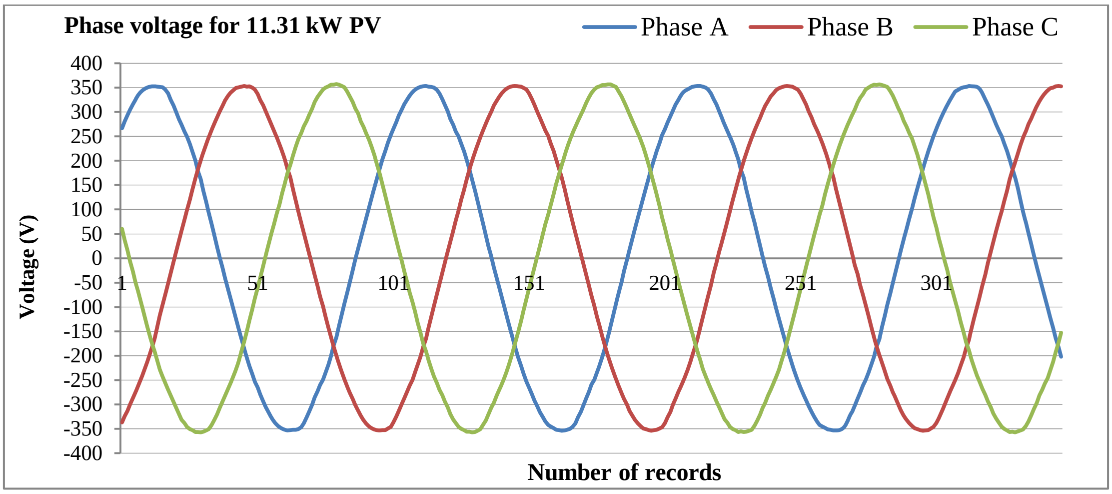

Figure 5:3 Phase voltage after integrating 11.31 kW PV with 63 kW load in Experiment-2

Figure 5.4 shows the comparison of the voltage waveform of the two experiments. It is now clear that voltage waveforms are not purely sine wave and the difference in amplitude is also clear between 7.5 kW and 11.31 kW PV integrated systems. As the PV was not uniformly distributed among phases it is therefore also clear from Figure 5.4 that the phase voltages are slightly out of phase. Voltage in phase-2 (V2) is slightly higher in 11.31kW PV integrated system than 7.5kW PV integrated system. Therefore it can be concluded that voltage increased with increased PV integration.

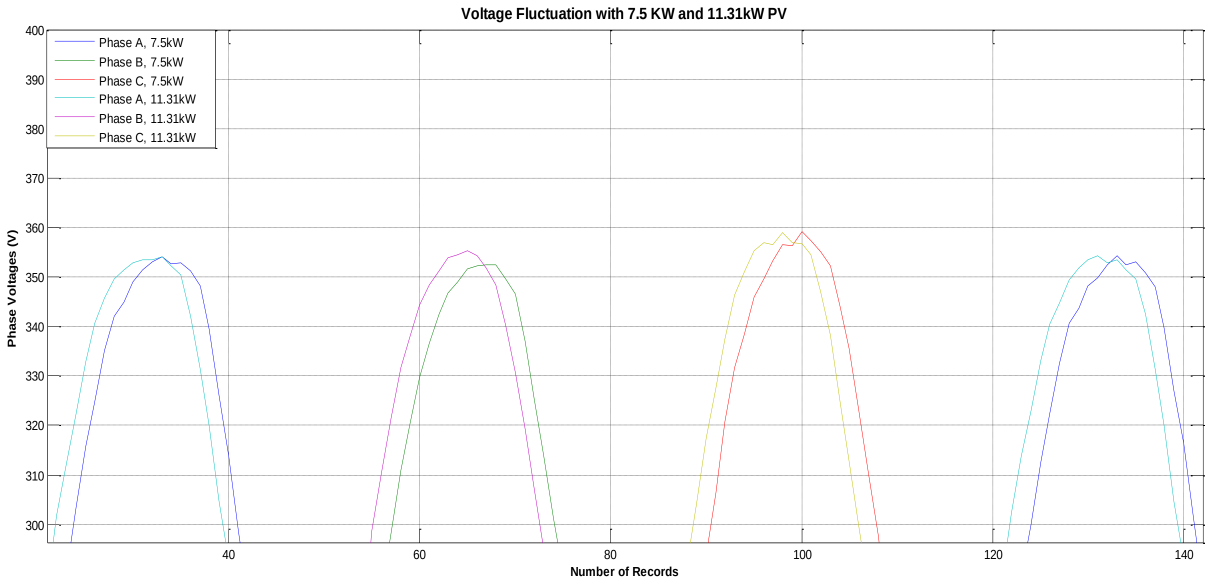

Figure 5:4 Comparison of the peak Phase voltages for 7.5kW and 11.31 kW PV integrated systems

5.1.2 Result and discussion - Model Simulation

A software model was developed in PSS SINCAL which mimics to the experimental setup as shown in Figure 5.5 highlighting the observed nodes which was also shown as Figure 4.39 in chapter 4. Three phase voltage was also considered as 430 V. PV, Load and storage connected to the network through distribution transformer (DT). The software model provides the flexibility to increase PV integration and to integrate energy storage (ES) into the network.

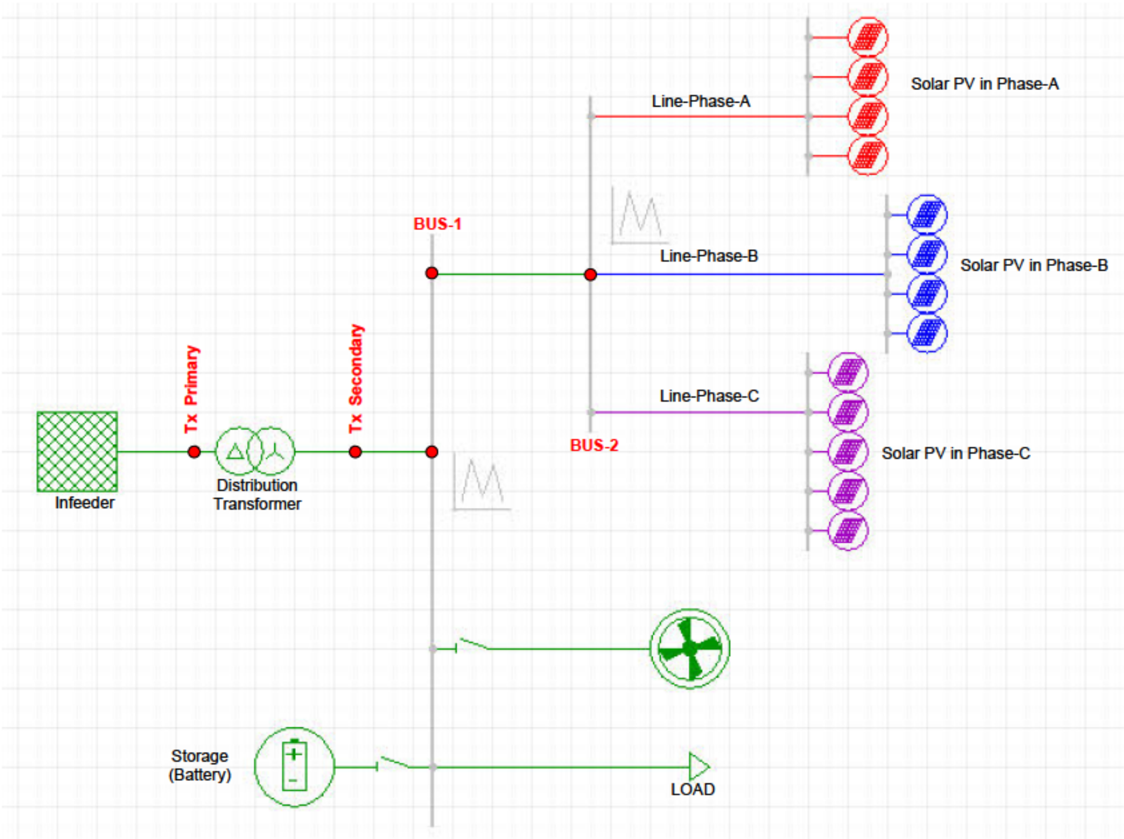

Figure 5:5 Software model mimic of experimental setup showing Observed nodes

5.1.2.1 Model without Energy Storage Condition

In the software model, solar PV was integrated in Phase-A, B and C as total installed PV capacity was 7.5 kW and 11.31 kW similar to Experiment 1 and 2. Each PV was connected to the network with an inverter. The connection layout of PV with inverter is shown in Figure 4.40 in Chapter 4. Three phase load was considered and a commercial load profile was used as shown in Figure 4.31(a) in chapter 4. The model was simulated under the following configurations and results are then compared:

- **Configuration-1:** 7.5 kW PV integration with 63 kW load
- **Configuration-2:** 11.31 kW PV integration with 63 kW load

Voltage was measured in BUS-2, BUS-1 and Tx_Secondary as shown in Figure 5.5. Load flow simulation was conducted in this experiment.

PV was connected in three different phases; therefore phase voltage is compared here. As mentioned earlier in Chapter 4 that in CSIRO three phase voltage was 430V therefore phase voltage was ideally 248.3 V. The simulation result compared the voltage regulation in three different nodes (Tx_secondary, BUS-1 and BUS-2) after integrating 7.5 kW PV and 11.31 kW PV. Comparing the phase voltage with the rated voltage (248.3 V), the voltage regulation shows that voltage increases more at the point where PV is connected i.e. at BUS-2 compared to BUS-1 and particularly phase-2 voltage or V2 was increased more in 11.31kW PV integrated condition than 7.5 kW PV integrated condition as shown in Figure 5.6. Earlier experimental results also found that phase-2 voltage increased more with 11.31 kW PV than 7.5 kW PV integrated condition as shown in Figure 5.4.

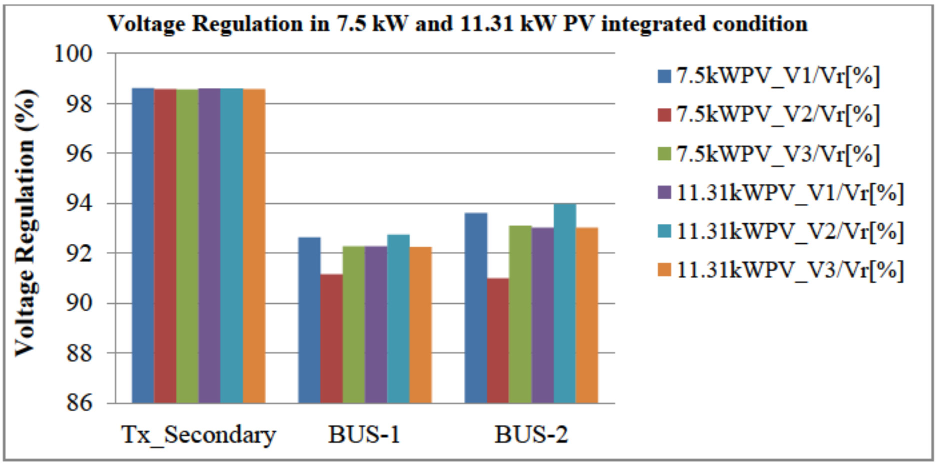

Figure 5:6 Voltage regulation comparison between 7.5 kW and 11.31 kW PV integrated condition

As the installed PV was not uniformly distributed among the three phases, the simulation result showed a phase unbalanced condition as seen in Figure 5.6. This phase unbalanced condition also changes the phase condition at Tx_Secondary node although the level of unbalanced condition is low at this node. Therefore it is clear from both the experimental and simulation result that, increased PV integration increases voltage at the point of connection or point of common coupling (PCC).

5.1.2.2 Model with Energy Storage Integrated Condition

In this case, the model was modified to investigate the impacts of adopting energy storage . The model layout is shown in Figure 5.5. It was explained earlier that storage is essential to take the benefit and for the effective use of solar and wind energy. In order to utilise storage there should be enough supply of energy as explained in Chapter 3. In such circumstances, PV daily output capacity should be 2.05 times the daily load capacity and storage capacity is 0.8 times the daily load capacity [91] for a typical residential load profile in Rockhampton, Australia. As for the commercial load of 63 kW, PV was considered 129 KW and 63 kW ES was integrated for best utilisation of PV energy and was simulated in the following configurations:

- Load Only (63 kW)
- Load with Solar PV (63 kW Load & 129 kW PV)
- Load with Solar PV and Storage (63 kW Load, 129 kW PV and 63 kW Storage)

Load profile and solar energy profile was considered as shown in Figure 4.31(a) and Figure 4.32 in chapter 4. Load flow (LF) simulation was done and voltage was measured at the LV side (Tx_Secondary) of the distribution transformer (DT) and at the point where load, storage and PV is connected i.e. at BUS-1. It was found that at BUS-1 there was a significant voltage drop in load only condition, but after adding enough PV the voltage at BUS-1 becomes more than the supply voltage, which is a risk for large scale PV integration. After adding storage, at BUS-1 voltage was dropped and at the same time improved the load side voltage and thus improved voltage regulation. Figure 5.7 and Figure 5.8 shows the voltage regulation (in percentage of rated voltage) and phase to ground voltage respectively at the observed nodes.

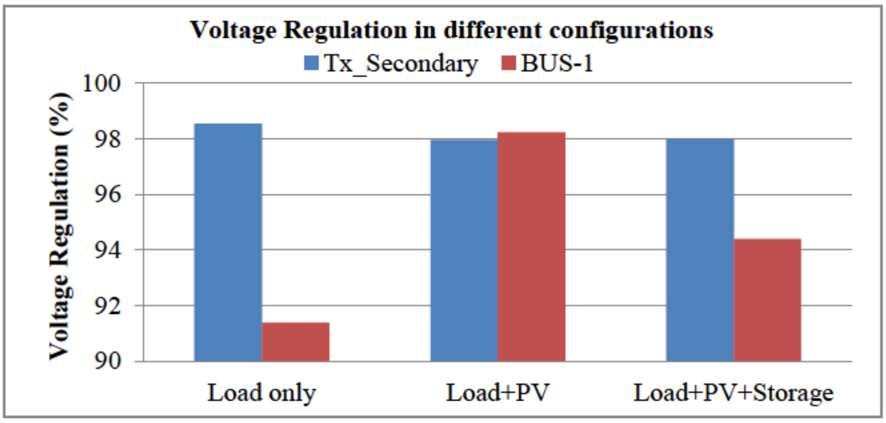

Figure 5:7 Voltage Regulations in different configurations

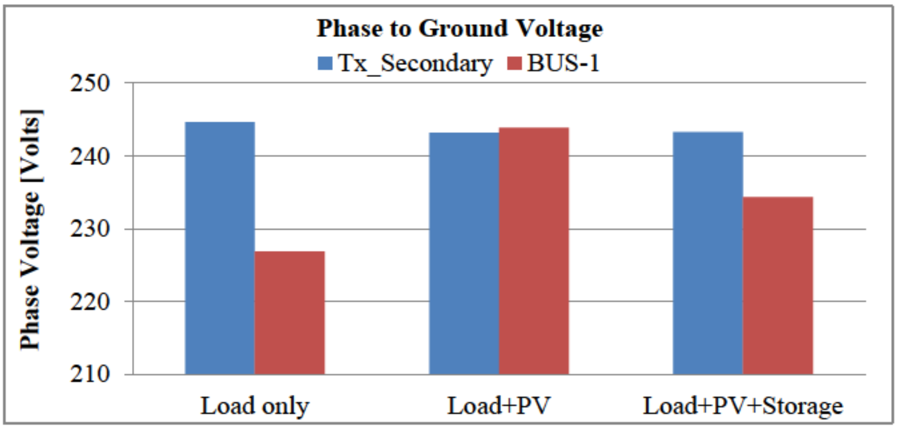

Figure 5:8 Phase Voltages in different configurations

To observe voltage variation with the load and generation profile, load curve (LC) analysis was done to view hourly variation in voltage in three configurations. In load only configuration i.e. when PV and storage was not connected to the network, at BUS-1 the voltage level drops significantly during the period 10:00AM to 18:00PM when load demand was high. Figure 5.9(a) shows the voltage profile at BUS-1 in load only configuration when the voltage level drops to 91.378% at 14:00PM.

When PV was integrated, the voltage at BUS-1 varies from 92.78% to 98.83% and maximum change/swing occurs during 08:00AM to 18:00PM as shown in Figure 5.9(b) and at 14:00PM voltage was measured at 98.10% of the rated voltage. After adding storage into the network, voltage at BUS-1 varied from 94.44% to 97.81% as shown in Figure 5.9 (c) and at 14:00PM voltage was 94.65% of rated voltage. The storage charge-discharge cycle is shown in Figure 5.9 (d).

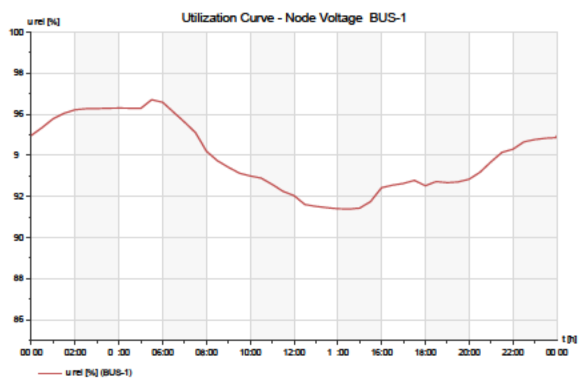

a: At BUS-1 Load only configuration

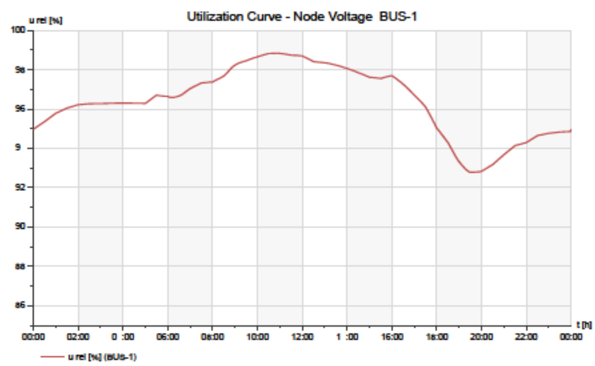

b: At BUS-1 Load with PV configuration

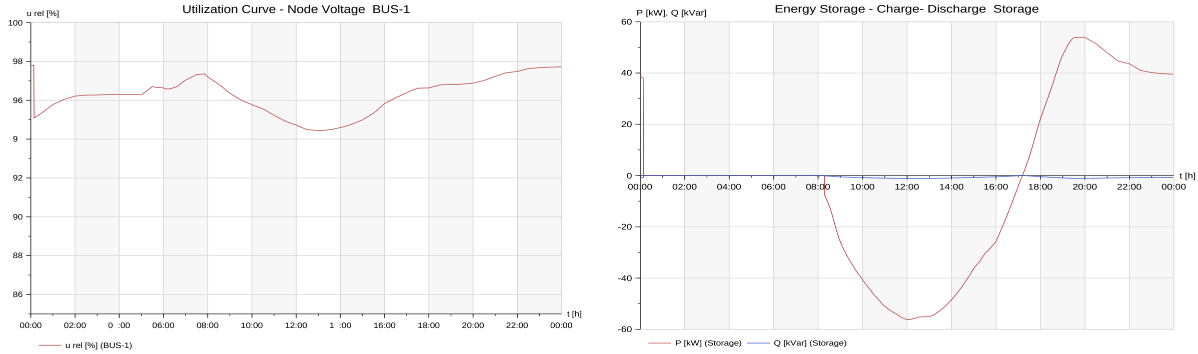

c: At BUS-1 Load with PV & Storage configuration d: Energy Storage (Charge and discharge)

Figure 5:9 Voltage variations at BUS-1 and Storage charge & discharge energy

The storage cycle in Figure 5.9(d) shows that storage stored energy during peak generation from PV during 09:00AM to 17:00PM and released stored energy during 18:00PM to 24:00PM. Therefore during the night when there was no PV generation, ES supported a part of load demand which eventually reduced the load on other network elements such as DT.

Element Utilization: Network elements are utilised according to the variation in load demand and variation in generation. Distribution Transformer (DT) is a key element that supports various loads, therefore proper utilisation of DT is of great importance. Daily utilisation of DT shows that after integrating PV, DT utilisation fluctuates and after adding storage this fluctuation is minimised and overall loading on DT also reduced. The installed DT capacity was 100 kVA. In load only condition maximum utilisation of DT was 76.6% and the minimum was 29.6% as shown in Figure 5.10 (a). In PV integrated condition loading on DT reduced during 07:00AM to 09:00AM and during 15:00PM to 17:00PM, however during 11:00AM to 14:00PM and 17:00PM to 21:00PM DT loading remains high as shown in Figure 5.10 (b). After adding ES into the network with PV, storage stored excess energy from PV and at the same time PV supports load demand during midday therefore DT utilization reduced and maximum DT utilization becomes 49.75% at 13:00PM, moreover during 18:00PM to 24:00AM storage support load demand which reduced loading on DT as shown in Figure 5.10 (c) and Figure 5.10 (d). Storage reduced DT loading swing and also reduced peak utilisation; therefore storage improved the DT loading capacity.

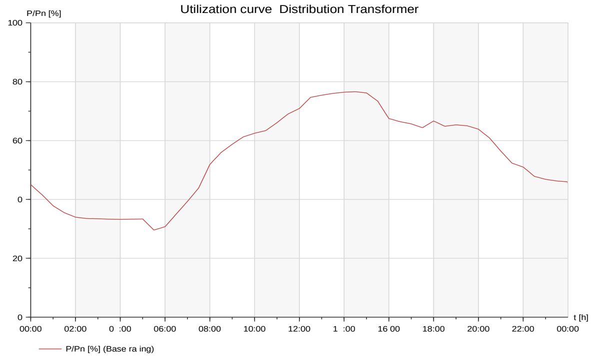

a: DT utilization in Load only configuration

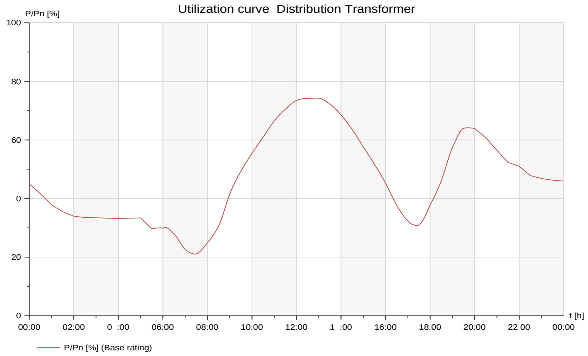

b: DT utilization in Load with PV configuration

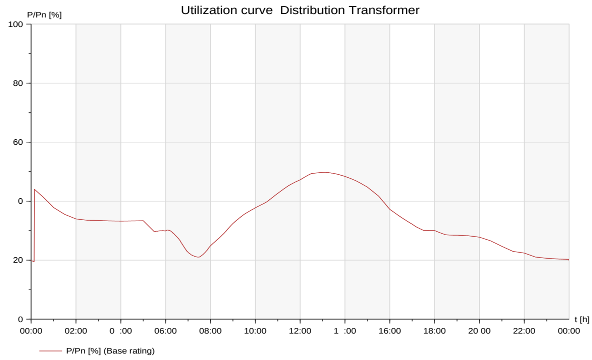

c: DT utilization in Load with PV and Storage configuration

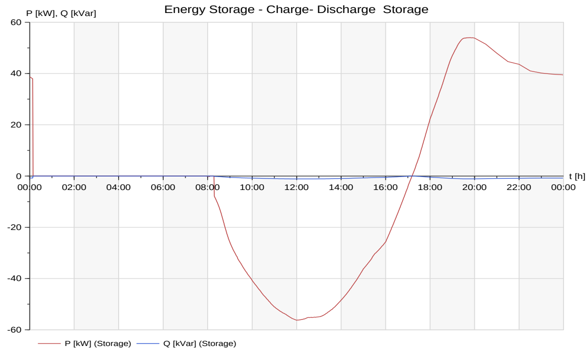

d: Charge-discharge cycle of ES

Figure 5:10 Distribution Transformer (DT) utilization is different configurations of network

Finally, the findings from the experimental and simulation investigation can be summarised as:

- Experimental and simulation results showed that PV increased voltage at PCC
- Phase voltage distortion occured when installed PV was not distributed uniformly among phases
- From simulation result it was found that storage reduced network voltage rise during peak generation from PV and increased voltage level when generation from PV was absent. Therefore storage helped in improving voltage regulation.
- Storage reduced loading on DT which helped to increase DT capacity and improve network performance.

The experiment and simulation was limited in a single 3-phase load; however in practical power network various single phase loads are connected especially the residential load. The next investigation describes voltage variation due to ES and RE integrated condition in a single phase distributed load network.

5.2 Results and Discussion of Investigation-2

In this study a model was developed considering single phase residential loads that are connected along a service line in a LV distribution network. Model setup, load, renewable energy (PV and wind turbine), storage allocation and required parameter settings were described in section 4.4.2 in Chapter 4. For the ease of understanding the findings, the model layout in Figure 4.42 in Chapter 4 is shown below as in Figure 5.11.

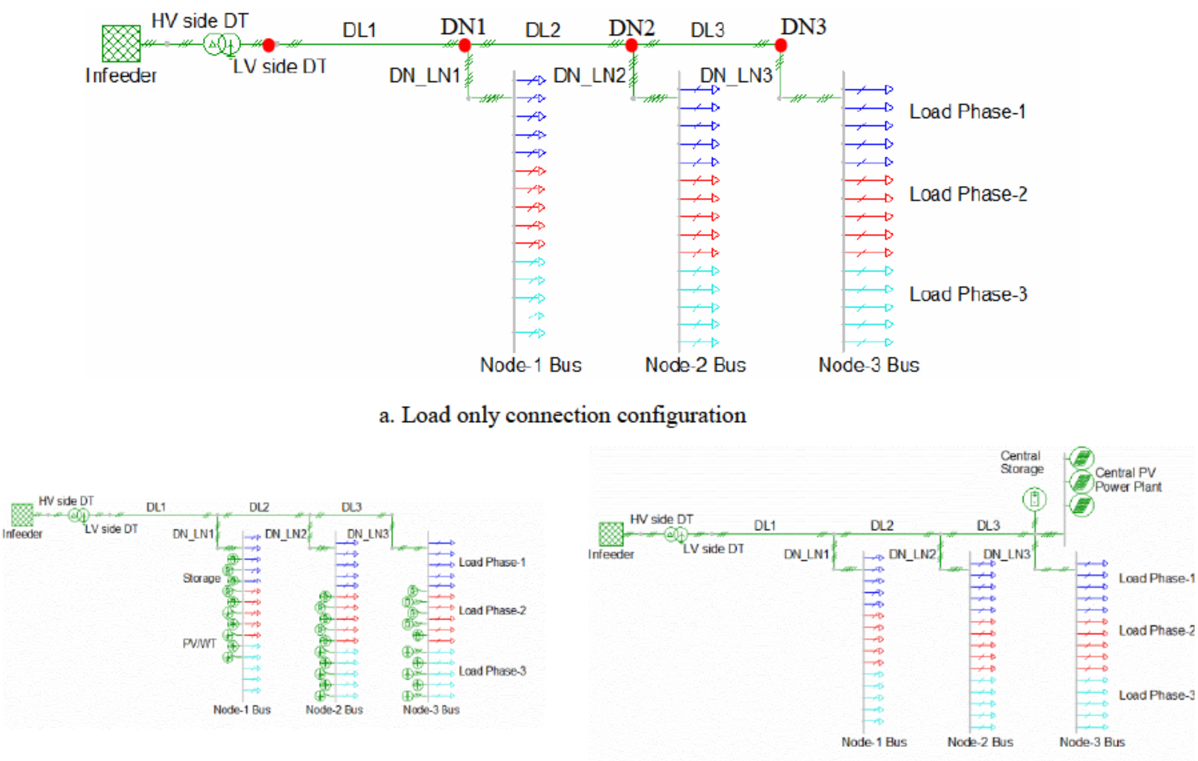

a. Load only connection configuration

b. PV/WT/Storage - distributed connection

c. PV/WT/Storage - centralised connection

Figure 5:11 A small network model

The model was simulated to evaluate the impacts of storage and RE on DT and DN. Load flow (LF) analysis was carried out to investigate the voltage regulation on the LV side of DT while load curve (LC) simulation was done to investigate voltage profile and loading on DT in various cases. Model was configured in the following 9 different cases and the findings are summarised below:

- Case-0: Load only
- Case-1: Load with Solar PV
- Case-2: Load with PV + Storage

- Case-3: Load with Large central PV power plant
- Case-4: Load with central PV power plant + Storage
- Case-5: Load with Wind turbine (WT)
- Case-6: Load with WT + Storage
- Case-7: Load with large central WT Power plant
- Case-8: Load with central WT Power plant + Storage

Load flow modelling of an unbalanced system showed that voltage dropped gradually from source side (Transformer secondary side) to the end node (DN3) as shown in Figure 5.12. In Case-0 voltage drops most at DN3 when no RE or storage was integrated. For the same capacity PV and WT in the network LF calculation is the same, therefore Case-1 and Case-5 provides the same results; similarly in Case-2 and Case-6. In the case of the centralised installation of PV or WT at the end of the service line where the lowest line voltage appears, like a RE power plant in case-3 and case-7, voltage improves at the end node (DN3) and also at higher nodes. But after adding centralised storage at the end node as in case-4 and case-8 node voltage improves further in all the nodes towards the source. Figure 5.13 shows the change in voltage in different case configurations. Therefore integrating PV or WT at the lowest voltage node is more beneficial and adding storage further improves the voltage towards the sending end voltage level, which is a better way to improve the voltage regulation problem rather than distributing PV or WT with all distributed loads.

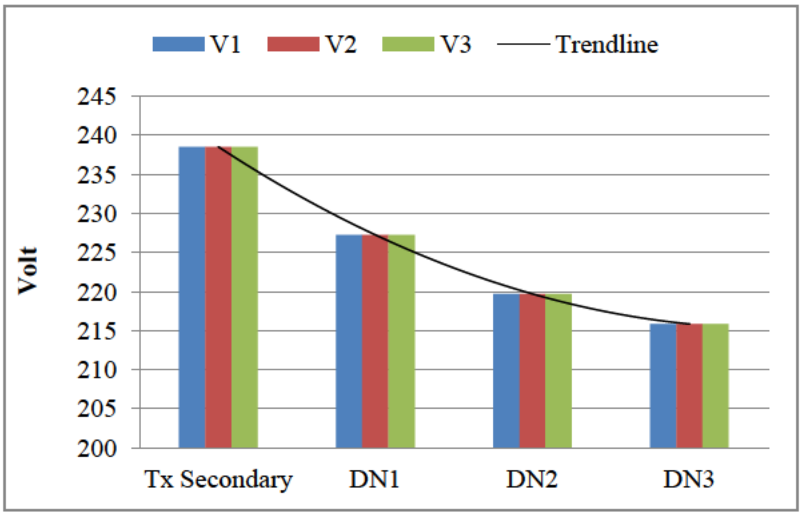

Figure 5:12 Voltage level at different point in the service line (Case-0)

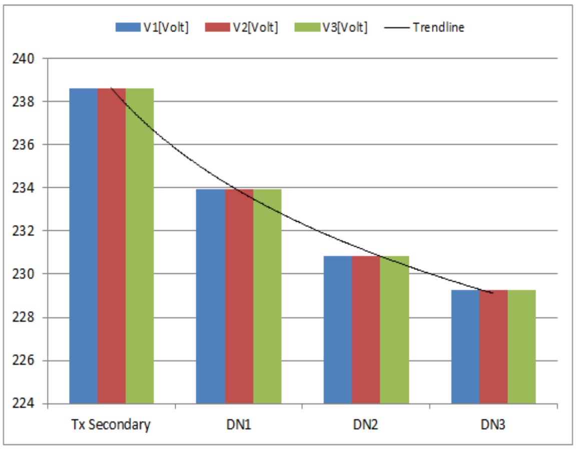

Case-1

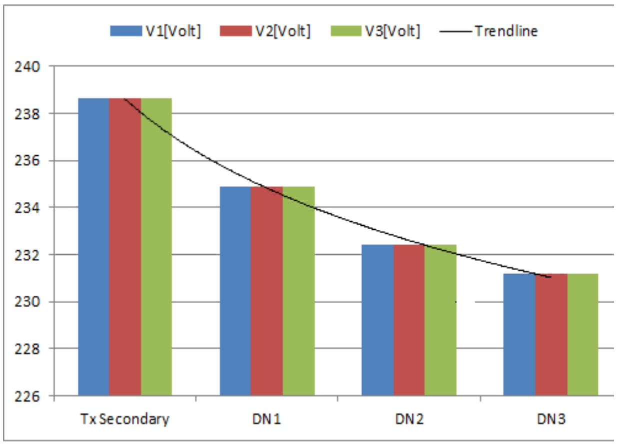

Case-2

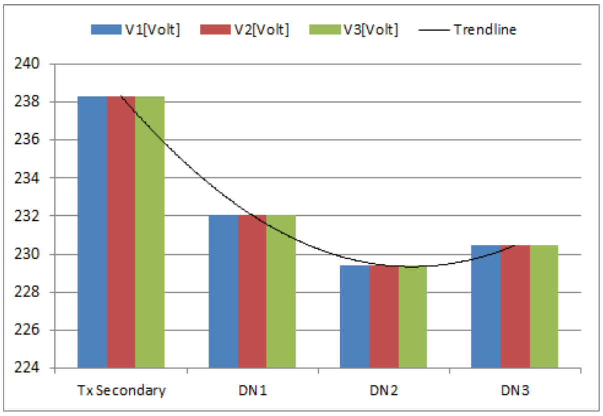

Case-3

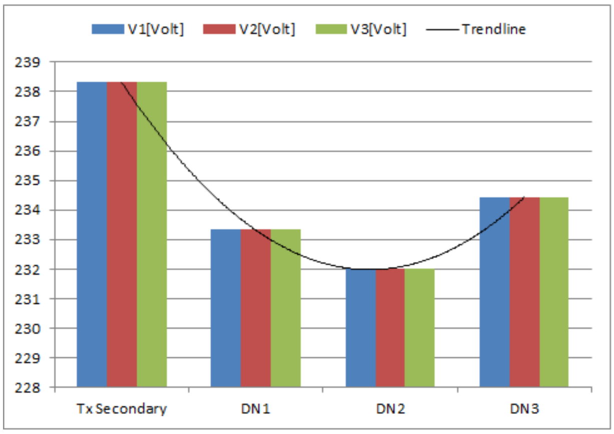

Case-4

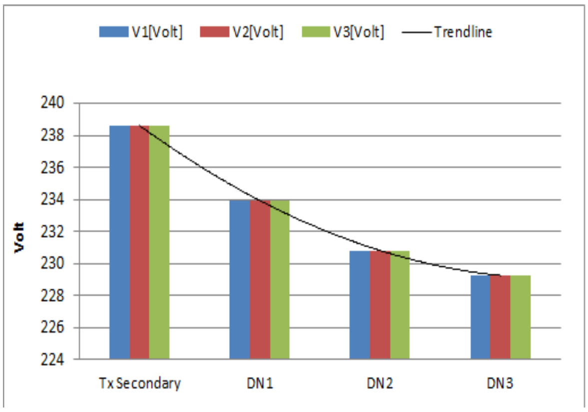

Case-5

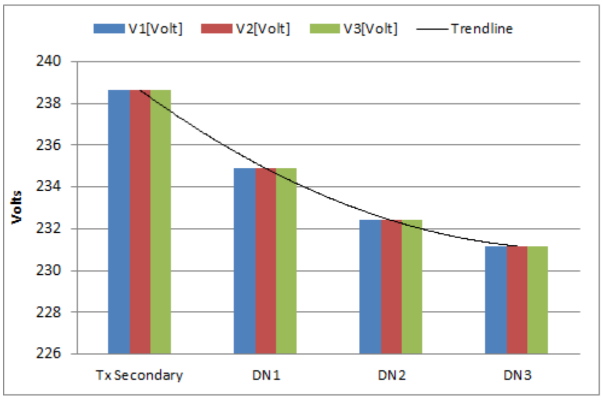

Case-6

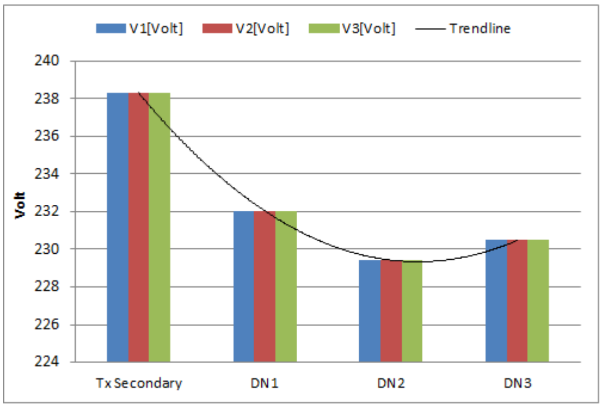

Case-7

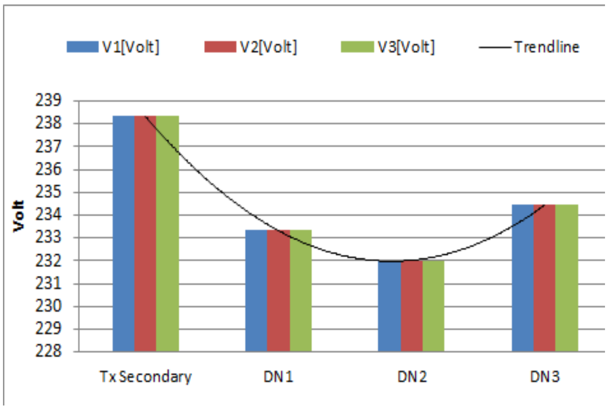

Case-8

Figure 5:13 Voltage level in different configuration of Load, PV/WT and Storage

Phase voltage variation from the secondary side of DT (Tx_Secondary) to the end node (DN3) of the service line in different case configurations is shown in Figure 5.14. It is clear from Figure 5.14 that PV or WT in distributed connection configuration improves the node voltage and integrating storage further improves the node voltage condition as shown in Case-2 and Case-6. In centralised connection configuration, storage improves the voltage at the PCC in a better way than in distributed connection configuration. Figure 5.14 shows the surface plot of phase voltage (V_1) in 2 volts interval for all cases.

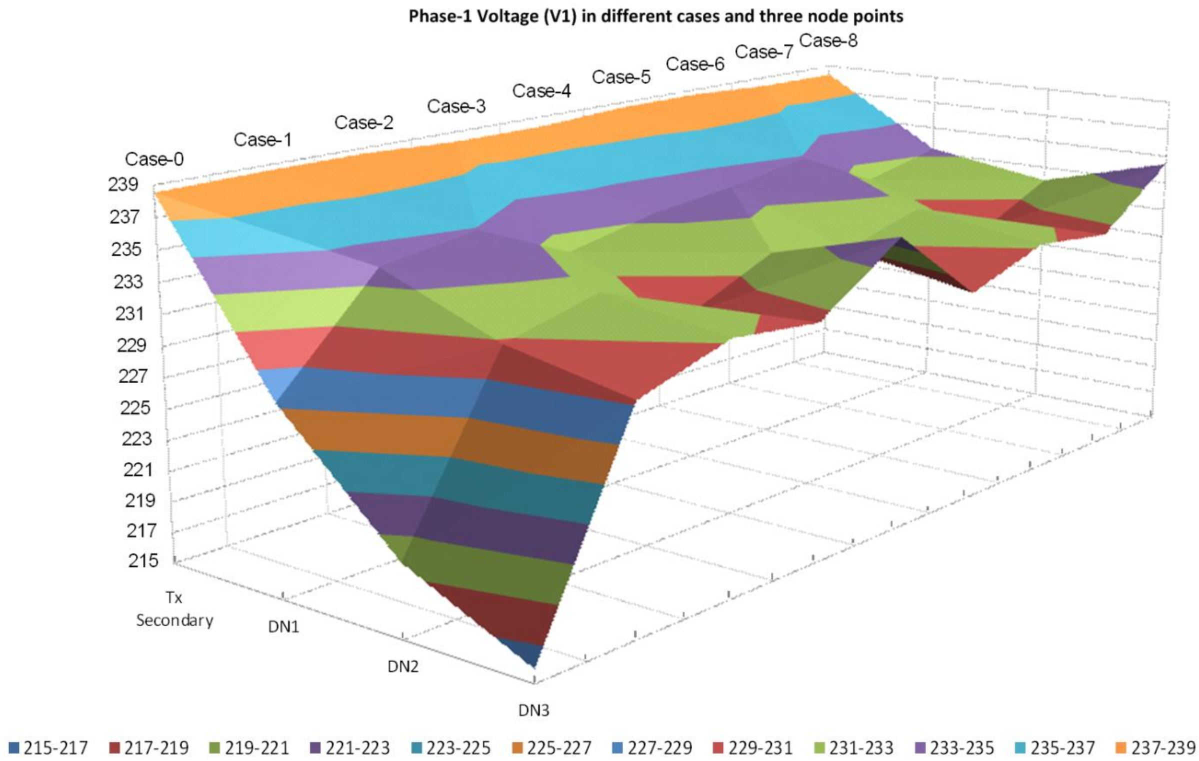

Figure 5:14 Changes in phase voltage in different case configurations

According to the voltage regulation standard followed [22] in Australia, the allowable lower voltage limit (V_{rll}) is 225.6V as marked in Figure 5.15, and compared to all other cases, in Case 4 and Case 8 i.e. RE power plant or centralised installation with large storage, it improves voltage along the whole service line and thus improves voltage regulation.

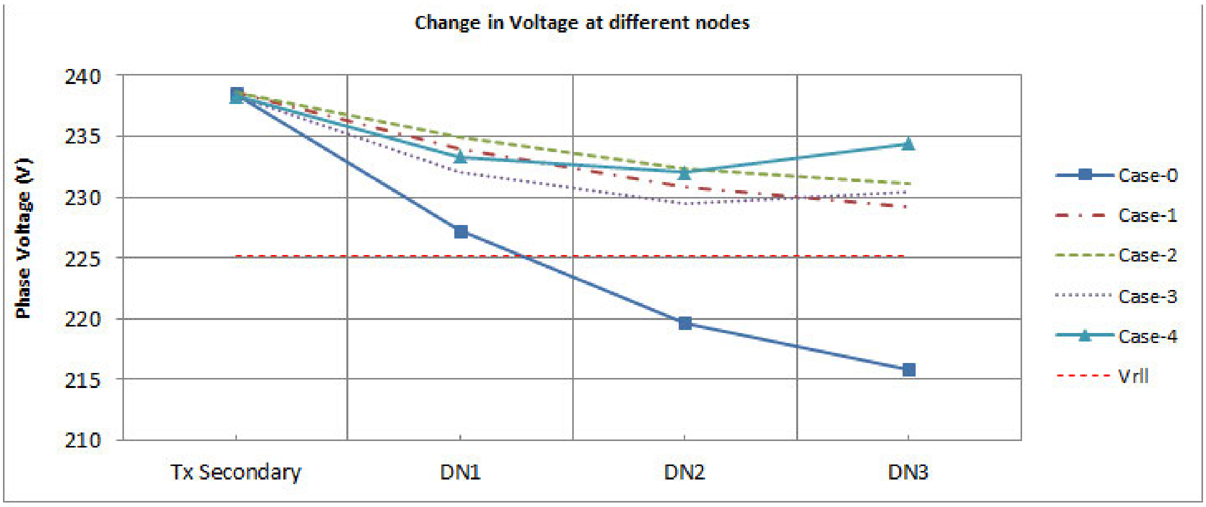

Figure 5:15 Change of voltage along the service line in different cases

The change in voltage due to PV or WT and ES is compared in distributed connection and centralised connection configurations in Figure 5.16 and 5.17 respectively. From both the figures it is clear that PV or WT increases voltage at a very high rate and ES slows down this increasing rate and that helps reducing sudden high changes in voltage levels and thus improves voltage regulation.

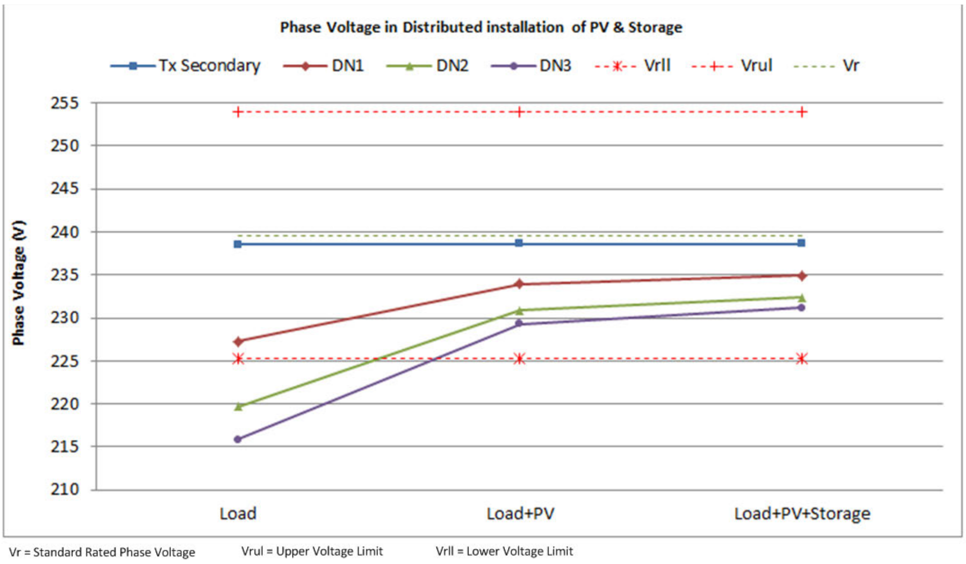

Figure 5:16 Voltage change compared to the limit in distributed installation of RE and storage

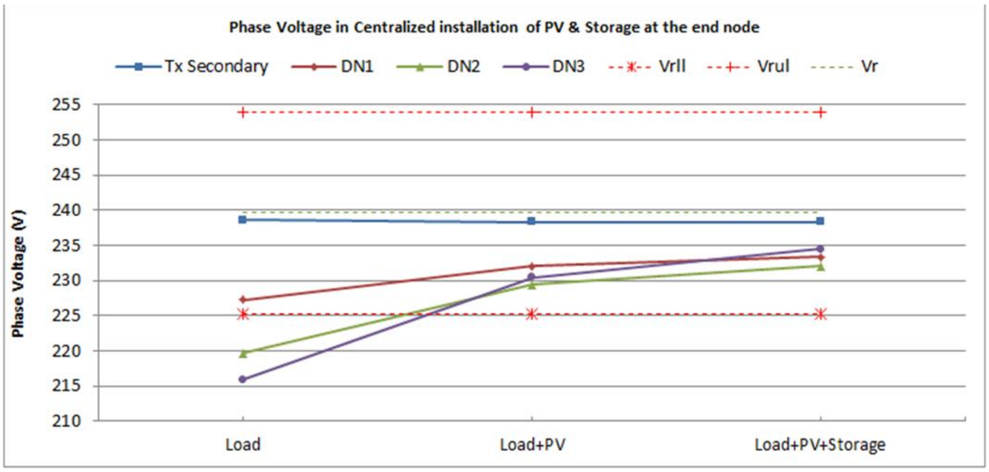

Vr = Standard Rated Phase Voltage Vrul = Upper Voltage Limit Vrll = Lower Voltage Limit

Figure 5:17 Voltage change compared to the limit in centralized installation of RE and storage

Load curve (LC) calculation provides a better view of voltage regulation for a specific time period. Figure 5.18 shows the daily voltage profile in all cases at the end node DN3. As mentioned earlier in Chapter 4, voltage regulation allows ± 6% of change in base voltage (240 V). Figure 5.18 shows that in Case-1, 3, 5 and 7 i.e. without storage condition voltage varied from a minimum 90.09% to a maximum 103.32% of base voltage. In storage integrated condition i.e. in Case 2, 4, 6 and 8 voltage varies from a minimum 92.13% to a maximum 101.09% of base voltage. However voltage regulation in centralised connection configuration is much better, as in Case-8 voltage varies from a minimum 94.05% to a maximum 99.87% of base voltage. Therefore storage improves voltage regulations and that improves the network element utilisation.

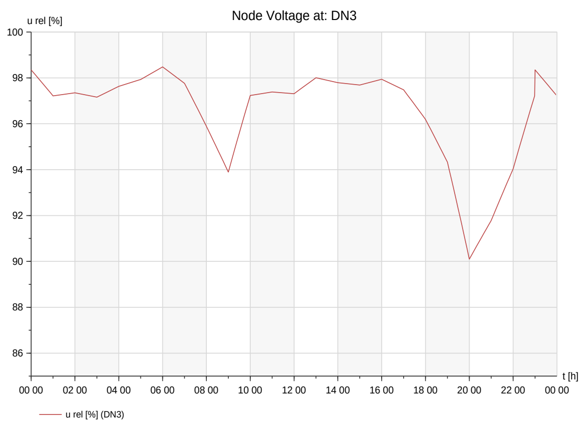

Case-0: Min 90.09% max 98.48% of base voltage

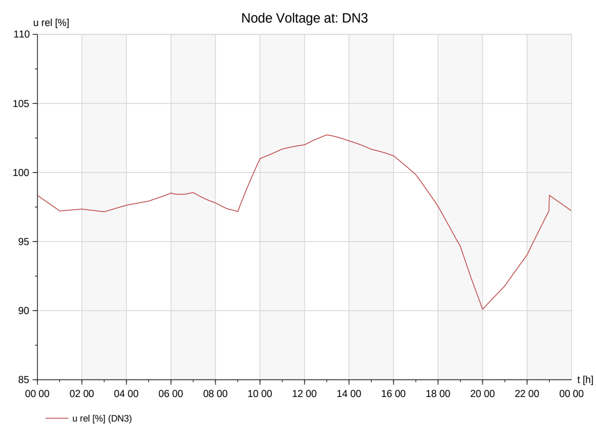

Case-1: Min 90.09% and max 102.72% of base voltage

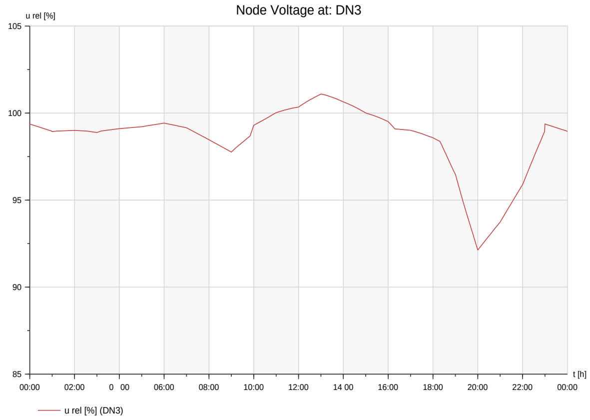

Case-2: Min 92.13% and max 101.09% of base voltage

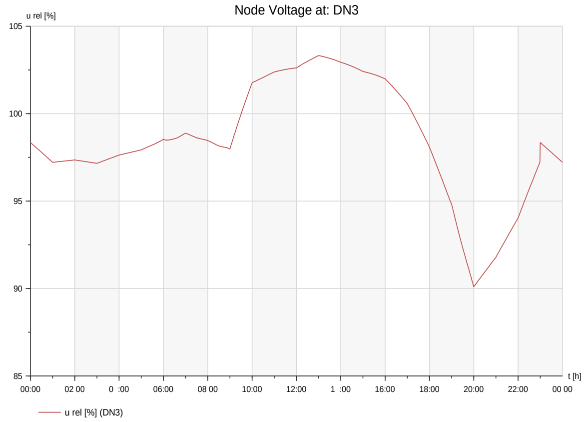

Case-3: Min 90.09% and max 103.32% of base voltage

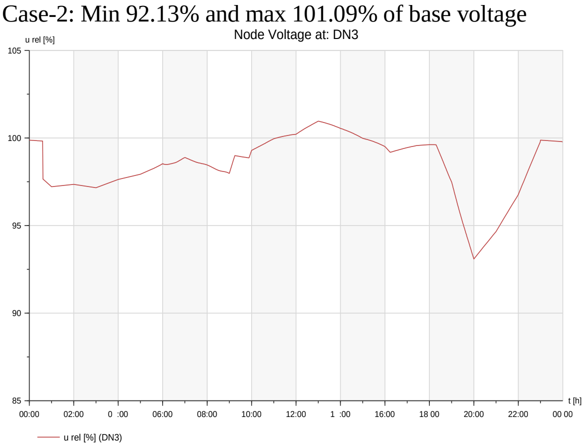

Case-4: Min 93.08% and max 100.95% of base voltage

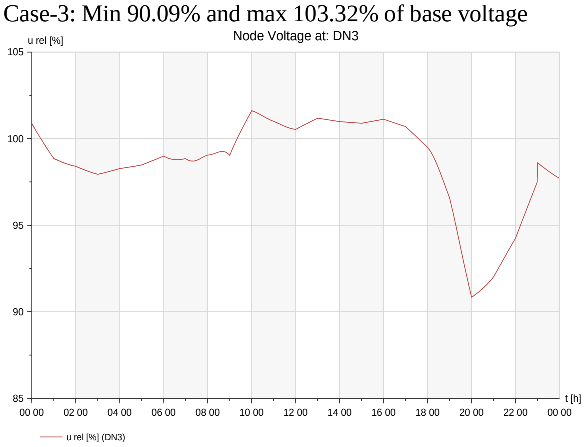

Case-5: Min 90.84% and max 101.61% of base voltage

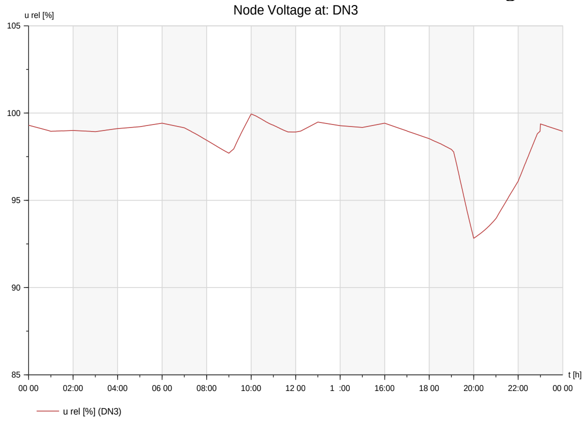

Case-6: Min 92.82% and max 99.94% of base voltage

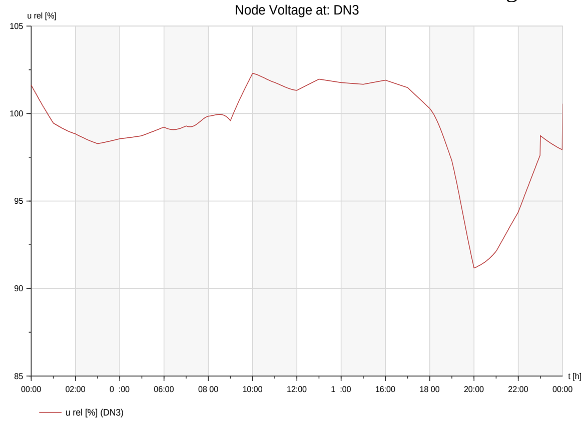

Case-7: Min 91.17% and max 102.29% of base voltage

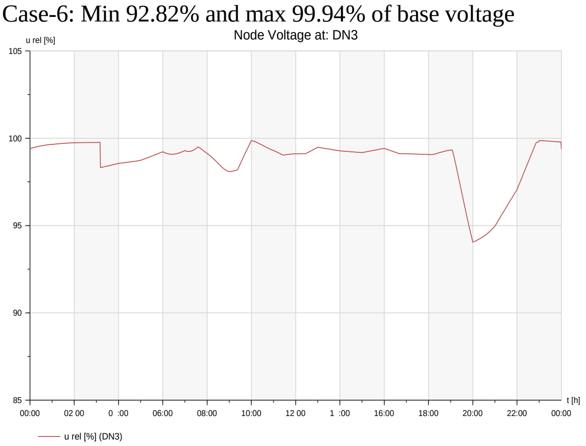

Case-8: Min 94.05% and max 99.87% of base voltage

Figure 5:18 Voltage profile at node 3 (DN3) in different case configurations

5.2.1 Element Utilisation

As mentioned earlier, DT is the key element in DN in supporting load and in this model a total 45 houses were connected to the service line that is connected from the LV side of the DT. The total load became 85.95 kVA, however due to line impedance, the total load on DT appeared more and peak DT utilisation became 93.33% in load connected condition as shown in Figure 5.19. Peak load demand appeared at 20:00PM; also in the morning (08:00AM to 10:00AM) load demand was high.

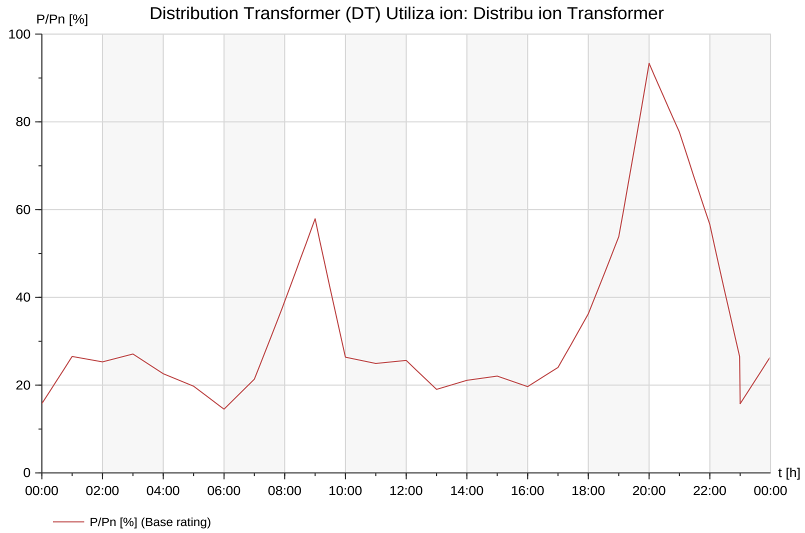

Figure 5:19 Distribution transformer utilisation in case-0

In the power network, DT utilised both ways when energy was supplied to the load from the HV side of DT and also when excess energy was generated by RE sources and exported back to the HV side of DT. Energy storage improved DT utilisation by reducing load during peak demand time at 20:00PM in all cases by supplying stored energy to support the load. Moreover storage also reduced the load on DT during mid day when load demand was low but RE generation was high and storage stored excess energy as shown in Figure 5.20.

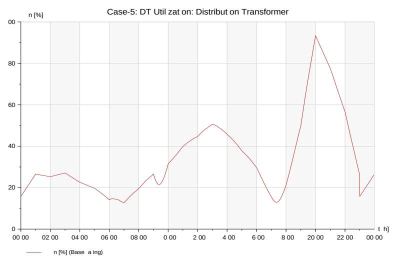

DT use in Case-1

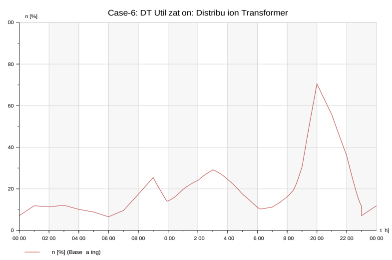

DT use in Case-2

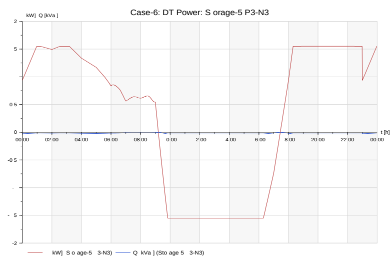

Storage use in Case-2

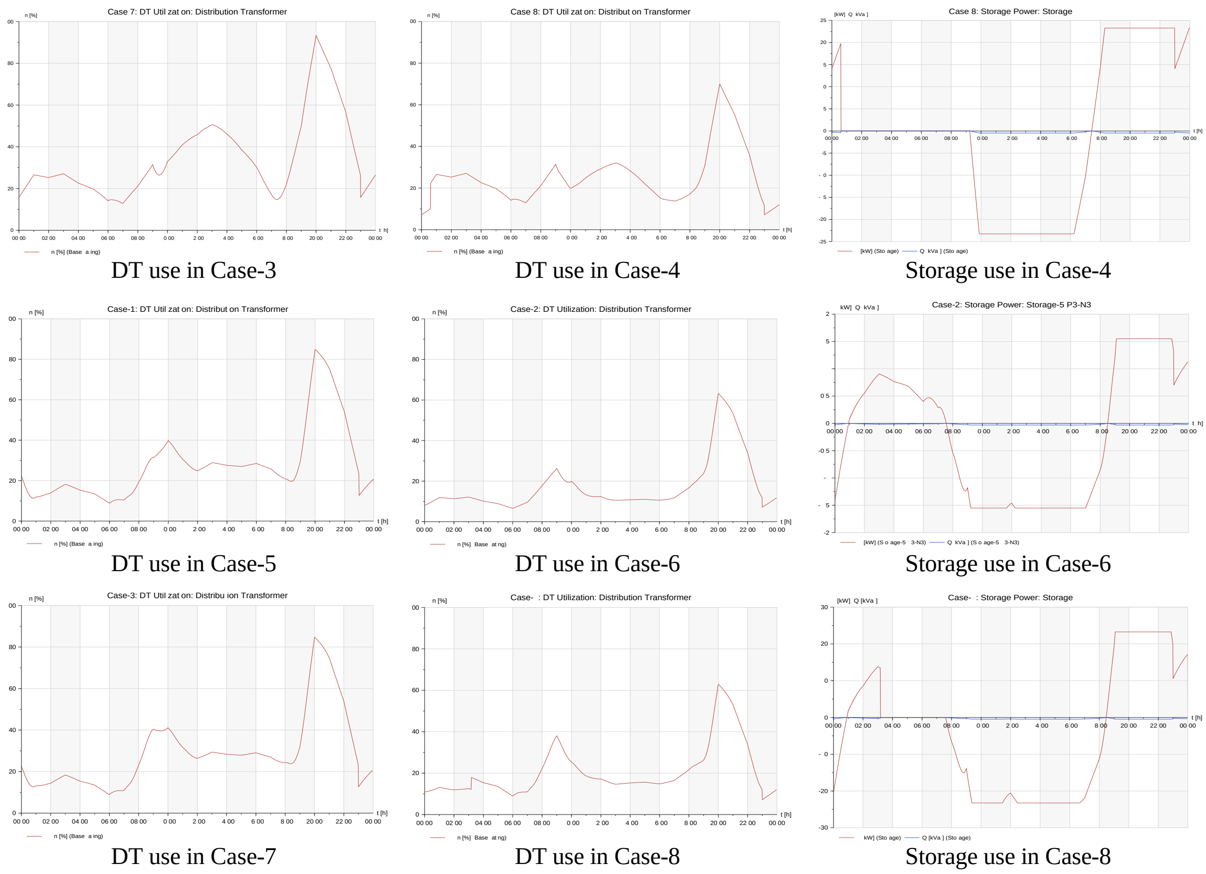

Figure 5:20 Storage support in DT utilisation is different cases

Figure 5.21 shows the comparative bar chart of DT utilisation in peak demand time in all cases. It is clear that storage with either PV or WT reduced load on distribution transformer and distribution network as shown in Case-4 and Case-8 in Figure 5.21.

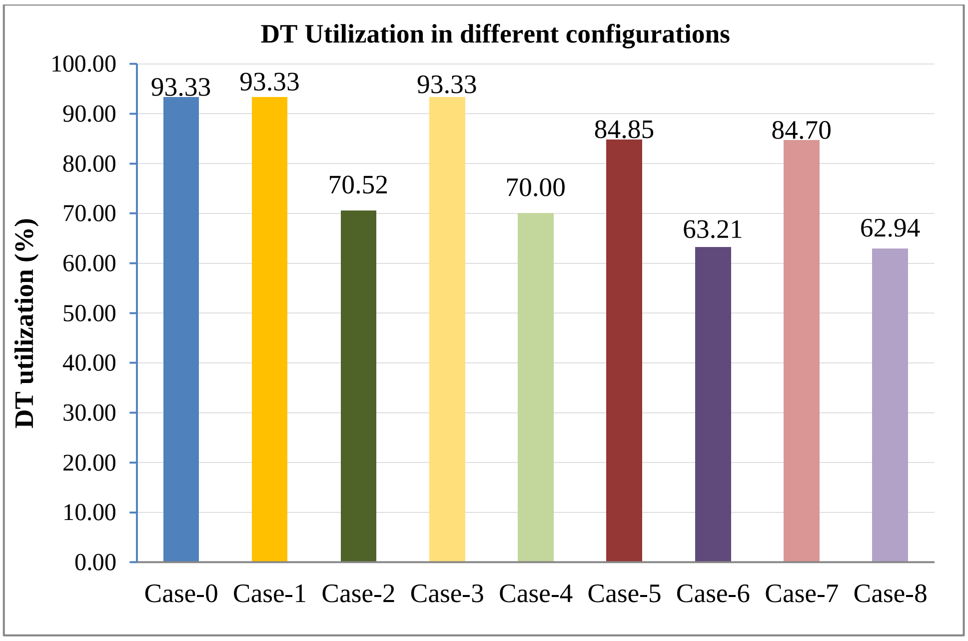

Figure 5:21 Distribution transformer utilisation in peak demand time

5.2.2 Storage Support during Energy Fluctuation

As mentioned earlier, solar radiation fluctuates for various reasons, same as for wind speed. Energy generated from these sources also fluctuates accordingly. Three different fluctuations (short continuous, short dip and long dip fluctuation) were defined in Chapter 4 in Figure 4.34. How storage supports load is illustrated by describing DT utilisation during these energy fluctuations. Figure 5.22 shows the storage support in the centralised connection configuration of PV and ES in Case-4. A similar response was found from storage when it was integrated with WT in Case-8. It is clear that due to these fluctuations DT utilisation also fluctuates and storage supported load demand during fluctuations and minimises the impact on DT loading.

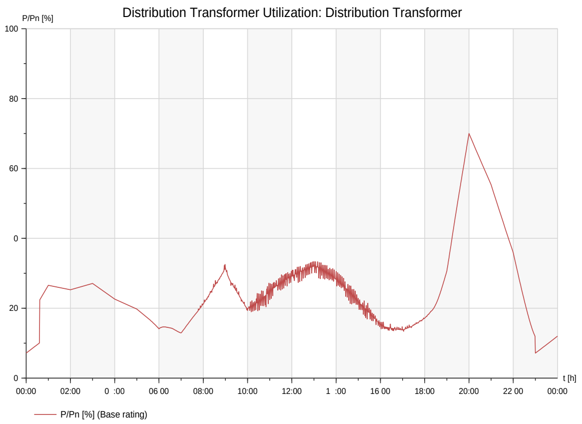

DT utilisation with short fluctuation in PV energy

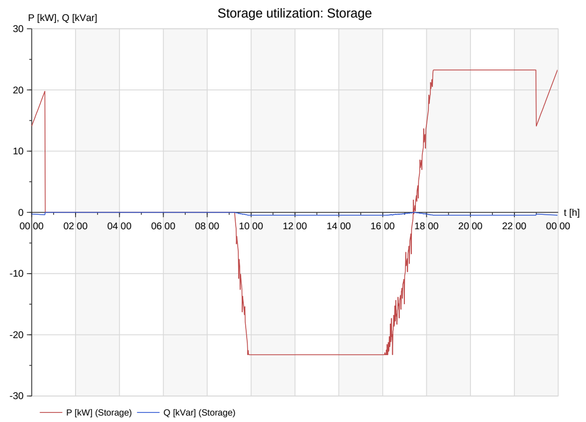

Storage response in short continuous fluctuation in PV energy

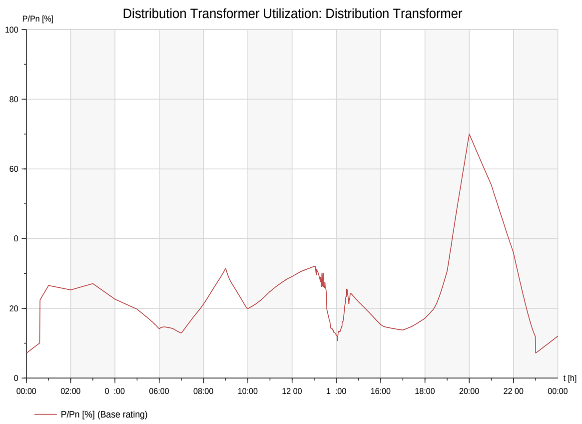

DT utilisation with short dip fluctuation in PV energy

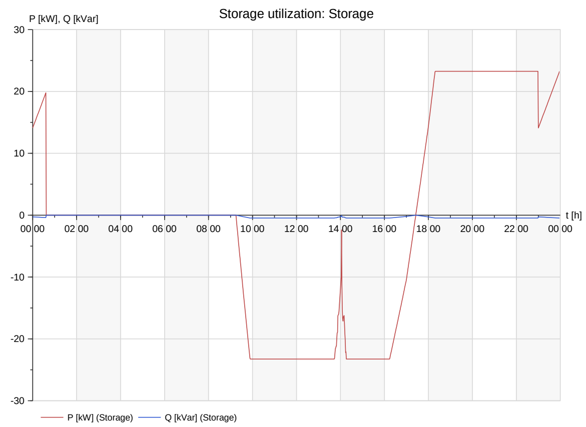

Storage response in short dip fluctuation in PV energy

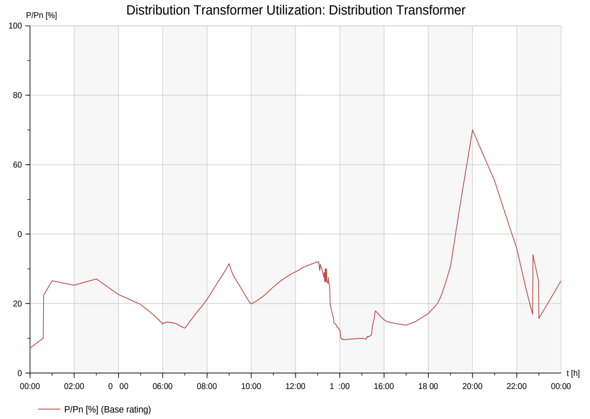

DT utilisation with long dip fluctuation in PV energy

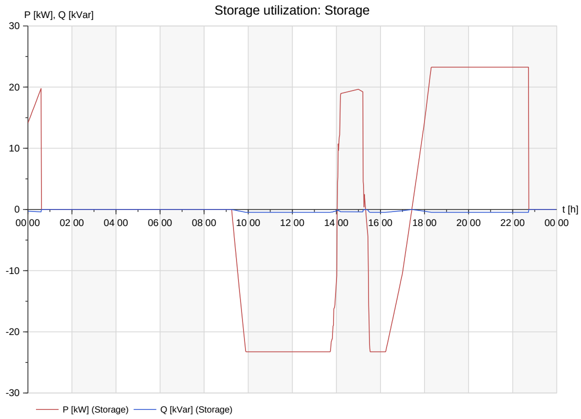

Storage response in long dip fluctuation in PV energy

Figure 5:22 Storage response during energy fluctuations

Therefore, integration of large scale ES and solar PV or Wind turbines within the distribution network in a distributed way introduced some technical challenges. These challenges are due to the intermittent nature of PV and WT, characteristics of inverter and converter, charging and discharging of storage and frequent use of inverter. Moreover if small scale RE sources and storage is connected in a distributed way near each load, like roof-top solar PV, then the risk is high. These small scale installations use an inverter more frequently and this involves all connected service lines allowing bi-directional power flow. On the other hand, if the same total capacity storage and PV or WT is installed at the end or near the end of the service line, that improves the voltage regulation and operates as a single plant and provides better use of RE and reduces the load on DT. Therefore the findings can be summarised as:

- Storage improves voltage regulation in RE integrated DN
- Storage improves DT utilisation by reducing load on DT
- Voltage regulation and DT utilisation achieved in a better way if RE and ES integrate into the DN as a centralised power plant, especially at the low voltage end of the service line.

Therefore in large networks, it will be a good idea to connect RE and storage at the end of each service line to minimise the effect on the power network.

5.3 Results and Discussion of Investigation-3

A small section of the power distribution network in Rockhampton was considered for this analysis. This section of the power network model was developed in PSS SINCAL to evaluate the impacts due to ES and solar PV on the DN. Network description and model setup was described in section 4.4.3 in Chapter 4. The network was divided into 7 load zones. This network was configured in distributed integration of PV and ES and centralised integration of PV and ES.

5.3.1 Distributed Integration of RE and ES

The power network in Kawana, a small part of Rockhampton, DN was modelled with real load and network parameter data. Load, PV and ES was integrated at the secondary side of the DT (11kV/415V) and the model was simulated in the following 7 configurations.

- Load only (no PV or storage installed)
- Load with PV (20% of load rating)
- Load with PV and storage (20% of load rating)
- Load with PV (50% of load rating)
- Load with PV and storage (50% of load rating)
- Load with PV (100% of load rating)
- Load with PV and storage (100% of load rating)

The model was simulated for load flow (LF) and load curve (LC) calculation and voltage variation was observed in several selected node points. The observed node points in the HV side of the network are shown in Figure 5.23 showing the starting node of each zone. The observation point of the LV side is the secondary side of the DT that connects load, PV and ES. The findings are summarised below:

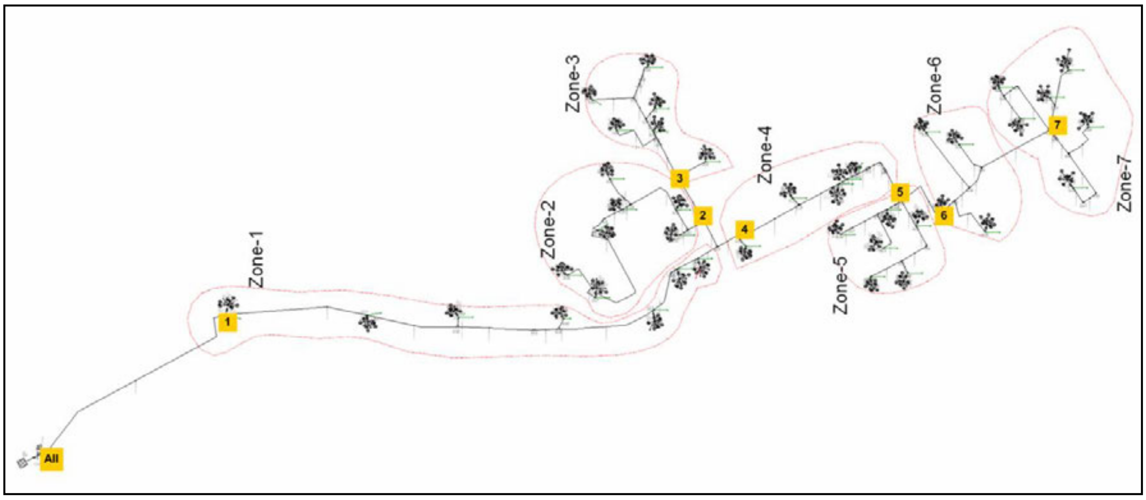

Figure 5:23 Observation node points on HV side of the feeder

The load flow modelling of an unbalanced system showed that voltage level gradually drops from infeeder (or source) to the end load i.e. from Zone-1 to Zone-7. Node marked “All” is the secondary side of transformer connected with the infeeder. Figure 5.24 shows the phase voltage drop at the high voltage (HV) side of the DT when no PV or storage was installed and Figure 5.25 shows the gradual voltage drop at the LV side of the DT of all nodes in 7 zones. LV side nodes are marked as; for example, a node “N002” in Zone-1 is marked as “LV_Z1_N002” and similarly other nodes in other zones.

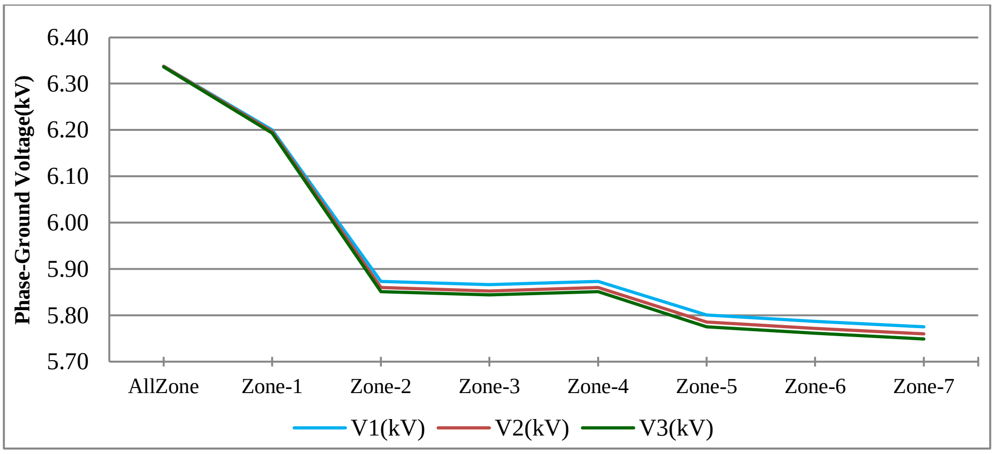

Figure 5:24 Voltage drop due to load from top to bottom zone (HV side of DT)

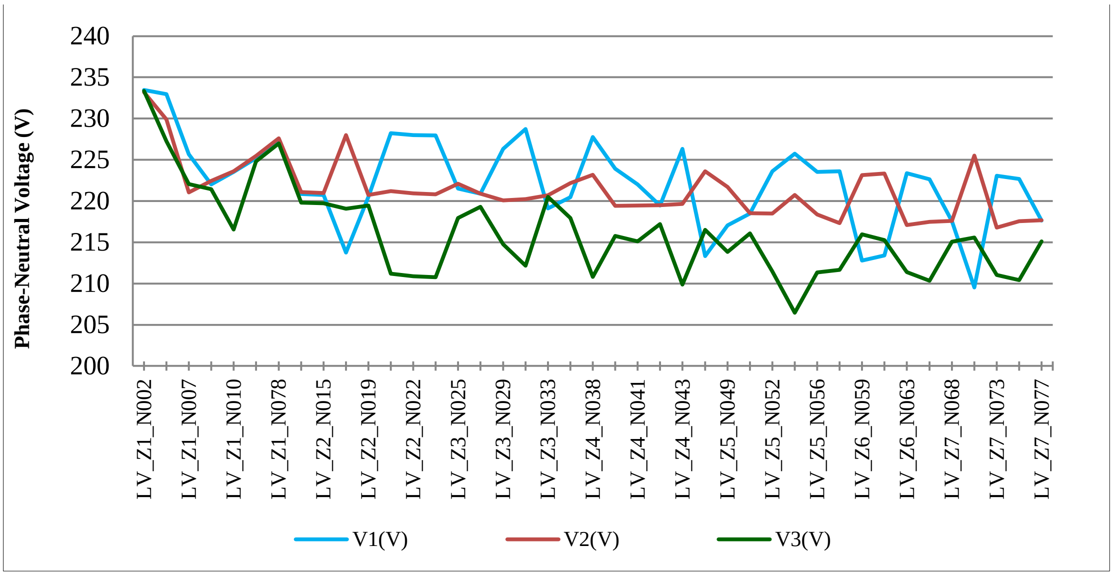

Figure 5:25 Voltage drop due to load in all nodes (LV side of all DT)

After adding PV into the DN, line-ground voltage increased and the percentage of increase is higher at the distant load zones as shown in Figure 5.26. PV was integrated at 20%, 50% and 100% of load rating into the network. The increase in voltage was found with increased PV sizes. A maximum 6.745% voltage rise was observed when PV was integrated at 100% of load rating compared to the no PV configuration voltage in the zone-7 as shown in Figure 5.26. According to Ergon Energy, increase in voltage due to PV should not be more than 1% of rated voltage [23].

At the LV side of DT, line-ground voltage increase was observed in all nodes and the increase in voltage was higher with increased PV capacity of 20%, 50% and 100% of load rating. Figure 5.27 shows the percentage increase of line to ground voltage in LV side of the DT. The effect of increased PV penetration was more in LV side and a maximum 9.67% of voltage rise was observed in Node-55 in Zone-5 at 100% PV integration, compared to the no PV integrated network configuration. The rate of voltage rise increased with increased PV penetration.

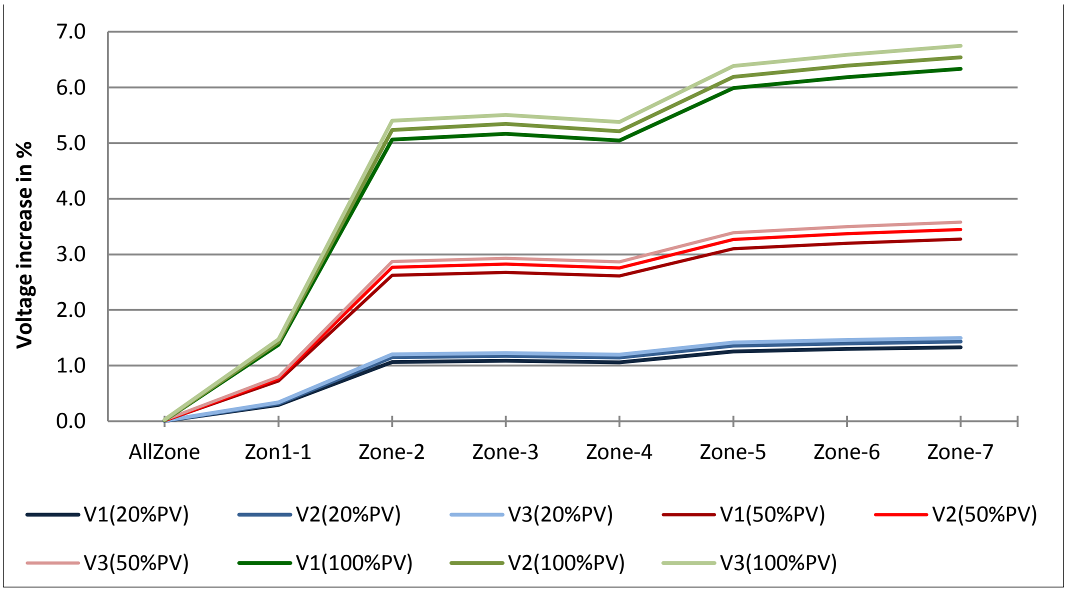

Figure 5:26 Voltage rise due to PV in different zones (HV side of DT)

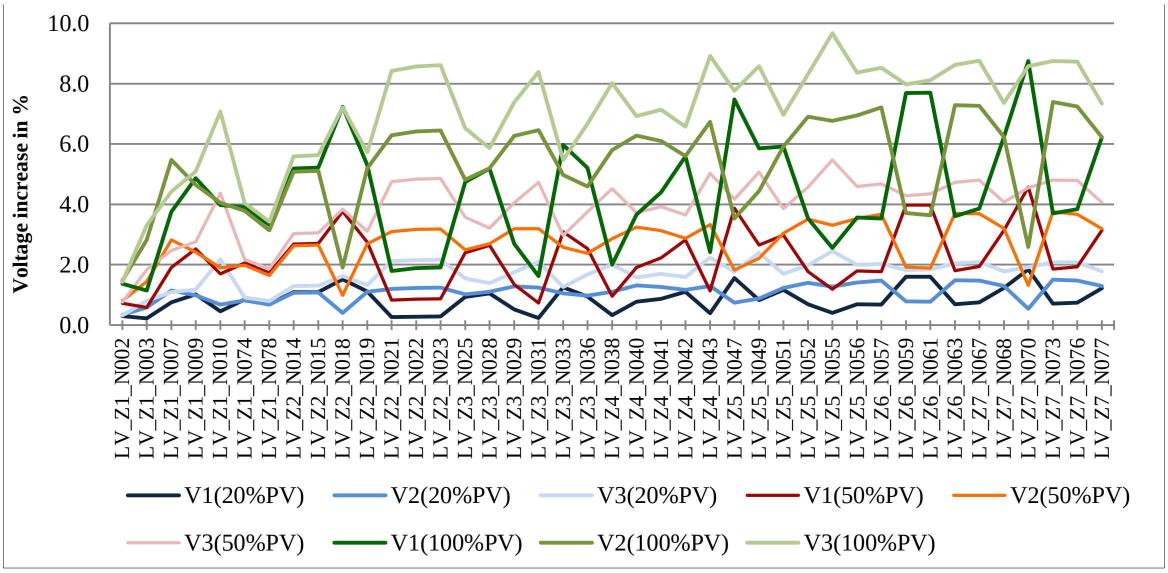

Figure 5:27 Voltage rise due to PV in different zones (LV side of DT)

After adding storage with all nodes in the network with the same capacity of PV i.e. 20%, 50% and 100% of the load rating, it was found that voltage started dropping in all zones compared to the system without storage. Figure 5.28 shows the HV side voltage drop at all the observation node points of all zones. However the percentage voltage drop was not as high as the voltage rise, because of the load management by ES and PV supply. Maximum voltage drop was 1.75% at Zone-7 when PV and storage was installed at 100% of the load rating.

At the LV side of DT voltage drop was observed in all nodes and it was found that voltage drop was higher at distant nodes. Figure 5.29 shows the voltage drop in LV side of DT when storage was integrated at 20%, 50% and 100% of the load rating with PV compared to the no storage integrated network. Maximum voltage drop of 2.23% was observed at node “LV_Z7_N070” in zone-7 compared with the no storage integrated condition.

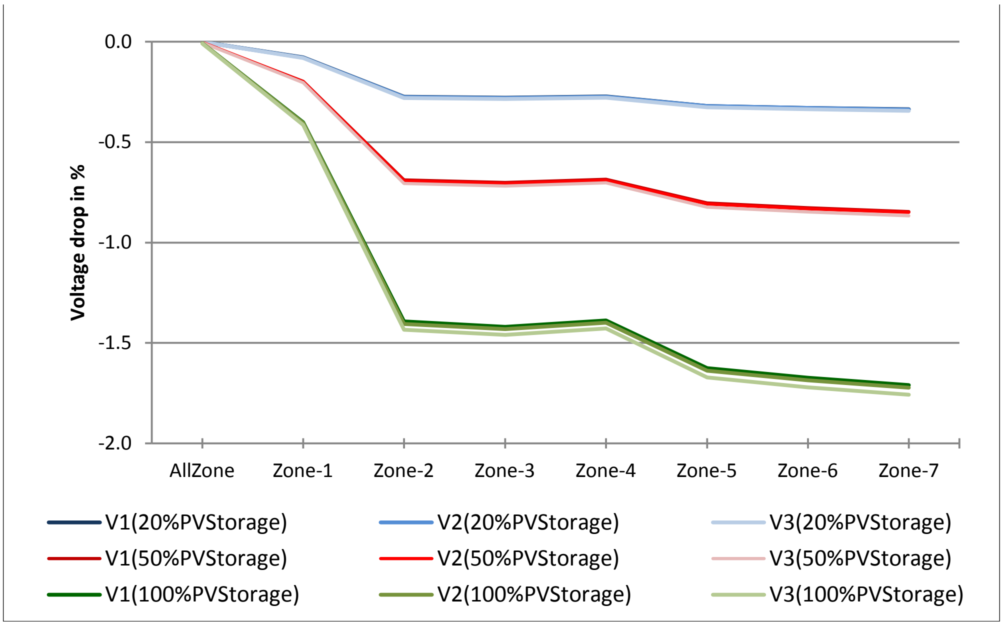

Figure 5:28 Voltage drop due to Storage in different zones (HV side of DT)

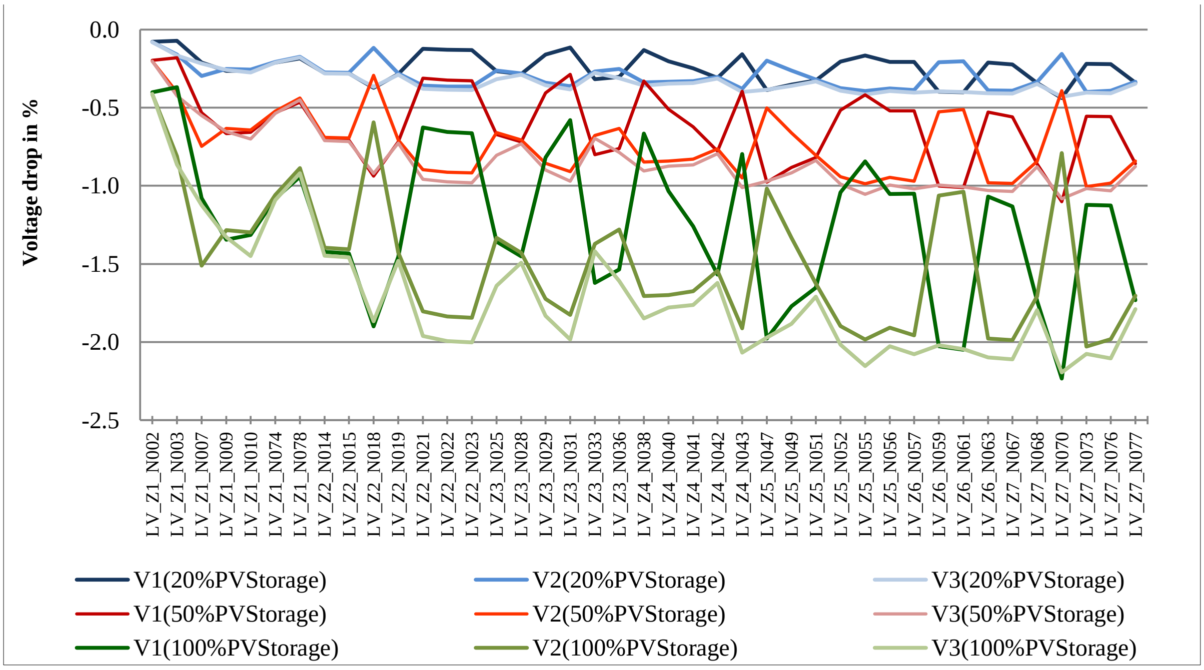

Figure 5:29 Voltage drop due to Storage in different zones (LV side of DT)

Therefore it is clear that in a service line or feeder, voltage drops from source to the end load due to line impedance and loads in various points along the feeder. By integrating PV into the network at various nodes, voltage starts rising and the maximum rise occurs at the distant nodes where voltage drop was higher in without PV condition. With the increase of PV into the network, voltage rise also increased. With the integration of Storage into the network voltage starts dropping as excess energy generated by PV was stored into the storage.

5.3.2 Centralised Integration of RE and ES

Considering the findings of investigation-2 described in section 5.2 the power network of Kawana described above was modified to integrate PV and ES in a centralised approach. However the load distribution was unchanged. As voltage dropped more in distant nodes, bulk size PV and storage was integrated into the distant nodes in each zone as shown in Figure 5.30. Observation nodes at the HV side remained same.

For this analysis, 500 kW of PV plant was installed in each Zone and to support best utilisation of PV 100 kW capacity of Energy storage was added in each zone. The PV and storage capacity against load in each zone as shown in Table 5.1:

Table 5:1 Load, PV and Storage in different zones

	Zone-1	**Zone-2**	**Zone-3**	**Zone-4**	**Zone-5**	**Zone-6**	**Zone-7**
Load (kVA)	1005.722	763.755	789.212	601.052	1111.004	407.336	763.755
PV (kW)	500	500	500	500	500	500	500
Storage (kW)	100	100	100	100	100	100	100

Load Flow calculation shows the voltage variation along the service line and level of voltage in the observation points were compared in load only, load with PV plant and finally load with PV and Storage plant in each zone as indicated (small blue circles in Figure) in Figure 5.30.

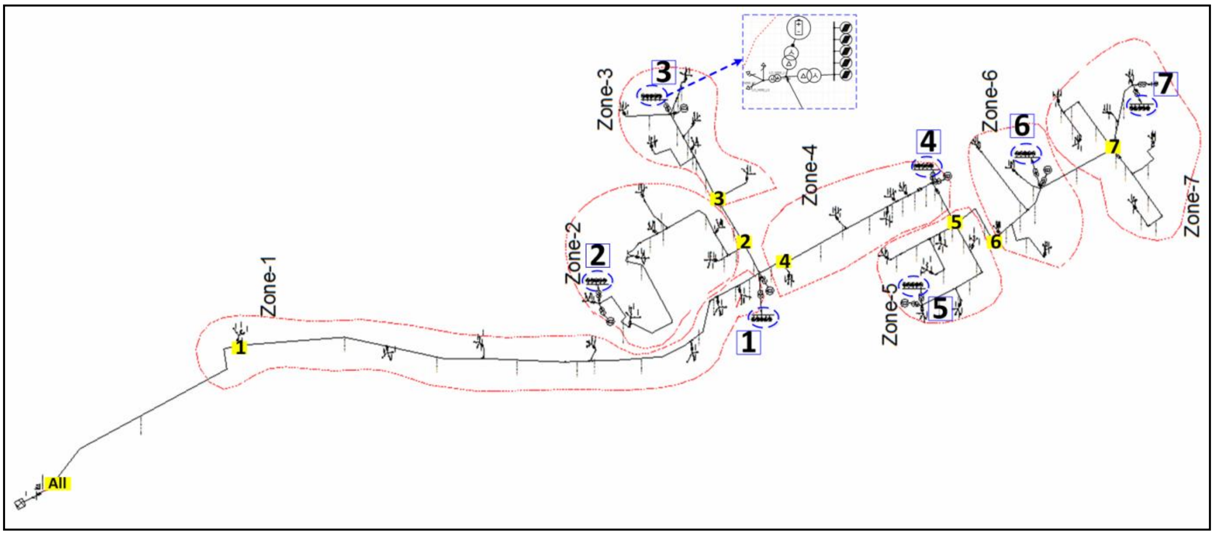

Figure 5:30 Power network of Kawana with the installation of bulk size PV and Storage in each zone

Load flow calculation provides the voltage level of the observed node based on the load demand and energy supply condition. It was found that in load only condition, phase voltage dropped gradually towards the end node in Zone-7 and phase voltage dropped 8.45% compared to the voltage at the observation node "All" near the Infeeder.

Figure 5.31 shows the phase-1 voltage in load only condition; load with PV plant and load with PV & storage plant in each zone of the DN. It was observed that by integrating PV plant at the end of each zone, phase voltage increased, especially in the distant nodes where voltage had a maximum drop in load only condition. After integrating storage, voltage levels further increased and that improved the operating conditions. However, the load flow does not reflect the condition over the whole day as the load demand and RE generation varies over time, therefore a load curve (LC) calculation was conducted to investigate the daily variation of phase voltages.

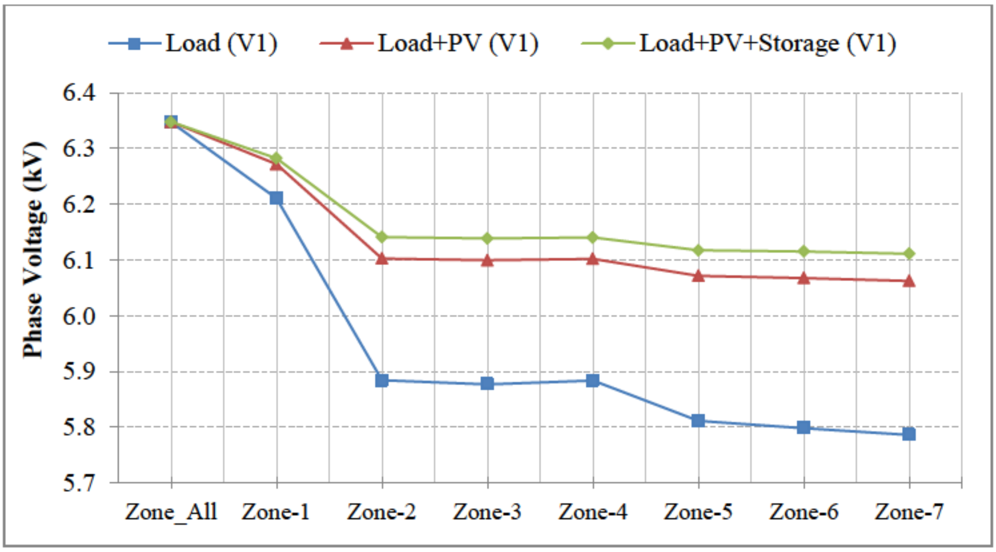

Figure 5:31 Observed phase voltage (V1) at the HV side of DT from Infeeder to the end node

Load curve calculation shows the variation of voltage level for the defined time period and Figure 5.32 showed the daily variation in voltage level at the HV side of observed nodes as indicated in Figure 5.30. Figure 5.32 shows the daily voltage regulation at the observed nodes in each zone and voltage varied from a minimum 90.715% to 99.70% of base voltage at 20:00PM and 06:00AM when load demand is maximum and minimum respectively. At 13:00PM maximum voltage level was 99.55% in Zone-1.

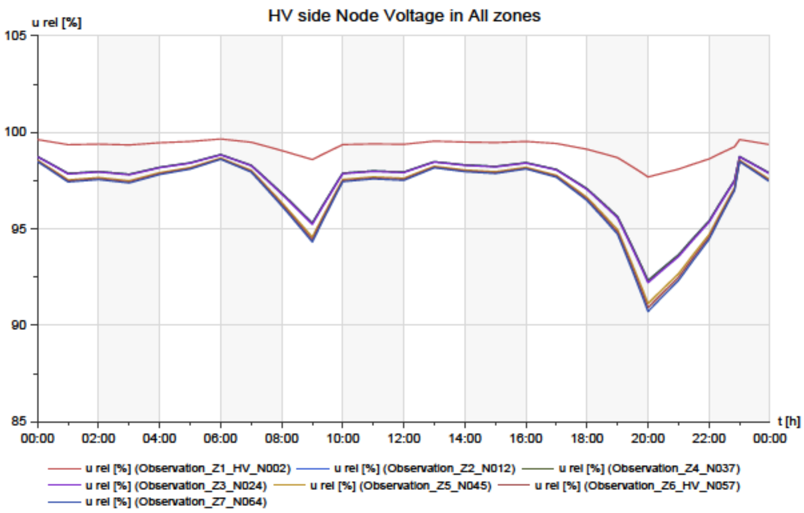

Figure 5:32 HV side - Variation in voltage level in load only condition in all zones

To observe the voltage variation at the LV side of the DT in load only condition, only Zone-7 nodes were observed as maximum voltage drop occurred in this zone. Figure 5.33 shows the voltage variation at 6 nodes in LV side of DT in Zone-7 and found that voltage varies from a minimum 87.634% to a maximum 98.569% of base voltage at 20:00PM and 06:00AM when load demand is a maximum and a minimum respectively. At 13:00PM the maximum voltage level was 98.15% of rated voltage.

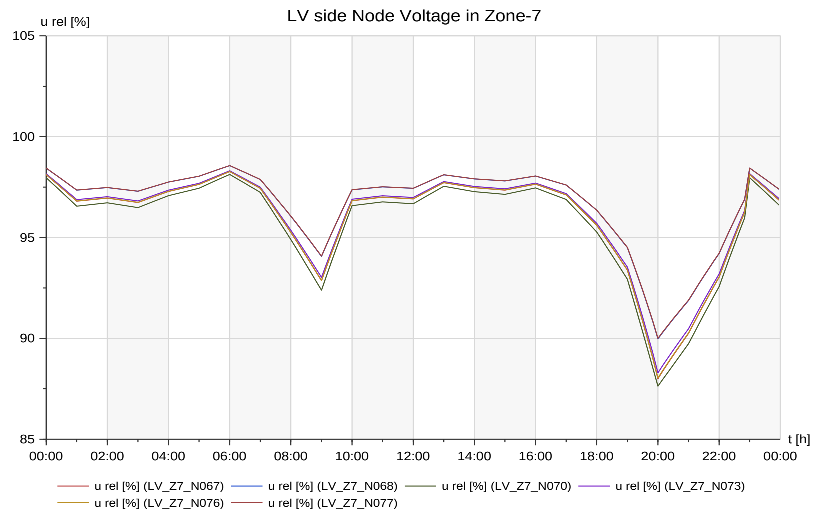

Figure 5:33 LV side - Variation of Voltage in Zone-7 in load only condition

After integrating 500 kW of PV plant at the distant node in each zone, the variation of voltage was observed at HV side and LV side of the network. Figure 5.34 shows the voltage variation in HV side of all zones. It was found that the voltage level increased after large integration of PV in the network and voltage level varied from a minimum 90.715% to a maximum 101.758% of base voltage at 20:00PM and 13:00PM respectively. Voltage level exceeds the rated level during 10:00AM to 16:00PM when PV generation is high as shown in Figure 5.34. Therefore after integrating PV (101.758 - 99.55) = 2.208% of increase in voltage was observed during the peak generation period of PV at 13:00PM.

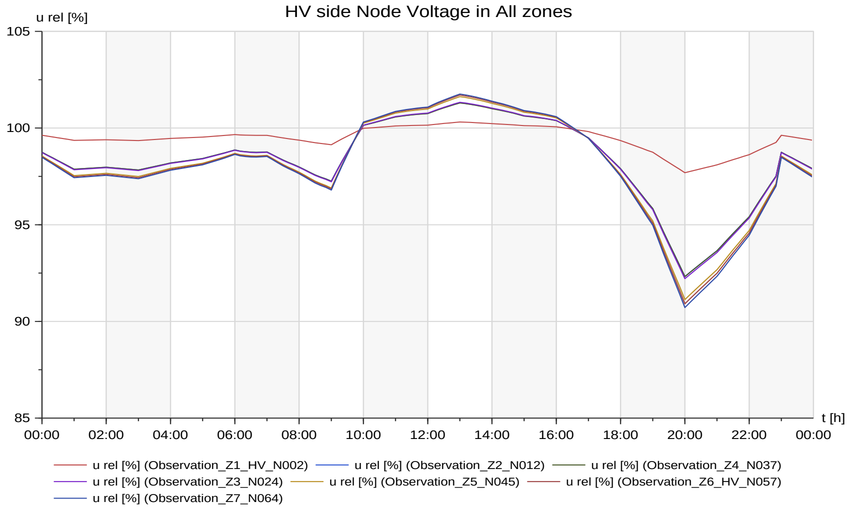

Figure 5:34 HV side - Variation in Voltage level after adding 500 kW PV in all zones

Similarly the variation in voltage was also observed in the LV side of the network after integrating PV plant in all zones. Figure 5.35 shows the variation in voltage at the secondary side of DT in six nodes in Zone-7. The change in voltage level observed a minimum 87.634% and a maximum 101.768% of base voltage at 20:00PM and 13:00PM respectively. During high PV generation time, the voltage level exceeded the rated voltage level during 10:00AM to 16:00PM. Therefore after integrating PV plant, (101.768 - 98.15) = 3.618% of increase in voltage was observed at 13:00PM at the LV side of the network.

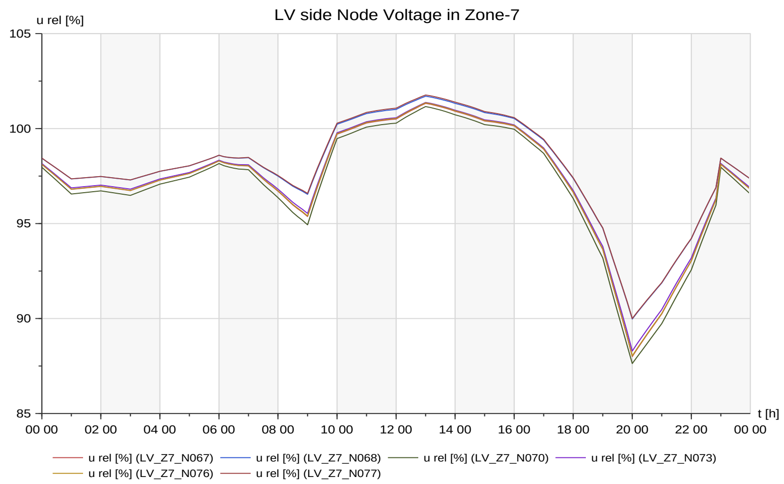

Figure 5:35 LV side - Variation in Voltage in Zone-7 after integrating PV plant

After integrating 100 kW capacity of Energy storage (Battery) in each zone near the installed PV plant, it showed that storage improved the lower voltage level during 18:00PM to 22:00PM by supporting the load demand and reduced the higher voltage level by storing energy during peak generation from PV from 10:00AM to 16:00PM. Figure 5.36 shows the variation in voltage level at the HV side of DT in all zones. It was found that voltage varies from a minimum 91.608% to a maximum 101.024%. This indicates that Storage increased the lower voltage by (91.608 - 90.715) = 0.893% at 20:00PM and also lowers the upper voltage level by (101.024 - 101.758) = (-) 0.734% at 13:00PM compared to the without storage integrated condition.

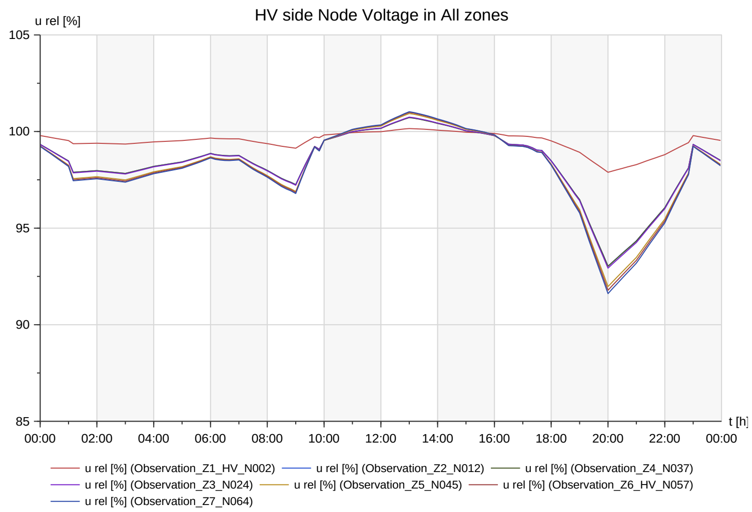

Figure 5:36 HV side - Variation in Voltage after integrating large PV and bulk storage

The variation in Voltage at the LV side was observed and Figure 5.37 shows the change in voltage variation at LV side of DT at Zone-7. Change in voltage varies from a minimum 88.565% and a maximum 101.021% of base voltage at 20:00PM and 13:00PM respectively. It was found that storage contributes the increase in the lower voltage by (88.565 - 87.634) = 0.931% at 20:00PM and lowers the upper voltage level by (101.021 - 101.768) = (-) 0.747% at 13:00PM compared to the without storage condition.

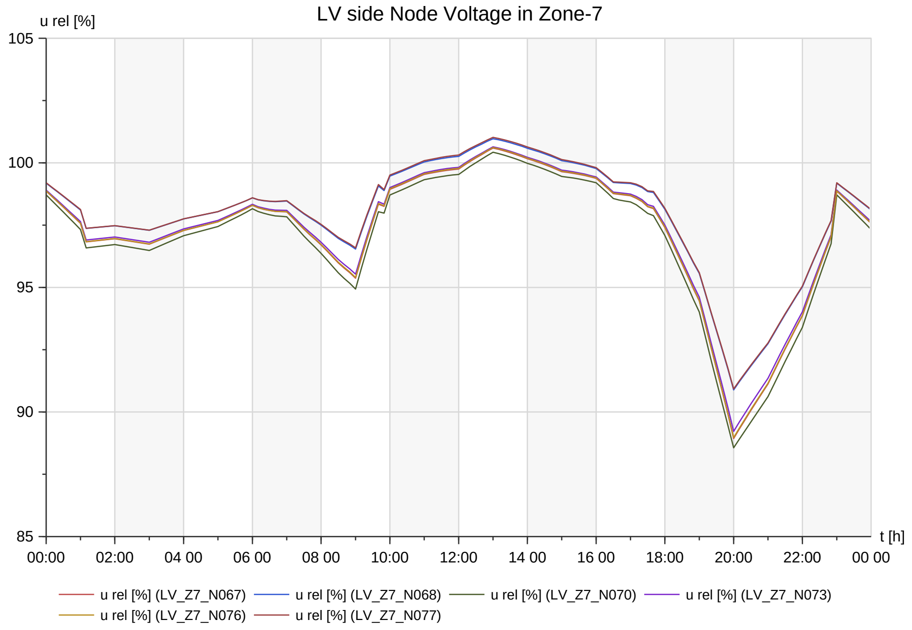

Figure 5:37 LV side - Variation in Voltage in Zone-7 after integrating large storage with PV

The findings of this investigation on small power network in Kawana, Rockhampton by integrating various capacities of RE sources and storage into the network are summarised below:

- Large integration of RE, such as Solar PV increased voltage level and during peak generation time of PV, the voltage level reached beyond the rated voltage
- Energy storage reduced this high increase in voltage during peak generation time by storing energy
- Storage increased voltage level by discharging stored energy when generation from PV was minimum or zero.

Therefore, storage improves voltage regulation with the large integration of RE into the distribution network in both HV side and LV side of the distribution network.

5.4 Results and Discussion of Investigation-4

The power network in Rockhampton was investigated to identify the impacts of storage on it and the results are discussed in this section. Details about power network in Rockhampton were discussed in chapter 4 and this network model building was also discussed in chapter 4. For the analysis, this power network was divided under 8 zone substations (ZS) as shown in

Figure 4.44 in chapter 4. Each ZS network was investigated separately and finally the combined total power network in Rockhampton was investigated. The power network model of Rockhampton covers the following 8 ZS networks:

1. Rockhampton Glenmore (RGL) ZS network
2. Pandoin (PAN) ZS network
3. Frenchville (FRN) ZS network
4. Parkhurst (PKH) ZS network
5. Berserker (BER) ZS network
6. Canning Street (CST) ZS network
7. Lakes Creek (LCR) ZS network
8. Rockhampton South (RSH) ZS network

Among the 8 ZS networks, LCR and RSH ZS network contains a part of the single phase SWER network which is a typical feature of Australian power networks. Other 6 ZS networks contain a 3 phase 11 kV distribution network that connects to the 66 kV sub-transmission part at Rockhampton Glenmore BSS and finally to the 132 kV transmissions line that connects the entire network to the main supply from Power Link.

Load is connected to the network through LV DT with 50% loaded condition. Load is connected to the LV side (415V line-line) of DT and in same node RE resources (solar PV or Wind turbine) was installed with the same capacity of load. It was discussed in Chapter-3 that for best utilisation of RE, ES is essential and estimation of required storage was also explained. Moreover in investigation-2 & 3 (in section 5.2 and 5.3) it was found that centralised installation of RE and ES have better influence in network voltage regulation. Therefore in this investigation, after integrating PV of 100% of load capacity in nodes, bulk size RE and storage was integrated in some selected nodes where voltage drop was higher. 500 kW PV or WT and 200 kW storage size was considered as was bulk size RE and storage installation. In each selected feeder 5 or 6 different observation nodes were selected and also each feeder integrated 5 different bulk size RE and storage as indicated in network figures.

The model allows switching off any network element as required. The investigation was conducted and results were compared in three network configuration modes:

1. Load only configuration
2. Load with RE configuration, and
3. Load with RE and Storage configuration

In each ZS network, the two longest feeders were selected for observation and simulated in the above three network configuration mode. The investigation of each ZS power network was conducted separately by observing selected feeders acting like a radial network. Load allocation and RE and storage distribution is listed in Appendix-A for each ZS power network. For load commercial summer load profile, summer solar PV generation and wind turbine generation was considered as shown in Figure 4.31 (a), 4.32 and 4.33 respectively in Chapter-4. The observed feeder length and load in each ZS power network is shown in Table 5.2. Feeder line parameter was explained in Chapter 4 in Table 4.4 in section 4.2.2.

Table 5:2 Feeder length & network loading information

Network	**Network Peak Load**	**Feeder-1**	**Feeder-2**
PAN	6,242 kVA	16.953 km	9.265 km
FRN	25,829 kVA	4.608605 km	10.879711 km
PKH	23,551 kVA	15.303296 km	5.561915 km
BER	18,364 kVA	3.702974 km	3.763271 km
RGL	23,422 kVA	14.475896 km	7.042022 km
LCR	17,465 kVA	10.641259 km	39.182575 km and 12.239363 km SWER-1 24.3267 km SWER-2
RSH	29,684 kVA	12.341789 km and 12.334163 km SWER	4.632956 km
CST	24,063 kVA	4.968 km	5.152002 km

The Load Flow (LF) and load curve (LC) simulation results of each ZS power network is explained below.

5.4.1 Rockhampton Glenmore (RGL) ZS Power Network

As mentioned earlier that Power Network in Rockhampton connected to the 132kV transmission line which was transformed into 66kV sub-transmission line and distributed to all zone substations. Glenmore ZS is the location where all the sub-transmission lines connected to the transmission line. ZS transformers connected the 66kV sub-transmission line to the 11 kV distribution line. The distribution network in Glenmore connects various capacity loads through several feeders and loads are connected to the 11kV distribution line through a 11kV/415V distribution transformer (DT). For the analysis it was considered loads, RE (PV or WT) and energy storage (ES) are connected to the LV side of distribution network i.e. at 415V. In order to investigate the impacts of ES on a Power network in the Glenmore ZS network, RE was integrated into all load connected nodes with 100% of load capacity. Moreover, two feeders were selected to observe the impacts where 5 nodes in each feeder were selected to observe voltage variation. The observation nodes are named as F1_N1 up to F1_N5 in Feeder-1 and F2_N1 up to F2_N5 in Feeder-2. The observation node at the beginning of each feeder named as F1_All and F2_All in Feeder-1 and Feeder-2 respective. In chapter 3, the required storage size was estimated for better utilisation of RE to support residential load demand. For solar radiation or wind speed of Rockhampton the required daily energy output from PV or WT should be 2.05 times or 1.7 times the daily load demand respectively. In this analysis, centralised RE generators of 500 KW and storage of 200 kW capacities was integrated in each 5 observation nodes in each feeder as shown in Figure 5.38. Therefore in this ZS network, RE was integrated in a distributed as well as a centralised way.

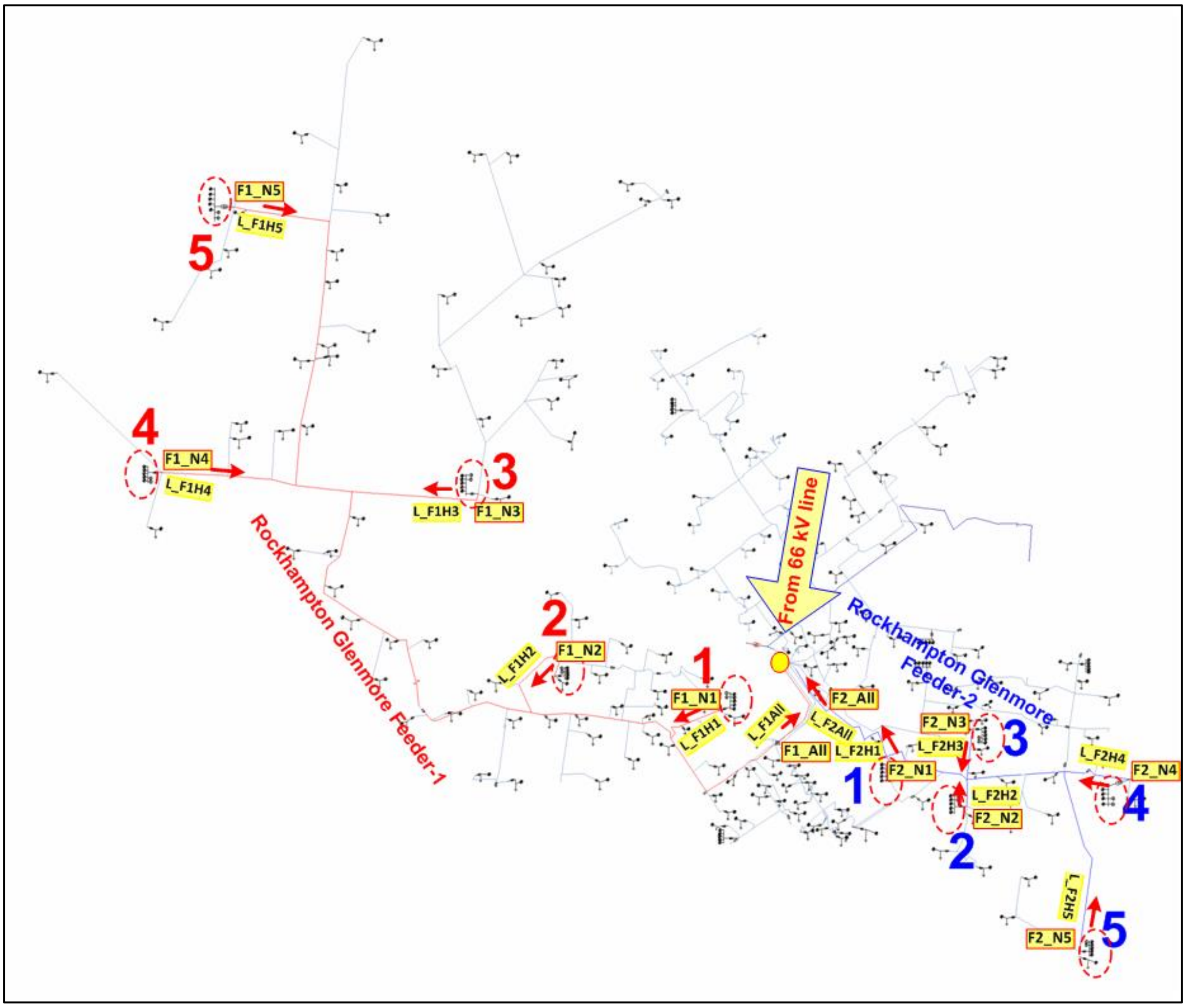

Figure 5:38 RGL ZS Power network - two feeders marked with selected observation nodes

The Load Flow (LF) calculation showed that the large integration of RE increased phase voltage, especially maximum swing was observed at distant nodes. This increase in voltage level was due to the excess energy generated by RE and the load being unable to consume all at the time of generation. On the other hand ES stored excess energy by charging storage batteries which caused the drop of the increased voltage level. Figure 5.39 and 5.40 shows the change in phase voltage in different observation nodes in Feeder-1 and 2 in load only, load with RE and load with RE and ES configurations mode.

It is clear from LF results that change in voltage or voltage swing maximum occurred at the distant nodes. In Feeder-1 at node "RGL_F1_N5", observed phase voltage was 6.1065 kV, 6.4620 kV and 6.3828 kV in Load only, load with RE and Load with RE and Storage configuration mode. In Feeder-2 at node "RGL_F2_N5", phase voltage was 6.2661 kV, 6.4067 kV and 6.3749 kV in Load only, Load with RE and Load with RE and Storage configuration mode.

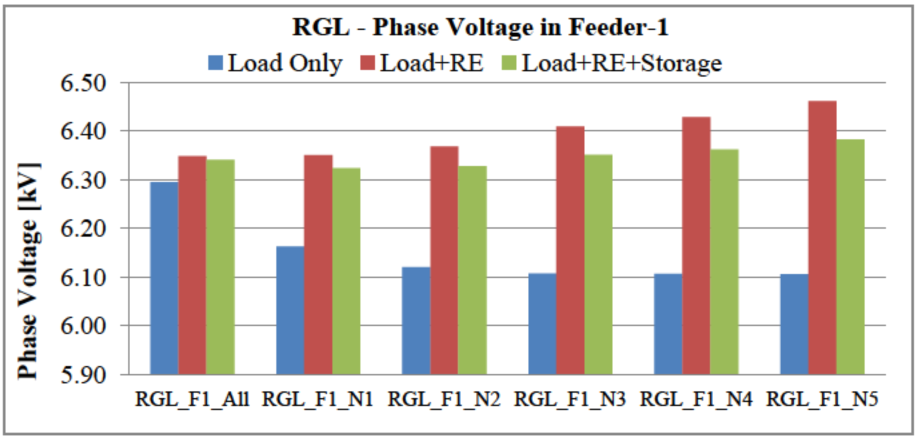

Figure 5:39 Phase voltage observed at various nodes in Feeder-1

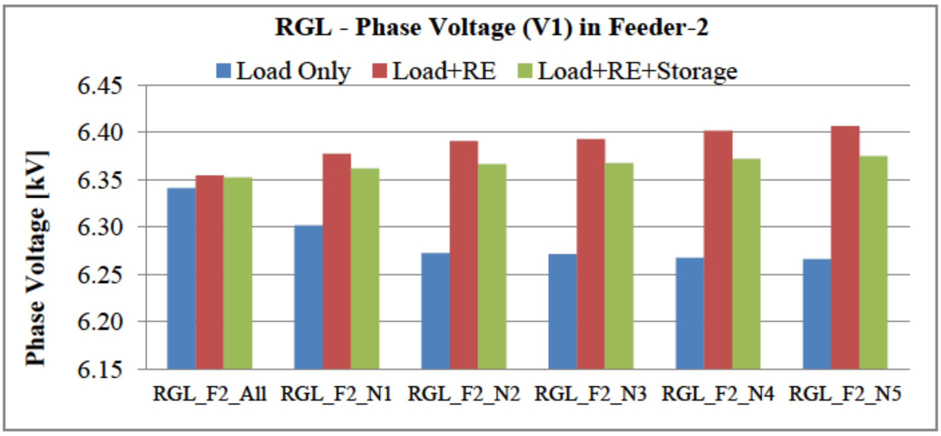

Figure 5:40 Phase voltage observed at various nodes in Feeder-2

Although Figure 5.39 and 5.40 clearly shows the change in voltage with RE and ES, but this doesn't explain timely behavior with load profile and generation profile and accordingly ES charge-discharge plays a vital role in voltage variation. Load curve (LC) calculation provides the opportunity to observe the voltage variation with time. Figure 5.41 shows the voltage variation at node "RGL_F1_All" and it is clear that the voltage level dropped during maximum load demand during mid day and the lowest voltage was 99.128% of rated voltage at 01:00PM. After integrating RE (PV) node, voltage increased as the PV generation was also maximum during mid day. At 01:00PM, 0.881% voltage increased as shown in Figure 5.41 (b). However after integrating storage voltage dropped at midday and increased voltage level a little during evening as shown in Figure 5.41 (c). Figure 5.41(d) shows the charge-discharge cycle of ES.

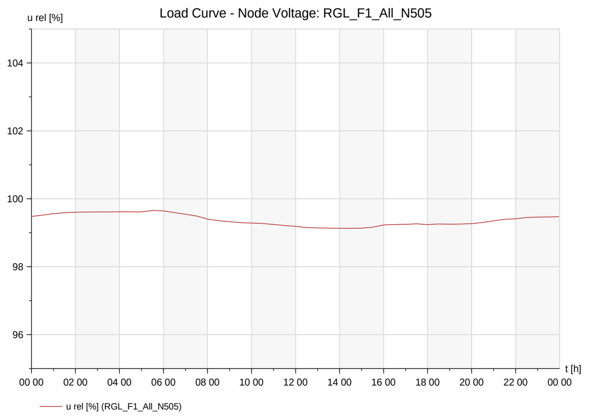

a. Load only

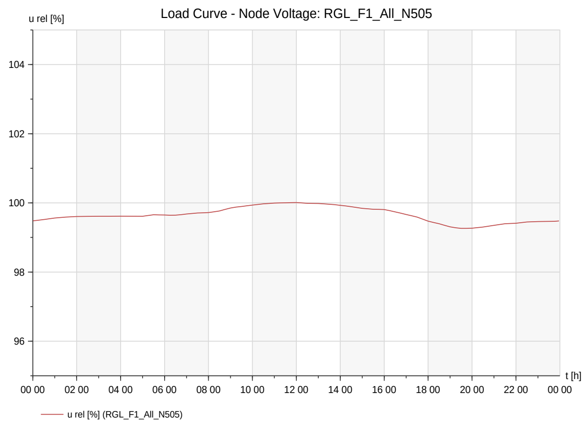

b. Load with RE

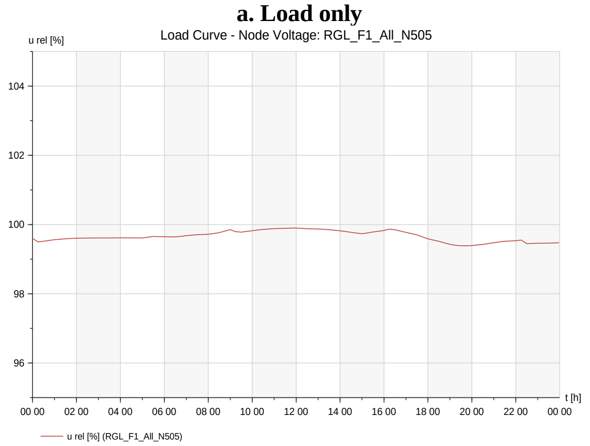

c. Load with RE and Storage

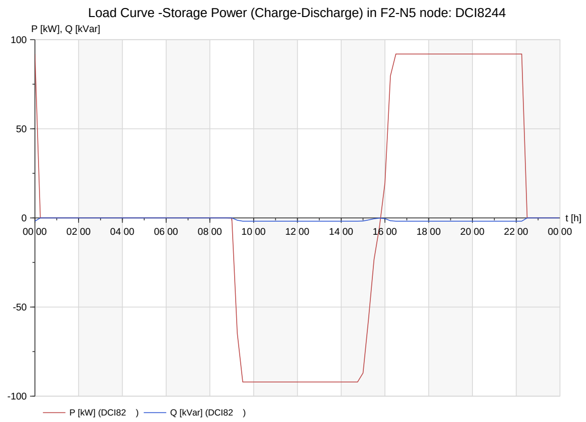

d. Storage Charge-discharge cycle

Figure 5:41 RGL ZS Power network - Voltage variation observed at node "F1_All" in Feeder-1

The change in voltage is greater in distant nodes and LC shows the variation with time. Figure 5.42 shows voltage variation in various observed nodes in Feeder-1 and Feeder-2. Minimum and maximum observed voltage levels are shown in Figure 5.42 for energy observed nodes.

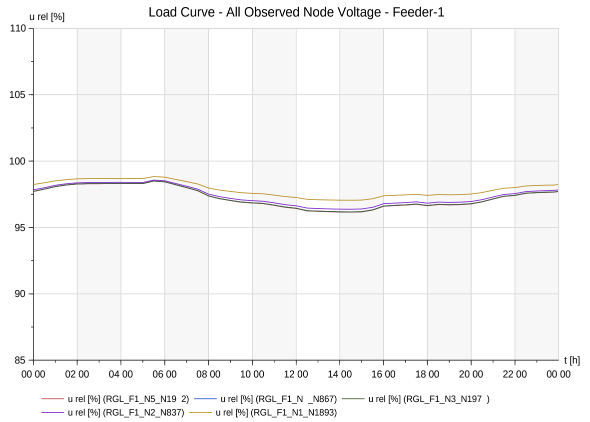

Feeder-1: Load only (96.153% to 98.834%)

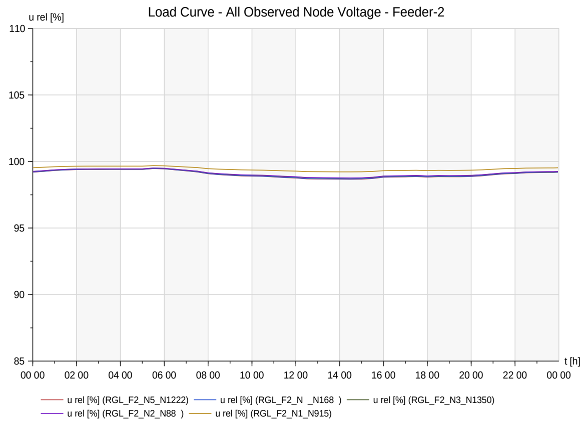

Feeder-2: Load only (98.66% to 99.69%)

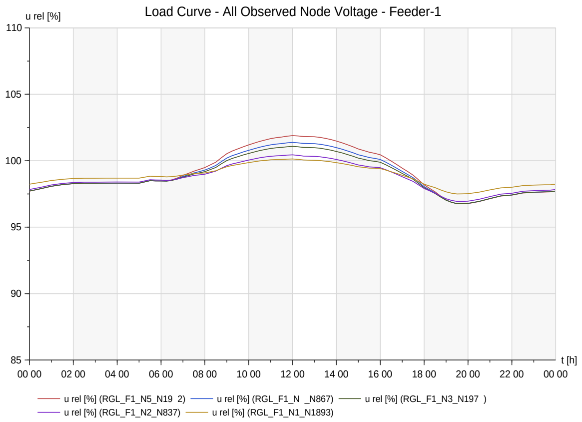

Feeder-1: Load with RE (99.26% to 100.009%)

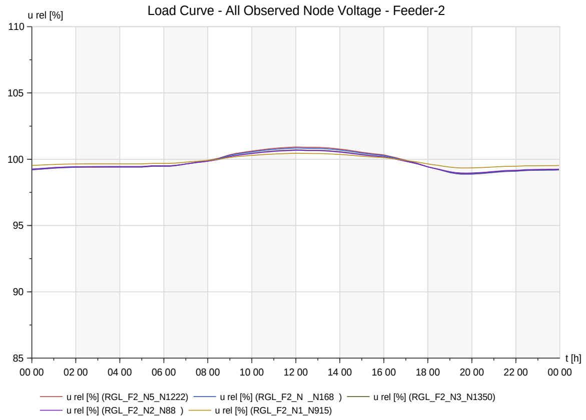

Feeder-2: Load with RE (98.87% to 100.92%)

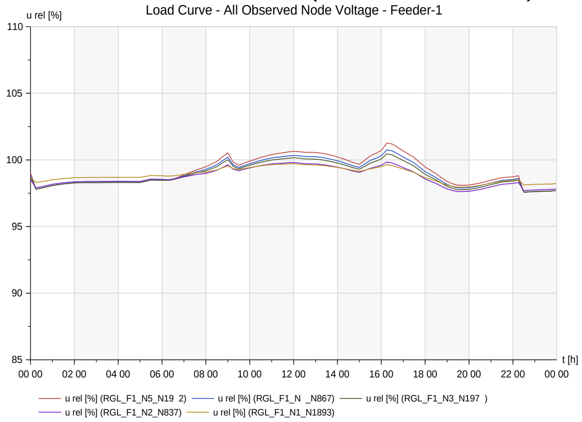

Feeder-1: Load with RE & Storage (97.57% to 101.26%)

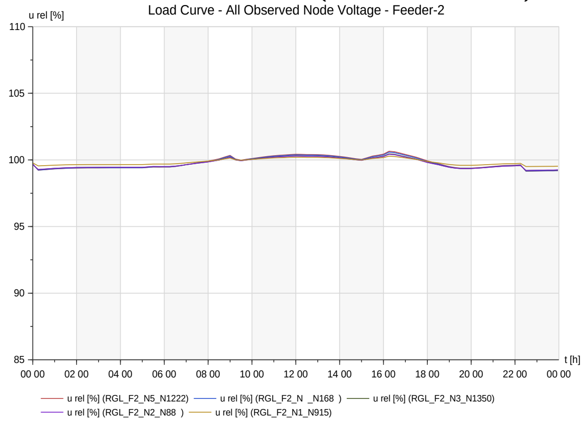

Feeder-2: Load with RE & Storage (99.15% to 100.653%)

Figure 5:42 RGL ZS power network - Voltage variation at different observed nodes

Therefore from the investigation on RGL ZS power network it was found that the impacts on distant nodes are higher. The LF and LC analysis showed that:

- Voltage drop was higher in distant nodes in load only condition
- LF analysis showed that voltage starts rising after integrating PV in the network. At distant node in Feeder-1 voltage rise was 5.8% and in Feeder-2 it was 2.24% after integrating PV compared to the load only condition
- After integrating storage voltage dropped in all observed nodes. At distant node it was found that voltage dropped 1.22% in Feeder-1 and 0.5% in Feeder-2 after integrating storage in the network
- LC analysis showed that during 09:00AM to 16:00PM voltage rise occurred due to PV. After integrating storage, voltage dropped during peak generation time around 12:00PM. It was also found that after 16:00PM storage discharge increased network voltage

5.4.2 Pandoin (PAN) ZS Power Network

The observation nodes and selected feeder in this ZS power network is shown in Figure 5.43. As the feeder is very long, there is enough power loss due to line impedance and enough voltage drops were observed at the distant nodes. In Feeder-1, 6 nodes and in Feeder-2, 5 nodes were selected to observe voltage variation. The observed nodes are named as F1_N1 up to F1_N6 in Feeder-1 and F2_N1 up to F2_N5 in Feeder-2. Both the feeders connected to a node that is marked as “All” in the Figure 5.43 where total impacts on the network were observed.

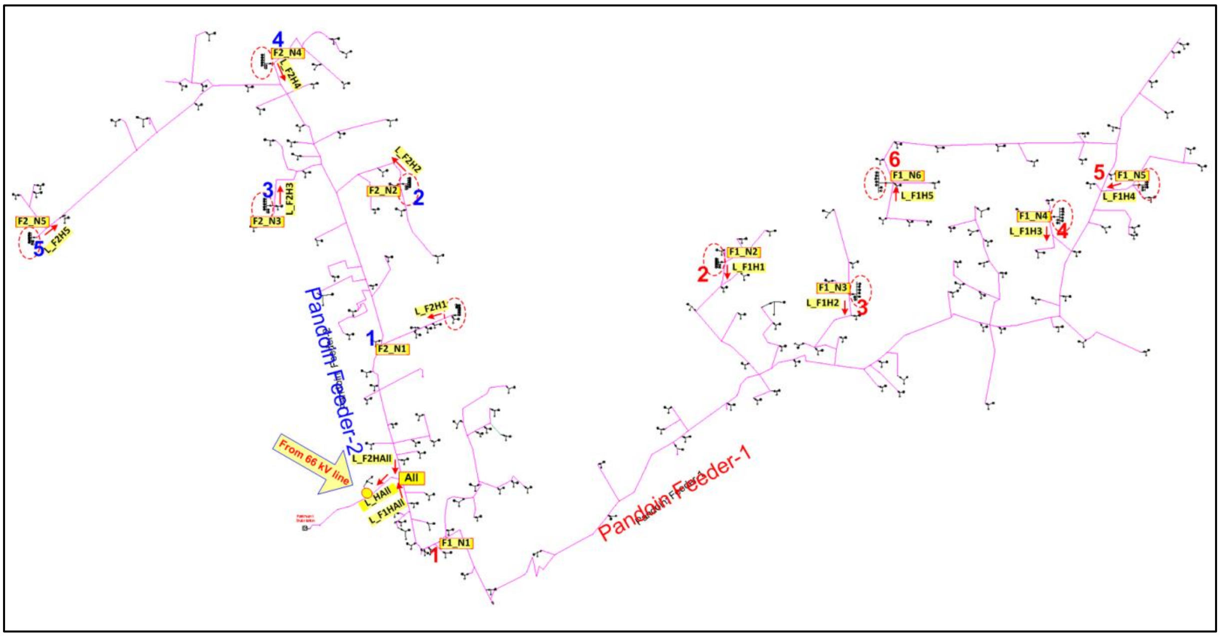

Figure 5:43 PAN ZS Power network - two feeders marked with selected observation nodes

Load Flow calculations showed that phase voltage decreased towards the end node in load only network configuration. After adding PV, phase voltage increased more at the distant nodes. Due to high PV penetration phase voltage became greater than the rated voltage of 6.35kV. After integrating storage, the increased phase voltage started dropping as did storage stored energy when PV was generating excess energy. Figure 5.44 and 5.45 shows the changes in phase voltage in load only, load with PV and load with PV and storage configuration mode.

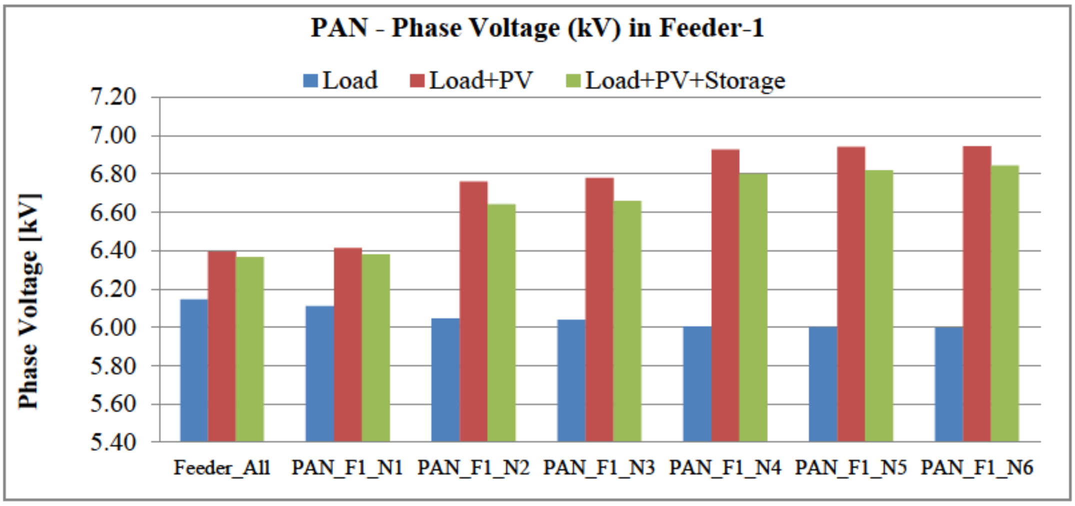

Figure 5:44Phase Voltage at various points in Feeder-1

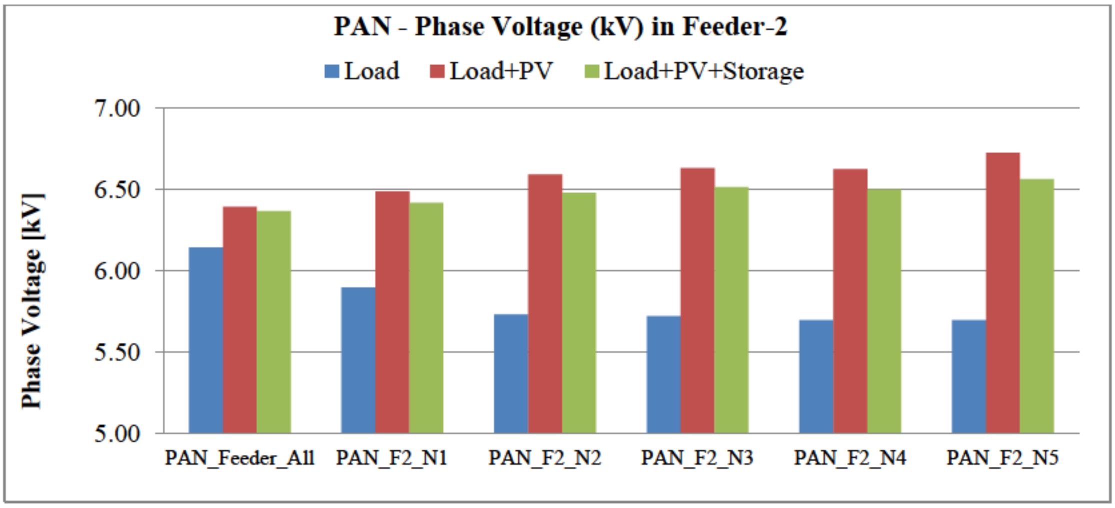

Figure 5:45 Phase Voltage at various points in Feeder-2

As the load demand varies over time and similarly energy generation from PV, therefore the load flow calculation is unable to show the variation of voltage with time. Load curve or load profile calculation provides the variation in voltage for 24 hours a day which provides the exact scenario of voltage variation for all three network configurations. For this analysis, load curve measured voltage in every 15 minutes interval for the whole day. Figure 5.46(a) shows the voltage regulation (percentage of voltage compared to rated voltage) in load only configuration at the node "All" where both feeders connected. As the load demand is very high during mid day therefore voltage dropped during that time and the minimum voltage appeared between 01:00PM to 3:00PM when voltage regulation was 96.732% and maximum voltage observed in the morning when voltage regulation was 98.512%.

After integrating distributed and bulk centralised PV the voltage regulation was changed. Figure 5.46(b) shows the voltage variation at the node point marked “All” and it is observed that the voltage level increased during PV generation time even if the load demand was high during the time 9:00AM to 18:00PM. Voltage regulation varied from 97.284% to 100.772% of rated voltage. It was identified that voltage level was increased 3.7% at 12:00PM compared to load only configuration.

When storage was integrated to the selected nodes where bulk PV was integrated, voltage level dropped when PV generates excess energy as compared to the load demand during mid day as shown in Figure 5.46(c). Voltage regulation was observed at the node point marked “All” and it was found that during 9:00AM to 15:00PM, storage stored excess energy in the network. However storage increased voltage level when PV generation stopped during evening by discharging stored energy to support load demand as shown in Figure 5.46(c). It was also observed that storage discharged completely at 23:00PM as shown in Figure 5.46(d) and voltage level drops at the observed node as a consequence.

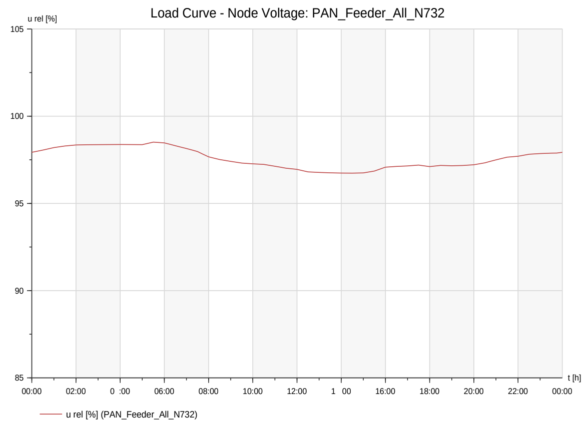

a. Load only configuration

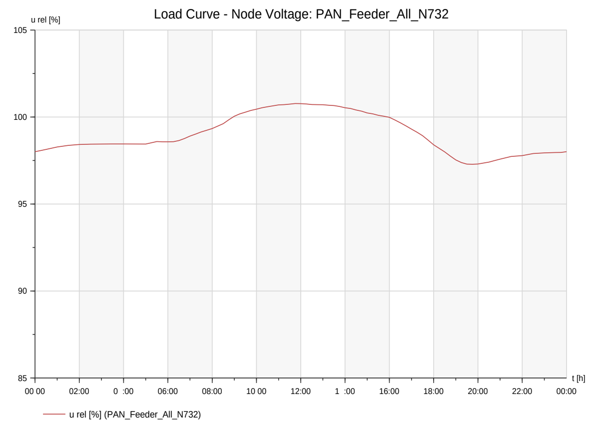

b. Load with PV configuration

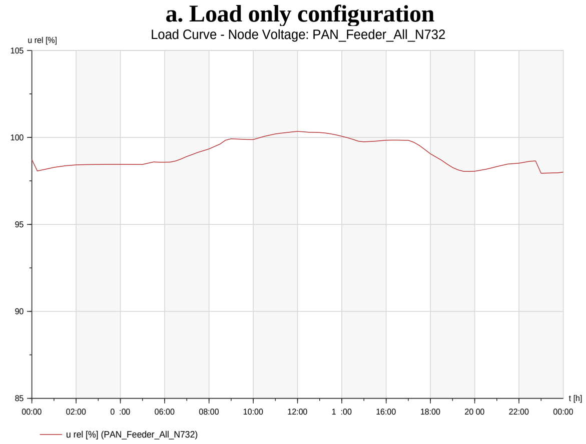

c. Load with PV & Storage configuration

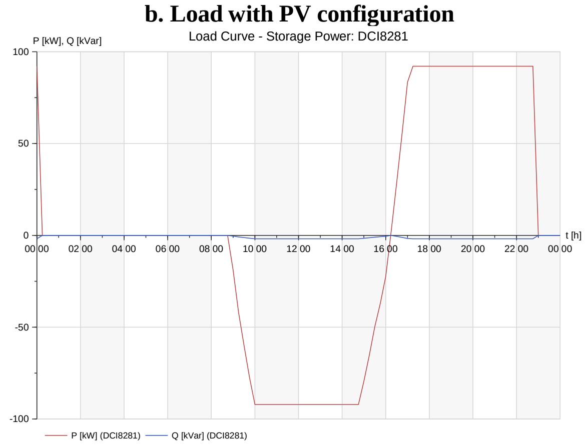

d. Storage charge-discharge cycle

Figure 5:46 Voltage variation observed at node "All" and storage charge-discharge cycle

The change in voltage or voltage variation was also observed in various observation nodes in Feeder-1 and Feeder-2 as shown in Figure 5.47. It was observed that voltage variation is much greater in distant nodes and it was also observed that storage reduced the higher voltage level that was experienced by the integration of large PV systems into the Pandoin ZS power network.

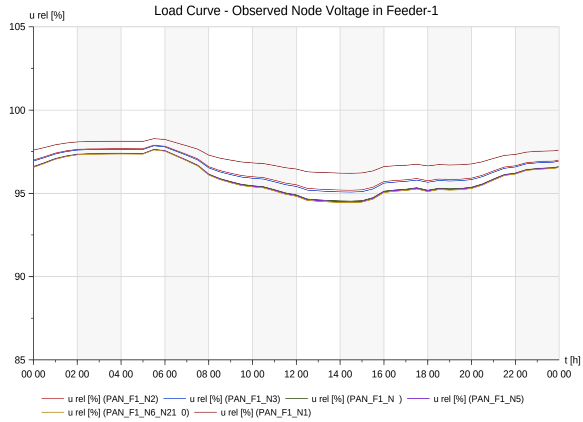

Feeder-1: Load Only

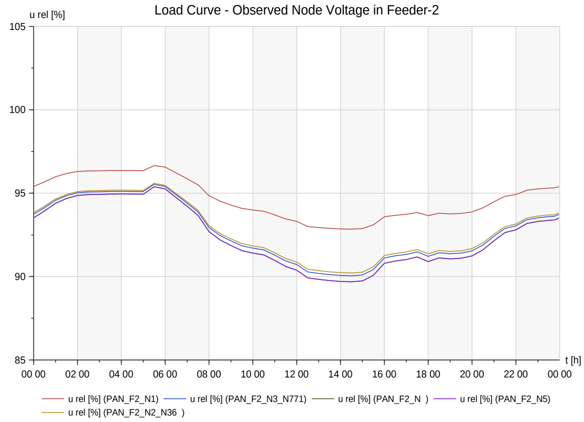

Feeder-2: Load Only

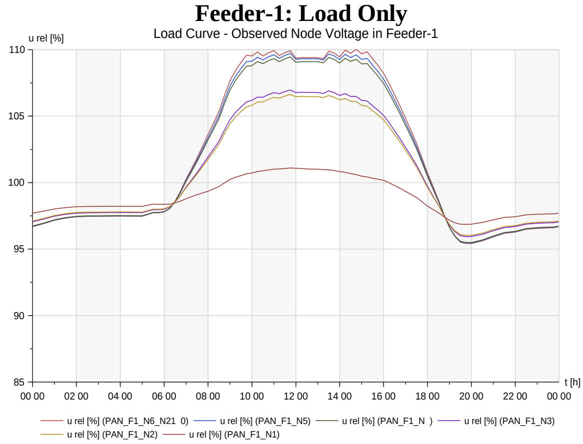

Feeder-1: Load with PV

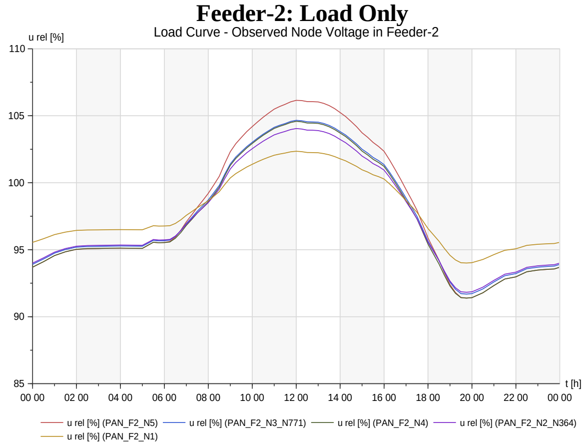

Feeder-2: Load with PV

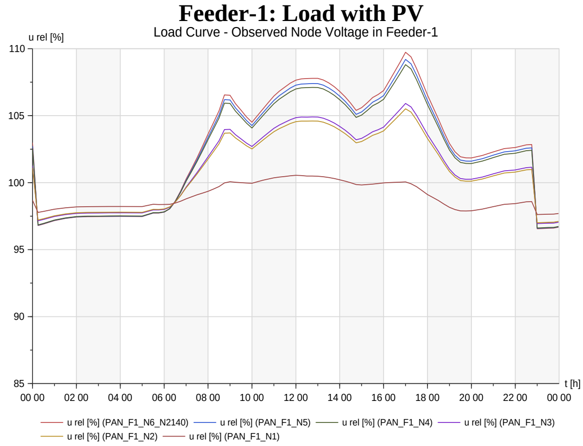

Feeder-1: Load with PV and Storage

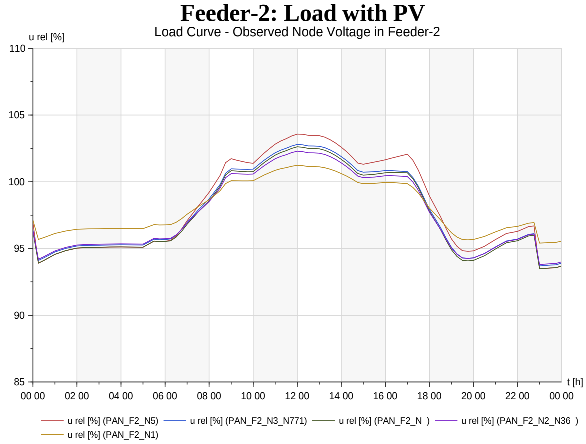

Feeder-2: Load with PV and Storage

Figure 5:47 Pandoin ZS Power network - Voltage variations at different observed nodes

The investigation on PAN ZS power network showed the similar result like RGL ZS power network. The LF and LC analysis showed that:

- Voltage drop was higher in distant nodes in load only condition
- LF analysis showed that voltage starts rising after integrating PV in the network. At distant node in Feeder-1 and in Feeder-2 voltage rise was above the rated voltage of 6.35kV
- After integrating storage voltage dropped in all observed nodes. At distant node it was found that voltage dropped maximum in both Feeder-1 and Feeder-2 after integrating storage in the network
- LC analysis showed that voltage level rise 3.7% at 12:00PM due to the integration of large PV compared to the load only configuration. After integrating storage, maximum voltage dropped during peak generation time around 12:00PM. It was also found that after 16:00PM storage discharge increased network voltage level

5.4.3 Frenchville (FRN) ZS Power Network

Two feeders and five nodes in each feeder were selected to observe the voltage variation in the Frenchville ZS power network as shown in Figure 5.48. Five observation nodes marked from 1 to 5 in Feeder-1 and 2 and named as “F1_N1 to F1_N5” and “F2_N1 to F2_N5” respectively. In each feeder, at five observation nodes, bulk size RE plant (PV or WT) and storage plant was installed. Feeder-2 covers very distant areas which is favourable for wind turbines, therefore in this feeder at node-4 and 5 500 kW WT and 200 kW storage was installed. However as mentioned earlier, all load connected nodes were integrated with PV of 100% load capacity. The power network model was simulated in load only, load with RE and load with RE and storage configuration mode.

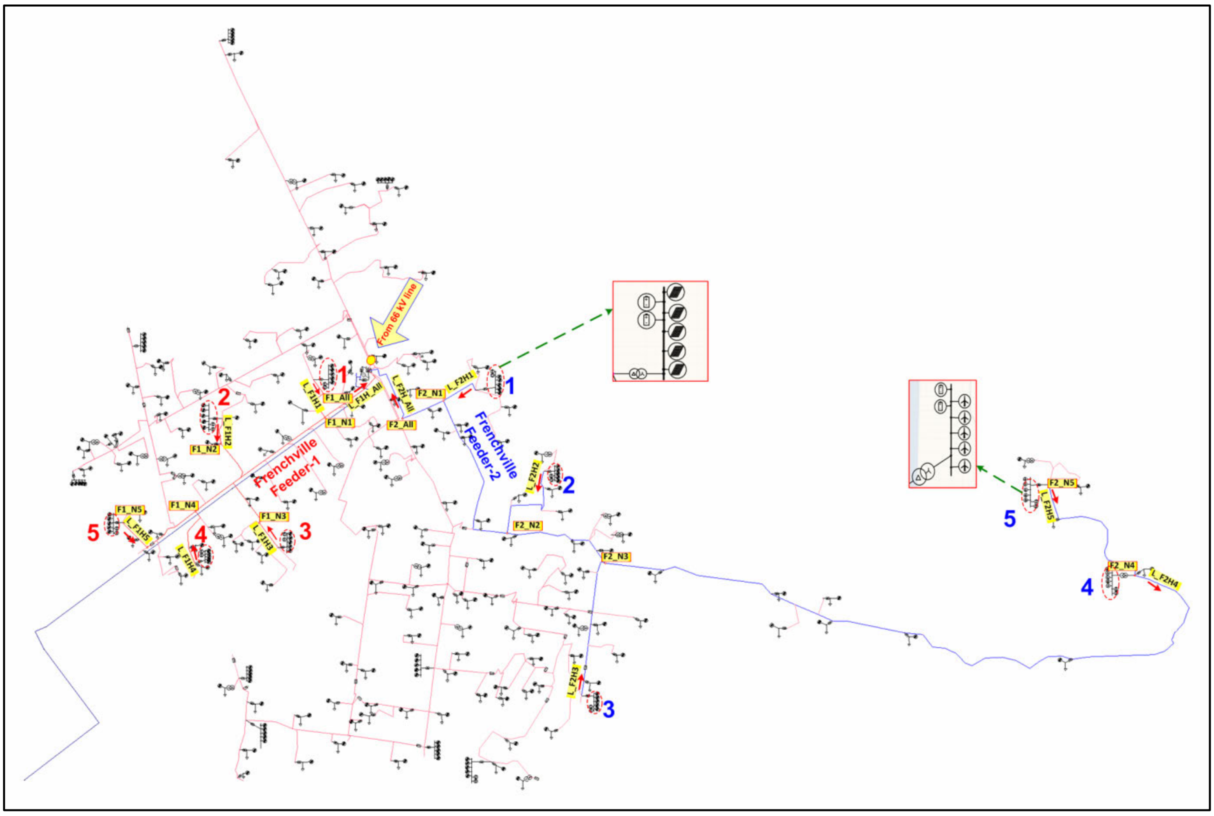

Figure 5:48 FRN ZS Power Network - two feeders marked with selected observation nodes

Load Flow (LF) calculations showed that phase voltage decreases towards the end node in load only configuration. Due to longer feeder length and therefore greater line impedance in Feeder-2, the voltage drop in distant nodes was more as compared to Feeder-1 (shown in Figure 5.49 and 5.50). After integrating RE (PV or WT), the node voltage increased and this increase was greater at distant nodes, therefore voltage swing is much greater in distant nodes. However after integrating storage, excess energy generated by RE that was stored in storage, eventually reduced the increased voltage level to a reasonable level as shown in Figure 5.49 and 5.50. For example at node “FRN_F2_N5” in load only condition phase, voltage was 6.0487 kV, in load with RE voltage was 6.467 kV and after integrating storage voltage became 6.383 kV.

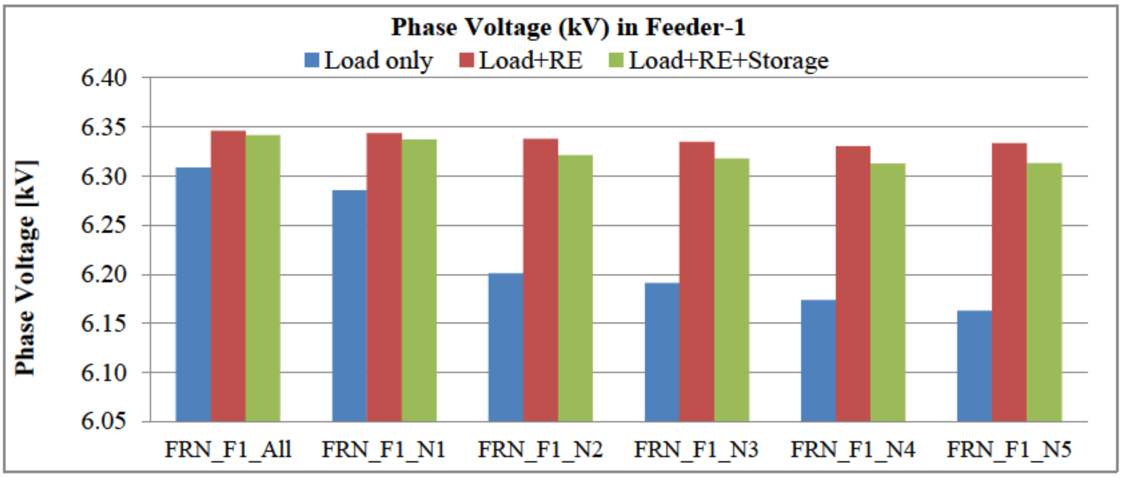

Figure 5:49 Phase Voltage at observation nodes in Feeder-1

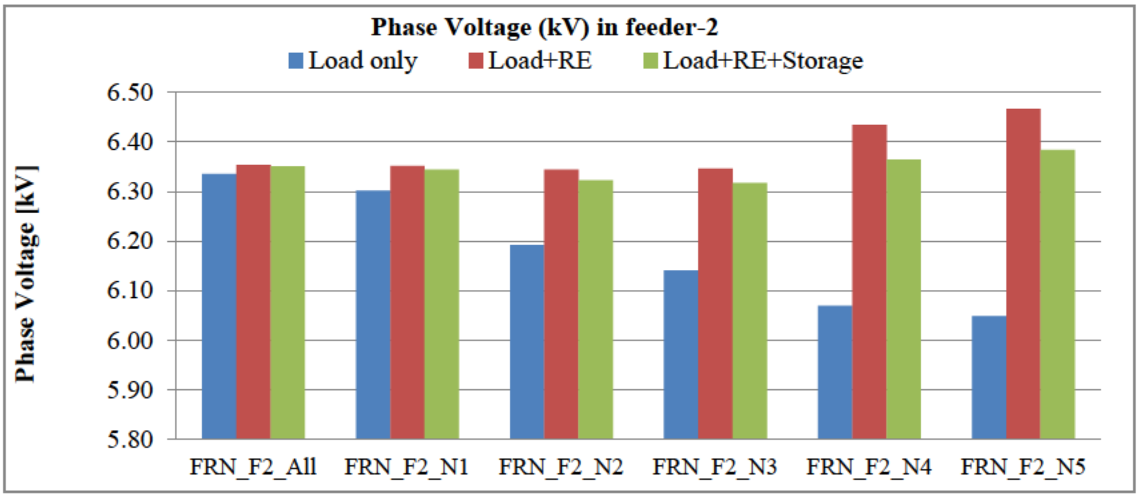

Figure 5:50 Phase Voltage at Observation nodes in Feeder-2

As the load demand varies with load profile and RE generation also varies, the Load curve (LC) calculation provides exact scenarios of voltage variation for 24 hours a day in all case configurations. Figure 5.51(a) shows the voltage regulation (percentage of voltage compared to the rated voltage) in load only configuration at the node "F1_All" in Feeder-1 and found that due to high load demand during mid day, voltage dropped during that time. The minimum voltage appeared between 12:00PM and 03:00PM when voltage regulation was 99.336% and the maximum voltage observed in the early morning at 05:30AM when voltage regulation was 99.736%.

After adding RE (PV and WT), voltage regulation was changed. During maximum generation from PV and WT the voltage level increased during mid day as shown in Figure 5.51 (b) at node F1_All" in Feeder-1. The voltage level increased during 09:00AM to

16:00PM even the high load demand during this time and voltage varied from a minimum 99.336% to 99.954% of rated voltage. Therefore at 01:00PM voltage increased 0.618% compared to the load only configuration.

After integrating battery as storage, excess energy stored into the storage during 09:00AM to 15:00PM, reduced the voltage level during that time. However storage increased voltage after 16:00PM by discharging stored energy to support load demand of the network. This activity of charging and discharging reduced the voltage and increased the voltage as observed in node F1_All and shown in Figure 5.51 (c). Figure 5.51 (d) shows the charging and discharging cycle of storage installed at node-5 in Feeder-1.

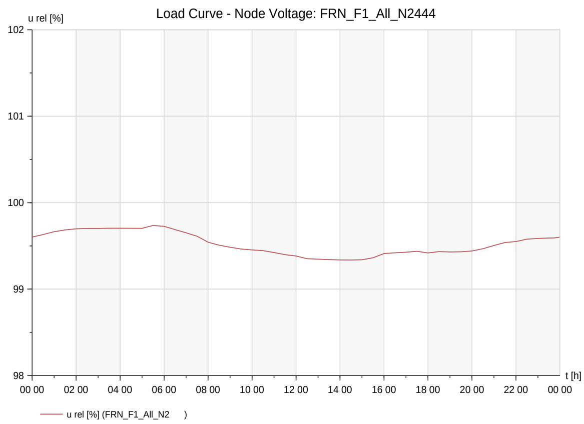

a. Load only configuration

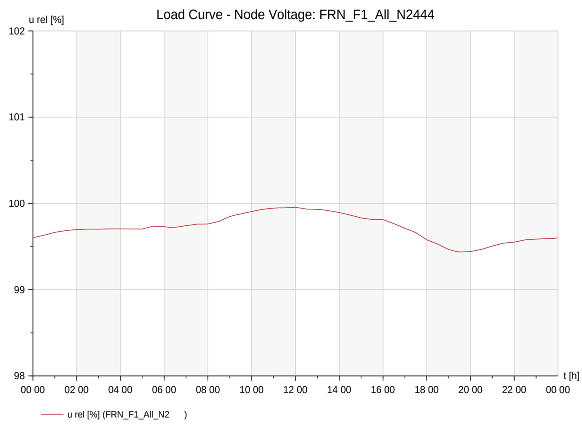

b. Load with RE configuration

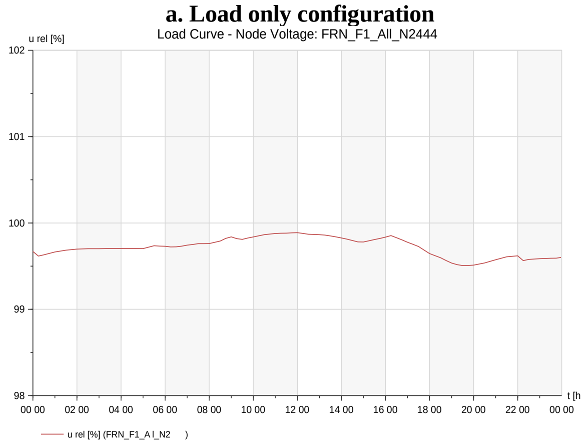

c. Load with RE and Storage

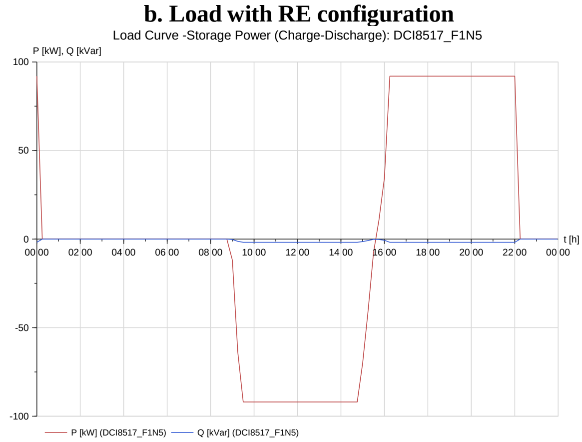

d. Storage Charge-discharge cycle

Figure 5:51 FRN ZS - Voltage variation observed at node "F1_All" and storage charge-discharge cycle

The change in voltage was also observed in various observation nodes in Feeder-1 and Feeder-2 of Frenchville ZS power network as shown in Figure 5.52. It was observed that voltage variation was much greater in distant nodes, however it was found that ES reduced the increased voltage level during peak generation time of RE, and also increased the voltage level when RE generation was absent.

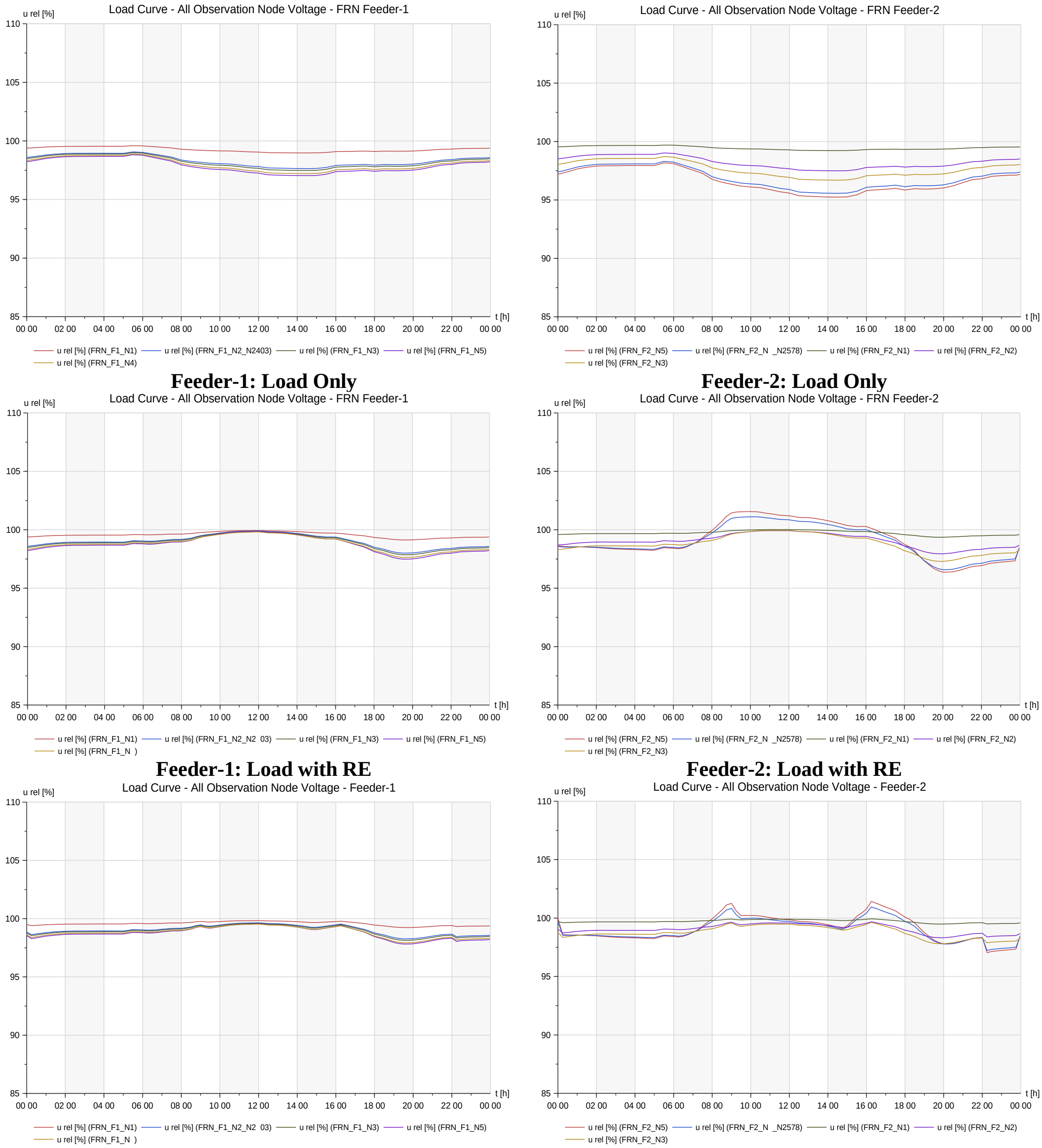

Feeder-1: Load Only **Feeder-2: Load Only**

Feeder-1: Load with RE **Feeder-2: Load with RE**

Feeder-1: Load with RE and Storage **Feeder-2: Load with RE and Storage**

Figure 5:52 Voltage variation observed at different node points in Frenchville ZS Power Network

FRN is a nearly uniform distributed load network and therefore minimum voltage variation was observed due to RE and storage in the network. The LF and LC analysis in the investigation on FRN ZS power network showed that:

- Phase voltage level decreases towards the distant nodes in load only condition

- LF analysis showed that voltage starts rising after integrating PV or WT in the network. A 6.91% voltage rise was observed at distant node in Feeder-2 after integrating PV and WT compared to the load only condition.
- After integrating storage with PV and WT voltage dropped in all observed nodes and 1.3% voltage drop was observed at distant node in Feeder-2.
- LC analysis showed that voltage level rise 0.618% at 01:00PM due to the integration of large PV and WT compared to the load only configuration. After integrating storage, maximum voltage dropped during peak generation time around 12:00PM. It was also found that after 16:00PM storage discharge increased network voltage level

5.4.4 Parkhurst (PKH) ZS Power Network

In Parkhurst, two long network feeders were considered for the analysis and Feeder-1 covered long distant loads. Feeder-1 runs on a line that follows Belmont Road and passes the Glendale area that covers distant small loads where wind speed is moderate and suitable for wind turbine installation, therefore WT was considered at Node-5 in Feeder-1. Due to the line impedance and low capacity load distributed at the distant nodes, there was enough power loss during supporting of the distant loads. Feeder-2 covered the load of the Kawana suburb and adjacent areas which have residential and commercial loads. In Feeder-1, 5 different observation nodes were selected where 500 kW RE and 200 kW storage was integrated. As Feeder-2 covers mostly populated areas, it is suitable for PV installations. In Feeder-2 500 kW size PV and 200 kW size storage was installed in 5 node points from “F2_N2 to F2_N6” or observation node 2 to 6 as indicated in Figure 5.53. The network was analysed in load only, load with RE and load with RE and storage configuration mode. Figure 5.53 shows the Parkhurst ZS power network with selected feeders and observation nodes in each feeder. In each feeder the first observation node was named as “F1_All and F2_All” in Feeder-1 and Feeder-2 respectively.

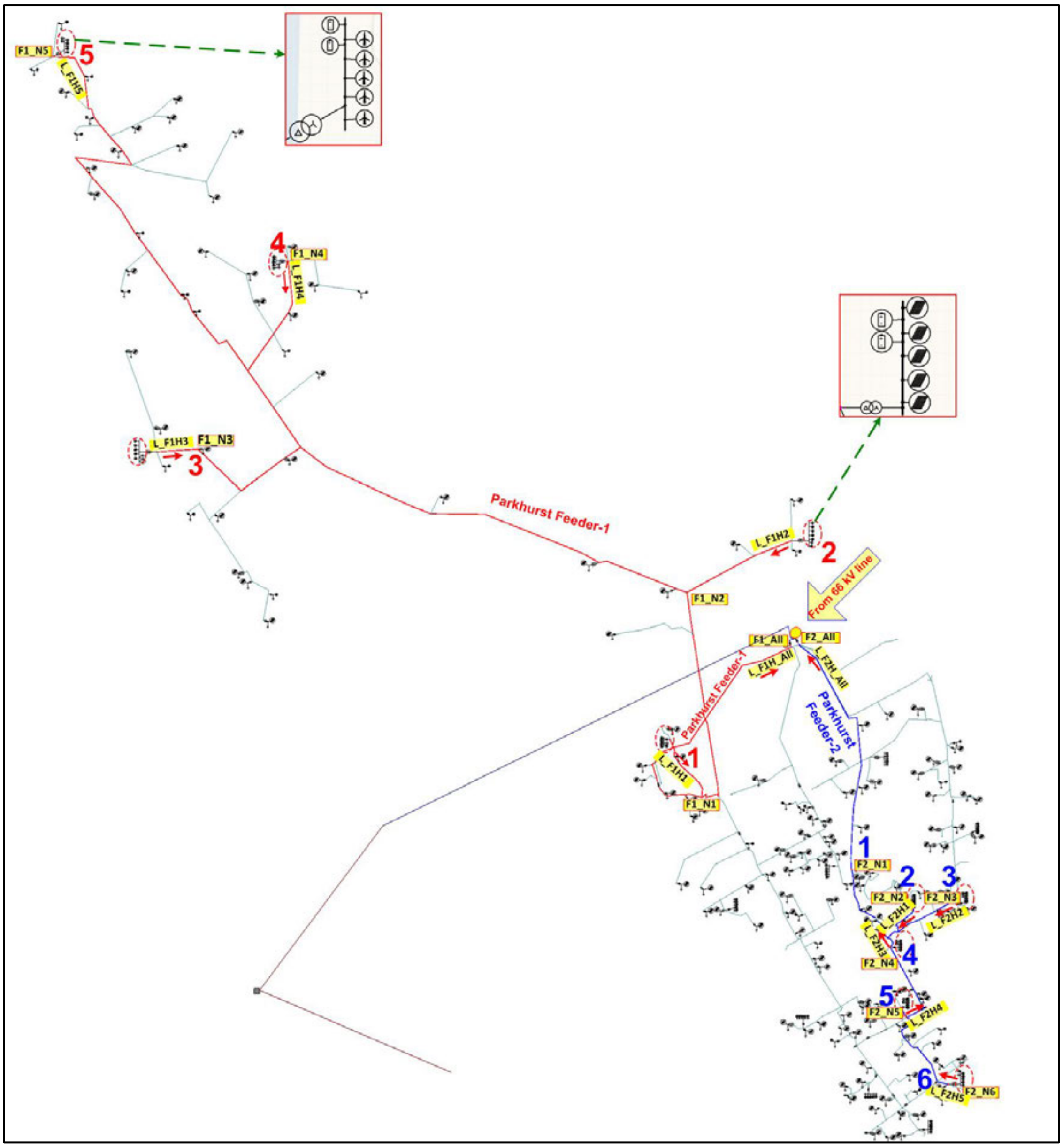

Figure 5:53 PKH ZS Power network - Observation feeders and nodes

Load flow (LF) calculations showed that phase voltage decreases from the supply source to the distant nodes in case of load only configuration. In Feeder-1 installed loads were of smaller capacity, therefore any voltage drop was mostly because of long line impedance. Due to high RE penetration phase voltage in Feeder-1 became greater than the rated voltage of 6.35 kV. In Feeder-1 at observation point 5 or at Node-5 the variation of voltage was observed as shown in Figure 5.54. It was found that at observation point 5 in Feeder-1 the voltage swing is high from load only to load with RE configuration and also after integrating storage. The node voltage was 6.1798 KV, 6.920kV and 6.6945 kV in load only, load with RE and load with RE and Storage configuration mode respectively.

In Feeder-2 comparatively large capacity loads were connected and a greater voltage drop was observed at the six observation nodes, as shown in Figure 5.55. After integrating RE, voltage started increasing in all observation nodes, however due to the high load demand this rise in voltage did not cross the rated voltage limit. Again, after integrating storage, voltage started dropping as storage stored excess energy from RE as shown in Figure 5.55. At node "F2_N6" i.e. at the distant node in Feeder-2 the observed voltage was 5.8 kV, 6.329 kV and 6.267 kV in load only, load with RE and load with RE and storage configuration mode respectively.

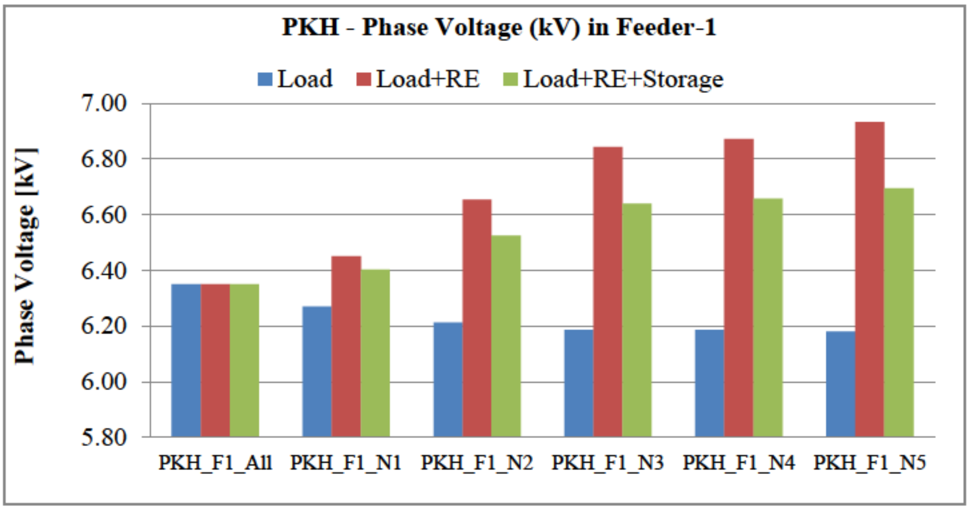

Figure 5:54 Phase Voltage at various points in Feeder-1

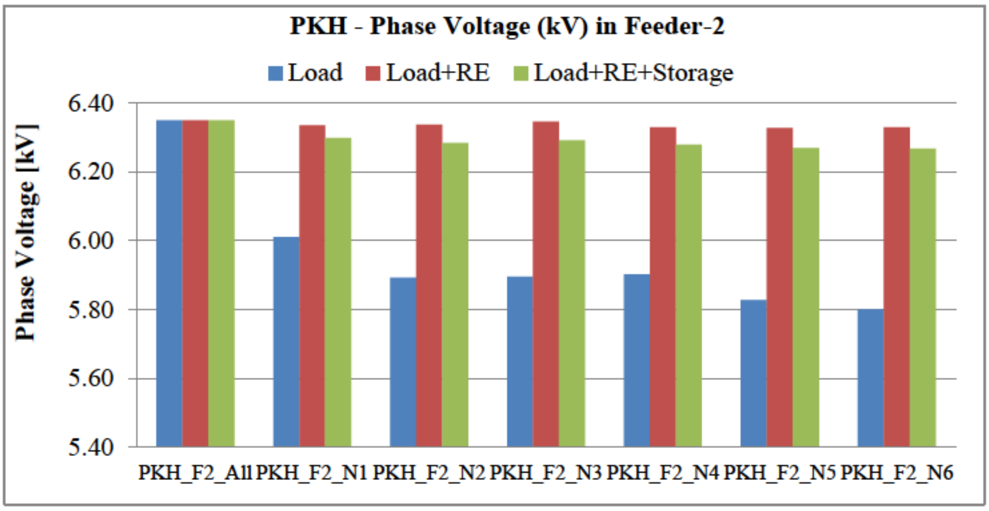

Figure 5:55 Phase Voltage at various points in Feeder-2

Load curve (LC) calculates LF in every 15 minutes for 24 hours a day which provides the exact scenario of the voltage variation with time. Figure 5.56 (a) shows the voltage regulation (percentage of voltage compared to rated voltage) in load only configuration at observation point 1 or at node "F1_N1" in Feeder-1 and it was found that due to high load demand during mid day, voltage dropped and minimum voltage appeared at 01:00PM to 03:00PM when voltage regulation was 98.713% and maximum voltage observed in the early morning at 05:30AM when voltage regulation was 99.514%.

After integrating RE, voltage regulation was changed. As the PV and WT generation profile has maximum generation during mid day, an increase in voltage was observed during mid day and Figure 5.56(b) showed this for node "F1_N1" in Feeder-1. It was found that the voltage level exceeds the rated voltage during 07:00AM to 18:00PM, and even the high load demand during this time and voltage varied from minimum 98.979% to 101.508% of rated voltage. Therefore at 13:00PM there was a voltage increase of 2.795% compared to load only condition.

After integrating battery as storage, excess energy stored into the storage during 09:00AM to 16:00PM reduced the voltage level during that time. At 13:00PM observed voltage was 101.0% of rated voltage. Therefore at 13:00PM storage reduced voltage by 0.508%. However storage increased voltage after 16:00PM by discharging stored energy to support load demand of the network. This activity of charging and discharging improved voltage regulation at the observed node "F1_N1" as shown in Figure 5.56 (c). Figure 5.56 (d) shows the installed storage charging and discharging cycle.

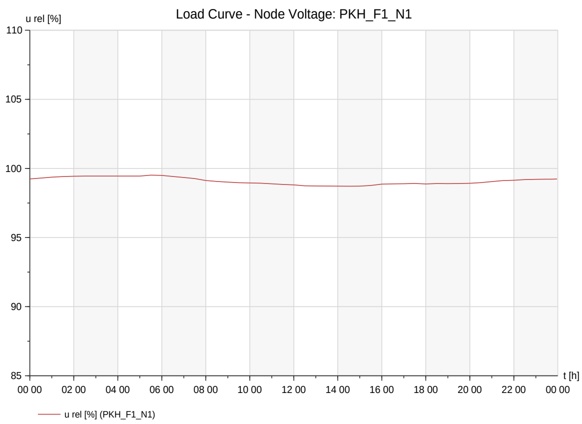

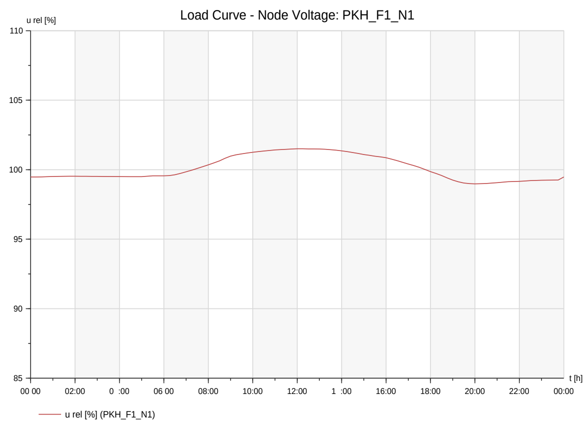

a. Load only **b. Load with RE**

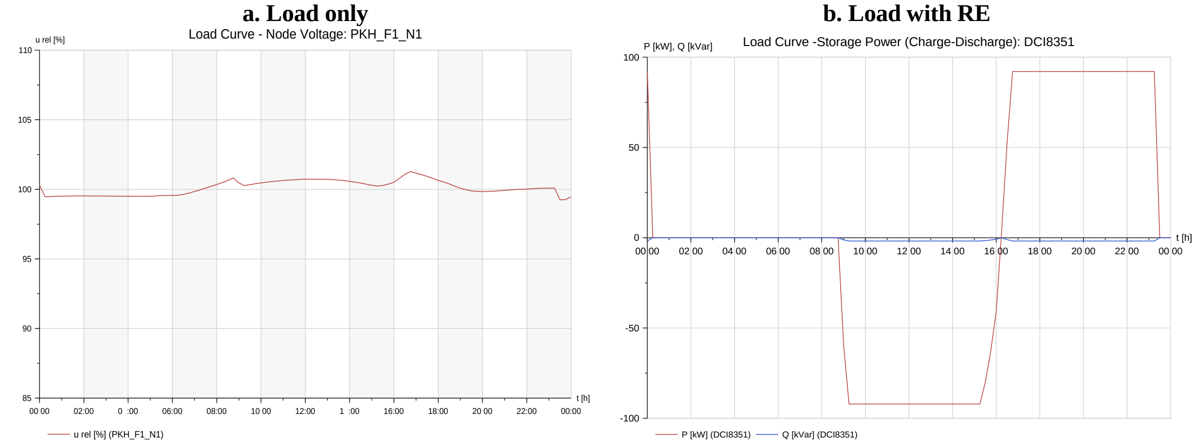

c. Load with RE and Storage **d. Storage charge-discharge cycle**

Figure 5:56 PKH ZS - Voltage variation observed at "F1_N1" in Feeder-1 & Storage charge-discharge cycle

Similarly, voltage variation was observed in Feeder-2 also. It was observed that voltage variation was greater in distant nodes during high load demand and also during maximum energy penetration from RE. It was also observed that storage reduced high voltage levels but increased voltage when RE generation was absent. Figure 5.57 shows the voltage variation at different observation nodes in Feeder-1 and feeder-2 in load only, load with RE and load with RE and storage configuration mode.

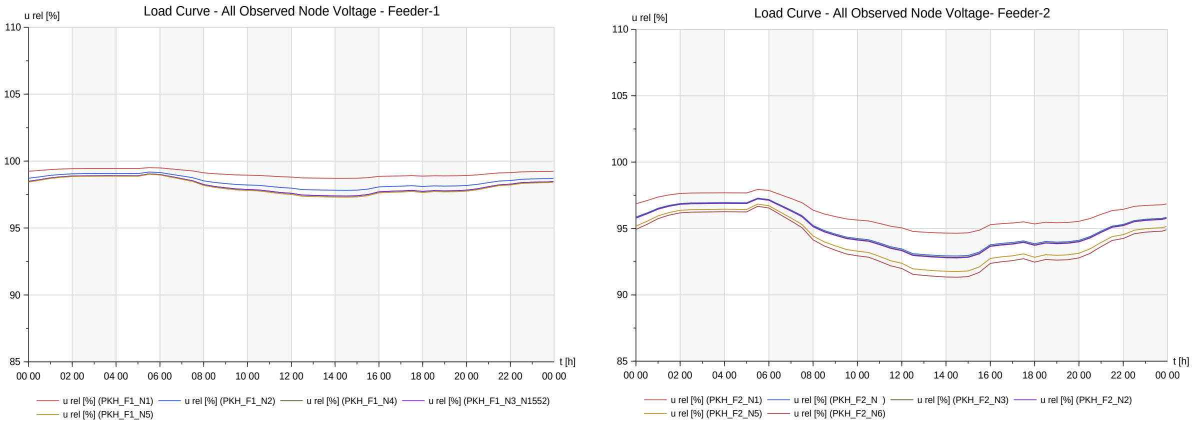

Feeder-1: Load only **Feeder-2: Load only**

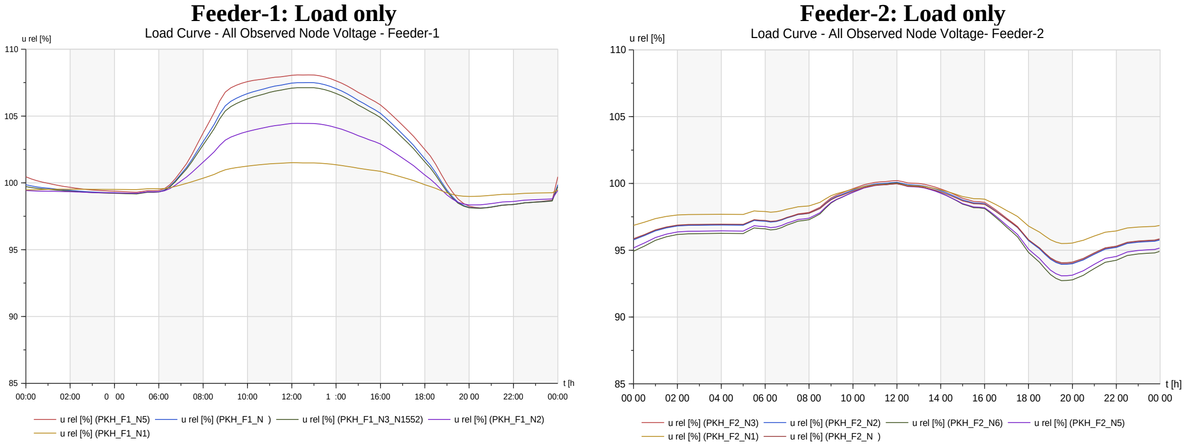

Feeder-1: Load with RE (PV & WT) **Feeder-2: Load with PV**

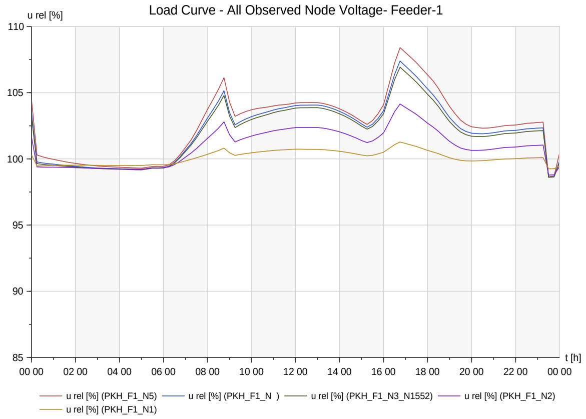

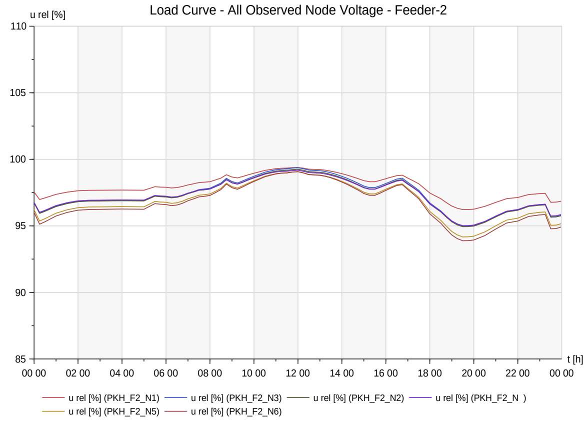

Feeder-1: Load with RE (PV&WT) and Storage **Feeder-2: Load with PV and Storage**

Figure 5:57 Voltage variation at different observed nodes in the Parkhurst ZS Power network

In PKH, Feeder-1 is much longer than Feeder-2 and load also distributed in vast areas covered by Feeder-1. The LF and LC analysis in the investigation on PKH ZS power network showed that:

- Phase voltage level decreases towards the distant nodes in load only condition
- LF analysis showed that voltage starts rising after integrating PV and WT in the network. A 11.97% and 9.12% voltage rise was observed at distant node in Feeder-1 and Feeder-2 respectively, after integrating PV and WT compared to the load only condition.
- After integrating storage with PV and WT voltage dropped in all observed nodes, 3.25% and 0.98% voltage drop was observed at distant node in Feeder-1 and Feeder-2 respectively.
- LC analysis showed that voltage level rise 2.795% at 13:00PM in Feeder-1due to the integration of large PV and WT compared to the load only configuration. After integrating storage, maximum voltage dropped during peak generation time and during 13:00PM 0.508% voltage drop was observed in Feeder-1. It was also found that after 16:00PM storage discharge increased the network voltage level.

5.4.5 Berserker (BER) ZS Power Network

Berserker ZS power network covers the urban area load. Two main feeders and 5 node points in each feeder were considered as indicated in Figure 5.58. The observation nodes are marked in the figure and nodes are named as “F1_N1 to F1_N5 and F2_N1 to F2_N5”, moreover the first observation node in each feeder is stated as “F1_All and F2_All”. Similar to other ZS power networks, this part of the network also simulated in load only, load with RE and load with RE and storage integrated mode.

The LF calculation showed that voltage dropped from source to the end node in both feeders in load only configuration and after integrating RE the voltage level increases in all observation nodes especially at the end node as shown in Figure 5.59 and 5.60. After integrating storage to the network, excess energy stored into the storage lowered the voltage level. At observation point 5 in Feeder-1 i.e. at node “F1_N5” the observed voltage was 6.2461 kV, 6.5265 kV and 6.5012 kV in load only, load with RE and load with RE and storage configuration mode.

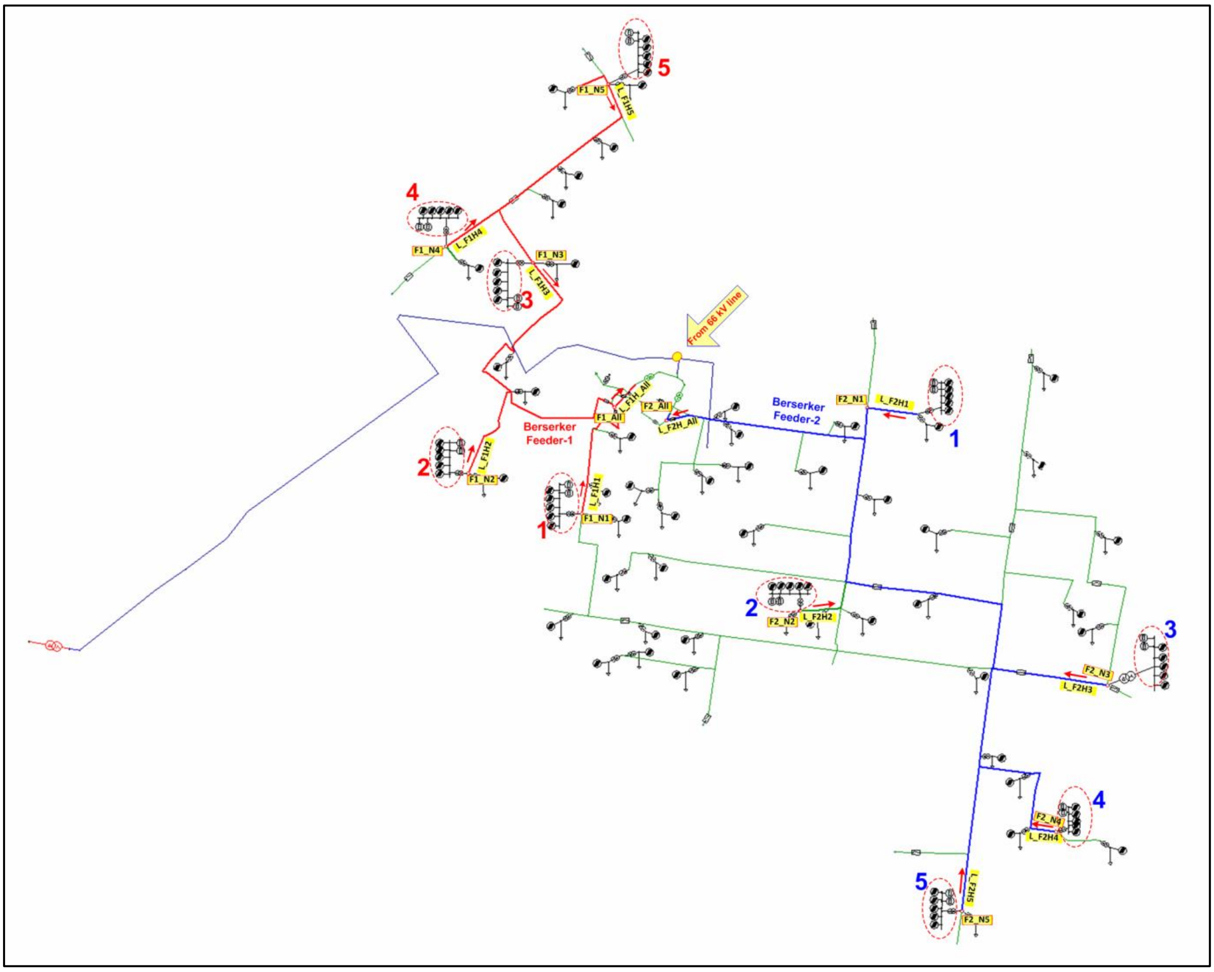

Figure 5:58 Berserker ZS power network showing observed feeders and nodes

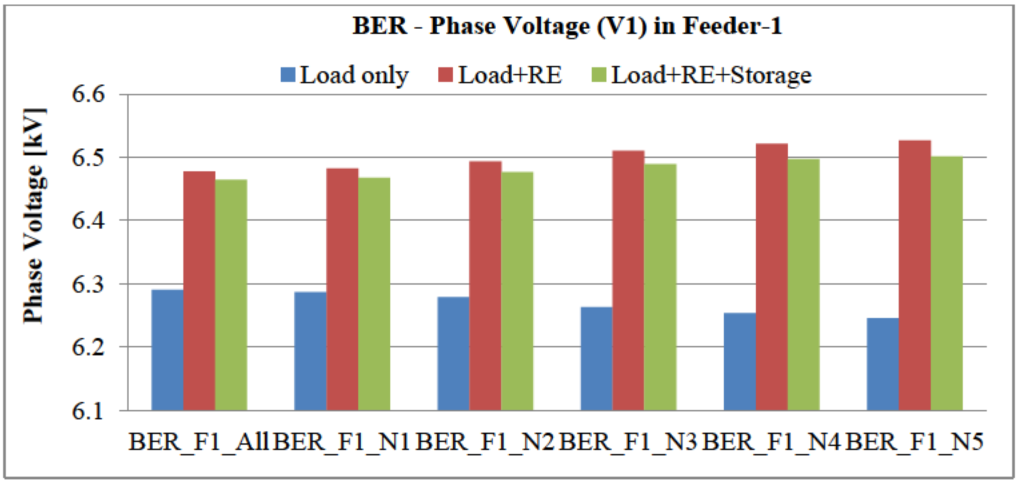

Figure 5:59 Phase Voltage at various points in Feeder-1

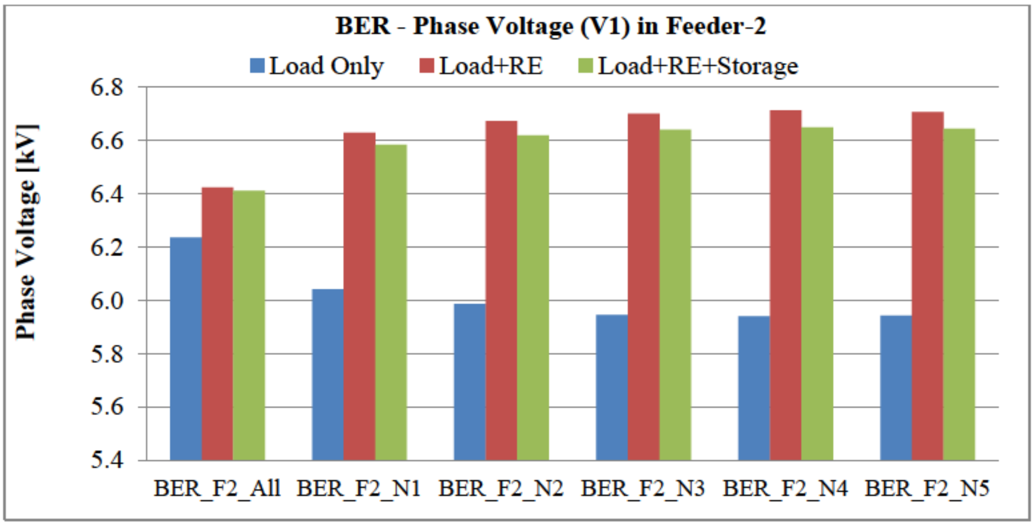

Figure 5:60 Phase Voltages at various points in Feeder-2

Load curve (LC) simulation provides the change in network voltage level in load only, load with RE and load with RE and storage configuration mode as shown in Figure 5.61. In load only configuration, the lowest voltage level observed was at 14:00PM due to peak load demand as shown in Figure 5.61 (a). After integrating RE, the voltage level increased in the network and at 14:00PM a 2.9% increase in voltage level was observed as shown in Figure 5.61 (b) compared to load only condition. After integrating storage to the network, the voltage level dropped and at 14:00PM a 0.25% voltage drop was observed at node “F1_All” as shown in Figure 5.61 (c) compared to load with RE configuration mode. Due to the large integration of RE, excess energy stored into the storage during 08:00AM to 17:00PM and from 17:00PM to 24:00AM storage released stored energy to support load demand as shown in Figure 5.61 (d).

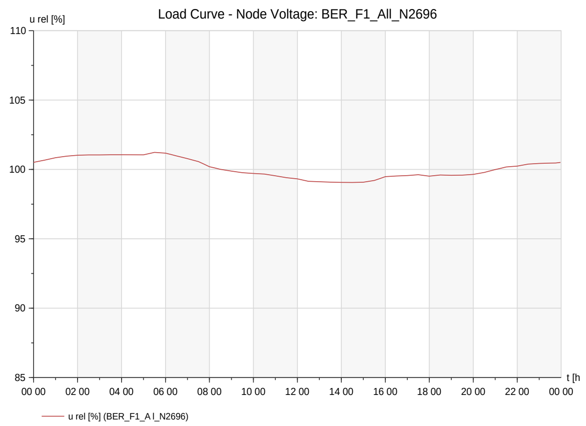

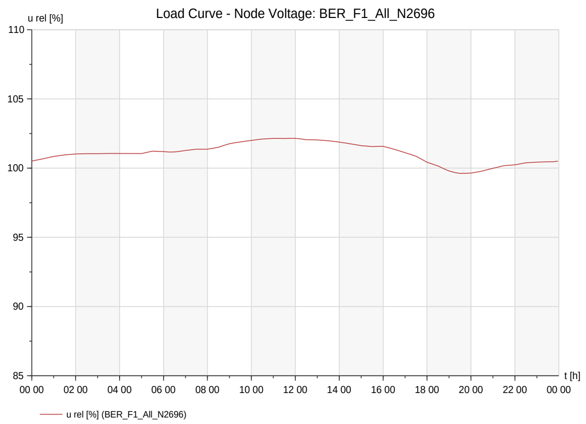

a. Load only **b. Load with RE**

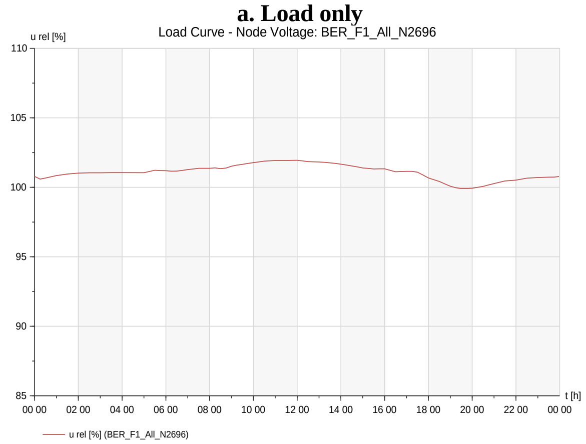

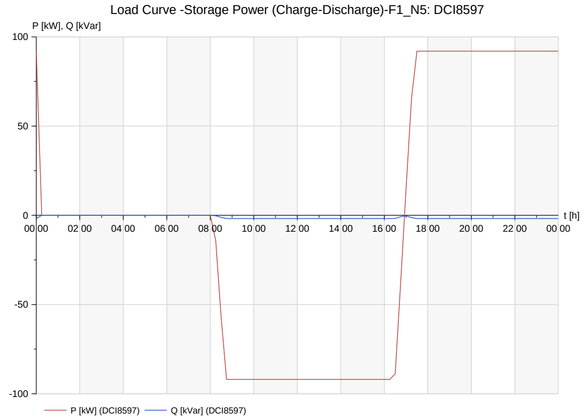

c. Load with RE and Storage **d. Storage charge-discharge cycle**

Figure 5:61 BER ZS - Voltage variation observed at "F1_All" in Feeder-1 & Storage charge-discharge cycle

The variation of voltage was better observed at the distant nodes. Figure 5.62 shows the voltage variation in different observation nodes in Feeder-1 and Feeder-2. More variation was observed in Feeder-2 nodes as Feeder-2 was heavily loaded compared to Feeder-1.

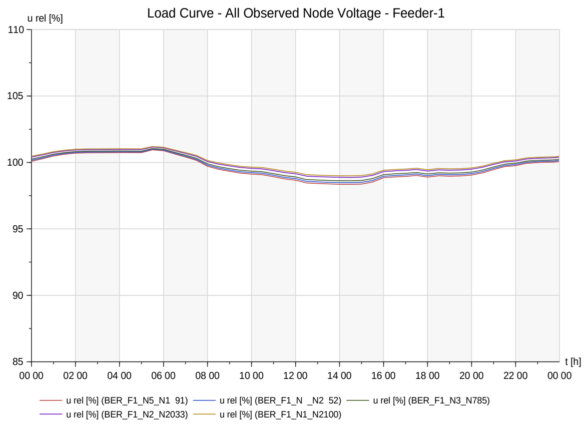

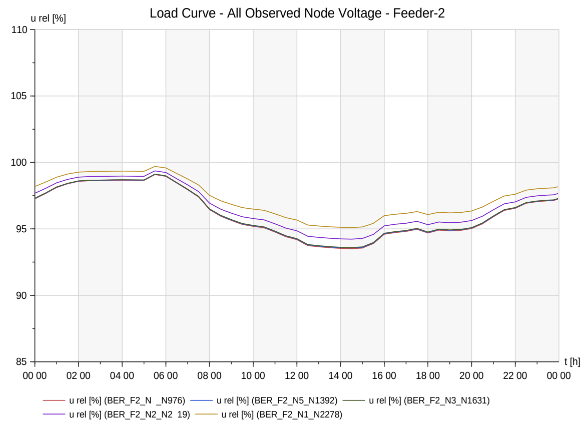

Feeder-1: Load only **Feeder-2: Load only**

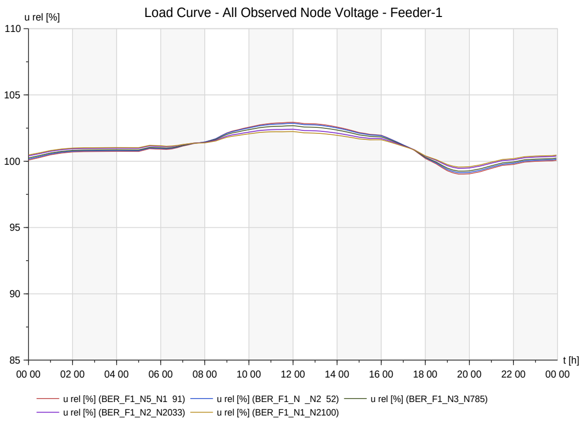

Feeder-1: Load with RE

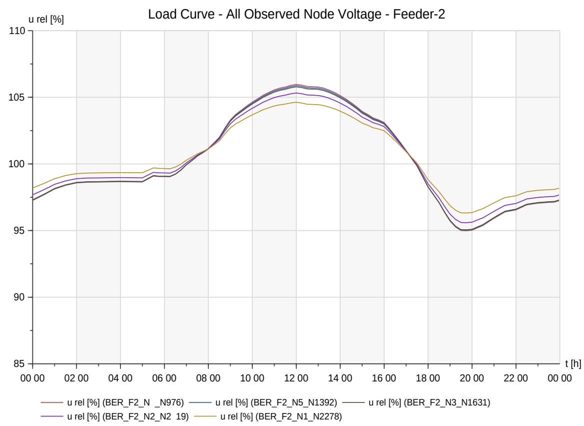

Feeder-2: Load with RE

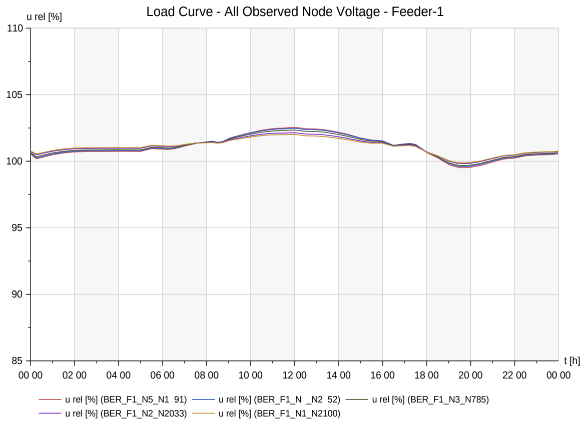

Feeder-1: Load with RE and Storage

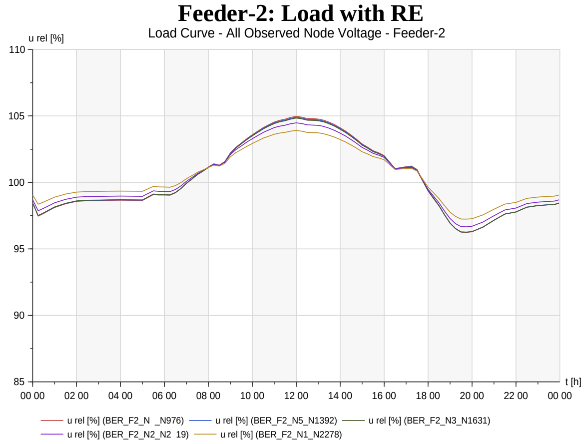

Feeder-2: Load with RE and Storage

Figure 5:62 Voltage variation observed at selected points in Berserker Power Network

In BER ZS network, Feeder-1 and Feeder-2 are similar in length and also load distributed uniformly. The LF and LC analysis in the investigation on BER ZS power network showed that:

- Phase voltage level decreases towards the distant nodes in load only condition
- LF analysis showed that voltage starts rising after integrating PV in the network. At the distant node in both feeders voltage rise was observed. Maximum 4.49% voltage increase was observed at distant node in Feeder-1 after integrating PV compared to the load only condition.
- After integrating storage with PV, voltage dropped in all observed nodes, maximum 0.38% voltage drop was observed at distant node in Feeder-1.
- LC analysis showed that voltage level rise 2.9% at 14:00PM in Feeder-1due to the integration of large PV compared to the load only configuration. After integrating storage, maximum voltage dropped during peak generation time and during 14:00PM 0.25% voltage drop was observed in Feeder-1. It was also found that after 17:00PM storage discharge increased the network voltage level.

5.4.6 Canning Street (CST) ZS Power Network

Like the observation in other ZS power network, in CST power network two feeders were selected to observe voltage variation. Figure 5.63 shows the selected feeders and observed nodes.

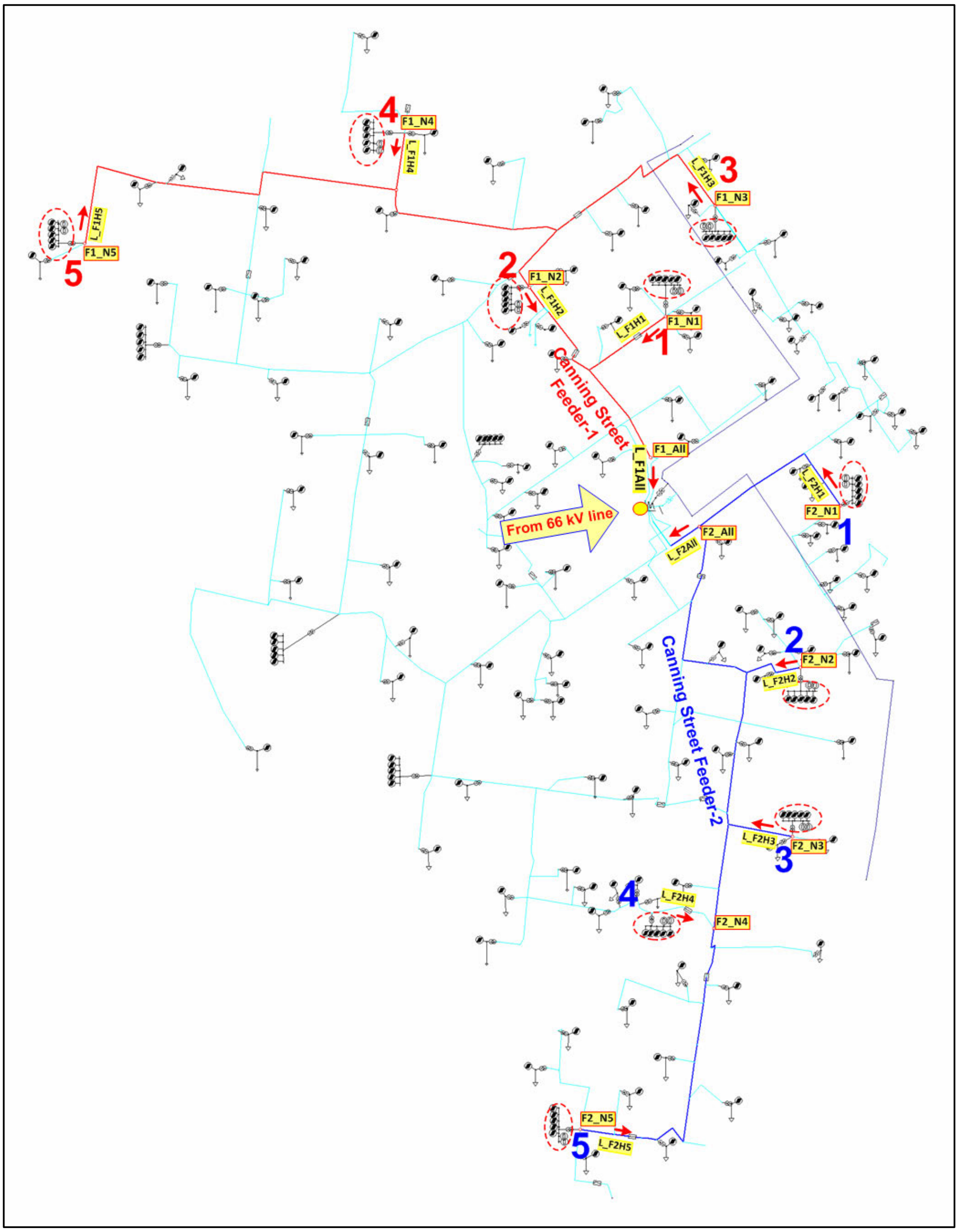

Figure 5:63 Canning street ZS power network showing observed feeders and nodes

In Feeder-1 five nodes were selected as "F1_N1 to F1_N5" and the node "F1_All" is close to the ZS Transformer where maximum voltage level of Feeder-1 was observed. Similarly in Feeder-2 five nodes were selected as "F2_N1 to F2_N5" and the node "F2_All" is close to the ZS Transformer where the maximum voltage level of Feeder-2 was observed. Similar to other ZS networks, bulk size RE (500kW) and Storage (200kW) was integrated in each 5 points in Feeder-1 and Feeder-2. Figure 5.64 and 5.65 shows the change in voltage in load only, load with RE and load with RE and Storage configuration in Feeder-1 and Feeder-2 respectively. It is found that the large integration of RE increases voltage levels and major swing appears at the distant nodes where voltage level was low in load only condition. During maximum power generation from RE sources, storage stored a portion of excess energy which caused a drop in voltage levels as observed in all nodes shown in Figure 5.64 and Figure 5.65.

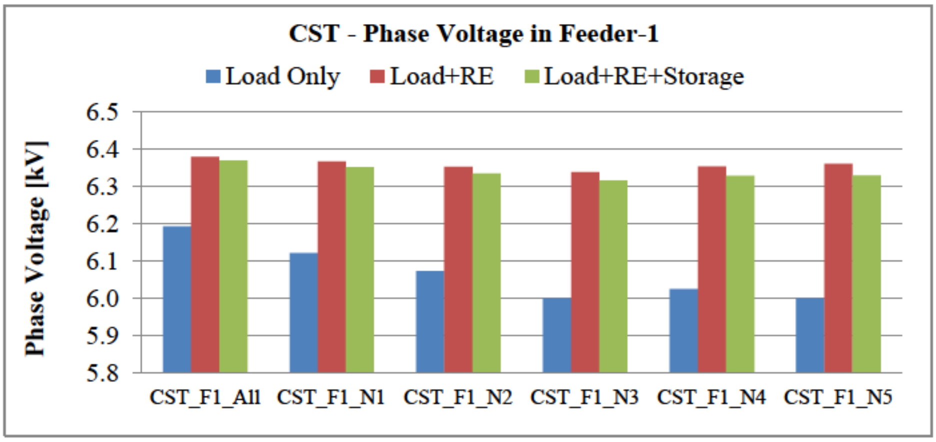

Figure 5:64 Phase Voltages in various observed nodes in Feeder-1

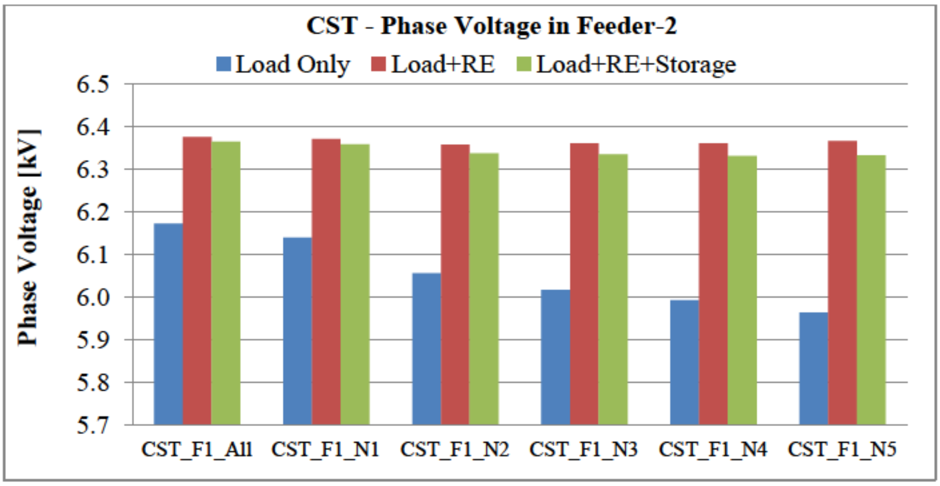

Figure 5:65 Phase Voltages in various observed nodes in Feeder-2

The RE generation varies with time and also load demand varies, however this variation is not matched which caused the variation in Voltage levels as observed in various nodes. Figure 5.66 (a) shows the percentage of observed voltage at node “F1_All” during 24 hours a day. It is clear that voltage levels dropped when load demand was high. After the large integration of RE in the network it was observed that the voltage level increased during mid day even at the high load demand time. It was found that in node “F1_All”, the voltage level increased 2.7% at 14:00PM as shown in Figure 5.66 (b). ES discharged stored energy and improved the voltage level during the evening. In node “F1_All” at 19:30PM, storage improved the voltage level by 0.232% of rated voltage compared to the without storage configuration as shown in Figure 5.66 (c). Figure 5.66 (d) shows the charging & discharging period of ES at Node-5 in Feeder-1. However the variation is clear in distant nodes for both feeders and Figure 5.67 shows the voltage variation observed at various nodes in Feeder-1 and feeder-2.

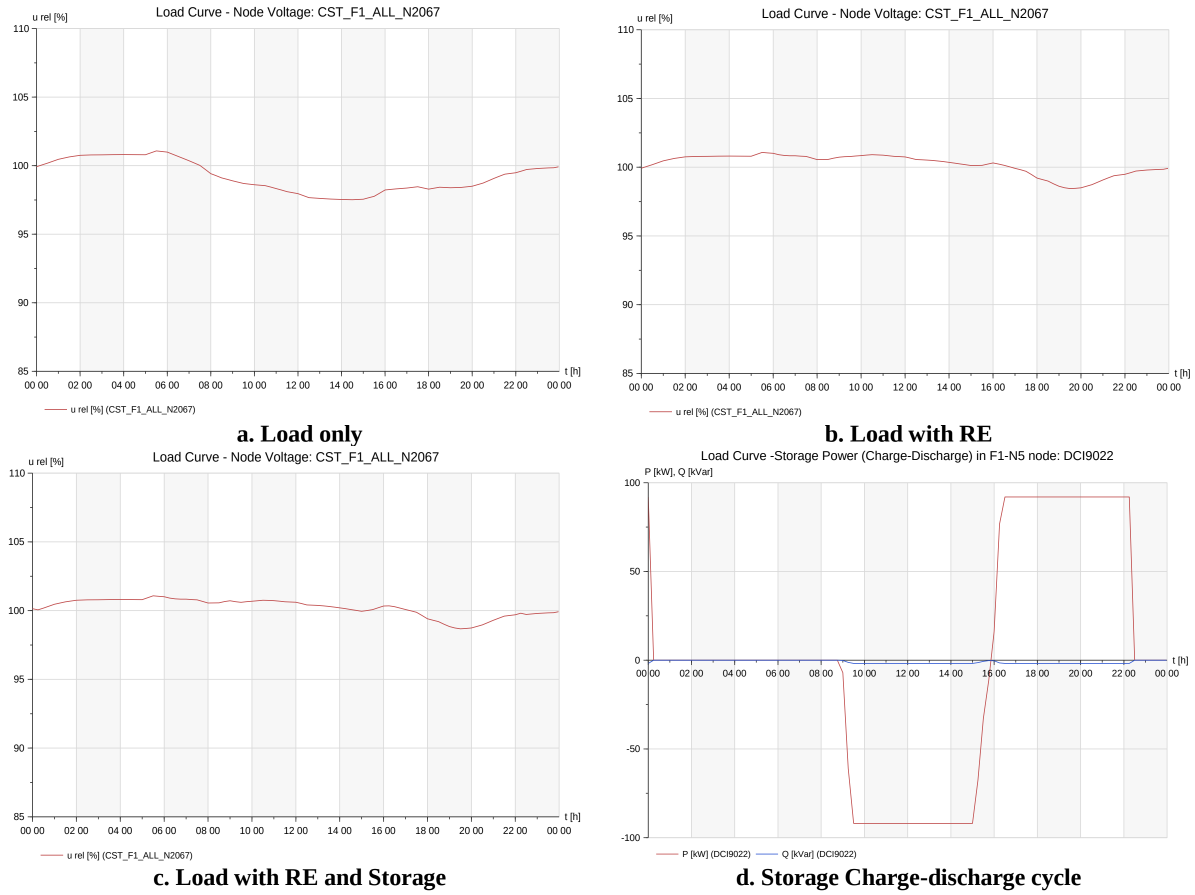

a. Load only **b. Load with RE**

c. Load with RE and Storage **d. Storage Charge-discharge cycle**

Figure 5:66 CST ZS - Voltage variation observed at "F1_All" in Feeder-1 & Storage charge-discharge cycle

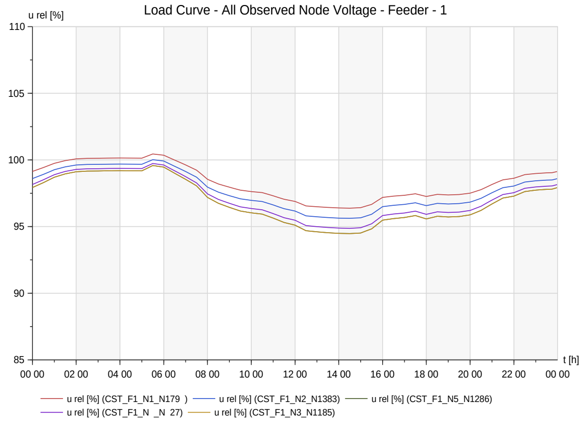

Feeder -1 : Load only (94.47% to 100.447%)

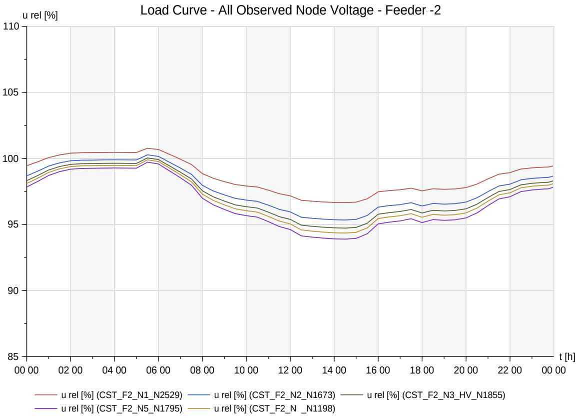

Feeder-2: Load only (93.89% to 100.227%)

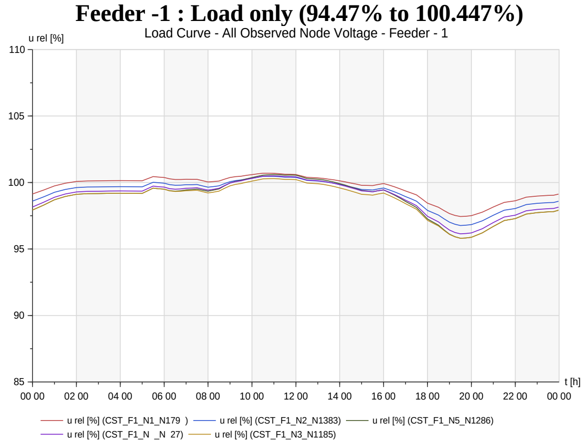

Feeder-1: Load with RE (95.80% to 100.70%)

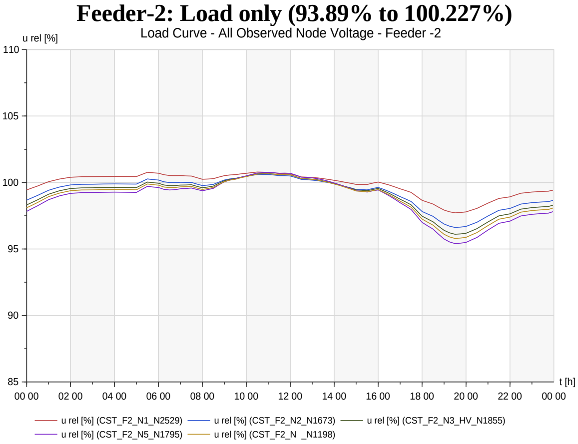

Feeder-2: Load with RE (95.408% to 100.789%)

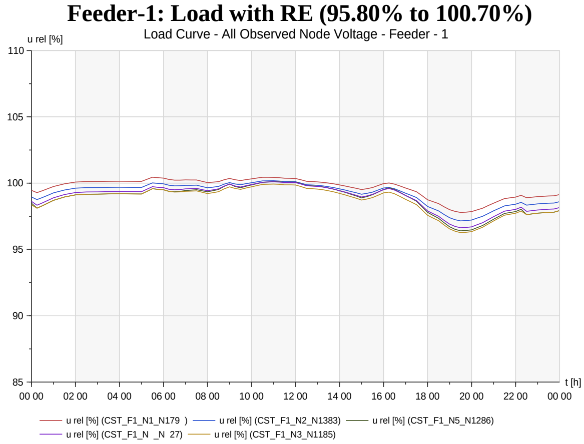

Feeder-1: Load with RE & Storage (96.27% to 100.447%)

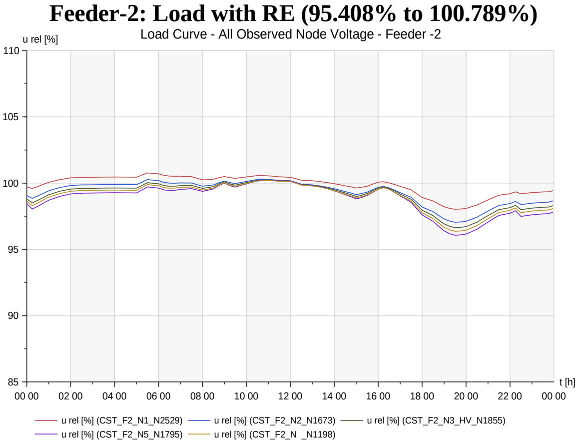

Feeder-2: Load with RE & Storage (96.06% to 100.77%)

Figure 5:67 CST ZS Power network - Voltage variations at different observation nodes

In CST ZS network, Feeder-1 and Feeder-2 are similar in length and in load distribution. The LF and LC analysis in the investigation on CST ZS power network showed that:

- Phase voltage level decreases towards the distant nodes in load only condition
- LF analysis showed that the maximum rise in voltage was at the distant node after integrating PV in the network, compared to the load only condition.
- After integrating storage with PV, voltage drop was observed in all nodes.

- LC analysis showed that voltage level rise 2.7% at 14:00PM in Feeder-1due to the integration of large PV. After integrating storage, maximum voltage dropped during peak generation time. However at 17:30PM storage discharge increased network voltage level by 0.232%.

5.4.7 Lakes Creek (LCR) ZS Power Network

In the Lakes Creek ZS power network, a portion of the network connects very distant loads via single phase SWER network. Therefore this ZS network provides a unique characteristic which is not commonly available. This network consists of both 3 phase and single phase lines at the voltage level of 11 kV and 12.7 kV respectively. Figure 5.68 shows the selected 5 observation nodes in Feeder-1 and installed PV of 500 kW capacity and storage of 200 kW capacity in each observation node.

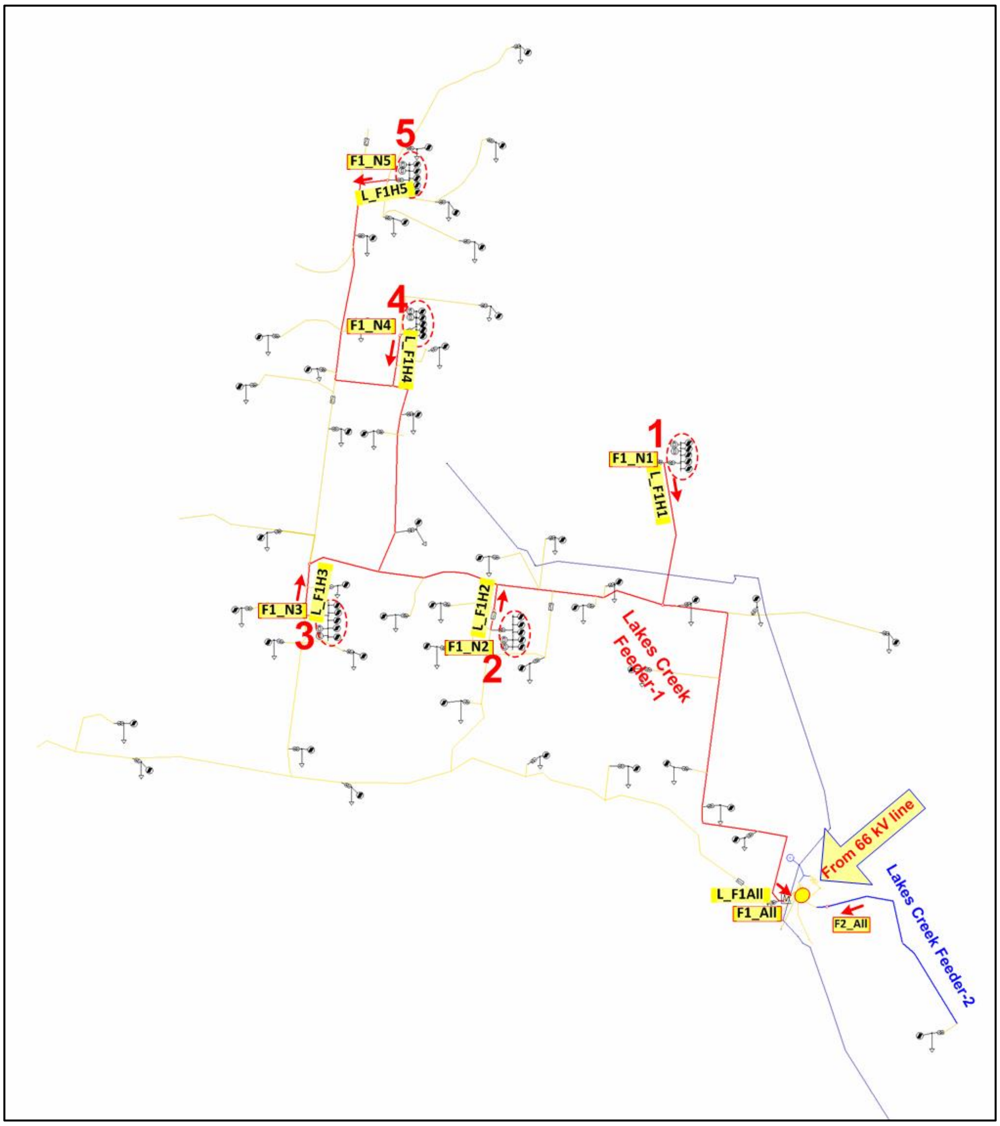

Figure 5:68 LCR ZS power network showing observed nodes in Feeder-1

In Feeder-2, 7 nodes were selected, however in 6 observation nodes 500 kW RE (PV or WT) and 200 kW storage was installed as indicated by small circles in Figure 5.69. Moreover 3 nodes (6A, 6B and 6C) in SWER network were selected to be investigated. This SWER network connected to the 3 phase network at two different points with a SWER isolator- a single phase transformer. This SWER line joins the 3 phase line at the nodes named "F2_N4" and "F2_N6A" in Feeder-2 and connects to phase-1. This configuration of 3 phase and a single phase network introduces phase unbalances in the network and that influences the whole network. Figure 5.70 shows the phase unbalance conditions that occurred in Feeder-2 due the SWER line integration into the Feeder in load only configuration. As the load on Phase-1 (V1) increased therefore voltage level of V1 reduced, as compared to other phases in all observed nodes.

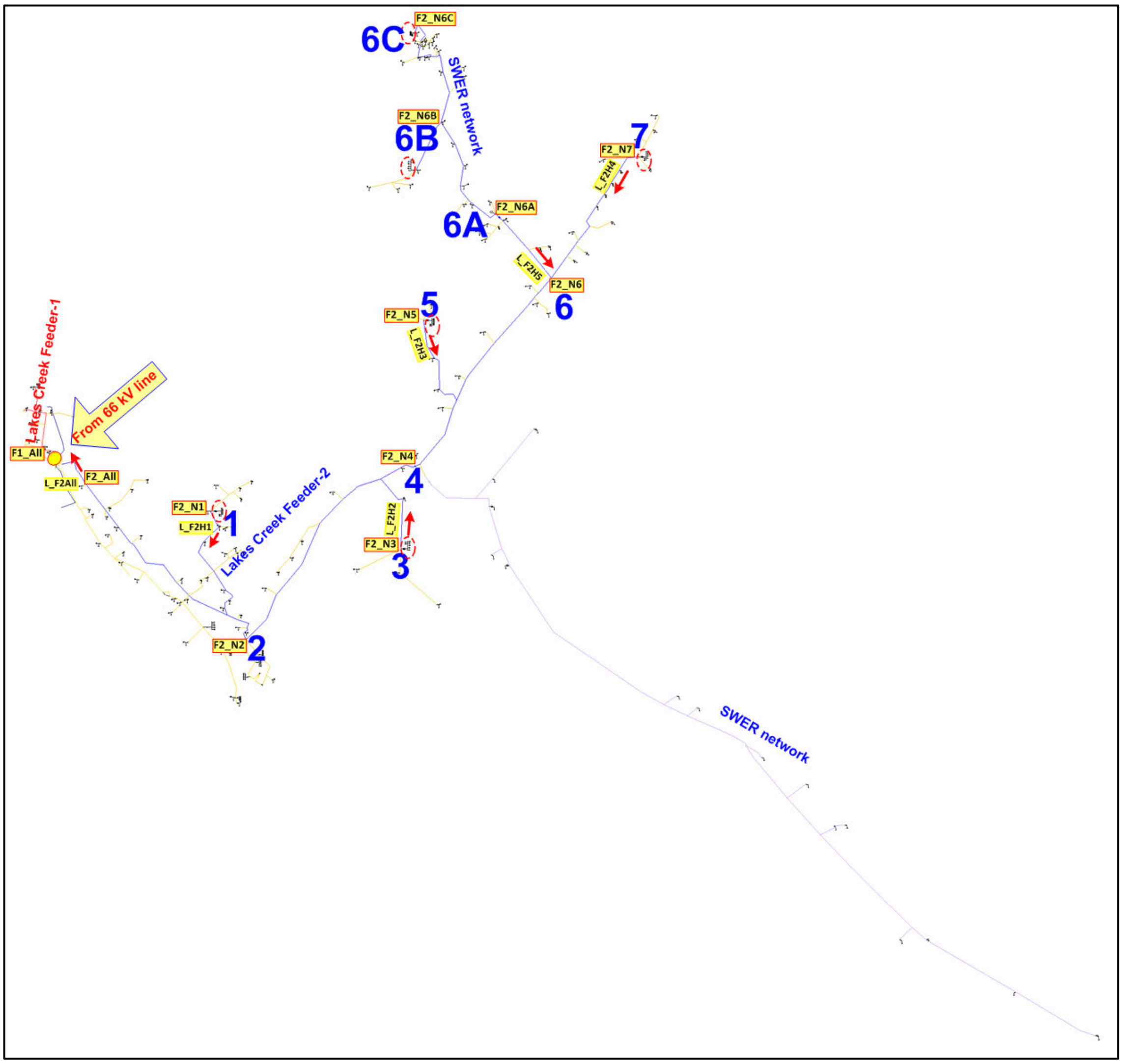

Figure 5:69 LCR ZS power network showing observed nodes in Feeder-2 and SWER network

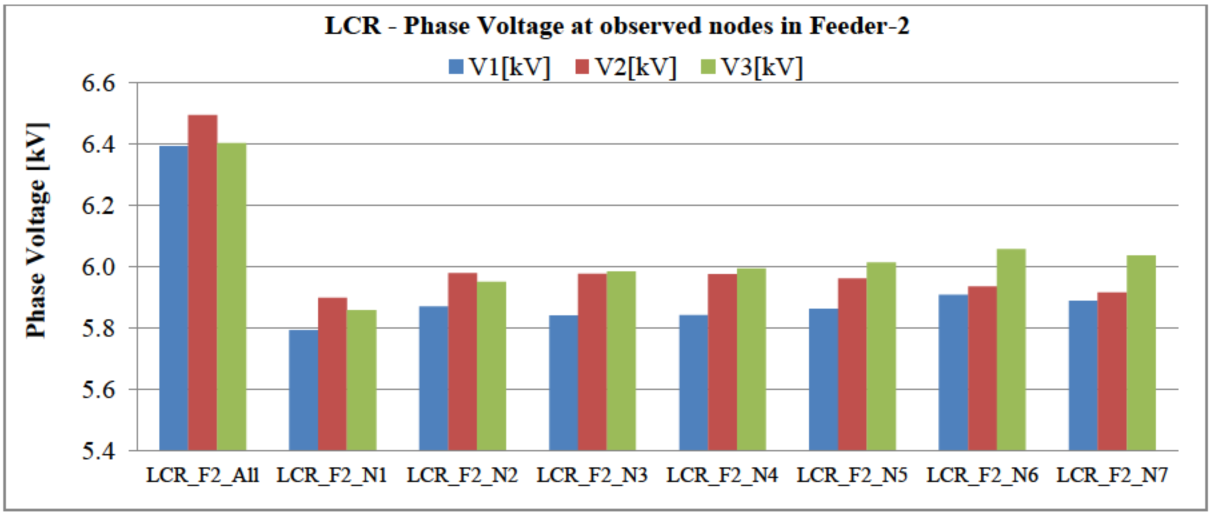

Figure 5:70 Phase voltages observed at different nodes of 3 phase part of Feeder-2

The impacts of storage and RE in phase voltage variations is explained below and also shows the comparison in phase-1 voltages for all observed nodes in the LCR network. Small size load was connected to the very long SWER line. Load Flow (LF) simulation results showed the variation of voltage due to RE and storage in Feeder-1 and Feeder-2. Figure 5.71 shows that voltage level increases in all observed nodes in Feeder-1 due to the large integration of RE, however after integrating Storage, this increased voltage starts decreasing. This variation is prominent at the distant nodes although the variation is less at the source end.

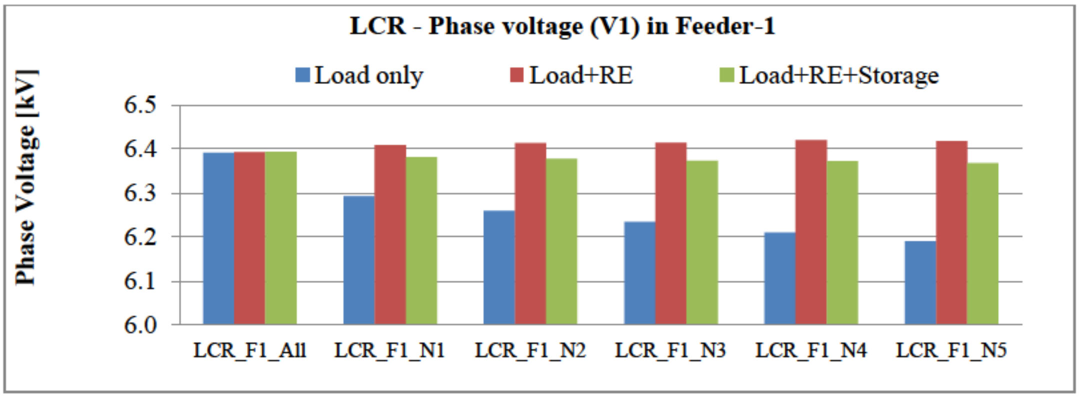

Figure 5:71 Phase voltages (V1) at observed nodes in Feeder-1

Similarly in Feeder-2, RE increases voltage levels in all observed nodes and storage reduced this increased voltage level. Figure 5.72 shows this variation in various observed nodes without showing the SWER part and Figure 5.73 shows this variation in the SWER part of the LCR network. At distant nodes in feeder-2 "F2_N7" the observed voltage was 5.889 kV, 6.186 kV and 6.1247 kV in load only, load with RE and load with RE and storage configuration mode. Due to the large RE integration, voltage increased 5.043% compared with load only condition and after integrating storage, voltage dropped 0.99% compared with load with RE condition. In the SWER part at node "F2_N6C" the observed voltage was 12.589 kV, 13.8595 kV and 13.4167 kV in load only, load with RE and load with RE and storage configuration mode. Therefore due to RE integration, the voltage level increased 10.09% as compared with load only condition. After integrating storage, voltage dropped 3.195% compared with RE condition. Therefore in single phase SWER network voltage fluctuation is much more due to RE and storage.

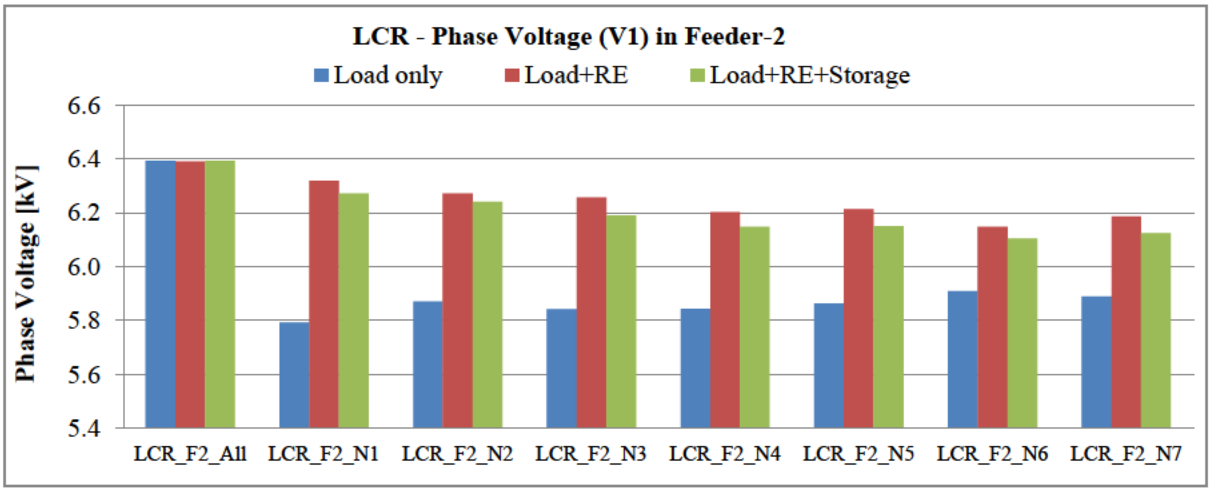

Figure 5:72 Phase Voltages (V1) at observed nodes in Feeder-2

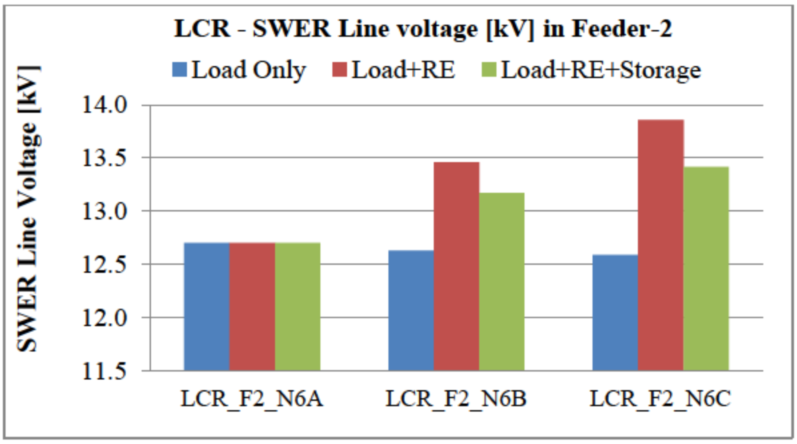

Figure 5:73 Voltage (V1) at observed nodes in SWER part of Feeder-2

Load curve (LC) or load profile calculation provides this variation in voltage level in details with time. As the Feeder-1 and Feeder-2 connects to the Transformer at ZS in LCR, the variations at node "F1_All and F2_All" are very close, however the variation at distant nodes are clearly evident. Figure 5.74 shows the voltage variation at different observed nodes in Feeder-1 and Feeder-2. It is clear that RE increases voltage levels during mid day when RE generation is high, however this variation is very high for the SWER single phase network. Storage reduces the voltage level during mid day by storing excess energy and increases voltage during peak load demand at the evening by discharging stored energy.

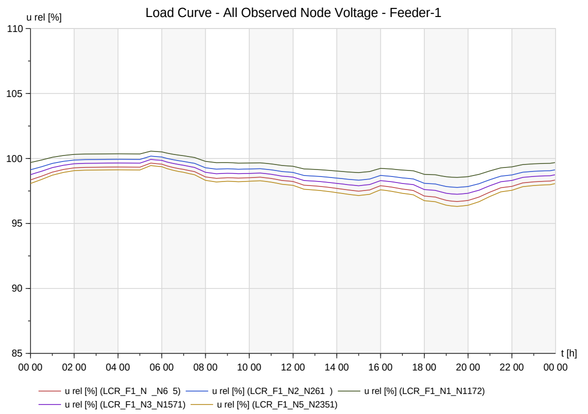

Feeder-1: Load only

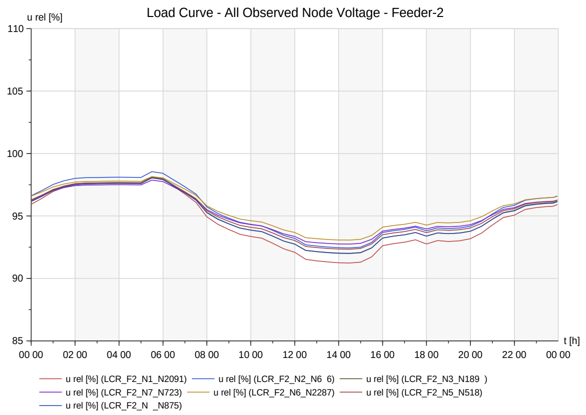

Feeder-2: Load only (without SWER part)

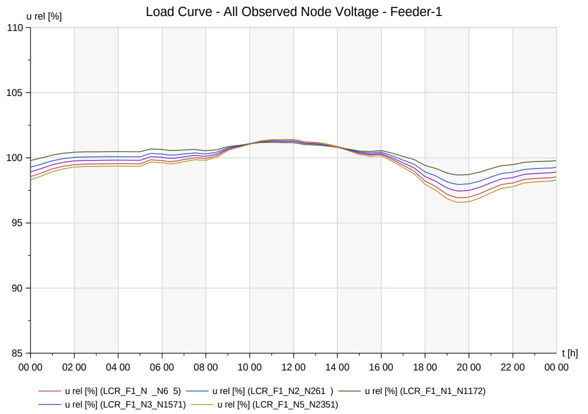

Feeder-1: Load with RE

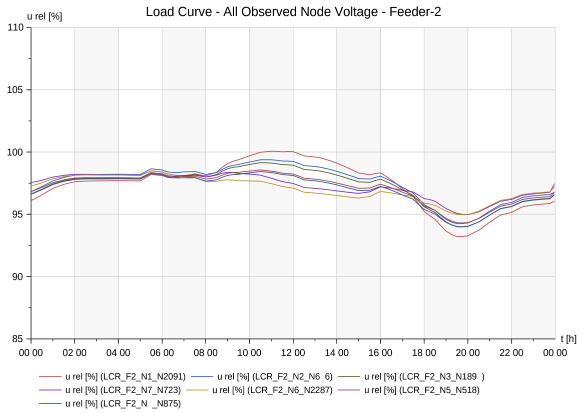

Feeder-2: Load with RE (without SWER part)

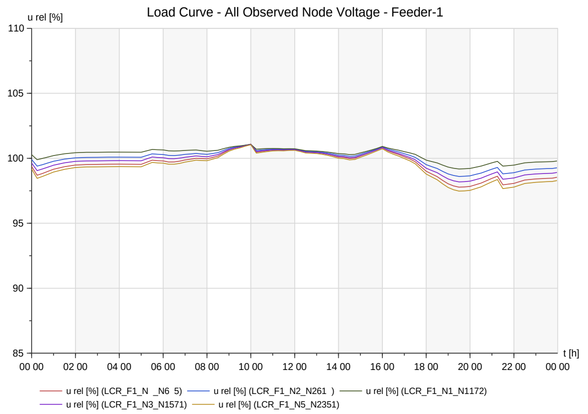

Feeder-1: Load with RE and Storage

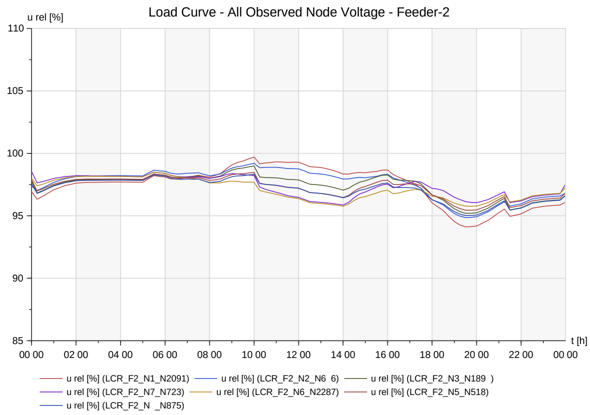

Feeder-2: Load with RE & Storage (without SWER part)

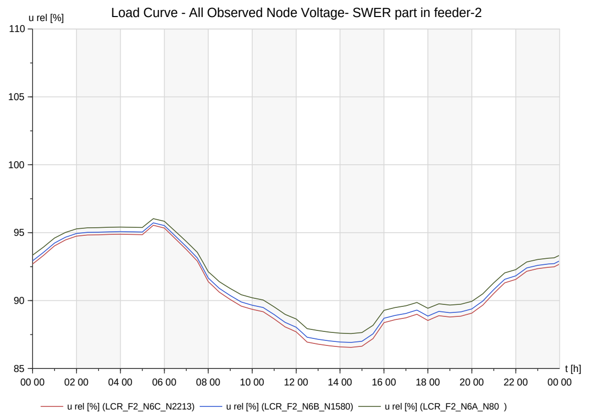

Feeder-2: SWER part in Load only configuration

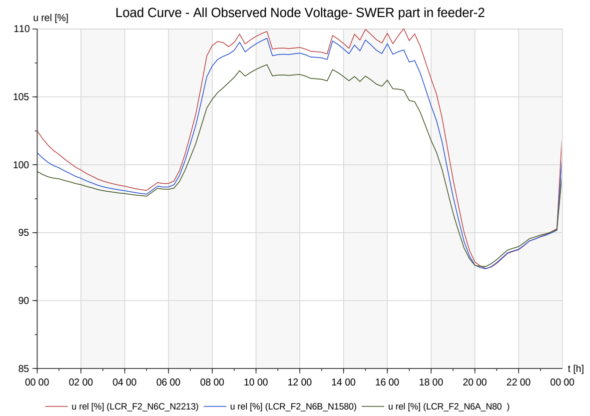

Feeder-2: SWER part- Load with RE

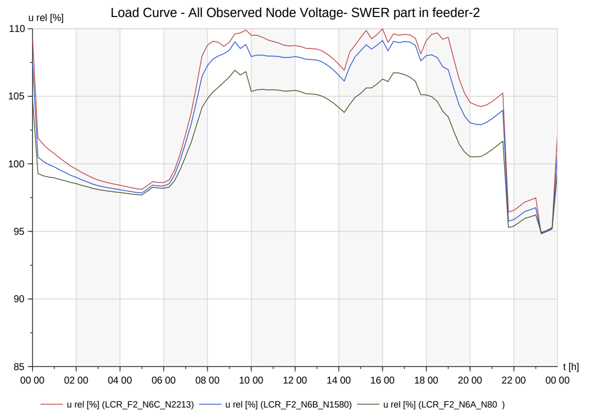

Feeder-2: SWER part- Load with RE and Storage

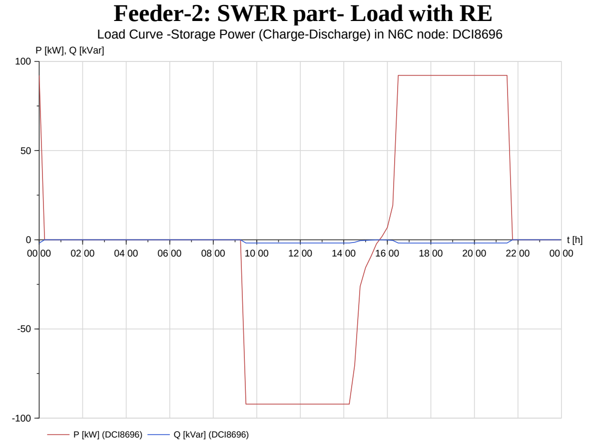

Feeder-2: Storage charge- discharge

Figure 5:74 LCR ZS Power network -Voltage variation at different observed nodes

In LCR ZS network consists of three phase and single phase lines. A SWER network was connected to Feeder-2. The LF and LC analysis in the investigation on LCR ZS power network showed that:

- Phase unbalanced condition occurred in Feeder-2 due to the SWER network
- Phase voltage level decreases towards the distant nodes in load only condition
- LF analysis showed that voltage increased after integrating RE in the network. At the distant node in Feeder-2 without SWER network part, 5.043% voltage increased at distant node and in the SWER network part 10.09% voltage increased after integrating RE compared to the load only condition.
- After integrating storage with RE, voltage dropped in all observed nodes, maximum 0.99% voltage drop was observed in Feeder-1 without SWER part and in SWER part 3.195% voltage drop was observed.
- LC analysis showed that the change in voltage level is higher in SWER part of the network during the peak generation time from RE.

5.4.8 Rockhampton South (RSH) ZS Power Network

Like LCR ZS power network, RSH ZS power network also contains a part of SWER network. Two feeders and 5 node points (F1_N1 up to F1_N5) in Feeder-1 was selected for observation. The single phase SWER network was connected to the Feeder-1 at node “F1_N2” as shown in Figure 5.75. The observation nodes on Feeder-2 are shown in Figure 5.76. To investigate the impacts of Storage, the network was integrated with a large scale RE installation. Like other network settings, initially PV was installed with 100% capacity of peak load demand, however as PV cannot supply energy 24 hours a day, a bulk size PV/WT plant was installed in nodes where voltage level drop is maximum. Each PV/WT plant is of 500kW capacity and a 200kW Energy Storage was installed to support load demand when RE generation was not available. In SWER part of the network in Feeder-1 500kW PV plant and 200kW Storage was installed in 2 nodes (F1_N4S and F1_N5S). All loads, PV and Storage are connected to the secondary side of distribution transformer (DT). In SWER part of the network all load, PV and Storage was connected in Phase-1 (V1) with single phase transformer of 22kV/415V, therefore the high voltage side of the transformer has a voltage of 12.7kV.

In Feeder-1, 5 observed nodes were selected in a 3-phase line and 3 observation nodes were selected in the SWER part of the network. Feeder-2 has 2 line segments and in each segment 3 nodes were selected for observation. The nodes are named as “F2_N1A, F2_N2A, F2_N3A” and “F2_N1B, F2_N2B, F2_N3B”.

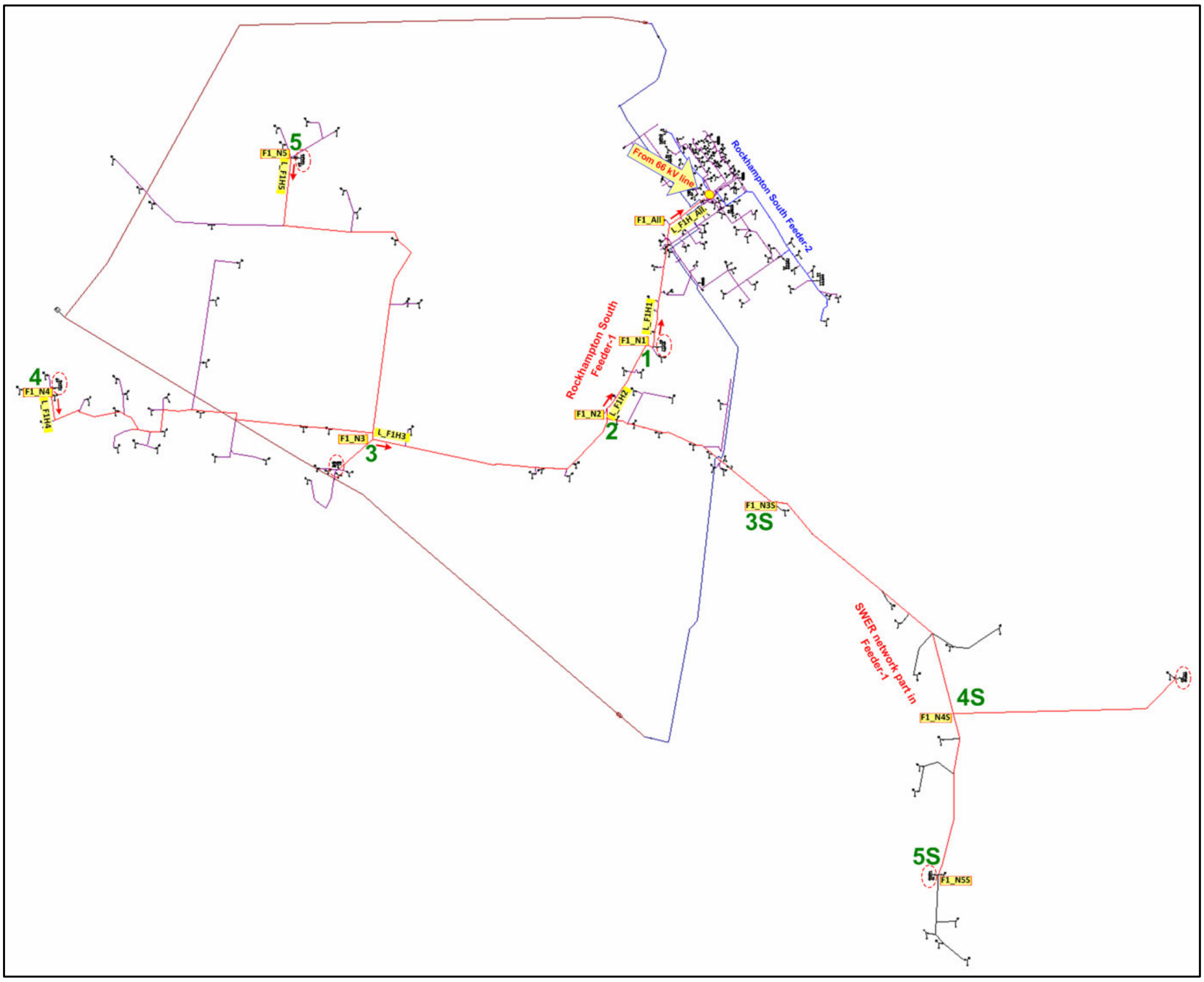

Figure 5:75 RSH ZS power network showing observed nodes in Feeder-1 and SWER network

Load Flow (LF) calculation was conducted to observe the change in voltage at the selected nodes in load only, load with RE and load with RE and Storage configuration mode of the network. Load Curve (LC) simulation was done to investigate the variation according to timely load demand, RE generation and Storage response. Figure 5.77 shows the change in voltage at the observed nodes after integrating large scale PV and Storage and it is clear that PV increased voltage most at the distant nodes where voltage dropped most in the load only case. Storage stored excess energy generated by PV which caused a drop in voltage levels and helped to keep the phase voltage within allowable limits. Similarly, in SWER part and in Feeder-2, RE or PV increased voltage level and Storage tried to limit this increase by storing excess energy as shown in Figure 5.78 and Figure 5.79.

Due to single phase SWER network connected to phase-1 (V1), more voltage drop was observed in phase-1 and as a consequence, phase unbalanced condition was observed in

Feeder-1. Also more fluctuation in voltage was observed in SWER part of the network. In SWER part, at node "F1_N5S" voltage was increased 10.4465% after integrating RE and decreased 2.895% after integrating storage into the network.

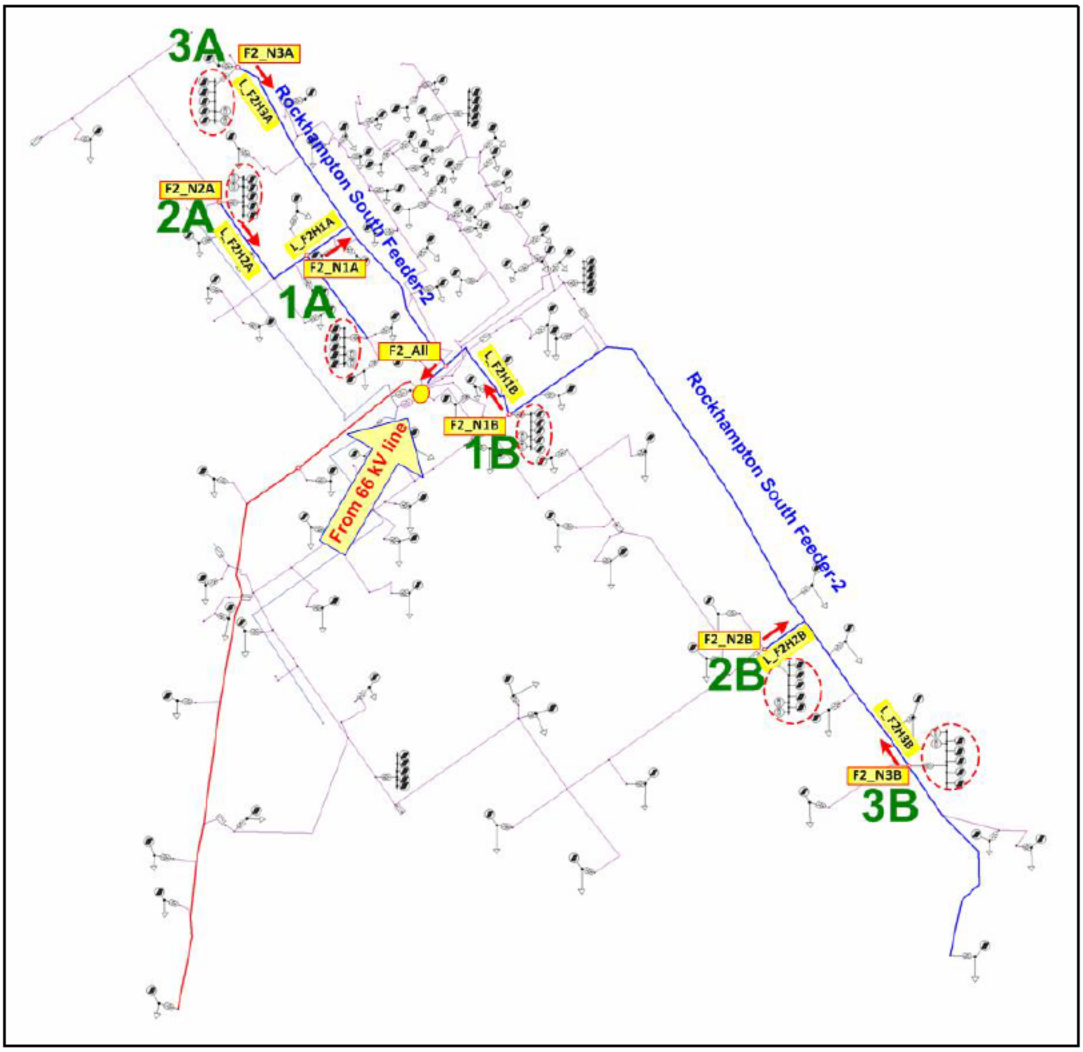

Figure 5:76 RSH ZS power network showing observed nodes in Feeder-2

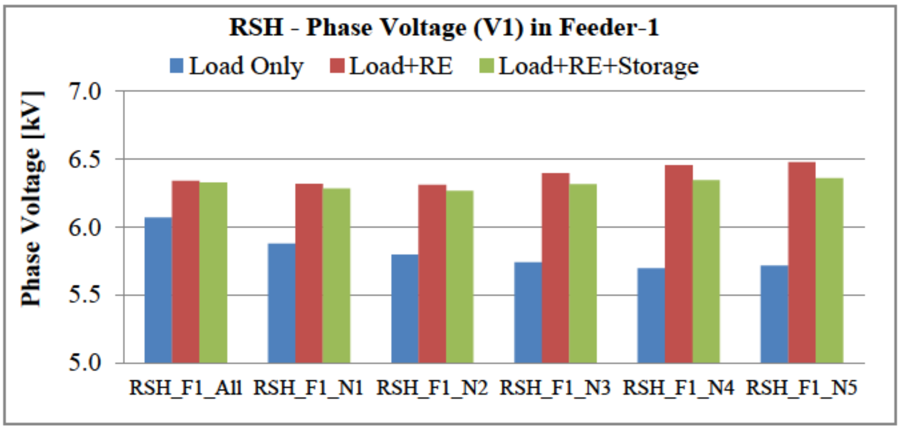

Figure 5:77 Phase Voltages at various nodes (without SWER Part) in Feeder-1

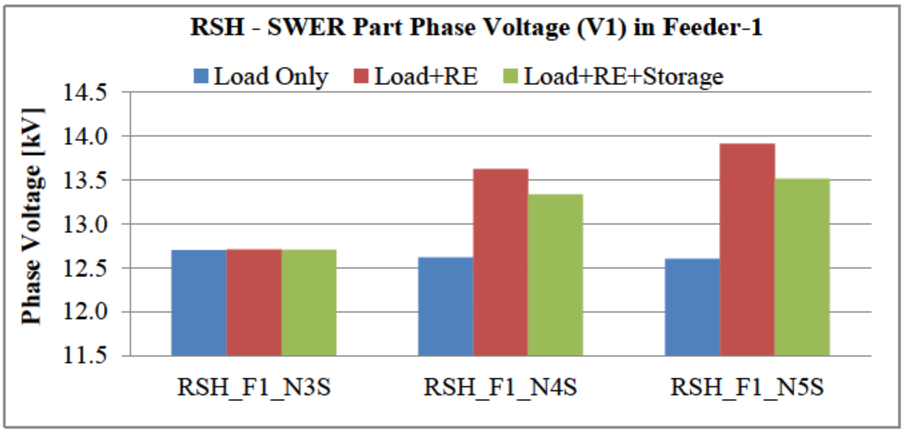

Figure 5:78 Line Voltage variations in SWER part of Feeder-1

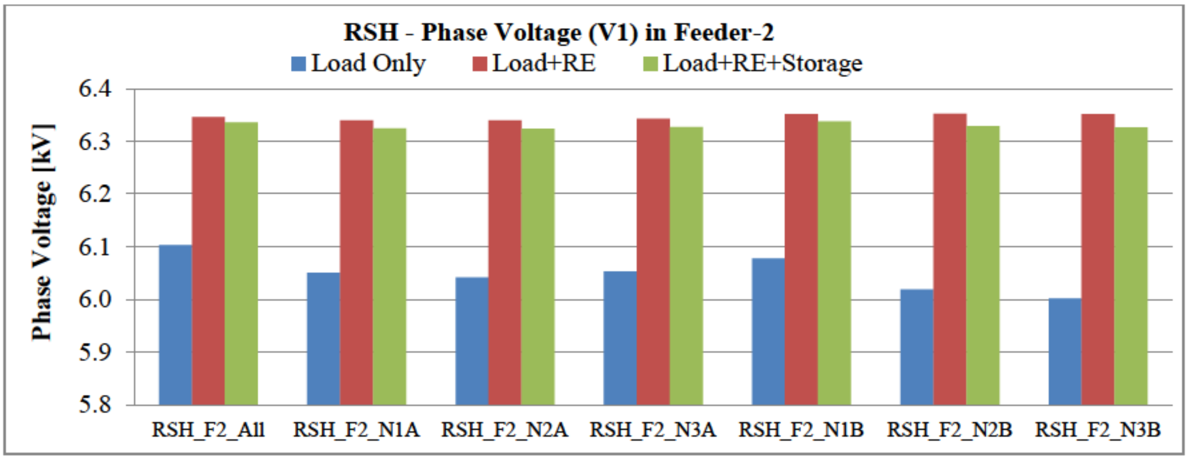

Figure 5:79 Voltage variations at various nodes in Feeder-2

As explained earlier Load Curve (LC) simulation considers load profile and the energy generation profile from RE and consequently storage behaviour in storing excess energy and releasing stored energy when load demand increases, provides the actual behavior of voltage variation in the network. Figure 5.80 (a, b, c) shows the voltage variation at node "F1_All" in load only, load with large installation of PV and load with PV and Storage integrated network condition. This is the node near to the transformer of ZS and the voltage level at this node remains very close to supply voltage. Figure 5.80 (a) shows the voltage at the node "F1_All" in load only condition and it is clear that voltage dropped 4.525% from the rated voltage at 14:00PM when load demand was high.

After integrating large scale PV into the network, high load demand was supported by energy generated by PV and excess energy forced an increase to the voltage level. Figure 5.80(b) shows that from 08:00AM to 17:00PM the voltage level increased and at 14:00PM the voltage level increased by 3.975% compared to load only condition. After integrating Energy Storage into the network, the voltage level drops during 10:00AM to 14:00PM and there is an increase in voltage level during 17:00PM to 21:00PM as shown in Figure 5.80(c). Figure 5.80 (d) shows the storage charge and discharge period for the storage installed at Node-5 in Feeder-1.

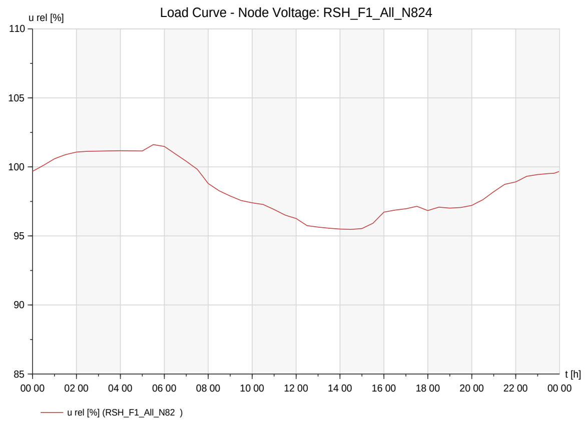

a. Load only

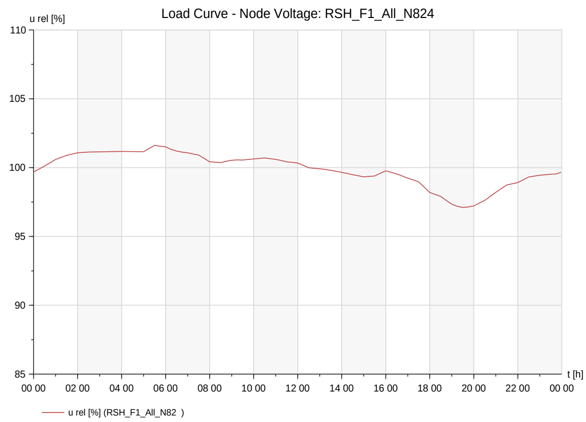

b. Load with RE

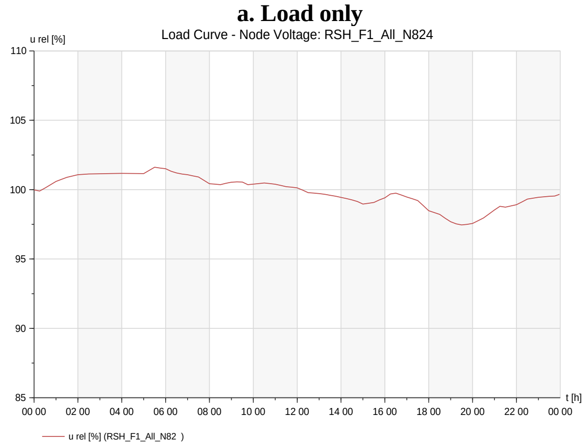

c. Load with RE and Storage

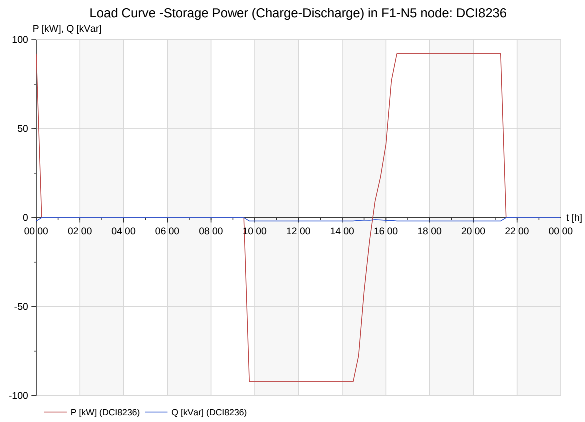

d. Storage Charge-discharge cycle

Figure 5:80 RSH ZS - Voltage variation observed at "F1_All" in Feeder-1 & Storage charge-discharge cycle

This change in voltage is more significant at the distant nodes of the network. Figure 5.81 shows the change in various nodes in Feeder-1 and Feeder-2 also showing the minimum and maximum voltage at observed nodes in each feeder. Voltage variation was high at the SWER part of the network.

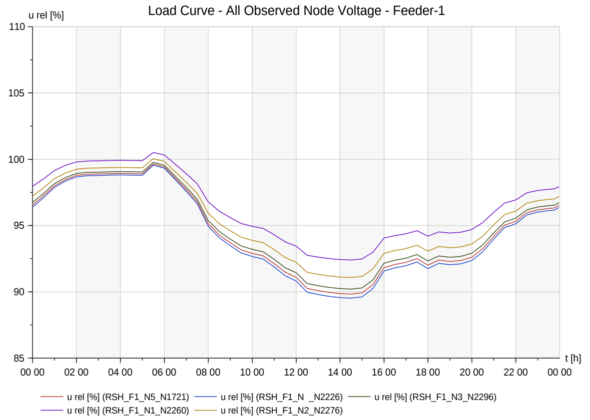

Feeder-1: Load only (89.524% to 100.507%)

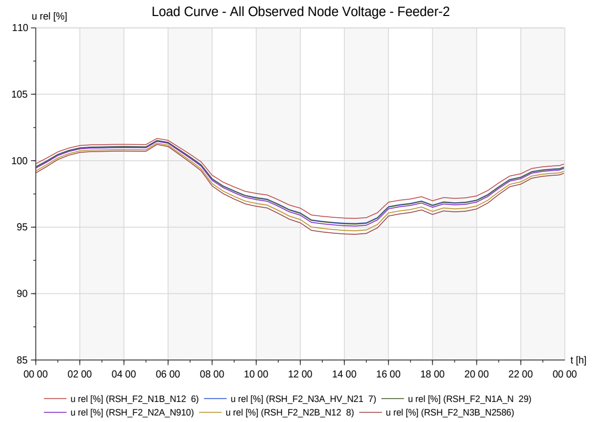

Feeder-2: Load only (94.464% to 101.675%)

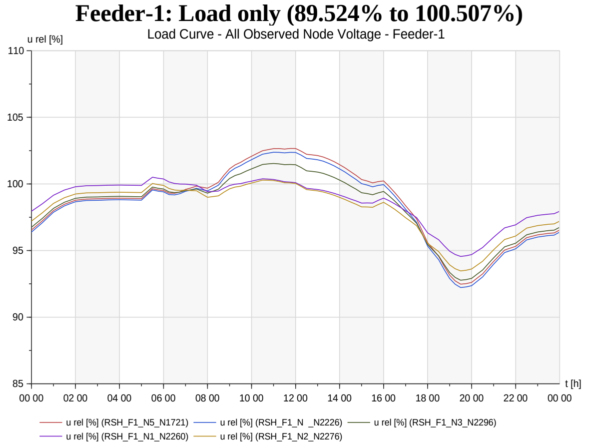

Feeder-1: Load with RE (92.226% to 102.662%)

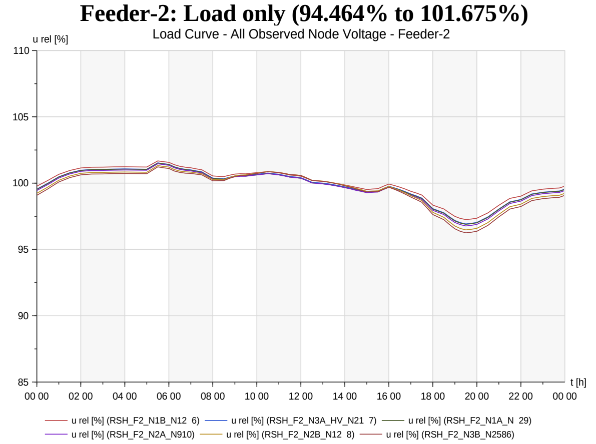

Feeder-2: Load with RE (96.253% to 101.675%)

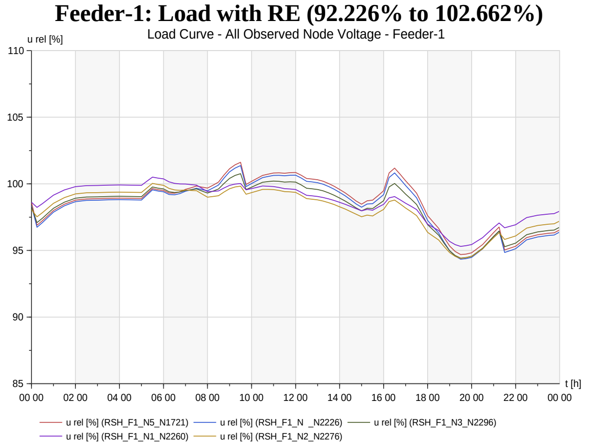

Feeder-1: Load with RE & Storage (93.344% to 101.618%)

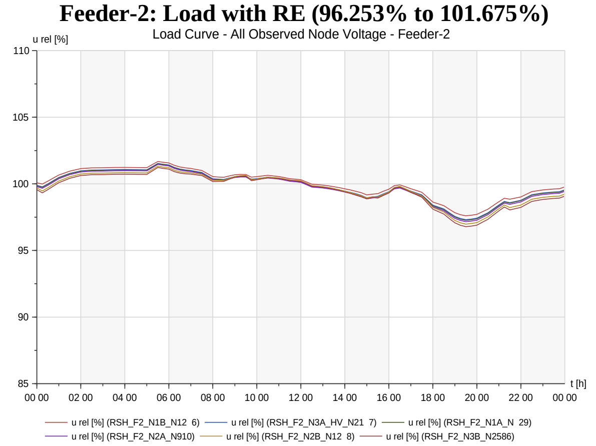

Feeder-2: Load with RE & Storage (96.786% to 101.675%)

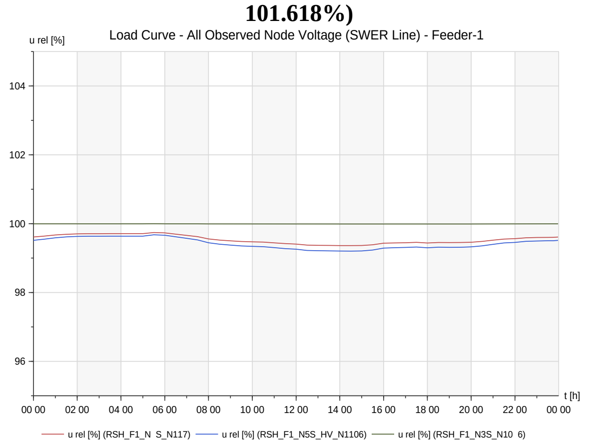

SWER Part: Load Only (99.203% to 99.995%)

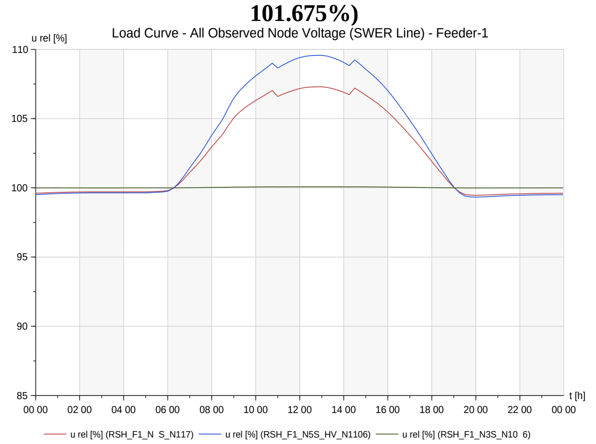

SWER Part: Load with RE (99.326% to 109.575%)

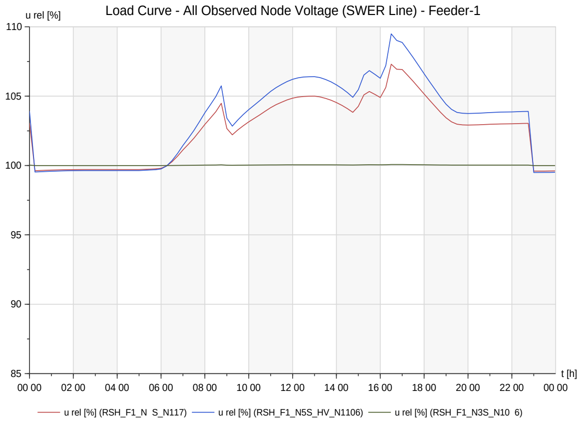

SWER Part: Load with RE & Storage (99.469% to 109.488%)

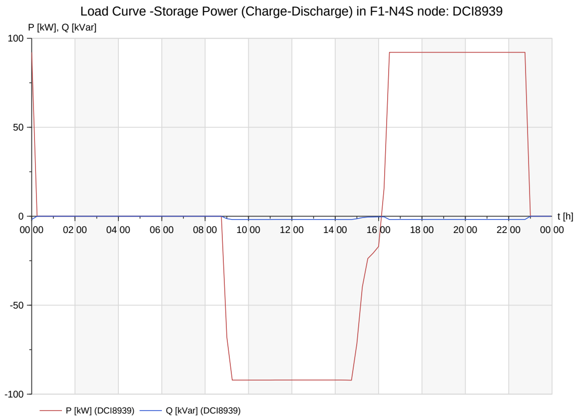

SWER Part: Charging & discharging in Storage at Node "RSH_F1_N4S"

Figure 5:81 RSH ZS network- Voltage variation observed at various observed nodes in Feeder-1 & Feeder-2

In RSH ZS network consists of three phase and single phase lines. A SWER network was connected to Feeder-1. The LF and LC analysis in the investigation on RSH ZS power network showed that:

- Phase unbalanced condition occurred in Feeder-1 due to the SWER network connection in Phase-1 only
- More fluctuation in voltage was observed in SWER part of the network and 10.4465% increase in voltage was observed after integrating RE. After integrating storage with RE 2.895% voltage drop was observed in SWER part of the network.
- LC analysis showed that the 4.525% voltage dropped during high demand time at 14:00PM in Feeder-1. After integrating PV voltage level increased during 08:00AM to 17:00PM and a maximum increase was observed at 14:00PM. A maximum 3.975% increase in voltage level was observed after integrating PV in Feeder-1. After integrating storage voltage level drops during 10:00AM to 14:00PM but during 17:00PM to 21:00PM voltage level increased due to discharge from storage.

5.4.9 Rockhampton Total Power Network

All the 8 ZS power networks and the impacts due to ES and RE were discussed separately when power flow was from source to load and then ES and RE also supplied power in the reverse direction in various load demand times. After integrating all 8 ZS power network together the network is not completely radial anymore, became partially meshed and this analysis gives the actual impacts on the complete network. However, observation nodes and lines are considered from the 11 kV nodes near each ZS transformer, than the 66 kV node where all 66 kV lines connected in the sub-transmission bus and finally at the node in the 132 kV transmission line. Load, RE and Storage remain connected at the LV side as discussed in 8 ZS power networks. Figure 5.82 indicates the nodes in observation in this case.

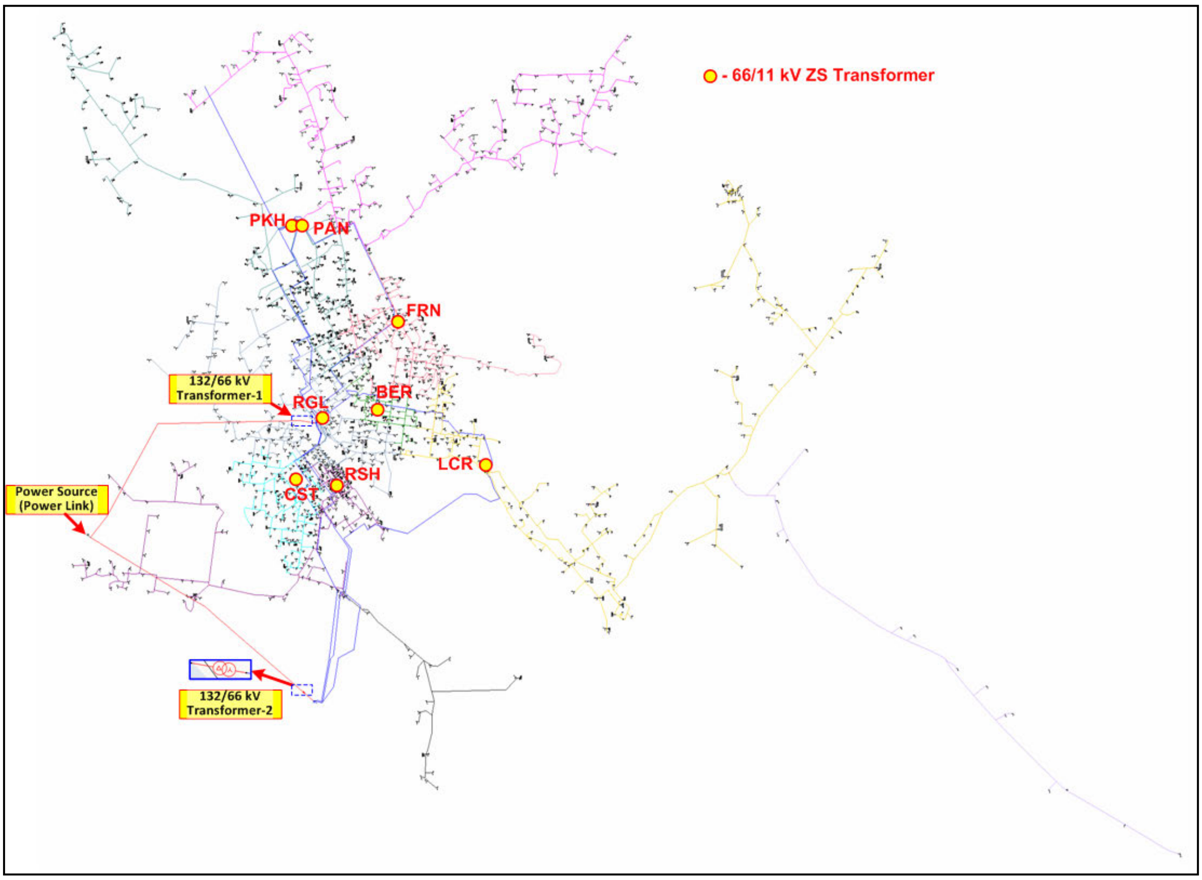

Figure 5:82 Rockhampton power network showing three observed network levels

LF calculation showed that due to the single phase SWER network in LCR and RSH, phase unbalance condition in these ZS network influenced other connecting ZS power networks. CST is very close to LCR and in this network, LCR influenced the phase voltage condition on CST, also phase voltage in BER was influenced by RSH. Interestingly, as all the ZS network connected close to the RGL network, therefore RGL was also influenced by the phase unbalanced situation. It was found that RE increased the phase voltage unbalanced condition; however storage helps in reducing this situation. For example, in LCR ZS, SWER covers a large part of the network so the difference in phase voltage was very clear. In load only condition V1= 6.285716 kV, V2= 6.282400kV, V3= 6.262372 kV and after integrating

RE, V1 increased 1.35718%, V2 1.82645% and V3 1.6182%. After integrating storage, voltage dropped slightly in all phases such as 0.0548% in V1, 0.1265% in V2 and 0.0959% in V3. It is clear that phase-2 voltage dropped a maximum which was increased to a maximum in load with RE configuration. Therefore large storage minimises the phase voltage unbalanced condition in the network. Figure 5.83 shows the phase voltage in Load only, load with RE and Load with RE and storage integrated condition at 11 kV side of the network.

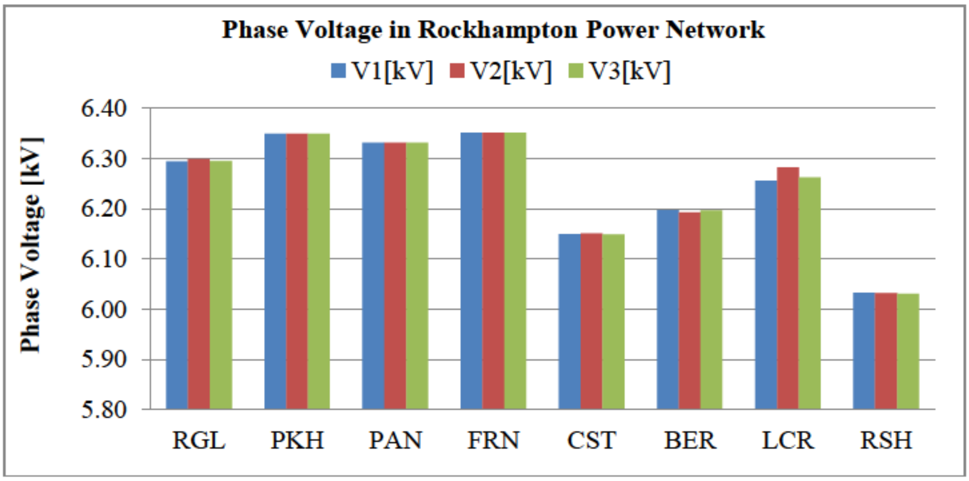

a. Load only condition

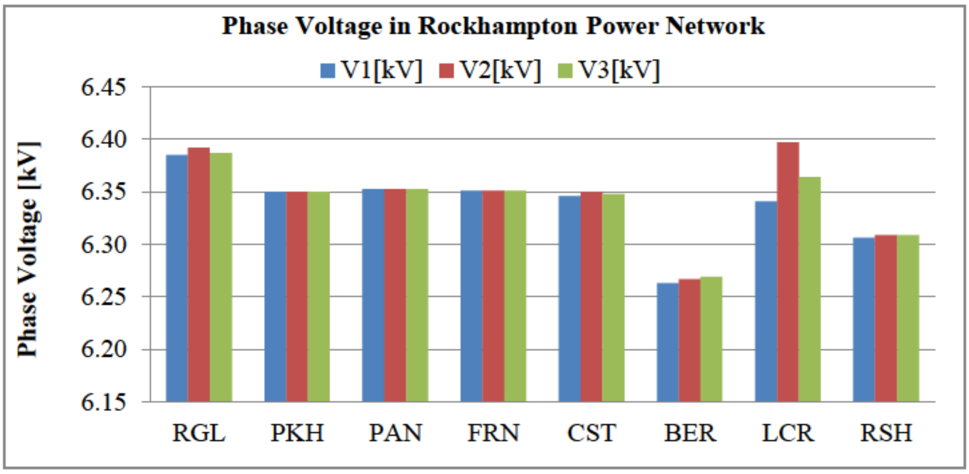

b. Load with RE condition

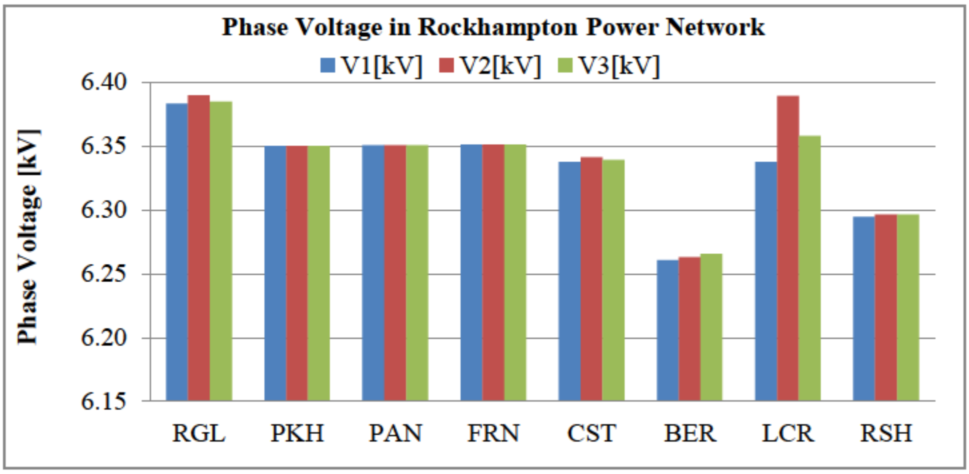

c. Load with RE and Storage integrated condition

Figure 5:83 Phase voltages at 8 ZS power networks in three configuration modes

By comparing the LF results it was found that RE (PV or WT) increased phase voltage and storage helped to reduce this increase in phase voltage. Figure 5.84 shows the phase-1 voltage (V1) in load only, load with RE and load with RE & storage integrated condition at 11 kV, 66 kV and 132 kV side of the network or compared at rated phase voltage of 6.35 kV, 38.1 kV and 76.21 kV respectively. It was found that voltage fluctuation is more at the lower voltage network and the installation of RE and storage at LV (415V) side of the network gradually influence the higher voltage level (11/66/132 kV) of the network. This change in higher voltage level can easily disturb the network performance of other networks that are connected from the higher voltage level network. It is seen that storage reduces the change in voltage and phase unbalance situation; therefore large scale storage will have positive impacts on power network in terms of voltage regulations.

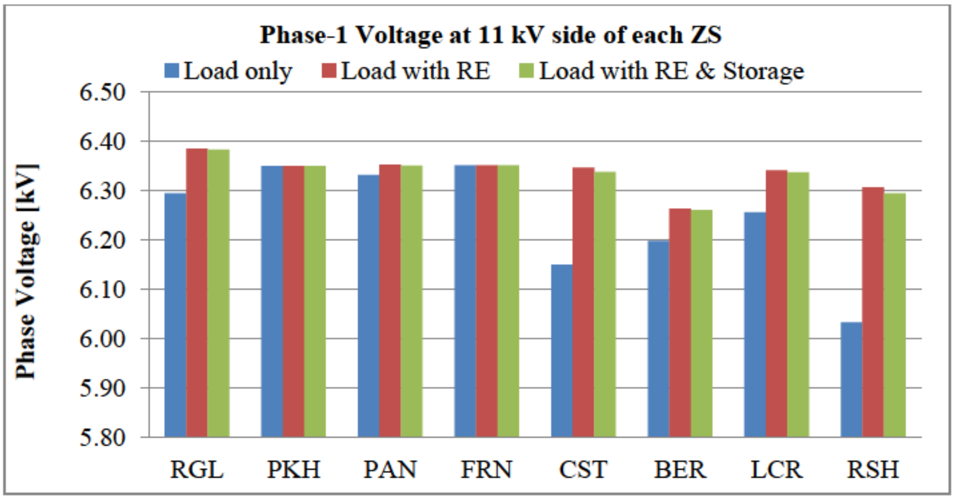

a. Phase-1 Voltage (V1) at 11 kV side of each ZS power network

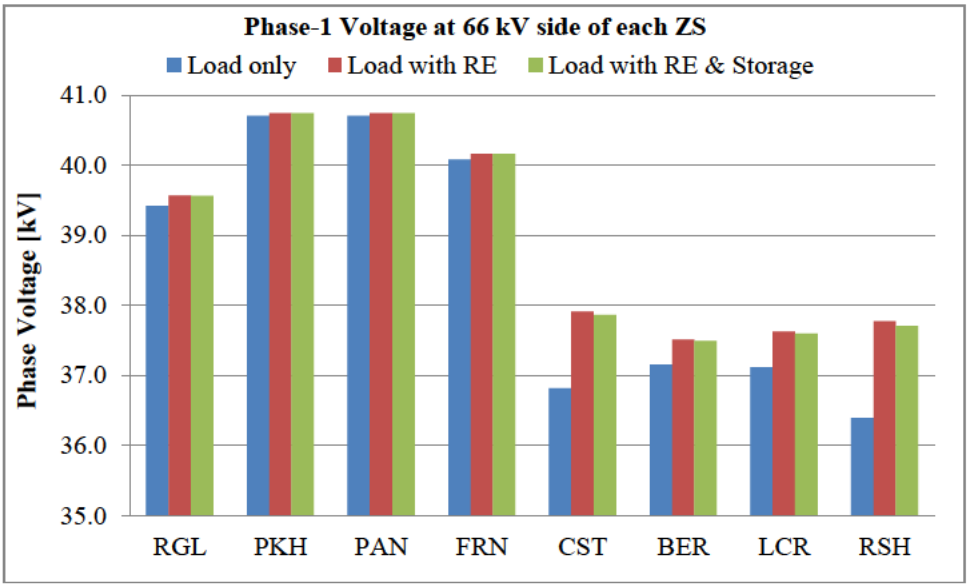

b. Phase-1 Voltage (V1) at 66 kV side of each ZS power network or Sub-Transmission line side

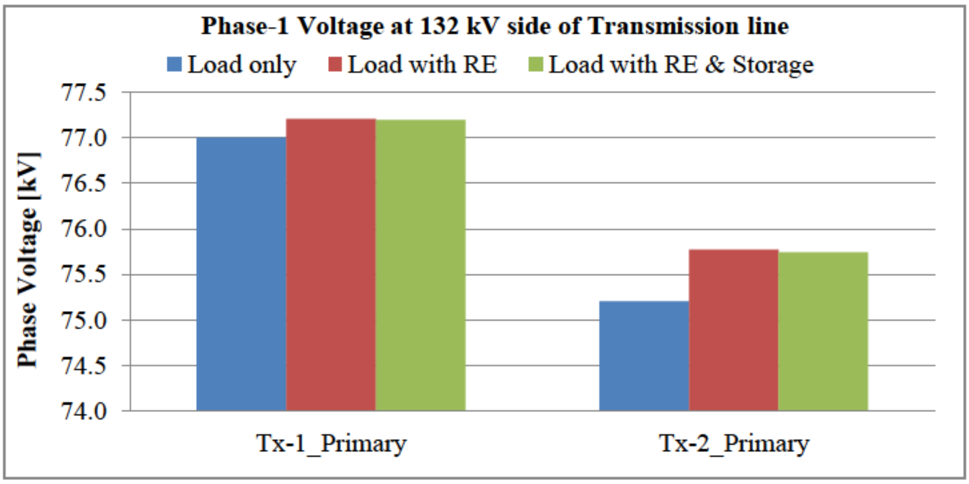

c. Phase-1 Voltage (v1) at 132 kV side of Transmission line

Figure 5:84 Phase-1 Voltage at 11, 66 & 132 kV network point

The LC calculation provides voltage variation with time and Figure 5.85 shows the voltage level at the 132 kV Transmission line measured at the primary side of the Transformer-1 and 2 between the transmission and sub-transmission lines. It is clear from Figure 5.85 (a & b) that RE increased voltage during mid day even at the high load demand time, however, after integrating storage the voltage level slightly dropped. At 14:00PM when load demand was high, the voltage level was 101.05%, 101.30% and 101.25% at 132 kV side of Transformer-1 and 98.65%, 99.40% and 99.35% at 132 kV side of Transformer-2 in load only, load with RE and load with RE & storage integrated condition. As the storage was installed at the LV side (415 V) of the network only at defined nodes in observed feeders, this network created more scope for additional storage into the network. However, the trend is clear that storage improves voltage level and has significant influence at the LV and distribution network as discussed earlier in each ZS power network.

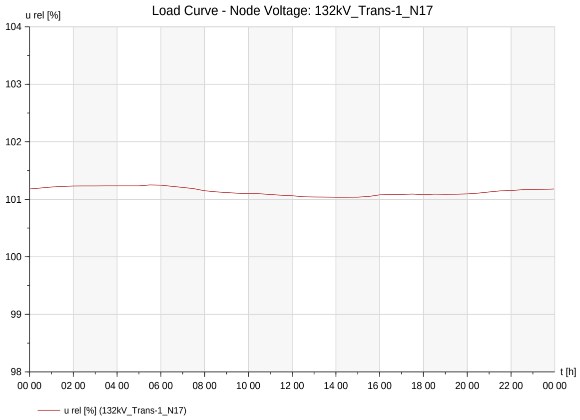

a. Load only (at 132kV side of Transformer-1)

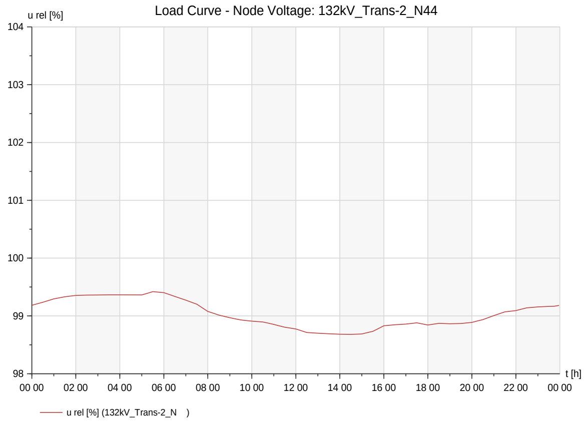

a. Load only (at 132kV side of Transformer-2)

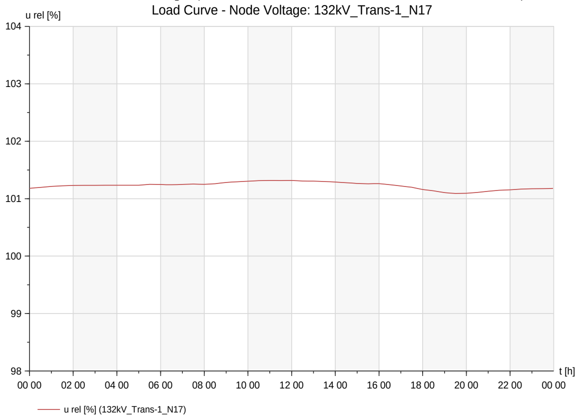

b. Load with RE (at 132kV side of Transformer-1)

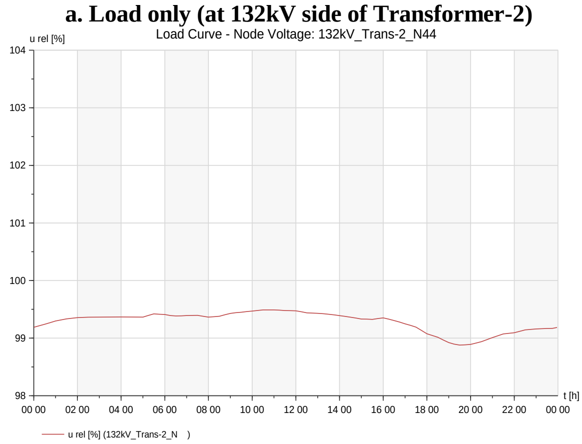

b. Load with RE (at 132kV side of Transformer-2)

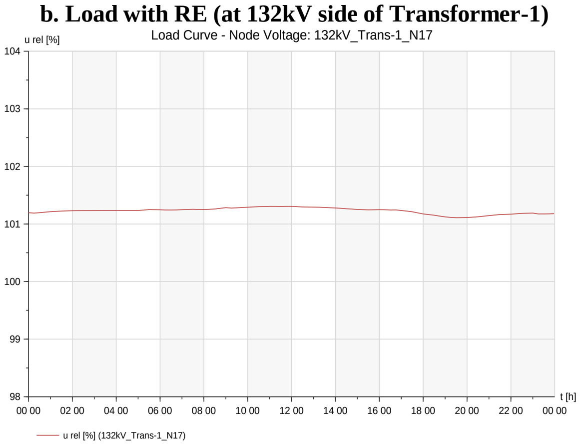

c. Load with RE & Storage (at 132kV side of Transformer-1)

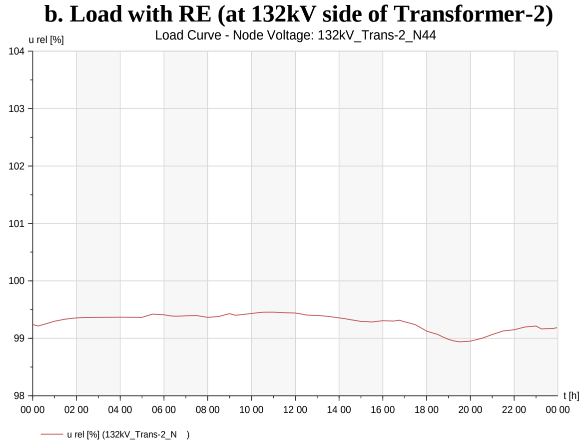

c. Load with RE & Storage (at 132kV side of Transformer-2)

Figure 5:85 Voltage variation observed at the HV side of Transmission line

Therefore large scale integration of RE and storage has greater impact in voltage regulation on LV and distribution networks which can influence the HV network as well and transmit the impact to other distribution networks connected from this transmission network.

PV or WT output increases the voltage level during high generation time and deteriorates unbalanced condition if installed in single phase line. Storage improves voltage regulation and phase unbalanced condition which improves the voltage regulation.

5.5 Conclusions

This chapter described the results of 4 different investigations of various network size and configurations and indentified the storage impacts on voltage regulation on the power network. The basic consideration was to identify the storage influence on the power network when the network was heavily integrated by various RE resources. In this analysis, solar PV and WT was considered as the RE sources. In investigation-1, the experiment on a controlled environment showed the amplitude of voltage waveform increased with increased PV penetration and a similar result was observed in model simulation. In simulated network, after integrating storage a voltage drop was observed at the PCC. Phase unbalance was observed in the experiment and in the simulation result as PV was not distributed symmetrically among phases. Investigation-2 considered a very small part of the power network, particularly a feeder or a service line from a distribution transformer (DT) to 45 number single phase distributed residential loads. This investigation was conducted by integrating RE and storage in distributed mode and then in centralised connection mode. Results showed that storage improved voltage regulation for both methods of connection, however centralised connection configuration showed better improvement. It was found that storage reduced load on DT and in centralised connection, configuration load on DT was a minimum which improved DT capacity. Moreover, in this investigation it was observed that storage minimises fluctuation from PV or WT and therefore improves voltage regulations. It was also observed that during short sudden fluctuations due to sudden change in solar radiation or wind speed, power generation from these sources changes instantly which causes transient fluctuations in the network. By supporting loads during that transient changes storage reduces the impacts on DT and on the network. In investigation-3, a part of the real power network in Rockhampton was considered. Various capacity PV and storage was integrated into the network and it was found that voltage levels increased with increased capacity of PV and this increase in voltage was more at distant nodes and in the low voltage network. A maximum of 6.745% and 9.67% of voltage increase was observed at the HV side and the low voltage side of the network respectively due to PV penetration. However storage minimises this increase in voltage. At the HV side 1.75%, and at the LV side, 2.23% voltage drop was observed respectively due to storage integration into the network. This network was further investigated by integrating centralised installation of large scale RE and storage at the distant nodes. LF analysis showed that ES increased voltage, however LC analysis showed that storage reduced voltage when RE generation exceeds load demand and increased voltage when RE generation failed to support load demand, therefore storage improved voltage regulation. Investigation-4 covered the total Rockhampton power network. For this ease of analysis, each ZS network was investigated separately and in that case feeders connected loads act as a radial network and power flows from HV source to the end node. In this investigation PV was initially integrated distributed way into the network and further PV or WT and ES was integrated into the network in a centralised way. Load, RE and storage was connected to the LV side the network. In each ZS network, 2 feeders were selected to observe and it was found that storage reduced the voltage level during high RE generation during mid day and improved voltage levels during the evening by releasing stored energy. Among 8 ZS power networks, Lakes Creek (LCR) and Rockhampton South (RSH) ZS power networks contain single phase SWER networks and due to this single phase network, phase unbalance in voltage was observed in the network. After integrating 8 ZS power network i.e. the complete Rockhampton power network was investigated which is a partial meshed network and found the similar result. It was found that the influence of storage was more visible at the LV and distribution network than HV network.

Chapter 6

Impacts of Storage on Network Harmonic Distortion

6.0 Introduction

Chapter 5 described the influence of storage on Voltage regulation in several network configuration scenarios. A detailed network scenario for experimental and model setup was described in Chapter 4. These networks were considered to analyse harmonic impacts of storage on power networks. This chapter describes the results of experimental and simulation work in terms of harmonic distortion in the network due to the integration of Energy Storage (ES) with RE into the power network. Four different cases were described in chapter 4 to investigate the impacts from a small scale to a large scale network. The results and discussion were presented for the small scale network that is based on experimental work to large scale network model. Similar to Chapter 5 this chapter also describes the result of the following 4 different scenarios:

Investigation-1: Harmonic distortion observation by

A. Experimental Investigation

B. Simulation based on experiment

(i) Without Energy storage

(ii) With Energy storage

Investigation-2: Harmonic distortion observation in a small Distributed load network

Investigation-3: Harmonic distortion observation in a small Power Network in Rockhampton

Investigation-4: Harmonic distortion observation in a large Rockhampton Power network

Section 6.1 provides the harmonic distortion results from the experiment and the same from a simulation investigation. Section 6.2 explains the investigation results of a network segment by integrating RE and storage in a distributed and a centralised way. Section 6.3

describes the results covering the practical network of Kawana in Rockhampton. Section 6.4 covers the complete power network of Rockhampton. Results are discussed by the separate analysis of 8 Zone Substations (ZS) and finally the results of the complete power network of Rockhampton. Section 6.5 provides the concluding remarks.

6.1 Results and Discussion on Investigation-1

This section covers two parts; (i) results of experimental investigation and (ii) simulation results without storage and with storage integrated configuration.

6.1.1 Result and discussion - Experimental Investigation

Detailed experimental setup was explained in Chapter 4, and the connection layout of the experiment was shown in Figure 4.38 in Chapter 4 and repeated in Figure 5.1 in Chapter 5. The experiment was conducted by increasing PV penetration.

Experimental data was collected from the data acquisition system in DAQ_PV at 5000 samples/sec for the following two experiments. As explained in Chapter 5, the PV was connected into the network in different sizes in different phases and showed the inverter connection layout in section 4.4.1.2 and Figure 4.40 in Chapter 4, but load was connected in a 3-phase line. SMA 1100W and SMA 1700W inverter was used to connect PV into the network.

- **Experiment-1:** 7.5 kW PV integration with varying load (23/43/53/63 KW)
- **Experiment-2:** 11.31 kW PV integration with varying load (23/43/53/63 kW)

Experimental data was captured by the data acquisition system “DAQ_PV” for both the experiments. From the experimental result it was found that the harmonic current increases with increased PV penetration.

Figure 6.1 and Figure 6.2 shows the phase currents of the PV system with the integration of 7.5 kW and 11.31 kW PV into the grid. The phase currents were not purely sine wave and ripples were clearly visible at peak value, also phase currents were not in same magnitude. Moreover magnitude of neutral current for 7.5 kW and 11.31 kW PV is very high and fluctuates significantly because of unbalanced PV generation which caused a significant amount of harmonics in the connected system. From the experimental result, it was observed that harmonic injection increased with increased PV penetration i.e. with increase of PV penetration from 7.5 kW to 11.31 kW. Figure 6.3 shows the neutral current of 7.5 kW and 11.31 kW PV systems. Neutral current of the PV system can be calculated from Equation 6.1.

$$I_N = \sqrt{I_A^2 + I_B^2 + I_C^2 - I_A I_B - I_B I_C - I_C I_A} \tag{6.1}$$

where I_N is the neutral current, I_A, I_B, and I_C are the RMS current of phase A, phase B and phase C respectively. Neutral current should be small however, as the phase current was not balanced neutral current increased. The experimental setup in connecting PV in different phases was not balanced therefore neutral current was found very high as shown in Figure 6.3.

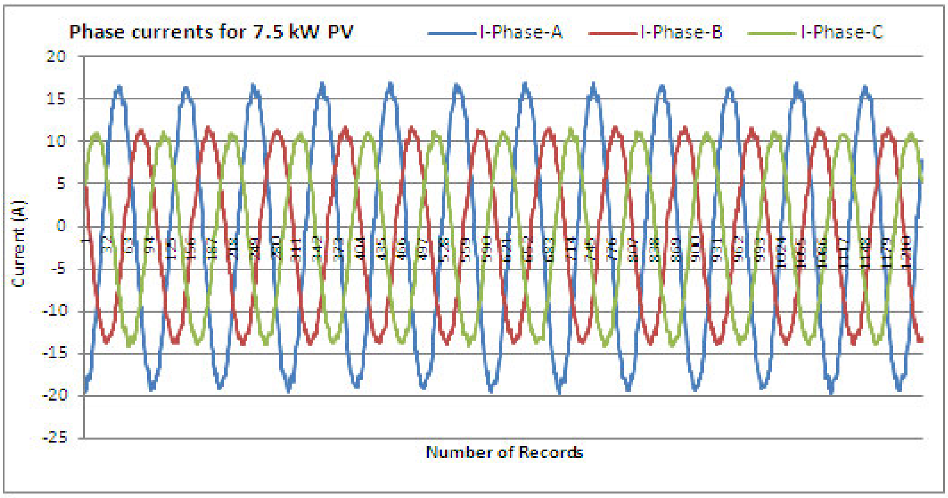

Figure 6:1 Phase current after 7.5 kW PV integration

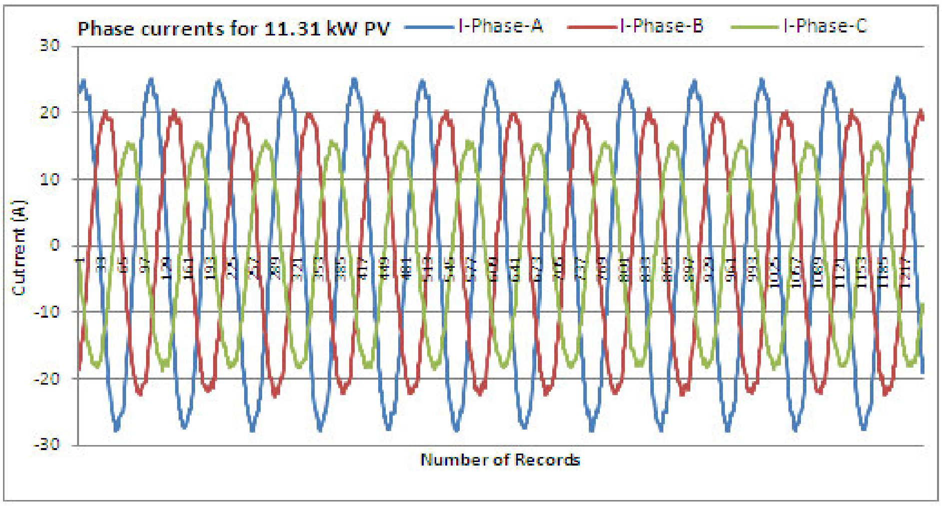

Figure 6:2 Phase current after 11.31 kW PV integration

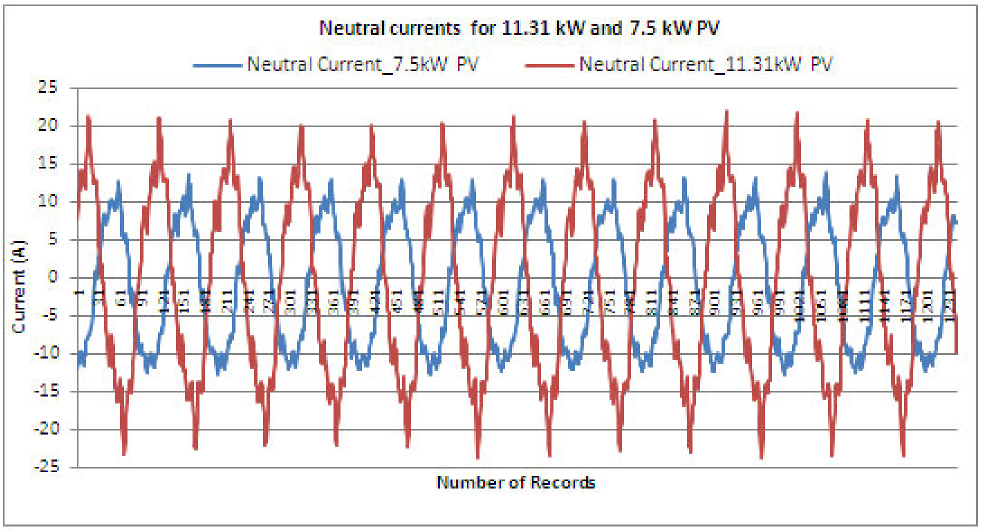

Figure 6:3 Neutral currents after 11.31 kW and 7.5 kW PV integration

Spectral analysis on experimental sampled data provides the amplitude of different harmonics present in the distribution network by applying Discrete Fourier Transform (DFT). DFT converts a discrete time signal from time domain to frequency domain. The Fast Fourier Transform (FFT) is an efficient method for computing the DFT and its inverse. For the analysis of harmonic emissions on experimental data, FFT was used considering 50Hz as the fundamental frequency. FFT found the presence of harmonic contents as the integral multiple of fundamental frequency.

In the experiment, data was collected at the rate of 5000 samples/sec or the sampling frequency was 5 kHz. MATLAB was used as a tool to apply FFT and to perform spectral analysis, harmonic effects were presented in a graphical representation. Figure 6.4 shows the time domain representation of the first 13 harmonics current. From the spectral analysis, it has been observed that with the integration of PV, current harmonics were injected into the network. Figure 6.5 shows the injected harmonics current in different frequencies with 7.5 kW of PV integration. Figure 6.5 shows that other than fundamental frequency, maximum current was found in the 3rd (150Hz) and the 9th (450Hz) harmonics. The magnitude of individual harmonics current (other than at fundamental frequency) after integrating 11.31 kW PV penetration is as shown in Figure 6.6. Harmonic injections from all even harmonics are very low and within the range of AS-4777 standard [144]. However, 3rd and 9th harmonics exceeded the regulatory standard limit [144] while 7th and 15th harmonics just touch the threshold level. Table 6.1 shows the observed harmonic current in terms of percentage of fundamental current at different harmonic frequencies.

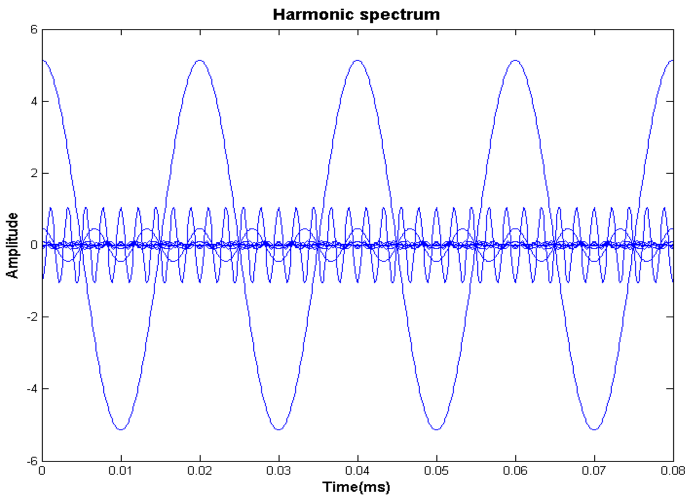

Figure 6:4 Time domain representations of first 13 harmonics

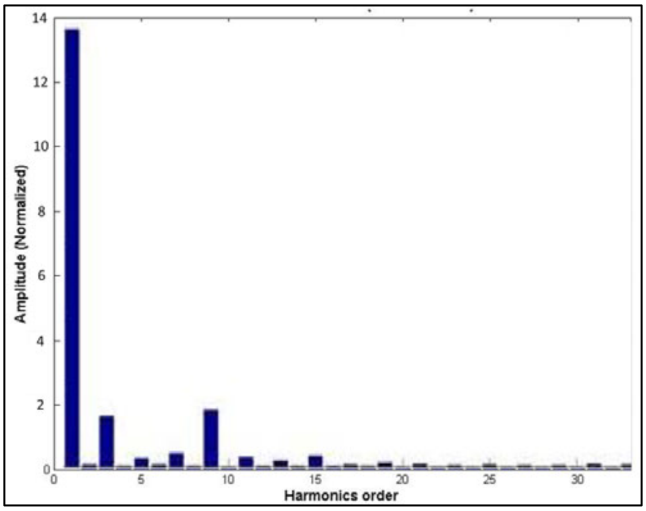

Figure 6:5 Amplitude of Harmonic current (with 7.5 kW PV)[145]

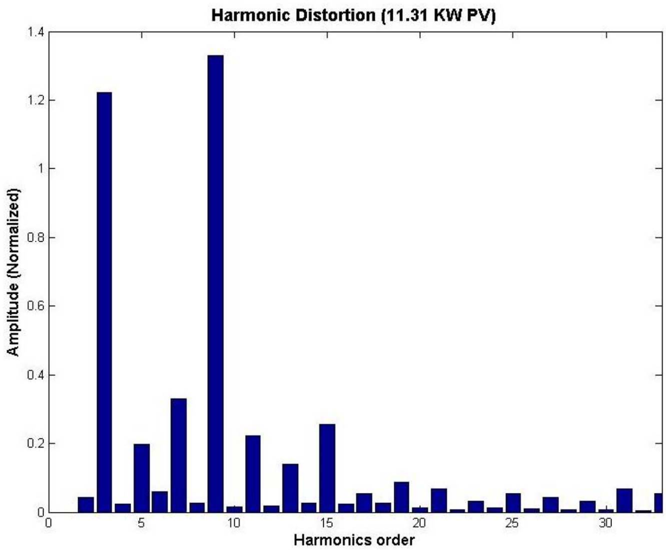

Figure 6:6 Amplitude of harmonic current with 11.31 kW PV (not showing the fundamental current)[145]

Table 6:1 Harmonic current at different harmonic frequencies[145]

Harmonic order (n)	Harmonic current (% of fundamental)	
	after integrating 7.5 kW PV	after integrating 11.31 kW PV
3	6.5810	11.8865
5	1.0145	1.9349
7	1.8473	3.2047
9	10.049	12.9414
11	2.6881	2.1572
13	0.5592	1.3458
15	2.5153	2.4919
All even harmonics	negligible	

Therefore, from Table 6.1 it is clear that harmonic current injection increases with increased PV into the power network. Total harmonic (current) distortion (THD) was calculated using harmonic distortion at each frequency and found THD of 17.63% for 11.31 kW PV integrated condition. As mentioned in section 5.1.1 in Chapter 5, the voltage waveform had flat peak, an indication of the presence of harmonic voltage. Minor voltage harmonics was observed due to PV and non linear load and THD was calculated as 1.28% in 11.31 kW PV integrated condition.

As the experiment was conducted without storage, a software model was developed, configured and simulated according to the experimental setup and then simulated after including battery as the energy storage.

6.1.2 Result and discussion - Model Simulation

A model was developed using PSS SINCAL which mimics to the experimental setup. Figure 6.7 shows the model, highlighting the line elements to observe current flow. Similar to the experimental setup PV was connected to the network with 1100W and 1700W capacity inverter. Harmonic current data for load, inverter and storage was included into the model. Harmonic data for SMA 1100W and SMA 1700W inverter was collected as shown in Table 4.14 in Chapter 4. Harmonic current data for load and storage are shown in Table 4.13 in Chapter 4. As the load harmonics data was not known in during the experiment, therefore there were some differences in the result of the harmonic calculation by experiment and by simulation.

The model setup was discussed in Chapter 4, moreover section 5.1.2 in Chapter 5 also described additional settings. As mentioned earlier, the SINCAL based model provides flexibility to increase PV integration and allows integrating energy storage (ES) into the network.

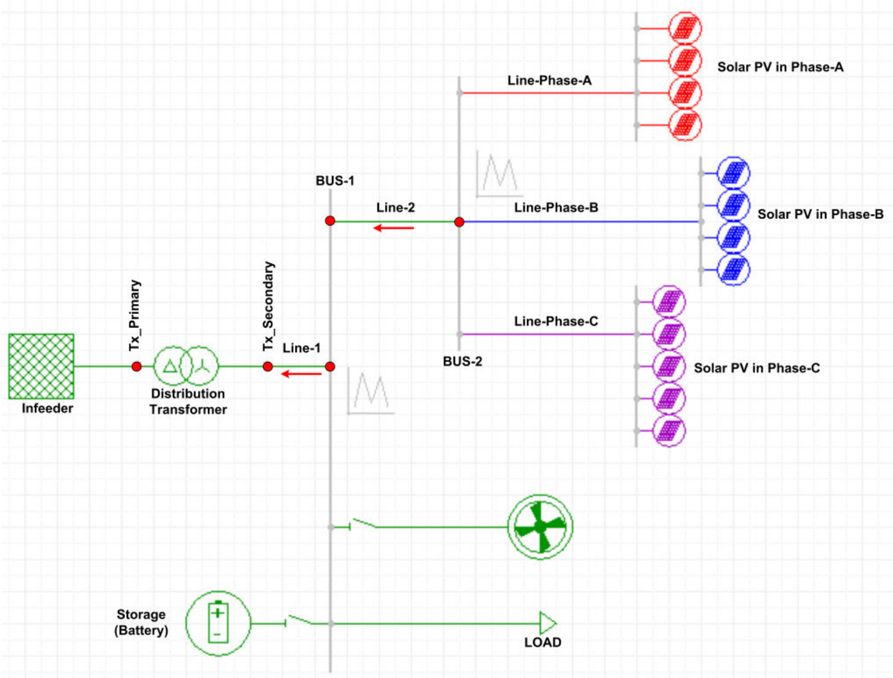

Figure 6:7 Software model mimic of experimental setup showing Observed lines

6.1.2.1 Model without Energy Storage condition

Similar to the experimental setup, in the model, solar PV was integrated in Phase-A, B and C as total installed PV capacity was 7.5 kW and 11.31 kW. Each PV was connected to the network with the inverter. The connection layout of PV via inverter is explained in section 4.4.1.2 and is shown in Figure 4.40 in Chapter 4. Three phase load was considered and commercial load profile was used as shown in Figure 4.31(a) in chapter 4. The model was simulated under the following configurations and results were compared:

- **Configuration-1:** 7.5 kW PV integration with 63 kW load
- **Configuration-2:** 11.31 kW PV integration with 63 kW load

Simulation was conducted and the harmonic current was measured at the observed lines (Line-1 and Line-2) as shown in Figure 6.7.

Harmonic Current:

Simulation results showed that harmonic current increases with the increased PV penetration in every harmonic order. The third harmonic was found to be very significant, even harmonics were very low therefore it was not shown and THD (up to 15th harmonics) is as shown in Figure 6.8. It is clear from the figure that harmonics is higher with the integration of 11.31 kW PV than 7.5 kW PV. Third harmonics exceeded the limit of AS-4777 (4%) and THD also exceeded AS-4777 limit (5%), although in this setup major harmonic contributor was the load where THD for load was 4.3%. However it is clear that increasing PV penetration increased harmonics distortion. Figure 6.8 shows the harmonic current in Line-1 i.e. from BUS-1 to Tx_Secondary node as indicated in Figure 6.7.

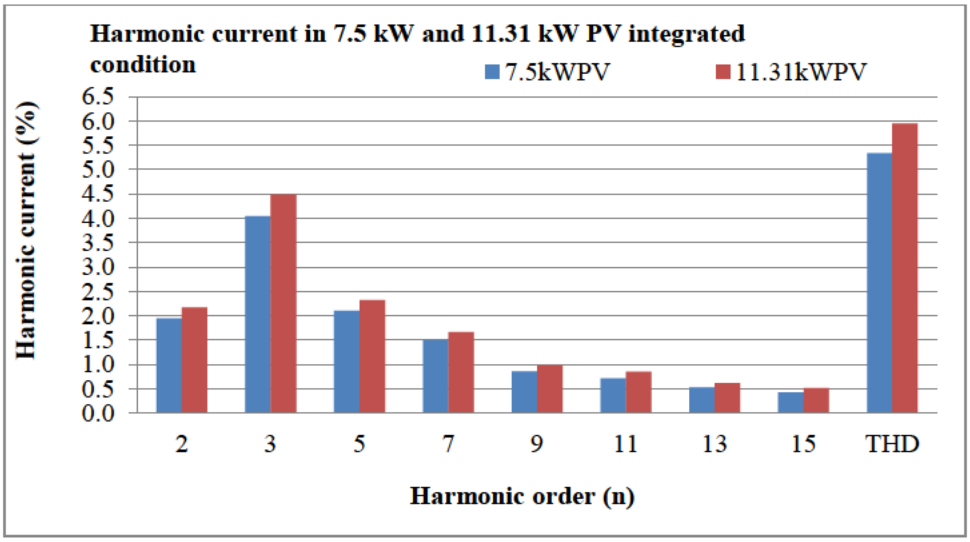

Figure 6:8 Harmonic current (% of fundamental) observed at Line-1 with different size PV penetration

Harmonic Voltage:

Harmonic voltage was measured at BUS-2 where all PV connected to the network and at Tx_Secondary node where all LV elements are connected. At BUS-2 THD voltage harmonics was calculated as 10.786% for 7.5 kW PV integrated condition and with 11.31 kW PV it was 12.014%. But at Tx_Secondary node, Transformer influenced the voltage condition and the harmonic voltage decreased, therefore THD for 7.5 kW and 11.31 kW PV becomes 0.6611%

and 0.6924% respectively as shown in Figure 6.9. Therefore voltage harmonics also increases with increased PV penetration.

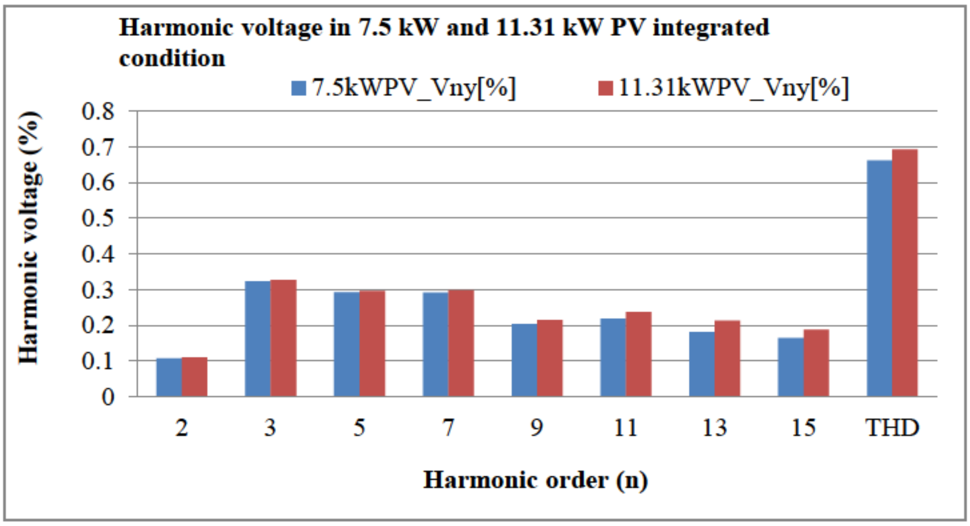

Figure 6:9 Harmonic voltage observed at Tx_Secondary node

6.1.2.2 Model with Energy Storage (ES) Integrated condition

In order to observe the storage impacts, the model was modified and ES was integrated into the model as explained in section 5.1.2.2 in Chapter 5. In this case a commercial load of 63 kW, PV 129 KW and 63 kW ES was integrated for the best utilisation of PV energy. The model was simulated as per the following configurations:

- Load Only (63 kW)
- Load with Solar PV (63 kW Load & 129 kW PV)
- Load with Solar PV and ES (63 kW Load, 129 kW PV and 63 kW Storage)

Harmonic Current:

As explained earlier in section 6.1.2.1, harmonic current increases with increased PV penetration. After adding storage it was found that storage increases more harmonics into the network. Figure 6.10 shows the harmonic current observed as a percentage of line current in Line-1 in three different configurations. In load only condition, total load current flows through Line-1 from Infeeder to load after integrating large PV into the network part of the load demand met by the PV which caused reduction in current flow through Line-1 and as a consequence, the percentage of harmonic current increased. Similarly after increasing ES into the network, additional load demand was met by the storage which caused further reduction in load current flow through Line-1. Furthermore harmonic current from load, PV inverter and storage injected into the network which caused increased THD in ES integrated condition.

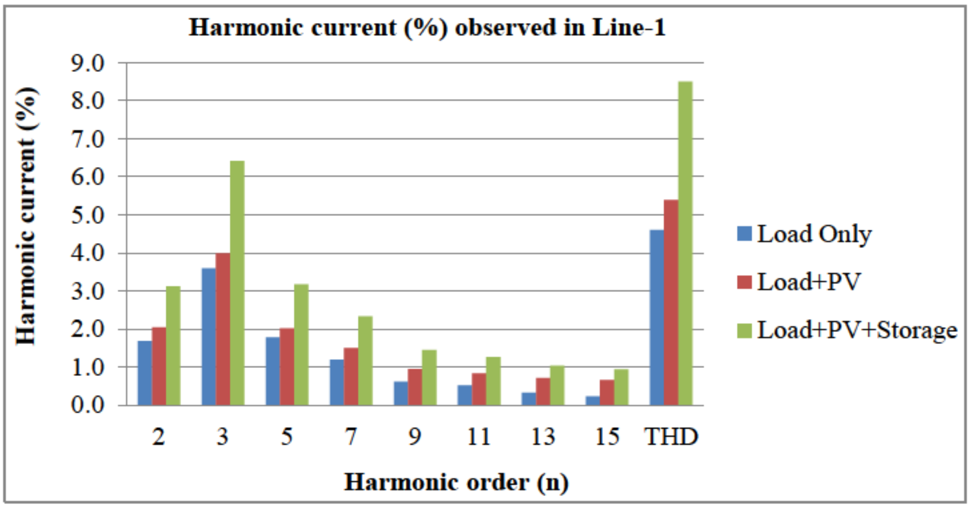

Figure 6:10 Harmonic current (% of line current) in Line-1 in different configurations

Harmonic Voltage:

As indicated earlier, harmonic current increases with the integration of PV and ES. Harmonic current into the network system causes harmonic voltage to rise [137], and the same consequence was observed in this experiment. It was observed from the simulation result that harmonic voltage slightly increased with storage integrated condition at the Tx_Secondary node as shown in Figure 6.11. However significant harmonic voltage was observed at BUS-1 where PV, Storage and loads are connected, particularly 3rd, 9th and 15th harmonics, although THD is still below the standard limit of 8% [22] as shown in Figure 6.12.

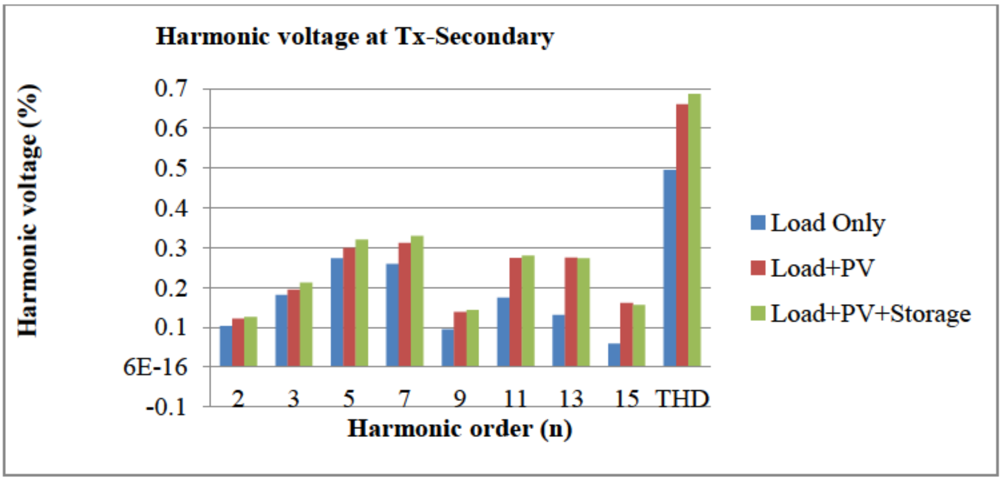

Figure 6:11 Harmonic Voltage (% of phase voltage) at Tx_Secondary node

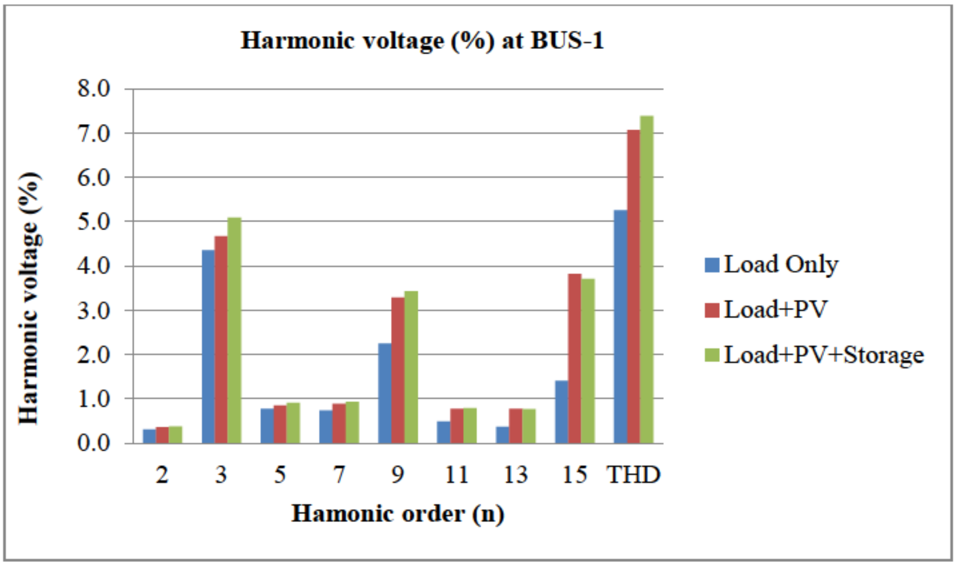

Figure 6:12 Harmonic Voltage (% of phase voltage) at BUS-1

Therefore, both experimental and simulation results clearly indicated that PV and ES increased harmonics current and harmonics voltage into the network, however the observed network level and integrated PV and ES was limited which kept the result close to the allowable limit. Large scale integration in a large network could have different result. This investigation covered only one 3-phase load, the next investigation describes harmonics due to ES and RE integrated condition in single phase distributed load network.

6.2 Results and Discussion on Investigation-2

In this investigation, Distributed single phase residential load was considered. Solar PV and wind turbine (WT) was considered as RE sources and Battery as ES. The model was configured such that solar PV or WT and storage were connected with distributed load in 3 node buses as shown in Figure 4.42 in Chapter 4. The model was modified to connect solar PV, WT and storage in a centralised way at the end node. The model setup, load, renewable energy (PV and wind turbine), storage allocation, installed elements harmonics data and required parameter settings were described in section 4.4.2 in Chapter 4. It was mentioned that a total of 45 houses were connected from 3 node buses and distributed among 3 phases. In each node bus, 5 houses installed 5 kW capacity PV/WT and 1.72 kW capacity ES, therefore a total of 15 houses installed PV/WT and ES. In the centralised connection of RE and storage total 75 kW capacity of PV/WT and 25.8 kW capacity ES was installed at the end node. For the ease of understanding the results from this investigation, the model layout in Figure 4.42 as detailed in Chapter 4 is shown below highlighting the lines indicating the observed flow of current (Figure 6.13). A total of 5 line elements were observed, as shown in Figure 6.13. These line elements are DL3, DL2, DL1, DT (from secondary side to primary side of DT) and infeeder (from primary side of DT to Infeeder).

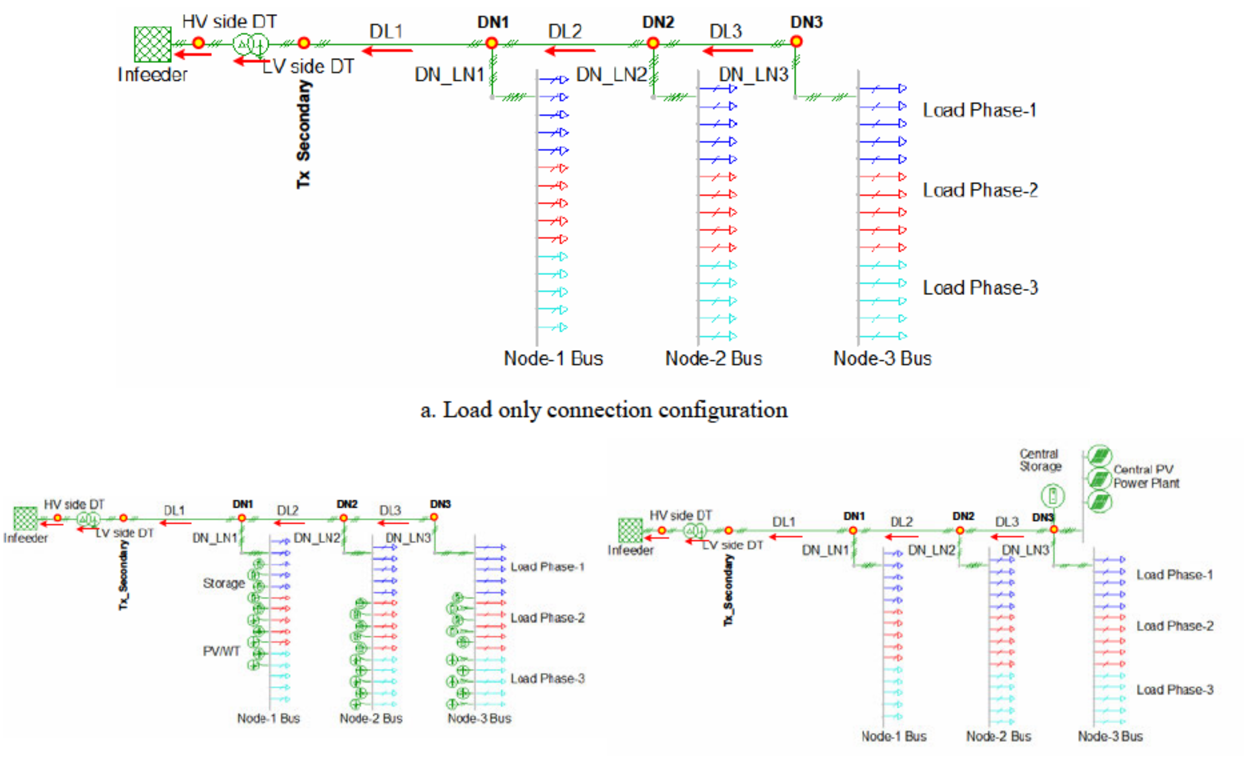

a. Load only connection configuration

b. PV/WT/Storage - distributed connection

c. PV/WT/Storage - centralized connection

Figure 6:13 A small network model showing observed lines

The model was simulated to evaluate the harmonic injection from RE and the storage into the network. Harmonic calculation was done in SINCAL and observed the flow of load current and harmonic current from load, RE and storage into the network and identified the harmonic emission due to storage. The model was configured in the following 9 different cases and the findings are summarised below:

- Case-0: Load only
- Case-1: Load with Solar PV
- Case-2: Load with PV + Storage
- Case-3: Load with Large central PV power plant
- Case-4: Load with central PV power plant + Storage

- Case-5: Load with Wind turbine (WT)
- Case-6: Load with WT + Storage
- Case-7: Load with large central WT Power plant
- Case-8: Load with central WT Power plant + Storage

Harmonic emission on DN was analysed by providing harmonic data of the inverter connecting PV and storage and converter harmonics data with wind turbine in the network model. Load harmonics data was scaled down to 25% of the maximum limit in AS/NZS 61000.3.2 [139] so as to view the harmonic emission from PV/WT and ES in a comparative way. After adding PV, WT and storage in different case configurations, the observed lines were investigated and harmonic current, load current data were noted. Based on this data, the percentage of harmonic current in different harmonic frequencies up to 25th harmonics were observed and finally, total harmonic (current) distortion (THD) was calculated using Equation 4.8 in Chapter 4.

Figure 6.14 shows the THD observed in 5 line segments in nine different case configurations. It was found that in all cases where RE and storage were integrated, THD exceeded the limit of AS-4777. In distributed connection configuration i.e. in Case-1, Case-2, Case-5 and Case-6 have the highest level of THD, therefore these connection configurations of RE and storage have great concern for power quality. When PV/WT was installed in a distributed way into the network, load current flow through the observed lines reduced as the load demand was partially met by the RE and when ES was integrated, further load demand met by the ES, which further reduced the flow of load current. On the other hand, the integration of these RE and ES adds harmonic currents into the network, also inverter operation increases which causes additional harmonic current into the network. This increases in harmonic current and a decrease in load current finally increased THD in the network. In centralised connection configuration i.e. in Case-3, Case-4, Case7 and Case-8, where PV, WT and storage connected to the network at the end point of service line, there is less harmonic emission compared to the distributed connection configuration as shown in Figure 6.14. In this case PV/WT and ES acts as a power plant at the other end of the feeder which supports the load demand and the flow of load current increased in the observed lines, especially through the end line (DL3) which cause reduced THD at that line and other observed lines compared to the distributed connection configuration. Moreover, the switching of the inverter was reduced which caused reduced of harmonic current into the network.

However, in both connection configurations it was found that storage increased THD in the network. It is clear from Figure 6.14 that Case-2 has a higher THD than in Case-1 and the same in Case-6 and Case-5 in the distributed connection configuration. Similarly, Case-4 has higher THD than Case-3 and also Case-8 has higher THD than Case-7. As ES adds additional harmonic current into the network and also by storing excess energy from PV/WT plant, there was reduction in the flow of load current and that caused the increase in THD.

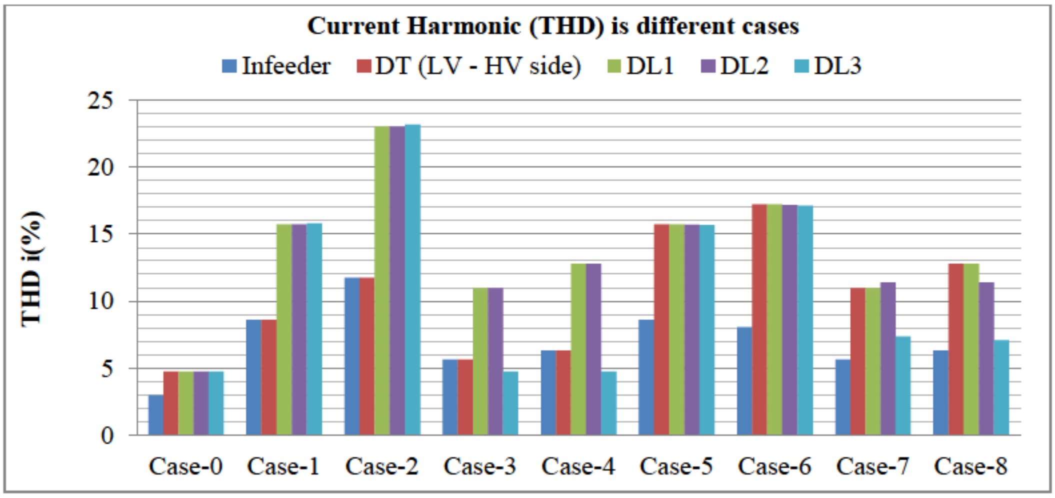

Figure 6:14 THD in different case configurations in different observed lines

As mentioned earlier the increase of harmonic current into the network causes the increase of harmonic voltage. Total harmonic voltage distortion (THD) of the complete LV side of the network i.e. from secondary side of DT to the end load, THD was measured as 24.5% and up to 25th harmonic frequency as shown in Figure 6.15. However at end node (DN3), the observed THD in Case-7 & 8 are 19.75% and 23.25% respectively.

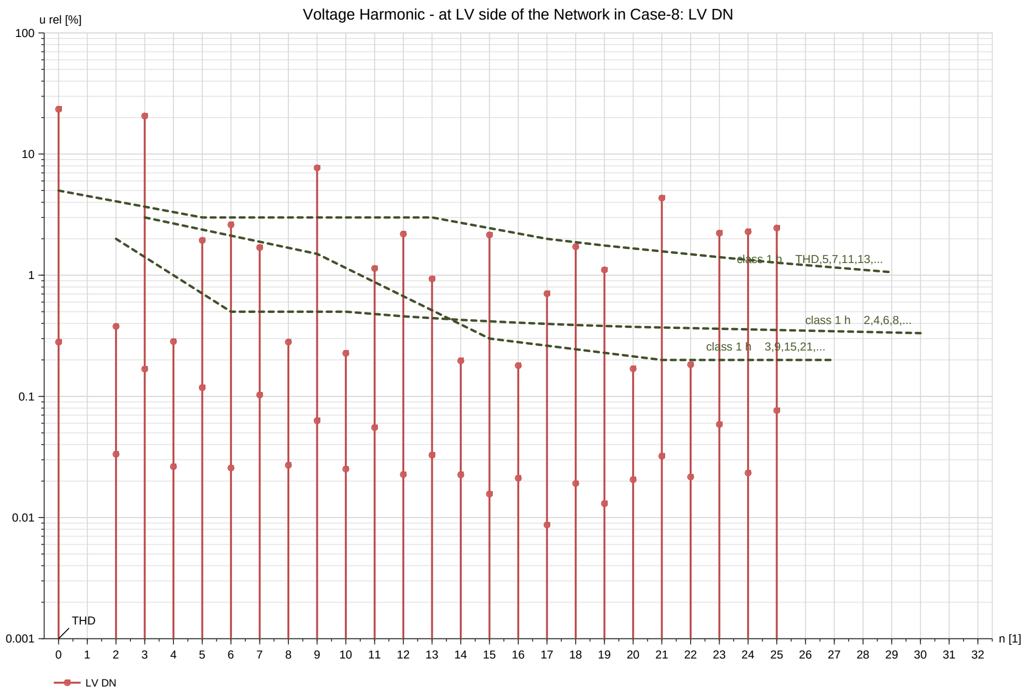

Figure 6:15 Harmonics Voltage distortion at the LV side of the network

Therefore, in all cases, storage adds additional harmonics to the network although it was found that in the centralised connection configuration, THD is less than for the distributed connection configuration. Voltage harmonic also increases with the integration of ES.

6.3 Results and Discussion on Investigation-3

In this investigation, a small section of the power network in Rockhampton was modelled in PSS SINCAL. A detailed model setup of Kawana, a suburb of Rockhampton, was discussed in section 4.4.3 in Chapter 4 and also in section 5.3 in Chapter 5. The network was divided into 7 load zones and loads were connected at the LV side of DT (11kV/415V) in each phase. Loads considered are residential loads and the load profile is shown in Figure 4.31(b) and for PV, summer solar radiation was considered as shown in Figure 4.32 in Chapter 4.

This network was configured in distributed integration of PV and ES and again centralised integration of PV and ES. Harmonic data for load, PV and ES was included into the model and the data shown in Tables 4.13 and 4.14 in Chapter 4.

6.3.1 Distributed Integration of RE and ES

This Power network of Kawana was modeled with real load and network parameter data. For the harmonic calculation, the model was simulated in the following three configurations.

- Load only (no PV or storage installed)
- Load with PV (PV 20% of load rating)
- Load with PV and storage (PV & Storage 20% of load rating)

As the load, PV and ES were distributed in LV side of all nodes in phases; therefore harmonic current was measured in only the line “All_Zone” that connects total network to the infeeder as shown in Figure 6.16. In load only condition total current harmonic distortion (THD) found was nearly 3%. This investigation was done after integrating PV and storage into the network at 20% of load rating and large load current still flowing through the observed line, a significant increase in harmonic current was not observed at the observed line. A detailed investigation was done after integrating PV and storage in centralised configuration in each zone.

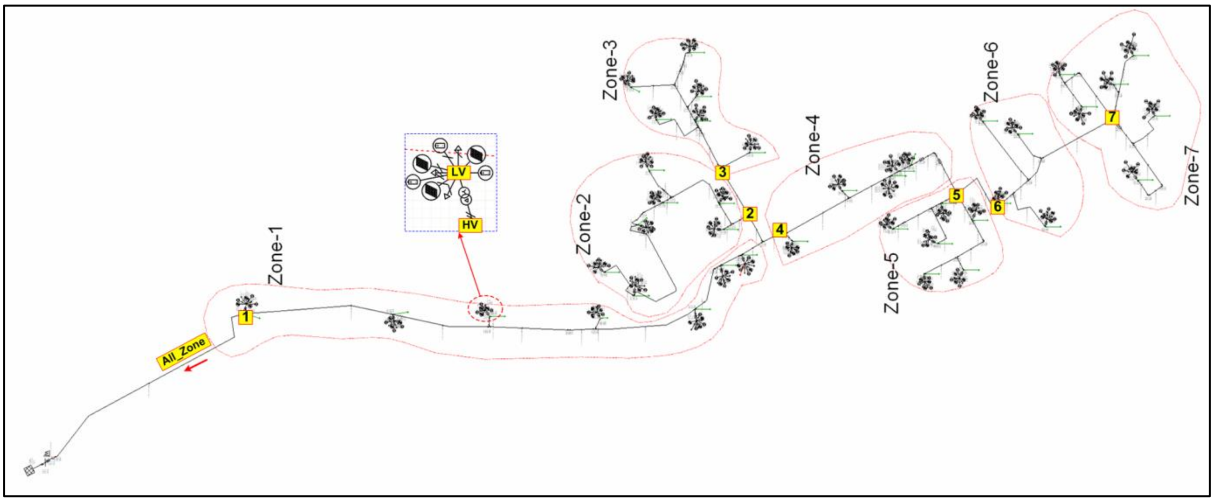

Figure 6:16 Distribution network of Kawana showing observed line

Voltage harmonics was observed on each node of the LV side of the DTs and the result is shown in Figure 6.17. Figure 6.16 highlighted one LV side of node showing load, PV and storage connected from DT. PV and storage was integrated at 20% of the load capacity. It was found that PV adds additional harmonics to the network and storage further adds harmonics to the network although the total harmonic voltage distortion (THD) was found to be within the acceptable limit of 8%[22].

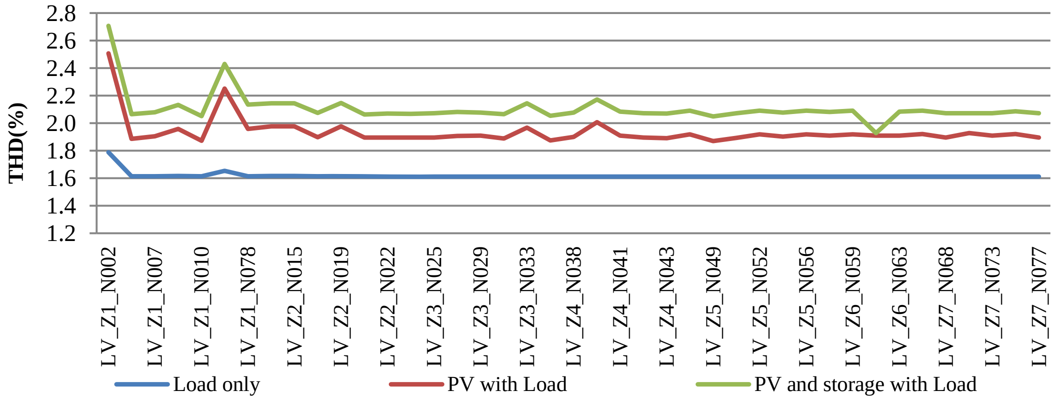

Figure 6:17 Observed harmonic voltage (THD) at the LV side of the network

Therefore, in distributed connection configuration both current harmonics and voltage harmonics increased with PV and ES. A further investigation on the Kawana network was done in centralised integration of PV and ES.

6.3.2 Centralized Integration of RE and ES

The power network of Kawana, described above, was modified to integrate PV and ES in a centralised approach. However the load distribution was kept unchanged. Bulk size PV and storage was integrated into the distant nodes in each zone as shown in Figure 6.18. For this analysis, 500 kW of PV plant was installed at the distant node of each zone and for the best utilisation of PV, 100 kW capacity of Energy storage was added in each zone. The installed PV and storage capacity against load in each zone is shown in Table 5.1 in Chapter 5. The harmonic calculation was done and the flow of harmonic current and load current was observed in the selected lines as shown in Figure 6.18.

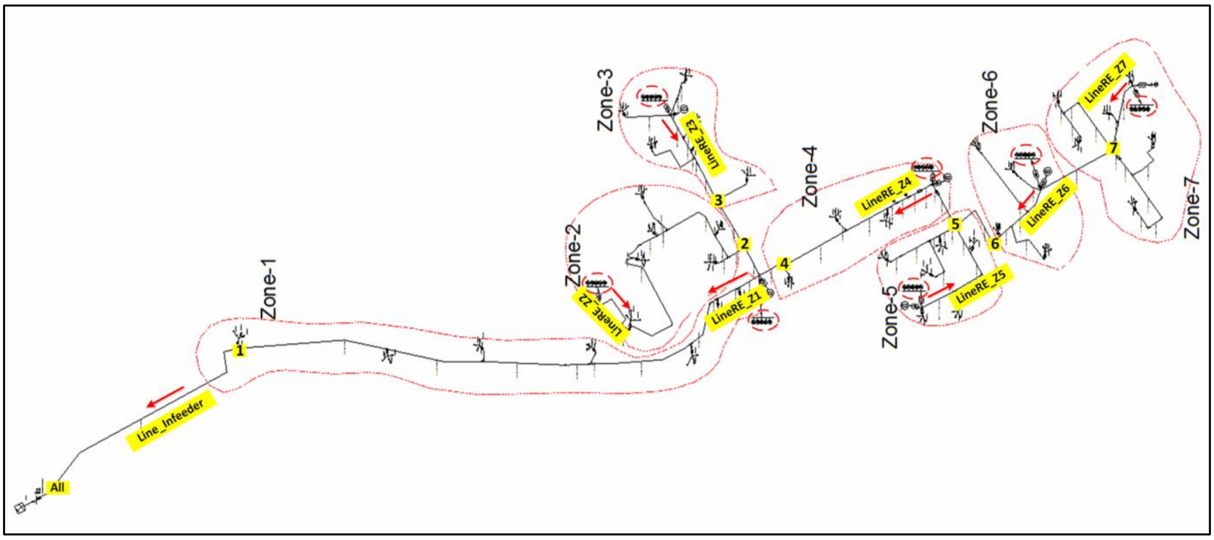

Figure 6:18 Power network of Kawana showing observed lines and bulk size PV and Storage in each zone

PV was integrated into the network with an inverter and considered as the current source element and similarly storage (Battery) was also integrated into the network. Harmonic current for the inverter was described Table 14 in Chapter 4 and the 10 kW inverter current harmonics data was scaled up for 100 kW capacity inverter for the analysis.

When PV generates energy and supplies to the network, this caused reduced load current flow from the infeeder and also PV injects harmonic current into the network. Similarly when ES stored excess energy that further reduced the flow of load current and when storage released energy to the network at that time PV was unable to supply energy. Hence, overall flow of load current remained the same. However harmonic current was injects into the network when PV and ES became active in the operation. The distribution of load among different zones is different however the same size solar PV and ES was integrated in all zones therefore load current and harmonic current was also not uniform among all zones.

Simulation for harmonic calculation was done in load only, load with PV and load with PV and storage integrated condition and results were compared. Figure 6.19 shows the Load current, Figure 6.20 shows the harmonic current and Figure 6.21 shows the total harmonic current distortion (THD) in three different configurations. The position of observed lines in Zone-1, Zone-4 and Zone-6 is such that current flows through these lines to the other part of the network, therefore flow of load current and harmonic current in these observed lines was high in load only condition. After integrating large PV in each zone, much of the load demand was met by PV, as a consequence flow of load current dropped significantly in these observed sections of the network, however PV injects additional harmonic currents into the network therefore harmonic current increases in these observation zone which caused THD to increase as can be seen in Figure 6.21. After integrating ES in each zone, some additional load demand was met by the storage which reduced the flow of load current further, however it increased the harmonic current and therefore THD was increased. The observed lines in Zone-2, Zone-3, Zone-5 and Zone-7 can see the flow of current only on those zones, therefore flow of load current and harmonic current was less in these lines, in load only configuration. After integrating large PV in these zones, energy generated from PV was supplied to the other loads therefore the observed lines see more current flowing through these lines, which caused an increase in load current also an increase in harmonic current. After integrating large storage in these zones, flow of load current increased in these lines which caused reduction in total harmonic distortion in these observed lines as seen in Figure 6.21.

The line “Line_Infeeder” can observe the flow of current of the complete network from infeeder to the end load, also harmonic current from all node to the infeeder in the reverse direction. Therefore this observation provides the overall impact on the complete network. It was found that after integrating PV in the network, flow of load current from the infeeder to the load dropped with big margin as PV supported load demand. After integrating ES, flow of load current further dropped as storage also supported some additional load demand. However, the flow of harmonic current increased on both occasions i.e. after integrating PV and storage, total harmonic current distortion increased on both occasions as illustrated in Figures 6.19, 6.20 and 6.21 and also THD exceeded the allowable limit of 5% mentioned in AS-4777.

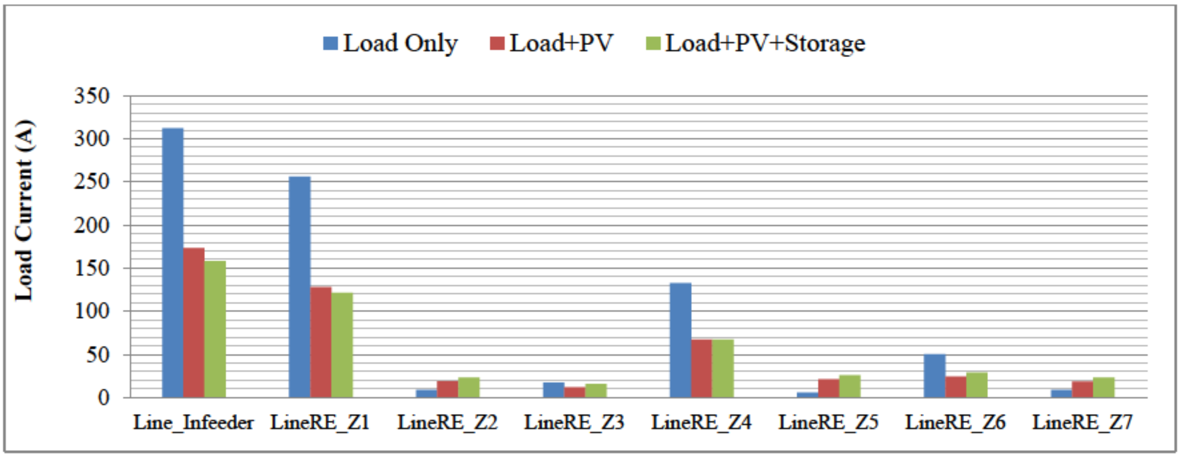

Figure 6:19 Load current in selected lines of observation in three configurations

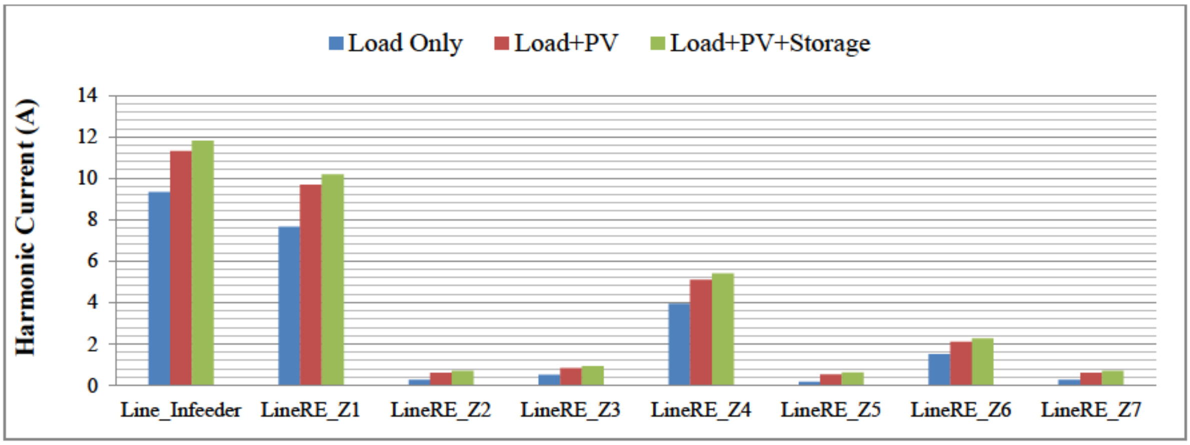

Figure 6:20 Harmonic current in selected lines of observation in three configurations

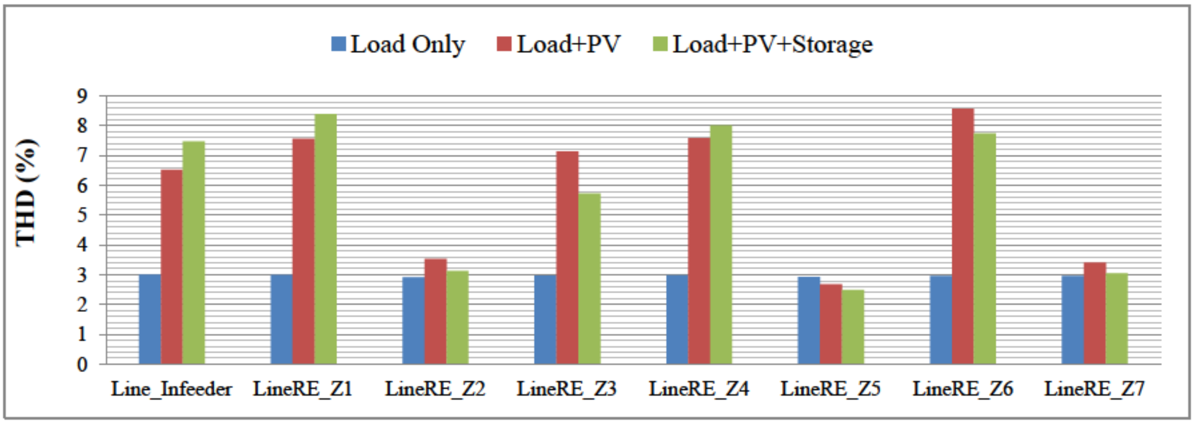

Figure 6:21 THD across selected lines of observation in three configurations

Therefore, this investigation on the power network in Kawana showed that total harmonic current distortion increases with the integration of RE such as PV, and ES further increased this level. Similarly total harmonic voltage distortion also increased with the integration of PV and ES.

6.4 Results and Discussion on Investigation-4

This investigation is considering the same network settings as described in section 5.4 in Chapter 5. However required harmonic data for load, inverter with PV and storage and also for WT was entered into the network model for network simulation to get the harmonic distortion in the network. This investigation covers the power network of Rockhampton which was divided into 8 zone substations (ZS) and finally combined to get the total power network model of Rockhampton for the investigation of harmonic impacts on the network due to ES. The power networks of the 8 ZS are listed below:

1. Rockhampton Glenmore (RGL) ZS network
2. Pandoin (PAN) ZS network
3. Frenchville (FRN) ZS network
4. Parkhurst (PKH) ZS network
5. Berserker (BER) ZS network
6. Canning Street (CST) ZS network
7. Lakes Creek (LCR) ZS network
8. Rockhampton South (RSH) ZS network

It was mentioned earlier that the networks contained a 3 phase 11 kV distribution network which connect to the 66 kV sub-transmission part at Rockhampton Glenmore BSS and finally to the 132 kV transmissions line that connects the entire network to the main supply from Power Link.

It was also mentioned in section 5.4 in Chapter 5 that load is connected to the network through LV DT with 50% loaded condition. Load is connected to the LV side (415V line-line) of DT and in the same node RE resources (solar PV or Wind turbine) was installed at the same capacity of load. In Chapter-3 it was mentioned that for best utilisation of RE, ES is essential and estimation of required storage was also explained. Moreover, in investigation-2 & 3, the distributed and centralised installation of RE and ES was evaluated. In this investigation after integrating PV of 100% of load capacity in nodes, bulk size RE and storage was integrated in some selected nodes where voltage drop was higher. 500 kW PV or

WT and 200 kW storage size was considered as bulk size RE and storage installation. This bulk size RE and storage were integrated at 5 or 6 different distant nodes in the selected feeder. In each ZS power network two feeders were selected and in each selected feeder 6 line segments were selected to observe current flow. The observed feeder, installed bulk size RE and storage and the flow of harmonic current are also indicated in the network figures.

The model allows switching on/off any network element as required. The investigation was conducted and results were compared in three network configuration modes:

1. Load only configuration
2. Load with RE configuration and
3. Load with RE and ES configuration

In each ZS network the two longest feeders were selected for observation and simulated in the above three network configuration modes.

The investigation of each ZS power network was conducted separately by observing selected feeders that act as a radial network. Load allocation, RE and storage distribution is listed in the Appendix-A for each ZS power network. For load, commercial summer load profile, summer solar and wind energy profile was considered as shown in Figure 4.31 (a), 4.32 and 4.33 respectively in Chapter-4. Line parameter were explained in Table 4.4 in section 4.2.2 and the harmonic data for load, PV, WT and ES was shown in Table 4.13 and 4.14 in Chapter 4. Each of the ZS power network model was simulated for harmonic calculations and the results are explained below.

6.4.1 Rockhampton Glenmore (RGL) ZS Power Network

The details of the Rockhampton Glenmore ZS power network have already been described in section 5.4.1 in Chapter 5. The selected feeders with installed bulk size RE (PV) and ES are highlighted in Figure 5.38 in Chapter 5. This investigation referred the same figure to observe the flow of harmonic current and load current through the highlighted line segments with an arrow sign. The arrow sign shows the flow of harmonic current from the installed RE and ES to the network. Two feeders were selected and in each feeder, 5 line segments were selected and named “L_F1H1 to L_F1H5” and “L_F2H1 to L_F2H5”. Another line segment “L_F1All and L_F2All”, also highlighted in Feeder-1 and Feeder-2 to observe the overall harmonic impacts on each feeder.

The network model in SINCAL was simulated for harmonic calculations in load only, load with RE and load with RE and ES configurations mode. Therefore, in comparison impacts of ES can be identified. Harmonic calculation was done up to the 25th harmonic frequency where 50Hz is the fundamental frequency. Total harmonic current up to 25th harmonics were compared and the total harmonic current distortion was evaluated for each observed line segment. Figure 6.22 shows the load current, harmonic current and total harmonic current distortion (THD) at the observed line segments in Feeder-1 and Feeder-2.

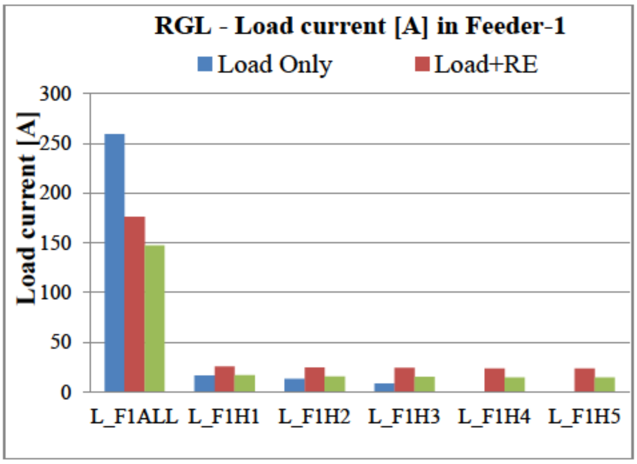

a-1. Load current in Feeder-1

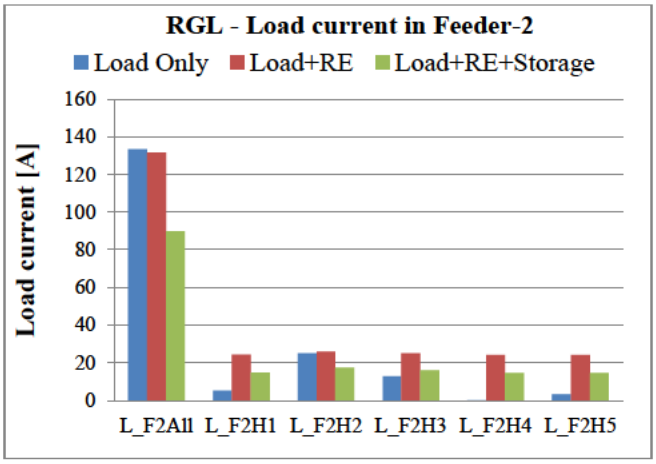

a-2. Load current in Feeder-2

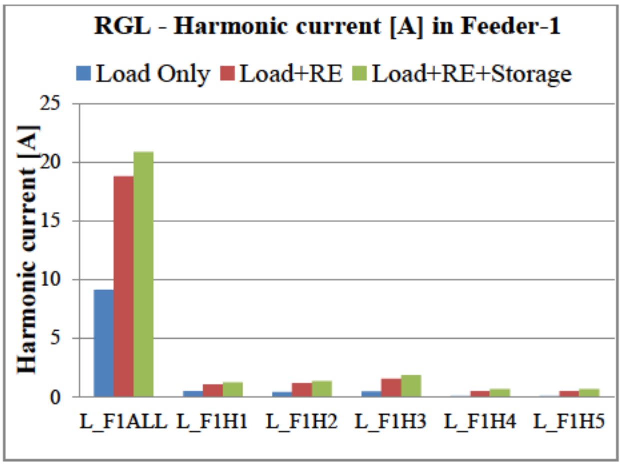

b-1. Harmonic current in Feeder-1

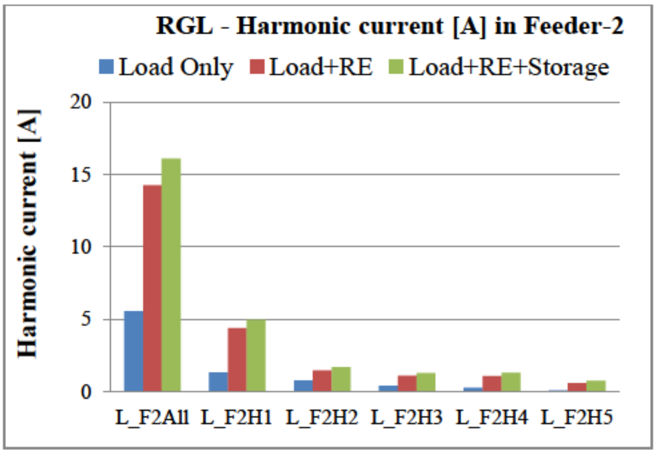

b-2. Harmonic current in Feeder-2

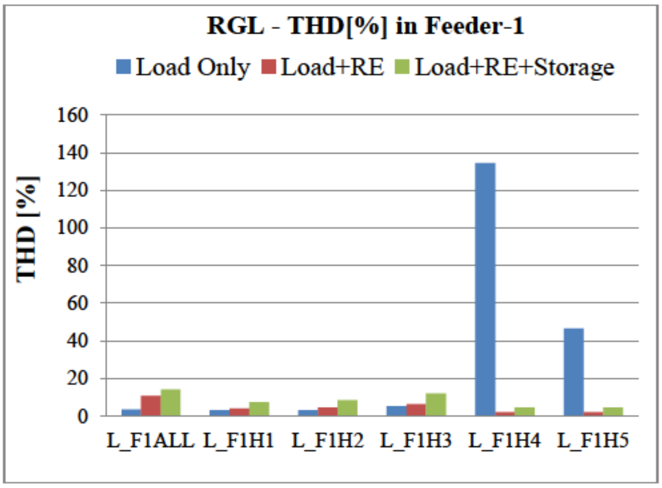

c-1. Total harmonic distortion in Feeder-1

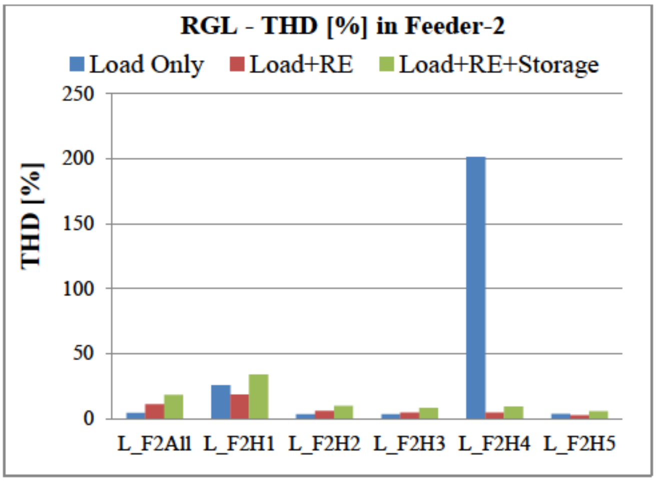

c-2. Total harmonic distortion in Feeder-2

Figure 6:22 RGL ZS - Harmonic current, load current & THD at observed lines in Feeder-1 and Feeder-2

ES and RE (PV) were installed at the end of the observed lines and load demand remains the same. However after integrating RE, the observed lines experienced additional flow of load current to the other part of the network. Therefore increase in load current was observed in lines (L_F1H1 to L_F1H5 and L_F2H1 to L_F2H5) after integrating RE into the network as seen in Figure 6.22 (a-1 and a-2). But overall flow of load current decreased in each feeder as the RE generated energy supports load demand that reduced power flows from the infeeder as observed in line "L_F1All and L_F2All" in feeder-1 and feeder-2. However after integrating ES, a part of the excess energy generated from RE was stored into the storage which reduced the flow of load current through the observed lines as seen in Figure 6.22 (a-1 and a-2).

PV or ES acts as a current source node element and after integrating RE, flow of harmonic current was increased in all the observed lines and ES further increased the harmonic current into the network as seen in Figure 6.22 (b-1 and b-2). Therefore the total harmonic current was increased in each feeder as observed in line "L_F1All and L_F2All" after integrating RE and ES.

Increase in harmonic current and decrease in load current increase the total harmonic current distortion (THD) in the network. It was observed that after integrating RE, THD was increased compared to the load only condition and after integrating ES, THD further increased as seen in Figure 6.22 (c-1 and c-2). In load only condition, line “L_F1H4, L_F1H5 and L_F2H4” observed very low load current flow as installed load beyond the observed lines was with very low capacity therefore THD increased in these observed lines in load only condition. However Fedder-1 and Feeder-2 observed THD as 3.50% and 4.17% in load condition, 10.65% and 10.82% in load with RE integrated condition and finally 14.14% and 17.89% in load with RE & ES integrated condition. Therefore ES increased the harmonic current distortion of the network.

Increase in harmonic current increased harmonic voltage distortion in the network. It was observed that total harmonic voltage distortion also increased with the integration of RE and ES. Harmonic voltage distortion was noticed in the nodes being observed for voltage regulation as shown in Figure 5.38 in Chapter 5. Total harmonic voltage distortion (THD) observed in Feeder-1 and Feeder-2 is summarised below in Table 6.2.

Table 6:2 THD (%v) observed in Feeder-1 and Feeder-2 in RGL ZS power network

Node	Load only	Load+RE	Load+RE+Storage
Feeder-1: RGL_F1_All	8.807%	27.767%	31.075%
Feeder-2: RGL_F2_All	8.615%	27.193%	30.423%

Therefore ES increases harmonic current distortion and harmonic voltage distortion in the network.

6.4.2 Pandoin (PAN) ZS Power Network

Pandoin ZS power network was described in section 5.4.2 in Chapter 5 and Figure 5.43 in Chapter 5 shows the line segments used to observe current flow and also highlights the nodes used to observe node voltages. There are 5 line segments in each feeder named “L_F1H1 to L_F1H5 and L_F2H1 to L_F2H5” in Feeder-1 and Feeder-2 respectively that were selected to observe current flow. Load current flows from the infeeder to end load, however power flow can reverse from RE installed at end node towards the infeeder which eventually reduces the flow of load current through the observed line segments. RE and ES acts as a current source element that injects harmonic current to the network and in Figure 5.43 arrow shows the flow harmonic current at the observed lines i.e. from RE or ES to the infeeder.

Two line segments named “L_F1All and L_F2All” were selected to observe the overall impacts on each selected feeder in the network. Load, RE (PV) and ES integration was discussed in section 5.4.2 in Chapter 5. In addition, harmonic data for load, inverter with RE and ES was applied in the network model and the model was simulated in load only, load with RE and load with RE and ES integrated condition. Figure 6.23 shows the observed load current, harmonic current and total harmonic current distortion (THD) in the observed line segments in load only, load with RE and load with RE and storage integrated condition.

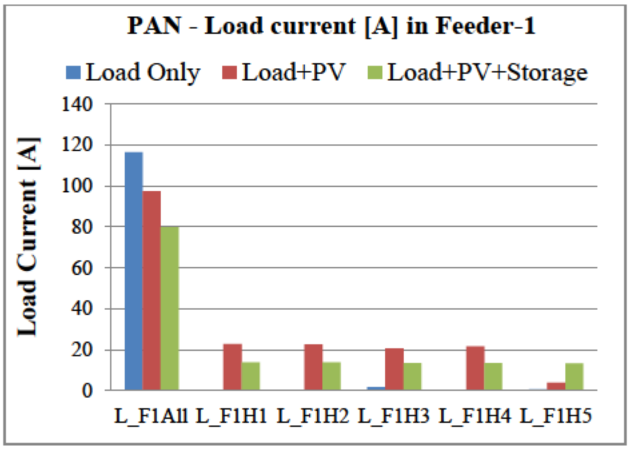

a-1. Load current in Feeder-1

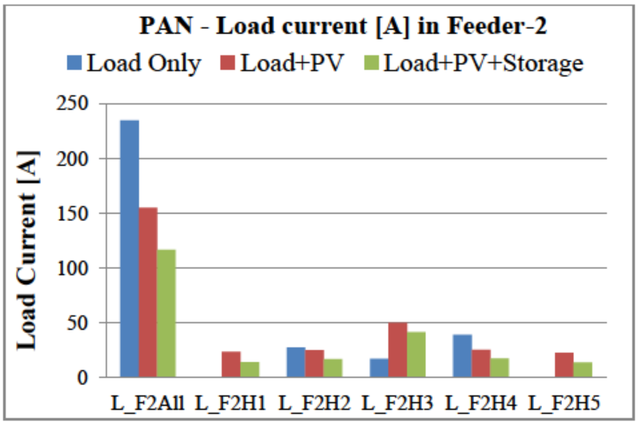

a-2. Load current in Feeder-2

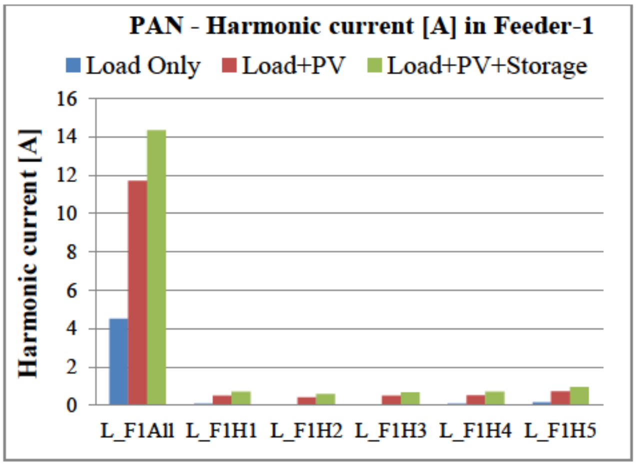

b-1. Harmonic current in Feeder-1

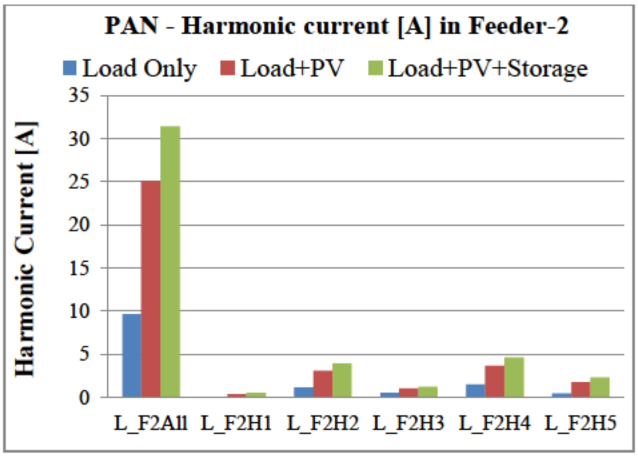

b-2. Harmonic current in Feeder-2

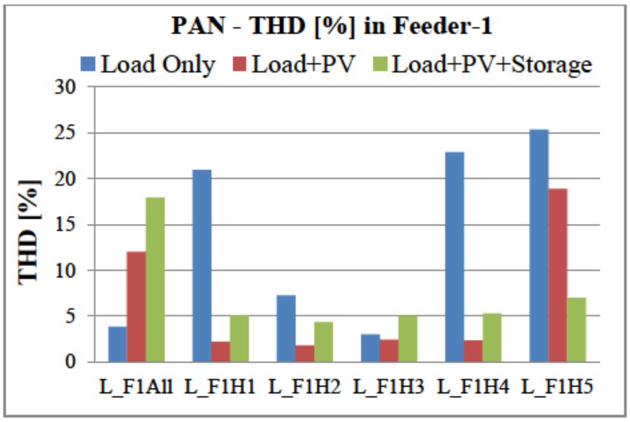

c-1. Total harmonic distortion in Feeder-1

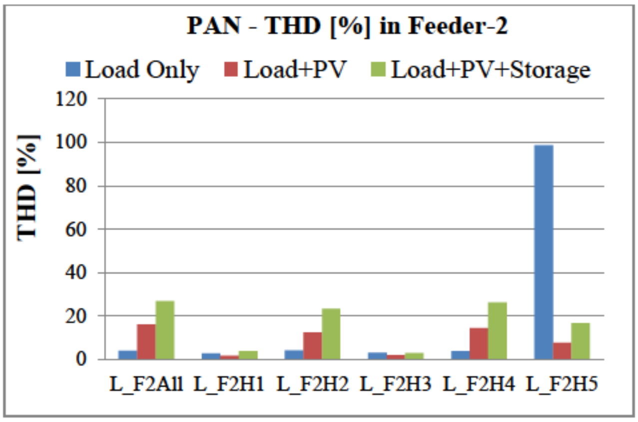

c-2. Total harmonic distortion in Feeder-2

Figure 6:23 PAN ZS - Harmonic current, load current & THD at observed lines in Feeder-1 and Feeder-2

It was found that in Feeder-1 and Feeder-2 overall load current flow decreased (in line "L_F1All & L_F2All) as the flow of power from RE sources increased. Also ES further decreased the flow of load current by supporting some additional load demand as shown in Figure 6.23 (a-1 and a-2). Although the other observed lines (L_F1H1 to L_F1H5 and L_F2H1 to L_F2H5) in both feeders show the increase in load current flow after integrating RE as the adjacent load demand is low therefore much of generated power from RE flow to the other part of the network through the observed lines, however ES reduced the load current flow by storing energy from RE as shown in Figure 6.23 (a-1 and a-2). Harmonic current flow increases with the integration of RE and ES as shown in Figure 6.23 (b-1 and b-2). Therefore the overall total harmonic current distortion (THD) was increased in both feeders after integrating ES into the network as shown in Figure 6.23 (c-1 and c-2).

As mentioned earlier, increases in harmonic current increase voltage distortion. It was observed that harmonic voltage distortion increased with the integration of RE and ES. At node "All" where both feeders join, the observed total harmonic voltage distortion (THD) was 3.5%, 10.1% and 13.09% in load only, load with RE and load with RE and ES integrated condition. Therefore ES increased harmonic current distortion and harmonic voltage distortion in the network.

6.4.3 Frenchville (FRN) ZS Power Network

In the Frenchville ZS power network, two feeders were selected and in each feeder 5 nodes were selected to observe voltage regulation. Also 5 line segments in each feeder were selected to observe flow of current as shown in Figure 5.48 in Chapter 5. At Node-4 and 5 in Feeder-2 500 kW WT and 200 kW ES was installed therefore in this network PV and WT both were installed as RE sources and ES was installed in each bulk size RE installed nodes. The details of the network are described in section 5.4.3 in Chapter 5. The harmonic data for load, PV, WT and ES up to 25th harmonics was described in Table 4.13 and 4.14 in Chapter 4. The power network model was simulated for harmonic calculation in load only, load with RE and load with RE and storage configuration mode.

Various capacity loads and inverter integrated elements are the source of harmonics. The installation of various capacity RE resources (Storage, PV or wind turbine) at various node points in the network, changes the flow of current, moreover the current flow also varies with electricity generation from the RE sources and the load demand which changes the load current and harmonic current level in various line elements.

The simulation result showed that the observed lines (L_F1H1 to L_F1H5 and L_F2H1 to L_F2H5) experienced additional flow of load current after integrating RE into the network. This increase in load current is due to the excess power generation from RE sources which passed to other loads in the network. However overall flow of load current from infeeder to load decreased as a sizable portion load demand was met by the RE as seen in Figure 6.24 (a-1 and a-2). Line "L_F1All and L_F2All" was selected to observe the overall flow of current in each feeder. After integrating ES into the network a portion of RE generated energy stored into the storage when RE generates excess energy and also supports load demand when RE sources stop generating power which reduces the load on the infeeder and as a consequence flow of load current from infeeder is reduced as seen from Figure 6.24 (a-1 and a-2).

The simulation result showed that harmonic current injection into the network increased with the installation of RE and ES in both the feeders as shown in Figure 6.24 (b-1 and b-2).

This increase in harmonic current increases the total harmonic current distortion (THD) in the network as shown in Figure 6.24 (c-1 and c-2). The overall THD in each feeder observed at line L_F1All and L-F2All was 3.06%, 7.33% and 8.93% in Feeder-1 and 3.61%, 13.60% and 18.94% in Feeder-2 in load only, load RE and load with RE and storage integrated condition.

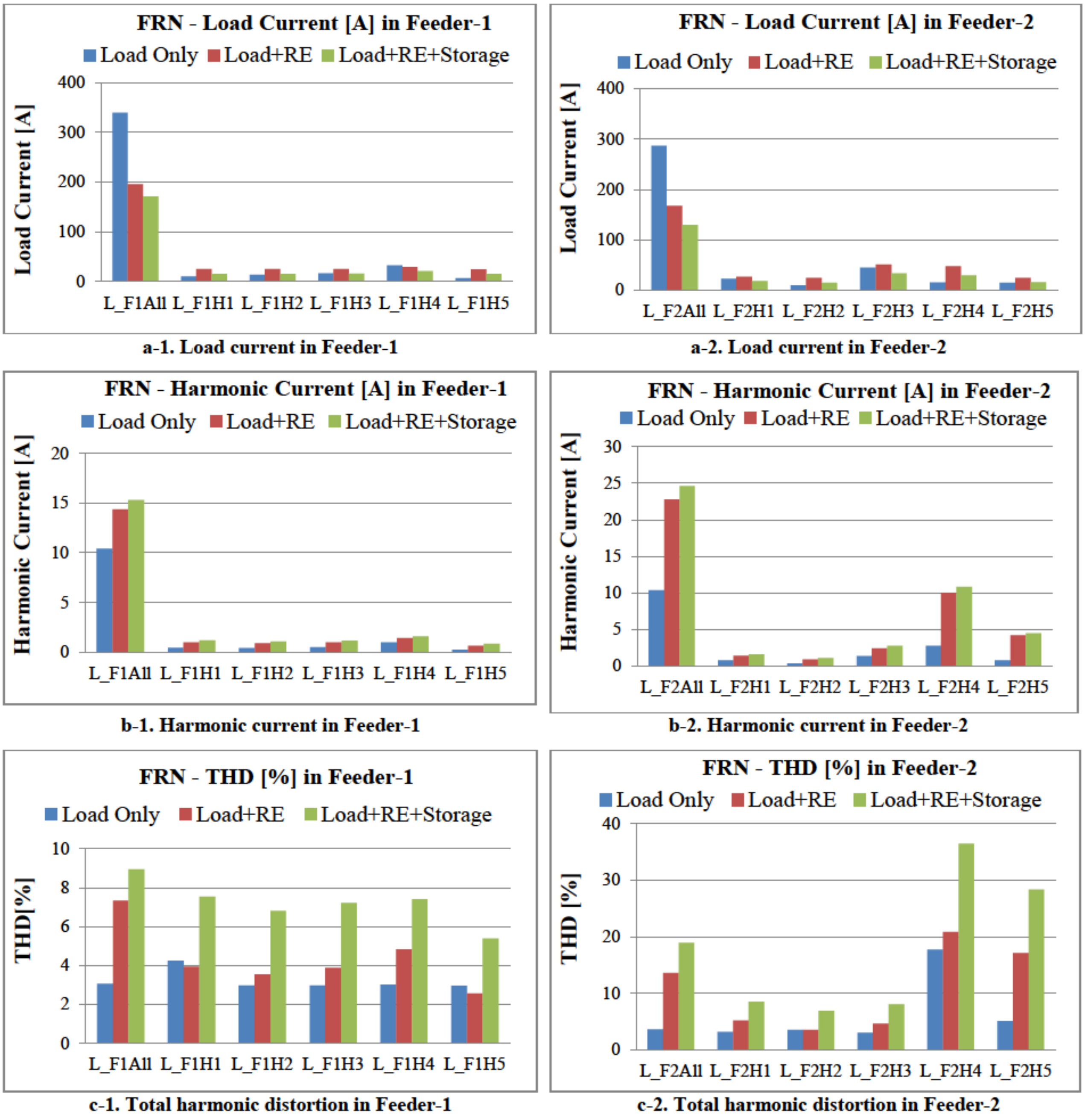

a-1. Load current in Feeder-1 **a-2. Load current in Feeder-2**

b-1. Harmonic current in Feeder-1 **b-2. Harmonic current in Feeder-2**

c-1. Total harmonic distortion in Feeder-1 **c-2. Total harmonic distortion in Feeder-2**

Figure 6:24 FRN ZS - Harmonic current, load current & THD at observed lines in Feeder-1 and Feeder-2

Harmonic Voltage distortion at the observed nodes in Feeder-1 and Feeder-2 was investigated and found that RE (PV or WT) increased total harmonic voltage distortion (THD) and storage further increases it. At node “F1_All” and “F2_All” in Feeder-1 and Feeder-2 the observed THD is as shown in Table 6.3.

Table 6:3 THD (%v) observed in Feeder-1 and Feeder-2

Node	Load only	Load+RE	Load+RE+Storage
Feeder-1: F1_All	5.86%	11.607%	12.625%
Feeder-2: F2_All	5.845%	11.589%	12.606%

Therefore, ES increased harmonic current distortion and the harmonic voltage distortion of the network.

6.4.4 Parkhurst (PKH) ZS Power Network

Like other ZS power networks, two feeders were selected to observe the flow of current in the network. Five line elements in each feeder were selected to be observe and assigned names were “L_F1H1 up to L_F1H5” and “L_F2H1 up to L_F2H5” in Feeder-1 and Feeder-2 respectively. These lines are next to the bulk installation of PV, WT & ES and the observed harmonic current flow direction was also indicated in Figure 5.53 in Chapter 5. Total current flow in Feeder-1 and Feeder-2 was observed at line segment “L_F1All” and “L_F2All” respectively. The effect of voltage harmonics was observed in nodes “F1_All and F2_All” in Feeder-1 and Feeder-2 respectively. In Feeder-2 WT was installed in Node-5. A detail of this network is available in section 5.4.4 in Chapter 5.

Harmonic data for load, inverter with RE and storage was considered in the model. Table 4.13 and 4.14 in Chapter 4 shows the considered harmonic data. The power network model was simulated in load only, load with RE and load with RE and storage integrated condition.

From simulation results it was found that flow of load current increased in all observed lines in Feeder-1 but in Feeder-2 the flow of load current decreased after integrating RE into the network. The length of Feeder-1 is more than Feeder-2, but concentration of load is less and the total loading also less in Feeder-1, therefore after installation of bulk size RE, power produced is greater than the load demand which forced excess electricity to flow to other part of the network and that was observed in all line segments in Feeder-1. In Feeder-2, although the length is less but loading is more than Feeder-1, in addition selected feeder-2 is connected to adjacent various capacity loads that consumed the power generated from RE and as a consequence load current demand from the infeeder was reduced after integrating RE into the network. However after integrating ES, excess energy from RE was stored in the storage also storage supports load demand which eventually reduced the flow of load current through the observed lines in both feeders as seen in Figure 6.25 (a-1 and a-2).

It was found that the flow of harmonic current increases in all the observed line elements in Feeder-1 and Feeder-2 after integrating RE (PV or WT) into the network. However after integrating ES, injection of harmonic current into the network was further increased as seen in Figure 6.25 (b-1 and b-2). Increase in harmonic current and decrease in load current increases total harmonic current distortion (THD) in the network. In observation line “L_F1H2”, load current was much less than harmonic current as the small size load was connected at the end of the line, therefore THD was very high in that line. It was observed that overall THD in Feeder-1 is 12.29%, 14.57% and 26.17% and in Feeder-2 it is 3.038%, 6.69% and 8.60% in load only, load with RE and load with RE and Storage integrated conditions respectively.

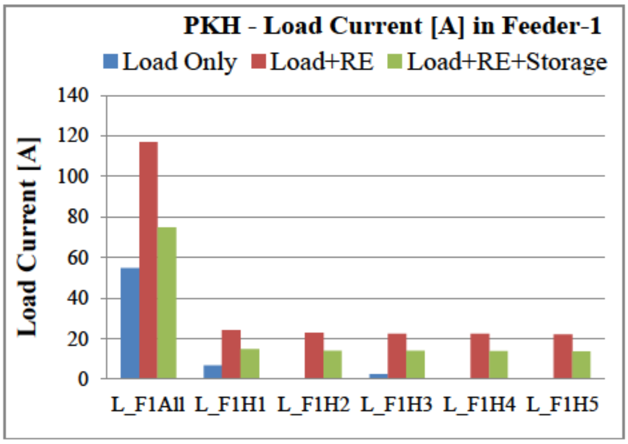

a-1. Load current in Feeder-1

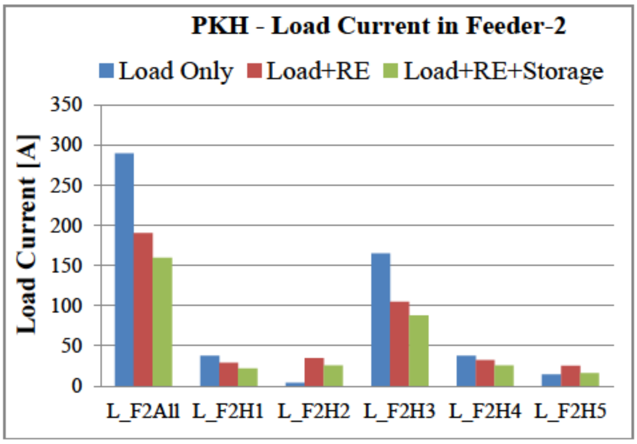

a-2. Load current in Feeder-2

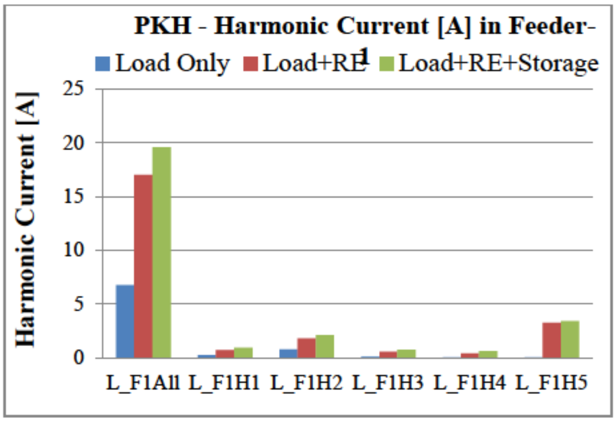

b-1. Harmonic current in Feeder-1

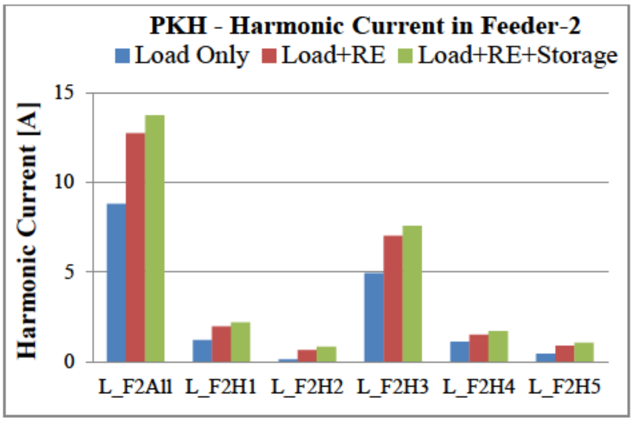

b-2. Harmonic current in Feeder-2

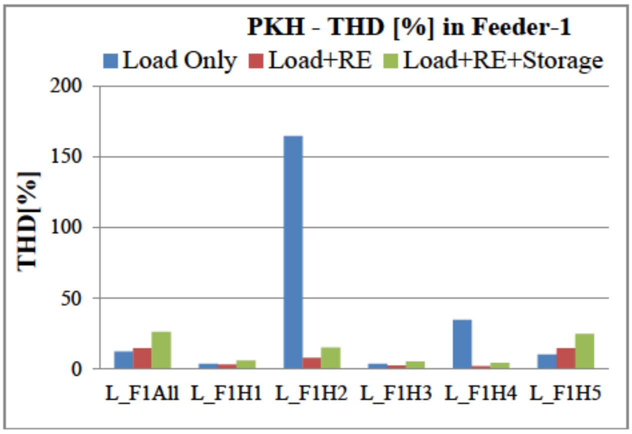

c-1. Total harmonic distortion in Feeder-1

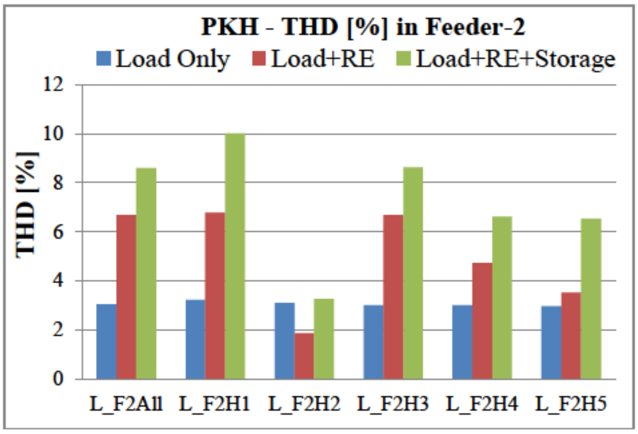

c-2. Total harmonic distortion in Feeder-2

Figure 6:25 PKH ZS - Harmonic current, load current & THD at observed lines in Feeder-1 and Feeder-2

Harmonic voltage distortion was observed in nodes "F1_All" and "F2_All" where both the 11 kV feeders started from the sub-transmission network of 66 kV. It was found that in load only condition THD was 4.1%. After large integration of RE in various nodes in both feeders the voltage harmonics level increased and THD becomes 8.33%. In order to maximise the RE utilisation energy storage was integrated with various nodes in both feeders and it was found that voltage harmonics increased in all frequency levels and THD reached to 9.239% and exceeded the allowable limit of 8% [22].

Therefore it is again found that ES increases harmonic current distortion and harmonic voltage distortion in the power network.

6.4.5 Berserker (BER) ZS Power Network

The power network under Berserker ZS was described in section 5.4.5 and the integration of bulk size RE and ES is shown in Figure 5.58 in Chapter 5. Two feeders were selected to be observed and in each feeder bulk size RE and ES was installed in 5 node points. Five line segments adjacent to the bulk installation of RE and ES in each feeder was selected to observe the flow of current.

The power network model was simulated for harmonic calculation and found that RE and ES increase total harmonic current distortion in the network. Similar to other ZS power network this part of the network also simulated in load only, load with RE and load with RE and storage integrated mode. Figure 6.26 shows the flow of load current, harmonic current and the total harmonic distortion (THD) in both feeders.

The total load on this network model is 18,364 kVA but the feeder length is less compared to other ZS power networks and it was found from the observation of voltage regulation in this network that available voltage was above the rated voltage and it further increased after integrating RE as discussed in section 5.4.5 in Chapter 5. This constant high voltage in all nodes of both feeders ensured that the flow of load current was high as shown in Figure 6.26 (a-1 and a-2). It was noted that in all observed lines experienced increased flow of load current and the overall flow of load current was also increased. However after integrating ES, this level of load current decreased in all observed lines as shown in Figure 6.26 (a-1 and a-2). Harmonic current increased with the integration of RE and ES into the network and the increase in harmonic current was observed in all lines. Therefore, increase in load current decreased total harmonic current distortion (THD) after integrating RE, however a decrease in load current after integrating ES increased THD in the network as seen in Figure 6.26 (c-1 and c-2).

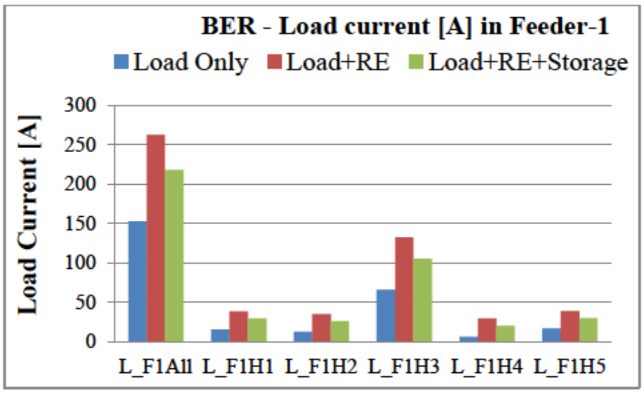

a-1. Load current in Feeder-1

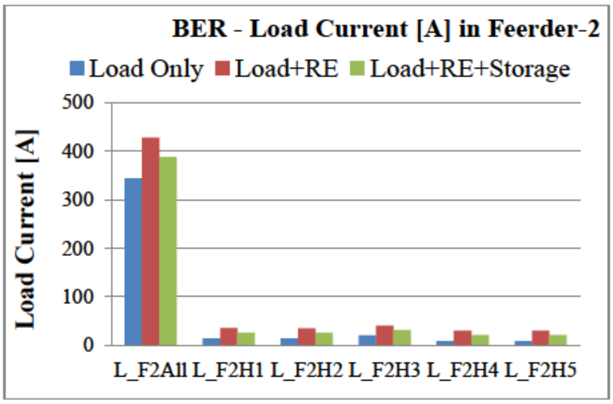

a-2. Load current in Feeder-2

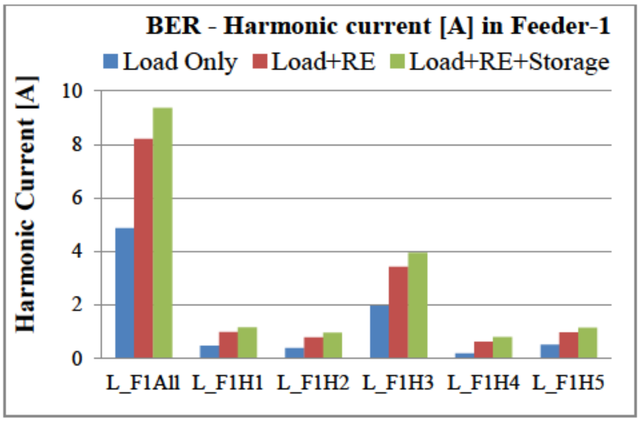

b-1. Harmonic current in Feeder-1

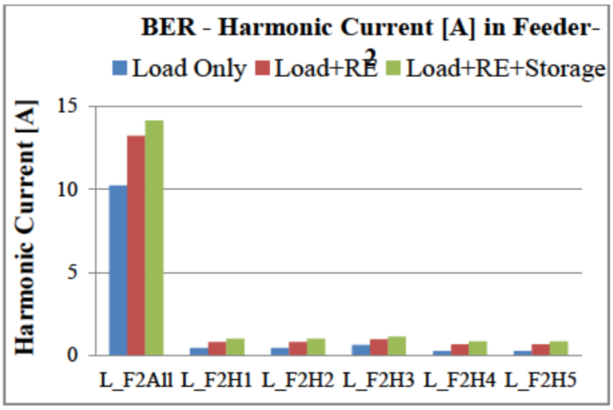

b-2. Harmonic current in Feeder-2

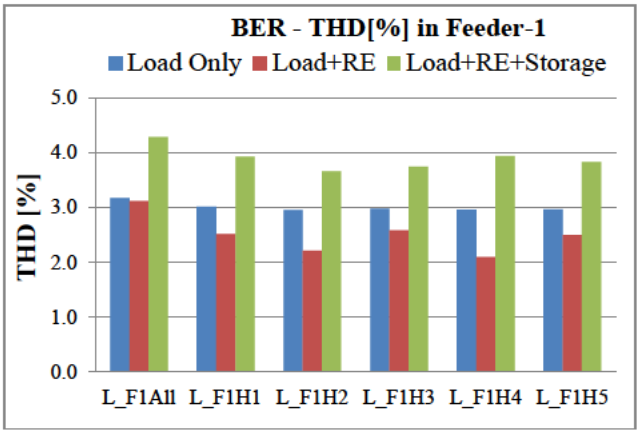

c-1. Total harmonic distortion in Feeder-1

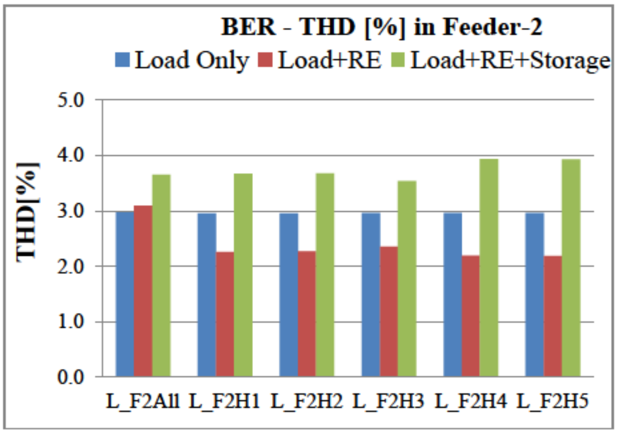

c-2. Total harmonic distortion in Feeder-2

Figure 6:26 BER ZS - Harmonic current, load current & THD at observed lines in Feeder-1 and Feeder-2

Increased harmonic current increases harmonic voltage distortion. It was observed that overall harmonic voltage distortion increases with the integration of RE and ES into the network. At the observed node "F1_All and F2_All" the beginning of both feeders experienced total harmonic voltage distortion which increased with ES as seen in Table 6.4.

Table 6:4 THD (%v) observed in Feeder-1 and Feeder-2 in BER ZS

Node	Load only	Load+RE	Load+RE+Storage
Feeder-1: F1_All	2.575%	6.57%	7.822%
Feeder-2: F2_All	7.968%	9.708%	10.543%

Therefore ES increased harmonic current distortion and harmonic voltage distortion in the network.

6.4.6 Canning Street (CST) ZS Power Network

Like the observations in other ZS power networks, in the CST power network two feeders were selected and in each feeder 5 line segments were selected to observe current flow.

Figure 5.63 in Chapter 5 shows the selected lines in the network model. These selected line segments are adjacent to the installed bulk RE and ES in the network and named as "L_F1H1 to L_F1H5 and L_F2H1 to L_F2H5" in Feeder-1 and Feeder-2 respectively. To observe the overall impacts, line "L_F1All and L_F2All" were selected at the starting of each feeder.

The power network model was simulated in load only, load with RE, load with RE and ES integrated condition. Simulation results showed that total harmonic distortion was increased with the integration of RE and ES. Figure 6.27 shows the load current, harmonic current and total harmonic distortion observed in both feeders.

There are two large loads near the observed line "L_F1H2" that caused a large amount of load current to flow through this line as shown in Figure 6.27 (a-1). After integrating a large RE source or RE plant into the network, flow of load current decreased in all observed lines in Feeder-1 and Feeder-2 as shown in Figure 6.27 (a-1 and a-2). ES stored energy during peak generation from RE sources and also supplied energy and supported load when RE sources were unable to support load. Therefore overall flow of load current reduced further as seen in Figure 6.27 (a-1 and a-2). Harmonic current injection increased with RE and ES as shown in Figure 6.27 (b-1 and b-2) therefore total harmonic current distortion was increased with RE and ES in both feeders as seen in Figure 6.27 (c-1 and c-2). The overall THD was observed in Feeder-1 at line L_F1All as 2.14%, 4.95% and 5.81% in load only, load RE and load RE and ES condition respectively and in Feeder-2 at line L_F2All as 2.99%, 7.26% and 8.31% in load only, load with RE and load with RE and ES integrated condition.

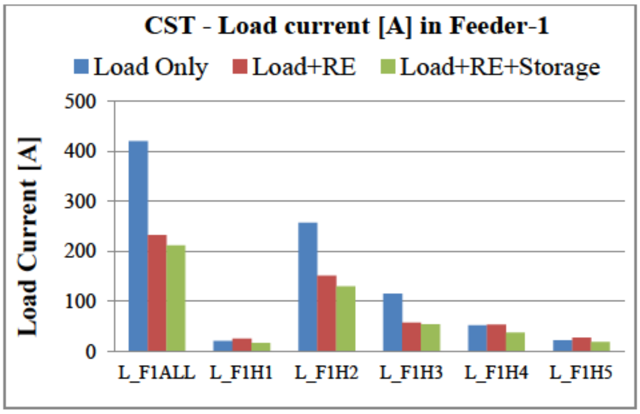

a-1. Load current in Feeder-1

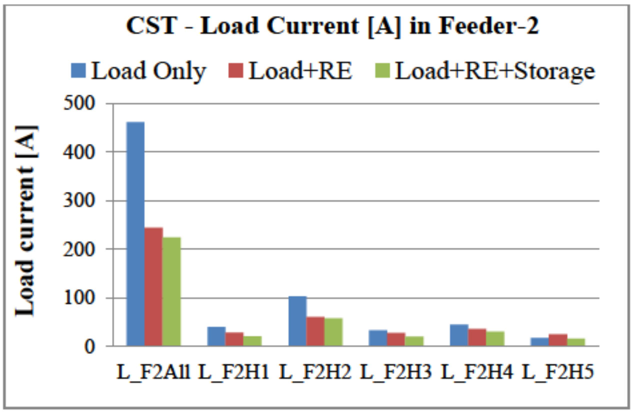

a-2. Load current in Feeder-2

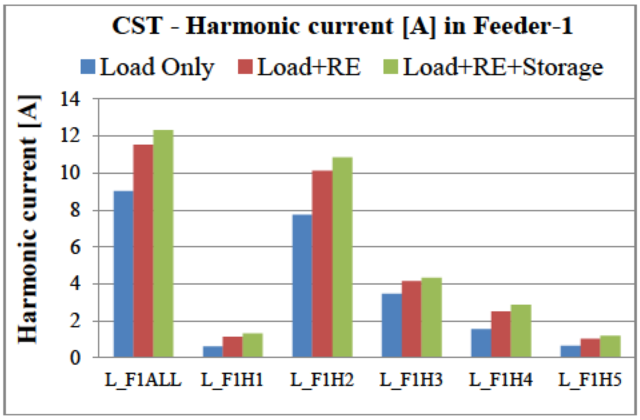

b-1. Harmonic current in Feeder-1

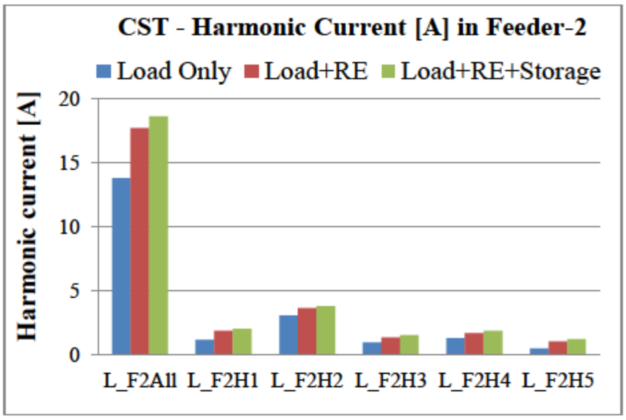

b-2. Harmonic current in Feeder-2

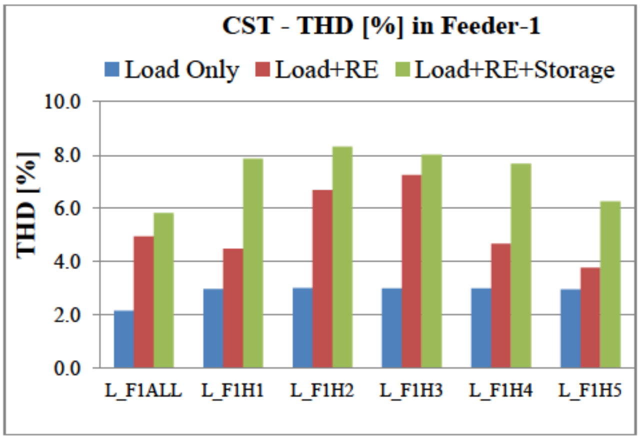

c-1. Total harmonic distortion in Feeder-1

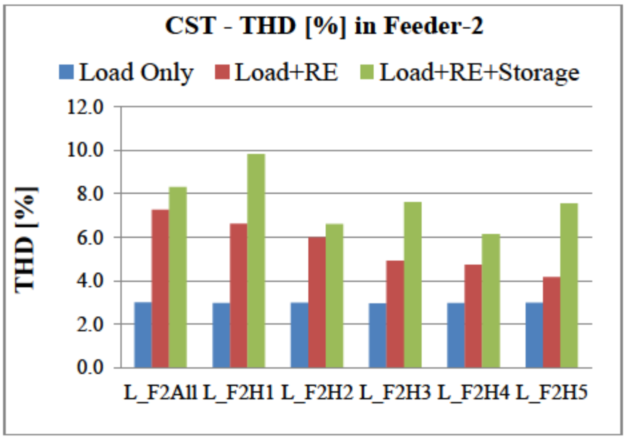

c-2. Total harmonic distortion in Feeder-2

Figure 6:27 CST ZS - Load current, Harmonic current & THD at observed lines in Feeder-1 and Feeder-2

Harmonic voltage distortion was observed in 5 observation nodes in each feeder as shown in Figure 5.63 in Chapter 5. Increased current harmonics caused voltage harmonic to increase with ES integrated condition. The overall harmonic voltage distortion (THD) in Feeder-1 and Feeder-2 was observed at node "F1_All and F2_All" and found that THD increased with RE and ES integrated condition as shown in Table 6.5.

Table 6:5 THD (%v) observed in Feeder-1 and Feeder-2 in CST ZS

Node	**Load only**	**Load+RE**	**Load+RE+Storage**
Feeder-1: CST_F1_All	12.208%	15.006%	15.731%
Feeder-2: CST_F2_All	12.237%	15.056%	15.785%

Therefore ES increases current harmonic distortion and voltage harmonic distortion in the network.

6.4.7 Lakes Creek (LCR) ZS Power Network

The power network model (single line diagram) of LCR ZS was described in section 5.4.7 in Chapter 5. In Feeder-1, 5 node points where bulk size RE and ES were installed and adjacent lines of this installation were selected to observe current flow. Lines are named as "L_F1H1 to L_F1H5" and the overall impact on Feeder-1 was observed at line "L_F1All" as shown in Figure 5.68 in Chapter 5. In Feeder-2, although bulk size RE and ES was installed in 6 node points, the flow of current was observed in 5 line segments marked with an arrow sign and named as "L_F2H1 to L_F2H5" as shown in Figure 5.69 in Chapter 5. The arrow sign shows the flow of harmonic current from RE and ES in Feeder-1 and Feeder-2. A part of SWER network connected to the Feeder-2. The network model was simulated in load only, load with RE and load with RE and ES integrated condition.

Simulation results showed that load current in Feeder-1 increased in all observed line segments after integrating RE into the network. Power generated from RE sources exceeded the local load demand, therefore the observed line segments experienced more flow of load current in Feeder-1 and the excess current flowed to the other loads. However overall flow of load current reduced in Feeder-2 after integrating RE into the network as seen in Figure 6.28 (a-1 and a-2). After integrating ES into the network, a part of the excess energy was stored in the storage and the ES also supported load demand when RE was unable to support it. Therefore overall flow of load current reduced in both Feeder-1 and Feeder-2 as seen in Figure 6.28 (a-1 and a-2).

Storage and RE both are current source elements that increase harmonic current flow in the network as seen in Figure 6.28 (b-1 and b-2). This increase in harmonic current increased total harmonic current distortion (THD) in the network as observed in both feeders as seen in Figure 6.28 (c-1 and c-2). The overall THD observed 6.52%, 7.15% and 10.07% in Feeder-1 and 6.47%, 18.69% and 26.17% in Feeder-2 load only, load with RE and load with RE and ES integrated condition.

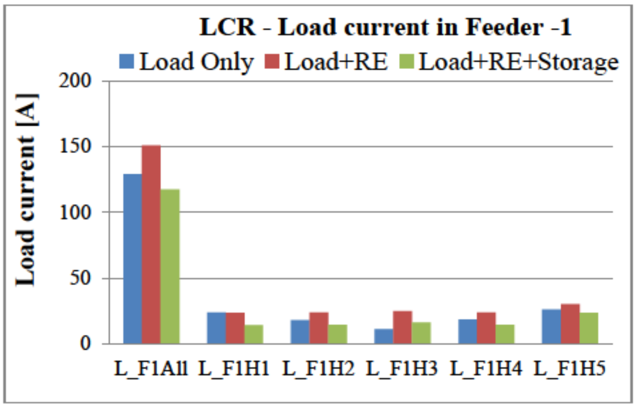

a-1. Load current in Feeder-1

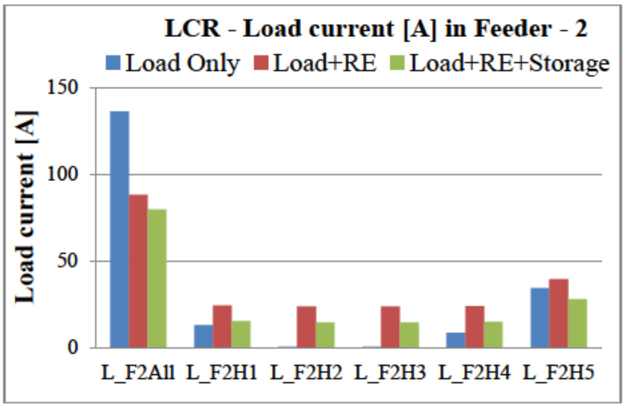

a-2. Load current in Feeder-2

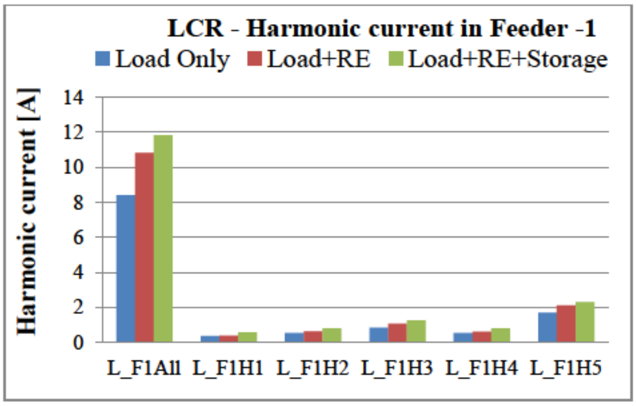

b-1. Harmonic current in Feeder-1

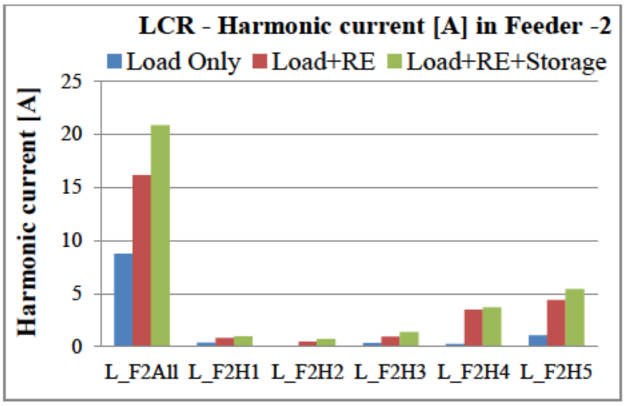

b-2. Harmonic current in Feeder-2

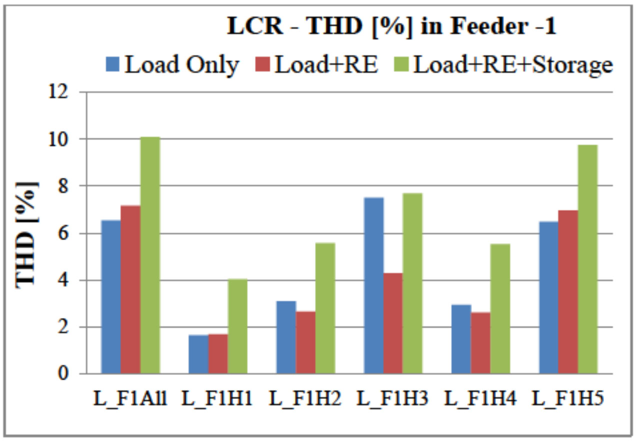

c-1. Total harmonic distortion in Feeder-1

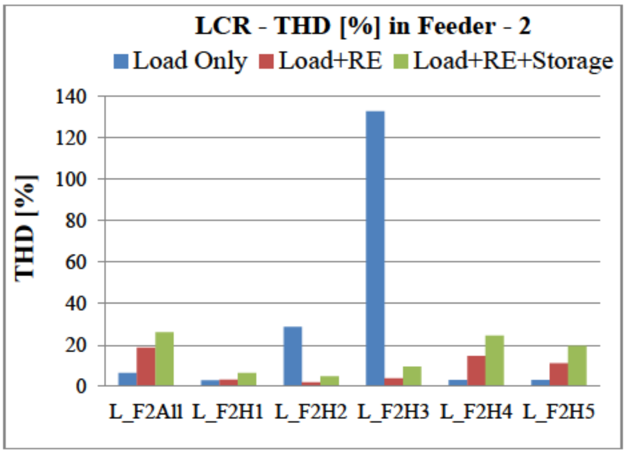

c-2. Total harmonic distortion in Feeder-2

Figure 6:28 LCR ZS - Load current, Harmonic current & THD at observed lines in Feeder-1 and Feeder-2

Various size load, large scale RE and ES in the network introduced harmonic current in the network which caused an increase in harmonic voltage in the network. The harmonic calculation was conducted up to the 25th harmonic values and the total harmonic voltage distortion (THD) was observed at node "F1_All and F2_All" in load only, load with RE and load with RE and ES integrated condition as shown in Table 6.6.

Table 6:6 THD (%v) observed in Feeder-1 and Feeder-2 in LCR ZS

Node	Load only	Load+RE	Load+RE+Storage
Feeder-1: LCR_F1_All	9.032%	12.851%	16.408%
Feeder-2: LCR_F2_All	9.2%	12.983%	16.545%

Therefore, ES increased harmonic current and voltage distortion in the power network.

6.4.8 Rockhampton South (RSH) ZS Power Network

The RSH ZS power network also contains a part of the SWER network. Two feeders and 5 line segments in Feeder-1 and 6 line segments in Feeder-2 were selected to observe the flow of current as shown in Figures 5.75 and 5.76 in Chapter 5. This power network was described in section 5.4.8 in Chapter 5. In Feeder-1, observed lines are named as “L_F1H1 to L_F1H5” and in Feeder-2 “L_F2H1A to L_F2H3A and L_F2H1B to L_F2H3B” as indicated in Figure 5.75 and 5.76 in Chapter 5. Total impacts on each feeder was observed in line “L_F1All and L_F2All” in Feeder-1 and Feeder-2 respectively.

The power network model was simulated in load only, load with RE and load with RE and ES integrated condition. It was found that flow of load current falls on most of the observed lines in both Feeder-1 and Feeder-2 after integrating RE into the network as the load demand was supported by power generated from RE. However the lines “L_F1H3, L_F1H4, L_F1H5” in Feeder-1 and lines “L_F2H3A and L_F2H2B” in Feeder-2 experienced increase in load current as the power generated from the bulk RE source at the end node of these lines was more than the load demand of those nodes. After integrating large storage into the network flow of load current dropped in all observed lines as storage supported additional load demand as seen in Figure 6.29 (a-1 and a-2).

Harmonic current increases in all observed lines after integrating RE into the network and further increases after integrating ES into the network as seen in Figure 6.29 (b-1 and b-2). The observed lines “L_F1H1 & L_F1H2” in Feeder-1 and “L_F2H1A & L_F2H1B” in Feeder-2 are in the path towards line L_F1All and L_F2All therefore these lines experienced the total flow of current behind these lines. Therefore load current and harmonic current in these lines was very high. As the harmonic current increased and load current decreased total harmonic current distortion (THD) was increased after integrating RE and ES further increased it in all observed lines as shown in Figure 6.29 (c-1 and c-2). The lines “L_F1H3, L_F1H4 and L_H1F5” in Feeder-1 observed low flow of load current as the load at the end of this line was very low however after integrating RE at the end of this line and excess power generated therefore flow of load current increased which reduced THD but after integrating ES flow of load current decreased which caused THD to increase. Overall THD was increased in both feeders after integrating RE and ES into the network. It was found that in Feeder-1 THD was 8.0%, 22.77% and 28.96% and in Feeder-2 THD was 3.02%, 6.19% and 7.51% in load only, load with RE and load with RE and ES integrated condition.

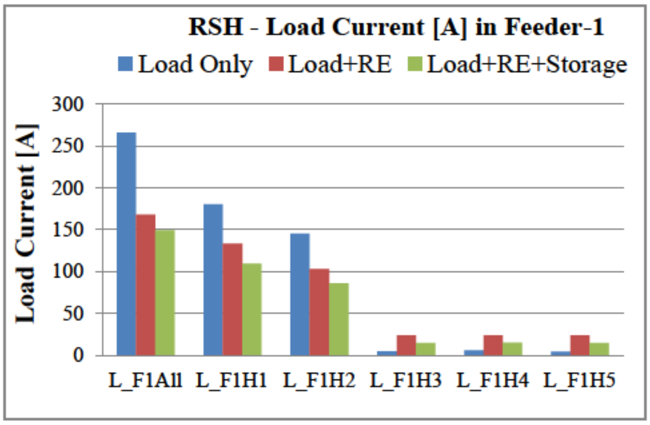

a-1. Load current in Feeder-1

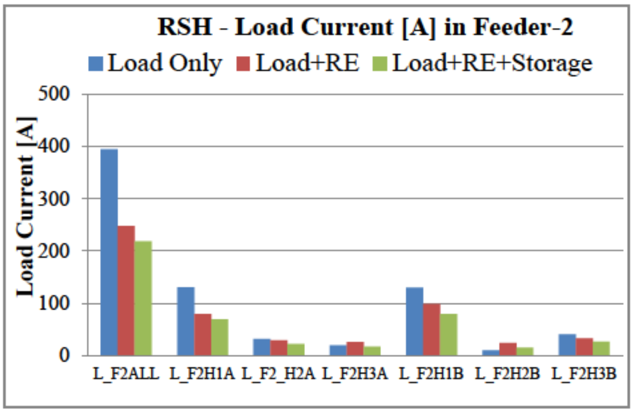

a-2. Load current in Feeder-2

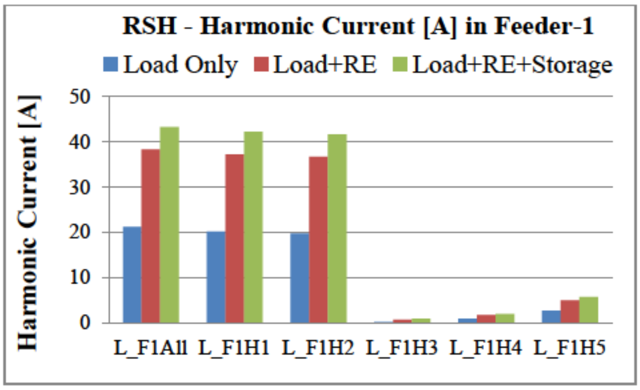

b-1. Harmonic current in Feeder-1

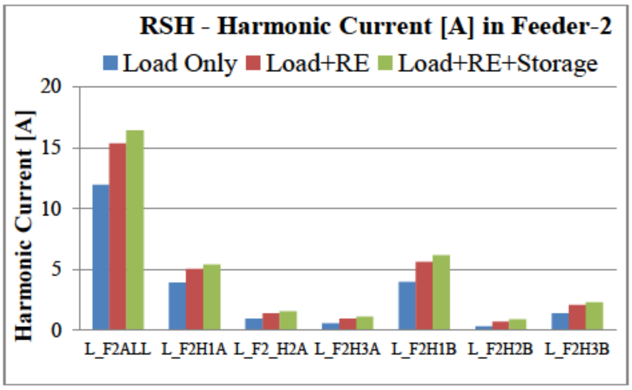

b-2. Harmonic current in Feeder-2

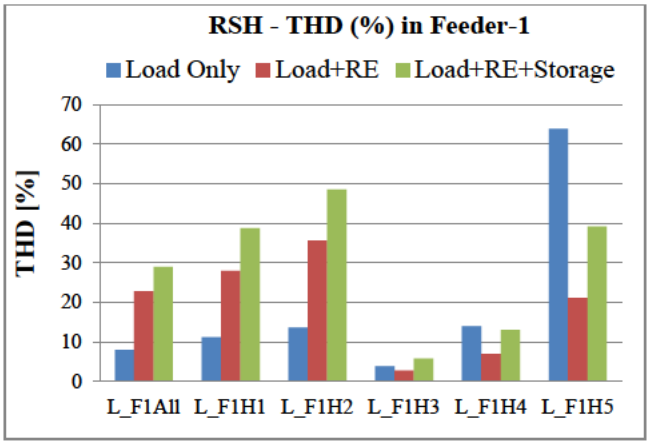

c-1. Total harmonic distortion in Feeder-1

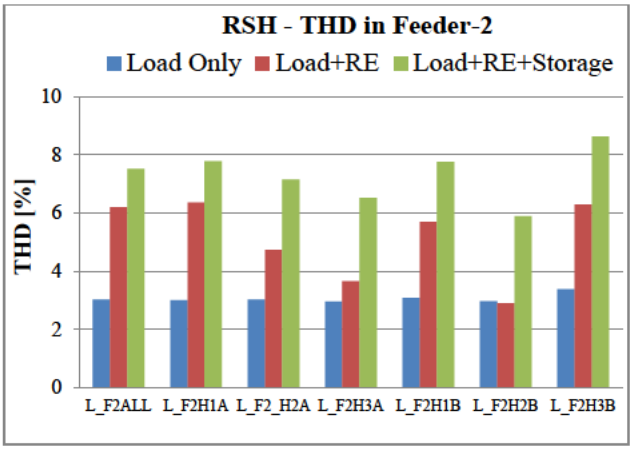

c-2. Total harmonic distortion in Feeder-2

Figure 6:29 RSH ZS - Load current, Harmonic current & THD at observed lines in Feeder-1 and Feeder-2

Harmonic voltage distortion was observed in all observed nodes as harmonic current distortion was found in all observed lines. The overall total harmonic voltage distortion increased with the integration of RE and ES in Feeder-1 and Feeder-2 as shown in Table 6.7.

Table 6:7 THD (%v) observed in Feeder-1 and Feeder-2 in RSH ZS

Node	Load only	Load+RE	Load+RE+Storage
Feeder-1: RSH_F1_All	9.465%	16.934%	19.025%
Feeder-2: RSH_F2_All	8.701%	15.552%	17.419%

Therefore harmonic current distortion and harmonic voltage distortion increased with the integration of ES.

6.4.9 Rockhampton total Power Network

After completing harmonic calculation of all 8 ZS power networks separately, the total impact on the HV power network was observed by integrating all 8 ZS networks together. Although the distribution network i.e. the network of 11 KV to the LV 415 V network was radial type but after integrating all network together some lines of one ZS power network connects to other ZS power network therefore it is not totally radial anymore although not completely meshed. The detail of this complete network was described in section 5.4.9 in Chapter 5 and the observed nodes were highlighted in Figure 5.82 in Chapter 5.

Harmonic distortion on distribution network due to RE and ES integration in the LV network was investigated in each ZS power network as explained above. The harmonic distortion on HV 66 kV sub-transmission and 132 kV transmission network due to the RE and ES in LV network was investigated. To observe harmonic distortion a 66kV line in each ZS was selected and 132 kV lines of two transformers connecting all 66 kV lines were selected. The Rockhampton power network model was simulated for harmonic calculation in load only, load with RE and Load with RE and ES integrated condition. It was found that in all 66 kV sub-transmission network load current reduces due to the integration of RE except the BER ZS network. RE installed in BER ZS network generated excess power that flowed to the other parts of the network and the observed line experienced increased flow of load current. However after integrating ES, the flow of load current reduced in all observed lines in sub-transmission network. In the 132 kV transmission line part, flow of load current decreases through Transformer-2 but increases through Transformer-1. Figure 6.30 shows the flow of load current in the transmission and sub-transmission network. By calculating total flow of load current, it was found that in load only condition a total of 487.54 A current passed from transmission to sub-transmission network. After integrating RE it was 380.09A and after integrating ES it was 372.24A, therefore overall flow of load current reduced after integrating ES into the network.

Harmonic current increased in all observed lines in the transmission and sub-transmission lines after integrating RE and ES in the power network as shown in Figure 6.31. This increase in harmonic current and decrease in load current increase the total harmonic current distortion (THD) in this part of the Rockhampton network as shown in Figure 6.32. The “66kV_BER” line i.e. the 66 kV power line that connects the 11 kV distribution line in Berserker, experienced high THD in load only condition as the load current demand was low however harmonic current injection was high. After the RE integration load current flow increased which eventually reduces THD, however after integrating ES, flow of load current reduced which caused an increase in THD. It was observed that in the transmission network i.e. in the two 132 kV lines with Transformer-1, THD was 10.07%, 12.86% and 13.74% in load only, load with RE and load with RE & ES integration condition and 132 kV line with Transformer-2, THD was 6.71%, 17.55% and 19.39% in load only, load with RE and load with RE and ES integrated condition. Therefore ES increased THD in transmission and sub-transmission network.

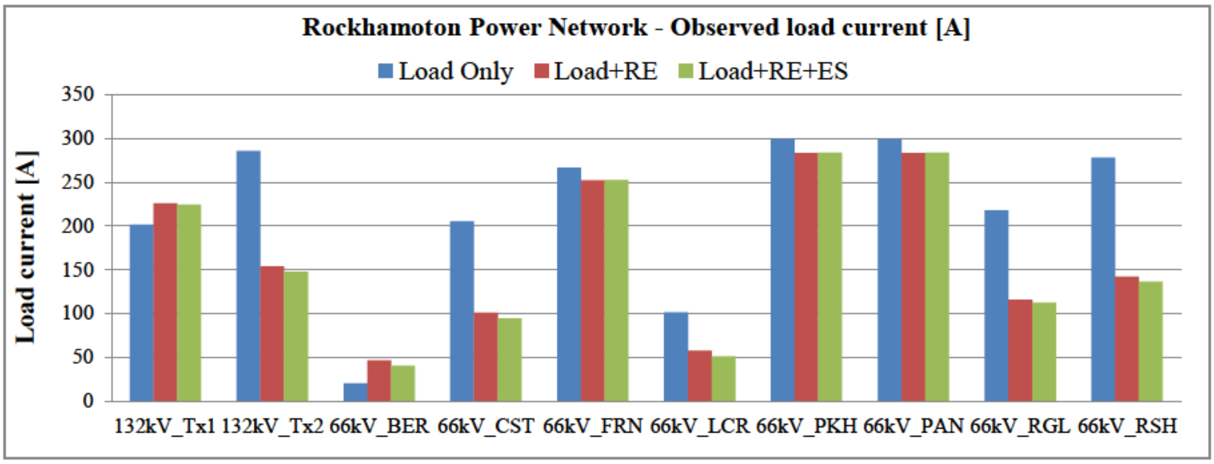

Figure 6:30 Load current - in selected lines in Transmission & sub-transmission network of Rockhampton

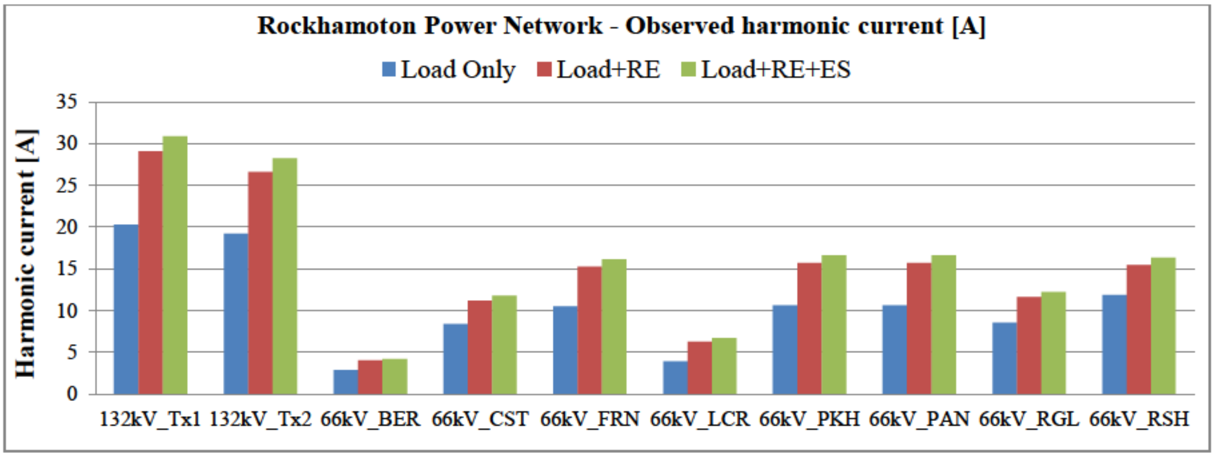

Figure 6:31 Harmonic current - in Transmission & sub-transmission part of Rockhampton network

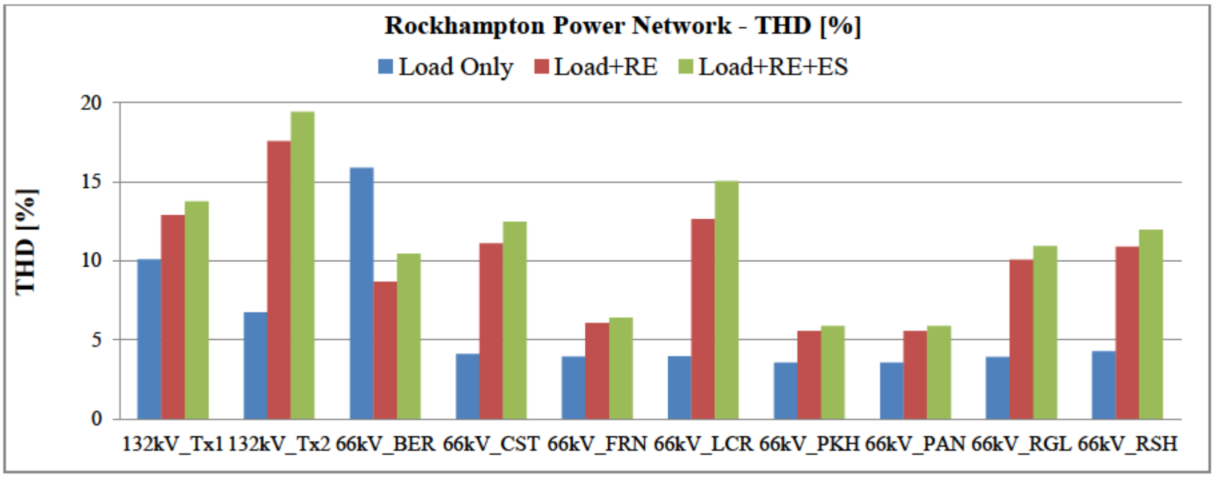

Figure 6:32 THD - in selected lines in Transmission & sub-transmission network of Rockhampton

High harmonic current increases voltage distortion in the power network. Total harmonic voltage distortion (THD) was observed at the 66 kV network as 22.38%, 31.59%, 33.72% and at 132 kV network it was observed at 18.46%, 25.98% and 27.76% in load only, load with RE and load with RE and ES integrated condition respectively.

Therefore large scale integration of ES into the LV network has the impact on the total power network. In this investigation, the harmonic current or voltage values for all network elements were based on the standard limit or from element data sheet maximum limits. Hence, results showed the high value in total harmonic distortion and exceeded the standard allowable limit.

6.5 Conclusions

Integration of large scale RE and ES has impacts on voltage regulation and it was discussed in Chapter 5. This chapter described harmonic distortion on power networks due to the large scale integration of ES. After integrating RE into the network, a part of the load demand was met by the energy generated from RE, therefore the flow of load current decreased. Moreover, ES stores excess energy generated from RE and that also supported a part of the load demand which further reduced the flow of load current in the network as the load demand was met from RE or ES locally. However harmonic current injects from load, RE and ES into the network. Therefore total harmonic distortion increases in the network.

From experimental investigation it was found that harmonic current distortion increases with the increased PV integration and nominal voltage distortion was also observed. Similar results observed from model simulation and model with ES showed that ES increases current and voltage harmonics in the network. Investigation with distributed installation of RE and ES in the network showed that harmonic current distortion exceeded the allowable limit of AS-4777 standard, however integrating RE and ES in a centralised way showed that harmonic current and voltage distortion reduce but exceeds the AS-4777 limit. Investigation of harmonic distortion on the power network on Kawana also showed that integration ES increased harmonic current and voltage distortion in the network. Lastly, large installation of

RE and ES in the LV side of power network in Rockhampton shows that ES increases harmonic current and voltage distortion in the network and influences the HV sub-transmission and transmission network.

Chapter 7

Conclusions and Future Work

7.0 Introduction

This Chapter details the major findings and accomplishments of this work and how the work addressed the aims and methodology as proposed in Chapter 1. Moreover, it presents the conclusions that are drawn from the findings and also notes the limitations of the study. Future research directions are also outlined in this chapter.

Modern Power systems are required to accommodate more and more RE from various sources, especially from solar and wind energy sources as nations around the world target to achieve certain amount of energy from RE sources. However both these energy sources have significant problem in timely load support, fluctuation in energy level or even unavailability of effective energy level. Energy storage is the building block for the effective utilisation and large scale integration of solar PV and wind energy into the power network.

In this thesis, the effects of deploying energy storage with the power network was examined particularly the power quality. Large scale integration of ES was examined for voltage regulation and harmonic distortion in the power network. Other influences such as distribution transformer loading and response in energy fluctuation from RE was also investigated. Moreover, environmental and economical advantages of ES were also examined.

First of all, the thesis looked at the storage requirement by examining the potential of solar and wind energy in Rockhampton; Australia. It also identified the environmental and economical benefit of energy storage. This thesis primarily addressed the major challenges associated with the integration of large scale ES with the solar and wind energy into the network. Experiment was conducted and impacts of solar PV were identified. In order to identify the impacts of ES in a typical distribution network, a power network model from small scale to large scale was developed. Modeling was done for Rockhampton distribution network for the present load condition. Performance of network in terms of voltage regulation and harmonic distortion was investigated in various sized power network models.

The major findings of this thesis, results and novel ideas have been presented in various publications listed in the list of publication section. Section 7.1 presents the general overview of the specific tasks carried out for the successful completion of this research. This section also described how the accomplished task addressed the aims mentioned in Chapter 1. Lastly, section 7.2 describes future research directions and possible future research where this study can be applied.

7.1 Summary and Achievements of the Research

The present power network structure, renewable energy potential in Queensland, and the benefit and limitations of renewable distributed generators (DG) were discussed in Chapter 2. Various energy storage technologies were investigated which helped in comprehending the possibilities of the large scale integration of ES into the future power network. The available regulatory standards were discussed in Chapter 2 that provided the insight of power quality that needed to be maintained.

The required size of energy storage in power networks depends on the energy generation from various RE sources and load demand. Chapter 3 described the detailed steps of the estimation process considering various standards. This estimation was done to support residential load with solar PV and wind turbines in grid connected mode. However these estimation steps can be applied to any other load types. The significance of storage was also investigated in Chapter 3 for economical and environmental advantages.

The primary objective of this work was to identify the impacts of energy storage in terms of two power quality indexes. In order to achieve this, the large power network model of Rockhampton was developed and the model database was populated with all real network parameter data collected from the utility operator in Rockhampton. The details of the development of the network were discussed in Chapter 4. This network can be utilised for any future investigation.

One of the major research findings is presented in Chapter 5. The experimental investigation and four different network models were evaluated for the change in voltage level due to the integration of energy storage. Experimental results showed that the network voltage level increases with increased PV penetration and also asymmetrical distribution of RE in phases introduces phase voltage unbalance condition. The experimental case was simulated in the software model and it found the same result. Therefore, the model was further extended by integrating energy storage and it was found that ES minimises the increased voltage by RE and also minimises the phase unbalance condition. Investigation was further extended to large networks up to the total power network of Rockhampton, and impacts of ES were evaluated by the large integration of RE and ES into the network.

Another key finding was presented in Chapter 6, which illustrates the harmonic distortion of ES on power networks. The experimental investigation showed that harmonic current and voltage distortion increase with increased PV integration. Models were developed that mimics the experimental setup, also showed that both PV and ES increase harmonic distortion in the network. For large scale integration, the large power network model of Rockhampton was considered and 8 zone substation supported networks were investigated separately and again collectively. It was found that the flow of load current decreases with the integration of RE. ES further reduces the flow of load current, however both RE and ES inject harmonic current to the network, therefore the overall harmonic distortion increases in the network and exceeds the limit as described in AS-4777.

Finally, based on the research undertaken, the followings have been achieved and noted:

1. An estimation process for the energy storage requirements with RE application in grid connected conditions. This has provided an idea of the required storage in a grid connected RE application.
2. Development of an accurate distribution network model which allows the integration of distributed renewable energy sources with energy storage. The model can be run for future load flow, load curve analysis and harmonic calculation.

3. Significant improvement in voltage regulation achieved after the integration of energy storage while the network is largely integrated with solar PV or wind turbines.
4. Significant improvement was also observed in the distribution transformer loading. Energy storage reduces loading on the distribution transformer which increases the network capacity and also reduces the risk of network capacity improvement.
5. Energy storage increases harmonic current and the total harmonic distortion in the network although the major harmonic contributor was load and RE.
6. Installation of storage and RE in the low voltage side of the network influences the change in voltage regulation and the harmonic distortion, not only in the LV network but also in the high voltage network.

7.2 Future Works

This thesis clearly identifies the merits of energy storage in terms of voltage regulation, phase balance and fluctuation reduction. However storage increases harmonics in the network which is a concern for a large scale practical network. Moreover, the experiment was conducted in a limited scale, therefore there are some scope for further investigation to improve the harmonic distortion caused by energy storage.

The thesis concluded with the scope of further research works as follows:

1. As the simulation result shows improvement for the network performance of power quality after the integration of storage into the network, therefore further experimental investigation with large scale ES and RE is required.
2. Although there are several techniques available to minimise harmonics in the power network, it can be further investigated after integrating large scale storage and RE in the power network.
3. There is scope to investigate the security risk of power networks after integrating storage and RE as distributed generators in various sites in the low voltage side of the power network.
4. Finally for the best utilisation, in large scale networks, large scale storage with RE should be investigated for a life cycle assessment.

REFERENCES

[1] REN21, "Renewables 2010, Global Status Report, Available [Online] at: http://www.ren21.net/Portals/97/documents/GSR/REN21_GSR_2010_full_revised%20Sept2010.pdf Accessed on July 04, 2011," 2010.

[2] REN21, "Renewables 2013. Global Status Report, Available [Online] at: http://www.ren21.net/Portals/0/documents/Resources/GSR/2013/GSR2013_lowres.pdf access date: 04 November 2013," 2013.

[3] Queensland-Government, "The Queensland Renewable Energy Plan, A clear energy future for Queensland, June 2009. Available [Online] at: http://www.cleanenergy.qld.gov.au/queensland_renewable_energy_plan.cfm," p. 32, June 2009 2009.

[4] "Energy in Australia 2010, Department of Resources, Energy and Tourism, Australia," April 2010 2010.

[5] Energy and Tourism Department of Resources, Australia, "Energy in Australia," p. 98, April 2010 2010.

[6] U.S. Energy Information Administration (EIA), "U.S. Energy Information Administration, International Energy Outlook 2010 - Highlights," *Report*, May 25, 2010 2010.

[7] "Queensland Energy Management Plan, Department of Employment, Economic Development and Innovation, Queensland Government, Available [Online] at: http://rti.cabinet.qld.gov.au/documents/2011/may/qld%20energy%20management%20plan/Attachments/Qld%20Energy%20Mgt%20Plan.pdf access date: 28/08/2012," *Report*, May 2011.

[8] "Australian Government, Department of Climate Change, 2009, 'National Greenhouse Gas Inventory—accounting for the KYOTO target May 2009', Department of Climate Change, http://www.climatechange.gov.au/climate-change/~/media/publications/greenhouse-report/national-greenhouse-gas-inventory-pdf.ashx, Accessed: 08-05-2010."

[9] N. Jenkins, R. Allan, P. Crossley, D. Kirschen, and G. Strbac, "Embedded Generation," *Institution of Engineering and Technology,* vol. ISBN:9780852967744, p. 292, October 2000.

[10] Mohammad Taufiqul Arif, Amanullah M. T. Oo, A B M Shawkat Ali, and GM Shafiullah, "Impacts of storage and solar photovoltaic on the distribution network," *Australasian Universities Power Engineering Conference (AUPEC2012), Denpasar-Bali, Indonesia*, 26-29 September 2012.

[11] "Bureau of Meteorology (2011), Australian Government. Available [Online] at: http://reg.bom.gov.au/ Data collected on 03/06/2011."

[12] Mohammad Taufiqul Arif, Amanullah M. T. Oo, and A B M Shawkat Ali, "Integration of Renewable Energy Resources into the Distribution Network - A Review on Required Power Quality," *International Journal on Energy and Power (IJEP), Science and Engineering Publishing Company,* vol. 1, pp. 37-48, November 2012.

[13] Estefanía Caamaño, Demet Suna, Jim Thornycroft, Sjef Cobben, Marcel Elswijk, Bruno Gaiddon, *et al.*, "Utilities experience and perception of PV distributed generation, Available [Online] at: http://www.pvupscale.org/IMG/pdf/WP4_D4-2_Utilities-Experience-PVDG_v5.pdf," 2007.

[14] StandardAustralia, "AS 61400.21-2006, Wind Turbinew, Part 21: Measurement and assessment of power quality characteristics of grid connected wind turbines," *Standard*, 2006.

[15] Joris Soens, "Impact of wind energy in a future power grid," *PhD Thesis, Katholieke Universiteit Leuven, Belgium, ISBN 90-5682-652-2*, December 2005.

[16] "Grid integration of large-capacity Renewable Energy sources and use of large-capacity Electrical Energy Storage, available [online] at: http://www.iec.ch/whitepaper/pdf/iecWP-gridintegrationlargecapacity-LR-en.pdf," *International Electrotechnical Commission, Geneva 20, Switzerland,* p. 116, October 2012.

[17] Daniel H. Doughty, Paul C. Butler, Abbas A. Akhil, Nancy H. Clark, and HJohn D. Boyes, "Batteries for Large-Scale Stationary Electrical Energy Storage," *The Electrochemical Society, Interface, available [Online] at:*

http://www.electrochem.org/dl/interface/fal/fal10/fal10_p049-053.pdf access date: 20/11/2012, Fall 2010.

[18] ErgonEnergy, "Distribution Current State Assessment (CSA) of Urban and SWER Network data for 2011, collected internally from Ergon Energy, date: 26/04/2012."

[19] ErgonEnergy, "Rockhampton Area Load:Bulk Supply Point total from 01/03/2010 to 28/02/2011, collected data from internal source of Ergon Energy, date: 12/05/2011."

[20] G. B. Shrestha and L. Goel, "A study on optimal sizing of stand-alone photovoltaic stations," *IEEE Transactions on Energy Conversion, Vol. 13, No. 4, December 1998*, 1998.

[21] StandardAustralia, "AS 4777.2-2005, Grid connection of energy systems via inverters, Part 2: Inverter requirements, Available [online] at: http://www.saiglobal.com/, access date: 18/06/2012," *Standard*, 2005.

[22] "Network Standard, Standard for Network Performance, Joint standard between ENERGEX and Ergon Energy," *Standard*.

[23] Andrew Thomas, "Photovoltaic planning criteria, Network planning and development distribution planning and capability, Ergon Energy, Australia," *Technical note*, 2011.

[24] V.J. Gosbell, "Harmonic distortion in the electric supply system, Power Quality Centre, Integral energy. Available [online] at: http://www.elec.uow.edu.au/pqaustralia/main/images/stories/pqrctechnotes/technote3.pdf access date: 01/06/2012," *Technical Note no. 3,* March 2000.

[25] Ergon Energy, "Distribution Feeder Database 2010. Collected information from Ergon Energy," 2010.

[26] Ergon Energy, "Network Configuration Diagram, available [Online] at: http://www.ergon.com.au/about-us/the-electricity-industry/electricity-distribution-pricing-methodologies/distribution-loss-factor-calculation-methodology#content-id-4876 access date: 10/10/2012."

[27] J. Duccan Glover, Mulukutla S. Sarma, and Thomas J. Overbye, "Power System Analysis and Design, 4th edition, Thompson Corporation," *Book,* p. 255, 2008.

[28] ActewAGL, "ActewAGL guidelines for grid-connected photovoltaic installations via inverter," 2009.

[29] Ryoichi Hara Motoki Akatsuka, Hiroyuki Kita, Takamitsu Ito, Yoshinobu Ueda, Yutaka Saito, "Estimation of battery capacity for suppression of PV power plant output fluctuation," *978-1-4244-5892-9/10 2010 IEEE*, 2010.

[30] Energy and Tourism Department of Resouces, Australia. (February 2012). *Energy in Australia 2012, Available [Online] at: http://www.bree.gov.au/documents/publications/energy-in-aust/energy-in-australia-2012.pdf access date: 05 September 2013*.

[31] "Australian Government, Department of Climate Change, 2009, 'National Greenhouse Gas Inventory—accounting for the KYOTO target May 2009', Department of Climate Change, http://www.climatechange.gov.au/climate-change/~/media/publications/greenhouse-report/national-greenhouse-gas-inventory-pdf.ashx, Accessed: June 30, 2011."

[32] United-Nations, "Kyoto Protocol to the United Nations Framework convention on climate change," p. 21, 1998.

[33] "Energy in Australia 2010, Australian Bureau of Agricultural and Resource Economics and Sciences, Department of Resources, Energy and Tourism, Australia. Available [Online] at: http://www.daff.gov.au/abares/publications_remote_content/publication_series/energy_in_australia?sq_content_src=%2BdXJsPWh0dHAlM0ElMkYlMkYxNDMuMTg4LjE3LjIwJTJGYW5yZGwlMkZEQUZGU2VydmljZSUyRmRpc3BsYXkucGhwJTNGZmlkJTNEcGVfYWJhcmVicnM5OTAxNDQ0NF8xMmEueG1sJmFsbD0x," April 2010 2010.

[34] Queensland-Government, "The Queensland Renewable Energy Plan, A clear energy future for Queensland, Available [Online] at: http://www.cleanenergy.qld.gov.au/queensland_renewable_energy_plan.cfm," p. 32, June 2009.

[35] NASA Report, "Biomass burning and the production of greenhouse gases. Available [Online] at: http://asd-www.larc.nasa.gov/biomass_burn/biomass.html."

[36] Geothermal-Resources-Council, "Geothermal Energy Reduces Greenhouse Gases. Available [Online] at: http://www.geothermal.org/articles/greenhousegases.pdf," *Report*, 2003.

[37] Energy Research Institute, "Australian Sustainable Energy, Zero Carbon Australia Stationary Energy Plan," p. 194, July 2010 2010.

[38] "Bureau of Meteorology, Australian Government. Available [Online] at: http://reg.bom.gov.au/."

[39] Energy Research Institute, "Australian Sustainable Energy, Zero Carbon Australia Stationary Energy Plan. Available [online] at: http://www.energy.unimelb.edu.au/ (access date: 10/02/2011)," p. 194, July 2010 2010.

[40] "Renewable Resourceful Victoria, Part 2 - Energy Resources, Available [Online] at: http://new.dpi.vic.gov.au/energy/future-energy/renewable/part-2," February 2010.

[41] Archer and Jacobson Z. Mark L. Cristina, "Evaluation of global wind power, Journal of Geophysical Research, Vol-110, D12110, doi:1029/2004JD005462," vol. 110, 2005.

[42] Queensland-Government, "Distributed Generation, Department of Energy and Water Supply, available [Online] at: http://www.cleanenergy.qld.gov.au/distributed-generation/default.htm access date: 10/10/2012."

[43] Mohammad Taufiqul Arif, Amanullah M. T. Oo, and A B M Shawkat Ali, "Investigation of Energy Storage Systems, Its Advantage and Requirement in Various Locations in Australia," *accepted for publication in the Journal of Renewable Energy, Hindawi Publishing Corporation,* vol. 2013, p. 15, 2013.

[44] H. Nfaoui, J. Buret, A.A.M. Sayigh, and P.D. Dunn, "Modelling of a wind/diesel system with battery storage for Tangiers, Morocco," *Renew Energy, Elsevier Ltd.*, vol. 4, pp. 155-167, 1994.

[45] Ahmad Zahedi, "Technical Analysis of Electric Power System Consisting of Solar PV Energy, Wind Power and Hydrogen Fuel Cell," *Australasian Universities Power Engineering Conference (AUPEC 2007), Perth, WA, Australia,* pp. 1-5, 2007.

[46] Saifur Rahman, "The Smart Grid, Its Opportunities and Challenges, Presentation at "Asia-Pacific Power & Energy Engineering Conference (IEEE PES APPEEC)," 29 March 2010.

[47] "Sydney buffeted by strong winds- Bureau of Meteorology, Sydney, NSW. Available [online] at: http://www.bom.gov.au/announcements/media_releases/nsw/20030825.shtml#graph access date: 30/07/2012," *media release, climate,* August 24 2003.

[48] Wind-Watch, "National Wind Watch, Presenting the facts about industrial wind power, Available [Online] at: http://www.wind-watch.org/faq-output.php access date: 30/07/2012."

[49] N. W. Miller, R. S. Zrebiec, R. W. Delmerico, and G. Hunt, "Design and commissioning of a 5 MVA, 2.5 MVA battery energy storage," *In the proceedings of IEEE Power Engineering Society Transmission and Distribution conference,* 1996.

[50] Alexandre Oudalov, D. Chartouni, C. Ohler, and G. Linhofer, "Value Analysis of Battery Energy Storage Applications in Power Systems," *PSCE-2006, IEEE,* 2006.

[51] Paulo F. Ribeiro, Brian K. Johnson, Mariesa L. Crow, Aysen Arsoy, and Yilu Liu, "Energy Storage Systems for Advanced Power Applications," *Proceedings of the IEEE,* vol. 89, p. 12, December 2001.

[52] N. Abi-Samra, C. Neft, A. Sundaram, and W. Malcolm, "The distribution system dynamic voltage restorer and its applications at industrial facilities with sensitive loads," *In the proceedings of 8th international Power Quality Solutions, Long Beach, CA,* Sep 9 - 15 1995.

[53] Sergio Vazquez, Srdjan M. Lukic, Eduardo Galvan, Leopoldo G. Franquelo, and Juan M. Carrasco, "Energy Storage Systems for Transport and Grid Applications," *IEEE Transactions on Industrial Electronics,* vol. 57, pp. 3881-3895, December 2010.

[54] "Renewable Green Energy Power, Solar Energy facts - Solar Energy Storage enables CSP and PV on the grid, Available [Online] at: http://www.renewablegreenenergypower.com/solar-energy-facts-solar-energy-storage-enables-csp-and-pv-on-the-grid/ access date: 05/11/2012."

[55] "Energy Storage, Alaska Energy Wiki, Available [Online] at: http://energy-alaska.wikidot.com/energy-storage access date: 04/11/2012."

[56] I.H. Wong, "An Underground Pumped Storage Scheme in the Bukit Timah Granit of Singapore.," *Tunnelling and Underground Space Technology, Elsevier,* vol. 11, pp. 485-489, 1996.

[57] F. Cristina Figueiredo and Peter C. Flynn, "Using Diurnal Power Price to Configure Pumped Storage," *IEEE Transactions on Energy Conversion*, vol. 21, pp. 804-809, September 2006.

[58] "Pumped Hydro Storage, First Hydro Company, Available [Online] at: http://www.fhc.co.uk/index.asp access date: 04/11/2012."

[59] Faancisco Diaz-Gonzalez, Andreas Sumper, and Oriol Gomis-Bellmunt, "A review of energy storage technologies for wind power applications," *Renewable and Sustainable Energy reviews, Elsevier*, vol. 16, pp. 2154-2171, February 2012.

[60] M. Korpass and C. Greiner, "Opportunities for hydrogen production in connection with wind power in weak grids," *Renewable Energy*, vol. 33, pp. 199-208, 2008.

[61] Mohammad Taufiqul Arif, Amanullah M. T. Oo, and A B M Shawkat Ali, "Estimation of required storage system for Solar PV and Wind energy and feasibility analysis of storage systems," *Energy Storage (ISBN 979-953-307-768-9) by InTech Online Publisher*, 2012.

[62] Faizur Rahman, Shafiqur Rehman, and Mohammad Arif Abdul-Majeed, "Overview of energy storage systems for storing electricity from renewable energy sources in Saudi Arabia," *Renewable and Sustainable Energy reviews, Elsevier*, vol. 16, pp. 274-283, January 2012.

[63] Marc Beaudin, Hamidreza Zareipour, Anthony Schellenberglabe, and William Rosehart, "Energy storage for mitigating the variability of renewable electric sources: An updated review," *Energy for Sustainable Development, Elsevier*, vol. 14, pp. 302-314, December 2010.

[64] Ioannis Hadjipaschalis, Andreas Poullikkas, and Venizelos Efthimiou, "Overview of current and future energy storage technologies for electric power applications," *Renewable and Sustainable Energy reviews, Elsevier*, vol. 13, pp. 1513-1522, August-September 2009.

[65] Eric Hittinger, J.F. Whitacre, and Jay Apt, "Compensating for wind variability using co-located natural gas generation and energy storage," *Energy Systems, Springer*, pp. 417-439, 2010.

[66] David Boutacoff, Daniel Rastler, and Haresh Kamath, "Energy Storage, Enabling Grid-ready solutions, EPRI, Available [Online] at: http://eepublishers.co.za/article/epri-144-01-energy-storage-enabling-grid-ready-solutions.html access date: 28/-8/2012," *Article*, 2010.

[67] "Technology Comparisons, Energy Storage Association (ESA), Available [Online] at: http://www.electricitystorage.org/images/uploads/static_content/technology/technology_resources/ratings_large.gif access date: 04/11/2012."

[68] Alexandre Oudalov, Tilo Buehler, and Daniel Chartouni, "Utility Scale Applications of Energy Storage," *IEEE Energy 2030, Atlanta, Georgia, USA*, 17-18 November 2008.

[69] Yuri Makarov, Pengwei Du, Michael CW Kintner-Meyer, Chunlian Jin, and Howard Illian, "Optimal Size of Energy Storage to Accomodate High Penetration of Renewable Resources in WECC System," *IEEE*, 2010.

[70] A.A. Solomon, D.Faiman, and G.Meron, "Properties and uses of storage for enhancing the grid penetration of very large photovoltaic systems," *Energy Policy, Elsevier*, vol. 38, pp. 5208–5222, 2010.

[71] Sharad W. Mohod and Mohan V. Aware, "Energy Storage to Stabilize the Weak Wind Generating Grid," *Power System Technology and IEEE Power India Conference, POWERCON 2008*, pp. 1-5, 2008.

[72] T. Tanabe, T. Sato, R. Tanikawa, I. Aoki, T. Funabashi, and R. Yokoyama, "Generation scheduling for eind power generation by storage battery system and meteorological forecast," *Power and Energy Society General Meeting - Conversion and Delivery of Electrical Enegy in the 21st Century, IEEE 2008*, pp. 1-7, 20-24 July 2008.

[73] H. Ibrahim, A. Ilinca, and J. Perron, "Energy storage systems - Characteristics and comparasions," *Renewable and Sustainable Energy reviews, Elsevier*, vol. 12, pp. 1221-1250, June 2008.

[74] Mohammad Taufiqul Arif, Amanullah M. T. Oo, and A B M Shawkat Ali, "Investigation of energy storage required for various location in Australia," *Central Regional Engineering Conference 2012, Engineers Australia, Queensland, Australia*, 10-11 August 2012.

[75] David Connolly, "The Integration of Fluctuating Renewable Energy using Energy Storage," *PhD Thesis, Department of Physica and Energy, University of Limerick, Available [Online] at:*

http://www.dconnolly.net/files/David%20Connolly,%20UL,%20Energy%20Storage%20Techniques,%20V3.pdf access date: 03/11/2012, December 2010.

[76] IEEE Standard, "IEEE Recommended Practice for Sizing Lead-Acid Batteries for Stand-Alone Photovoltaic (PV) Systems, Available [Online] at: http://ieeexplore.ieee.org/stamp/stamp.jsp?tp=&arnumber=4280849," *IEEE Standard 1013™-2007*.

[77] "Solar Energy Grid Integration Systems (SEGIS), Program Concept Paper, Available [Online] at: http://www.docstoc.com/docs/22916131/SOLAR-ENERGY-GRID-INTEGRATION-SYSTEMS," *Sandia National Laboratories, U.S. Department of Energy, Energy Efficiency and Renewable Energy*, October 2007.

[78] ABB Report, "Connecting renewable energy to the Grid, Available [Online] at: http://www.abb.com/cawp/seitp326/377dbeff7a3a6aedc12577c20033dbf5.aspx," *Web Information*, Access date: 01/11/2012.

[79] IEEE Standard, "IEEE Std 1547-2003, IEEE Standard for Interconnecting Distributed Resources With Electric Power Systems," *Standard*, pp. 1-16., 2003.

[80] IEEE, "IEEE P2030.2 Draft Guide for the Interoperability of Energy Storage Systems Integrated with the Electric Power Infrastructure, Available [Online] at: http://grouper.ieee.org/groups/scc21/2030.2/2030.2_index.html access date: 05/11/2012," 2012.

[81] StandardAustralia, "AS 4777.1-2005, Grid connection of energy systems via inverters, Part 1: Installation requirements, Available [online] at: http://www.saiglobal.com/, access date: 18/06/2012," *Standard*, 2005.

[82] StandardAustralia, "AS 610038-2000, Standard voltages, Available [online] at: http://www.saiglobal.com/, access date: 18/06/2012," *Standard*, 2000.

[83] StandardAustralia, "AS/NZS 61000.3.3:2006, Electromagnetic compatibility (EMC) Part 3.3: Limits - Limitation of voltage changes, voltage fluctuations and flicker in public low-voltage supply systems for equipment with rated current less than or equal to 16A per phase," *Standard*, 2006.

[84] StandardAustralia, "AS 61000.3.100-2011, Electromagnetic compatibility (EMC), part 3.100: Limits - Steady state voltage limits in public electricity systems, Available [online] at: http://www.saiglobal.com/ " *Australian Standard*, 2011.

[85] IEEE Standards, "IEEE Std 1159-1995, IEEE Recommended practice for monitoring electric power quality," *Standard*, June, 1995.

[86] Holttinen, Hannele, Lemstrom, Bettina, Peter, Binder, *et al.*, "Design and operation of power systems with large amounts of wind power, state-of-art report, VTT working papers 82, VTT, Finland," October 2007.

[87] Yu Ru, Jan Kleissl, and Sonia Martinez, "Storage Size Determination for Grid-Connected Photovoltaic Systems," *IEEE Transactions on Sustainable Energy*, pp. 1-14, June 2012.

[88] Jeroen Tant, Frederik Geth, Daan Six, Peter Tant, and Johan Driesen, "Multiobjective Battery Storage to Improve PV Integration in Residential Distribution Grids," *IEEE Transactions on Sustainable Energy*, pp. 1-10, July 2012.

[89] Matthew Zillmann, Ruifeng Yan, and Tapan Kumar Saha, "Regulation of Distribution Network Voltage Using Dispersed Nattery Storage Systems: A Case Study of Rural Network," *Power and Energy Society General Meeting, IEEE, San Diego, CA*, pp. 1-8, 24-29 July 2011.

[90] Paul Denholm and Maureen Hand, "Grid flexibility and storage required to achieve very high penetration of variable renewable electricity," *Energy Policy*, vol. 39, pp. 1817-1830, 2011.

[91] Mohammad Taufiqul Arif, Amanullah M. T. Oo, and A B M Shawkat Ali, "Estimation of Energy Storage and Its Feasibility Analysis, Energy Storage - Technologies and Applications, Dr. Ahmed Zobaa (Ed.), ISBN: 978-953-51-0951-8, InTech, DOI: 10.5772/52218. Available from: http://www.intechopen.com/books/energy-storage-technologies-and-applications/estimation-of-energy-storage-and-its-feasibility-analysis," 2013.

[92] Mohammad Taufiqul Arif, Amanullah M. T. Oo, GM Shafiullah, and A B M Shawkat Ali, "Significance of Storage on Solar Photovoltaic System - a Residential Load Case Study in

Australia," *accepted for publication in the International Journal of Smart Grid and Renewable Energy (SGRE), Vol. 4 No. 2, May 2013*.

[93] Tom Lambert, "How HOMER Calculates the PV Array Power Output, Software available [Online] at: http://homerenergy.com/," *Homer Help file*, 2007.

[94] Priscilla N. John Ahmed M.A. Haidar, Mohd Shawal, "Optimal configuration assessment of renewable energy in Malaysia," *Renewable Energy 36 (2011) 881-888*, 2011.

[95] David Sharpe Tony Burton, Nick Jenkins, Ervin Bossanyi, "Wind Energy Handbook, John Wiley & Sons Ltd. 2001."

[96] Katherine Klink Aaron Knoll, "Residential and Commercial scale distributed wind energy in North Dakota, USA. Wind Energy, 2009."

[97] Gilbert M. Masters, "Renewable and Efficient Electric Power Systems," *John Wiley & Sons, Inc.*, 2004.

[98] Charles J. Hanley Dan T. Ton, Georgianne H. Peek, and John D. Boyes, "Solar Energy Grid Integration Systems –Energy Storage (SEGIS-ES)," *SANDIA REPORT, SAND2008-4247, Unlimited Release, July 2008*, 2008.

[99] Souhir SALLEM Nabiha BRAHMI, Maher CHAABENE, "Sizing of a mini autonomous hybrid electric grid," *International Renewable Energy Congress*, 2009.

[100] IEEE Standard, "IEEE Std 1561-2007, IEEE Guide for Optimizing the Performance and Life of Lead-Acid Batteries in Remote Hybrid Power Systems.," *Standard*, 2007.

[101] IEEE Standard, "IEEE Standard for Interconnecting Distributed Resources With Electric Power Systems, in IEEE Std 1547-2003. p. 0_1-16.," *Standard*, 2003.

[102] EnergyMatters, "Average household electricity consumption per day in Australia, Available [Online] at: http://www.energymatters.com.au/climate-data/grid-electricity-usage.php access date: 04/07/2012," 2012.

[103] The Infinite power of Texas Renewable Energy, "Estimating PV System Size and Cost," *SECO FACT SHEET NO. 24*.

[104] Energy Matters, "SMA Sunny Boy 3800W Grid-connected Inverter, Available [Online] at: http://www.energymatters.com.au/sma-sunny-boy-3800watt-grid-connect-inverter-p-412.html."

[105] LG PV, "LG Polycrystalline PV Module, Available [Online] at: http://futuresustainability.rtrk.com.au/?scid=80507&kw=4858156&pub_cr_id=17164703877 (access date: 20/03/2012)."

[106] HOMER, "Analysis of micro powersystem options, Available [Online] at: https://analysis.nrel.gov/homer/."

[107] G.J., "Dalton, Lockington, D. A. & Baldock, T. E. (2008) Feasibility analysis of stand-alone renewable energy supply options for a large hotel. Renewable Energy, vol 33, issue 7, P-1475-1490.."

[108] Celik, "A.N., Techno-economic analysis of autonomous PV-Wind hybrid energy systems using different sizing methods. Energy Conversion and Management, 2003. 44(12): P. 1951-1968.."

[109] Barley, "DC, Winn BC. Optimal dispatch strategy in remote hybrid power systems, Solar Energy 1996;58:1 65-79."

[110] PV-Price, "Sun Solar System, Available [Online] at: www.sunsolarsystem.com.au (access date: 15/03/2012)."

[111] PV-Price, "Goodhew Electrical and Solar, Available [Online] at: http://www.goodhewsolar.com.au/customPages/goodhew-electrical-%26-solar-offers-homeowners-the-most-affordable-quality-solar-systems-on-the-market.?subSiteId=1 (access date: 15/03/2012)."

[112] Inverter-Cost, "SMA Sunny Boy Grid tie Inverter 7000W SB7000US price, Available [Online] at: http://www.google.com/products/catalog?hl=en&q=sunny+boy+grid+tie+inverter+price&gs_sm=3&gs_upl=2378l7840l1l8534l11l10l0l1l1l0l223l2055l0.3.7l11l0&bav=on.2,or.r_gc.r_pw.,cf.osb&biw=1680&bih=831&um=1&ie=UTF-8&tbm=shop&cid=10871923140935237408&sa=X&ei=z0g6T-T0LayziQfnkZGQCg&ved=0CGkQ8wIwAQ (access date: 16/03/2012)."

[113] Inverter-Cost, "SMA Sunny Boy 1700 Price, Available [Online] at: http://www.solarmatrix.com.au/special-offers/sunny-boy-1700?ver=gg&gclid=CMO0gIOzna4CFYVMpgod7T1OHg (access date: 16/03/2012)."

[114] Bergey WindPower, "Wind Turbine Retail Price list, Available [Online[at: http://production-images.webapeel.com/bergey/assets/2012/3/6/98837/PriceList-March.pdf Access date: 09/04/2012."

[115] Winturbine_Price, "Ecodirect, Clean Energy Solution, Windturbine Price, Available [Online] at: http://www.ecodirect.com/Bergey-Windpower-BWC-10kW-p/bergey-windpower-bwc-10kw-ex.htm Access date: 29/02/2012," *Online Information*.

[116] ErgonEnergy, "Electricity tariffs and prices, available [Online] at: http://www.ergon.com.au/your-business/accounts--and--billing/electricity-prices."

[117] ALTE-Store, "Battery Price, Trojan T-105 6V, 225AH (20HR) Flooded Lead Acid Battery, Available [Online] at: http://www.altestore.com/store/Deep-Cycle-Batteries/Batteries-Flooded-Lead-Acid/Trojan-T-105-6V-225AH-20HR-Flooded-Lead-Acid-Battery/p1771/."

[118] RedEnergy, "Pricing definition for Electricity customers, NSW, Available [Online] at: http://www.redenergy.com.au/docs/NSW-Pricing-DEFINITIONS-0311.pdf," 2011.

[119] Future_Sustainability, "Rebates for Solar Power, Available [Online]at: http://futuresustainability.rtrk.com.au/?scid=80507&kw=4858156&pub_cr_id=17164703877. "

[120] Economic Development & Innovation Depertment of Employment, Queensland, "Solar Bonus Scheme, Queensland Government, Office of Clean Energy, Available [Online] at: http://www.cleanenergy.qld.gov.au/demand-side/solar-bonus-scheme.htm?utm_source=WWW2BUSINESS&utm_medium=301&utm_campaign=redirection."

[121] ErgonEnergy, "Energy Conservation, Renewable energy sources, available [Online] at: http://www.ergon.com.au/energy-conservation/what-are-we-doing/renewable-energy-sources , access date: 01/01/2013."

[122] ErgonEnergy, "Network Management Plan Part A: Electricity Supply for Regional Queensland 2012/13 to 2016/17, Available [Online] at: http://www.ergon.com.au/__data/assets/pdf_file/0009/6786/NMP-2012-17-Part-A-FINAL.pdf ,access date: 01/01/2013," 2012.

[123] *Australian Energy Market Operator (AEMO), National Electricity Forecasting Report (NEFR) for the National Electricity Market (NEM) 2012, Available [Online] at: http://www.aemo.com.au/Electricity/Planning/Forecasting/National-Electricity-Forecasting-Report-2012*.

[124] "Community profile, Rockhampton Region, Rockhampton Regional Council, Availavle [Online] at: http://profile.id.com.au/rockhampton , access date: 05/01/2013."

[125] EasyPower, "PowerFlow - Load Flow analysis Software, available [Online] at: http://www.easypower.com/products/EasyPower/features/PowerFlow/PowerFlow_overview.php access date: 07/01/2012."

[126] ETAP website report, "Power System Software, Network Analysis Software, Available [Online] at: http://etap.com/network-analysis/network-analysis.htm access date: 08/01/2013."

[127] ETAP website report, "Renewable Energy Software, available [Online] at: http://etap.com/renewable-energy/photovoltaic-array-solar-panel.htm access date: 07/01/2013."

[128] DINIS website report, "Distribution Network Information System, available [Online] at: http://www.dinis.com/products.htm access date: 07/01/2013."

[129] SimTec, "PSS SINCAL, available [Online] at: http://www.simtec-gmbh.at/sites_en/sincal.asp access date: 01/02/2011."

[130] "Hill Michael, Strategic Engineering, Power System Analysis Package Available [Online] at: http://www.hmac.com.au/index.php/software/power-system-analysis-packages/."

[131] SINCAL, "Help File, PSS SINCAL, description available from software CD."

[132] Stephen J. Chapman, " (2005). Electric Machinery Fundamentals. McGraw Hill. pp. 100, 263.. ISBN 978-0-07-246523-5.."

[133] ErgonEnergy, "Voltage range, Low Voltage network design, available [Online] at: http://www.ergon.com.au/__data/assets/pdf_file/0018/64233/Section-15-LV-Network-Design.pdf access date: 20/06/2012," p. 5/11.

[134] StandardAustralia, "AS 61400.21 - 2006: Wind turbines part 21: Measurement and assessment of power quality characteristics of grid connected wind turbines," *Standard*, 2006.

[135] V.J. Gosbell, "Voltage unbalance, Power quality centre, Integral energy, Available [online] at: http://www.elec.uow.edu.au/pqaustralia/main/images/stories/pqrctechnotes/technote6.pdf access date: 01/06/2012," *Technical Note no. 6*, October 2002.

[136] Allen-Bradley, "Power System Harmonics, A Reference guide to causes, effects and corrective measures, www.rockwellautomation.com," April 2001.

[137] StandardAustralia, "IEC 61000.3.6:2012, Electromagnetic compatibility (EMC) Part 3.6: Limits - Assessment of emission limits for the connection of distorting installations to MV, HV and EHV power systems," *Standard (Technical Report)*, 2012.

[138] W. Mack Grady, "Harmonics and how they relate to power factor," *Proceedings of the EPRI Power Quality Issues and Opportunities Conference (PQA' 93), San Diego, CA, USA*, November 1993.

[139] StandardAustralia, "AS/NZS 61000.3.2:2003, Electromagnetic compatibility (EMC) Part 3.2: Limits - Limits for harmonic current emissions (equipment input current less than or equal to 16A per phase)," *Standard*, 2003.

[140] "SMA Solar, Emission of Harmonic Currents, Grid connected inverter, Collected data from Service Manager SMA Solar Technology, 67 Epping Road, North Ryde, NSW-2113, Australia."

[141] Copper Development Association, "Power Quality Application Guide, Voltage disturbances, Standard EN 50160, available [Online] at: http://www.copperinfo.co.uk/power-quality/downloads/pqug/542-standard-en-50160-voltage-characteristics-in.pdf accedd date: 20/06/2012," 2004.

[142] SMA Inverters, "Sunny Boy SB 1100/1700 Inverter Test certificate result sheet, available [Online] at: http://www.rexelrenewableenergy.co.uk/FileDepository/TechDocs/Inverters/Test%20Certificate.pdf access date: 18/06/2012," 2012.

[143] SMA Solar Technology, "Inverter Efficiency, Sunny Boy 3000TL/4000TL/5000TL, available [Online] at: http://www.sma-australia.com.au/en_AU/products/solar-inverters/sunny-boy/sunny-boy-3000tl-4000tl-5000tl.html access date: 18/06/2012."

[144] StandardAustralia, "AS 4777.3-2005, Grid connection of energy systems via inverters, Part 3: Grid protection requirements, Available [online] at: http://www.saiglobal.com/, access date: 18/06/2012," 2005.

[145] GM Shafiullah, Amanullah M. T. Oo, ABM Shawkat Ali, Salahuddin Azad, Mohammad Arif, and Tim Moore, "Experimental Analysis of Harmonics on Utility Grid with PV Penetration," *IIn the proceedings of the International Conference on Electrical and Computer Systems, Ontario, Canada*, 22-24 August 2012.

Appendix-A

A-1: Load, RE and ES Data

Tables below shows the data of load, PV, WT and ES installed in various nodes in different ZS Power network in Rockhampton. It also shows the installed distribution transformer (DT) capacity.

Rockhampton Glenmore (RGL) ZS Power Network:

#	Node1	Element	S[kVA]	cosphi	PV[kW]	DT[kVA]	Bulk RE & ES
1	RGL_N156	RGL_LO100	0.57	0.9	0.55670103	1.14	RGL_F1_N1
2	RGL_N2040	RGL_LO1005	33.959	0.8	29.4814976	67.918	500 kW PV
3	RGL_N157	RGL_LO101	0.856	0.9	0.83602821	1.712	200 kW ES
4	RGL_N2055	RGL_LO1013	143.2	0.9	139.858926	286.4	
5	RGL_N2066	RGL_LO1015	251.297	0.9	245.433858	502.594	RGL_F1_N2
6	RGL_N158	RGL_LO102	0.57	0.9	0.55670103	1.14	500 kW PV
7	RGL_N2081	RGL_LO1024	67.918	0.8	58.9629951	135.836	200 kW ES
8	RGL_N2087	RGL_LO1025	450	0.8	390.66739	900	
9	RGL_N2092	RGL_LO1028	192.159	0.95	198.102062	384.318	RGL_F1_N3
10	RGL_N160	RGL_LO103	1.426	0.9	1.39272925	2.852	500 kW PV
11	RGL_N2095	RGL_LO1030	50	0.9	48.8334238	100	200 kW ES
12	RGL_N2125	RGL_LO1038	157.5	0.95	162.371134	315	
13	RGL_N2130	RGL_LO1041	84.898	0.95	87.5237113	169.796	RGL_F1_N4
14	RGL_N2144	RGL_LO1045	372.321	0.95	383.836082	744.642	500 kW PV
15	RGL_N2175	RGL_LO1059	67.918	0.95	70.0185567	135.836	200 kW ES
16	RGL_N2185	RGL_LO1065	0.57	0.95	0.58762887	1.14	
17	RGL_N2208	RGL_LO1070	102.16	0.95	105.319588	204.32	RGL_F1_N5
18	RGL_N2219	RGL_LO1075	0.57	0.9	0.55670103	1.14	500 kW PV
19	RGL_N2239	RGL_LO1082	45.318	0.95	46.7195876	90.636	200 kW ES
20	RGL_N2247	RGL_LO1088	388.305	0.9	379.245252	776.61	
21	RGL_N2255	RGL_LO1093	0.57	0.9	0.55670103	1.14	
22	RGL_N2305	RGL_LO1111	90.635	0.95	93.4381443	181.27	
23	RGL_N2324	RGL_LO1121	1.141	0.9	1.11437873	2.282	RGL_F2_N1
24	RGL_N2334	RGL_LO1124	102.16	0.9	99.7764514	204.32	500 kW PV
25	RGL_N2348	RGL_LO1130	33.959	0.9	33.1666848	67.918	200 kW ES
26	RGL_N2377	RGL_LO1141	118.729	0.95	122.401031	237.458	
27	RGL_N2384	RGL_LO1144	192.159	0.9	187.675638	384.318	RGL_F2_N2
28	RGL_N2387	RGL_LO1145	33.959	0.9	33.1666848	67.918	500 kW PV
29	RGL_N2397	RGL_LO1151	0.57	0.9	0.55670103	1.14	200 kW ES
30	RGL_N2409	RGL_LO1159	128.106	0.95	132.068041	256.212	

31	RGL_N2417	RGL_LO1163	45.318	0.9	44.260662	90.636	RGL_F2_N3
32	RGL_N2418	RGL_LO1164	239.832	0.9	234.236354	479.664	500 kW PV
33	RGL_N2434	RGL_LO1172	169.795	0.9	165.833424	339.59	200 kW ES
34	RGL_N2485	RGL_LO1199	84.898	0.95	87.5237113	169.796	
35	RGL_N2488	RGL_LO1200	125	0.9	122.083559	250	RGL_F2_N4
36	RGL_N2509	RGL_LO1204	59.406	0.95	61.243299	118.812	500 kW PV
37	RGL_N2512	RGL_LO1206	101.877	0.9	99.5000543	203.754	200 kW ES
38	RGL_N2556	RGL_LO1226	101.877	0.9	99.5000543	203.754	
39	RGL_N2568	RGL_LO1231	128.106	0.95	132.068041	256.212	RGL_F2_N5
40	RGL_N2623	RGL_LO1255	178.093	0.95	183.601031	356.186	500 kW PV
41	RGL_N2646	RGL_LO1266	67.918	0.9	66.3333695	135.836	200 kW ES
42	RGL_N2654	RGL_LO1269	90.635	0.9	88.5203473	181.27	
43	RGL_N2676	RGL_LO1280	102.16	0.9	99.7764514	204.32	
44	RGL_N216	RGL_LO140	67.918	0.8	58.9629951	135.836	
45	RGL_N238	RGL_LO153	150	0.9	146.500271	300	
46	RGL_N239	RGL_LO154	101.877	0.9	99.5000543	203.754	
47	RGL_N249	RGL_LO160	33.959	0.9	33.1666848	67.918	
48	RGL_N250	RGL_LO161	67.918	0.9	66.3333695	135.836	
49	RGL_N251	RGL_LO162	33.959	0.9	33.1666848	67.918	
50	RGL_N253	RGL_LO163	100	0.9	97.6668475	200	
51	RGL_N266	RGL_LO173	100	0.8	86.8149756	200	
52	RGL_N282	RGL_LO177	100	0.8	86.8149756	200	
53	RGL_N288	RGL_LO178	192.159	0.9	187.675638	384.318	
54	RGL_N293	RGL_LO180	157.5	0.95	162.371134	315	
55	RGL_N294	RGL_LO181	100	0.8	86.8149756	200	
56	RGL_N296	RGL_LO182	100	0.9	97.6668475	200	
57	RGL_N368	RGL_LO221	1.426	0.95	1.47010309	2.852	
58	RGL_N388	RGL_LO227	67.918	0.9	66.3333695	135.836	
59	RGL_N391	RGL_LO228	118.812	0.95	122.486598	237.624	
60	RGL_N393	RGL_LO229	45.318	0.95	46.7195876	90.636	
61	RGL_N399	RGL_LO231	372.321	0.95	383.836082	744.642	
62	RGL_N400	RGL_LO232	0.856	0.9	0.83602821	1.712	
63	RGL_N409	RGL_LO236	67.918	0.8	58.9629951	135.836	
64	RGL_N433	RGL_LO244	640	0.8	555.615844	1280	
65	RGL_N435	RGL_LO245	372.321	0.9	363.634183	744.642	
66	RGL_N441	RGL_LO249	128.106	0.9	125.117092	256.212	
67	RGL_N465	RGL_LO259	1.426	0.95	1.47010309	2.852	
68	RGL_N476	RGL_LO264	2.852	0.8	2.4759631	5.704	
69	RGL_N481	RGL_LO267	128.106	0.9	125.117092	256.212	
70	RGL_N500	RGL_LO274	800	0.9	781.33478	1600	
71	RGL_N502	RGL_LO275	6.196	0.95	6.38762887	12.392	
72	RGL_N504	RGL_LO277	6.297	0.9	6.15008139	12.594	
73	RGL_N506	RGL_LO278	101.877	0.9	99.5000543	203.754	
74	RGL_N520	RGL_LO284	33.959	0.9	33.1666848	67.918	
75	RGL_N522	RGL_LO286	118.812	0.9	116.039935	237.624	

76	RGL_N534	RGL_LO290	450	0.8	390.66739	900
77	RGL_N579	RGL_LO303	255.399	0.95	263.297938	510.798
78	RGL_N595	RGL_LO309	90.635	0.9	88.5203473	181.27
79	RGL_N601	RGL_LO312	0.57	0.95	0.58762887	1.14
80	RGL_N626	RGL_LO323	1.426	0.9	1.39272925	2.852
81	RGL_N639	RGL_LO330	67.918	0.8	58.9629951	135.836
82	RGL_N647	RGL_LO334	90.635	0.95	93.4381443	181.27
83	RGL_N682	RGL_LO350	128.106	0.95	132.068041	256.212
84	RGL_N683	RGL_LO351	100	0.9	97.6668475	200
85	RGL_N686	RGL_LO353	1.426	0.8	1.23798155	2.852
86	RGL_N703	RGL_LO362	153.239	0.95	157.978351	306.478
87	RGL_N704	RGL_LO363	135.953	0.8	118.027564	271.906
88	RGL_N717	RGL_LO369	2.852	0.8	2.4759631	5.704
89	RGL_N719	RGL_LO370	280	0.95	288.659794	560
90	RGL_N728	RGL_LO374	426.535	0.95	439.726804	853.07
91	RGL_N743	RGL_LO382	255.446	0.95	263.346392	510.892
92	RGL_N754	RGL_LO388	0.57	0.95	0.58762887	1.14
93	RGL_N59	RGL_LO39	40	0.95	41.2371134	80
94	RGL_N759	RGL_LO392	153.239	0.9	149.6637	306.478
95	RGL_N766	RGL_LO394	2.852	0.95	2.94020619	5.704
96	RGL_N787	RGL_LO403	255.446	0.95	263.346392	510.892
97	RGL_N800	RGL_LO405	192.159	0.95	198.102062	384.318
98	RGL_N815	RGL_LO413	45.318	0.9	44.260662	90.636
99	RGL_N825	RGL_LO417	0.856	0.9	0.83602821	1.712
100	RGL_N839	RGL_LO423	51.08	0.95	52.6597938	102.16
101	RGL_N846	RGL_LO426	113.294	0.9	110.650678	226.588
102	RGL_N849	RGL_LO428	67.918	0.9	66.3333695	135.836
103	RGL_N874	RGL_LO440	102.16	0.9	99.7764514	204.32
104	RGL_N879	RGL_LO441	0.57	0.9	0.55670103	1.14
105	RGL_N886	RGL_LO443	1.426	0.9	1.39272925	2.852
106	RGL_N891	RGL_LO445	2.519	0.9	2.46022789	5.038
107	RGL_N907	RGL_LO453	33.959	0.95	35.0092784	67.918
108	RGL_N911	RGL_LO454	1.141	0.9	1.11437873	2.282
109	RGL_N918	RGL_LO457	372.321	0.9	363.634183	744.642
110	RGL_N933	RGL_LO465	45.318	0.95	46.7195876	90.636
111	RGL_N939	RGL_LO469	118.812	0.9	116.039935	237.624
112	RGL_N947	RGL_LO473	113.294	0.95	116.797938	226.588
113	RGL_N965	RGL_LO485	1.141	0.9	1.11437873	2.282
114	RGL_N74	RGL_LO51	50	0.95	51.5463918	100
115	RGL_N1020	RGL_LO513	59.364	0.9	57.9789474	118.728
116	RGL_N75	RGL_LO52	20	0.9	19.5333695	40
117	RGL_N77	RGL_LO53	80	0.9	78.133478	160
118	RGL_N1059	RGL_LO533	67.918	0.9	66.3333695	135.836
119	RGL_N1062	RGL_LO535	153.239	0.9	149.6637	306.478
120	RGL_N1072	RGL_LO539	90.635	0.9	88.5203473	181.27

121	RGL_N1096	RGL_LO549	0.57	0.95	0.58762887	1.14
122	RGL_N1099	RGL_LO551	128.106	0.9	125.117092	256.212
123	RGL_N1103	RGL_LO553	423.873	0.95	436.982474	847.746
124	RGL_N1104	RGL_LO554	2.852	0.95	2.94020619	5.704
125	RGL_N82	RGL_LO56	140	0.9	136.733587	280
126	RGL_N1114	RGL_LO560	1.426	0.9	1.39272925	2.852
127	RGL_N1144	RGL_LO579	2.852	0.95	2.94020619	5.704
128	RGL_N84	RGL_LO58	200	0.95	206.185567	400
129	RGL_N1147	RGL_LO581	0.57	0.9	0.55670103	1.14
130	RGL_N86	RGL_LO59	145	0.9	141.616929	290
131	RGL_N1170	RGL_LO591	160.133	0.95	165.085567	320.266
132	RGL_N1199	RGL_LO606	6.297	0.95	6.49175258	12.594
133	RGL_N1213	RGL_LO611	2.852	0.95	2.94020619	5.704
134	RGL_N1219	RGL_LO614	45.318	0.95	46.7195876	90.636
135	RGL_N1250	RGL_LO628	212.673	0.95	219.250515	425.346
136	RGL_N1261	RGL_LO632	166.277	0.8	144.353337	332.554
137	RGL_N1271	RGL_LO640	550	0.8	477.482366	1100
138	RGL_N1276	RGL_LO642	90.635	0.95	93.4381443	181.27
139	RGL_N1287	RGL_LO647	50.939	0.8	44.2226804	101.878
140	RGL_N1296	RGL_LO653	33.959	0.95	35.0092784	67.918
141	RGL_N1307	RGL_LO662	90.635	0.95	93.4381443	181.27
142	RGL_N1309	RGL_LO664	372.321	0.9	363.634183	744.642
143	RGL_N1314	RGL_LO667	51.08	0.9	49.8882257	102.16
144	RGL_N109	RGL_LO67	385	0.8	334.237656	770
145	RGL_N1330	RGL_LO672	169.795	0.9	165.833424	339.59
146	RGL_N1335	RGL_LO676	153.239	0.95	157.978351	306.478
147	RGL_N1343	RGL_LO680	423.873	0.95	436.982474	847.746
148	RGL_N1350	RGL_LO683	102.16	0.95	105.319588	204.32
149	RGL_N1353	RGL_LO684	33.959	0.95	35.0092784	67.918
150	RGL_N1357	RGL_LO686	150	0.9	146.500271	300
151	RGL_N1361	RGL_LO688	67.918	0.9	66.3333695	135.836
152	RGL_N1437	RGL_LO723	128.106	0.95	132.068041	256.212
153	RGL_N1459	RGL_LO731	128.106	0.95	132.068041	256.212
154	RGL_N1464	RGL_LO735	67.918	0.95	70.0185567	135.836
155	RGL_N1467	RGL_LO736	0.285	0.95	0.29381443	0.57
156	RGL_N1470	RGL_LO739	600	0.8	520.889853	1200
157	RGL_N1472	RGL_LO740	0.57	0.95	0.58762887	1.14
158	RGL_N1486	RGL_LO746	143.2	0.9	139.858926	286.4
159	RGL_N1497	RGL_LO754	128.106	0.95	132.068041	256.212
160	RGL_N1498	RGL_LO755	90.635	0.95	93.4381443	181.27
161	RGL_N1516	RGL_LO763	0.57	0.9	0.55670103	1.14
162	RGL_N1528	RGL_LO767	166.277	0.8	144.353337	332.554
163	RGL_N124	RGL_LO77	40	0.95	41.2371134	80
164	RGL_N1544	RGL_LO774	100	0.9	97.6668475	200
165	RGL_N125	RGL_LO78	100	0.8	86.8149756	200

166	RGL_N1584	RGL_LO796	135.953	0.9	132.781009	271.906	
167	RGL_N1612	RGL_LO809	67.918	0.95	70.0185567	135.836	
168	RGL_N1620	RGL_LO813	157.5	0.95	162.371134	315	
169	RGL_N1651	RGL_LO826	2.852	0.95	2.94020619	5.704	
170	RGL_N1652	RGL_LO827	101.877	0.95	105.027835	203.754	
171	RGL_N1654	RGL_LO829	33.959	0.95	35.0092784	67.918	
172	RGL_N1665	RGL_LO831	0.57	0.95	0.58762887	1.14	
173	RGL_N1693	RGL_LO844	6.196	0.95	6.38762887	12.392	
174	RGL_N1695	RGL_LO846	200.651	0.95	206.856701	401.302	
175	RGL_N1714	RGL_LO858	160.284	0.95	165.241237	320.568	
176	RGL_N1718	RGL_LO860	157.5	0.95	162.371134	315	
177	RGL_N1726	RGL_LO865	2.519	0.9	2.46022789	5.038	
178	RGL_N1752	RGL_LO877	102.16	0.95	105.319588	204.32	
179	RGL_N1763	RGL_LO881	0.57	0.9	0.55670103	1.14	
180	RGL_N1768	RGL_LO883	128.106	0.9	125.117092	256.212	
181	RGL_N1802	RGL_LO897	102.16	0.9	99.7764514	204.32	
182	RGL_N1807	RGL_LO901	118.729	0.8	103.074552	237.458	
183	RGL_N1822	RGL_LO908	102.16	0.95	105.319588	204.32	
184	RGL_N1825	RGL_LO909	1.426	0.95	1.47010309	2.852	
185	RGL_N141	RGL_LO91	45	0.95	46.3917526	90	
186	RGL_N1842	RGL_LO918	128.106	0.95	132.068041	256.212	
187	RGL_N1863	RGL_LO929	118.729	0.95	122.401031	237.458	
188	RGL_N1865	RGL_LO930	1.426	0.95	1.47010309	2.852	
189	RGL_N1869	RGL_LO933	320.266	0.9	312.793706	640.532	
190	RGL_N1897	RGL_LO942	0.57	0.95	0.58762887	1.14	
191	RGL_N1909	RGL_LO946	212.673	0.95	219.250515	425.346	
192	RGL_N1917	RGL_LO949	67.918	0.8	58.9629951	135.836	
193	RGL_N1929	RGL_LO955	102.16	0.95	105.319588	204.32	
194	RGL_N1935	RGL_LO958	67.918	0.9	66.3333695	135.836	
195	RGL_N1953	RGL_LO964	0.57	0.9	0.55670103	1.14	
196	RGL_N1967	RGL_LO967	33.959	0.8	29.4814976	67.918	
197	RGL_N150	RGL_LO97	157.5	0.95	162.371134	315	
198	RGL_N1973	RGL_LO971	128.106	0.9	125.117092	256.212	
199	RGL_N1977	RGL_LO972	143.2	0.95	147.628866	286.4	
200	RGL_N1978	RGL_LO973	0.57	0.95	0.58762887	1.14	
201	RGL_N1989	RGL_LO978	2.478	0.9	2.42018448	4.956	
202	RGL_N154	RGL_LO98	1.426	0.9	1.39272925	2.852	
203	RGL_N1995	RGL_LO981	423.873	0.9	413.983397	847.746	
204	RGL_N2001	RGL_LO984	90.635	0.95	93.4381443	181.27	
205	RGL_N155	RGL_LO99	0.57	0.9	0.55670103	1.14	
206	RGL_N2025	RGL_LO998	128.106	0.95	132.068041	256.212	

Pandoin (PAN) ZS Power Network:

#	Node1	Element	S[kVA]	cosphi	PV[kW]	DT[kVA]	Bulk RE & ES
1	PAN_N2123	PAN_LO1037	6.163	1	6.688008681	12.326	PAN_F1_N1
2	PAN_N2131	PAN_LO1042	2.465	0.980019	2.621537531	4.93	500 kW PV
3	PAN_F1_N6_N2140	PAN_LO1044	2.465	0.980019	2.621537531	4.93	200 kW ES
4	PAN_N2153	PAN_LO1048	2.465	0.980019	2.621537531	4.93	
5	PAN_N2164	PAN_LO1054	2.465	0.980019	2.621537531	4.93	PAN_F1_N2
6	PAN_N2170	PAN_LO1057	12.327	0.980019	13.10981466	24.654	500 kW PV
7	PAN_N2228	PAN_LO1079	120.341	0.980019	127.9831432	240.682	200 kW ES
8	PAN_N2249	PAN_LO1089	2.465	0.980019	2.621537531	4.93	
9	PAN_N2261	PAN_LO1096	2.465	0.980019	2.621537531	4.93	PAN_F1_N3
10	PAN_N2279	PAN_LO1101	2.465	1	2.674986435	4.93	500 kW PV
11	PAN_N2289	PAN_LO1107	2.465	0.980019	2.621537531	4.93	200 kW ES
12	PAN_N2315	PAN_LO1117	2.465	0.980019	2.621537531	4.93	
13	PAN_N2340	PAN_LO1128	2.465	0.980019	2.621537531	4.93	PAN_F1_N4
14	PAN_N181	PAN_LO116	150	0.9	146.5002713	300	500 kW PV
15	PAN_N2425	PAN_LO1167	36.102	0.95	37.2185567	72.204	200 kW ES
16	PAN_N182	PAN_LO117	157.5	0.95	162.371134	315	
17	PAN_N183	PAN_LO118	2	0.9	1.953336951	4	PAN_F1_N5
18	PAN_N2454	PAN_LO1183	2.465	0.980019	2.621537531	4.93	500 kW PV
19	PAN_N2457	PAN_LO1185	2.465	0.980019	2.621537531	4.93	200 kW ES
20	PAN_N184	PAN_LO119	150	0.9	146.5002713	300	
21	PAN_N2477	PAN_LO1194	4.931	0.980019	5.244138566	9.862	
22	PAN_N2482	PAN_LO1197	60.17	0.980019	63.99103986	120.34	
23	PAN_N185	PAN_LO120	150	0.9	146.5002713	300	PAN_F2_N1
24	PAN_N2518	PAN_LO1209	4.931	0.980019	5.244138566	9.862	500 kW PV
25	PAN_N186	PAN_LO121	100	0.9	97.66684753	200	200 kW ES
26	PAN_N2537	PAN_LO1216	2.465	0.980019	2.621537531	4.93	
27	PAN_N187	PAN_LO122	100	0.9	97.66684753	200	PAN_F2_N2
28	PAN_N2554	PAN_LO1225	2.465	1	2.674986435	4.93	500 kW PV
29	PAN_N2560	PAN_LO1227	2.465	0.980019	2.621537531	4.93	200 kW ES
30	PAN_N188	PAN_LO123	50	0.9	48.83342377	100	
31	PAN_N2576	PAN_LO1235	2.465	0.980019	2.621537531	4.93	PAN_F2_N3
32	PAN_N2584	PAN_LO1239	2.465	0.980019	2.621537531	4.93	500 kW PV
33	PAN_N190	PAN_LO124	157.5	0.95	162.371134	315	200 kW ES
34	PAN_N2587	PAN_LO1241	2.465	0.980019	2.621537531	4.93	
35	PAN_N2600	PAN_LO1246	2.465	1	2.674986435	4.93	PAN_F2_N4
36	PAN_N2603	PAN_LO1248	60.17	1	65.29571351	120.34	500 kW PV
37	PAN_N191	PAN_LO125	2	0.9	1.953336951	4	200 kW ES
38	PAN_N2619	PAN_LO1252	6.163	0.980019	6.55437558	12.326	
39	PAN_N193	PAN_LO126	5	0.9	4.883342377	10	PAN_F2_N5
40	PAN_N194	PAN_LO127	27	0.95	27.83505155	54	500 kW PV
41	PAN_N196	PAN_LO128	2	0.9	1.953336951	4	200 kW ES

42	PAN_N198	PAN_LO129	2	0.9	1.953336951	4
43	PAN_N199	PAN_LO130	2	0.9	1.953336951	4
44	PAN_N200	PAN_LO131	2	0.9	1.953336951	4
45	PAN_N201	PAN_LO132	50	0.9	48.83342377	100
46	PAN_N202	PAN_LO133	5	0.9	4.883342377	10
47	PAN_N203	PAN_LO134	5	0.9	4.883342377	10
48	PAN_N204	PAN_LO135	150	0.9	146.5002713	300
49	PAN_F2_N2_N364	PAN_LO218	180.511	0.980019	191.9741831	361.022
50	PAN_N380	PAN_LO225	2.465	0.980019	2.621537531	4.93
51	PAN_N404	PAN_LO233	2.465	0.980019	2.621537531	4.93
52	PAN_N415	PAN_LO239	4.931	0.980019	5.244138566	9.862
53	PAN_N447	PAN_LO251	180.511	0.980019	191.9741831	361.022
54	PAN_N448	PAN_LO252	2.465	0.980019	2.621537531	4.93
55	PAN_N454	PAN_LO254	6.163	0.980019	6.55437558	12.326
56	PAN_N462	PAN_LO257	2.465	0.980019	2.621537531	4.93
57	PAN_N477	PAN_LO265	2.465	0.980019	2.621537531	4.93
58	PAN_N489	PAN_LO270	235.868	0.980019	250.8465779	471.736
59	PAN_N508	PAN_LO279	2.465	0.980019	2.621537531	4.93
60	PAN_N513	PAN_LO282	2.465	0.980019	2.621537531	4.93
61	PAN_N516	PAN_LO283	60.17	0.980019	63.99103986	120.34
62	PAN_N521	PAN_LO285	2.465	0.980019	2.621537531	4.93
63	PAN_N567	PAN_LO297	2.465	0.980019	2.621537531	4.93
64	PAN_N588	PAN_LO305	2.465	0.980019	2.621537531	4.93
65	PAN_N591	PAN_LO307	60.17	1	65.29571351	120.34
66	PAN_N603	PAN_LO313	180.511	0.980019	191.9741831	361.022
67	PAN_N614	PAN_LO316	2.465	0.980019	2.621537531	4.93
68	PAN_N633	PAN_LO326	2.465	0.980019	2.621537531	4.93
69	PAN_N656	PAN_LO338	180.511	0.980019	191.9741831	361.022
70	PAN_N663	PAN_LO342	2.465	0.980019	2.621537531	4.93
71	PAN_N54	PAN_LO35	70	0.9	68.36679327	140
72	PAN_N684	PAN_LO352	2.465	0.980019	2.621537531	4.93
73	PAN_N693	PAN_LO358	120.341	1	130.5925122	240.682
74	PAN_N697	PAN_LO360	120.341	0.980019	127.9831432	240.682
75	PAN_N57	PAN_LO38	300	0.8	260.4449267	600
76	PAN_N757	PAN_LO390	2.465	0.980019	2.621537531	4.93
77	PAN_F2_N3_N771	PAN_LO396	60.17	0.980019	63.99103986	120.34
78	PAN_N793	PAN_LO404	3.698	0.980019	3.932838049	7.396
79	PAN_N831	PAN_LO420	2.465	0.980019	2.621537531	4.93
80	PAN_N848	PAN_LO427	2.465	0.980019	2.621537531	4.93
81	PAN_N860	PAN_LO434	2.465	0.980019	2.621537531	4.93
82	PAN_N868	PAN_LO436	50	0.9	48.83342377	100
83	PAN_N870	PAN_LO437	2.465	0.980019	2.621537531	4.93
84	PAN_N889	PAN_LO444	2.465	1	2.674986435	4.93
85	PAN_N916	PAN_LO456	4.931	0.980019	5.244138566	9.862
86	PAN_N929	PAN_LO461	2.465	0.980019	2.621537531	4.93

87	PAN_N944	PAN_LO471	2.465	0.980019	2.621537531	4.93
88	PAN_N977	PAN_LO490	2.465	0.980019	2.621537531	4.93
89	PAN_N996	PAN_LO499	235.868	0.980019	250.8465779	471.736
90	PAN_N1016	PAN_LO509	235.868	0.980019	250.8465779	471.736
91	PAN_N1019	PAN_LO512	6.163	0.980019	6.55437558	12.326
92	PAN_N1022	PAN_LO515	2.465	1	2.674986435	4.93
93	PAN_N1026	PAN_LO517	12.327	1	13.37710255	24.654
94	PAN_N1035	PAN_LO522	2.465	0.980019	2.621537531	4.93
95	PAN_N1039	PAN_LO525	2.465	0.980019	2.621537531	4.93
96	PAN_N1052	PAN_LO529	2.46	0.98	2.616169289	4.92
97	PAN_N1066	PAN_LO536	2.465	0.980019	2.621537531	4.93
98	PAN_N1079	PAN_LO542	235.868	0.980019	250.8465779	471.736
99	PAN_N1095	PAN_LO548	2.465	0.980019	2.621537531	4.93
100	PAN_N1105	PAN_LO555	2.465	0.980019	2.621537531	4.93
101	PAN_N1145	PAN_LO580	2.465	0.980019	2.621537531	4.93
102	PAN_N1158	PAN_LO585	2.465	0.980019	2.621537531	4.93
103	PAN_N1168	PAN_LO590	2.465	0.980019	2.621537531	4.93
104	PAN_N1189	PAN_LO601	120.341	1	130.5925122	240.682
105	PAN_N1192	PAN_LO602	4.931	0.980019	5.244138566	9.862
106	PAN_N1223	PAN_LO616	6.163	1	6.688008681	12.326
107	PAN_N1227	PAN_LO618	12.327	0.980019	13.10981466	24.654
108	PAN_N1245	PAN_LO625	2.465	0.980019	2.621537531	4.93
109	PAN_N1264	PAN_LO635	50	0.9	48.83342377	100
110	PAN_N1283	PAN_LO646	120.341	0.980019	127.9831432	240.682
111	PAN_N1305	PAN_LO660	2.465	0.980019	2.621537531	4.93
112	PAN_N1306	PAN_LO661	27	0.95	27.83505155	54
113	PAN_N1320	PAN_LO670	256.559	0.980019	272.8515406	513.118
114	PAN_N1321	PAN_LO671	50	0.9	48.83342377	100
115	PAN_N1332	PAN_LO674	2.465	0.980019	2.621537531	4.93
116	PAN_N1341	PAN_LO678	2.465	0.980019	2.621537531	4.93
117	PAN_N1354	PAN_LO685	2.465	0.980019	2.621537531	4.93
118	PAN_N114	PAN_LO69	180	0.9	175.8003256	360
119	PAN_N115	PAN_LO70	150	0.9	146.5002713	300
120	PAN_N1418	PAN_LO714	235.868	0.980019	250.8465779	471.736
121	PAN_N1426	PAN_LO718	2.465	0.980019	2.621537531	4.93
122	PAN_N1435	PAN_LO722	4.931	0.980019	5.244138566	9.862
123	PAN_N1457	PAN_LO730	2.465	0.980019	2.621537531	4.93
124	PAN_N1489	PAN_LO749	2.465	0.980019	2.621537531	4.93
125	PAN_N1492	PAN_LO751	100	0.9	97.66684753	200
126	PAN_N1500	PAN_LO756	4.931	0.980019	5.244138566	9.862
127	PAN_N1513	PAN_LO761	2.465	0.980019	2.621537531	4.93
128	PAN_N1537	PAN_LO772	27	0.95	27.83505155	54
129	PAN_N1550	PAN_LO778	2.465	0.980019	2.621537531	4.93
130	PAN_N1555	PAN_LO781	6.163	1	6.688008681	12.326
131	PAN_N1561	PAN_LO784	2.465	0.980019	2.621537531	4.93

132	PAN_N1572	PAN_LO788	6.163	1	6.688008681	12.326
133	PAN_N1573	PAN_LO789	2.465	0.980019	2.621537531	4.93
134	PAN_N1577	PAN_LO792	2.465	0.980019	2.621537531	4.93
135	PAN_N1585	PAN_LO797	2.465	0.980019	2.621537531	4.93
136	PAN_N1586	PAN_LO798	2.465	0.980019	2.621537531	4.93
137	PAN_N1587	PAN_LO799	2.465	0.980019	2.621537531	4.93
138	PAN_N1607	PAN_LO807	2.465	0.980019	2.621537531	4.93
139	PAN_N1613	PAN_LO810	4.931	0.980019	5.244138566	9.862
140	PAN_N1671	PAN_LO833	4.931	0.980019	5.244138566	9.862
141	PAN_N1674	PAN_LO834	2.465	0.980019	2.621537531	4.93
142	PAN_N1682	PAN_LO837	2.465	0.980019	2.621537531	4.93
143	PAN_N1700	PAN_LO849	2.465	0.980019	2.621537531	4.93
144	PAN_N1705	PAN_LO852	180.511	0.9	176.2994031	361.022
145	PAN_N1713	PAN_LO857	2.465	0.980019	2.621537531	4.93
146	PAN_N1760	PAN_LO879	2.465	0.980019	2.621537531	4.93
147	PAN_N1772	PAN_LO886	2.465	0.980019	2.621537531	4.93
148	PAN_N1815	PAN_LO904	2.465	1	2.674986435	4.93
149	PAN_N1841	PAN_LO917	180.511	0.980019	191.9741831	361.022
150	PAN_N1844	PAN_LO919	2.465	0.980019	2.621537531	4.93
151	PAN_N144	PAN_LO94	150	0.9	146.5002713	300
152	PAN_N1891	PAN_LO940	2.465	0.980019	2.621537531	4.93
153	PAN_N1908	PAN_LO945	2.465	1	2.674986435	4.93
154	PAN_N1919	PAN_LO951	2.465	0.980019	2.621537531	4.93
155	PAN_N1920	PAN_LO952	2.465	0.980019	2.621537531	4.93
156	PAN_N1931	PAN_LO956	4.931	0.980019	5.244138566	9.862
157	PAN_N1940	PAN_LO960	2.465	0.980019	2.621537531	4.93
158	PAN_N1944	PAN_LO961	2.465	0.980019	2.621537531	4.93
159	PAN_N1968	PAN_LO969	4.931	0.980019	5.244138566	9.862
160	PAN_N1990	PAN_LO979	6.163	0.980019	6.55437558	12.326
161	PAN_N2005	PAN_LO986	12.327	1	13.37710255	24.654

Frenchville (FRN) ZS Power Network:

#	Node1	Element	S[kVA]	cosphi	PV[kW]	DT[kVA]	Bulk RE & ES
1	FRN_N2048	FRN_LO1011	117.281	0.9	114.5446555	234.562	FRN_F1_N1
2	FRN_N2062	FRN_LO1014	102.046	0.9	99.66511123	204.092	500 kW PV
3	FRN_N2070	FRN_LO1017	153.068	0.9	149.4966902	306.136	200 kW ES
4	FRN_N2071	FRN_LO1018	51.023	0.9	49.83255562	102.046	
5	FRN_N2127	FRN_LO1040	12.731	0.95	13.12474227	25.462	FRN_F1_N2
6	FRN_N2138	FRN_LO1043	125.578	0.95	129.4618557	251.156	500 kW PV
7	FRN_N2157	FRN_LO1050	192.202	0.95	198.1463918	384.404	200 kW ES
8	FRN_N2160	FRN_LO1052	117.281	0.95	120.9082474	234.562	
9	FRN_N2166	FRN_LO1055	128.135	0.95	132.0979381	256.27	FRN_F1_N3
10	FRN_N2168	FRN_LO1056	188.366	0.9	183.971134	376.732	500 kW PV
11	FRN_N2177	FRN_LO1061	100	0.9	97.66684753	200	200 kW ES
12	FRN_N2179	FRN_LO1062	188.366	0.95	194.1917526	376.732	
13	FRN_N2227	FRN_LO1078	102.046	0.8	88.59120998	204.092	FRN_F1_N4
14	FRN_N2254	FRN_LO1092	153.068	0.9	149.4966902	306.136	500 kW PV
15	FRN_N2272	FRN_LO1099	221.66	0.9	216.4883342	443.32	200 kW ES
16	FRN_N2283	FRN_LO1105	125.578	0.95	129.4618557	251.156	
17	FRN_N2290	FRN_LO1108	192.202	0.9	187.7176343	384.404	FRN_F1_N5
18	FRN_N2313	FRN_LO1115	331.904	0.95	342.1690722	663.808	500 kW PV
19	FRN_N2321	FRN_LO1120	331.904	0.95	342.1690722	663.808	200 kW ES
20	FRN_N2352	FRN_LO1132	188.366	0.95	194.1917526	376.732	
21	FRN_N2362	FRN_LO1135	61.952	0.9	60.50656538	123.904	
22	FRN_N2382	FRN_LO1143	125.578	0.9	122.6480738	251.156	
23	FRN_N2390	FRN_LO1147	251.155	0.9	245.2951709	502.31	FRN_F2_N1
24	FRN_N2401	FRN_LO1153	64.067	0.95	66.04845361	128.134	500 kW PV
25	FRN_N2403	FRN_LO1154	123.905	0.95	127.7371134	247.81	200 kW ES
26	FRN_N2414	FRN_LO1161	125.578	0.9	122.6480738	251.156	
27	FRN_N2429	FRN_LO1169	128.135	0.95	132.0979381	256.27	FRN_F2_N2
28	FRN_N2435	FRN_LO1173	6.365	0.95	6.56185567	12.73	500 kW PV
29	FRN_N2444	FRN_LO1179	123.905	0.95	127.7371134	247.81	200 kW ES
30	FRN_N2448	FRN_LO1180	6.365	0.9	6.216494845	12.73	
31	FRN_N2463	FRN_LO1188	102.046	0.95	105.2020619	204.092	FRN_F2_N3
32	FRN_N2534	FRN_LO1215	185.857	0.9	181.5206728	371.714	500 kW PV
33	FRN_N2553	FRN_LO1224	64.067	0.95	66.04845361	128.134	200 kW ES
34	FRN_N2575	FRN_LO1234	64.067	0.9	62.57221921	128.134	
35	FRN_N2578	FRN_LO1236	6.365	0.8	5.525773196	12.73	FRN_F2_N4
36	FRN_N2621	FRN_LO1253	819.791	0.9	800.664026	1639.582	500 kW PV
37	FRN_N2628	FRN_LO1259	352.057	0.9	343.8429734	704.114	200 kW ES
38	FRN_N2633	FRN_LO1261	125.578	0.95	129.4618557	251.156	
39	FRN_N2648	FRN_LO1267	153.068	0.9	149.4966902	306.136	FRN_F2_N5
40	FRN_N2651	FRN_LO1268	192.202	0.9	187.7176343	384.404	500 kW PV
41	FRN_N2657	FRN_LO1271	160.168	0.9	156.4310364	320.336	200 kW ES
42	FRN_N2659	FRN_LO1272	12.731	0.95	13.12474227	25.462	

43	FRN_N2702	FRN_LO1283	102.046	0.9	99.66511123	204.092
44	FRN_N208	FRN_LO138	157.5	0.95	162.371134	315
45	FRN_N256	FRN_LO165	150	0.9	146.5002713	300
46	FRN_N258	FRN_LO167	100	0.9	97.66684753	200
47	FRN_N259	FRN_LO168	100	0.8	86.81497558	200
48	FRN_N261	FRN_LO169	600	0.8	520.8898535	1200
49	FRN_N263	FRN_LO170	600	0.8	520.8898535	1200
50	FRN_N264	FRN_LO171	102.046	0.8	88.59120998	204.092
51	FRN_N267	FRN_LO174	100	0.9	97.66684753	200
52	FRN_N270	FRN_LO176	100	0.9	97.66684753	200
53	FRN_N292	FRN_LO179	100	0.9	97.66684753	200
54	FRN_N305	FRN_LO187	100	0.9	97.66684753	200
55	FRN_N307	FRN_LO188	50	0.9	48.83342377	100
56	FRN_N309	FRN_LO189	160.722	0.95	165.6927835	321.444
57	FRN_N311	FRN_LO190	153.068	0.9	149.4966902	306.136
58	FRN_N312	FRN_LO191	150	0.9	146.5002713	300
59	FRN_N314	FRN_LO192	100	0.9	97.66684753	200
60	FRN_N328	FRN_LO204	153.068	0.9	149.4966902	306.136
61	FRN_N330	FRN_LO205	153.068	0.9	149.4966902	306.136
62	FRN_N331	FRN_LO206	160.722	0.95	165.6927835	321.444
63	FRN_N333	FRN_LO207	102.046	0.8	88.59120998	204.092
64	FRN_N335	FRN_LO208	153.068	0.9	149.4966902	306.136
65	FRN_N336	FRN_LO209	102.046	0.8	88.59120998	204.092
66	FRN_N340	FRN_LO212	117.281	0.9	114.5446555	234.562
67	FRN_N360	FRN_LO216	123.905	0.95	127.7371134	247.81
68	FRN_N425	FRN_LO242	331.904	0.9	324.1601736	663.808
69	FRN_N440	FRN_LO248	188.366	0.95	194.1917526	376.732
70	FRN_N460	FRN_LO256	125.578	0.9	122.6480738	251.156
71	FRN_N466	FRN_LO260	125.578	0.95	129.4618557	251.156
72	FRN_N469	FRN_LO261	123.905	0.95	127.7371134	247.81
73	FRN_N593	FRN_LO308	192.202	0.9	187.7176343	384.404
74	FRN_N600	FRN_LO311	128.135	0.9	125.1454151	256.27
75	FRN_N627	FRN_LO324	125.578	0.9	122.6480738	251.156
76	FRN_N643	FRN_LO333	62.789	0.95	64.73092784	125.578
77	FRN_N650	FRN_LO335	128.135	0.95	132.0979381	256.27
78	FRN_N668	FRN_LO343	156.972	0.9	153.3096039	313.944
79	FRN_N674	FRN_LO345	6.365	0.8	5.525773196	12.73
80	FRN_N688	FRN_LO354	84.981	0.95	87.60927835	169.962
81	FRN_N689	FRN_LO355	128.135	0.9	125.1454151	256.27
82	FRN_N694	FRN_LO359	153.068	0.9	149.4966902	306.136
83	FRN_N711	FRN_LO366	221.66	0.95	228.5154639	443.32
84	FRN_N744	FRN_LO383	221.66	0.95	228.5154639	443.32
85	FRN_N746	FRN_LO385	153.068	0.9	149.4966902	306.136
86	FRN_N779	FRN_LO398	12.24	0.95	12.6185567	24.48
87	FRN_N781	FRN_LO399	2.511	0.9	2.452414542	5.022

88	FRN_N806	FRN_LO409	125.578	0.95	129.4618557	251.156
89	FRN_N808	FRN_LO410	102.046	0.95	105.2020619	204.092
90	FRN_N858	FRN_LO433	221.66	0.95	228.5154639	443.32
91	FRN_N883	FRN_LO442	123.905	0.95	127.7371134	247.81
92	FRN_N893	FRN_LO446	128.135	0.9	125.1454151	256.27
93	FRN_N904	FRN_LO451	185.857	0.95	191.6051546	371.714
94	FRN_N930	FRN_LO462	102.046	0.8	88.59120998	204.092
95	FRN_N934	FRN_LO466	123.905	0.95	127.7371134	247.81
96	FRN_N951	FRN_LO476	102.046	0.95	105.2020619	204.092
97	FRN_N961	FRN_LO482	64.067	0.95	66.04845361	128.134
98	FRN_N971	FRN_LO488	123.905	0.95	127.7371134	247.81
99	FRN_N979	FRN_LO491	62.789	0.95	64.73092784	125.578
100	FRN_N988	FRN_LO496	125.578	0.95	129.4618557	251.156
101	FRN_N1001	FRN_LO503	185.857	0.9	181.5206728	371.714
102	FRN_N1015	FRN_LO508	127.557	0.95	131.5020619	255.114
103	FRN_N1018	FRN_LO511	185.857	0.9	181.5206728	371.714
104	FRN_N1031	FRN_LO519	192.202	0.9	187.7176343	384.404
105	FRN_N1032	FRN_LO520	100	0.9	97.66684753	200
106	FRN_N1037	FRN_LO524	1.005	0.9	0.981551818	2.01
107	FRN_N1088	FRN_LO546	62.789	0.95	64.73092784	125.578
108	FRN_N1108	FRN_LO557	123.905	0.95	127.7371134	247.81
109	FRN_N1126	FRN_LO565	125.578	0.95	129.4618557	251.156
110	FRN_N1129	FRN_LO567	100	0.9	97.66684753	200
111	FRN_N83	FRN_LO57	600	0.9	586.0010852	1200
112	FRN_N1138	FRN_LO575	192.202	0.8	166.8601194	384.404
113	FRN_N1139	FRN_LO576	125.578	0.95	129.4618557	251.156
114	FRN_N1142	FRN_LO578	128.135	0.95	132.0979381	256.27
115	FRN_N1160	FRN_LO586	450	0.8	390.6673901	900
116	FRN_N1164	FRN_LO588	157.5	0.95	162.371134	315
117	FRN_N1240	FRN_LO623	5.023	0.9	4.905805751	10.046
118	FRN_N1249	FRN_LO627	123.905	0.9	121.0141074	247.81
119	FRN_N1253	FRN_LO629	188.366	0.9	183.971134	376.732
120	FRN_N1262	FRN_LO633	125.578	0.95	129.4618557	251.156
121	FRN_N1270	FRN_LO639	128.135	0.95	132.0979381	256.27
122	FRN_N1273	FRN_LO641	100	0.9	97.66684753	200
123	FRN_N1295	FRN_LO652	60.116	0.95	61.97525773	120.232
124	FRN_N1308	FRN_LO663	185.857	0.95	191.6051546	371.714
125	FRN_N1317	FRN_LO669	62.789	0.9	61.3240369	125.578
126	FRN_N1338	FRN_LO677	185.857	0.95	191.6051546	371.714
127	FRN_N1393	FRN_LO700	153.068	0.9	149.4966902	306.136
128	FRN_N1399	FRN_LO704	125.578	0.95	129.4618557	251.156
129	FRN_N1412	FRN_LO711	123.905	0.95	127.7371134	247.81
130	FRN_N1417	FRN_LO713	50	0.9	48.83342377	100
131	FRN_N1423	FRN_LO717	94.183	0.95	97.09587629	188.366
132	FRN_N1462	FRN_LO733	100	0.9	97.66684753	200

133	FRN_N1463	FRN_LO734	185.857	0.9	181.5206728	371.714
134	FRN_N1474	FRN_LO742	12.558	0.9	12.26500271	25.116
135	FRN_N1529	FRN_LO768	150	0.9	146.5002713	300
136	FRN_N1594	FRN_LO802	464.637	0.9	453.7963104	929.274
137	FRN_N129	FRN_LO81	160	0.9	156.266956	320
138	FRN_N1629	FRN_LO817	100	0.9	97.66684753	200
139	FRN_N130	FRN_LO82	157.5	0.95	162.371134	315
140	FRN_N132	FRN_LO83	100	0.8	86.81497558	200
141	FRN_N1677	FRN_LO835	255.114	0.9	249.1618014	510.228
142	FRN_N135	FRN_LO84	215	0.95	221.6494845	430
143	FRN_N1694	FRN_LO845	192.202	0.9	187.7176343	384.404
144	FRN_N136	FRN_LO85	250	0.8	217.037439	500
145	FRN_N1703	FRN_LO850	128.135	0.9	125.1454151	256.27
146	FRN_N1708	FRN_LO854	185.857	0.9	181.5206728	371.714
147	FRN_N1722	FRN_LO862	153.068	0.95	157.8020619	306.136
148	FRN_N1732	FRN_LO868	125.578	0.95	129.4618557	251.156
149	FRN_N1744	FRN_LO873	313.944	0.95	323.6536082	627.888
150	FRN_N1750	FRN_LO876	192.202	0.95	198.1463918	384.404
151	FRN_N1791	FRN_LO893	100	0.9	97.66684753	200
152	FRN_N1812	FRN_LO902	102.046	0.95	105.2020619	204.092
153	FRN_N1820	FRN_LO907	185.857	0.9	181.5206728	371.714
154	FRN_N1829	FRN_LO912	188.366	0.9	183.971134	376.732
155	FRN_N1831	FRN_LO913	102.046	0.9	99.66511123	204.092
156	FRN_N1835	FRN_LO914	309.762	0.9	302.5347802	619.524
157	FRN_N1853	FRN_LO925	185.857	0.9	181.5206728	371.714
158	FRN_N1862	FRN_LO928	123.905	0.95	127.7371134	247.81
159	FRN_N1866	FRN_LO931	102.046	0.95	105.2020619	204.092
160	FRN_N1880	FRN_LO937	521.453	0.9	509.2867065	1042.906
161	FRN_N1915	FRN_LO948	62.789	0.95	64.73092784	125.578
162	FRN_N145	FRN_LO95	345	0.8	299.5116658	690
163	FRN_N1969	FRN_LO970	123.905	0.95	127.7371134	247.81
164	FRN_N1996	FRN_LO982	150	0.9	146.5002713	300
165	FRN_N2009	FRN_LO989	51.023	0.9	49.83255562	102.046
166	FRN_N2014	FRN_LO990	188.366	0.9	183.971134	376.732
167	FRN_N2016	FRN_LO991	188.366	0.95	194.1917526	376.732
168	FRN_N2019	FRN_LO994	153.068	0.9	149.4966902	306.136

Parkhurst (PKH) ZS Power Network:

#	Node1	Element	S[kVA]	cosphi	PV[kW]	DT[kVA]	Bulk RE & ES
1	PKH_N2034	PKH_LO1002	50.917	0.95	52.49175258	101.834	PKH_F1_N1
2	PKH_N2037	PKH_LO1003	1.465	0.9	1.430819316	2.93	500 kW PV
3	PKH_N2046	PKH_LO1010	159.432	0.9	155.7122084	318.864	200 kW ES
4	PKH_N2072	PKH_LO1019	26.978	0.95	27.81237113	53.956	
5	PKH_N2076	PKH_LO1021	1.099	0.9	1.073358654	2.198	PKH_F1_N2
6	PKH_N2077	PKH_LO1022	101.834	0.95	104.9835052	203.668	500 kW PV
7	PKH_N2122	PKH_LO1036	85.644	0.8	74.35181769	171.288	200 kW ES
8	PKH_N167	PKH_LO104	3.663	0.95	3.77628866	7.326	
9	PKH_N168	PKH_LO105	0.733	0.9	0.715897992	1.466	PKH_F1_N3
10	PKH_N169	PKH_LO106	0.733	0.9	0.715897992	1.466	500 kW PV
11	PKH_N2183	PKH_LO1064	0.733	0.9	0.715897992	1.466	200 kW ES
12	PKH_N2205	PKH_LO1069	214.11	0.9	209.1144872	428.22	
13	PKH_N170	PKH_LO107	0.733	0.9	0.715897992	1.466	PKH_F1_N4
14	PKH_N2210	PKH_LO1071	53.144	0.9	51.90406945	106.288	500 kW PV
15	PKH_N2223	PKH_LO1077	1.465	0.9	1.430819316	2.93	200 kW ES
16	PKH_N171	PKH_LO108	26.978	0.95	27.81237113	53.956	
17	PKH_N172	PKH_LO109	1.831	0.9	1.788279978	3.662	PKH_F1_N5
18	PKH_N173	PKH_LO110	0.733	0.9	0.715897992	1.466	500 kW PV
19	PKH_N2282	PKH_LO1104	101.834	0.95	104.9835052	203.668	200 kW ES
20	PKH_N174	PKH_LO111	0.733	0.9	0.715897992	1.466	
21	PKH_N2309	PKH_LO1114	3.663	0.9	3.577536625	7.326	
22	PKH_N2316	PKH_LO1118	3.663	0.9	3.577536625	7.326	
23	PKH_N2319	PKH_LO1119	42.822	0.95	44.14639175	85.644	PKH_F2_N1
24	PKH_N175	PKH_LO112	1.831	0.9	1.788279978	3.662	500 kW PV
25	PKH_N177	PKH_LO113	159.432	0.9	155.7122084	318.864	200 kW ES
26	PKH_N2350	PKH_LO1131	0.366	0.95	0.377319588	0.732	
27	PKH_N2365	PKH_LO1136	128.466	0.9	125.4686923	256.932	PKH_F2_N2
28	PKH_N178	PKH_LO114	106.288	0.9	103.8081389	212.576	500 kW PV
29	PKH_N2392	PKH_LO1149	85.644	0.95	88.29278351	171.288	200 kW ES
30	PKH_N179	PKH_LO115	160.388	0.95	165.3484536	320.776	
31	PKH_N2406	PKH_LO1156	1.099	0.9	1.073358654	2.198	PKH_F2_N3
32	PKH_N2416	PKH_LO1162	1.831	0.95	1.887628866	3.662	500 kW PV
33	PKH_N2437	PKH_LO1175	450	0.8	390.6673901	900	200 kW ES
34	PKH_N2438	PKH_LO1176	42.822	0.9	41.82289745	85.644	
35	PKH_N2451	PKH_LO1182	85.644	0.95	88.29278351	171.288	PKH_F2_N4
36	PKH_N2484	PKH_LO1198	85.644	0.9	83.6457949	171.288	500 kW PV
37	PKH_N2496	PKH_LO1202	0.982	0.9	0.959088443	1.964	200 kW ES
38	PKH_N2511	PKH_LO1205	1	0.9	0.976668475	2	
39	PKH_N2543	PKH_LO1219	50.917	0.95	52.49175258	101.834	PKH_F2_N5
40	PKH_N2565	PKH_LO1229	3880	0.8	3368.421053	7760	500 kW PV
41	PKH_N2611	PKH_LO1250	106.288	0.8	92.27390125	212.576	200 kW ES
42	PKH_N2622	PKH_LO1254	152.751	0.9	149.1870863	305.502	

43	PKH_N2642	PKH_LO1265	1.831	0.95	1.887628866	3.662
44	PKH_N2664	PKH_LO1274	1.831	0.9	1.788279978	3.662
45	PKH_N2668	PKH_LO1275	1.831	0.9	1.788279978	3.662
46	PKH_N265	PKH_LO172	85.644	0.9	83.6457949	171.288
47	PKH_N298	PKH_LO183	101.834	0.9	99.45805751	203.668
48	PKH_N299	PKH_LO184	85.644	0.9	83.6457949	171.288
49	PKH_N300	PKH_LO185	85.644	0.8	74.35181769	171.288
50	PKH_N321	PKH_LO198	101.834	0.9	99.45805751	203.668
51	PKH_N322	PKH_LO199	152.751	0.9	149.1870863	305.502
52	PKH_N324	PKH_LO200	42.822	0.9	41.82289745	85.644
53	PKH_N325	PKH_LO201	134.889	0.95	139.0608247	269.778
54	PKH_N326	PKH_LO202	85.644	0.8	74.35181769	171.288
55	PKH_N327	PKH_LO203	85.644	0.9	83.6457949	171.288
56	PKH_N366	PKH_LO220	0.733	0.9	0.715897992	1.466
57	PKH_N410	PKH_LO237	2.5	0.9	2.441671188	5
58	PKH_N458	PKH_LO255	3.663	0.9	3.577536625	7.326
59	PKH_N482	PKH_LO268	265.72	0.9	259.5203473	531.44
60	PKH_N523	PKH_LO287	152.751	0.8	132.6107434	305.502
61	PKH_N540	PKH_LO292	127.292	0.95	131.228866	254.584
62	PKH_N544	PKH_LO293	0.733	0.9	0.715897992	1.466
63	PKH_N556	PKH_LO295	3100	0.8	2691.264243	6200
64	PKH_N585	PKH_LO304	152.751	0.9	149.1870863	305.502
65	PKH_N599	PKH_LO310	53.144	0.9	51.90406945	106.288
66	PKH_N608	PKH_LO314	1.831	0.9	1.788279978	3.662
67	PKH_N610	PKH_LO315	159.432	0.95	164.3628866	318.864
68	PKH_N624	PKH_LO321	107.055	0.9	104.5572436	214.11
69	PKH_N625	PKH_LO322	106.288	0.95	109.5752577	212.576
70	PKH_N676	PKH_LO346	159.432	0.9	155.7122084	318.864
71	PKH_N692	PKH_LO357	106.288	0.95	109.5752577	212.576
72	PKH_N701	PKH_LO361	3.663	0.95	3.77628866	7.326
73	PKH_N714	PKH_LO367	132.86	0.95	136.9690722	265.72
74	PKH_N721	PKH_LO371	152.751	0.9	149.1870863	305.502
75	PKH_N730	PKH_LO376	0.733	0.9	0.715897992	1.466
76	PKH_N736	PKH_LO378	101.834	0.95	104.9835052	203.668
77	PKH_N738	PKH_LO379	1.831	0.9	1.788279978	3.662
78	PKH_N739	PKH_LO380	1.099	0.9	1.073358654	2.198
79	PKH_N748	PKH_LO386	101.834	0.95	104.9835052	203.668
80	PKH_N758	PKH_LO391	128.466	0.95	132.4391753	256.932
81	PKH_N764	PKH_LO393	106.288	0.8	92.27390125	212.576
82	PKH_N63	PKH_LO41	300	0.8	260.4449267	600
83	PKH_N817	PKH_LO414	1.099	0.95	1.132989691	2.198
84	PKH_N830	PKH_LO419	0.733	0.9	0.715897992	1.466
85	PKH_N64	PKH_LO42	157.5	0.95	162.371134	315
86	PKH_N833	PKH_LO421	1.473	0.95	1.518556701	2.946
87	PKH_N873	PKH_LO439	1500	0.8	1302.224634	3000

88	PKH_N896	PKH_LO447	152.751	0.8	132.6107434	305.502
89	PKH_N924	PKH_LO458	128.466	0.9	125.4686923	256.932
90	PKH_N948	PKH_LO474	152.751	0.9	149.1870863	305.502
91	PKH_N953	PKH_LO477	152.751	0.9	149.1870863	305.502
92	PKH_N954	PKH_LO478	214.11	0.9	209.1144872	428.22
93	PKH_N957	PKH_LO480	85.644	0.9	83.6457949	171.288
94	PKH_N962	PKH_LO483	85.644	0.9	83.6457949	171.288
95	PKH_N966	PKH_LO486	1.831	0.95	1.887628866	3.662
96	PKH_N980	PKH_LO492	1.053	0.95	1.08556701	2.106
97	PKH_N994	PKH_LO498	134.889	0.95	139.0608247	269.778
98	PKH_N998	PKH_LO501	42.822	0.9	41.82289745	85.644
99	PKH_N1009	PKH_LO507	0.733	0.9	0.715897992	1.466
100	PKH_N1036	PKH_LO523	42.822	0.9	41.82289745	85.644
101	PKH_N1044	PKH_LO528	1.831	0.95	1.887628866	3.662
102	PKH_N1056	PKH_LO531	128.466	0.9	125.4686923	256.932
103	PKH_N79	PKH_LO54	330	0.8	286.4894194	660
104	PKH_N1073	PKH_LO540	152.751	0.95	157.4752577	305.502
105	PKH_N1092	PKH_LO547	30.55	0.95	31.49484536	61.1
106	PKH_N1101	PKH_LO552	101.834	0.95	104.9835052	203.668
107	PKH_N1115	PKH_LO561	50.917	0.9	49.72902876	101.834
108	PKH_N1124	PKH_LO564	1.099	0.95	1.132989691	2.198
109	PKH_N1130	PKH_LO568	0.733	0.9	0.715897992	1.466
110	PKH_N1133	PKH_LO570	0.733	0.9	0.715897992	1.466
111	PKH_N1136	PKH_LO573	265.72	0.9	259.5203473	531.44
112	PKH_N1141	PKH_LO577	265.72	0.9	259.5203473	531.44
113	PKH_N1177	PKH_LO594	50.917	0.9	49.72902876	101.834
114	PKH_N1181	PKH_LO595	3.663	0.95	3.77628866	7.326
115	PKH_N1182	PKH_LO596	85.644	0.95	88.29278351	171.288
116	PKH_N1184	PKH_LO598	101.834	0.9	99.45805751	203.668
117	PKH_N1187	PKH_LO600	101.834	0.9	99.45805751	203.668
118	PKH_N1218	PKH_LO613	0.982	0.9	0.959088443	1.964
119	PKH_N1221	PKH_LO615	0.733	0.9	0.715897992	1.466
120	PKH_N1243	PKH_LO624	159.432	0.9	155.7122084	318.864
121	PKH_N1265	PKH_LO636	3.663	0.9	3.577536625	7.326
122	PKH_N1292	PKH_LO649	1.831	0.9	1.788279978	3.662
123	PKH_N93	PKH_LO65	617	0.8	535.6483993	1234
124	PKH_N1301	PKH_LO658	42.822	0.95	44.14639175	85.644
125	PKH_N1303	PKH_LO659	50.917	0.95	52.49175258	101.834
126	PKH_N1310	PKH_LO665	85.644	0.9	83.6457949	171.288
127	PKH_N1331	PKH_LO673	128.466	0.9	125.4686923	256.932
128	PKH_N112	PKH_LO68	250	0.95	257.7319588	500
129	PKH_N1345	PKH_LO681	101.834	0.95	104.9835052	203.668
130	PKH_N1358	PKH_LO687	101.834	0.95	104.9835052	203.668
131	PKH_N1367	PKH_LO690	0.733	0.9	0.715897992	1.466
132	PKH_N1395	PKH_LO701	128.466	0.9	125.4686923	256.932

133	PKH_N1396	PKH_LO702	1.099	0.95	1.132989691	2.198
134	PKH_N1400	PKH_LO705	106.288	0.9	103.8081389	212.576
135	PKH_N1402	PKH_LO706	1.099	0.95	1.132989691	2.198
136	PKH_N1403	PKH_LO707	0.733	0.9	0.715897992	1.466
137	PKH_N116	PKH_LO71	160	0.9	156.266956	320
138	PKH_N119	PKH_LO73	150	0.9	146.5002713	300
139	PKH_N1461	PKH_LO732	152.751	0.9	149.1870863	305.502
140	PKH_N1473	PKH_LO741	254.584	0.9	248.6441671	509.168
141	PKH_N1483	PKH_LO744	85.644	0.95	88.29278351	171.288
142	PKH_N1487	PKH_LO747	0.733	0.9	0.715897992	1.466
143	PKH_N1488	PKH_LO748	300	0.8	260.4449267	600
144	PKH_N121	PKH_LO75	110	0.9	107.4335323	220
145	PKH_N1494	PKH_LO752	0.733	0.9	0.715897992	1.466
146	PKH_N1496	PKH_LO753	0.733	0.9	0.715897992	1.466
147	PKH_N1508	PKH_LO759	1.831	0.9	1.788279978	3.662
148	PKH_N122	PKH_LO76	300	0.95	309.2783505	600
149	PKH_N1542	PKH_LO773	1.831	0.9	1.788279978	3.662
150	PKH_N1547	PKH_LO777	0.733	0.9	0.715897992	1.466
151	PKH_N1552	PKH_LO779	0.366	0.9	0.357460662	0.732
152	PKH_N1563	PKH_LO785	101.834	0.9	99.45805751	203.668
153	PKH_N127	PKH_LO79	115	0.9	112.3168747	230
154	PKH_N128	PKH_LO80	15	0.9	14.65002713	30
155	PKH_N1601	PKH_LO805	85.644	0.9	83.6457949	171.288
156	PKH_N1630	PKH_LO818	50.917	0.95	52.49175258	101.834
157	PKH_N1643	PKH_LO823	3.663	0.95	3.77628866	7.326
158	PKH_N1690	PKH_LO843	3.663	0.9	3.577536625	7.326
159	PKH_N1696	PKH_LO847	106.288	0.9	103.8081389	212.576
160	PKH_N1720	PKH_LO861	316.882	0.95	326.6824742	633.764
161	PKH_N138	PKH_LO87	160	0.9	156.266956	320
162	PKH_N139	PKH_LO89	600	0.8	520.8898535	1200
163	PKH_N1816	PKH_LO905	128.466	0.95	132.4391753	256.932
164	PKH_N1818	PKH_LO906	85.644	0.95	88.29278351	171.288
165	PKH_N1828	PKH_LO911	0.733	0.9	0.715897992	1.466
166	PKH_N1837	PKH_LO915	5.265	0.95	5.427835052	10.53
167	PKH_N143	PKH_LO93	140	0.9	136.7335865	280
168	PKH_N1885	PKH_LO939	85.644	0.9	83.6457949	171.288
169	PKH_N1918	PKH_LO950	152.751	0.9	149.1870863	305.502
170	PKH_N147	PKH_LO96	500	0.8	434.0748779	1000
171	PKH_N1985	PKH_LO976	19.644	0.95	20.25154639	39.288
172	PKH_N1993	PKH_LO980	0.733	0.9	0.715897992	1.466
173	PKH_N2023	PKH_LO996	0.733	0.9	0.715897992	1.466
174	PKH_N2024	PKH_LO997	152.751	0.9	149.1870863	305.502

Berserker (BER) ZS Power Network:

#	Node1	Element	S[kVA]	cosphi	PV[kW]	DT[kVA]	Bulk RE & ES
1	BER_N2033	BER_LO1001	239.832	0.9	234.2363538	479.664	BER_F1_N1
2	BER_N2044	BER_LO1009	192.159	0.95	198.1020619	384.318	500 kW PV
3	BER_N2088	BER_LO1026	102.16	0.95	105.3195876	204.32	200 kW ES
4	BER_N2202	BER_LO1068	255.446	0.95	263.3463918	510.892	
5	BER_N2211	BER_LO1072	102.16	0.95	105.3195876	204.32	BER_F1_N2
6	BER_N2241	BER_LO1083	118.729	0.95	122.4010309	237.458	500 kW PV
7	BER_N2258	BER_LO1095	102.16	0.9	99.77645144	204.32	200 kW ES
8	BER_N2266	BER_LO1097	401.302	0.95	413.7134021	802.604	
9	BER_N2277	BER_LO1100	51.08	0.9	49.88822572	102.16	BER_F1_N3
10	BER_N2333	BER_LO1123	1.677	0.9	1.637873033	3.354	500 kW PV
11	BER_N2339	BER_LO1127	439.296	0.9	429.0465545	878.592	200 kW ES
12	BER_N2419	BER_LO1165	255.446	0.9	249.4860553	510.892	
13	BER_N2462	BER_LO1187	150	0.9	146.5002713	300	BER_F1_N4
14	BER_N2515	BER_LO1207	118.812	0.95	122.4865979	237.624	500 kW PV
15	BER_N2517	BER_LO1208	118.729	0.95	122.4010309	237.458	200 kW ES
16	BER_N2533	BER_LO1214	118.812	0.95	122.4865979	237.624	
17	BER_N254	BER_LO164	157.5	0.95	162.371134	315	BER_F1_N5
18	BER_N257	BER_LO166	201.767	0.95	208.0072165	403.534	500 kW PV
19	BER_N318	BER_LO196	100	0.9	97.66684753	200	200 kW ES
20	BER_N319	BER_LO197	50	0.9	48.83342377	100	
21	BER_N339	BER_LO211	340.99	0.9	333.0341834	681.98	
22	BER_N358	BER_LO215	439.604	0.9	429.3473684	879.208	
23	BER_N486	BER_LO269	153.239	0.9	149.6637005	306.478	BER_F2_N1
24	BER_N490	BER_LO271	150	0.9	146.5002713	300	500 kW PV
25	BER_N637	BER_LO329	363.519	0.9	355.0375475	727.038	200 kW ES
26	BER_N52	BER_LO34	4000	0.9	3906.673901	8000	
27	BER_N56	BER_LO37	90	0.9	87.90016278	180	BER_F2_N2
28	BER_N785	BER_LO402	89.046	0.95	91.8	178.092	500 kW PV
29	BER_N66	BER_LO43	260	0.9	253.9338036	520	200 kW ES
30	BER_N856	BER_LO432	153.239	0.9	149.6637005	306.478	
31	BER_N67	BER_LO44	100	0.9	97.66684753	200	BER_F2_N3
32	BER_N928	BER_LO460	118.729	0.9	115.9588714	237.458	500 kW PV
33	BER_N935	BER_LO467	439.604	0.9	429.3473684	879.208	200 kW ES
34	BER_N1040	BER_LO526	5150	0.78	4359.196961	10300	
35	BER_N1078	BER_LO541	118.812	0.9	116.0399349	237.624	BER_F2_N4
36	BER_N1134	BER_LO571	150	0.9	146.5002713	300	500 kW PV
37	BER_N1211	BER_LO610	439.604	0.9	429.3473684	879.208	200 kW ES
38	BER_N1239	BER_LO622	192.159	0.9	187.6756375	384.318	
39	BER_N1372	BER_LO692	150	0.9	146.5002713	300	BER_F2_N5
40	BER_N1392	BER_LO699	153.239	0.9	149.6637005	306.478	500 kW PV
41	BER_N1449	BER_LO725	153.239	0.95	157.9783505	306.478	200 kW ES
42	BER_N1491	BER_LO750	128.106	0.8	111.2151926	256.212	

43	BER_N1517	BER_LO764	102.16	0.95	105.3195876	204.32
44	BER_N1536	BER_LO771	153.239	0.95	157.9783505	306.478
45	BER_N1560	BER_LO783	153.239	0.95	157.9783505	306.478
46	BER_N1581	BER_LO794	106.83	0.9	104.3374932	213.66
47	BER_N1592	BER_LO800	178.093	0.95	183.6010309	356.186
48	BER_N1644	BER_LO824	320.266	0.9	312.7937059	640.532
49	BER_N1730	BER_LO867	169.901	0.95	175.1556701	339.802
50	BER_N1766	BER_LO882	212.673	0.95	219.2505155	425.346
51	BER_N1840	BER_LO916	255.446	0.9	249.4860553	510.892
52	BER_N1898	BER_LO943	102.16	0.95	105.3195876	204.32

Canning Street (CST) ZS Power Network:

#	Node1	Element	S[kVA]	cosphi	PV[kW]	DT[kVA]	Bulk RE & ES
1	CST_HV_N2042	CST_LO1007	400	0.85	368.9636462	800	CST_F1_N1
2	CST_HV_N2116	CST_LO1034	157.5	0.95	162.371134	315	500 kW PV
3	CST_HV_N2242	CST_LO1084	117.852	0.9	115.1023332	235.704	200 kW ES
4	CST_HV_N2243	CST_LO1085	1170	0.85	1079.218665	2340	
5	CST_HV_N2246	CST_LO1087	289.982	0.9	283.2162778	579.964	CST_F1_N2
6	CST_HV_N2251	CST_LO1091	400	0.8	347.2599023	800	500 kW PV
7	CST_HV_N2267	CST_LO1098	221.562	0.95	228.414433	443.124	200 kW ES
8	CST_HV_N2306	CST_LO1112	221.562	0.95	228.414433	443.124	
9	CST_HV_N2329	CST_LO1122	117.852	0.9	115.1023332	235.704	CST_F1_N3
10	CST_HV_N2353	CST_LO1133	119.152	0.9	116.3720022	238.304	500 kW PV
11	CST_HV_N2370	CST_LO1137	200.668	0.8	174.2098752	401.336	200 kW ES
12	CST_HV_N2373	CST_LO1139	381.286	0.9	372.3900163	762.572	
13	CST_HV_N2375	CST_LO1140	595.044	0.9	581.1607162	1190.088	CST_F1_N4
14	CST_HV_N2381	CST_LO1142	115.993	0.95	119.5804124	231.986	500 kW PV
15	CST_HV_N2395	CST_LO1150	173.989	0.8	151.0485079	347.978	200 kW ES
16	CST_HV_N2407	CST_LO1157	278.655	0.95	287.2731959	557.31	
17	CST_HV_N2441	CST_LO1177	119.152	0.95	122.8371134	238.304	CST_F1_N5
18	CST_HV_N2443	CST_LO1178	59.576	0.9	58.18600109	119.152	500 kW PV
19	CST_HV_N2478	CST_LO1195	117.852	0.95	121.4969072	235.704	200 kW ES
20	CST_HV_N2544	CST_LO1220	332.344	0.95	342.6226804	664.688	
21	CST_HV_N2547	CST_LO1222	221.562	0.95	228.414433	443.124	
22	CST_HV_N2562	CST_LO1228	119.152	0.95	122.8371134	238.304	
23	CST_HV_N2567	CST_LO1230	119.152	0.9	116.3720022	238.304	CST_F2_N1
24	CST_HV_N2591	CST_LO1243	115.993	0.9	113.2867065	231.986	500 kW PV
25	CST_HV_N2594	CST_LO1244	6.103	0.95	6.291752577	12.206	200 kW ES
26	CST_HV_N2602	CST_LO1247	12.756	0.95	13.15051546	25.512	
27	CST_HV_N2670	CST_LO1277	130	0.95	134.0206186	260	CST_F2_N2
28	CST_HV_N2679	CST_LO1281	59.576	0.95	61.4185567	119.152	500 kW PV
29	CST_HV_N221	CST_LO144	157.5	0.95	162.371134	315	200 kW ES
30	CST_HV_N222	CST_LO145	100	0.9	97.66684753	200	
31	CST_HV_N230	CST_LO148	150	0.9	146.5002713	300	CST_F2_N3
32	CST_HV_N232	CST_LO149	157.5	0.95	162.371134	315	500 kW PV
33	CST_HV_N233	CST_LO150	100	0.9	97.66684753	200	200 kW ES
34	CST_HV_N241	CST_LO155	100	0.8	86.81497558	200	
35	CST_HV_N243	CST_LO156	100	0.9	97.66684753	200	CST_F2_N4
36	CST_HV_N245	CST_LO157	150	0.9	146.5002713	300	500 kW PV
37	CST_HV_N246	CST_LO158	50	0.9	48.83342377	100	200 kW ES
38	CST_HV_N248	CST_LO159	100	0.8	86.81497558	200	
39	CST_HV_N377	CST_LO224	173.989	0.9	169.9295714	347.978	CST_F2_N5
40	CST_HV_N398	CST_LO230	57.996	0.9	56.64286489	115.992	500 kW PV
41	CST_HV_N430	CST_LO243	241.265	0.9	235.6359197	482.53	200 kW ES
42	CST_HV_N439	CST_LO247	100	0.9	97.66684753	200	

43	CST_HV_N451	CST_LO253	115.993	0.95	119.5804124	231.986
44	CST_HV_N480	CST_LO266	124.4	0.95	128.2474227	248.8
45	CST_HV_N553	CST_LO294	88.389	0.9	86.32674986	176.778
46	CST_HV_N557	CST_LO296	119.152	0.95	122.8371134	238.304
47	CST_HV_N617	CST_LO317	600	0.8	520.8898535	1200
48	CST_HV_N655	CST_LO337	115.993	0.9	113.2867065	231.986
49	CST_HV_N661	CST_LO340	190.812	0.9	186.3600651	381.624
50	CST_HV_N662	CST_LO341	402.495	0.9	393.104178	804.99
51	CST_HV_N672	CST_LO344	125	0.9	122.0835594	250
52	CST_HV_N681	CST_LO349	59.576	0.9	58.18600109	119.152
53	CST_HV_N55	CST_LO36	40.5	0.95	41.75257732	81
54	CST_HV_N724	CST_LO372	117.852	0.9	115.1023332	235.704
55	CST_HV_N735	CST_LO377	124.4	0.9	121.4975583	248.8
56	CST_HV_N740	CST_LO381	402.495	0.9	393.104178	804.99
57	CST_HV_N767	CST_LO395	228.771	0.9	223.4334238	457.542
58	CST_HV_N62	CST_LO40	200	0.95	206.185567	400
59	CST_HV_N802	CST_LO407	440.862	0.9	430.5760174	881.724
60	CST_HV_N872	CST_LO438	186.6	0.9	182.2463375	373.2
61	CST_HV_N902	CST_LO449	100	0.9	97.66684753	200
62	CST_HV_N903	CST_LO450	124.4	0.9	121.4975583	248.8
63	CST_HV_N932	CST_LO464	127.208	0.95	131.142268	254.416
64	CST_HV_N945	CST_LO472	186.599	0.95	192.3701031	373.198
65	CST_HV_N955	CST_LO479	12.206	0.95	12.58350515	24.412
66	CST_HV_N1004	CST_LO504	119.152	0.95	122.8371134	238.304
67	CST_HV_N1055	CST_LO530	119.152	0.95	122.8371134	238.304
68	CST_HV_N1057	CST_LO532	62.2	0.95	64.12371134	124.4
69	CST_HV_N1071	CST_LO538	59.576	0.95	61.4185567	119.152
70	CST_HV_N1081	CST_LO543	278.655	0.9	272.153554	557.31
71	CST_HV_N1127	CST_LO566	119.152	0.95	122.8371134	238.304
72	CST_HV_N1137	CST_LO574	332.343	0.8	288.5234943	664.686
73	CST_HV_N1166	CST_LO589	117.852	0.95	121.4969072	235.704
74	CST_HV_N1186	CST_LO599	412.483	0.85	380.4780792	824.966
75	CST_HV_N87	CST_LO60	400	0.8	347.2599023	800
76	CST_HV_N88	CST_LO61	180	0.95	185.5670103	360
77	CST_HV_N1258	CST_LO631	12.756	0.95	13.15051546	25.512
78	CST_HV_N1263	CST_LO634	332.344	0.95	342.6226804	664.688
79	CST_HV_N1269	CST_LO638	124.4	0.95	128.2474227	248.8
80	CST_HV_N1279	CST_LO643	332.344	0.95	342.6226804	664.688
81	CST_HV_N1294	CST_LO651	115.993	0.8	100.6992946	231.986
82	CST_HV_N1299	CST_LO656	119.152	0.95	122.8371134	238.304
83	CST_HV_N1342	CST_LO679	115.993	0.95	119.5804124	231.986
84	CST_HV_N1397	CST_LO703	497.599	0.8	431.9904504	995.198
85	CST_HV_N1410	CST_LO710	332.344	0.95	342.6226804	664.688
86	CST_HV_N1429	CST_LO719	124.4	0.9	121.4975583	248.8
87	CST_HV_N1432	CST_LO720	89.364	0.955	92.61271839	178.728

88	CST_HV_N1451	CST_LO727	147.315	0.95	151.871134	294.63	
89	CST_HV_N1456	CST_LO729	157.5	0.95	162.371134	315	
90	CST_HV_N120	CST_LO74	300	0.8	260.4449267	600	
91	CST_HV_N1479	CST_LO743	228.771	0.95	235.8463918	457.542	
92	CST_HV_N1510	CST_LO760	497.599	0.8	431.9904504	995.198	
93	CST_HV_N1518	CST_LO765	124.4	0.95	128.2474227	248.8	
94	CST_HV_N1554	CST_LO780	62.2	0.95	64.12371134	124.4	
95	CST_HV_N1570	CST_LO787	58.926	0.95	60.74845361	117.852	
96	CST_HV_N1576	CST_LO791	553.906	0.9	540.9825285	1107.812	
97	CST_HV_N1593	CST_LO801	115.993	0.9	113.2867065	231.986	
98	CST_HV_N1598	CST_LO803	1170	0.85	1079.218665	2340	
99	CST_HV_N1608	CST_LO808	124.4	0.95	128.2474227	248.8	
100	CST_HV_N1614	CST_LO811	200	0.95	206.185567	400	
101	CST_HV_N1616	CST_LO812	150	0.9	146.5002713	300	
102	CST_HV_N1622	CST_LO814	124.4	0.9	121.4975583	248.8	
103	CST_HV_N1633	CST_LO820	115.993	0.9	113.2867065	231.986	
104	CST_HV_N1653	CST_LO828	157.5	0.95	162.371134	315	
105	CST_HV_N1697	CST_LO848	63.604	0.9	62.1200217	127.208	
106	CST_HV_N1728	CST_LO866	241.265	0.9	235.6359197	482.53	
107	CST_HV_N1757	CST_LO878	160.07	0.9	156.3353228	320.14	
108	CST_HV_N1761	CST_LO880	400	0.8	347.2599023	800	
109	CST_HV_N1782	CST_LO889	241.265	0.8	209.4541508	482.53	
110	CST_HV_N1826	CST_LO910	464.011	0.9	453.1849159	928.022	
111	CST_HV_N142	CST_LO92	120	0.9	117.200217	240	
112	CST_HV_N1848	CST_LO922	127.208	0.9	124.2400434	254.416	
113	CST_HV_N1855	CST_LO926	124.4	0.95	128.2474227	248.8	
114	CST_HV_N1868	CST_LO932	278.655	0.9	272.153554	557.31	
115	CST_HV_N1870	CST_LO934	124.4	0.95	128.2474227	248.8	
116	CST_HV_N1882	CST_LO938	58.926	0.95	60.74845361	117.852	
117	CST_HV_N1932	CST_LO957	115.993	0.95	119.5804124	231.986	
118	CST_HV_N1954	CST_LO965	88.389	0.95	91.12268041	176.778	
119	CST_HV_N1966	CST_LO966	124.4	0.95	128.2474227	248.8	
120	CST_HV_N2018	CST_LO993	297.879	0.9	290.9290288	595.758	

Lakes Creek (LCR) ZS Power Network:

#	Node1	Element	S[kVA]	cosphi	PV[kW]	DT[kVA]	Bulk RE & ES
1	LCR_HV_N2039	LCR_LO1004	6.271	0.9	6.124688009	12.542	LCR_F1_N1
2	LCR_HV_N2091	LCR_LO1027	2.509	0.9	2.450461205	5.018	500 kW PV
3	LCR_HV_N2121	LCR_LO1035	1.254	0.9	1.224742268	2.508	200 kW ES
4	LCR_HV_N2145	LCR_LO1046	6.231	0.9	6.08562127	12.462	
5	LCR_HV_N2189	LCR_LO1067	121.173	0.9	118.3458492	242.346	LCR_F1_N2
6	LCR_HV_N2212	LCR_LO1073	2.509	0.9	2.450461205	5.018	500 kW PV
7	LCR_HV_N2221	LCR_LO1076	381.484	0.95	393.2824742	762.968	200 kW ES
8	LCR_HV_N2231	LCR_LO1081	90.646	0.9	88.53109061	181.292	
9	LCR_HV_N2257	LCR_LO1094	2.509	0.9	2.450461205	5.018	LCR_F1_N3
10	LCR_HV_N2285	LCR_LO1106	2.509	0.9	2.450461205	5.018	500 kW PV
11	LCR_HV_N2291	LCR_LO1109	6.193	0.9	6.048507868	12.386	200 kW ES
12	LCR_HV_N2298	LCR_LO1110	2.509	0.9	2.450461205	5.018	
13	LCR_HV_N2314	LCR_LO1116	2.509	0.9	2.450461205	5.018	LCR_F1_N4
14	LCR_HV_N2405	LCR_LO1155	2.509	0.9	2.450461205	5.018	500 kW PV
15	LCR_HV_N2436	LCR_LO1174	2.509	0.9	2.450461205	5.018	200 kW ES
16	LCR_HV_N2461	LCR_LO1186	3.763	0.9	3.675203473	7.526	
17	LCR_HV_N2471	LCR_LO1190	2.509	0.9	2.450461205	5.018	LCR_F1_N5
18	LCR_HV_N2473	LCR_LO1192	2.492	0.9	2.43385784	4.984	500 kW PV
19	LCR_HV_N2474	LCR_LO1193	3.763	0.9	3.675203473	7.526	200 kW ES
20	LCR_HV_N2494	LCR_LO1201	2.492	0.9	2.43385784	4.984	
21	LCR_HV_N2498	LCR_LO1203	121.173	0.95	124.9206186	242.346	
22	LCR_HV_N2520	LCR_LO1210	213.701	0.95	220.3103093	427.402	
23	LCR_HV_N2523	LCR_LO1211	3.738	0.9	3.650786761	7.476	LCR_F2_N1
24	LCR_HV_N2569	LCR_LO1232	121.173	0.9	118.3458492	242.346	500 kW PV
25	LCR_HV_N2572	LCR_LO1233	2.509	0.9	2.450461205	5.018	200 kW ES
26	LCR_HV_N2579	LCR_LO1237	2.509	0.9	2.450461205	5.018	
27	LCR_HV_N2585	LCR_LO1240	12.543	0.9	12.25035269	25.086	LCR_F2_N2
28	LCR_HV_N2596	LCR_LO1245	465	0.8	403.6896365	930	500 kW PV
29	LCR_HV_N2606	LCR_LO1249	2.509	0.9	2.450461205	5.018	200 kW ES
30	LCR_HV_N2625	LCR_LO1256	2.509	0.9	2.450461205	5.018	
31	LCR_HV_N2637	LCR_LO1262	2.509	0.9	2.450461205	5.018	LCR_F2_N3
32	LCR_HV_N2639	LCR_LO1263	2.509	0.9	2.450461205	5.018	500 kW PV
33	LCR_HV_N2655	LCR_LO1270	12.543	0.9	12.25035269	25.086	200 kW ES
34	LCR_HV_N2672	LCR_LO1279	2.509	0.9	2.450461205	5.018	
35	LCR_HV_N2681	LCR_LO1282	2.509	0.9	2.450461205	5.018	LCR_F2_N4
36	LCR_HV_N268	LCR_LO175	121.106	0.9	118.2804124	242.212	500 kW PV
37	LCR_HV_N302	LCR_LO186	50	0.9	48.83342377	100	200 kW ES
38	LCR_HV_N315	LCR_LO193	125	0.9	122.0835594	250	
39	LCR_HV_N316	LCR_LO194	157.5	0.95	162.371134	315	LCR_F2_N5
40	LCR_HV_N317	LCR_LO195	157.5	0.95	162.371134	315	500 kW PV
41	LCR_HV_N338	LCR_LO210	632.174	0.9	617.4244167	1264.348	200 kW ES
42	LCR_HV_N361	LCR_LO217	6.271	0.9	6.124688009	12.542	

43	LCR_HV_N365	LCR_LO219	121.173	0.95	124.9206186	242.346
44	LCR_HV_N372	LCR_LO222	6.271	0.9	6.124688009	12.542
45	LCR_HV_N386	LCR_LO226	6.271	0.9	6.124688009	12.542
46	LCR_HV_N411	LCR_LO238	6.231	0.9	6.08562127	12.462
47	LCR_HV_N423	LCR_LO241	121.173	0.95	124.9206186	242.346
48	LCR_hv_N436	LCR_LO246	155.102	0.9	151.4832339	310.204
49	LCR_HV_N492	LCR_LO272	314.876	0.95	324.614433	629.752
50	LCR_HV_N498	LCR_LO273	2.509	0.9	2.450461205	5.018
51	LCR_HV_N511	LCR_LO281	2.509	0.9	2.450461205	5.018
52	LCR_HV_N568	LCR_LO298	90.646	0.9	88.53109061	181.292
53	LCR_HV_N573	LCR_LO301	2.509	0.9	2.450461205	5.018
54	LCR_HV_N619	LCR_LO318	6.193	0.9	6.048507868	12.386
55	LCR_HV_N620	LCR_LO319	314.876	0.95	324.614433	629.752
56	LCR_HV_N623	LCR_LO320	60.587	0.9	59.17341291	121.174
57	LCR_HV_N635	LCR_LO327	2.509	0.9	2.450461205	5.018
58	LCR_HV_N640	LCR_LO331	2.509	0.9	2.450461205	5.018
59	LCR_HV_N657	LCR_LO339	121.173	0.9	118.3458492	242.346
60	LCR_HV_N729	LCR_LO375	60.587	0.95	62.46082474	121.174
61	LCR_HV_N776	LCR_LO397	142.126	0.9	138.8099837	284.252
62	LCR_HV_N829	LCR_LO418	6.271	0.9	6.124688009	12.542
63	LCR_HV_N835	LCR_LO422	2.509	0.9	2.450461205	5.018
64	LCR_HV_N842	LCR_LO424	2.509	0.9	2.450461205	5.018
65	LCR_HV_N844	LCR_LO425	5000	0.74	4015.192621	10000
66	LCR_HV_N925	LCR_LO459	70.552	0.9	68.90591427	141.104
67	LCR_HV_N69	LCR_LO46	300	0.95	309.2783505	600
68	LCR_HV_N931	LCR_LO463	2.509	0.9	2.450461205	5.018
69	LCR_HV_N936	LCR_LO468	302.765	0.9	295.7010309	605.53
70	LCR_HV_N70	LCR_LO47	55	0.9	53.71676614	110
71	LCR_HV_N940	LCR_LO470	2.509	0.9	2.450461205	5.018
72	LCR_HV_N964	LCR_LO484	2.509	0.9	2.450461205	5.018
73	LCR_HV_N983	LCR_LO494	6.271	0.9	6.124688009	12.542
74	LCR_HV_N986	LCR_LO495	3.763	0.9	3.675203473	7.526
75	LCR_HV_N993	LCR_LO497	2.509	0.9	2.450461205	5.018
76	LCR_HV_N73	LCR_LO50	100	0.9	97.66684753	200
77	LCR_HV_N1021	LCR_LO514	1.254	0.9	1.224742268	2.508
78	LCR_HV_N1034	LCR_LO521	464	0.8	402.8214867	928
79	LCR_HV_N1061	LCR_LO534	2.509	0.9	2.450461205	5.018
80	LCR_HV_N1068	LCR_LO537	2.509	0.9	2.450461205	5.018
81	LCR_HV_N1087	LCR_LO545	181.76	0.95	187.3814433	363.52
82	LCR_HV_N1118	LCR_LO562	121.106	0.95	124.8515464	242.212
83	LCR_HV_N1161	LCR_LO587	60.587	0.9	59.17341291	121.174
84	LCR_HV_N1176	LCR_LO593	2.509	0.9	2.450461205	5.018
85	LCR_HV_N1234	LCR_LO620	12.461	0.9	12.17026587	24.922
86	LCR_HV_N1280	LCR_LO644	6.231	0.9	6.08562127	12.462
87	LCR_HV_N1282	LCR_LO645	1.254	0.9	1.224742268	2.508

88	LCR_HV_N1290	LCR_LO648	155.102	0.9	151.4832339	310.204
89	LCR_HV_N1293	LCR_LO650	181.76	0.95	187.3814433	363.52
90	LCR_HV_N1300	LCR_LO657	2.509	0.9	2.450461205	5.018
91	LCR_HV_N1315	LCR_LO668	121.173	0.95	124.9206186	242.346
92	LCR_HV_N1348	LCR_LO682	121.173	0.95	124.9206186	242.346
93	LCR_HV_N1378	LCR_LO695	2.509	0.9	2.450461205	5.018
94	LCR_HV_N1404	LCR_LO708	2.509	0.9	2.450461205	5.018
95	LCR_HV_N1421	LCR_LO715	12.543	0.9	12.25035269	25.086
96	LCR_HV_N1422	LCR_LO716	121.173	0.95	124.9206186	242.346
97	LCR_HV_N1445	LCR_LO724	142.126	0.9	138.8099837	284.252
98	LCR_HV_N1455	LCR_LO728	130.474	0.95	134.5092784	260.948
99	LCR_HV_N1505	LCR_LO757	121.173	0.9	118.3458492	242.346
100	LCR_HV_N1527	LCR_LO766	2.509	0.9	2.450461205	5.018
101	LCR_HV_N1545	LCR_LO775	6.193	0.8	5.376451438	12.386
102	LCR_HV_N1546	LCR_LO776	121.173	0.95	124.9206186	242.346
103	LCR_HV_N1600	LCR_LO804	121.173	0.9	118.3458492	242.346
104	LCR_HV_N1606	LCR_LO806	45.323	0.9	44.26554531	90.646
105	LCR_HV_N1623	LCR_LO815	1.254	0.9	1.224742268	2.508
106	LCR_HV_N1637	LCR_LO821	121.173	0.9	118.3458492	242.346
107	LCR_HV_N1649	LCR_LO825	2.509	0.9	2.450461205	5.018
108	LCR_HV_N1658	LCR_LO830	2.509	0.9	2.450461205	5.018
109	LCR_HV_N1666	LCR_LO832	12.461	0.9	12.17026587	24.922
110	LCR_HV_N1683	LCR_LO838	2.509	0.9	2.450461205	5.018
111	LCR_HV_N1685	LCR_LO839	2.5	0.9	2.441671188	5
112	LCR_HV_N1686	LCR_LO840	2.509	0.9	2.450461205	5.018
113	LCR_HV_N1688	LCR_LO841	12.387	0.95	12.77010309	24.774
114	LCR_HV_N1704	LCR_LO851	121.173	0.9	118.3458492	242.346
115	LCR_HV_N1710	LCR_LO855	2.509	0.9	2.450461205	5.018
116	LCR_HV_N1715	LCR_LO859	100	0.8	86.81497558	200
117	LCR_HV_N1736	LCR_LO870	2600	0.8	2257.189365	5200
118	LCR_HV_N1741	LCR_LO872	394.806	0.9	385.5945741	789.612
119	LCR_HV_N1749	LCR_LO875	121.173	0.95	124.9206186	242.346
120	LCR_HV_N1770	LCR_LO884	151.466	0.95	156.1505155	302.932
121	LCR_HV_N1771	LCR_LO885	12.543	0.95	12.93092784	25.086
122	LCR_HV_N1784	LCR_LO890	60.587	0.9	59.17341291	121.174
123	LCR_HV_N1792	LCR_LO894	226.615	0.9	221.3277265	453.23
124	LCR_HV_N1804	LCR_LO899	60.587	0.9	59.17341291	121.174
125	LCR_HV_N1846	LCR_LO921	2.509	0.9	2.450461205	5.018
126	LCR_HV_N1849	LCR_LO923	12.543	0.9	12.25035269	25.086
127	LCR_HV_N1896	LCR_LO941	233.864	0.9	228.4075963	467.728
128	LCR_HV_N1911	LCR_LO947	2.509	0.9	2.450461205	5.018
129	LCR_HV_N1928	LCR_LO954	30.675	0.95	31.62371134	61.35
130	LCR_HV_N1939	LCR_LO959	12.543	0.9	12.25035269	25.086
131	LCR_HV_N1948	LCR_LO962	157.438	0.95	162.3072165	314.876
132	LCR_HV_N1988	LCR_LO977	2.509	0.9	2.450461205	5.018

133	LCR_HV_N2007	LCR_LO987	6.271	0.9	6.124688009	12.542
134	LCR_HV_N2017	LCR_LO992	6.271	0.9	6.124688009	12.542
135	LCR_HV_N2020	LCR_LO995	233.864	0.9	228.4075963	467.728
136	LCR_HV_N2094	LCR_LO1029	2.509	0.9	2.450461205	5.018
137	LCR_HV_N2213	LCR_LO1074	2.509	0.9	2.450461205	5.018
138	LCR_HV_N2338	LCR_LO1126	2.509	0.9	2.450461205	5.018
139	LCR_HV_N2545	LCR_LO1221	2.509	0.9	2.450461205	5.018
140	LCR_HV_N2627	LCR_LO1258	2.509	0.9	2.450461205	5.018
141	LCR_HV_N357	LCR_LO214	5.017	0.9	4.899945741	10.034
142	LCR_HV_N472	LCR_LO262	2.509	0.9	2.450461205	5.018
143	LCR_HV_N529	LCR_LO289	2.509	0.9	2.450461205	5.018
144	LCR_HV_N678	LCR_LO347	6.271	0.9	6.124688009	12.542
145	LCR_HV_N690	LCR_LO356	2.509	0.9	2.450461205	5.018
146	LCR_HV_N710	LCR_LO365	2.509	0.9	2.450461205	5.018
147	LCR_HV_N755	LCR_LO389	2.509	0.9	2.450461205	5.018
148	LCR_HV_N804	LCR_LO408	2.509	0.9	2.450461205	5.018
149	LCR_HV_N855	LCR_LO431	2.509	0.9	2.450461205	5.018
150	LCR_HV_N863	LCR_LO435	2.509	0.9	2.450461205	5.018
151	LCR_HV_N970	LCR_LO487	2.509	0.9	2.450461205	5.018
152	LCR_HV_N1024	LCR_LO516	2.509	0.9	2.450461205	5.018
153	LCR_HV_N1123	LCR_LO563	2.509	0.9	2.450461205	5.018
154	LCR_HV_N1135	LCR_LO572	2.509	0.9	2.450461205	5.018
155	LCR_HV_N1183	LCR_LO597	5.017	0.9	4.899945741	10.034
156	LCR_HV_N1209	LCR_LO609	5.017	0.9	4.899945741	10.034
157	LCR_HV_N1229	LCR_LO619	5.017	0.9	4.899945741	10.034
158	LCR_HV_N1298	LCR_LO655	5.017	0.9	4.899945741	10.034
159	LCR_HV_N1468	LCR_LO737	2.509	0.9	2.450461205	5.018
160	LCR_HV_N1469	LCR_LO738	2.509	0.9	2.450461205	5.018
161	LCR_HV_N1558	LCR_LO782	2.509	0.9	2.450461205	5.018
162	LCR_HV_N1580	LCR_LO793	2.509	0.9	2.450461205	5.018
163	LCR_HV_N1632	LCR_LO819	2.509	0.9	2.450461205	5.018
164	LCR_HV_N1724	LCR_LO863	2.509	0.9	2.450461205	5.018
165	LCR_HV_N1779	LCR_LO888	2.509	0.9	2.450461205	5.018
166	LCR_HV_N1845	LCR_LO920	2.509	0.9	2.450461205	5.018
167	LCR_HV_N1981	LCR_LO974	2.509	0.9	2.450461205	5.018
168	LCR_HV_N1997	LCR_LO983	2.509	0.9	2.450461205	5.018
169	RAG_N2617	RAG_LO1251	2.509	0.9	2.450461205	5.018
170	RAG_N2671	RAG_LO1278	2.509	0.9	2.450461205	5.018
171	RAG_N408	RAG_LO235	2.509	0.9	2.450461205	5.018
172	RAG_N784	RAG_LO401	2.509	0.9	2.450461205	5.018
173	RAG_N897	RAG_LO448	2.509	0.9	2.450461205	5.018
174	RAG_N72	RAG_LO49	20	0.9	19.53336951	40
175	RAG_N1214	RAG_LO612	2.509	0.9	2.450461205	5.018
176	RAG_N90	RAG_LO63	31.5	0.95	32.4742268	63
177	RAG_N1366	RAG_LO689	2.509	0.9	2.450461205	5.018

178	RAG_N1565	RAG_LO786	2.509	0.9	2.450461205	5.018	
179	RAG_N1706	RAG_LO853	5.017	0.9	4.899945741	10.034	
180	RAG_N137	RAG_LO86	35	0.95	36.08247423	70	
181	RAG_N1725	RAG_LO864	2.509	0.9	2.450461205	5.018	
182	RAG_N1788	RAG_LO892	2.509	0.9	2.450461205	5.018	
183	RAG_N1800	RAG_LO896	2.509	0.9	2.450461205	5.018	

Rockhampton South (RSH) ZS Power Network:

#	Node1	Element	S[kVA]	cosphi	PV[kW]	DT[kVA]	Bulk RE & ES
1	RSH_HV_N2030	RSH_LO1000	176.275	0.9	172.1622355	352.55	RSH_F1_N1
2	RSH_HV_N2041	RSH_LO1006	12.599	0.9	12.30504612	25.198	500 kW PV
3	RSH_HV_N2043	RSH_LO1008	459.445	0.95	473.6546392	918.89	200 kW ES
4	RSH_HV_N2051	RSH_LO1012	12.599	0.9	12.30504612	25.198	
5	RSH_HV_N2069	RSH_LO1016	113.951	0.8	98.92653283	227.902	RSH_F1_N2
6	RSH_HV_N2074	RSH_LO1020	6.3	0.9	6.153011394	12.6	500 kW PV
7	RSH_HV_N2080	RSH_LO1023	12.599	0.9	12.30504612	25.198	200 kW ES
8	RSH_HV_N2099	RSH_LO1031	10.577	0.9	10.33022246	21.154	
9	RSH_HV_N2114	RSH_LO1033	347.924	0.9	339.8064026	695.848	RSH_F1_N3
10	RSH_HV_N2126	RSH_LO1039	140.7	0.95	145.0515464	281.4	500 kW PV
11	RSH_HV_N2147	RSH_LO1047	347.924	0.9	339.8064026	695.848	200 kW ES
12	RSH_HV_N2154	RSH_LO1049	3.78	0.9	3.691806837	7.56	
13	RSH_HV_N2163	RSH_LO1053	250.5	0.95	258.2474227	501	RSH_F1_N4
14	RSH_HV_N2172	RSH_LO1058	6.3	0.9	6.153011394	12.6	500 kW PV
15	RSH_HV_N2176	RSH_LO1060	113.951	0.95	117.4752577	227.902	200 kW ES
16	RSH_HV_N2182	RSH_LO1063	324.207	0.98	344.7887792	648.414	
17	RSH_HV_N2186	RSH_LO1066	180.458	0.8	156.6645686	360.916	RSH_F1_N5
18	RSH_HV_N2229	RSH_LO1080	221.665	0.8	192.4384156	443.33	500 kW PV
19	RSH_HV_N2245	RSH_LO1086	58.758	0.9	57.38708627	117.516	200 kW ES
20	RSH_HV_N2250	RSH_LO1090	281.4	0.95	290.1030928	562.8	
21	RSH_HV_N2280	RSH_LO1102	117.517	0.9	114.7751492	235.034	
22	RSH_HV_N2281	RSH_LO1103	12.599	0.9	12.30504612	25.198	
23	RSH_HV_N2344	RSH_LO1129	227.377	0.95	234.4092784	454.754	RSH_F2_N1
24	RSH_HV_N2354	RSH_LO1134	35.255	0.95	36.34536082	70.51	500 kW PV
25	RSH_HV_N2371	RSH_LO1138	12.599	0.9	12.30504612	25.198	200 kW ES
26	RSH_HV_N2388	RSH_LO1146	58.758	0.9	57.38708627	117.516	
27	RSH_HV_N2391	RSH_LO1148	117.517	0.9	114.7751492	235.034	RSH_F2_N2
28	RSH_HV_N2400	RSH_LO1152	12.599	0.9	12.30504612	25.198	500 kW PV
29	RSH_HV_N2408	RSH_LO1158	2.52	0.9	2.461204558	5.04	200 kW ES
30	RSH_HV_N2410	RSH_LO1160	2.52	0.9	2.461204558	5.04	
31	RSH_HV_N2424	RSH_LO1166	153.934	0.95	158.6948454	307.868	RSH_F2_N3
32	RSH_HV_N2428	RSH_LO1168	2.52	0.9	2.461204558	5.04	500 kW PV
33	RSH_HV_N2431	RSH_LO1170	6.3	0.9	6.153011394	12.6	200 kW ES
34	RSH_HV_N2432	RSH_LO1171	98.518	0.9	96.21942485	197.036	
35	RSH_HV_N2449	RSH_LO1181	2.52	0.9	2.461204558	5.04	RSH_F2_N4
36	RSH_HV_N2455	RSH_LO1184	113.951	0.8	98.92653283	227.902	500 kW PV
37	RSH_HV_N2464	RSH_LO1189	2.52	0.9	2.461204558	5.04	200 kW ES
38	RSH_HV_N2472	RSH_LO1191	58.758	0.9	57.38708627	117.516	
39	RSH_HV_N2479	RSH_LO1196	12.599	0.9	12.30504612	25.198	RSH_F2_N5
40	RSH_HV_N2531	RSH_LO1212	168.84	0.95	174.0618557	337.68	500 kW PV
41	RSH_HV_N2532	RSH_LO1213	430	0.8	373.304395	860	200 kW ES
42	RSH_HV_N2539	RSH_LO1217	184.721	0.9	180.4111774	369.442	

43	RSH_HV_N2541	RSH_LO1218	411.97	0.95	424.7113402	823.94
44	RSH_HV_N2551	RSH_LO1223	560	0.85	516.5491047	1120
45	RSH_HV_N2580	RSH_LO1238	216.55	0.9	211.4975583	433.1
46	RSH_HV_N2641	RSH_LO1264	411.97	0.95	424.7113402	823.94
47	RSH_HV_N2663	RSH_LO1273	362.052	0.95	373.2494845	724.104
48	RSH_HV_N2669	RSH_LO1276	760	0.85	701.0309278	1520
49	RSH_HV_N205	RSH_LO137	5	0.9	4.883342377	10
50	RSH_HV_N215	RSH_LO139	157.5	0.95	162.371134	315
51	RSH_HV_N217	RSH_LO141	100	0.9	97.66684753	200
52	RSH_HV_N219	RSH_LO142	157.5	0.95	162.371134	315
53	RSH_HV_N220	RSH_LO143	50	0.9	48.83342377	100
54	RSH_HV_N225	RSH_LO146	125	0.9	122.0835594	250
55	RSH_HV_N227	RSH_LO147	600	0.8	520.8898535	1200
56	RSH_HV_N234	RSH_LO151	227.377	0.95	234.4092784	454.754
57	RSH_HV_N236	RSH_LO152	227.377	0.95	234.4092784	454.754
58	RSH_HV_N374	RSH_LO223	113.951	0.9	111.2923494	227.902
59	RSH_HV_N405	RSH_LO234	113.951	0.9	111.2923494	227.902
60	RSH_HV_N419	RSH_LO240	56.975	0.9	55.64568638	113.95
61	RSH_HV_N445	RSH_LO250	6.3	0.9	6.153011394	12.6
62	RSH_HV_N463	RSH_LO258	2.52	0.9	2.461204558	5.04
63	RSH_HV_N475	RSH_LO263	2.52	0.9	2.461204558	5.04
64	RSH_HV_N503	RSH_LO276	2.52	0.9	2.461204558	5.04
65	RSH_HV_N510	RSH_LO280	800	0.85	737.9272925	1600
66	RSH_HV_N525	RSH_LO288	2.52	0.9	2.461204558	5.04
67	RSH_HV_N537	RSH_LO291	162.104	0.8	140.730548	324.208
68	RSH_HV_N571	RSH_LO299	2.52	0.9	2.461204558	5.04
69	RSH_HV_N572	RSH_LO300	124.4	0.9	121.4975583	248.8
70	RSH_HV_N575	RSH_LO302	117.517	0.8	102.0223549	235.034
71	RSH_HV_N628	RSH_LO325	12.599	0.95	12.98865979	25.198
72	RSH_HV_N636	RSH_LO328	2.52	0.9	2.461204558	5.04
73	RSH_HV_N642	RSH_LO332	113.951	0.8	98.92653283	227.902
74	RSH_HV_N680	RSH_LO348	6.3	0.9	6.153011394	12.6
75	RSH_HV_N715	RSH_LO368	12.599	0.8	10.93781877	25.198
76	RSH_HV_N725	RSH_LO373	58.758	0.9	57.38708627	117.516
77	RSH_HV_N745	RSH_LO384	430	0.85	396.6359197	860
78	RSH_HV_N750	RSH_LO387	232.43	0.8	201.7840477	464.86
79	RSH_HV_N782	RSH_LO400	12.599	0.95	12.98865979	25.198
80	RSH_HV_N801	RSH_LO406	2.52	0.9	2.461204558	5.04
81	RSH_HV_N812	RSH_LO411	324.207	0.8	281.4602279	648.414
82	RSH_HV_N813	RSH_LO412	170.926	0.9	166.9380358	341.852
83	RSH_HV_N819	RSH_LO415	324.207	0.8	281.4602279	648.414
84	RSH_HV_N850	RSH_LO429	12.599	0.9	12.30504612	25.198
85	RSH_HV_N905	RSH_LO452	168.84	0.95	174.0618557	337.68
86	RSH_HV_N912	RSH_LO455	500	0.8	434.0748779	1000

87	RSH_HV_N71	RSH_LO48	145	0.9	141.6169289	290
88	RSH_HV_N960	RSH_LO481	117.517	0.9	114.7751492	235.034
89	RSH_HV_N973	RSH_LO489	2.52	0.9	2.461204558	5.04
90	RSH_HV_N981	RSH_LO493	411.97	0.95	424.7113402	823.94
91	RSH_HV_N997	RSH_LO500	362.052	0.8	314.3153554	724.104
92	RSH_HV_N1000	RSH_LO502	411.97	0.95	424.7113402	823.94
93	RSH_HV_N1017	RSH_LO510	347.924	0.8	302.0501356	695.848
94	RSH_HV_N1027	RSH_LO518	600	0.9	586.0010852	1200
95	RSH_HV_N1043	RSH_LO527	324.207	0.8	281.4602279	648.414
96	RSH_HV_N1084	RSH_LO544	113.951	0.95	117.4752577	227.902
97	RSH_HV_N81	RSH_LO55	100	0.9	97.66684753	200
98	RSH_HV_N1097	RSH_LO550	186.6	0.9	182.2463375	373.2
99	RSH_HV_N1109	RSH_LO558	600	0.8	520.8898535	1200
100	RSH_HV_N1112	RSH_LO559	12.599	0.95	12.98865979	25.198
101	RSH_HV_N1152	RSH_LO583	194.524	0.9	189.9854585	389.048
102	RSH_HV_N1154	RSH_LO584	362.052	0.9	353.6047748	724.104
103	RSH_HV_N1174	RSH_LO592	6.3	0.9	6.153011394	12.6
104	RSH_HV_N1193	RSH_LO603	2.52	0.9	2.461204558	5.04
105	RSH_HV_N1196	RSH_LO604	47.007	0.8	40.80911557	94.014
106	RSH_HV_N1197	RSH_LO605	117.517	0.9	114.7751492	235.034
107	RSH_HV_N1200	RSH_LO607	170.926	0.9	166.9380358	341.852
108	RSH_HV_N1201	RSH_LO608	184.721	0.9	180.4111774	369.442
109	RSH_HV_N89	RSH_LO62	140	0.9	136.7335865	280
110	RSH_HV_N1237	RSH_LO621	140.7	0.95	145.0515464	281.4
111	RSH_HV_N1247	RSH_LO626	2.52	0.9	2.461204558	5.04
112	RSH_HV_N1257	RSH_LO630	180	0.8	156.266956	360
113	RSH_HV_N91	RSH_LO64	750	0.8	651.1123169	1500
114	RSH_HV_N1297	RSH_LO654	184.721	0.95	190.4340206	369.442
115	RSH_HV_N1313	RSH_LO666	347.924	0.8	302.0501356	695.848
116	RSH_HV_N1334	RSH_LO675	362.052	0.9	353.6047748	724.104
117	RSH_HV_N1370	RSH_LO691	144.367	0.9	140.9986978	288.734
118	RSH_HV_N1375	RSH_LO693	6.3	0.9	6.153011394	12.6
119	RSH_HV_N1376	RSH_LO694	310.999	0.8	269.9937059	621.998
120	RSH_HV_N1382	RSH_LO697	430	0.8	373.304395	860
121	RSH_HV_N1385	RSH_LO698	400	0.8	347.2599023	800
122	RSH_HV_N1405	RSH_LO709	411.97	0.95	424.7113402	823.94
123	RSH_HV_N1416	RSH_LO712	600	0.9	586.0010852	1200
124	RSH_HV_N1434	RSH_LO721	459.445	0.95	473.6546392	918.89
125	RSH_HV_N1507	RSH_LO758	411.97	0.95	424.7113402	823.94
126	RSH_HV_N1515	RSH_LO762	2000	0.85	1844.818231	4000
127	RSH_HV_N1531	RSH_LO769	284.877	0.9	278.2303852	569.754
128	RSH_HV_N1533	RSH_LO770	35.255	0.95	36.34536082	70.51
129	RSH_HV_N1583	RSH_LO795	6.3	0.9	6.153011394	12.6
130	RSH_HV_N1681	RSH_LO836	800	0.85	737.9272925	1600

131	RSH_HV_N1689	RSH_LO842	266.499	0.95	274.7412371	532.998	
132	RSH_HV_N1734	RSH_LO869	170.926	0.8	148.3893652	341.852	
133	RSH_HV_N1738	RSH_LO871	12.599	0.9	12.30504612	25.198	
134	RSH_HV_N1745	RSH_LO874	6.3	0.9	6.153011394	12.6	
135	RSH_HV_N1785	RSH_LO891	117.517	0.9	114.7751492	235.034	
136	RSH_HV_N1797	RSH_LO895	459.445	0.95	473.6546392	918.89	
137	RSH_HV_N1803	RSH_LO898	290.177	0.8	251.9170917	580.354	
138	RSH_HV_N140	RSH_LO90	400	0.8	347.2599023	800	
139	RSH_HV_N1805	RSH_LO900	459.445	0.9	448.7254476	918.89	
140	RSH_HV_N1813	RSH_LO903	275.027	0.95	283.5329897	550.054	
141	RSH_HV_N1852	RSH_LO924	58.758	0.8	51.01074335	117.516	
142	RSH_HV_N1860	RSH_LO927	2.52	0.9	2.461204558	5.04	
143	RSH_HV_N1876	RSH_LO936	180.458	0.9	176.2476397	360.916	
144	RSH_HV_N1904	RSH_LO944	56.975	0.9	55.64568638	113.95	
145	RSH_HV_N1926	RSH_LO953	2.52	0.9	2.461204558	5.04	
146	RSH_HV_N1949	RSH_LO963	170.926	0.9	166.9380358	341.852	
147	RSH_HV_N1982	RSH_LO975	117.517	0.9	114.7751492	235.034	
148	RSH_HV_N2003	RSH_LO985	2.454	0.9	2.396744438	4.908	
149	RSH_HV_N2008	RSH_LO988	144.367	0.8	125.3321758	288.734	
150	RSH_HV_N2626	RSH_LO1257	2.52	0.9	2.461204558	5.04	
151	RSH_HV_N653	RSH_LO336	2.52	0.9	2.461204558	5.04	
152	RSH_HV_N821	RSH_LO416	2.52	0.9	2.461204558	5.04	
153	RSH_HV_N853	RSH_LO430	2.52	0.9	2.461204558	5.04	
154	RSH_HV_N950	RSH_LO475	2.52	0.9	2.461204558	5.04	
155	RSH_HV_N1006	RSH_LO505	2.52	0.9	2.461204558	5.04	
156	RSH_HV_N1007	RSH_LO506	2.52	0.9	2.461204558	5.04	
157	RSH_HV_N1106	RSH_LO556	18.803	0.9	18.36429734	37.606	
158	RSH_HV_N1380	RSH_LO696	2.52	0.9	2.461204558	5.04	
159	RSH_HV_N118	RSH_LO72	25	0.9	24.41671188	50	
160	RSH_HV_N1450	RSH_LO726	2.52	0.9	2.461204558	5.04	
161	RSH_HV_N1485	RSH_LO745	2.52	0.9	2.461204558	5.04	
162	RSH_HV_N1574	RSH_LO790	2.52	0.9	2.461204558	5.04	
163	RSH_HV_N1639	RSH_LO822	2.52	0.9	2.461204558	5.04	
164	RSH_HV_N1711	RSH_LO856	2.52	0.9	2.461204558	5.04	

A-2: Power Network of Rockhampton

The complete power network of Rockhampton developed in PSS SINCAL is shown in next page.

Rockhampton Power Network